



Université catholique de Louvain

Earth and Life Institute-Agronomy (ELI-A)

Groupe de Recherche en Physiologie Végétale (GRPV)

**Interest of hemp for phytomanagement of
heavy metal contaminated agricultural soil:
putative impact of silicon in relation to fibre
production**

Marie LUYCKX

Doctoral thesis in Agronomical sciences and biological engineering

PhD committee

Prof. Stanley Lutts, UCLouvain (supervisor)

Dr Gea Guerriero, LIST (supervisor)

Prof. Pierre Bertin, UCLouvain

Prof. Christophe Waterlot, ISA Lille

Prof. Muriel Quinet, UCLouvain

Prof. Richard Lambert, UCLouvain

Dr Aricia Evlard, ValBiom

Abstract

Cannabis sativa L. is a promising species for non-food production on moderate heavy metal (HM)-contaminated farmland soils and considered as a potential crop for cleaning the soil from HM because of its high biomass production, its long root system and its capacity to absorb and accumulate HM. However, until now, “soil remediation” is usually considered independently of “soil production”, and there is an obvious lack of information regarding the possibility to conciliate phytomanagement and obtaining valuable marketable products. The global aim of the present thesis is to contribute to fill this gap, with specific attention to hemp fibres, the most economically valuable part of the plant. Using two different growing systems (nutrient solution or contaminated agricultural soil), we investigated the contaminant concentration and distribution in hemp raw material, hemp HM tolerance, and the impact of HM on fibre production and quality, considering for the first time industrial standards.

We showed that *C. sativa* is suited for fibre production associated with HM management due to its extraction potential. However, this strategy should be limited to soils with a moderate content of HM, considering that high HM bioavailability negatively impacted plant growth and development. The management of moderately HM-contaminated soils with hemp can contribute to reduce the dispersion of HM in the environment through its high biomass yield and its important root system. Besides, HM impacted fibre elongation and thickening, but not their mechanical properties, and were mainly accumulated in trichomes rather than in fibres. Fibres could thus be used in special products like insulating material and cements, with a specific attention to the stability of these material regarding the erosion of the final product.

To devise agricultural strategies aimed at improving crop yield, the effect of silicon (Si) on plants' stress resistance was also considered. Overall, we demonstrated that the addition of Si had numerous physiological impacts on the plant behavior occurring rapidly after HM stress application and before any modification in terms of growth. The main beneficial effects involved HM sequestration, improved oxidative response, and stimulation of energy metabolism. Si thus has the potential of enabling the plant to react adaptively against HM stress responses and promotes tolerance. Si also accumulated in bast fibres and influenced the timing of fibre elongation and transition from elongation to thickening. Si application can thus have an impact on fibres' final properties after harvest.

Remerciements

Je voudrais d'abord remercier le Professeur Stanley Lutts pour la confiance qu'il m'a accordée lorsque j'ai décidé de me lancer dans cette grande aventure qu'est la thèse. Son soutien, l'ampleur de ses compétences scientifiques, ainsi que sa grande humanité m'ont permis de mener à bien ce projet.

Je voudrais ensuite remercier le Dr Gea Guerriero pour toutes les merveilleuses opportunités d'apprendre qu'elle m'a apportées, que ce soit au niveau de la rédaction d'articles auxquels elle m'a proposé de participer, ou des techniques de biologie moléculaire que j'ai pu aborder lorsqu'elle m'a prise sous son aile au LIST.

Je remercie également les membres de mon jury de thèse : Prof. Muriel Quinet, Dr. Aricia Evlard, Prof. Pierre Bertin, Prof. Christophe Waterlot, et Prof. Richard Lambert. A tous, merci pour vos conseils et commentaires constructifs.

Je ne peux évidemment pas oublier l'aide précieuse des membres du GRPV ! Que ce soit pour la mise en place des cultures en serres (merci Jacques et Baudouin), pour l'aide lors de différents dosages (Brigitte et Marie-Eve), ou encore pour la magnifique ambiance de travail (un grand merci à tous !) dont j'ai pu profiter au cours de ces 6 années de thèse. Je remercie particulièrement Muriel pour ses nombreux bons conseils, particulièrement dans la dernière ligne droite de la thèse. J'ai par ailleurs une pensée affectueuse pour la dream-team du bureau : Servane et Mathilde, sans qui les super-nanas n'existeraient pas, mais également tous les autres chercheurs que j'ai pu rencontrer et apprécier (Audrey, Lauranne, Willy, Hermann, Emna, Christophe, ...). Je remercie également Béatrice, Lindsay et Adeline pour leur aide administrative. Je remercie enfin M. Lejeune pour sa bonne humeur et les discussions passionnantes tournant bien évidemment autour de sujets en biologie, on ne se refait pas !

Je remercie également ma famille pour son soutien sans failles, en particulier mes parents, mon frère et ma soeur pour leur confiance et les nombreux encouragements, la chouette sortie de terrain avec ma maman et la curiosité scientifique insatiable de mon papa.

Je remercie bien sûr mes amis, et ceux parmi eux qui sont devenus comme une seconde famille : Mélissa, Julien, Maëlle et Ricky. Les parties de jeu de société, la bonne cuisine mauritienne et liégeoise de Ricky et Maëlle, les

desserts à tomber par terre de Julien, les nombreuses séances de badminton avec Mélissa, et tous ces bons moments passés avec vous, ont rythmé, mais surtout égayé les soirées en semaine.

La personne que je tiens le plus à remercier est Frédéric, mon compagnon, témoin de mes moments de joie, mais aussi de doutes. Tu n'as jamais cessé de m'encourager tout au long de mon parcours universitaire, et d'être présent quand j'en avais besoin. Merci pour toute la joie et le grain de folie que tu apportes à mon quotidien, et merci tout simplement de faire partie de ma vie :).

Thesis achievements

Luyckx, M., Hausman, J. F., Lutts, S., & Guerriero, G. (2017). Impact of silicon in plant biomass production: focus on bast fibres, hypotheses, and perspectives. *Plants*, *6*, 37.

Luyckx, M., Hausman, J. F., Lutts, S., & Guerriero, G. (2017). Silicon and plants: current knowledge and technological perspectives. *Frontiers in Plant Science*, *8*, 411.

Berni, R., Luyckx, M., Xu, X., Legay, S., Sergeant, K., Hausman, J. F., ... & Guerriero, G. (2019). Reactive oxygen species and heavy metal stress in plants: Impact on the cell wall and secondary metabolism. *Environmental and experimental botany*, *161*, 98-106.

Luyckx, M., Berni, R., Cai, G., Lutts, S., & Guerriero, G. (2019). Impact of heavy metals on non-food herbaceous crops and prophylactic role of Si. In *Plant Metallomics and Functional Omics* (pp. 303-321). Springer, Cham.

Luyckx, M., Hausman, J.F., Isenborghs, A., Guerriero, G., Lutts, S. (2021). Impact of cadmium and zinc on proteins and cell wall-related gene expression in young stems of hemp (*Cannabis sativa* L.) and influence of exogenous silicon. *Environmental and experimental botany*, *183*, 104363.

Luyckx, M., Hausman, J. F., Blanquet, M., Guerriero, G., & Lutts, S. (2021). Silicon reduces cadmium absorption and increases root-to-shoot translocation without impacting growth in young plants of hemp (*Cannabis sativa* L.) on a short-term basis. *Environmental Science and Pollution Research*, 1-15.

Luyckx, M., Hausman, J. F., Sergeant, K., Guerriero, G., & Lutts, S. (2021). Molecular and biochemical insights into hemp early responses to Cd and Zn exposure and the potential effect of Si on stress response. *Frontiers in plant science*, accepted manuscript.

Table of Contents

Abstract	3
Remerciements	4
Thesis achievements.....	6
Table of Contents	7
List of main abbreviations	13
Bibliographical review.....	15
1. Heavy metals.....	15
1.1. Sources of heavy metals and soil quality	15
1.2. Harmful effects for human health	18
1.3. Remediation methods.....	20
2. Phytomanagement.....	21
2.1. Definition	21
2.2. Candidate plants for HM- phytomanagement	23
2.3. Phytomanagement limitations.....	25
2.4. Strategy to increase plant resistance	28
3. Silicon	28
3.1. Silicon abundance and plant uptake.....	28
3.2. Si priming	29
3.3. Si and HM stress alleviation	30
4. Hemp.....	33
4.1. Hemp and humankind	33
4.2. Valorisation of hemp.....	35
4.3. Agronomy of hemp	42
4.4. Phytomanagement potential	45
4.5. Which uses for HM- and Si –containing biomass?	47
5. Objectives	57
Chapter 1: Studying hemp potential as a non-food crop for phytomanagement of contaminated agricultural soils by heavy metals in combination with biochar and compost.....	75

1. Introduction.....	76
2. Material and Methods	79
2.1. Growing conditions.....	79
2.2. Soil characterization.....	81
2.3. Plant material	82
2.4. Photosynthesis-related parameters	83
2.5. Mineral concentrations in plants	84
2.6. Fibre's and hurds' characterization.....	84
2.7. Statistical analysis.....	85
3. Results.....	85
3.1. Plant physiology	85
3.2. HM accumulation in hemp.....	89
3.3. Soil properties after hemp cultivation	93
3.4. Influence of management methods on utilizable hemp biomass.....	94
4. Discussion.....	98
5. Conclusion	104
Chapter 1: Highlights and Perspectives.....	111
Chapter 2: Studying the influence of Silicon application on hemp physiological properties and the impact on fibres' final properties after harvest.....	113
1. Introduction.....	114
2. Material and methods.....	116
2.1. Growth conditions.....	116
2.2. Soil characterization.....	117
2.3. Plant material	117
2.4. Photosynthesis-related parameters	118
2.5. Fibre's and hurds' characterization.....	118
2.6. Mineral concentration in stems, leaves, fibres and hurd	118
2.7. Statistical analysis.....	119
3. Results.....	119
3.1. Yield	119

3.2. Photosynthesis-related parameters	120
3.3. Si accumulation in hemp	121
3.4. HM accumulation in hemp.....	122
3.5. Fibres and hurds characterization	124
4. Discussion.....	128
5. Conclusion	133
Chapter 2: Highlights and Perspectives.....	135
Chapter 3: Studying the impact of a high bioavailability of Cd, as well as the short-term impact of silicon (Si) on biomass production	137
1. Introduction.....	138
2. Material and methods.....	141
2.1. Plant material and growing conditions.....	141
2.2. Mineral concentration	142
2.3. Photosynthesis-related parameters	143
2.4. Malondialdehyde content and total antioxidant activities	143
2.5. Glutathione and total non-protein thiols	144
2.6. Statistical analysis.....	144
3. Results.....	145
3.1. Plant growth and morphological parameters.....	145
3.2. Plant mineral content	147
3.3. Photosynthesis-related parameters	149
3.4. Oxidative stress-related parameters and phytochelatin estimation	150
4. Discussion.....	152
5. Conclusions.....	159
Chapter 3: Highlights and Perspectives.....	161
Chapter 4: Studying the impact of a high bioavailability of Zn, as well as the short-term impact of silicon (Si) on biomass production	163
1. Introduction.....	164
2. Material and methods.....	166
2.1. Plant material and growing conditions.....	166
2.2. Physiological measurements	167

2.3. Mineral concentration	168
2.4. Malondialdehyde (MDA) content and total antioxidant activities	168
2.5. Glutathione and total non-protein thiols	168
2.6. Statistical analysis	168
3. Results.....	169
3.1. Plant growth.....	169
3.2. Mineral concentrations.....	171
3.3. Photosynthesis-related parameters	173
3.4. Plant water and oxidative status.....	174
4. Discussion.....	176
5. Conclusion	181
Chapter 4: Highlights and Perspectives.....	183
Chapter 5: Molecular and biochemical clues of Cd and Zn toxicity and response in hemp' roots and stems, and the potential effect of Si on stress response	185
1. Introduction.....	186
2. Material and methods.....	189
2.1. Plant material and growth conditions.....	189
2.2. Ion content, glutathione, phytochelatin and proline concentration	190
2.3. Targeted gene expression analysis	190
2.4. Proteomic analysis	191
2.5. Determination of lignification and Cd deposition in leaves an roots	193
2.6. Statistical analysis.....	193
3. Results.....	194
3.1. Heavy metal impacts on plant growth.....	194
3.2. Ion accumulation, glutathione, phytochelatin and proline content.....	194
3.3. Gene expression in leaves and roots	196
3.4. Proteomics	200
3.5. Determination of lignification and Cd deposition in leaves and roots	211
4. Discussion.....	214
5. Conclusion	223

Chapter 5: Highlights and Perspectives.....	227
Chapter 6: Proteins and cell wall-related gene expression in young stems of hemp in relation to Cd, Zn and/or Si exposure.....	229
1. Introduction.....	230
2. Material and Methods	234
2.1. Plant material and growing conditions.....	234
2.2. Mineral concentration	235
2.3. Gene expression analysis	235
2.4. Proteomic analysis	236
2.5. Confocal microscope observation	236
2.6. Immunohistochemistry	236
2.7. Statistical analysis.....	237
3. Results.....	237
3.1. Impact of Cd and Zn on plant physiological parameters.....	237
3.2. Mineral content	238
3.3. Gene expression in the stem	239
3.4. Proteomics	241
3.5. Confocal microscopy and immunohistochemistry	250
4. Discussion.....	255
5. Conclusion	263
Chapter 6: Highlights and Perspectives.....	267
Chapter 7: Impact of Silicon and Heavy Metals on Hemp (<i>C. sativa</i> L.) ions distribution in roots, stems and leaves at tissue and cell level	269
1. Introduction.....	270
2. Material and Methods	272
2.1. Plant material and growing conditions.....	272
2.2. Sample preparation for micro-PIXE analysis	273
2.3. Micro-PIXE analysis.....	273
2.4. Scanning electron microscopy (SEM-EDX)	274
2.5. Microscopic determination of lignification in stems.....	275
3. Results.....	275

3.1. Histological description of root, stem and leaf in hemp.....	275
3.2. Element concentration and distribution within root tissues	276
3.3. Element concentration and distribution within stem tissues	282
3.4. Element concentration and distribution within leaf tissues	288
3.5. EDX analysis of Si distribution in roots, stems and leaves.....	294
3.6. Cellulose and lignin detection in stems.....	297
4. Discussion.....	298
4.1. Roots.....	298
4.2. Stems.....	300
4.3. Leaves.....	301
5. Conclusion	302
References (Chapter 1 to 7).....	303
General Discussion.....	329
Conclusion and perspectives.....	347
Appendix.....	357
Appendix 1: Futura 75 grown in controlled conditions, in 5L pots filled with soil samples (BB, CLL) from the <i>in situ</i> experiment, and with or without foliar application of Si	357
1. Material and Methods	357
2. Results.....	359
3. Discussion.....	363
4. Conclusion	365
Appendix 2: Comparison of Santhica 27 and Futura 75 cultivars	367
1. Material and Methods	368
2. Results.....	370
3. Discussion.....	375
4. Conclusion	377

List of main abbreviations

Φ_{PSII}	Actual PSII efficiency
Ψ_s	Osmotic potential
<i>A</i>	Instantaneous CO ₂ assimilation
AOAD	Antioxidant activity measured in methanol extract
BF	Bioaccumulation factor
Chl	Chlorophyll
DW	Dry weight
<i>E</i>	Instantaneous transpiration
FRAP	Ferric reducing ability of plasma
F_v/F_m	Maximal quantum yield of PSII
FW	Fresh weight
<i>g_s</i>	Stomatal conductance
GSH	Reduced glutathione
GSHt	Total glutathione
GSSG	Oxidized glutathione
HM	Heavy metals
HPLC	High liquid pressure chromatography
MDA	Malondialdehydes
MT	Metallothioneins
NPQ	Non-photochemical-quenching
PC	Phytochelatins
PCW	Primary cell wall
PSII	Photosystème II
qP	Photochemical quenching
ROS	Reactive oxygen species
RUBISCO	Ribulose 1,5-bisphosphate carboxylase/oxidase
SCW	Secondary cell wall
SP	Internode containing the snap point
TF	Translocation factor
WC	Water content

Bibliographical review

Adapted from the published articles:

Luyckx, M., Hausman, J. F., Lutts, S., & Guerriero, G. (2017). Impact of silicon in plant biomass production: focus on bast fibres, hypotheses, and perspectives. *Plants*, 6, 37.

Luyckx, M., Hausman, J. F., Lutts, S., & Guerriero, G. (2017). Silicon and plants: current knowledge and technological perspectives. *Frontiers in Plant Science*, 8, 411.

Berni, R., Luyckx, M., Xu, X., Legay, S., Sergeant, K., Hausman, J. F., ... & Guerriero, G. (2019). Reactive oxygen species and heavy metal stress in plants: Impact on the cell wall and secondary metabolism. *Environmental and experimental botany*, 161, 98-106.

Luyckx, M., Berni, R., Cai, G., Lutts, S., & Guerriero, G. (2019). Impact of heavy metals on non-food herbaceous crops and prophylactic role of Si. In *Plant Metallomics and Functional Omics* (pp. 303-321). Springer, Cham.

1. Heavy metals

1.1. Sources of heavy metals and soil quality

Soil plays a central role in food safety as it determines the possible composition of food and feed at the basis of the food chain (Tóth et al., 2016). However, since several decades various anthropogenic activities have negatively affected the quality of soil. Heavy metals (HM) are one of the key factors that constitute an important environmental problem. Chemically speaking, HM refer to naturally occurring metals having atomic number greater than 20 and an elemental density greater than 5 g.cm^{-3} , such as cadmium (Cd), mercury (Hg), copper (Cu), arsenic (As), lead (Pb), chromium (Cr), nickel (Ni), and zinc (Zn) (Ali & Khan, 2018; Li et al., 2019). Whereas, from a biological perspective, “heavy” describes a series of metals, in some cases metalloids (elements with intermediate properties between those of typical metals and non-metals, such as arsenic and antimony), that even in low concentrations can be toxic for plants, and animals are also included (Ayangbenro & Babalola, 2017; Li et al., 2019). The term “heavy metal” is a matter for debate, but it is widely employed by the scientific community and will, therefore, be used as well in this thesis.

Table 1: Source and harmful effects of some heavy metals on human health (Ayangbenro and Babalola, 2017).

Heavy Metal	Source	Effects on Human
Cd	Fertilizer, mining, pesticide, plastic, refining, welding	Bone disease, coughing, emphysema, headache, hypertension, itai-itai disease, kidney conditions, lung and prostate cancer, lymphocytosis, microcytic hypochromic anemia, testicular atrophy, vomiting
Hg	Batteries, coal combustion, geothermal activities, mining, paint industries, paper industry, volcanic eruption, weathering of rocks	Ataxia, attention deficit, blindness, deafness, decrease rate of fertility, dementia, dizziness, dysphasia, gastrointestinal irritation, gingivitis, kidney problem, loss of memory, pulmonary edema, reduced immunity, sclerosis
Cu	Copper polishing, mining, paint, plating, printing operations	Abdominal pain, anemia, diarrhea, headache, liver and kidney damage, metabolic disorders, nausea, vomiting
As	Atmospheric deposition, mining, pesticides, rock sedimentation, smelting	Brain damage, cardiovascular and respiratory disorder, conjunctivitis, dermatitis, skin cancer
Pb	Coal combustion, electroplating, manufacturing of batteries, mining, paint, pigments	Anorexia, chronic nephropathy, damage to neurons, high blood pressure, hyperactivity, insomnia, learning deficits, reduced fertility, renal system damage, risk factor for Alzheimer's disease, shortened attention span
Cr	Dyeing, electroplating, paints production, steel fabrication, tanning, textile	Bronchopneumonia, chronic bronchitis, diarrhea, emphysema, headache, irritation of the skin, itching of respiratory tract, liver diseases, lung cancer, nausea, renal failure, reproductive toxicity, vomiting
Ni	Electroplating, non-ferrous metal, paints, porcelain enameling	Cardiovascular diseases, chest pain, dermatitis, dizziness, dry cough and shortness of breath, headache, kidney diseases, lung and nasal cancer, nausea
Zn	Brass manufacturing, mining, oil refinery, plumbing	Ataxia, depression, gastrointestinal irritation, hematuria, icterus, impotence, kidney and liver failure, lethargy, macular degeneration, metal fume fever, prostate cancer, seizures, vomiting

Naturally occurring HM are typically present in insoluble forms, like in mineral structures, or in precipitated or complex forms that are not readily available for living organisms (Ayangbenro & Babalola, 2017). Except for natural processes (comets, erosion, volcanic eruptions, and the weathering of minerals), HM contaminants are inadvertently introduced to soils through anthropogenic activities (Ayangbenro & Babalola, 2017; Liu et al., 2018): mining activities, metallurgical and petrochemical industries, fertilizers and pesticides are increasing the dissemination and mobilization of HM (Table 1).

Different guideline values have been set for industrial and transport areas (higher guideline value) and for all other land uses (lower guideline value) (Table 2, Tóth et al., 2016). If this is exceeded, the area has a contamination level which presents ecological or health risks (Table 2).

Table 2: The guideline values defined on the basis of either ecological risks (e) or health risks (t) (Tóth et al., 2016).

Substance (symbol)	Threshold value mg/kg	Lower guideline value mg/kg	Higher guideline value mg/kg
Antimony (Sb) (p)	2	10 (t)	50 (e)
Arsenic (As) (p)	5	50 (e)	100 (e)
Mercury (Hg)	0.5	2 (e)	5 (e)
Cadmium (Cd)	1	10 (e)	20 (e)
Cobalt (Co) (p)	20	100 (e)	250 (e)
Chrome (Cr)	100	200 (e)	300 (e)
Copper (Cu)	100	150 (e)	200 (e)
Lead (Pb)	60	200 (t)	750 (e)
Nickel (Ni)	50	100 (e)	150 (e)
Zinc (Zn)	200	250 (e)	400 (e)
Vanadium (V)	100	150 (e)	250 (e)

In Europe, approximately 137,000 km² of agricultural land have been estimated to be contaminated by HM to a certain degree (Figure 1; Tóth et al., 2016).

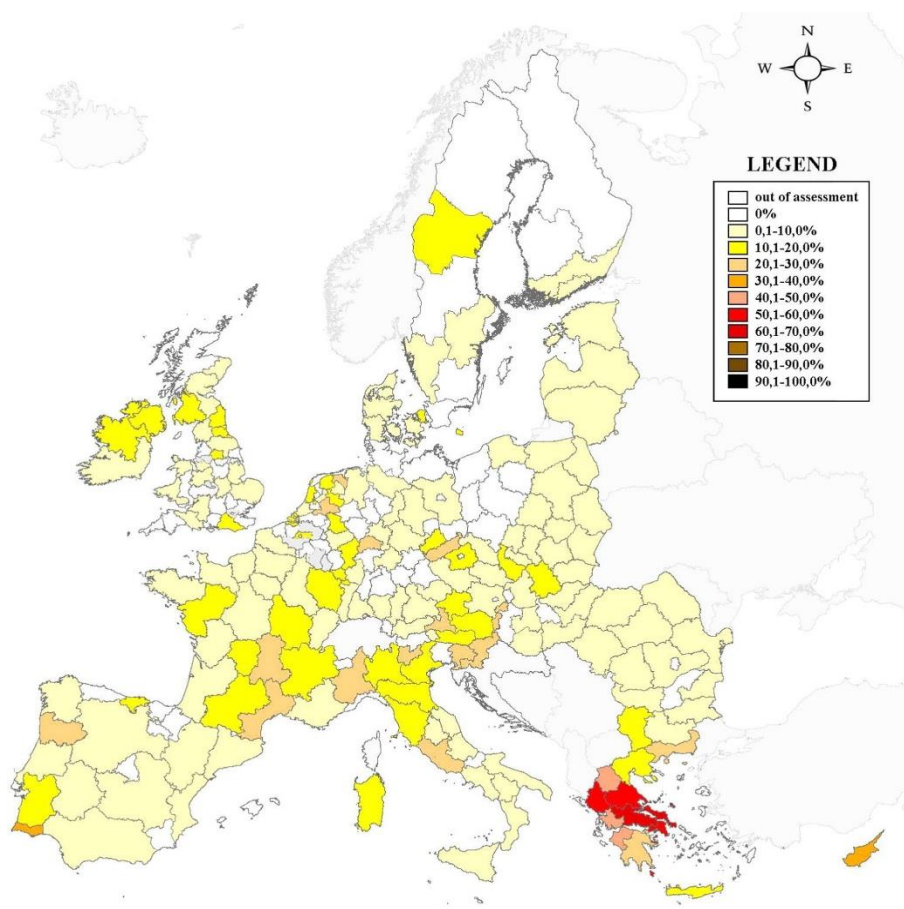


Figure 1 : Percentage of samples with concentrations above the lower guideline value from lands devoted to agricultural practices (Tóth et al., 2016).

1.2. Harmful effects for human health

Heavy metal pollution is currently a major environmental problem because, unlike organic pollutants (e.g. fuel oil, plastic products, and polycyclic aromatic hydrocarbons), metal ions persist in the environment due to their non-degradable nature (Ayangbenro & Babalola, 2017; Upcraft & Guo, 2019). Moreover, HM from anthropogenic sources typically have a high bioavailability due to their soluble and mobile reactive forms (Ayangbenro & Babalola, 2017). Heavy metal pollution not only degrades the quality of water bodies, atmosphere, and food crops, but also poses a great threat to the health of living organisms (Li et al., 2019): the majorities of HM are toxic at low concentrations (Ali et al., 2013; Ayangbenro & Babalola, 2017). The toxicity of HM mainly depends upon their relative oxidation state, responsible for

physiological bio-toxic effects (Mishra et al., 2019). When they enter into the living organisms, they combine with proteins, enzymes, and DNA molecules, thus forming highly stable bio-toxic compounds ultimately altering their proper functioning and subtracting them from the bioreactions (Mishra et al., 2019). Some HM are carcinogens, mutagens, teratogens and endocrine disruptors, while others cause neurological and behavioral changes especially in children (Ali et al., 2013). The harmful effects of specific HM for human health are presented in Table 1.

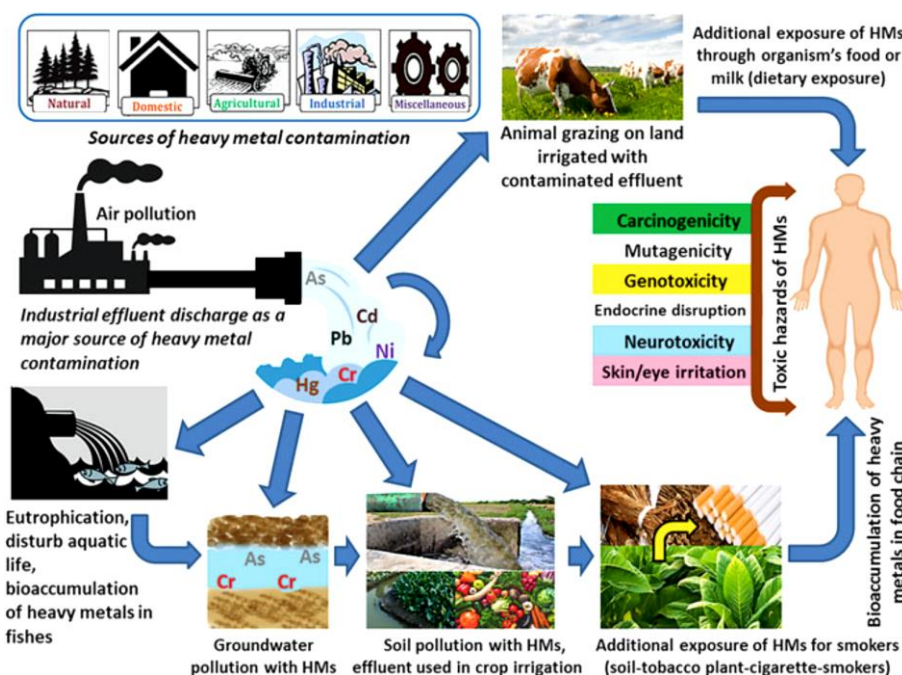


Figure 2: Trophic transfer of toxic HM from soil to plants, to humans, and food to humans (Saxena et al., 2019).

The population can be exposed directly, via ingestion as well as inhalation of contaminated soil particles, but also indirectly, via the consumption of contaminated plant foods: the cations of these pollutants bond with soil particles, enter into solution, and are then absorbed by the roots and transferred to the edible parts of the plant, thus entering the food chain (Figure 2; Di Candito et al., 2004; Bidar, 2007; Saxena et al., 2019). As a consequence, an important proportion of HM-contaminated sites is not suitable and even prohibited for food crops' cultivation. Besides, the world's population continues to rise: a population of around 8 billion is expected to increase to about 10 billion by 2050 (ONU, 2019). By this time, another one billion tonnes of cereals and 200 million extra tonnes of livestock products will need to be

produced every year (Dubois, 2011). Moreover, the production of feedstock for biofuels competes with food production on significant areas of prime cultivated land. Remediation of soil pollution is thus one of the main environmental challenges today.

1.3. Remediation methods

Various *in-situ* and *ex-situ* remediation methods have been developed for HM-contaminated soils. These remediation techniques employ containment (capping, encapsulation, landfilling), extraction/removal (soil washing, flushing, electrokinetic extraction), and immobilization (solidification, vitrification, chemical stabilization) mechanisms to reduce the contamination effects through physical, chemical, electrical, and thermal remedy processes (Figure 3; Ayangbenro & Babalola, 2017; Liu et al., 2018). In general, *in-situ* soil remediation is more cost-effective than *ex-situ* treatment, and contaminant removal/extraction is more favorable than immobilization and containment (Liu et al., 2018).

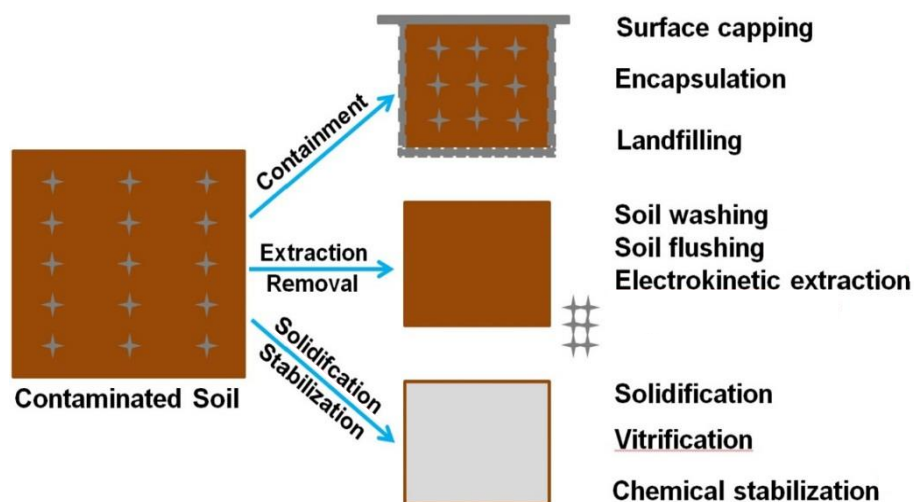


Figure 3: Remediation techniques for heavy metal-contaminated soils (Liu et al., 2018).

However, these techniques are both invasive, ineffective when metal concentrations in solution are less than 100 mg/L, and depend on field conditions (weather, soil permeability, contamination depth, potential deep leaching of chemicals) (Ayangbenro & Babalola, 2017; Liu et al., 2018). Furthermore, physicochemical remediation technologies influence soil properties, fertility, and biodiversity. For example, in vitrification, high

temperature ($>1500\text{ }^{\circ}\text{C}$) is given to the soil zone which melts the soil, and after cooling HM are entrapped in a glassy matrix (Shah, & Daverey, 2020). Such treated soil is not able to grow plants and cannot be used for agriculture purpose. Thus, there is a need to develop alternative techniques that are environment friendly, suitable, applicable to the local conditions, and able to meet the established permissible limits (Ayangbenro & Babalola, 2017).

The recent development of phytomanagement technologies, where plants and associated soil microbes are used to extract, degrade or immobilize various contaminants from polluted soils, marks significant progress in this field (Barceló & Poschenrieder, 2003; Citterio et al., 2003; Meers et al., 2005; Ali et al., 2013). It differs from traditional remediation techniques in that it can be used for the reclamation of contaminated soil without disturbing the soil fertility and biodiversity, it is novel, and solar-driven technology with good public acceptance (Ali et al., 2013; Shah, & Daverey, 2020). Moreover, phytomanagement is more feasible and applicable than physical and chemical strategies, particularly for treating large, diffuse areas with fine-textured, high organic matter content soils (Liu et al., 2018).

2. Phytomanagement

2.1. Definition

Phytomanagement consists of six main processes, illustrated in Figure 4.

Phytoextraction and rhizofiltration (accumulation of HM absorbed by plant from soil/water in shoots and leaves), as well as phytostabilization (HM immobilization in soil by plant roots), are used for the management of soils contaminated by HM. Phytostabilization will not remove HM from soil, but it prevents the dispersal of particle-bound pollutants by wind and water erosion and reduce the export of dissolved contaminants by reducing surface runoff and water flow into the subsurface, especially for the areas lacking natural vegetation due to HM concentrations (Evangelou et al., 2015; Liu et al., 2018). Organic pollutants, depending on their nature, can be degraded by rhizospheric microorganisms (bacteria and fungi) associated with the plant cover (phytodegradation and rhizodegradation) (Bert et al., 2017). Phytovolatilization is used for the removal of volatile organic compounds, as well as elements such as mercury, selenium and tritium (Ghosh & Singh, 2005).

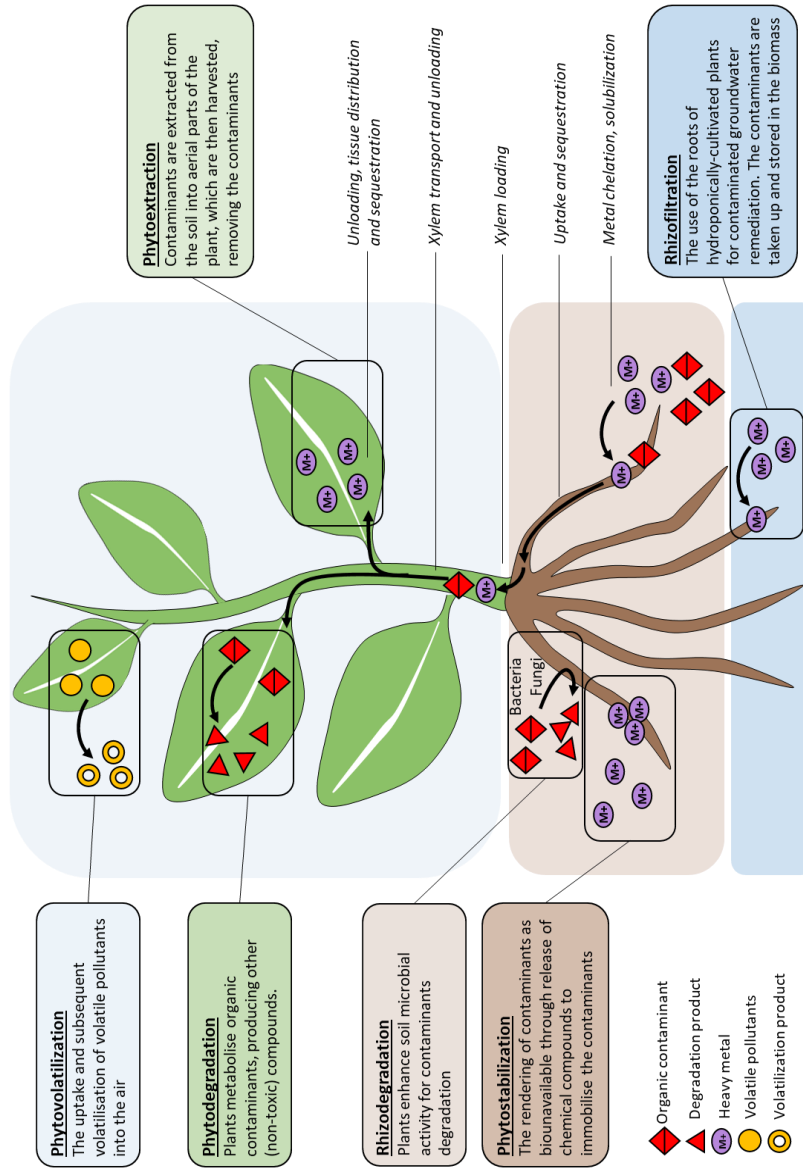


Figure 4: Schematic representation of the types of phytomanagement processes performed by plants for soil remediation (adapted from Upcraft and Guo, 2019).

Phytomanagement has become much popular in the recent past (~50% papers are published in the last six years, 2015–2021) especially in China, India and United States (Figure 5).

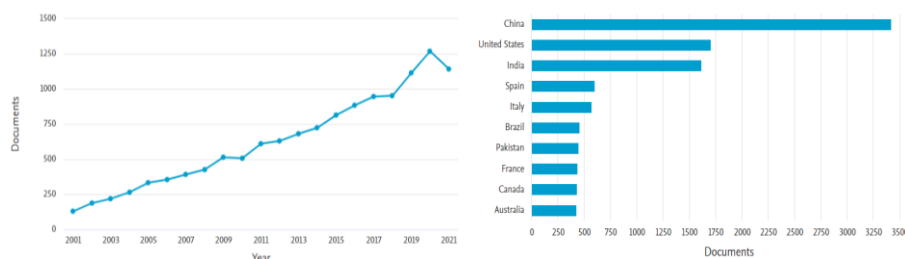


Figure 5: Number of papers published on phytomanagement in the last 20 years (2001–2021) according to Scopus® database (Elsevier B.V.): (a) paper published each year; (b) paper published by different countries (countries with ≥ 295 papers in the last 20 years).

These techniques are, however, still emerging on the markets of polluted sites' management techniques, in particular due to a lack of operational hindsight and information on the possibilities of valuing the biomass produced and the associated costs and benefits (Bert et al., 2017). Moreover, there are some limitations such as soil properties (e.g., pH, buffering capacity, texture, clay minerals, organic matter content, fertility, and cation exchange capacity), contaminant (e.g., metal species, content and speciation), climate (e.g., precipitation, temperature), geography (slope and aspect), and finally plant used (species, growth, biomass, sensitivity for HM) (Liu et al., 2018; Shah & Daverey, 2020).

2.2. Candidate plants for HM- phytomanagement

Phytoextraction

Plants used for HM extraction can be divided into two groups: metal hyperaccumulators and biomass producers:

- Metal hyperaccumulators (e.g. Brassicaceae and Thlaspi species) are plants capable of concentrating $>10 \text{ g kg}^{-1}$ (1%) Mn or Zn, $>1 \text{ g kg}^{-1}$ (0.1%) As, Co, Cr, Cu, Ni, Pb, Sb, Se or Tl, and $>0.1 \text{ g kg}^{-1}$ (0.01%) Cd in aboveground biomass without suffering from phytotoxic damage. However, these plants are typically metal-selective, limited to their native habitats and tend to have limited aboveground biomass and root penetration depth ultimately limiting their applicability (Di Candito et al., 2004; Meers et al., 2005; Ali et

al., 2013; Wang et al., 2017; Liu et al., 2018; Rhey et al., 2020). Furthermore, the phytoaccumulation of HM is correlated with the available concentration in the soil (Liu et al., 2018). To accelerate phytoextraction, the use of chelating agent (e.g. EDTA, DTPA) has been proposed, nevertheless many of them are resistant to biodegradation and may be leached to deep soil and groundwater (Liu et al., 2018).

- Biomass producers (e.g. *Brassica juncea*, *Salix* and *Populus* species) include plants tolerant to HM with lower metal uptake capacity comparatively to hyperaccumulators, which is compensated by a high production capacity and growth rate (Wang et al., 2017). These plants, though not metal hyperaccumulators, demonstrate overall comparable metal extraction capability (Liu et al., 2018).

After each cropping, the plant is removed from the site, and the biomass obtained has to be stored or disposed of appropriately, so that it does not pose any risk to the environment (Ghosh & Singh, 2005; Abdel-Shafy & Mansour, 2018). However, legislation that stipulates management of biomass after phytoremediation, promotes recycling of biomass with known environmental risks, and includes specific policies developed for managers is still lacking (Song and Park, 2017).

Phytostabilization

Plants used for phytostabilization (e.g. *Agrostis tenuis*, *Festuca rubra* L.) are tolerant to HM, have high root biomass production, and a limited translocation of absorbed HM from roots to shoots (Liu et al., 2018). The vegetation cap reduces the mobility and bioavailability of HM in the environment, the plant canopy reduces aeolian dispersion, while plant roots prevent water erosion, immobilize HM, and prevent leaching (Wang et al., 2017). The technique, however, cannot be applied on extremely contaminated sites or soils with poor agronomic potential, in which plant growth and survival are barely possible (Bert et al., 2017; Liu et al., 2018). For these reason, the technique is frequently employed in combination with soil amendments (e.g., lime, phosphates, compost, biochar), added to soil to reduce bioavailability and biotoxicity of HM and favor the establishment of a plant cover (Peralta-Videa et al., 2009; Chowdhury et al., 2016; Bert et al., 2017; Luo et al., 2017; Liu et al., 2018; Meena et al., 2018;). The term “assisted phytostabilization” will then be used (Bert et al., 2017).

New plants of interest

Two specific limitations determine the phytomanagement success: remediation time and cost (Upcraft & Guo, 2019). Time required for phytomanagement is assumed not to improve significantly in the coming decades, therefore increasingly active research has been directed toward studying the phytomanagement capabilities of non-edible crop of commercial interest to valorise marginal farmland soils: they grow rapidly, produce high biomass, and HM accumulation in harvestable parts does not eliminate their potential conversion into value-added bioproducts. For example, there are no current standards for HM content in building materials, and numerous investigations tend to show that the risk of alternative materials incorporation in the production of the cement increase the quantity and the leachable fraction of HM it contains is nonexistent (reviewed by Marion et al., 2005). Moreover, the use of phytoremediating-plants to produce biofuels, timber and innovative materials does not compete with the agricultural sector, because contaminated lands, which are not suitable for food production and not at all used economically are used instead (Evangelou et al., 2015). This strategy could provide incomes for the farmers or, at least, counteract the cost and time needed for phytomanagement (Di Candito et al., 2004; Fernando et al., 2015; Tóth et al., 2016; Feng et al., 2020). However, it implies that biomass production is not compromised by HM from a quantitative point of view and that the properties of the harvested biomass remain compatible with the requirements of industry from a qualitative point of view.

2.3. Phytomanagement limitations

HM bioavailability

There are various environmental factors such as pH, temperature, soil type, and texture, nutrient amendments and O₂, which influence the bioremediation process (Mishra et al., 2019). In particular, soil composition, pH and structure strongly affect HM bioavailability (Vardhan et al., 2019).

Bioavailability can be considered as a complex dynamic process comprising three steps, namely (1) *environmental availability*, i.e. the total amount of HM, including both actual and potential fractions which can be physico-chemically desorbed from the soil matrix into the pore water, (2) *environmental bioavailability*, i.e. the amount of the environmentally available fraction which an organism can take up through physiologically

driven processes, and (3) *toxicological bioavailability*, i.e. the amount of HM which can physiologically induce bioaccumulation or other effects within plants depending on translocation, metabolism, and detoxification (Figure 6; *ISO 17402:2008(en)*; Kim et al., 2015). For each HM, differences in solubility and hence mobility in the soil as well as the translocation within the plants are dominated by specific and non-specific adsorption, as well as different complexation affinities for inorganic and organic ligands which to a large degree depend on soil pH (Kim et al., 2015; Vardhan et al., 2019). As a result, at common soil pH ranges, Cd, Ni, and Zn exhibit relatively high mobility and Cu, Cr, and Pb exhibit relatively low mobility (Kim et al., 2015).

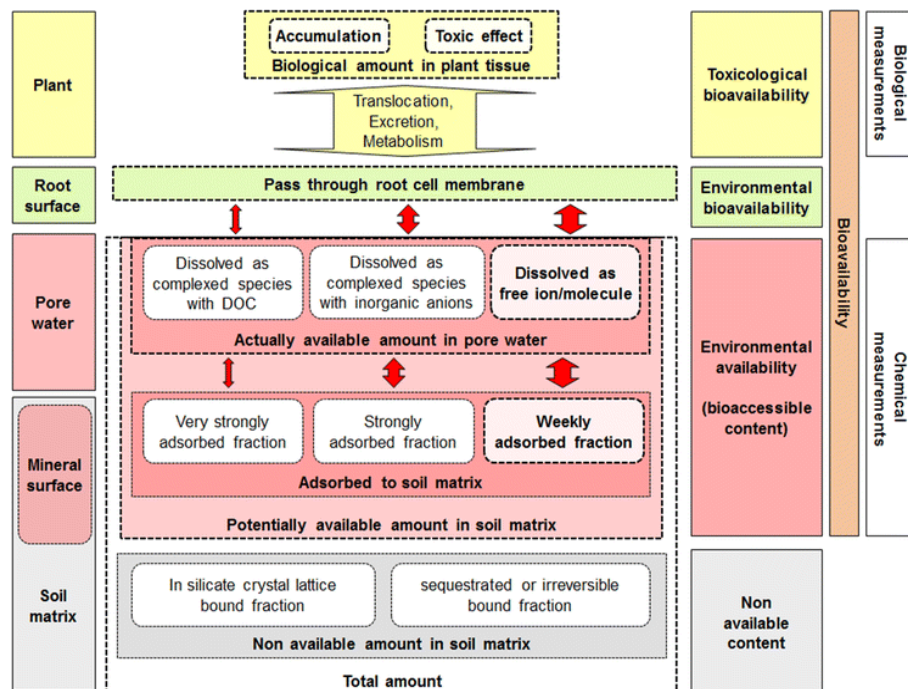


Figure 6: Three-step concept of heavy metal bioavailability in soils for plants (thick arrows indicate the most important factors affecting bioavailability) (Kim et al., 2015).

HM toxicity

The crop sensitivity to HM also constitutes one of the major limitations of phytomanagement techniques (Shah & Daverey, 2020). Metals such as Cu, Zn, Mn, Ni and Fe are considered fundamental plant micronutrients when present in low concentrations. The principal functions of essential HM include participation in the redox reaction of cellular processes and other molecular activities by being an integral part of several enzymes (Emamverdian et al.,

2015; Bhat et al., 2019). The presence of both essential and non-essential HM (e.g. Cd, Pb, Ni or Hg) in excess may induce a wide range of morphological changes associated with altered water status, absorption of essential elements, as well as basic metabolic reactions (photosynthesis, respiration, homeostasis), with a direct consequence on crop growth and yield (Figure 7; Rucińska-Sobkowiak, 2016; Jalmi et al., 2018).

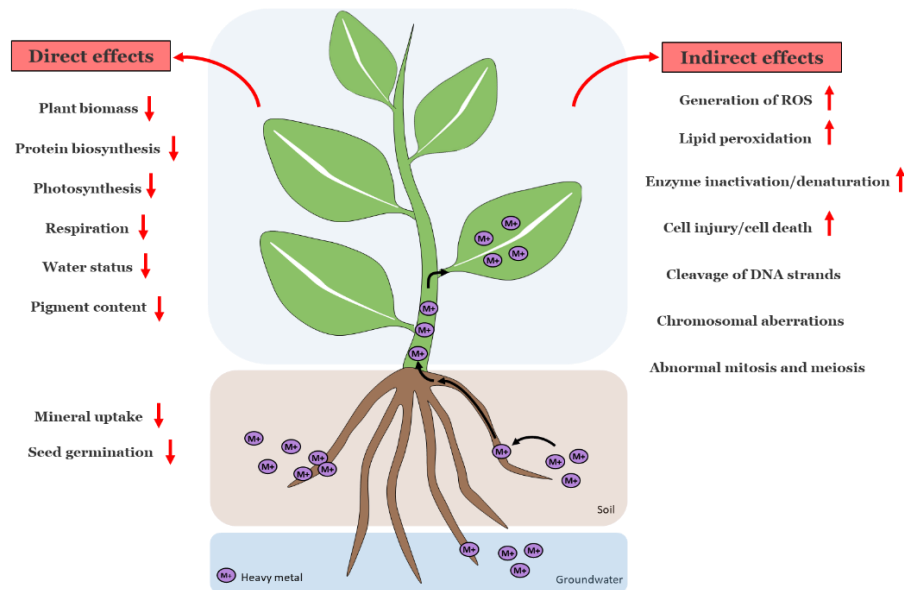


Figure 7: Heavy metal uptake by plant roots and their possible direct and indirect negative effects on crop productivity. The sign ↓ indicates decrease and the sign ↑ indicates increase (adapted from Bhat et al., 2019).

On a biochemical level, HM inactivate or denature various important enzymes and other proteins, and disturb the integrity of membranes (Ghori et al., 2019; Mishra et al., 2019). Moreover, the production of reactive oxygen species (ROS) is strongly hastened by HM (Fryzova et al., 2017). These highly reactive species lead to lipid peroxidation, especially of the cellular membranes causing them to leak, damage of biomolecules and also cleavage of DNA strands, phenomena collectively known as oxidative stress (Ghori et al., 2019 and references therein).

To minimize the detrimental effects of HM exposure and their accumulation, plants have evolved various molecular and physiological mechanisms (Yadav, 2010). Some of these mechanisms are part of the homeostatic process and hence are constitutive, while others are exclusive and activated only when a certain metal toxicity is encountered (Ghori et al., 2019). The initial step of plant cells behavior towards any environmental

constraint is stress sensing (Hossain and Komatsu, 2013): changes in ambient conditions are sensed by receptors at the plasma membrane inducing signaling pathways transferring stress signal from the plasma membrane to nucleus and leading to changes in gene expression (Singh et al., 2016; Kosová et al., 2018). Then, the first line of defense provided by a plant is to reduce the uptake of HM with help of cellular and root exudates, and then to restrict the metals from entering the cell by increasing efflux or biosorption to cell walls (classified as avoidance mechanism) (Ghori et al., 2019). Many plants have exclusive mechanisms that are classified as tolerance mechanisms for individual metal ions: during this, a complex is formed between metal ions and a chelant (e.g. phytochelatins, metallothionein) and the complex is transported to the vacuoles where metal ions can no longer affect cells' functioning (Cobbett, 2000; Hopkins, 2003; Fernández et al., 2014; Ye et al., 2012; Jost-Tse, 2018; Ghori et al., 2019; Nawaz et al., 2019). Furthermore, the increased abundance of defense proteins for effective ROS scavenging, the accumulation of heat shock proteins (HSPs) and chaperones for re-establishing normal protein conformation and accumulation of soluble N compounds to regulate osmotic potential, help HM-stressed plants maintain redox homeostasis (Hossain & Komatsu, 2013). Using these mechanisms, many plant species have the ability to grow on contaminated sites and some of them are able to accumulate high concentrations of HM in their tissues.

2.4. Strategy to increase plant resistance

As mentioned earlier, soil amendments (e.g., lime, phosphates, compost, biochar) can be added to soil to reduce the bioavailability and biotoxicity of HM and favor the establishment of a plant cover (Peralta-Videa et al., 2009; Chowdhury et al., 2016; Bert et al., 2017; Luo et al., 2017; Liu et al., 2018; Meena et al., 2018). Besides, any other sustainable strategy helping the plant to cope with HM toxicity could be usefully integrated in a phytomanagement scheme and this is especially the case for silicon application.

3. Silicon

3.1. Silicon abundance and plant uptake

Silicon (Si) is the second most abundant element in soils and can be found at high concentration in many terrestrial plants (Epstein, 1994; Keeping & Reynolds, 2009). Differently to micronutrients, Si is considered non-essential

(or quasi-essential, Epstein & Bloom, 2005) for plant growth and development. Plants develop well in its absence, although in some cases, e.g., the silicifier horsetail and rice, the absence of Si triggers susceptibility to fungal infection (Datnoff & Rodrigues, 2005; Law & Exley, 2011). However, numerous studies correlate Si uptake with enhanced vigor and resistance of plants to various biotic (Guerrero et al., 2018) and abiotic stress, including HM toxicity (Imtiaz et al., 2016), but the mechanisms of Si function remain still elusive. Its use in phytomanagement could therefore be considered to improve the biomass yield of economically important cultivated plants.

Silicon is taken up by plants as silicic acid Si(OH)_4 via aquaporin-type channels (Nod26-like intrinsic proteins, NIPs) (Ma et al., 2006; Grégoire et al., 2012; Deshmukh et al., 2015). A specific 108 amino acid spacing between the conserved NPA domains determines Si(OH)_4 permeability (Deshmukh et al., 2015). Plants are classified into accumulators, excluders and intermediate type (Mitani & Ma, 2005), depending on the amount of biogenic silica found in their tissues. Most dicots accumulate less than 0.1% Si on a dry weight basis, but many grass species are able to accumulate as much as 10% (Montpetit et al., 2012; Trembath-Reichert et al., 2015; Vivancos et al., 2015), and rice is often considered as the most effective Si-accumulating plant (Ma et al., 2002).

3.2. Si priming

Si acts as a “tonic” by priming plants, i.e., by preparing the defence responses which are then fully deployed at the onset of the stress. The effects of Si under normal conditions are indeed latent: no major modifications, e.g., in gene expression, are observed (Van Bockhaven, 2014). Under control conditions Si probably activates the metabolic status of the plant, by making it more efficient in responding to exogenous stimuli. In rice, a Si-accumulator, Si causes alterations of C/N balance in the source-sink relationship under unstressed conditions, by favouring a remobilization of amino acids to support the increased N demand during grain development (Detmann et al., 2012; Detmann et al., 2013). These data support the hypothesis that Si has a signalling role in plant cells. Si was indeed suggested to have a role as second messenger by binding to the hydroxyl groups of proteins involved in cell signalling, thereby partaking in the signal transduction (Fauteux et al., 2005). It is important to mention that Si primes defence responses also in Si non-accumulators, i.e., tomato (Ghareeb et al., 2011): tomato is protected against *Ralstonia solanacearum* by Si which causes an upregulation, upon infection,

of genes involved in ethylene and jasmonic acid signalling, i.e., *JERF3*, *TRSF1*, *ACCO*, as well as genes involved in stress response, i.e., trehalose phosphatase, late embryogenesis abundant protein, ferritin. In this study, the authors also observed an increased expression of a negative regulator of the jasmonic acid signal, *JAZ1*, together with a ubiquitin protein-ligase: the authors propose that *JAZ1* helps in preventing the eventual damage caused by the stimulation of defense-related compounds and that the ubiquitin protein-ligase may degrade *JAZ1*. In tomato challenged by *R. solanacearum*, Si also upregulates a MAPK (*MAPK19*), a WRKY transcription factor and genes encoding linker histones (H1 and H5). These findings corroborate the role of Si in intracellular signalling and suggest its involvement in transcription too (Ghareeb et al., 2011). Silicon was shown to upregulate the expression of a leucine rich repeat receptor-like kinase (LRR-RLK) in rice (Fleck et al., 2011), which is a protein involved in intracellular signal transduction. High-throughput technologies relying on *-omics* will help shed light on the missing genes/proteins involved in the signal transduction underlying Si priming (the so-called “primeomics”; Balmer et al., 2015).

3.3. Si and HM stress alleviation

Si assumes key functions in the plant response to numerous environmental constraints. Two major processes contributing to stress resistance are commonly considered (i) a physical and mechanical protection mediated by SiO₂ deposits and (ii) a biochemical response triggering metabolic changes (Figure 8).

In HM-polluted soil, Si may influence the bioavailability of toxic elements. The presence of soil sodium metasilicate or alkaline Si-containing material may induce a rise in the rhizospheric pH leading to a decrease in available HM concentration in the soil (Jia-Wen et al., 2013). Soluble silicate hydrolyzes to generate gelatinous metasillicic acid (H₂SiO₃) retaining HM (Gu et al., 2011). Si-treated plants may also exude phenolics such as catechin and quercetin having strong Al-chelating abilities (Kidd et al., 2001). The formation of hydroxyaluminosilicates in the apoplast also contributes to Al detoxification (Wang et al., 2004).

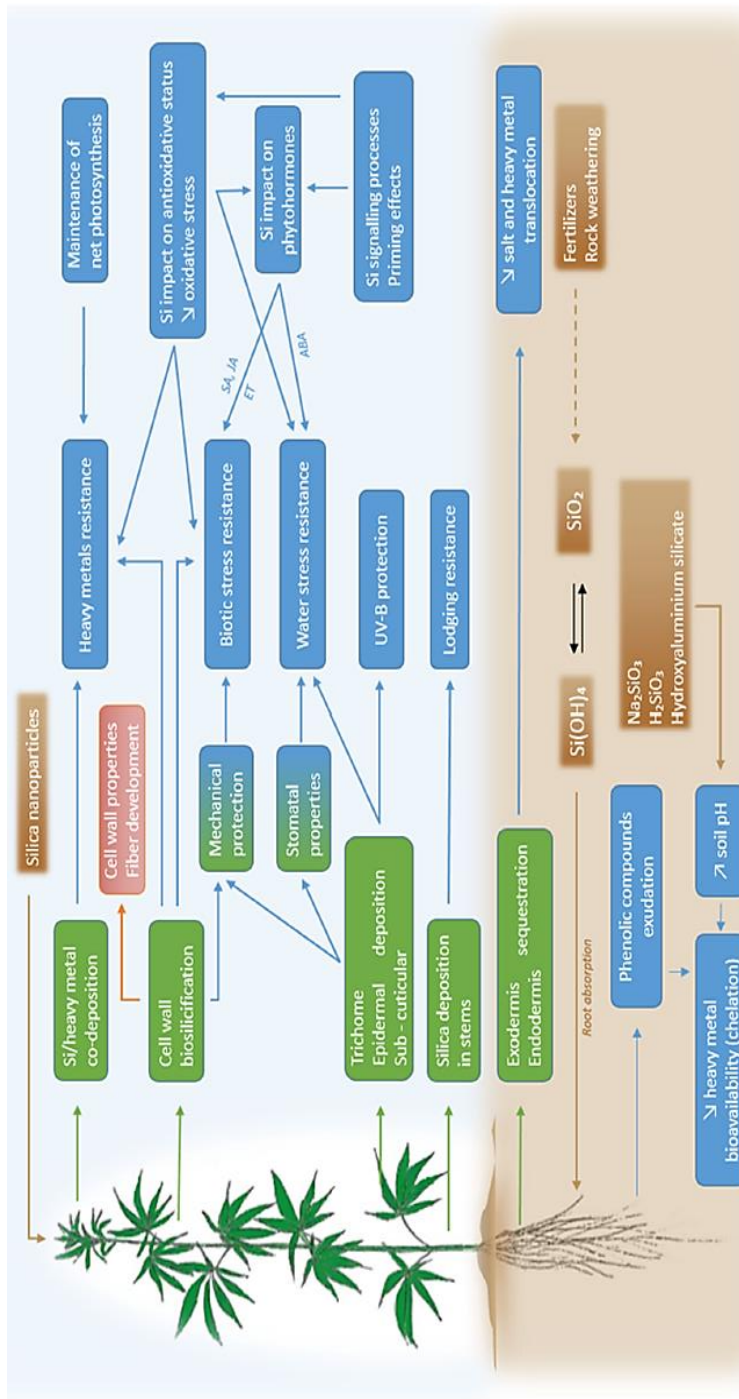


Figure 8: Global overview of Si impact on hemp (*Cannabis sativa* L.), here depicted as a model plant in light of its economic importance as a source of bast fibres. Speciation of Si in soil and application of SiO₂ nanoparticles are indicated in brown boxes and possible sites of Si deposit in the plant are indicated in green boxes. Resulting consequences of Si accumulation in terms of stress resistance and underlying physiological processes are indicated in blue boxes.

Compartmentation of toxic ions is an important process in HM tolerance. Si is known to affect plant cell wall properties by precipitating as amorphous opaline silica (SiO_2), thereby associating with wall components (Guerriero et al., 2018). In roots of several plant species, silicification mainly occurs in the endodermis and enhances the function of this crucial cell layer as an apoplasmic barrier (Fleck et al., 2011; Lukačová et al., 2013; Keller et al., 2015). Quantifying the precise impact of root silicification process on HM retention in the root system requires additional experimental approaches and such knowledge is essential to develop management practices for non-food crop production on contaminated soils. If Si contributes to restrict the upward movement of HM, this may determine that the aerial fraction of the plant can be further valorised for energy or fibre production (Fernando et al., 2015). However, it has also been reported that Si(OH)_4 moves via the transpiration stream and deposits as biogenic silica (SiO_2) when water evaporates in the aerial parts (Trembath-Reichert et al., 2015). In the leaf, Si treatment may increase HM accumulation in epidermis and trichomes (Iwasaki & Matsumura, 1999; Doncheva et al., 2009). Besides transpiration, still undetermined biological factors influence Si(OH)_4 polymerization in the cell wall (Kumar et al., 2017). Since the cell wall also constitutes a major site of HM deposits (Guerriero et al., 2016; Luyckx et al., 2017a), thus preventing them from entering the cytoplasm (Krzyszowska, 2011), an interaction between Si and HM cannot be ruled out which could have some impact on fibre differentiation or properties of the ligno-cellulosic biomass. Controversial data are available in the literature regarding co-precipitation of Si with HM. However, a mechanism of co-deposition of Si and Cd in the rice cell walls via a [Si-wall matrix]Cd complexation has been identified, which may explain a Si-induced decrease in the Cd influx in cells (He et al., 2013), and a hemicellulose-bound form of Si with a net negative charge could be responsible for the inhibition of Cd uptake (Ma et al., 2015).

Si remaining in the form of soluble silicic acid (Si(OH)_4) may also be involved in biochemical/molecular processes contributing to growth stimulation and stress resistance in relation to the oversynthesis of stress hormones such as salicylic acid (SA), jasmonic acid (JA) and ethylene (Fauteux et al., 2005; Yin et al., 2014). Moreover, numerous studies reported that Si alleviation of damages caused by toxic ions (salt and HM stress) also includes the regulation of genes involved in their uptake and translocation; stimulation of antioxidant enzymatic activities (SOD, POD, CAT, GR), and

non-enzymatic antioxidant synthesis; and maintenance of net photosynthesis relying on the stabilization of chloroplast structures, photosystem II (PSII) integrity and increased pigment concentration (Liang et al., 2003; Nwugo & Huerta, 2008; Vaculík et al., 2012; Adrees et al., 2015; Cao et al., 2015; Tripathi et al., 2015; Xu et al., 2015; Bu et al., 2016; Imtiaz et al., 2016; Ma et al., 2016; Sanglard et al., 2016).

Si may thus be of paramount importance in triggering adapted plant responses, but the precise molecular cues involved in the adaptative processes still need to be clearly identified. In the literature, there is only a handful of studies concerning the role of Si in non-food herbaceous crops.

4. Hemp

4.1. Hemp and humankind

Cannabis sativa (hemp) is a herbaceous annual plant belonging to the family of Cannabaceae (Spano et al., 2020). Originating from Central Asia, hemp use is estimated to have begun with a first harvest around 8500 years ago, and active cultivation has occurred for over four to six millennia (Fike, 2016). Through the Middle Ages and until the end of the sailing ship period, hemp was an important crop in many European countries, including the UK, France, The Netherlands, Germany, Spain and Italy (Carus & Sarmiento, 2016). The most important applications for the strong fibre were canvas and ropes for sailing boats, as well as textile and paper industries (Ranalli & Venturi, 2004; Carus & Sarmiento, 2016). Notably, the first copies of the Bible were made of hemp paper (Ranalli & Venturi, 2004).

In Europe, flax and hemp were the most important fibre crops from the 16th to the 18th century. In the 19th century, hemp area under production started to decline in response to lowered cotton processing costs, importation of jute and abaca fibres from overseas, and the competition of steam engines over sailing ships (Struik et al., 2000; Bouloc, 2006; Fike, 2016; Mark & Will, 2019). Hemp's fall from grace was hastened by concerns over its use for hallucinogenic purposes: in the first half of the 20th century, several multilateral treaties started to prohibit the use of drugs (e.g., cocaine, heroin and *Cannabis*) (Ranalli & Venturi, 2004; Bouloc, 2006; Behr, 2018). In 1961, the single convention on narcotic drugs prohibited hemp cultivation in the USA and Western Europe (except France) (Kozlowski et al., 2005).

Moreover, the beginning of the petrol era and the synthetic fibre production competed with natural fibre production (Boulloc, 2006; Fike, 2016; Behr, 2018).

However, since about the last thirty years, there has been a renewed interest for hemp (Figure 9).

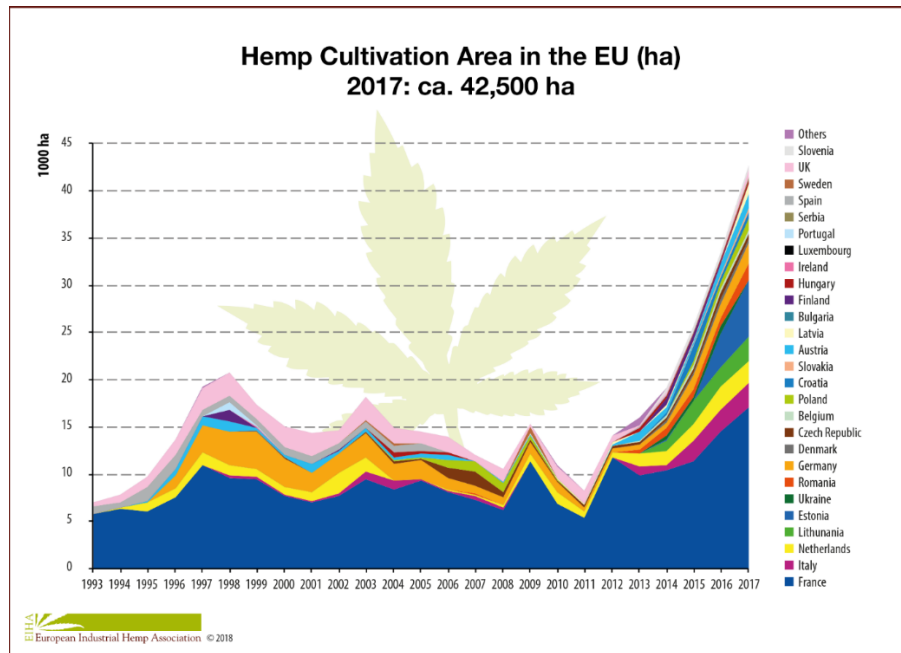


Figure 9: Hemp Cultivation Area in the European Union from 1993 to 2017. Source: EU Commission and nova-Institute surveys (nova/EIHA 2018)

This recent comeback of hemp in the European fields can be explained by the legalisation in most EU member states of *C. sativa* cultivars producing low quantity of Δ^9 -tetrahydrocannabinol (THC), the chemical chiefly responsible for the psychoactive properties in marijuana (Crini et al., 2020; Spano et al., 2020), as well as the search of alternatives to food crops and alternatives sources of renewable resources (Kozłowski et al., 2005; Faux, 2014; Carus, 2017; Mark & Will, 2019; Crini et al., 2020). Hemp has indeed been rediscovered as an interesting ‘new’ crop with a large agro-ecological plasticity and high yield compared with many other crops which produce a wide variety of renewable resources (Struik et al., 2000).

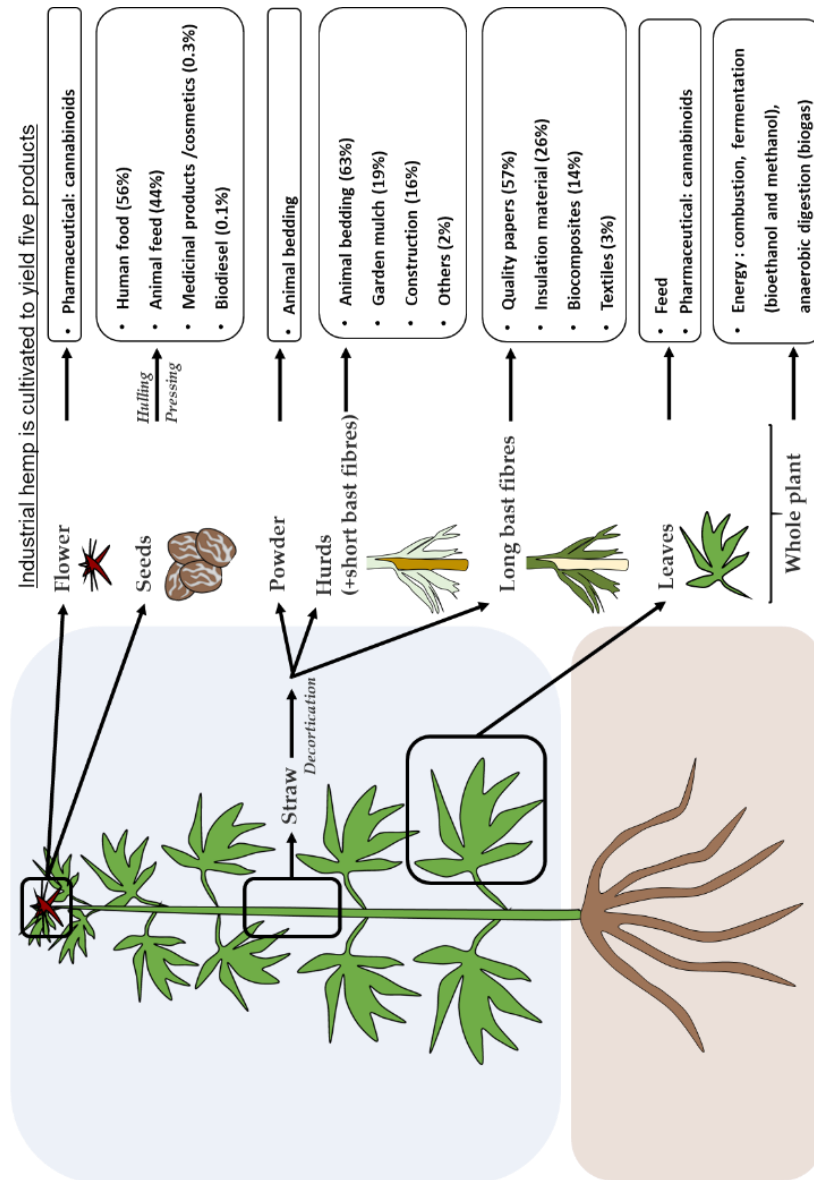


Figure 10: Hemp is cultivated to yield five products: bast fibres, hurd fibres, seeds, leaves and flower (illustration: Marie Luyckx). % = applications for European Hemp Fibre in 2016 (Carus & Sarmento, 2016).

4.2. Valorisation of hemp

Industrial hemp is cultivated to yield five products: bast fibres, hurd fibres, the seed, the leaves and the flower (

). There are 25,000 estimated products derived from industrial hemp (Crini et al., 2020).

a) Bast fibres and hurd

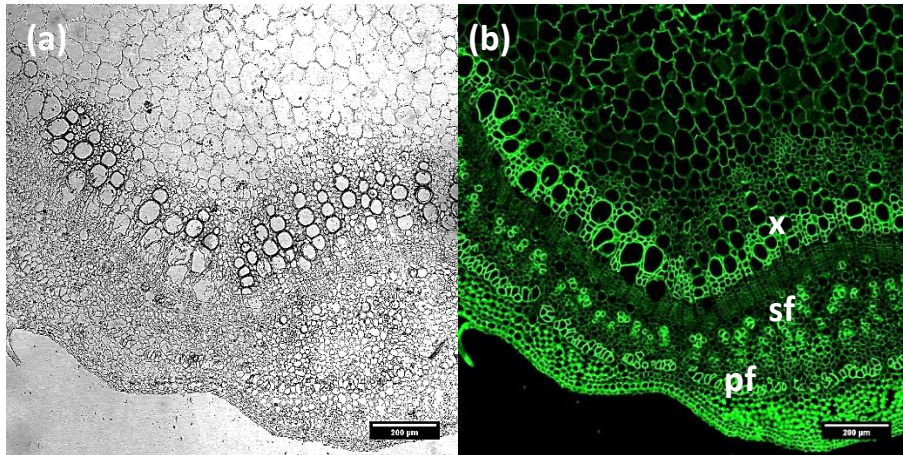


Figure 11: Confocal microscope observation (a) and immunodetection of the CBM3a epitope specific for crystalline cellulose (b) in stem sections of *C. sativa* (cv. Santhica 27). Primary bast fibre (pf), secondary bast fibre (sf), xylem (x). Scale bar: 200 µm.

The majority of the aboveground hemp biomass comes from the plant stem (Rheay et al., 2020). Nowadays, fibre is the main product derived from the hemp stem (Crini et al., 2020). Hemp fibres have some of the best mechanical properties of all natural fibres (Carus & Sarmiento, 2016). Hemp is the source of two types of fibres: (i) primary and secondary bast fibres (20-40% of hemp stem) associated with the conductive elements of phloem and bundles held together by pectins and lignin, and (ii) woody short core fibres (60-80% of hemp stem), called hurds or shives, located in the xylem (Figure 11; Rheay et al., 2020; Luyckx et al., 2021a).

The bast fibres initially elongate through intrusive growth, then cease elongation and start to thicken by secondary cell wall (SCW) deposition (Guerriero et al., 2017a; Behr, 2018). Plant fibre primary cell wall (PCW) consists mainly of cellulose, hemicelluloses and pectin (Pejic et al., 2009). Secondary xylem, primary and secondary bast fibres undergo SCW deposition after the beginning of secondary growth (Behr, 2018). The composition of SCW is not similar for xylem- and phloem-located fibres. Xylem fibres differentiate a xylan-type SCW, while in the phloem fibres, SCW is of gelatinous (G-layer) type (Gorshkova et al., 2012). The CW of xylan-type fibres are lignified, contain predominantly xylan as hemicellulose constituent

and show a typical layered structure (S1–S3, Figure 12) because of the different orientation of the cellulose microfibrils (van den Broeck et al., 2008; Neutelings, 2011; Mikshina et al., 2013; Stevulova et al., 2014; Chakraborty et al., 2015). The SCW of gelatinous fibres is also deposited in three layers, S1 and S2 compositions being similar to xylan-type wall while the G-layer has a very different organization (Figure 12): the major part of the G-layer is characterized by a high abundance of crystalline cellulose (up to 90%) embedded in a rhamnogalacturonan-I (RG-I) matrix and a low content of xylan and lignin (e.g., ca. 4% in hemp) (Guerriero et al., 2013, 2017b; Behr, 2018; Chernova et al., 2018).

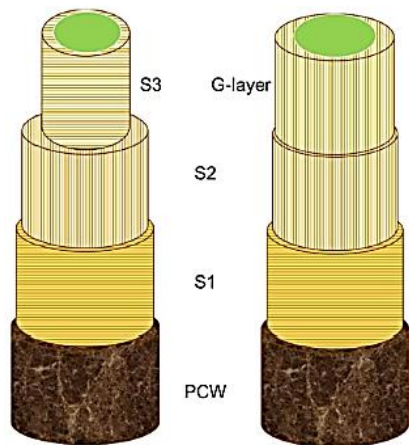


Figure 12: Schematised structure of the cell wall with a xylan-type SCW (S1, S2 and S3, left) and a G-type SCW (S1, S2 and G-layer). S1, S2 and S3 are mainly made of cellulose, glucuronoxylan and lignin, with minor amount of pectins. The G-layer displays a high content of cellulose (> 75 % and up to 90 %) embedded in a rhamnogalacturonan-I (RGI = pectin) matrix, but does not contain xylan nor lignin. Each layer has a specific angle between cellulose microfibrils and the longitudinal cell axis (Behr, 2018).

The transition from bast fibre elongation via intrusive growth to SCW deposition occurs at a specific area called the “snap point” (SP) (Gorshkova et al., 2003). The formation of SCW in hemp phloem fibres begins with the deposition of the Gn-layer (“gelatinous-new”) (Chernova et al., 2018). During further CW development, the Gn-layer is transformed to a “solid” G-layer: enzymatic digestion of the pectic matrix leads to the compaction of cellulose microfibrils and final organization of the G-layer (Chernova et al., 2018). It was also recently reported that in the young hemp hypocotyl, the G-layer has a loose structure (Gf) and that it gets compacted at later stages of development (Figure 13, Behr et al., 2019).

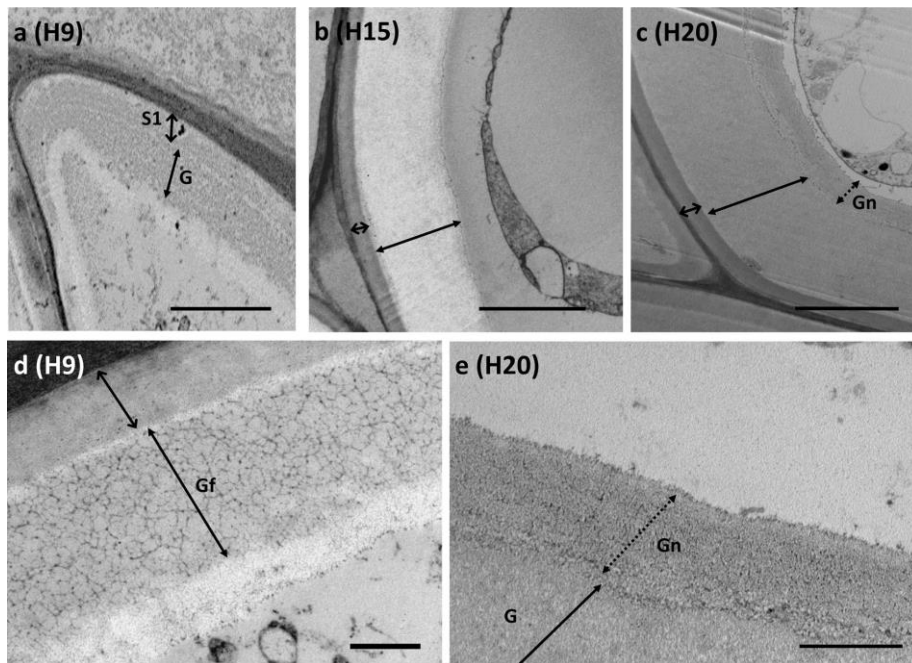


Figure 13 : Ultrastructural analysis of bast fibers in hemp stems at different developmental stages. a After 9 days of growth (H9), bast fiber cells already highlight the presence of secondary cell wall and it is possible to distinguish a first layer (S1, double arrow) and the initial gelatinous layer (G-layer, indicated by the double full arrow). b Bast fibers at the stage of development H15, where the increase in thickness of the G-layer is clear. c At the developmental stage H20, the increase in thickness of the G-layer (double full arrow) is most noticeable. At this stage, it is possible to notice the presence of an additional fibrillar layer, which presumably corresponds to the Gn-layer. Bars a–c: 2 μm . d Early stage of development in which the G-layer is characterized by a messy intertwined array of fibrils (which is defined as “Gf layer”). e Detail of a more compact G-layer and of the fibrillar layer Gn, in which it is possible to recognize its cellulosic nature. Bars in d, e: 500 nm (from Behr et al., 2019).

Bast fibres

Primary bast fibres, which extend nearly to the entire length of the stalk and are coarser than secondary bast fibres, are the most valuable part of the stalk (Crini et al., 2020). In Europe, hemp stems are processed mostly in the “disordered line” producing not aligned bast fibre bundles (often incorrectly identified as “technical fibre”) used for lightweight papers (57% of the European hemp fibres market), insulation material (26% of the market) and biocomposites (14% of the applications) (Carus & Sarmiento, 2016; Musio et al., 2018). The possibility to obtain long aligned fibre bundles for textile and

high-added value applications is limited by the lack of dedicated harvesting machines that can mow hemp stems, lay them on the field in aligned swaths and cut them in 1 m long portions, so that they can be fed in flax scutching (decortication) lines (Musio et al., 2018).

Surging demands from the automotive and construction industries to develop eco-friendly and renewable materials triggered the growth of the biocomposite market in recent years (Shahzad, 2012). The biocomposite industry is interested in the use of natural fibres (e.g., hemp bast fibres) as natural substitutes of synthetic fibers such as glass, carbon or metallic fibers: plant fibres are cheaper, renewable, biodegradable, have a low C footprint (Table 3), and, compared to glass fibres, they raise no health-related concerns (Guerriero et al., 2014; Andre et al., 2016; Carus & Sarmiento, 2016; Guerriero et al., 2016; Musio et al., 2018; Crini et al., 2020).

Table 3: Environmental parameters in the production of 1 kg of fibres (Mougin, 2006).

Parameters	Hemp fibre	Glass fibre
Power consumption (MJ)	3.4	48.3
CO ₂ emission (kg)	0.64	20.4
SO _x emission (g)	1.2	8.8
NO _x emission (g)	0.95	2.9
BOD (mg)	0.265	1.75

Moreover, they show favourable mechanical properties of rigidity and strength (25.0% to 30.0% stronger than glass fibers), in combination with low density. Additionally, the molding process of natural fibre composites (NFC) consumes less energy than that of glass fibres, which reduces the production cost by 10.0% (*Natural Fiber Composites Market Size | NFC Industry Report, 2018-2024*, s. d.; Crini et al., 2020). Hemp composites have comparable flexural strength properties (54 MPa) than glassfibre composites with propylene matrix (60 MPa), and the specific flexural strength of hempcomposite (36.5) is higher than that of glass fibre composite (Shahzad, 2012). However, moisture sensitivity of these biocomposites and weak bonding with polymer matrices are anticipated to hamper the growth of the market. Therefore, their application in the automotive industry is limited to car interiors only (*Natural Fiber Composites Market Size | NFC Industry Report, 2018-2024*, s. d.). The global NFC market size was valued at USD 4.46 billion in 2016, and is likely to register a compound annual growth rate

(CAGR) of 11.8% from 2016 to 2024 (*Natural Fiber Composites Market Size / NFC Industry Report, 2018-2024*, s. d.).

Besides, graphitic carbon nanosheets, prepared by hydrothermal carbonization combined with activation of hemp bast fibre, presents a great potential for facile large-scale production of high-performance carbons for a variety of diverse applications including energy storage: they display some of the best power–energy characteristics (on an active mass normalized basis) ever reported in the literature for an electrochemical capacitor (Wang et al., 2013).

Hurds

Hurds are used for animal bedding (63% of hemp hurd applications) and construction (16% of the market; Guerriero et al., 2014; Andre et al., 2016; Carus & Sarmiento, 2016; Guerriero et al., 2016).

Urbanization emanating from rapid population growth in developing countries and new technical needs in industrial regions have put pressure on the demand for adapted building materials. Biomaterials may constitute, in numerous cases, a suitable option offering a source of renewable material and interesting rheological properties (Moroz et al., 2014). An important example is hempcrete/hemp-lime, perhaps the most researched bio-based building material (Crini et al., 2020). This material is a mixture of hemp woody fibres and lime products. Hempcrete is commonly used in the construction sector, e.g. as a lightweight insulating material, hurd board, additive to bricks or loam construction, or as pour-in insulation (Crini et al., 2020). Insulation is the second important application for hemp fibers today (Carus & Sarmiento, 2016). These fibers can also be used for acoustic and soundproofing purposes (Crini et al., 2020).

The industrial process of stalk also provides dust (10–15%) that can be used as fuel and soil improver in powder form, or as granulated animal bedding (Carus & Sarmiento, 2016; Crini et al., 2020).

b) Seeds

Hemp seeds, with a high nutritional value, can be consumed raw or pressed into hemp seed oil (25%–35% of the total seed mass) which has an excellent and unique fatty acid profile (α - and γ -linolenic acid, n-3:n-6 ratio about 3:1) (Carus & Sarmiento, 2016; Behr, 2018; Rheay et al., 2020). The composition of seeds (20%–35% protein, 20%–30% carbohydrates, and fibre) allows hemp

to be used for human food and animal feed, medicinal products, personal care products, and fuel (Small & Marcus, 2002; Żuk-Gołaszewska & Gołaszewski, 2020; Rheay et al., 2020).

Traditionally harvested at full flowering for textile destinations, nowadays hemp is mainly harvested at seed maturity to maximise the economic value of hemp by exploiting all plant biomass (stems, inflorescences and seeds) (Musio et al., 2018). This implies to adapt agronomic techniques and genotypes to preserve fibre quality during grain ripening (Amaducci et al., 2015; Musio et al., 2018).

c) Flower

While fibre and seed are the main products, there is a growing interest over the valorization of hemp secondary metabolites (Amaducci et al., 2015). Hemp inflorescences and vegetative organs are rich in various unique bioactive secondary metabolites, namely cannabinoids (C₂₁ terpenophenolic compounds), terpenoids and flavonoids (Amaducci et al., 2015). The cannabinoids, which are unique to *Cannabis* plants, and primarily the non-psychoactive cannabinoid (cannabidiol-CBD) fraction, is gaining more and more interest in pharmaceutical and food supplement industries (Carus & Sarmiento, 2016; Rheay et al., 2020). Naturally dioecious, breeding and selection efforts have led to the development of monoecious *C. sativa* varieties specific to different end-uses: fibre hemp, seed/grain hemp, and CBD hemp (Rheay et al., 2020). Since CBD is mainly concentrated in female flowers, the plants used for CBD production are often started in greenhouses from propagated female clones and are transplanted two to four weeks after establishment. The use of hemp for generating CBD has not received much consideration as of now, although there is a growing commercial interest in using hemp plants for this purpose (Adesina et al., 2020).

d) The whole plant

Hemp biomass may also be used for energy production: fuel properties of hemp are either similar or superior to other solid biofuels such as cereal straw, wood, etc. (Adesina et al., 2020). For example, the heat of hemp combustion (18.4–19.1 MJ/kg) is comparable to maize-*Zea mays* (18 MJ.kg⁻¹) and slightly lower than *Miscanthus* sp. (19.8 MJ.kg⁻¹) (Adesina et al., 2020; Żuk-Gołaszewska & Gołaszewski, 2020). Additionally, both wet and ensiled hemp biomass can be transformed into biogas and ethanol. Hemp also emits

comparatively low sulfur compounds and has low ash content (Adesina et al., 2020; Żuk-Gołaszewska & Gołaszewski, 2020).

4.3. Agronomy of hemp

The plant is an annual plant sown in spring and harvested from the end of August (not threshed: stem harvesting) to the end of September (threshed: stems and seeds harvesting), and reproduces via seed propagation (Bouloc, 2006; Rhey et al., 2020). Plants can grow to heights of up to 4 m with an average diameter of 1 to 3 cm and develop a tap root penetrating up to 2 m into the soil (Bouloc, 2006; Rhey et al., 2020). Only cultivars with THC content lower than 0.2% (w/w) can be cultivated in Europe (RÈGLEMENT (UE) n°1307/2013).

From an agronomic point of view, crop yield, quality and uses are affected by several features:

a) Plant cultivars

Hemp is a naturally dioecious plant with highly variable sexual phenotype (Faux, 2014; Struik et al., 2000). Female plants are usually used for seeds and phytocannabinoid production, while males are preferred for fibre production (Schlottenhofer & Yuan, 2017). Hemp is wind pollinated and the flowering of male and female plants in dioecious cultivars is not synchronised, male plants tending to flower and senesce earlier (Behr, 2018; Struik et al., 2000), which makes the mechanical harvest of the seed difficult (Faux, 2014). A small percentage of monoecious plant can naturally occur, particularly in short-day conditions (Amaducci et al., 2015). Today the cultivation of multipurpose cultivars, with joint production of seeds and stems, is a minimum requirement for hemp farmers. In Europe, most of the registered industrial hemp cultivars (e.g. Santhica, Futura) are monoecious. Monoecious cultivars are considered particularly suitable for this type of use, as they allow greater uniformity, easier mechanical harvesting, and higher seed yield to produce both stems and seeds simultaneously thanks to growth homogeneity (Baldini et al., 2018). However, monoecious accessions tend to show a wide range in sex ratios within the crop, including unisexual plants, and may gradually return to natural dioecy after a few generations (Faux, 2014; Faux and Bertin, 2014; Petit et al., 2020). Constant strict selection (manual elimination of residual male plants and strongly masculinized plants before flowering) of monoecious plants is therefore needed to maintain monoecy during the seed multiplication (Moliterni et al., 2004; Behr, 2018; Petit et al., 2020).

b) The flowering induction

Hemp is a short-day plant implying that the flowering induction occurs below a critical photoperiod threshold. The cultivars that are grown in Europe have a critical photoperiod between 14 and 15.5 h (Struik et al., 2000). This behaviour affects crop production, because the maximum fibre yield, strength and quality are reached shortly after flowering (Kozłowski et al., 2005; Faux, 2014). However, if hemp is grown for both fibre and seeds or only seeds, it has to be harvested at full maturity phase, when the seeds in the middle part of the panicle are mature. The fibres obtained are stronger and not suitable for textile production (Kozłowski et al., 2005). The precocity of the variety has therefore to be adapted to the eco-region where it is grown (Behr, 2018).

c) Soil preparation and requirements

Preparation of a fine and homogenous seed-bed is an important condition to obtain a uniform establishment and a homogeneous crop presenting the desired plant density (Struik et al., 2000). Soil preparation for hemp is similar to that of other break crops: winter ploughing followed by preparation of a fine seedbed in the spring are the recommended tillage practices for hemp, especially on clay soils (Amaducci et al., 2015). Besides, hemp has specific soil requirements: the soils must be fertile, structural, with no excess of water during early stages of growth, with ground temperature of at least 8-10°C, and optimum pH between 6 and 8 (Struik et al., 2000; Kozłowski et al., 2005; Amaducci et al., 2015). Nevertheless, hemp is appreciated by organic growers for its adaptability to a wide range of agronomic conditions, ease of production, low fertilization needs, and rapid growth (Crini et al., 2020). The data published by the ITC (Institut Technique du Chanvre en France) in 2007, indicated that the fertilization needs of a hemp crop producing 8 T. ha⁻¹ of straw and 1 T. ha⁻¹ of seeds are of 120, 100, 300 and 320 kg.ha⁻¹ for N, P, K, and Ca respectively. Moreover, hemp cultivation has always been considered an excellent crop to include in crop rotation because of its beneficial effects on following crops (up to 10-15% yield increase), the crop requires no irrigation, and herbicides are not considered necessary because hemp's fast growth can inhibit weed growth (Citterio et al., 2003; Ranalli & Venturi, 2004; Crini et al., 2020; Żuk-Gołaszewska & Gołaszewski, 2020). Hemp is also often considered a crop mostly free of pathogens, possibly because of the presence of essential oils (e.g. α -pinene and limonene) and cannabinoids in hemp, that act as insects' deterrent (Kozłowski et al., 2005).

d) Sowing density

Fibre content and quality strongly rely on sowing density: increasing sowing density increases the bast fibre content, as well as the proportion of primary bast fibres (Struik et al., 2000). Current recommended seeding rates ranges from 40 to 65 kg ha⁻¹ to reach 200–300 plant m⁻² for fibre hemp, decreasing to 20 kg ha⁻¹ for seed hemp (ITC, 2007).

e) Harvesting and retting process

The harvesting time and the retting duration of the stems affect the maturity and the mechanical properties of the fibres, and dictate the selection of further processing devices for hemp stems, as well as the economics of fibres production (Jörg et al., 2020).

The hemp crop harvesting systems involves threshed and unthreshed methods. Unthreshed harvesting consists of collecting the stems, while threshed harvesting collects the seeds and leave the stems on the field in a disordered swath. Following the latter system, the farmer can benefit from the income derived from the sale of seeds and fibres (Jörg et al., 2020). However, in this system, harvesting is carried out considering seed ripening and not fibre quality: the fibres obtained are more suitable for lower value applications, such as the production of paper and pulp, short fibre/fibre bundle reinforced thermoplastics or perhaps non-woven textiles (needle felts or fleeces) (reviewed by Jörg et al., 2020). Furthermore, when plants are harvested too late, the lignification of the fibres makes fibre extraction more challenging and affects the integrity of the properties of the fibres (Jörg et al., 2020).

The retting of hemp is another area needing attention. Retting is a “biochemical process in which enzymes produced by microorganisms attack the pectins that glue together fibre cells, aiding the separation of fibre bundles within the bast fibre and of hurds from bast fibre” (Musio et al., 2018). Retting has a strong influence on several fibre properties: (i) the removal of unwanted elements, such as residues of other tissues, cuticle and encrustations, (ii) the easy separation of the fibres from other tissues, (iii) the fibre quantity and (iv) the residual pectin, hemicellulose and lignin content of the fibre walls (Di Candilo et al., 2010 and references therein). Retting is well mastered and controlled for flax, but more subjectively and inconsistently implemented for hemp (Jörg et al., 2020). This leads to fibres with significant heterogeneity in terms of retting degree: retting time should be long enough to disaggregate

lignin, pectin and waxes while preventing the degradation of the cellulose (Behr, 2018). It is also important that swathes of retted stems dry quickly when conditions are favourable so as to avoid over-retting. Removal of the leaves and flower heads before the stems are swathed is likely to promote more even retting by better exposing the whole length of the stems to drying (Bruce et al., 2001). Hemp stems are usually retted on the soil (dew retting) or submerged in water tanks (water retting), both methods being carried out by pectic enzymes secreted by indigenous microflora (Tamburini et al., 2004; Jankauskienė & Gruzdevienė, 2013; Nair et al., 2013). After retting, fibres are mechanically separated from other material by scutching (Tamburini et al., 2004).

Dew retting is carried out on the field, where the stems are left after harvesting, and is considered to be the oldest method of retting (Nair et al., 2013; Musio et al., 2018). This process is widespread in Europe due to low labor costs and high fiber yield (Jankauskienė & Gruzdevienė, 2013; ; Nair et al., 2013; Musio et al., 2018). However, dew retting is time consuming (3-4 weeks) and highly dependent on microclimatic conditions: over-retting and under-retting can occur frequently, resulting in poor fibre quality and un-homogeneous results (Nair et al., 2013; Musio et al., 2018). In order to avoid degradation of cellulose, a mixture of selected enzymes or fungi can be spread on the stems resulting in a reduced dew retting duration characterized by a low cellulosic activity (Musio et al., 2018 and references therein).

Water retting produces the highest quality fiber, but the environmental pollution caused by it forced the industries to regulate the procedure and find other alternatives, like steam explosion and electromagnetic energy-assisted retting (Nair et al., 2013). However, the impact of water retting is reduced in the case of controlled warm water retting, where the retting process is optimized with target bacterial inoculum and the best fibre quality being obtained after 3–4 days of retting (Di Candilo et al., 2010).

Among the other methods, the chemical retting and the mechanical separation of fibres are not suitable because the process is expensive and produces poor quality fibres (Tamburini et al., 2004; Di Candilo et al., 2010).

4.4. Phytomanagement potential

Growing hemp for phytomanagement on marginal farmland soils has the potential to alleviate many of the current constraints of phytomanagement. Compared to many wild plant species tested for phytomanagement purposes,

hemp has a greater adaptability to different soils and climatic conditions, it has deep roots allowing the treatment of large soil volumes and has substantial aboveground biomass production with options for value-added industrial products that do not introduce toxins into the consumer marketplace (Linger et al., 2002; Citterio et al., 2003; Piotrowska-Cyplik & Czarnecki, 2003; Meers et al., 2005; Rheay et al., 2020). In addition, its agro-technology and industrial processing are well-known and applied in many countries (Citterio et al., 2003). Hemp could thus integrate a crop rotation with other non-food crops, used for biodiesel production (rapeseed, soybean, cotton) for example, on moderately contaminated substrates. The major factors that impact the usability of the hemp biomass for phytomanagement purposes include the contaminant type and concentration in the biomass, the type of product use and regulatory standards/guidelines on acceptable product quality (Rheay et al., 2020).

A multitude of research has shown that hemp is capable to extract HM from soil and to accumulate it in different concentrations throughout the entire plant (Citterio et al., 2003; Czarnecki, 2003; Meers et al., 2005; Piotrowska-Cyplik & Rheay et al., 2020).

Hemp is considered as an excellent candidate for phytostabilization: hemp roots are able to sequester/phytostabilize HM from polluted soils, with minimal HM translocation to the shoot (Citterio et al., 2003; Shi & Cai, 2009; Shi et al., 2012). The use of hemp in phytoextraction strategies involves the uptake of contaminants into harvestable materials. If hemp accumulates most of the metals in its root system, its use for phytoextraction purposes would allow only slow restoration of soils. However, hemp deep root system allows the treatment of large soil volumes and its great aboveground biomass production compensates lower metal uptake and translocation capacity (Citterio et al., 2003). Moreover, with the perspective of exploiting useless polluted soils for hemp cultivation, the HM uptake per year and the remediation time assume a minor importance because no expenses for soil restoration must be met. On the contrary, productive economical activity could start up and improve the environment (Citterio et al., 2003). Besides, hemp has been tested with favorable results as phytoextractor in areas where lands were contaminated with various pollutants such as metals, radioactive elements, organics, including pesticides and fertilizers, oils and solvents (reviewed by Crini et al., 2020) with a phytoextraction potential of $126\text{--}684 \text{ g (ha vegetation period)}^{-1}$ for Cd (Linger et al., 2002; Citterio et al., 2003). Phytoextraction is dependent on the contaminant's identity and concentration,

as well as soil characteristics (Rheay et al., 2020). The use of chelating agents such as EDTA (ethylene diamine tetraacetate) or biodegradable EDDS (ethylenediamine-*N,N'*-disuccinic acid) may strongly improve the use of hemp to clean up contaminated soils, but an important percentage of the mobilized HM may be lost by uncontrolled leaching of the pollutant before absorption by the plant (Kos & Leštan, 2004; Meers et al., 2005).

Phytomanagement also requires the use of plant species displaying HM tolerance. Hemp growth is generally not inhibited by moderate contamination of heavy metals in the soil (Rheay et al., 2020). Hemp was reported to tolerate up to 27 mg kg⁻¹ soil of Cd, and up to 800 mg Cd kg⁻¹ DW had no major effects on growth, fibres' and hurds' quality, although high Cd content in the leaves had detrimental effects on chlorophyll synthesis, water splitting apparatus and energy distribution in PSII. The tolerance of hemp to HM is likely linked to an increase in reduced glutathione and phytochelatins (Linger et al., 2002, 2005; Citterio et al., 2003; Ahmad et al., 2015; Ahmad et al., 2016a).

4.5. Which uses for HM- and Si –containing biomass?

In addition to the restoration of soil quality and functions, phytotechnologies can produce valuable biomass. Industrial utilisation of the harvested biomass will depend on the phytotechnology applied on the polluted site: phytoextraction produces biomass enriched in HM, while (assisted) phytostabilisation will produce biomass with HM concentrations close to their physiological concentrations (Bert et al., 2017). Heavy metal-contaminated hemp raw material may thus integrate, under the conditions set by the regulations, many kinds of industrial products with added value, which significantly decreases the cost of potential phytomanagement (Di Candito et al., 2004; Griga & Bjelková, 2013; Rheay et al., 2020).

Depending on the HM content in hemp biomass, the following industrial processing could be considered (Griga & Bjelková, 2013 and references therein):

- The biomass contains excessive amounts of HM: energy use (combustion, recycling of ash HM);
- Fibres' HM content exceeds the limits for garment textiles (STANDARD 100 by OEKO-TEX®, Table 4): composite materials, paper industry, geotextile and other industrial applications;

- Fibres contain acceptable amounts of HM (STANDARD 100 by OEKO-TEX®) or HM are mainly concentrated in stem tissues other than fibres: garment textile industry, hurds either burnt or used for other industrial applications.

Table 4: OEKO-TEX® Limit values of extractable heavy metals (mg kg⁻¹).

Product Class	I Baby	II In direct contact with skin	III With no direct contact with skin	IV Decoration material
Sb (Antimony)	30.0	30.0	30.0	/
As (Arsenic)	0.2	1.0	1.0	1.0
Pb (Lead)	0.2	1.0 ^a	1.0 ^a	1.0 ^a
Cd (Cadmium)	0.1	0.1	0.1	0.1
Cr (Chromium)	1.0	2.0	2.0	2.0
Cr (VI)	0.5	0.5	0.5	0.5
Co (Cobalt)	1.0	4.0	4.0	4.0
Cu (Copper)	25.0 ^b	50.0 ^b	50.0 ^b	50.0 ^b
Ni (Nickel) ^c	1.0 ^d	4.0 ^e	4.0 ^e	4.0 ^e
Hg (Mercury)	0.02	0.02	0.02	0.02

^a No requirement for accessories made from glass

^b No requirement for accessories and yarns made from inorganic materials

^c Including the requirement by REACH-Regulation Annex XVII, Entry 27

^d For metallic accessories and metallized surfaces: 0.5 mg kg⁻¹

^e For metallic accessories and metallized surfaces: 1.0 mg kg⁻¹

Only food and feed production would represent some risks to health and should be avoided (Linger et al., 2002; Griga & Bjelková, 2013).

Besides, this implies to control HM emissions in order to prevent transfers into the environment (Bert et al., 2017). In this respect, hemp dew retting should be avoided or carefully monitored: retting in water tanks is strongly recommended to avoid HM transfers from stem to soils or from soils to the stems. The process is more expensive than dew retting, due to high water use and high oxygen demand of the waste waters, but the quality of water-retted fibre is superior than dew-retted fibre, allowing them to be used in special products (Griga & Bjelková, 2013; Nair et al., 2013; Musio et al., 2018). After retting, the obtained straws can be mechanically separated from other material by scutching to obtain clean long fibres (Tamburini et al., 2004). To lower the cost of water retting and maintain hemp as an attractive crop for farmers, stems can also be directly decorticated without any retting, but decortication of non-retted stems results in fibres of inferior quality with

impurities on them, because fibres are glued together and to the stem with chemical bonds such as those mediated by pectins, which cannot be broken completely by applying mechanical pressure (Di Candilo et al., 2010; Nair et al., 2013).

a) Sources of energy

Hemp can be cultivated as source of energy and used for the production of biofuels, bioethanol or material for combustion. This use of hemp biomass could contribute to the objectives of Directive 2009/28/EC (amended by Directive 2015/1513/EC) on the promotion of the use of energy from renewable sources (non-fossil fuels) in the European Union (EU). The directive's objective is to further reduce greenhouse gas emissions and the significant contribution that road transport fuels make to those emissions. A first objective has been set by the Directive: the share of energy from renewable sources in all forms of transport in 2020 is at least 10 % of the final consumption of energy in transport in Member States. Plant biomass has the great advantage over other renewable energy forms; it is currently the only renewable source of fixed carbon and thus is the only source in the long term for the production of transport fuels (Evangelou et al., 2015).

Nevertheless, there is a risk of pollutant dissemination that needs to be carefully considered. This risk is probably limited for biodiesel production because seeds are commonly used for this purpose and most angiosperms drastically limit HM accumulation in these crucial structures. Moreover, hemp-derived biofuels can replace gasoline for diesel engines without any needed modifications and they produce less greenhouse gas carbon monoxide, potentially helping relieve global warming (Crini et al., 2020). In contrast, the risk for HM dispersal is by far higher when vegetative parts (in the form of briquettes, pellets, ...) are used for combustion at high temperatures, but there is still a lack of reliable data regarding the quantification of this risk, and filters have to be installed to retain the volatile HM (Evangelou et al., 2015). This process also concentrates the pollutants in the ash and thus enables them to be recovered with relatively low costs; the process considerably reduces the volumes of contaminated material and thus disposal cost (Di Candito et al., 2004).

The vegetative parts can also be used to produce bioethanol from fermentation and biogas via anaerobic digestion (Crini et al., 2020). These processes are more suitable than combustion because they give the possibility of controlling the fate of the extracted HM and prevent the emission of HM

oxides (Werle et al., 2017). However, the risk originating from the HM contained in the digestate after biogas or ethanol production have to be mitigated.

Si may have a critical role in the biomass combustion process and causes a number of serious problems to power plants through slagging, corrosion and fouling. Hence, besides its beneficial biological effects, Si can negatively impact the thermoconversion of biomass energy. Amorphous structures of phytolith disappear at high temperatures and biomass should accordingly be pyrolyzed below 600 °C. The cell wall quality is essential for plant biomass conversion to biofuels and is influenced by genotype and environmental conditions (da Costa et al., 2014). The determination of the precise impact of Si and HM on cell wall properties in energy crops is consequently of paramount importance. In this regard, Guerriero et al. (2019 and 2020) recently showed, via SIMS nano-analysis, that in hemp bast fibres Si accumulates in a specific region of the G-layer closest to the lumen and, preferentially, on the distal side facing the cortex. This preferential accumulation was interpreted by invoking a purely mechanical principle: the impregnation of the distal cell walls of bast fibres with silica results in the formation of a ring strengthening the whole stem.

b) Composites and plastic alternatives

In the literature, there is no evidence of fibre damage (fibre fineness and strength) due to HM contamination (Linger et al., 2002; Griga & Bjelková, 2013). Arru et al. (2004) used an X-ray microanalysis to investigate the localization of Cu in *C. sativa* and found that this element accumulated preferentially in the upper leaf epidermal cell and in the abaxial trichomes, but the primary bast fibres were not involved in Cu accumulation. Moreover, in composite materials, fibres are embedded in polymers, HM could thus probably not be set free.

The major difficulty which limits an extended use of natural fibers is their hydrophilic nature: cell wall polymers often bear hydrophilic hydroxyl groups able to form new hydrogen bonds with water molecules, which hinders hydroxyl groups from reacting with the polar matrix of the composites (Mwaikambo & Ansell, 2002). This property affects the degree of interfacial adhesion between fibers and the hydrophobic matrix (of polymeric nature), and results in a decrease in the mechanical properties (especially durability, and toughness) of the resulting composite material (Rachini et al., 2012). Thus, modification of the fiber surface is generally used to reduce the

hydrophilic character of natural fibers for incorporation mostly in organic matrix (Rachini et al., 2012). Silane is an inorganic compound (SiH_4) commonly used to improve the tensile strength and thermal stability of natural fibres (Abdelmouleh et al., 2004) which may be due to Si-O-C and Si-O-Si links on the cellulose surface (Lu et al., 2013). Other Si-based treatments, including siloxane and nano Si dioxide are also used for similar purposes (Kabir et al., 2012; Orue et al., 2016; Siengchin & Dantungee, 2014). Si beneficial influence on natural fibre properties is thus confirmed by the use of Si-containing compounds during industrial processing of harvested fibres.

Besides a direct influence of HM and Si on the physical properties of the biomaterial, an indirect effect may also result from their influence on cell wall formation and fibre development. In this regard, Si can have an influence on the endogenous phytohormones (Figure 14). Plant hormones play important roles in the establishment of (pro)cambial cells, which then differentiate the (primary/secondary) xylem and phloem fibres (reviewed by Guerriero et al., 2014): auxin, for example, is crucial in the determination of procambial precursor cells, as well as in secondary growth (Nieminen et al., 2015) and cytokinins regulate cambial activity during secondary development (Nieminen et al., 2008). An increased (pro)cambial activity triggered by Si can lead to an increased bast fibre differentiation in hemp stems. In addition to that, Si may affect the phytohormone balance regulating important stages of bast fibre development, notably intrusive growth and cell wall thickening. It was recently showed that, in elongating hemp bast fibres, transcripts related to the indole glucosinolate metabolic process were upregulated (Guerriero et al., 2017b). Indole glucosinolate synthesis may be related to the wound hormone jasmonic acid (JA) and may regulate the phase of intrusive growth (Guerriero et al., 2017b). Interestingly, a relationship has been reported in the literature between Si and JA: Si primes JA-mediated defense response in rice (Ye et al., 2013).

Additionally, Si is known to boost plant secondary metabolites such as phenols, which can scavenge the apoplastic ROS produced in the cell walls of adjacent cells during the invasion of their middle lamellas (Figure 14; Ahanger et al., 2020; Vega et al., 2020). Besides, fibre elongation requires optimal H_2O_2 levels. Tang and colleagues observed that blocking the activity of the NADPH oxidase with diphenyleneiodonium (DPI) inhibits ROS formation and fibre cell elongation (Tang et al., 2014), while another study identified a high accumulation of a gene encoding a cytosolic ascorbate peroxidase (GhAPX1) during cotton fibre elongation likely to detoxify H_2O_2

(Li et al., 2007). One way in which ROS (hydroxylradicals) regulate growth is through the scission of xyloglucan polymers, decreasing the resistance of the wall to the pressure from the expanding protoplast (Gapper and Dolan, 2006). It may thus be hypothesized that Si treatment *in vivo* during fibre development (and not only *ex planta* on harvested mature fibres) may lead to several promising applications. A field study already provided evidences that soil application of silicate could improve the size of fibre by increasing cell elongation and fineness (Khan & Roy, 1964). This exciting goal, however, requires a multidisciplinary approach to gain a better understanding of Si influence on the modalities of fibre development. Moreover, given the positive effects on plants, the use of Si for fibre crop growth may provide an enhanced biomass yield and, therefore, an increased production of bast fibres.

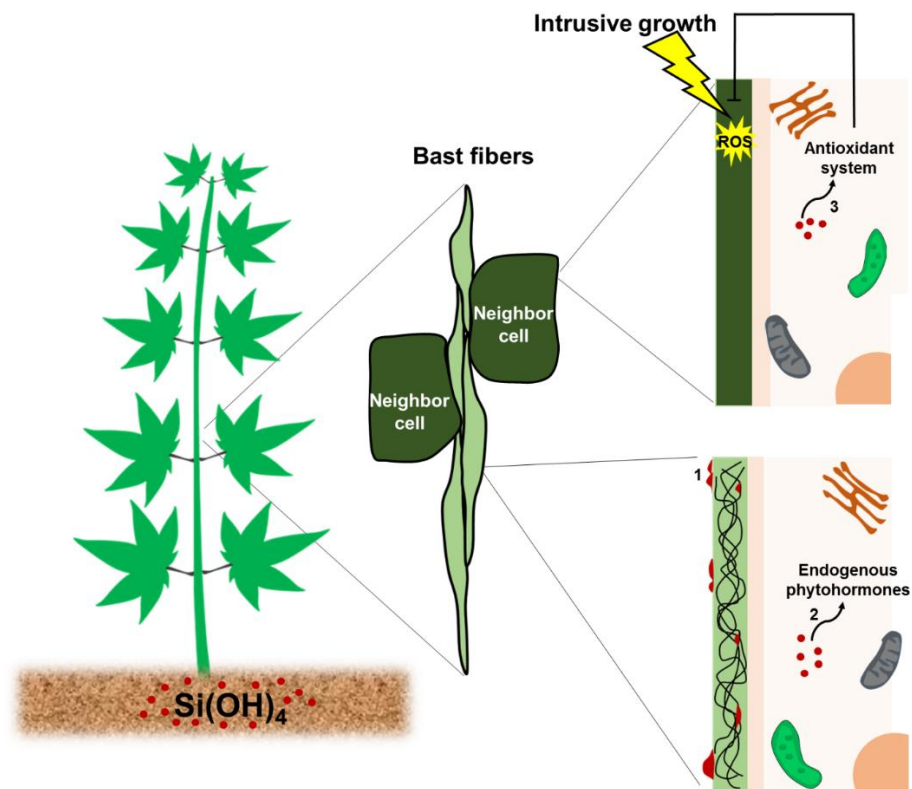


Figure 14: Effects of Si on fibre crops (textile hemp is represented in the picture). Silica (in red) in the cell walls of bast fibres (1) contributes to improve the mechanical properties of the fibres; Si (red dots) can have an effect on the synthesis of endogenous phytohormones, resulting in improved growth (2). Si in the cells neighbouring intrusively growing bast fibres stimulates secondary metabolism and the formation of antioxidant molecules scavenging the reactive oxygen species (ROS) formed in the apoplast, due to the invasion of the middle lamellas (3).

c) Building and Construction

A strong body of evidence in the literature has demonstrated a role of the cell wall in the response of plants to toxic concentrations of HM: besides acting as a “reservoir” for the accumulation of HM (via ion exchange mechanism with components of the cell wall containing –COOH groups, notably low methyl-esterified homogalacturonans), the plant cell wall is remodeled at the onset of HM stress (Krzesłowska, 2011; Gall et al., 2015; Parrotta et al., 2015). The remodeling of pectins, i.e. an increase in low methyl-esterified (acidic) pectins sequestering HM in the egg-box” structure, in primary cell walls, upon HM stress has already been reviewed (Hu et al., 2010; Parrotta et al., 2015; Gutsch et al., 2018).

The presence of metals in hempcrete may influence numerous parameters conditioning the structural performance, such as maximum ductility, tensile strength and durability (Hassan et al., 2010; Cattaneo et al., 2012). Moreover, the presence of HM, especially Zn and Pb, in bioconcretes may represent a risk of dispersal and adapted coating needs to be applied to prevent runoff from porous material (Harada & Yanbe, 2018). Besides, HM-containing sludges have the potential to be utilized as alternative raw materials in cement production: leaching test shows that the trapped elements in hydrated samples would not cause leaching hazard (Shih et al., 2005). We may thus expect that hemp could also be used in cement without health hazard.

The presence of SiO₂ in hemp hurds favours the formation of a lightweight material, once in contact with lime binder. The resulting hempcrete is very light, but also durable, since the presence of SiO₂ protects it against the attack of chewing insects, termites, fungi, rodents. SiO₂ is additionally fire-retardant (Branda et al., 2016). The presence of Si could also indirectly influence the longitudinal reinforcement ratio, the shear span-to-depth ratio and the maximum size of the coarse aggregate (Arunya et al., 2017; Muñoz et al., 2014). The association of SiO₂ with woody fibres cell walls may thus provide new properties, notably, as increased durability.

d) Removal of HM from wastewater

Another interesting environmental field is the removal of pollutants present in aqueous solution by hemp-based biosorbents (Crini et al., 2020). Technologies such as chemical precipitation, flotation, ion exchange, electrolyte recovery and membrane separation are available for the removal

of HM from wastewater, but most of them are economically expensive and present high energy requirements.

An increased production of hemp fibres results in an increased amount of waste, namely short and entangled fibres that are not suitable for industrial processes. This material demonstrates a high affinity for metals such as Cd, Co, Cr, Cu, Mn, Ni, Pb and Zn (Pejic et al., 2009; Crini et al., 2020) and offers cheap and eco-friendly methods for effluent treatment. Strong bonding of metal ions by carboxylic (primarily present in hemicelluloses, pectins and lignin), phenolic (lignin) and, to some extent, hydroxylic and carbonyl groups are responsible of the adsorption through chemisorption (Pejic et al., 2009). The applicability of hemp-based biosorbents, derived from plant harvested on contaminated soil, depends on HM contents in hemp: the biomass harvested has to be free of pollutants to be used in this purpose. The performance of hemp-based biosorbents also depends on the residual concentration of the metals in solution (Crini et al., 2020).

The chemical transformation of the fibres may improve their efficiency for biosorption processes. The surface transformation of waste textile fibres by carboxymethylation introduces carboxyl binding sites, thereby allowing the fibres to retain a higher amount of Cd^{2+} (Bediako et al., 2016). Similarly, the treatment of short hemp fibres with 0.7% NaClO_2 at the boiling temperature for 5 min improved their capacity to retain Pb^{2+} , Cd^{2+} and Zn^{2+} (Pejic et al., 2011). Carbonized hemp fibres show a large sorption capacity linked to a well-developed internal pore structure, a large specific surface and the presence of a wide spectrum of surface functional groups (Vukcevic et al., 2014; Vukčević et al., 2014). Treatments of fibres with Si-containing compounds, such as silane, during the industrial processing of harvested fibres, modify their structural properties, suggesting that Si-treatments during fibre development in plants may induce new interesting properties for their use in sorption processes (Luyckx et al., 2017b).

e) Phytomining and catalysts in organic chemistry

Phytomining is an exciting phytoextraction-based technology that uses the ability of certain plants to uptake valuable metals (i.e. gold, nickel, thallium, rhenium), producing a bio-ore from the harvested biomass that allows metal recovery through smelting. Once applied at large scale, phytomining may either function as a standalone operation to retrieve the desired element or jointly with phytoremediation, financing the costs of the latter (Novo et al., 2017). The procedure has to be applied on a site (mine

tailings, mineralized or polluted soils) with sub-economic levels of the target metal, with high biomass yield plant species able to accumulate elevated amounts of the target metal and tolerate other coexisting metals. The harvested plant biomass is incinerated to retrieve the bio-ore, from which the target metal can be recovered through smelting (Novo et al., 2017).

Besides, it is also possible to address the direct use of zinc-, nickel- and manganese-enriched biomass to produce catalysts used in organic synthesis for the production of molecules with high added value for fine and industrial chemicals (Grison, 2015). With the development of this new concept metallic wastes are becoming new ecofriendly and efficient catalytic systems. The approach opens greener and broader perspectives in terms of new environmental and socioeconomic challenges. Studies are underway to determine the concentration of HM in biomass that would make it worth exploiting for catalysis (Grison, 2015).

Available Si fertilizers are costly and usually poor in soluble Si. Biochars, produced from the pyrolysis of phytolith-rich biomass is thus a promising alternative Si source for plants (Li & Delvaux, 2019). Indeed, the solubility of amorphous silica is higher (1.8–2 mM Si) than its crystalline counterpart quartz (0.1–0.25 mM Si). The Si release from crop biochar will depend on the amplitude of plant Si uptake, soil pH, buffer capacity, and pyrolysis temperature. The biomass has to be pyrolyzed below 500–800 °C to avoid the disappearance of the amorphous structure of phytoliths (Houben et al., 2014).

5. Objectives

Cannabis sativa L. is a promising species for non-food production on moderate heavy metal (HM)-contaminated substrates (Hussain et al., 2019a; Pietrini et al., 2019) and considered as a potential crop for cleaning the soil from HM-because of its high biomass production, its long root system and its capability to absorb and accumulate HM (Ahmad et al., 2016a; Kumar et al., 2017). Until now, “soil remediation” is usually considered independently of “soil production” and there is an obvious lack of information regarding the possibility to conciliate phytomanagement and obtaining valuable marketable products. The global aim of the present thesis is to contribute to fill this gap.

After hemp straw processing, different plant fractions are obtained: fibres (27-30% of above-ground biomass), hurds (45-55%) and powder (15-24%). In this thesis, a specific attention has been paid to the most economically valuable part of the plant: fibres (50% of the plant economic value; InterChanvre, 2017). The major factors that will impact the possibility to combine soil management with hemp plants for fibres production include: the contaminant concentration and distribution in hemp raw material, hemp HM tolerance, and the impact of HM on fibre yield and quality, although there is still of paucity of information regarding the last aspects.

Besides, the young plant stage is often considered the most sensitive one to HM. To devise agricultural strategies aimed at improving crop yield, the effect of silicon (Si) on plants’ stress resistance, as well as the use of amendments (green waste compost, miscanthus biochar and their combination), should be considered as promising strategies. The beneficial effects of Si fertilizers on plant growth and crop yields are well documented in the literature (Keeping and Reynolds, 2009; Bhat et al., 2019). However, to the best of our knowledge, no data are available regarding Si impact on HM-treated young plants of hemp.

Based on the above-mentioned observations, this thesis aims at answering the following questions:

1. What is the capability of hemp to absorb and accumulate HM from a soil management perspective?
2. What are the physiological consequences of accumulated HM?
3. Do HM have an impact on fibre differentiation and properties in relation to HM accumulation in young stem?
4. What is the short-term impact of Si on hemp responses and fibre development in stressed and unstressed plants?

These questions will be addressed using two different strategies: the first one consists to analyze the behaviour of hemp growing on a moderately contaminated agricultural soil for the whole growing period and to apply Si by foliar spraying. The second one implies to expose young plants for a short period on nutrient solution containing high concentrations of pollutants and to apply Si through the root system. Although these two approaches may appear somewhat contradictory, they are in fact complementary but are rarely compared in terms of efficiency.

Chapter 1 investigated the phytomanagement potential of hemp cultivated on agricultural soil contaminated by Cd and Zn, and the impact of soil amendements on the plant growth potential. Moreover, the impact of these treatments on the fibre HM contents and major mechanical properties was addressed considering for the first time industrial standards. In Chapter 2, we investigated the influence of Si application on hemp physiological properties and the impact on fibres' final properties after harvest.

Chapters 3 and 4 more deeply investigated the short-term physiological consequences of Cd, Zn and Si exposure, as well as the maximal phytoextraction capacity, through the use of nutrient solution where the bioavailability Cd, Zn and Si is high.

The main events accompanying hemp' response to high bioavailability of Cd, Zn and Si, at the root and leaves levels, was investigated with a transcriptomic and a proteomic approach in Chapter 5.

As we intend to combine phytomanagement with non-food production, data regarding the precise impact of element such as Cd and Zn on genes involved in fibres development *in planta* are of crucial importance. In Chapter 6, we therefore investigated the impact of Cd and Zn, in the presence or absence of Si, on the expression of genes regulating fibre development and characterized the proteome of hypocotyls. This innovative approach should help us to more deeply understand the relationship between plant molecular adaptation and subsequent plant production.

Management of harvested products requires to precise the distribution of toxic HM within plants tissues, but only data regarding total ion concentration in plant organs are available in the literature. In order to provide new information regarding this crucial point, we conducted a sophisticated micro-PIXE approach to obtain reliable mapping of accumulated HM (Chapter 7).

The thesis structure is presented in a schematic way in Figure 15.

References

- Abdelmouleh, M., Boufi, S., Belgacem, M. N., Duarte, A. P., Salah, A. B., & Gandini, A. (2004). Modification of cellulosic fibres with functionalised silanes: Development of surface properties. *International Journal of Adhesion and Adhesives*, *24*, 43-54.
- Abdel-Shafy, H. I., & Mansour, M. S. (2018). Phytoremediation for the elimination of metals, pesticides, PAHs, and other pollutants from wastewater and soil. In *Phytobiont and ecosystem restitution* (pp. 101-136). Springer, Singapore.
- Adesina, I., Bhowmik, A., Sharma, H., & Shahbazi, A. (2020). A Review on the Current State of Knowledge of Growing Conditions, Agronomic Soil Health Practices and Utilities of Hemp in the United States. *Agriculture*, *10*, 129.
- Adrees, M., Ali, S., Rizwan, M., Zia-ur-Rehman, M., Ibrahim, M., Abbas, F., Farid, M., Qayyum, M. F., & Irshad, M. K. (2015). Mechanisms of silicon-mediated alleviation of heavy metal toxicity in plants: A review. *Ecotoxicology and Environmental Safety*, *119*, 186-197.
- Ahanger, M. A., Bhat, J. A., Siddiqui, M. H., Rinklebe, J., & Ahmad, P. (2020). Integration of silicon and secondary metabolites in plants: a significant association in stress tolerance. *Journal of experimental botany*, *71*, 6758-6774.
- Ahmad, A., Hadi, F., & Ali, N. (2015). Effective phytoextraction of cadmium (Cd) with increasing concentration of total phenolics and free proline in *Cannabis sativa* (L) plant under various treatments of fertilizers, plant growth regulators and sodium salt. *International journal of phytoremediation*, *17*, 56-65.
- Ahmad, R., Tehsin, Z., Malik, S. T., Asad, S. A., Shahzad, M., Bilal, M., Shah, M. M., & Khan, S. A. (2016). Phytoremediation potential of hemp (*Cannabis sativa* L.): Identification and characterization of heavy metals responsive genes. *CLEAN–Soil, Air, Water*, *44*, 195-201.
- Ali, H., Khan, E., & Sajad, M. A. (2013). Phytoremediation of heavy metals— Concepts and applications. *Chemosphere*, *91*, 869-881.
- Ali, H., & Khan, E. (2018). What are heavy metals? Long-standing controversy over the scientific use of the term ‘heavy metals’ – proposal of a comprehensive definition. *Toxicological & Environmental Chemistry*, *100*, 6-19.
- Andre, C. M., Hausman, J.-F., & Guerriero, G. (2016). *Cannabis sativa*: The plant of the thousand and one molecules. *Frontiers in plant science*, *7*, 19.
- Arru, L., Rognoni, S., Baroncini, M., Bonatti, P. M., & Perata, P. (2004). Copper localization in *Cannabis sativa* L. grown in a copper-rich solution. *Euphytica*, *140*, 33-38.
- Arunya, A., Sarayu, K., Murthy, A., & Iyer, N. (2017). Enhancement of durability properties of bioconcrete incorporated with nano silica. *International Journal of Civil Engineering and Technology*, *8*, 1388-1394.

- Ayangbenro, A. S., & Babalola, O. O. (2017). A new strategy for heavy metal polluted environments: A review of microbial biosorbents. *International journal of environmental research and public health*, *14*, 94.
- Baldini, M., Ferfuaia, C., Piani, B., Sepulcri, A., Dorigo, G., Zuliani, F., ... & Cattivello, C. (2018). The performance and potentiality of monoecious hemp (*Cannabis sativa* L.) cultivars as a multipurpose crop. *Agronomy*, *8*, 162.
- Balmer, A., Pastor, V., Gamir, J., Flors, V., & Mauch-Mani, B. (2015). The ‘prime-ome’: Towards a holistic approach to priming. *Trends in plant science*, *20*, 443-452.
- Barceló, J., & Poschenrieder, C. (2003). Phytoremediation: Principles and perspectives. *Contributions to science*, 333-344.
- Bediako, J. K., Wei, W., & Yun, Y.-S. (2016). Conversion of waste textile cellulose fibers into heavy metal adsorbents. *Journal of Industrial and Engineering Chemistry*, *43*, 61-68.
- Behr, M., Faleri, C., Hausman, J. F., Planchon, S., Renaut, J., Cai, G., & Guerriero, G. (2019). Distribution of cell-wall polysaccharides and proteins during growth of the hemp hypocotyl. *Planta*, *250*(5), 1539-1556.
- Behr, M. (2018). *Molecular investigation of cell wall formation in hemp stem tissues* [PhD Thesis]. Université catholique de Louvain.
- Bert, V., Douay, F., & Faure, O. (2017). *Les phytotechnologies appliquées aux sites et sols pollués : Nouveaux résultats de recherche et démonstration*. ADEME.
- Bhat, J. A., Shivaraj, S. M., Singh, P., Navadagi, D. B., Tripathi, D. K., Dash, P. K., Solanke, A. U., Sonah, H., & Deshmukh, R. (2019). Role of silicon in mitigation of heavy metal stresses in crop plants. *Plants*, *8*, 71.
- Bidar, G. (2007). *Intérêt du phytomanagement dans la gestion durable des sols pollués : Recherche des mécanismes biologiques de transfert et de localisation de Cd, Pb, Zn dans les strates herbacées et arborées*.
- Bouloc, P. (2006). *Le chanvre industriel : Production et utilisations*. France Agricole Editions.
- Branda, F., Malucelli, G., Durante, M., Piccolo, A., Mazzei, P., Costantini, A., ... & Bifulco, A. (2016). Silica treatments: A fire retardant strategy for hemp fabric/epoxy composites. *Polymers*, *8*, 313.
- Bruce, D. M., Hobson, R. N., White, R. P., & Hobson, J. (2001). PM—Power and Machinery: Stripping of Leaves and Flower Heads to improve the Harvesting of Fibre Hemp. *Journal of agricultural engineering research*, *78*, 43-50.
- Bu, R., Xie, J., Yu, J., Liao, W., Xiao, X., Lv, J., Wang, C., Ye, J., & Calderón-Urrea, A. (2016). Autotoxicity in cucumber (*Cucumis sativus* L.) seedlings is alleviated by silicon through an increase in the activity of antioxidant enzymes and by mitigating lipid peroxidation. *Journal of Plant Biology*, *59*, 247-259.
- Cao, B., Ma, Q., Zhao, Q., Wang, L., & Xu, K. (2015). Effects of silicon on absorbed light allocation, antioxidant enzymes and ultrastructure of chloroplasts in

tomato leaves under simulated drought stress. *Scientia Horticulturae*, 194, 53-62.

- Carus, M., & Sarmiento, L. (2016). The European Hemp Industry: Cultivation, processing and applications for fibres, shivs, seeds and flowers. *European Industrial Hemp Association*, 1-9.
- Carus, M. (2017). Record cultivation of industrial hemp in Europe in 2016. *Eiha*. Available at: <http://eih.org/document/record-cultivation-of-industrial-hemp-in-europe-in-2016>.
- Cattaneo, S., Giussani, F., & Mola, F. (2012). Flexural behaviour of reinforced, prestressed and composite self-consolidating concrete beams. *Construction and Building Materials*, 36, 826-837.
- Chakraborty, A., Sarkar, D., Satya, P., Karmakar, P. G., & Singh, N. K. (2015). Pathways associated with lignin biosynthesis in lignomaniac jute fibres. *Molecular Genetics and Genomics*, 290, 1523-1542.
- Chernova, T. E., Mikshina, P.V., Salnikov, V.V., Ibragimova, N.N., Sautkina, O.V., Gorshkova, T.A., 2018. Development of distinct cell wall layers both in primary and secondary phloem fibers of hemp (*Cannabis sativa* L.). *Industrial Crops and Products*, 117, 97-109.
- Chowdhury, S., Mazumder, M. J., Al-Attas, O., & Husain, T. (2016). Heavy metals in drinking water: Occurrences, implications, and future needs in developing countries. *Science of the total Environment*, 569, 476-488.
- Citterio, S., Santagostino, A., Fumagalli, P., Prato, N., Ranalli, P., & Sgorbati, S. (2003). Heavy metal tolerance and accumulation of Cd, Cr and Ni by *Cannabis sativa* L. *Plant and Soil*, 256, 243-252.
- Cobbett, C. S. (2000). Phytochelatin and their roles in heavy metal detoxification. *Plant physiology*, 123, 825-832.
- Crini, G., Lichtfouse, E., Chanet, G., & Morin-Crini, N. (2020). Traditional and new applications of hemp. In *Sustainable Agriculture Reviews 42* (p. 37-87). Springer.
- da Costa, R. M., Lee, S. J., Allison, G. G., Hazen, S. P., Winters, A., & Bosch, M. (2014). Genotype, development and tissue-derived variation of cell-wall properties in the lignocellulosic energy crop *Miscanthus*. *Annals of Botany*, 114, 1265-1277.
- Datnoff, L. E., & Rodrigues, F. A. (2005). The Role of Silicon in Suppressing Rice Diseases. *APSnet Feature Articles*. <https://doi.org/10.1094/APSnetFeature-2005-0205>
- Deshmukh, R. K., Vivancos, J., Ramakrishnan, G., Guérin, V., Carpentier, G., Sonah, H., Labbé, C., Isenring, P., Belzile, F. J., & Bélanger, R. R. (2015). A precise spacing between the NPA domains of aquaporins is essential for silicon permeability in plants. *The Plant Journal*, 83, 489-500.
- Detmann, K. C., Araújo, W. L., Martins, S. C., Sanglard, L. M., Reis, J. V., Detmann, E., Rodrigues, F. Á., Nunes-Nesi, A., Fernie, A. R., & DaMatta, F. M. (2012). Silicon nutrition increases grain yield, which, in turn, exerts a feed-forward

- stimulation of photosynthetic rates via enhanced mesophyll conductance and alters primary metabolism in rice. *New Phytologist*, 196, 752-762.
- Detmann, K., Araújo, W., Martins, S., Fernie, A. R., & DaMatta, F. (2013). Metabolic alterations triggered by silicon nutrition: Is there a signaling role for silicon? *Plant signaling & behavior*, 8, e22523.
- Di Candilo, M., Bonatti, P. M., Guidetti, C., Focher, B., Grippo, C., Tamburini, E., & Mastromei, G. (2010). Effects of selected pectinolytic bacterial strains on water-retting of hemp and fibre properties. *Journal of Applied Microbiology*, 108, 194-203.
- Di Candito, M., Ranalli, P., & Dal Re, L. (2004). Heavy metal tolerance and uptake of Cd, Pb and Tl by hemp. *Advances in Horticultural Science*, 138-144.
- Doncheva, S. N., Poschenrieder, C., Stoyanova, Z., Georgieva, K., Velichkova, M., & Barceló, J. (2009). Silicon amelioration of manganese toxicity in Mn-sensitive and Mn-tolerant maize varieties. *Environmental and Experimental Botany*, 65, 189-197.
- Dubois, O. (2011). *The state of the world's land and water resources for food and agriculture: Managing systems at risk*. Earthscan.
- Emamverdian, A., Ding, Y., Mokhberdoran, F., & Xie, Y. (2015). Heavy metal stress and some mechanisms of plant defense response. *The Scientific World Journal*.
- Epstein, E. (1994). The anomaly of silicon in plant biology. *Proceedings of the National Academy of Sciences*, 91, 11-17.
- Epstein, E., & Bloom, A. J. (2005). *Mineral Nutrition of Plants: Principles and Perspectives, 2nd Edn* (Sunderland: Sinauer Associates Inc).
- Evangelou, M. W. H., Papazoglou, E. G., Robinson, B. H., & Schulin, R. (2015). Phytomanagement: Phytoremediation and the Production of Biomass for Economic Revenue on Contaminated Land. In A. A. Ansari, S. S. Gill, R. Gill, G. R. Lanza, & L. Newman (Éds.), *Phytoremediation: Management of Environmental Contaminants, Volume 1* (p. 115-132). Springer International Publishing.
- Fauteux, F., Rémus-Borel, W., Menzies, J. G., & Bélanger, R. R. (2005). Silicon and plant disease resistance against pathogenic fungi. *FEMS Microbiology letters*, 249, 1-6.
- Faux, A.-M. (2014). *Quantitative approach of the genetic determinism of sex expression in monoecious hemp (Cannabis sativa L.), and its relationship with flowering phenology and stem and seed yields* [PhD Thesis]. Dissertation. Université Catholique de Louvain Earth and Life Institute 2014.
- Faux, A. M., and Bertin, P. (2014). Modelling approach for the quantitative variation of sex expressions in monoecious hemp (*Cannabis sativa* L.). *Plant Breed.* 133, 679–793. doi: 10.1111/pbr.12208.
- Feng, W., Guo, Z., Xiao, X., Peng, C., Shi, L., Ran, H., & Xu, W. (2020). A dynamic model to evaluate the critical loads of heavy metals in agricultural soil. *Ecotoxicology and environmental safety*, 197, 110607.

- Fernández, R., Fernández-Fuego, D., Bertrand, A., & González, A. (2014). Strategies for Cd accumulation in *Dittrichia viscosa* (L.) Greuter: Role of the cell wall, non-protein thiols and organic acids. *Plant Physiology and Biochemistry*, *78*, 63-70.
- Fernando, A. L., Duarte, M. P., Vatsanidou, A., & Alexopoulou, E. (2015). Environmental aspects of fiber crops cultivation and use. *Industrial Crops and Products*, *68*, 105-115.
- Fike, J. (2016). Industrial Hemp: Renewed Opportunities for an Ancient Crop. *Critical Reviews in Plant Sciences*, *35*, 406-424.
- Fleck, A. T., Nye, T., Repenning, C., Stahl, F., Zahn, M., & Schenk, M. K. (2011). Silicon enhances suberization and lignification in roots of rice (*Oryza sativa*). *Journal of Experimental Botany*, *62*, 2001-2011.
- Fryzova, R., Pohanka, M., Martinkova, P., Cihlarova, H., Brtnicky, M., Hladky, J., & Kynicky, J. (2017). Oxidative stress and heavy metals in plants. *Reviews of environmental contamination and toxicology volume 245*, 129-156.
- Gall, L. H., Philippe, F., Domon, J. M., Gillet, F., Pelloux, J., & Rayon, C. (2015). Cell wall metabolism in response to abiotic stress. *Plants*, *4*, 112-166.
- Gapper, C., & Dolan, L. (2006). Control of plant development by reactive oxygen species. *Plant physiology*, *141*, 341-345.
- Ghareeb, H., Bozsó, Z., Ott, P. G., Repenning, C., Stahl, F., & Wydra, K. (2011). Transcriptome of silicon-induced resistance against *Ralstonia solanacearum* in the silicon non-accumulator tomato implicates priming effect. *Physiological and Molecular Plant Pathology*, *75*, 83-89.
- Ghori, N.-H., Ghori, T., Hayat, M. Q., Imadi, S. R., Gul, A., Altay, V., & Ozturk, M. (2019). Heavy metal stress and responses in plants. *International Journal of Environmental Science and Technology*, *16*, 1807-1828.
- Ghosh, M., & Singh, S. P. (2005). A review on phytoremediation of heavy metals and utilization of it's by products. *Asian J Energy Environ*, *6*, 18.
- Gorshkova, T.A., Sal'nikov, V.V., Chemikosova, S.B., Ageeva, M.V., Pavlencheva, N.V., Van Dam J.E.G., (2003). The snap point: a transition point in *Linum usitatissimum* bas fiber development. *Industrial Crops and Products*, *18*, 213-221.
- Gorshkova, T., Brutch, N., Chabbert, B., Deyholos, M., Hayashi, T., Lev-Yadun, S., ... & Pilate, G. (2012). Plant fiber formation: state of the art, recent and expected progress, and open questions. *Critical Reviews in Plant Sciences*, *31*, 201-228.
- Grégoire, C., Rémus-Borel, W., Vivancos, J., Labbé, C., Belzile, F., & Bélanger, R. R. (2012). Discovery of a multigene family of aquaporin silicon transporters in the primitive plant *Equisetum arvense*. *The Plant Journal*, *72*, 320-330.
- Griga, M., & Bjelková, M. (2013). Flax (*Linum usitatissimum* L.) and Hemp (*Cannabis sativa* L.) as Fibre Crops for Phytoextraction of Heavy Metals: Biological, Agro-technological and Economical Point of View. In D. K. Gupta (Éd.), *Plant-Based Remediation Processes* (p. 199-237). Springer.

- Grison, C. (2015). Combining phytoextraction and ecocatalysis: a novel concept for greener chemistry, an opportunity for remediation.
- Gu, H.-H., Qiu, H., Tian, T., Zhan, S.-S., Chaney, R. L., Wang, S.-Z., Tang, Y.-T., Morel, J.-L., & Qiu, R.-L. (2011). Mitigation effects of silicon rich amendments on heavy metal accumulation in rice (*Oryza sativa* L.) planted on multi-metal contaminated acidic soil. *Chemosphere*, *83*, 1234-1240.
- Guerriero, G., Sergeant, K., Hausman, J.F., (2013). Integrated-omics: a powerful approach to understanding the heterogeneous lignification of fibre crops. *International Journal of Molecular Sciences*, *14*, 10958-10978.
- Guerriero, G., Sergeant, K., & Hausman, J.-F. (2014). Wood biosynthesis and typologies: A molecular rhapsody. *Tree physiology*, *34*, 839-855.
- Guerriero, G., Hausman, J.-F., & Legay, S. (2016). Silicon and the plant extracellular matrix. *Frontiers in Plant Science*, *7*, 463.
- Guerriero, G., Behr, M., Legay, S., Mangeot-Peter, L., Zorzan, S., Ghoniem, M., Hausman, J.F., (2017a). Transcriptomic profiling of hemp bast fibres at different developmental stages. *Scientific Reports*, *7*, 4961.
- Guerriero, G., Law, C., Stokes, I., Moore, K. L., & Exley, C. (2018). Rough and tough. How does silicic acid protect horsetail from fungal infection? *Journal of Trace Elements in Medicine and Biology*, *47*, 45-52.
- Guerriero, G., Deshmukh, R., Sonah, H., Sergeant, K., Hausman, J. F., Lentzen, E., ... & Exley, C. (2019). Identification of the aquaporin gene family in *Cannabis sativa* and evidence for the accumulation of silicon in its tissues. *Plant Science*, *287*, 110167.
- Guerriero, G., Stokes, I., Valle, N., Hausman, J. F., & Exley, C. (2020) Visualising silicon in plants: histochemistry, silica sculptures and elemental imaging. *Cells*, *9*,1066.
- Gutsch, A., Keunen, E., Guerriero, G., Renaut, J., Cuypers, A., Hausman, J. F., & Sergeant, K. (2018). Long-term cadmium exposure influences the abundance of proteins that impact the cell wall structure in *Medicago sativa* stems. *Plant Biology*, *20*, 1023-1035.
- Harada, S., & Yanbe, M. (2018). Adsorption by and artificial release of zinc and lead from porous concrete for recycling of adsorbed zinc and lead and of porous concrete to reduce urban non-point heavy metal runoff. *Chemosphere*, *197*, 451-456.
- Hassan, A. A. A., Hossain, K. M. A., & Lachemi, M. (2010). Structural assessment of corroded self-consolidating concrete beams. *Engineering Structures*, *32*, 874-885.
- He, C., Wang, L., Liu, J., Liu, X., Li, X., Ma, J., Lin, Y., & Xu, F. (2013). Evidence for 'silicon' within the cell walls of suspension-cultured rice cells. *New Phytologist*, *200*, 700-709.
- Hopkins, W. G. (2003). *Physiologie végétale*. De Boeck Supérieur.

- Hossain, Z., & Komatsu, S. (2013). Contribution of proteomic studies towards understanding plant heavy metal stress response. *Frontiers in Plant Science*, 3, 310.
- Houben, D., Sonnet, P., & Cornelis, J. T. (2014). Biochar from Miscanthus: a potential silicon fertilizer. *Plant and soil*, 374(1), 871-882.
- Hu, G., Huang, S., Chen, H., Wang, F., (2010). Binding of four heavy metals to hemicelluloses from rice bran. *Food Research International*, 43, 203-206.
- Hussain R, Weeden H, Bogush D, Degushi M, Soliman M, Potlakayala S, Katam R, Goldman S, Rudrabhatia S (2019) Enhanced tolerance of industrial hemp (*Cannabis sativa* L.) plants on abandoned mineland soil leads to overexpression of cannabinoids. *PLoS ONE* 14: e0221570
- Imtiaz, M., Rizwan, M. S., Mushtaq, M. A., Ashraf, M., Shahzad, S. M., Yousaf, B., Saeed, D. A., Rizwan, M., Nawaz, M. A., & Mehmood, S. (2016). Silicon occurrence, uptake, transport and mechanisms of heavy metals, minerals and salinity enhanced tolerance in plants with future prospects: A review. *Journal of environmental management*, 183, 521-529.
- InterChanvre (2017) : Plan filière de l'interprofession du chanvre, Plan submitted to the French Ministry of Agriculture—Recherche Google.* (s. d.). https://www.google.com/search?q=InterChanvre+%282017%29%3A+Plan+fili%C3%A8re+de+l%E2%80%99interprofession+du+chanvre%2C+Plan+submitted+to+the+French+Ministry+of+Agriculture&rlz=1C1PNJJ_frBE929BE929&sxsrf=ALeKk01BLuwSuiUo0zWTxFLDQ844QTXuRw%3A1619788994105&ei=wgSMYJr1BcicsAeyhZTgBA&oq=InterChanvre+%282017%29%3A+Plan+fili%C3%A8re+de+l%E2%80%99interprofession+du+chanvre%2C+Plan+submitted+to+the+French+Ministry+of+Agriculture&gs_lcp=Cgdnd3Mtd2l6EANQgqYKWIKmCmC_rApoAHACeACAAQCI AQCSAQCYAQQgAQKgAQGqAQdnd3Mtd2l6wAEB&sclient=gws-wiz&ved=0ahUKEwia3uqciKbwAhVIDuwKHbICBUwQ4dUDCA4&uact=5 (Accessed 29 April 2021)
- ISO 17402:2008(en), Soil quality—Requirements and guidance for the selection and application of methods for the assessment of bioavailability of contaminants in soil and soil materials.* (s. d.). Consulté 14 avril 2021, à l'adresse <https://www.iso.org/obp/ui/#iso:std:iso:17402:ed-1:v1:en:fig:2>
- Iwasaki, K., & Matsumura, A. (1999). Effect of silicon on alleviation of manganese toxicity in pumpkin (*Cucurbita moschata* Duch cv. Shintosa). *Soil Science and Plant Nutrition*, 45, 909-920.
- Jalmi, S. K., Bhagat, P. K., Verma, D., Noryang, S., Tayyeba, S., Singh, K., Sharma, D., & Sinha, A. K. (2018). Traversing the links between heavy metal stress and plant signaling. *Frontiers in plant science*, 9, 12.
- Jankauskienė, Z., & Gruzdevienė, E. (2013). Physical parameters of dew retted and water retted hemp (*Cannabis sativa* L.) fibres. *Zemdirbyste-Agriculture*, 100, 71-80.

- Jia-Wen, W. U., Yu, S. H. I., Yong-Xing, Z. H. U., Yi-Chao, W., & Hai-Jun, G. (2013). Mechanisms of enhanced heavy metal tolerance in plants by silicon: A review. *Pedosphere*, *23*, 815-825.
- Jörg, M., Amaducci, S., Alain, B., Johnny, B., & Shah, D. U. (2020). Transdisciplinary top-down review of hemp fibre composites: From an advanced product design to crop variety selection.
- Jost-Tse, Y.-C. (2018). *Les plantes hyperaccumulatrices de métaux lourds : Une solution à la pollution des sols et de l'eau ?* Editions Publibook.
- Kabir, M. M., Wang, H., Lau, K. T., Cardona, F., & Aravinthan, T. (2012). Mechanical properties of chemically-treated hemp fibre reinforced sandwich composites. *Composites Part B: Engineering*, *43*, 159-169.
- Keeping, M. G., & Reynolds, O. L. (2009). Silicon in agriculture: New insights, new significance and growing application. *Annals of Applied Biology*, *155*, 153.
- Keller, C., Rizwan, M., Davidian, J.-C., Pokrovsky, O. S., Bovet, N., Chaurand, P., & Meunier, J.-D. (2015). Effect of silicon on wheat seedlings (*Triticum turgidum* L.) grown in hydroponics and exposed to 0 to 30 μ M Cu. *Planta*, *241*, 847-860. <https://doi.org/10.1007/s00425-014-2220-1>.
- Khan, D. H., & Roy, A. C. (1964). Growth, p-uptake, and fibre cell dimensions of jute plant as affected by silicate treatment. *Plant and Soil*, 331-336.
- Kidd, P. S., Llugany, M., Poschenrieder, C. H., Gunse, B., & Barcelo, J. (2001). The role of root exudates in aluminium resistance and silicon-induced amelioration of aluminium toxicity in three varieties of maize (*Zea mays* L.). *Journal of experimental botany*, *52*, 1339-1352.
- Kim, R.-Y., Yoon, J.-K., Kim, T.-S., Yang, J. E., Owens, G., & Kim, K.-R. (2015). Bioavailability of heavy metals in soils: Definitions and practical implementation—a critical review. *Environmental geochemistry and health*, *37*, 1041-1061.
- Kos, B., & Leštan, D. (2004). Soil washing of Pb, Zn and Cd using biodegradable chelator and permeable barriers and induced phytoextraction by *Cannabis sativa*. *Plant and soil*, *263*, 43-51.
- Kosová, K., Vítámvás, P., Urban, M. O., Prášil, I., T., and Renaut, J. (2018). Plant abiotic stress proteomics: the major factors determining alterations in cellular proteome. *Frontiers in Plant Science*, *9*, 122.
- Kozłowski, R., Baraniecki, P., & Barriga-Bedoya, J. (2005). Bast fibres (flax, hemp, jute, ramie, kenaf, abaca). *Biodegradable and sustainable fibres*, 36-88.
- Krzesłowska, M. (2011). The cell wall in plant cell response to trace metals: Polysaccharide remodeling and its role in defense strategy. *Acta Physiologiae Plantarum*, *33*, 35-51.
- Kumar, S., Milstein, Y., Bami, Y., Elbaum, M., & Elbaum, R. (2017). Mechanism of silica deposition in sorghum silica cells. *New Phytologist*, *213*, 791-798.
- Law, C., & Exley, C. (2011). New insight into silica deposition in horsetail (*Equisetum arvense*). *BMC plant biology*, *11*, 1-9.

- Li, Z., & Delvaux, B. (2019). Phytolith-rich biochar: A potential Si fertilizer in desilicated soils. *Gcb Bioenergy*, *11*, 1264-1282.
- Li, H. B., Qin, Y. M., Pang, Y., Song, W. Q., Mei, W. Q., & Zhu, Y. X. (2007). A cotton ascorbate peroxidase is involved in hydrogen peroxide homeostasis during fibre cell development. *New Phytologist*, *175*, 462-471.
- Li, C., Zhou, K., Qin, W., Tian, C., Qi, M., Yan, X., & Han, W. (2019). A review on heavy metals contamination in soil: Effects, sources, and remediation techniques. *Soil and Sediment Contamination: An International Journal*, *28*, 380-394.
- Liang, Y., Chen, Q. I. N., Liu, Q., Zhang, W., & Ding, R. (2003). Exogenous silicon (Si) increases antioxidant enzyme activity and reduces lipid peroxidation in roots of salt-stressed barley (*Hordeum vulgare*L.). *Journal of plant physiology*, *160*, 1157-1164.
- Linger, P., Müssig, J., Fischer, H., & Kobert, J. (2002). Industrial hemp (*Cannabis sativa* L.) growing on heavy metal contaminated soil: Fibre quality and phytoremediation potential. *Industrial Crops and Products*, *16*, 33-42.
- Liu, L., Li, W., Song, W., & Guo, M. (2018). Remediation techniques for heavy metal-contaminated soils: Principles and applicability. *Science of the Total Environment*, *633*, 206-219.
- Lu, T., Jiang, M., Jiang, Z., Hui, D., Wang, Z., & Zhou, Z. (2013). Effect of surface modification of bamboo cellulose fibers on mechanical properties of cellulose/epoxy composites. *Composites Part B: Engineering*, *51*, 28-34.
- Lukačová, Z., Švubová, R., Kohanová, J., & Lux, A. (2013). Silicon mitigates the Cd toxicity in maize in relation to cadmium translocation, cell distribution, antioxidant enzymes stimulation and enhanced endodermal apoplasmic barrier development. *Plant Growth Regulation*, *70*, 89-103.
- Luo, R., Li, J., Zhao, Y., Fan, X., Zhao, P., & Chai, L. (2017). A critical review on the research topic system of soil heavy metal pollution bioremediation based on dynamic co-words network measures. *Geoderma*, *305*, 281-292.
- Luyckx, M., Hausman, J.-F., Lutts, S., & Guerriero, G. (2017a). Impact of silicon in plant biomass production: Focus on bast fibres, hypotheses, and perspectives. *Plants*, *6*, 37.
- Luyckx, M., Hausman, J.-F., Lutts, S., & Guerriero, G. (2017b). Silicon and plants: Current knowledge and technological perspectives. *Frontiers in Plant Science*, *8*, 411.
- Luyckx, M., Hausman, J.-F., Isenborghs, A., Guerriero, G., & Lutts, S. (2021). Impact of cadmium and zinc on proteins and cell wall-related gene expression in young stems of hemp (*Cannabis sativa* L.) and influence of exogenous silicon. *Environmental and Experimental Botany*, *183*, 104363.
- Ma, J. F., Tamai, K., Ichii, M., & Wu, G. F. (2002). A rice mutant defective in Si uptake. *Plant Physiology*, *130*, 2111-2117.

- Ma, J. F., Tamai, K., Yamaji, N., Mitani, N., Konishi, S., Katsuhara, M., Ishiguro, M., Murata, Y., & Yano, M. (2006). A silicon transporter in rice. *Nature*, *440*, 688-691.
- Ma, J., Cai, H., He, C., Zhang, W., & Wang, L. (2015). A hemicellulose-bound form of silicon inhibits cadmium ion uptake in rice (*Oryza sativa*) cells. *New Phytologist*, *206*, 1063-1074.
- Ma, J., Sheng, H., Li, X., & Wang, L. (2016). ITRAQ-based proteomic analysis reveals the mechanisms of silicon-mediated cadmium tolerance in rice (*Oryza sativa*) cells. *Plant Physiology and Biochemistry*, *104*, 71-80.
- Marion, A. M., De Lanève, M., & De Grauw, A. (2005). Study of the leaching behaviour of paving concretes: quantification of heavy metal content in leachates issued from tank test using demineralized water. *Cement and Concrete Research*, *35*, 951-957.
- Mark, T. B., & Will, S. (2019). Economic Issues and Perspectives for Industrial Hemp. *Industrial hemp as a modern commodity crop*, 107-118.
- Meena, R. A. A., Sathishkumar, P., Ameen, F., Yusoff, A. R. M., & Gu, F. L. (2018). Heavy metal pollution in immobile and mobile components of lentic ecosystems—A review. *Environmental Science and Pollution Research*, *25*, 4134-4148.
- Meers, E., Ruttens, A., Hopgood, M., Lesage, E., & Tack, F. M. G. (2005). Potential of *Brassica rapa*, *Cannabis sativa*, *Helianthus annuus* and *Zea mays* for phytoextraction of heavy metals from calcareous dredged sediment derived soils. *Chemosphere*, *61*, 561-572.
- Mikshina, P., Chernova, T., Chemikosova, S., Ibragimova, N., Mokshina, N., & Gorshkova, T. (2013). Cellulosic fibers: Role of matrix polysaccharides in structure and function. *Cellulose—fundamental aspects. Rijeka: InTech*, 91-112.
- Mishra, S., Bharagava, R. N., More, N., Yadav, A., Zainith, S., Mani, S., & Chowdhary, P. (2019). Heavy metal contamination: An alarming threat to environment and human health. In *Environmental biotechnology: For sustainable future* (p. 103-125). Springer.
- Mitani, N., & Ma, J. F. (2005). Uptake system of silicon in different plant species. *Journal of experimental botany*, *56*, 1255-1261.
- Moliterni, V. M. C., Cattivelli, L., Ranalli, P., and Mandolino, G. (2004). The sexual differentiation of *Cannabis sativa* L.: a morphological and molecular study. *Euphytica* *140*, 95–106.
- Montpetit, J., Vivancos, J., Mitani-Ueno, N., Yamaji, N., Rémus-Borel, W., Belzile, F., Ma, J. F., & Bélanger, R. R. (2012). Cloning, functional characterization and heterologous expression of TaLsi1, a wheat silicon transporter gene. *Plant molecular biology*, *79*, 35-46.
- Moroz, J. G., Lissel, S. L., & Hagel, M. D. (2014). Performance of bamboo reinforced concrete masonry shear walls. *Construction and Building Materials*, *61*, 125-137.

- Mougin, G. (2006). *Natural-fibre composites—Problems and solutions*, 43, 32-35.
- Muñoz, J. F., Yao, Y., Youtcheff, J., & Arnold, T. (2014). Mixtures of silicon and aluminum oxides to optimize the performance of nanoporous thin films in concrete. *Cement and Concrete Composites*, 48, 140-149.
- Musio, S., Müssig, J., & Amaducci, S. (2018). Optimizing Hemp Fiber Production for High Performance Composite Applications. *Frontiers in Plant Science*, 9.
- Mwaikambo, L. Y., & Ansell, M. P. (2002). Chemical modification of hemp, sisal, jute, and kapok fibers by alkalization. *Journal of applied polymer science*, 84, 2222-2234.
- Nair, G. R., Singh, A., Zimmiewska, M., & Raghavan, V. (2013). Comparative Evaluation of Physical and Structural Properties of Water Retted and Non-retted Flax Fibers. *Fibers*, 1, 59-69.
- Natural Fiber Composites Market Size | NFC Industry Report, 2018-2024*. (s. d.). Consulté 9 avril 2021, à l'adresse <https://www.grandviewresearch.com/industry-analysis/natural-fiber-composites-market>
- Nawaz, M. A., Zakharenko, A. M., Zemchenko, I. V., Haider, M. S., Ali, M. A., Imtiaz, M., Chung, G., Tsatsakis, A., Sun, S., & Golokhvast, K. S. (2019). Phytolith formation in plants: From soil to cell. *Plants*, 8, 249.
- Neutelings, G. (2011). Lignin variability in plant cell walls: contribution of new models. *Plant Science*, 181, 379-386.
- Nieminen, K., Immanen, J., Laxell, M., Kauppinen, L., Tarkowski, P., Dolezal, K., ... & Helariutta, Y. (2008). Cytokinin signaling regulates cambial development in poplar. *Proceedings of the National Academy of Sciences*, 105, 20032-20037.
- Nieminen, K., Blomster, T., Helariutta, Y., & Mähönen, A. P. (2015). Vascular cambium development. *The Arabidopsis book/American Society of Plant Biologists*, 13.
- Novo, L. A., Castro, P. M., Alvarenga, P., & da Silva, E. F. (2017). Phytomining of rare and valuable metals. *Phytoremediation*, 469-486.
- Nwugo, C. C., & Huerta, A. J. (2008). Silicon-induced cadmium resistance in rice (*Oryza sativa*). *Journal of plant nutrition and soil science*, 171, 841-848.
- Orue, A., Jauregi, A., Unsuain, U., Labidi, J., Eceiza, A., & Arbelaz, A. (2016). The effect of alkaline and silane treatments on mechanical properties and breakage of sisal fibers and poly (lactic acid)/sisal fiber composites. *Composites Part A: Applied Science and Manufacturing*, 84, 186-195.
- Parrotta, L., Guerriero, G., Sergeant, K., Cai, G., Hausman, J.-F., (2015). Target or barrier? The cell wall of early- and later-diverging plants vs cadmium toxicity: differences in the response mechanisms. *Frontiers in Plant Science*, 6, 133.
- Pejic, B., Vukcevic, M., Kostic, M., & Skundric, P. (2009). Biosorption of heavy metal ions from aqueous solutions by short hemp fibers: Effect of chemical composition. *Journal of Hazardous Materials*, 164, 146-153.

- Pejic, B. M., Vukcevic, M. M., Pajic-Lijakovic, I. D., Lausevic, M. D., & Kostic, M. M. (2011). Mathematical modeling of heavy metal ions (Cd^{2+} , Zn^{2+} and Pb^{2+}) biosorption by chemically modified short hemp fibers. *Chemical engineering journal*, *172*, 354-360.
- Peralta-Videa, J. R., Lopez, M. L., Narayan, M., Saupe, G., & Gardea-Torresdey, J. (2009). The biochemistry of environmental heavy metal uptake by plants: Implications for the food chain. *The international journal of biochemistry & cell biology*, *41*, 1665-1677.
- Petit, J., Salentijn, E. M., Paulo, M. J., Denneboom, C., & Trindade, L. M. (2020). Genetic architecture of flowering time and sex determination in hemp (*Cannabis sativa* L.): A genome-wide association study. *Frontiers in plant science*, *11*, 1704.
- Pietrini, F., Passatore, L., Patti, V., Francocci, F., Giovannozzi, A., & Zacchini, M. (2019). Morpho-physiological and metal accumulation responses of hemp plants (*Cannabis Sativa* L.) grown on soil from an agro-industrial contaminated area. *Water*, *11*, 808.
- Piotrowska-Cyplik, A., & Czarnecki, Z. (2003). Phytoextraction of Heavy Metals by Hemp during Anaerobic Sewage Sludge Management in the Non-Industrial Sites. *Polish Journal of Environmental Studies*, *12*.
- Rachini, A., Le Troedec, M., Peyratout, C., & Smith, A. (2012). Chemical modification of hemp fibers by silane coupling agents. *Journal of applied polymer science*, *123*, 601-610.
- Ranalli, P., & Venturi, G. (2004). Hemp as a raw material for industrial applications. *Euphytica*, *140*, 1-6.
- Rheay, H. T., Omondi, E. C., & Brewer, C. E. (2020). Potential of hemp (*Cannabis sativa* L.) for paired phytoremediation and bioenergy production. *GCB Bioenergy*.
- Rucińska-Sobkowiak, R. (2016). Water relations in plants subjected to heavy metal stresses. *Acta Physiologiae Plantarum*, *38*, 1-13.
- Sanglard, L. M., Detmann, K. C., Martins, S. C., Teixeira, R. A., Pereira, L. F., Sanglard, M. L., Fernie, A. R., Araújo, W. L., & DaMatta, F. M. (2016). The role of silicon in metabolic acclimation of rice plants challenged with arsenic. *Environmental and Experimental Botany*, *123*, 22-36.
- Saxena, G., Purchase, D., Mulla, S. I., Saratale, G. D., & Bharagava, R. N. (2019). Phytoremediation of heavy metal-contaminated sites: Eco-environmental concerns, field studies, sustainability issues, and future prospects. *Reviews of Environmental Contamination and Toxicology Volume 249*, 71-131.
- Schluttenhofer, C., & Yuan, L. (2017). Challenges towards revitalizing hemp: A multifaceted crop. *Trends in plant science*, *22*(11), 917-929.
- Shah, V., & Daverey, A. (2020). Phytoremediation: A multidisciplinary approach to clean up heavy metal contaminated soil. *Environmental Technology & Innovation*, *18*, 100774.

- Shahzad, A. (2012). Hemp fiber and its composites—a review. *Journal of composite materials*, *46*, 973-986.
- Shi, G., & Cai, Q. (2009). Cadmium tolerance and accumulation in eight potential energy crops. *Biotechnology Advances*, *27*, 555-561.
- Shi, G., Liu, C., Cui, M., Ma, Y., & Cai, Q. (2012). Cadmium tolerance and bioaccumulation of 18 hemp accessions. *Applied biochemistry and biotechnology*, *168*, 163-173.
- Shih, P.-H., Chang, J.-E., Lu, H.-C., & Chiang, L.-C. (2005). Reuse of heavy metal-containing sludges in cement production. *Cement and Concrete Research*, *35*, 2110-2115.
- Siengchin, S., & Dangtungee, R. (2014). Polyethylene and polypropylene hybrid composites based on nano silicon dioxide and different flax structures. *Journal of Thermoplastic Composite Materials*, *27*, 1428-1447.
- Singh, S., Parihar, P., Singh, R., Singh, V., P., and Prasad, S., M. (2016). Heavy metal tolerance in plants: role of transcriptomics, proteomics, metabolomics, and ionomics. *Frontiers in Plant Science*, *6*, 1143.
- Small, E., & Marcus, D. (2002). *Hemp: A new crop with new uses for North America*. Trends in new crop and news uses, ASHS Press, Alexandria, VA, USA.
- Song, U., & Park, H. (2017). Importance of biomass management acts and policies after phytoremediation. *Journal of Ecology and Environment*, *41*, 1-6.
- Spano, M., Di Matteo, G., Rapa, M., Ciano, S., Ingallina, C., Cesa, S., Menghini, L., Carradori, S., Giusti, A. M., & Di Sotto, A. (2020). Commercial Hemp Seed Oils: A Multimethodological Characterization. *Applied Sciences*, *10*, 6933.
- Stevulova, N., Cigasova, J., Estokova, A., Terpakova, E., Geffert, A., Kacik, F., Singovszka, E., & Holub, M. (2014). Properties characterization of chemically modified hemp hurds. *Materials*, *7*, 8131-8150.
- Struik, P. C., Amaducci, S., Bullard, M. J., Stutterheim, N. C., Venturi, G., & Cromack, H. T. H. (2000). Agronomy of fibre hemp (*Cannabis sativa* L.) in Europe. *Industrial crops and products*, *11*, 107-118.
- Tamburini, E., León, A. G., Perito, B., Di Candilo, M., & Mastromei, G. (2004). Exploitation of bacterial pectinolytic strains for improvement of hemp water retting. *Euphytica*, *140*, 47-54.
- Tang, W., Tu, L., Yang, X., Tan, J., Deng, F., Hao, J., ... & Zhang, X. (2014). The calcium sensor GhCaM7 promotes cotton fiber elongation by modulating reactive oxygen species (ROS) production. *New phytologist*, *202*, 509-520.
- Tóth, G., Hermann, T., Da Silva, M. R., & Montanarella, L. (2016). Heavy metals in agricultural soils of the European Union with implications for food safety. *Environment international*, *88*, 299-309.
- Trembath-Reichert, E., Wilson, J. P., McGlynn, S. E., & Fischer, W. W. (2015). Four hundred million years of silica biomineralization in land plants. *Proceedings of the National Academy of Sciences*, *112*, 5449-5454.
- Tripathi, D. K., Singh, V. P., Prasad, S. M., Chauhan, D. K., Dubey, N. K., & Rai, A. K. (2015). Silicon-mediated alleviation of Cr (VI) toxicity in wheat seedlings

as evidenced by chlorophyll fluorescence, laser induced breakdown spectroscopy and anatomical changes. *Ecotoxicology and environmental safety*, 113, 133-144.

- Upcraft, T., & Guo, M. (2019). Phytoremediation Value Chains and Modeling. *Hou. Sustainable Remediation of Contaminated Soil and Groundwater: Materials, Processes, and Assessment*, 1st ed. Elsevier, 325-366.
- Vaculík, M., Landberg, T., Greger, M., Luxová, M., Stoláriková, M., & Lux, A. (2012). Silicon modifies root anatomy, and uptake and subcellular distribution of cadmium in young maize plants. *Annals of Botany*, 110, 433-443.
- Van Bockhaven, J. (2014). *Silicon-induced resistance in rice (Oryza sativa L.) against the brown spot pathogen Cochliobolus miyabeanus* (Doctoral dissertation, Ghent University).
- van den Broeck, H. C., Maliepaard, C., Ebskamp, M. J. M., Toonen, M. A. J., & Koops, A. J. (2008). Differential expression of genes involved in C1 metabolism and lignin biosynthesis in wooden core and bast tissues of fibre hemp (*Cannabis sativa* L.). *Plant Science*, 174, 205-220.
- Vardhan, K. H., Kumar, P. S., & Panda, R. C. (2019). A review on heavy metal pollution, toxicity and remedial measures: Current trends and future perspectives. *Journal of Molecular Liquids*, 290, 111197.
- Vega, I., Rumpel, C., Ruíz, A., Mora, M. D. L. L., Calderini, D. F., & Cartes, P. (2020). Silicon Modulates the Production and Composition of Phenols in Barley under Aluminum Stress. *Agronomy*, 10, 1138.
- Vivancos, J., Labbé, C., Menzies, J. G., & Bélanger, R. R. (2015). Silicon-mediated resistance of A rabidopsis against powdery mildew involves mechanisms other than the salicylic acid (SA)-dependent defence pathway. *Molecular Plant Pathology*, 16, 572-582.
- Vukčević, M., Pejić, B., Kalijadis, A., Pajić-Lijaković, I., Kostić, M., Laušević, Z., & Laušević, M. (2014). Carbon materials from waste short hemp fibers as a sorbent for heavy metal ions—Mathematical modeling of sorbent structure and ions transport. *Chemical Engineering Journal*, 235, 284-292.
- Vukcevic, M., Pejic, B., Lausevic, M., Pajic-Lijakovic, I., & Kostic, M. (2014). Influence of chemically modified short hemp fiber structure on biosorption process of Zn²⁺ ions from waste water. *Fibers and Polymers*, 15, 687-697.
- Wang, Y., Stass, A., & Horst, W. J. (2004). Apoplastic binding of aluminum is involved in silicon-induced amelioration of aluminum toxicity in maize. *Plant physiology*, 136, 3762-3770.
- Wang, H., Xu, Z., Kohandehghan, A., Li, Z., Cui, K., Tan, X., ... & Mitlin, D. (2013). Interconnected carbon nanosheets derived from hemp for ultrafast supercapacitors with high energy. *ACS nano*, 7, 5131-5141.
- Wang, L., Ji, B., Hu, Y., Liu, R., & Sun, W. (2017). A review on in situ phytoremediation of mine tailings. *Chemosphere*, 184, 594-600.

- Werle, S., Ziolkowski, L., Bisorca, D., Pogrzeba, M., Krzyzak, J., & Milandru, A. (2017). Fixed-Bed Gasification Process–The Case of the Heavy Metal Contaminated Energy Crops. *Chemical Engineering Transactions*, *61*, 1393-1398.
- Xu, C. X., Ma, Y. P., & Liu, Y. L. (2015). Effects of silicon (Si) on growth, quality and ionic homeostasis of aloe under salt stress. *South African Journal of Botany*, *98*, 26-36.
- Yadav, S. K. (2010). Heavy metals toxicity in plants: An overview on the role of glutathione and phytochelatin in heavy metal stress tolerance of plants. *South African journal of botany*, *76*, 167-179.
- Ye, J., Yan, C., Liu, J., Lu, H., Liu, T., & Song, Z. (2012). Effects of silicon on the distribution of cadmium compartmentation in root tips of *Kandelia obovata* (S., L.) Yong. *Environmental Pollution*, *162*, 369-373.
- Ye, M., Song, Y., Long, J., Wang, R., Baerson, S. R., Pan, Z., ... & Zeng, R. (2013). Priming of jasmonate-mediated antiherbivore defense responses in rice by silicon. *Proceedings of the National Academy of Sciences*, *110*, E3631-E3639.
- Yin, L., Wang, S., Liu, P., Wang, W., Cao, D., Deng, X., & Zhang, S. (2014). Silicon-mediated changes in polyamine and 1-aminocyclopropane-1-carboxylic acid are involved in silicon-induced drought resistance in *Sorghum bicolor* L. *Plant Physiology and Biochemistry*, *80*, 268-277.
- Żuk-Gołaszewska, K., & Gołaszewski, J. (2020). Hemp production. *Sustainable Agriculture Reviews*, *42*, 1-36.

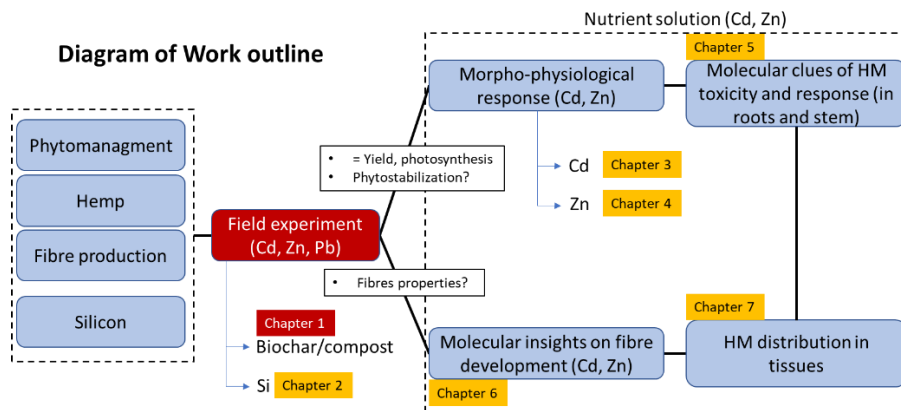
Chapter 1

Studying hemp potential as a non-food crop for phytomanagement of contaminated agricultural soils by heavy metals in combination with biochar and compost.

Marie Luyckx, Mathilde Blanquet, Arnaud Isenborghs, Gea Guerriero, Géraldine Bidar, Christophe Waterlot, Francis Douay, Stanley Lutts.

Author's contributions

ML and SL designed the methodology; ML performed the whole experiment, treated, and analyzed the data; MB and AI contributed to mineral analysis; SL supervised the whole research process; ML and SL wrote the original draft. All authors reviewed the manuscript.



Abstract

The present study aims to determine the suitability of textile hemp (*Cannabis sativa* L.) for phytomanagement and non-food production on agricultural soils contaminated by heavy metals. To devise agricultural strategies aimed at improving non-food crop yield, the use of soils amendments (biochar and/or compost) was also considered. Experiments were conducted in natural field conditions on an agricultural soil previously contaminated by atmospheric fallout from a lead and zinc smelter closed in 2003. Except for a slight yield decrease, hemp was found to be unaffected by soil contamination and showed the same photosynthetic fitness and fibres' quality as control plants. Hemp phytoextraction capacity was limited by the low environmental availability of heavy metals. The vegetation cover may reduce the dispersion of heavy metals from dusts in the environment suggesting that hemp could be used as a suitable crop for phytostabilization strategies. Biochar and compost were found to be interesting options to improve yield, reduce heavy metals' contents in valuable biomass and promote the production of thicker and more resistant fibres.

Keywords: Phytostabilization • biochar • compost • bast fibres

1. Introduction

In many regions across the world, past industrial activities, together with the increasing use of heavy metals (HM) have resulted in a growing number of contaminated areas (Linger et al., 2002; Saxena et al., 2019). Besides former industrial and mining areas, agricultural soils may also be impacted by moderate pollution as a result of atmospheric contamination from surrounding areas and use of low quality fertilisers or pesticides (Ayangbenro & Babalola, 2017; Liu et al., 2018). These areas may no longer be suitable for food production since toxic metals are not biodegradable, and their accumulation in soils can affect the soil physicochemical and biological properties, thereby representing a threat to plants and animals and ultimately constituting a major risk for human health (Linger et al., 2005; Saxena et al., 2019; Jaskulak et al., 2020).

Some of these moderately contaminated agricultural soils may nevertheless still be used for non-food production purposes. With the perspective of maintaining an agricultural activity on these soils, the possibility to combine soil management with plants (phytomanagement) for

non-food production has emerged as a cost-efficient and eco-sustainable solution (Saxena et al., 2019; Jaskulak et al., 2020). The field applicability of this strategy can however be limited by the concentration of HM in the biomass and the slower growth rate of cultivated plant. The use of soil amendments may consequently be recommended to better guarantee the establishment of a plant cover (Peralta-Videa et al., 2009; Chowdhury et al., 2016; Luo et al., 2017; Meena et al., 2018). In this respect, there is a growing body of evidence and enthusiasm concerning the use of biochars and composts in soil management (Filiberto and Gaunt, 2013; Mudhoo et al., 2020; Barquilha and Braga, 2021).

Biochars are organic materials combusted under low oxygen conditions, resulting in a porous, low density carbon-rich material (Beesley et al., 2011). When applied to the soil, biochars can neutralise soil acidity, enhance cation exchange capacity (CEC), improve soil water retention capacity and provide suitable conditions for the colonization of beneficial microorganisms (Biederman & Harpole, 2013; Rodríguez-Vila et al., 2016; El-Naggar et al., 2019; Wang et al., 2020). Liu et al. (2013a) reviewed the published data on 59 pot experiments and 57 field experiments from 21 countries and found that biochar soil amendment (BSA) lower than 30 t ha⁻¹ may increase crop productivity by 11.0 % on average. The impact of BSA on soil fertility and crop productivity is highly dependent on biochar characteristics (the source raw materials and pyrolysis temperatures, doses applied, etc.) and the physicochemical parameters of the soils (El-Naggar et al., 2019). Biochars can also reduce the mobility of some organic and inorganic pollutants in soil: their large surface areas and CEC, determined to a large extent by the source raw materials and pyrolysis temperatures, enable the enhanced sorption of both organic and inorganic contaminants present in soils in their most mobile forms (Beesley et al., 2011; Janus et al., 2017). This is however not the case for arsenic (As), since biochar increases the soil pH and consequently also As bioavailability in soils (Beesley et al., 2011). Moreover, biochar does not appreciably decompose in soil, thus a single application can provide positive effects over several growing seasons in the field, which is not usually the case for manures, compost, and conventional fertilizers (Filiberto and Gaunt, 2013). Among the different types of biochar cited in the literature, the one produced from *Miscanthus* is of particular interest for contaminated soil management: in addition to its interest for enhancing both soil HM sequestration and soil fertility, it could also be regarded as a potential source of bioavailable silicon (Si) (Houben et al., 2014;

Pidlisnyuk et al., 2021). Silicon is largely recognized as a beneficial element able to improve plant growth subjected to various biotic and abiotic stresses (Etesami and Jeong, 2018).

Composts are produced from a range of organic materials (OM) including food, animal manure, sewage sludge, paper residues and other wastes (Rodríguez-Vila et al., 2016). Addition of compost to soil can improve soil water retention capacity, contribute to the supply of carbon (C) and essential nutrients, and increase the biomass and diversity of soil microorganisms (Forján et al., 2016; Rodríguez-Vila et al., 2016; Ai et al., 2020). However, the organic C in compost is quickly lost due to its relatively low recalcitrance (Forján et al., 2016). Also, composts can reduce the bioavailability of metals through the formation of stable complexes with the organic matter (Forján et al., 2016; Mudloo et al., 2020).

Since modern contaminants' management strategies increasingly focus on the effects of the most toxicologically relevant fractions of these contaminants, biochars and composts could represent suitable candidates for remediation trials (Beesley et al., 2011). Remediation also requires maintenance of soil quality and ultimately material conditions conducive to plant growth (Beesley et al., 2011). In some cases, biochars can immobilise essential macro-nutrients, while, in composts, pollutants fixed on organic matter (OM) may be released over time due to the low recalcitrance of OM and thus OM degradation. Therefore, biochars or composts alone may be ineffective for long-term sustainable remediation. The joint use of biochars and composts could thus synergize their beneficial individual effects and provides their most effective way of deployment to soils: composts provide nutrients and biochars are recalcitrant in soils (Beesley et al., 2011). Besides, as biochar applications provide greater nutrient retention, limited amounts of other amendments (i.e. compost) need to be applied because of reduced nutrient loss by leaching (Filiberto and Gaunt, 2013; Busch and Glaser, 2015).

The success of phytomanagement requires the use of plant species exhibiting HM tolerance, HM accumulation in above-ground harvestable organs, high biomass production, and producing non-food resources (Ali et al., 2013; Griga & Bjelková, 2013; Linger et al., 2002; Tóth et al., 2016). During last 20 years, fibre crops have been gaining more and more interest for this purpose: *Cannabis sativa* L. (hemp) appears as an ideal candidate due to its ability to extract HM from the soil and the possibility of industrial processing of contaminated biomass (Citterio et al., 2003; Griga and Bjelková, 2013; Linger et al., 2002; Zielonka et al., 2020). After hemp straw processing,

different plant fractions are obtained: fibres (27-30% of above-ground biomass), hurds (45-55%) and powder (15-24%). These fractions represent mean values of 50%, 27% and 2% of the plant economic value, respectively (InterChanvre, 2017): all above-ground biomass produced can be used, thus not generating any waste as defined by EU regulations (Bono et al., 2020). Fibres are mainly used in paper production (56%), insulation (29%) and bio-based plastics (9%), while hurds are mainly used as animal litters (50%), in building industry (hemp crete, lightweight particle panels, 14%) and horticultural mulching (22%). Moreover, the high aerial biomass of hemp can be used as a combustible raw material for energy production (Griga and Bjelková, 2013; Parvez et al., 2021). Not all these applications are necessarily suitable for hemp biomass produced on contaminated substrates. The major factors that will impact the usability of the hemp biomass produced in the presence of soil contamination include: (a) the contaminant type and concentration in the biomass, (b) the type of product use, and (c) regulatory standards/guidelines on acceptable product quality (Rheay et al., 2020).

Produced mainly in Europe and more specifically in France (which accounts for 40% of the European production), hemp also constitutes a local resource that does not require the use of phytosanitary products. Moreover, hemp helps to regenerate the soil structure and fertility through its deep root system, making it a plant with low environmental impact (InterChanvre, 2017; EIHA, 2019; Bono et al., 2020).

The general objectives of the current study are i) to evaluate the phytomanagement potential of hemp cultivated on agricultural soil formerly contaminated by Cd and Zn, ii) to determine the impact of amendments (green waste compost, *Miscanthus* biochar and their combination) on the plant growth potential and iii) to assess the impact of these treatments on the bast fibres' HM contents and their major mechanical properties.

2. Material and Methods

2.1. Growing conditions

Two agricultural sites (Courcelles-lès-Lens, CLL (50°24'58.2"N 3°01'40.0"E), and Bois-Bernard, BB (50°22'52.0"N 2°55'11.3"E); France) were selected: CLL is located near (about 1 km to the southeast) a former lead and zinc smelter (Metaleurop), while BB is far enough from it (about 9 km southwest) not to be influenced by contaminated dust fallout and was taken as

a control. The lead and zinc smelter Metaleurop closed in 2003 but previously released in the environment, during decades, dust particles responsible for HM contamination (mainly Cd, Zn and Pb) in the surroundings.

Before the beginning of the experiment (T0), 3 soil samples from ploughed layer (0 - 25 cm) from each site were characterized (Table S1.1). Total HM concentrations in CLL soil (5.5 ± 0.2 mg Cd, 396 ± 32 mg Zn, 298 ± 21 mg Pb kg^{-1} soil) exceeded, for Zn and Pb, the permissible limits (PL) recommended for agricultural use (10 mg Cd kg^{-1} , 250 mg Zn kg^{-1} , and 200 mg Pb kg^{-1} ; Tóth et al., 2016), while in BB, Cd and Zn concentrations were 5 times lower than in CLL and below the PL for Cd and Zn (1.1 ± 0.1 mg Cd, 80.9 ± 3.9 mg Zn per kg of soil; MisChar program). The presence of Pb in the topsoil of BB (285 ± 95 mg kg^{-1}) is linked to the presence of some shrapnel issued from World War I. Detailed soil analyses for both sites are provided in Table S1.1 (supplemental data). In both BB and CLL, HM extraction with CaCl_2 0.01 M revealed very low environmental availability of Cd and Pb, since their extractable concentration were below the detection limits of the flame atomic absorption spectrometer (0.05 mg kg^{-1} for Cd, 0.65 mg kg^{-1} for Pb). In both sites, the CEC was between 17.3 and 19.8 cmol kg^{-1} , and soil pH in CLL (7.9 ± 0.1) was slightly more alkaline than in BB (7.0 ± 0.2).

For each site, four blocks of 18 m * 10 m, separated by 1-meter wide band were set up. Each block corresponded to a specific treatment and each of them was divided into 2 contiguous areas (9 m * 10 m), one for industrial hemp and the other for wheat to establish a crop rotation (Figure 1.1). From year to year, hemp and wheat were alternate at the 2 joint areas of each block (Figure 1.1), but only hemp will be considered in this study. Eight treatments were defined, considering soil contamination (site) and the concomitant presence/absence of soil amendment, and will hereafter be referred to as BB (control, unamended), CLL (contaminated, unamended), BBbio (BB amended with biochar), BBcomp (BB amended with compost), BBmix (BB amended with biochar and compost), CLLbio, CLLcomp, CLLmix.

Soils were amended before plant sowing with *Miscanthus* biochar (5.2 $\text{kg m}^{-2} \approx 2\%$ m/m, *miscanthus* pyrolysis at 500°C for 15 min, produced by ETIA in France), and/or green waste compost (2 $\text{kg m}^{-2} \approx 20$ T/ha, from the Cucq platform in France, managed by Agriopale). The doses applied are in the range of those usually cited in the literature for biochar (2 - 10% m/m; Janus et al., 2015), and corresponds, for compost, to agronomic practices conventionally implemented in the region. The physicochemical parameters of the produced biochar and compost are detailed in Tables S1.2 and S1.3. The

determination of total HM contents revealed traces of Cd and Pb in both biochar and compost, but they cannot be regarded as a potential source of HM in amended soils: as described in the results below, they did not lead to an increase of HM pseudo-total concentration in the experimental sites.

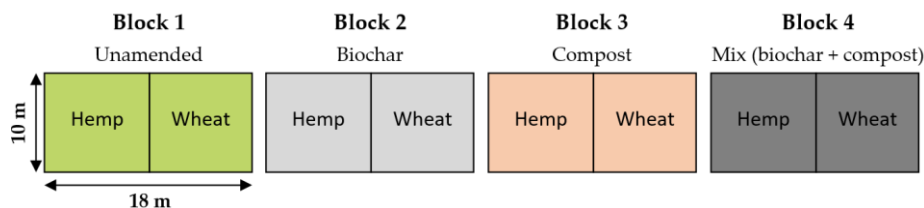


Figure 1.1: Overview of the experimental blocks set up in Bois-Bernard and Courcelles-lès-Lens.

The field study was carried out in 2018 and 2019. 2018 was drier and warmer than 2019 (Lille-Lesquin weather station). The accumulated rainfall over the period of physiological measurements, as well as over the entire vegetation period in 2019 exceeded that of 2018, while average temperatures were higher in 2018 than in 2019 (detailed parameters overtime in Table S1.4).

2.2. Soil characterization

Soil samples were collected before plant sowing in 2018 (T0), after plant harvest in 2018 (T1), and after plant harvest in 2019 (T2). We analyzed HM pseudo-total concentrations, HM concentrations after CaCl_2 0.01 M extraction (HM environmental availability), CEC and pH.

For pseudo-total concentrations, 300 mg DM (dry matter) of soil samples were ground to powder (250 μm), placed in a tube with a mix of HCl 37%- HNO_3 68% (3:1, v/v), heated to 95 $^\circ\text{C}$ for 1h30, dissolved in distilled water, and finally filtered through Whatman n°1 filter papers. The environmental available metal concentrations were evaluated using 3 g of ground soil samples, placed in a tube with 30 mL of CaCl_2 (0.01 M), mixed for 2 h before centrifugation (4500 g – 20 min), and finally filtered on Whatman n°1 filter paper. Total and environmental available heavy metals were quantified by flame atomic absorption spectrometry following the recommendations in Waterlot and Hechelski (2019).

For CEC determination (NF X31-130), 2.5 g DM of soil samples were ground to powder (2 mm), placed in a percolation tube, and rinsed four times with a solution of ammonium acetate (1M). Residues of ammonium acetate solution were then eliminated with ethanol 95%, and the tube was dried 24 h

at room temperature. Then, samples were transferred in centrifugation tubes with 50 mL NaCl 1 M and agitated during 1 h. The solution was centrifuged (3000 g, 15 min) and filtered (Minisart filter, 0.45 μm cellulose acetate). Then, CEC was determined according to the Berthelot reaction: 400 μL of the solution obtained was mixed with 4 mL of a color reagent (130 g sodium salicylate, 130 g trisodium citrate dihydrate, 970 mg sodium nitroprusside, adjusted to 1 L with distilled water), 4 mL of sodium dichloroisocyanurate (32 g NaOH in 500 mM distilled water, cooled at room temperature and mixed with 2 g of DIC, before volume adjustment to 1 L with distilled water) and adjusted to 40 mL with distilled water. Samples were then agitated and heated 60 min at 25 $^{\circ}\text{C}$ before absorbance measurement (655 nm).

For pH determination, a volume of 6 mL of dry soil ground to powder (2 mm) was placed in a tube with 30 mL of distilled water and agitated 1 h at 750 rpm. pH was measured 2 h after agitation for the soil particles' sedimentation.

2.3. Plant material

Seeds of a monoecious hemp fibre variety (*Cannabis sativa* cv. Futura 75) were sown in the end of April (2018 and 2019), with a sowing density of 50 kg ha⁻¹. No fertilization nor weeding were applied. Harvests were performed 4 months after the seeds were sown, at the full mature stage. For each treatment, 3 areas of 1 m² were randomly defined to collect the plants (Figure 1.2).

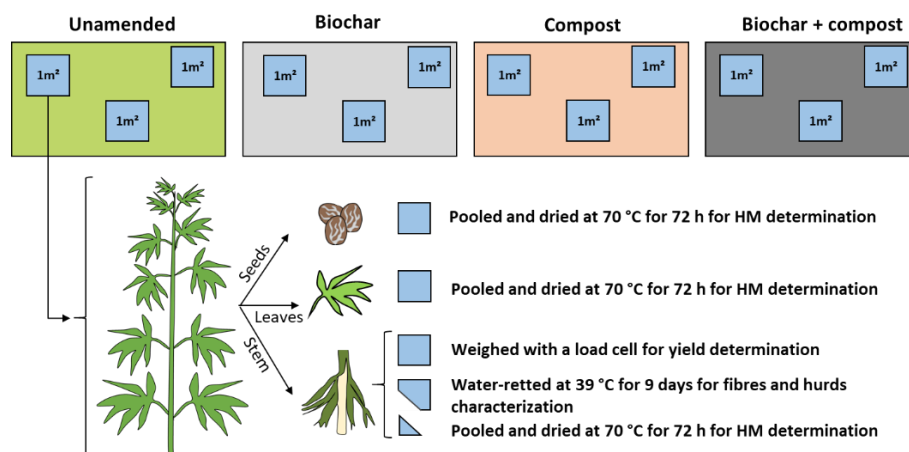


Figure 1.2: Harvesting criterion and details on samples' preparation. Valid for plants grown in Bois-Bernard and Courcelles-lès-Lens.

Plants from these areas were cut 5 cm above the ground, and seeds and leaves were then separated from the stem. Leaves and seeds from the same area were pooled and dried at 70 °C for 72 h for Cd, Pb and Zn determination. Stems from the same area were weighed with a load cell for yield determination, and then pooled and water-retted for fibres and hurds characterization, except for subsamples dried at 70 °C for 72 h for HM determination (Figure 1.2).

2.4. Photosynthesis-related parameters

Before plant harvest, 11-week old, 15-week old and 17-week old plants were used to assess treatments' effects on photosynthesis. Photosynthesis-related parameters were measured on 5 plants per treatment, on the middle portion of the leaf blades constituting the second fully formed leaves from the top.

Chlorophyll fluorescence was measured using a fluorescence monitoring system (FMS2; Hansatech, King's Lynn, UK). Blade portions were acclimated to darkness for 20 min. The minimal fluorescence level (F_0) was obtained by measuring the modulated light ($0.1 \mu\text{mol m}^{-2} \text{s}^{-1}$). The maximal fluorescence level (F_m) with all photosystem II (PSII) reaction centres open was determined by a 0.8-s saturating pulse at $8500 \mu\text{mol m}^{-2} \text{s}^{-1}$ in dark-adapted leaves. The leaves were then continuously illuminated with white actinic light ($320 \mu\text{mol m}^{-2} \text{s}^{-1}$), during 3 min; the steady-state value of fluorescence (F_s) was recorded. A second saturating pulse at $8500 \mu\text{mol m}^{-2} \text{s}^{-1}$ was imposed to determine maximal fluorescence level in the light-adapted state (F_m'). The actinic light was removed and the minimal fluorescence level in the light-adapted state (F_0') was determined by illuminating the leaf with a 3-s pulse of far-red light. The following fluorescence-related parameters were calculated (Maxwell and Johnson 2000): F_v/F_m (maximal efficiency of PSII photochemistry in the dark-adapted state), q_p (photochemical quenching coefficient), NPQ (non-photochemical quenching), Φ_{PSII} (actual PSII efficiency).

Leaf stomatal conductance (g_s) was measured using an AP4 diffusion porometer (Delta-TDevices Ltd., Cambridge, UK). The instantaneous CO_2 assimilation under ambient conditions (400 ppm CO_2) (A) and instantaneous transpiration (E) were measured using an infrared gas analyser (LCA4 8.7 ADC, Bioscience, Hertfordshire, UK). Gas exchanges were measured using a Parkinson leaf cuvette on intact leaves for 1 min (20 records

min⁻¹) with an air flow of 300 mL min⁻¹. All measurements were performed around midday (between 10 a.m. and 2 p.m).

The intrinsic (A/g_s), and instantaneous (A/E) water use efficiency were also calculated.

2.5. Mineral concentrations in plants

Plant samples were ground to powder (250 μ m), and 500 mg DM were placed in an oven and heated to 500 °C for 48 h. The ashes were then digested in 68% HNO₃ and acid evaporated to dryness on a sand bath at 80 °C. Minerals were incubated with a mix of HCl 37%-HNO₃ 68% (3:1) and the mixture was slightly evaporated and dissolved in distilled water, and filtered on Whatman n°1 filter paper. Heavy metals were quantified by Inductively Coupled Plasma-Optical Emission Spectroscopy (Varian, type MPX).

BF (bioaccumulation factor) = HM concentration in aerial plant parts (mg kg⁻¹)/HM total concentration in the soil (mg kg⁻¹)

Phytoextraction potential (g. ha⁻¹) = [hemp stem yield (T. ha⁻¹) x HM concentration in stem (g. T⁻¹)] + [hemp leaves yield (T. ha⁻¹) x HM concentration in leaves (g. T⁻¹)].

2.6. Fibre's and hurds' characterization

Stems were water-retted to separate fibres from hurds: stems were placed in 70 cm-long water-filled containers and incubated 9 days at 39 °C. Fibres were then separated manually by combing (Réquillé et al., 2018).

Fibre bundles' title and tensile strength were determined according to MO 123 and XP 25-501-3 T standards respectively (CELABOR). Fibre tensile strength was evaluated using a Zwick tensile bench with 10 N and 500 N load cell, a test speed of 7.5 mm min⁻¹, a pretension of 0.1 N, and a gap between the clamps of 75 mm.

Subsequently, we determined lignin, cellulose, hemicellulose through near-infrared spectrometry (NIRS) as well as HM contents in fibres and hurds. NIIRS was performed using XDS system (Foss Master Lab Rapid Content) with ISIScan software and a spectral range from 400 to 2498 nm. Stem samples were preliminary dried at 60 °C for 48 h and ground to provide homogenous powder with particle size lower than 1 mm. The analysis was performed with a dual detector system at a data acquisition rate of 2 scan/sec and a spectral resolution of 2 nm.

2.7. Statistical analysis

Five replicates were analyzed for each treatment. ANOVA tests were performed separately for each year. Normality of the data was verified using Shapiro-Wilk tests and the data were log-transformed when required. Homogeneity of the data was verified using Levene's tests. Two-way ANOVA was performed at a significant level of P -value < 0.05 using R (version 3.3.1) considering the soil contamination (BB, CLL) and the amendment applied as main factors. Means were compared using Tukey's HSD all-pairwise comparisons at 5% level as a post-hoc test.

3. Results

3.1. Plant physiology



Figure 1.3: Experimental blocks in Bois-Bernard and Courcelle-lès-Lens sites, 3 months after plant sowing.

As illustrated in Figures 1.3 and 1.4, neither the soil contamination nor the amendments applied significantly impacted plant development and yield.

However, several trends persisted over time: (i) a lower hemp yield in CLL (32 T ha⁻¹ in 2018, 19 T ha⁻¹ in 2019) compared to BB (40 T ha⁻¹ in 2018, 25 T ha⁻¹ in 2019); (ii) a yield decrease in BBbio treatment, and conversely, a yield increase in CLLbio and CLLcomp (significant in 2019) treatments compared to the unamended block of each site. It should also be noted that hemp yield was higher in 2018 than in 2019, and that the weed *Chenopodium album* L. infested both experimental sites before hemp sowing in 2019. In 2018, the mix treatment provided the highest yield in BB site but the lowest one in CLL.

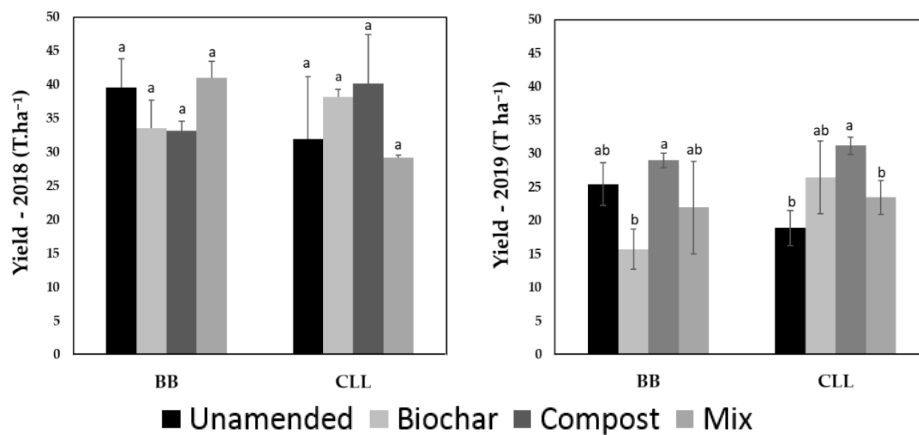


Figure 1.4: Hemp yield (T ha⁻¹) in 2018 and 2019. Plants were grown 4 months on HM contaminated soil of Courcelles-lès-Lens (CLL) or on control soil of Bois-Bernard (BB), in the presence or in the absence of biochar (Bio), compost (Comp), or biochar and compost (Mix). Data are means \pm standard errors ($n=3$). The different letters indicate that the values are significantly different from each other ($P < 0.05$; Tukey's HSD all-pairwise comparisons).

The mean stem length decreased significantly in BBbio treatment compared to the unamended block of BB, while addition of compost in CLL significantly increased stem length as illustrated in Figure 1.5.

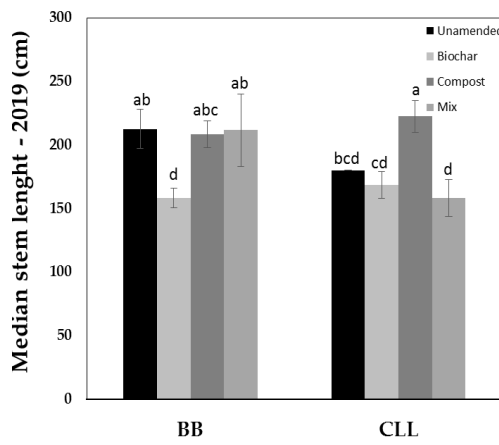


Figure 1.5: Hemp stem mean length (cm). Plants were grown during 4 months on HM contaminated soil of Courcelles-lès-Lens (CLL) or on control soil of Bois-Bernard (BB), in the presence or in the absence of biochar (Bio), compost (Comp), or biochar and compost (Mix). Data are means \pm standard errors ($n=3$). The different letters indicate that the values are significantly different from each other ($P < 0.05$; Tukey's HSD all-pairwise comparisons).

Table 1.1: Light-dependent parameters of photosynthesis of *C. sativa* (cv Futura 75), mean of values recorded 11, 15 and 17 weeks after plant sowing. Plants were grown on HM-contaminated soil of Courcelles-lès-Lens (CLL) or on control soil of Bois-Bernard (BB) in the presence or in the absence of biochar, compost or biochar and compost (Mix). Maximal efficiency of PSII photochemistry in the dark-adapted state (F_v/F_m), actual PSII efficiency (Φ_{PS2}), photochemical quenching coefficient (q_p), non-photochemical quenching (NPQ). Data are means \pm standard errors ($n=5$). For each column, values with different letters are significantly different at $P < 0.05$ according to the Tukey's HSD all-pairwise comparisons.

		2018				2019			
Site	Block	F_v/F_m	Φ_{PS2}	q_p	NPQ	F_v/F_m	Φ_{PS2}	q_p	NPQ
BB	Unamended	0.85 \pm 0.02 a	0.75 \pm 0.04 a	0.92 \pm 0.04 a	0.31 \pm 0.14 a	0.85 \pm 0.05 a	0.70 \pm 0.10 a	0.93 \pm 0.04 a	0.47 \pm 0.64 a
	Biochar	0.80 \pm 0.04 a	0.70 \pm 0.06 a	0.96 \pm 0.08 a	0.38 \pm 0.29 a	0.81 \pm 0.06 a	0.66 \pm 0.15 a	0.97 \pm 0.03 a	0.59 \pm 0.57 a
	Compost	0.86 \pm 0.03 a	0.77 \pm 0.03 a	0.95 \pm 0.05 a	0.21 \pm 0.10 a	0.85 \pm 0.02 a	0.74 \pm 0.08 a	0.95 \pm 0.03 a	0.40 \pm 0.25 a
	Mix	0.83 \pm 0.05 a	0.75 \pm 0.07 a	0.93 \pm 0.08 a	0.27 \pm 0.16 a	0.85 \pm 0.04 a	0.69 \pm 0.12 a	0.93 \pm 0.03 a	0.48 \pm 0.56 a
	Unamended	0.81 \pm 0.03 a	0.72 \pm 0.03 a	0.96 \pm 0.04 a	0.34 \pm 0.18 a	0.83 \pm 0.03 a	0.76 \pm 0.06 a	0.96 \pm 0.04 a	0.28 \pm 0.16 a
	Biochar	0.84 \pm 0.05 a	0.73 \pm 0.06 a	0.93 \pm 0.09 a	0.31 \pm 0.13 a	0.82 \pm 0.05 a	0.73 \pm 0.14 a	0.95 \pm 0.03 a	0.29 \pm 0.16 a
	Compost	0.84 \pm 0.06 a	0.78 \pm 0.03 a	0.94 \pm 0.03 a	0.30 \pm 0.19 a	0.84 \pm 0.04 a	0.74 \pm 0.06 a	0.94 \pm 0.04 a	0.27 \pm 0.17 a
	Mix	0.83 \pm 0.05 a	0.73 \pm 0.06 a	0.95 \pm 0.05 a	0.24 \pm 0.09 a	0.83 \pm 0.03 a	0.74 \pm 0.07 a	0.96 \pm 0.04 a	0.34 \pm 0.17 a

During the whole experiment (2018 and 2019), parameters of chlorophyll fluorescence (F_v/F_m , Φ_{PS2} , q_P , NPQ) were not significantly influenced by HM contamination nor soil amendments (Table 1.1, detailed results in Table S1.5). Moreover, values recorded in 2018 were similar to those recorded in 2019.

Parameters involved in light-independent reactions of photosynthesis were also evaluated (C_i , E , A , g_s , Table 1.2; detailed results overtime in Table S1.5): only few statistical effects were reported. The CO_2 concentration in intercellular spaces (C_i) of plants cultivated on the unamended block of CLL was significantly lower than the C_i of plants cultivated on the unamended block of BB. Only biochar seemed to have an impact on light-independent reactions of photosynthesis: in BB, instantaneous transpiration (E) was higher (significant in 2018), while net photosynthesis tended to increase (during both years) compared to the unamended block of the site. As detailed in Table S1.4, E decreased and A and g_s tended to decrease over time in 2019 in both BB and CLL sites (amended or not), but none of these results were significant. Besides, C_i , E , A , and g_s values were statistically similar between 2018 and 2019.

Plant's water use efficiency (WUE) tended to be lower in CLL than BB in 2018, while we observed the opposite trend in 2019 (Table 1.2). Soil amendments had contrasting effects on WUE in CLL and BB, and the trends observed in 2018 were not similar in 2019. In 2019, the highest WUE in BB was observed in response to compost application, while in CLL it was observed for the unamended site. As far as intrinsic water use efficiency is concerned, the highest value in BB was observed for biochar, while in CLL it was observed for the compost-amended sites both in 2018 and 2019 (data not shown).

3.2.HM accumulation in hemp

Cadmium, Pb and Zn were detected in plants cultivated in BB and CLL, with generally higher concentrations in the leaves than in the stem (Table 1.3). Foliar concentrations of Cd, Pb and Zn were significantly higher in plants sampled in CLL compared to those sampled in BB. The same trend was recorded for stems. Besides, leaves and stems HM concentrations tended to be higher in 2019 than in 2018.

Table 1.2: Light-independent parameters of photosynthesis of *C. sativa* (cv Futura 75), mean of values recorded 11, 15 and 17 weeks after plant sowing. Plants were grown on HM-contaminated soil of Courcelles-lès-Lens (CLL) or on control soil of Bois-Bernard (BB) in the presence or in the absence of biochar, compost or biochar and compost (Mix). CO₂ in intercellular spaces (*C_i*), instantaneous evapotranspiration (*E*), net photosynthesis (*A*), stomatal conductance (*g_s*), water use efficiency (*A/E*). Data are means ± standard errors (*n*=5). For each column, values with different letters are significantly different at *P* < 0.05 according to the Tukey's HSD all-pairwise comparisons. Color code: significant impact of the site (CLL vs BB; blue) or, for each site, of the amendment (biochar, compost, mix) applied comparatively to the unamended block (green).

Site	Block	2018					2019				
		<i>C_i</i> (μmol mol ⁻¹)	<i>E</i> (mmol H ₂ O m ⁻² s ⁻¹)	<i>A</i> (μmol CO ₂ m ⁻² s ⁻¹)	<i>g_s</i> (mmol m ⁻² s ⁻¹)	<i>A/E</i>	<i>C_i</i> (μmol mol ⁻¹)	<i>E</i> (mmol H ₂ O m ⁻² s ⁻¹)	<i>A</i> (μmol CO ₂ m ⁻² s ⁻¹)	<i>g_s</i> (mmol m ⁻² s ⁻¹)	<i>A/E</i>
BB	Unamended	258 ± 63 a	2.22 ± 0.53 ab	6.12 ± 1.97 ab	255 ± 179 ab	2.76	355 ± 40 d	1.56 ± 0.90 a	2.61 ± 2.32 a	212 ± 117 a	1.67
	Biochar	252 ± 39 a	3.25 ± 1.31 c	8.04 ± 4.34 b	204 ± 82 ab	2.47	307 ± 59 ad	1.86 ± 1.45 a	5.13 ± 5.87 a	172 ± 111 a	2.76
	Compost	260 ± 51 a	2.57 ± 0.91 bc	6.95 ± 3.35 ab	277 ± 159 ab	2.70	343 ± 58 cd	1.53 ± 1.05 a	5.17 ± 5.80 a	262 ± 180 a	3.38
	Mix	269 ± 56 a	2.71 ± 0.52 bc	6.44 ± 4.22 ab	353 ± 235 b	2.38	334 ± 58 bd	1.96 ± 1.12 a	4.43 ± 4.08 a	173 ± 90 a	2.26
CLL	Unamended	263 ± 72 a	1.87 ± 1.01 ab	3.18 ± 2.21 a	141 ± 151 a	1.70	247 ± 67 a	1.89 ± 1.04 a	6.90 ± 4.87 a	221 ± 164 a	3.65
	Biochar	277 ± 61 a	1.32 ± 1.47 a	3.05 ± 3.09 a	144 ± 90 a	2.31	267 ± 66 ab	1.73 ± 1.33 a	4.77 ± 4.17 a	226 ± 143 a	2.76
	Compost	272 ± 63 a	1.87 ± 0.61 ab	4.88 ± 3.12 ab	125 ± 110 a	2.61	277 ± 49 abc	2.25 ± 1.80 a	6.16 ± 5.01 a	175 ± 100 a	2.74
	Mix	239 ± 48 a	2.14 ± 0.63 ab	5.14 ± 2.20 ab	116 ± 76 a	2.40	265 ± 71 ab	1.80 ± 1.35 a	4.27 ± 3.64 a	236 ± 145 a	2.37

Table 1.3: Cadmium, lead and zinc concentrations (in mg kg⁻¹ DW) in leaves and stems of *C. sativa* (cv Futura 75) and the bioaccumulation factor (BF). Plants were grown during 4 months (in 2018 and 2019) on HM-contaminated soil of Courcelles-lès-Lens (CLL) or on control soil of Bois-Bernard (BB), in the presence or in the absence of biochar, compost, or biochar and compost (Mix). Data are means ± standard errors (*n*=5). For each element, organ and year, values with different letters are significantly different at *P* < 0.05 according to the Tukey's HSD all-pairwise comparisons. code: significant impact of the site (CLL vs BB; blue) or, for each site, of the amendment (biochar, compost, mix) applied comparatively to the unamended block (green).

		2018			2019			
	Site	Block	Cd	Pb	Zn	Cd	Pb	Zn
Leaves	BB	Unamended	0.018 ± 0.003 b	1.10 ± 0.22 ab	25.27 ± 4.10 a	0.075 ± 0.032 ab	2.72 ± 1.03 ab	41.74 ± 6.35 a
		Biochar	0.011 ± 0.000 a	0.77 ± 0.05 a	27.34 ± 0.94 a	0.091 ± 0.030 abc	3.37 ± 0.73 ab	47.05 ± 4.04 ab
		Compost	0.028 ± 0.003 c	1.02 ± 0.05 ab	24.96 ± 3.19 a	0.056 ± 0.008 a	2.57 ± 0.36 ab	42.64 ± 7.22 a
		Mix	0.031 ± 0.000 c	1.72 ± 0.04 cd	26.92 ± 0.92 a	0.062 ± 0.015 a	2.12 ± 0.27 a	37.43 ± 3.61 a
	CLL	Unamended	0.058 ± 0.004 ef	2.17 ± 0.07 cde	42.69 ± 1.65 bc	0.165 ± 0.040 d	3.72 ± 0.39 b	65.67 ± 5.06 c
		Biochar	0.036 ± 0.000 d	1.63 ± 0.47 bc	39.45 ± 4.70 b	0.134 ± 0.030 cd	3.28 ± 0.39 ab	70.23 ± 2.24 c
		Compost	0.058 ± 0.003 f	2.09 ± 0.09 cd	41.83 ± 1.33 bc	0.159 ± 0.024 d	3.66 ± 0.56 b	69.99 ± 6.49 c
		Mix	0.048 ± 0.004 e	2.90 ± 0.00 ef	50.73 ± 0.54 c	0.127 ± 0.013 bc	3.29 ± 0.84 ab	59.21 ± 11.33 bc
Stems	BB	Unamended	0.026 ± 0.002 a	0.92 ± 0.01 a	20.47 ± 3.68 a	0.039 ± 0.017 a	1.16 ± 0.23 a	4.94 ± 2.01 a
		Biochar	0.019 ± 0.001 a	0.85 ± 0.23 a	11.25 ± 5.40 a	0.028 ± 0.008 a	1.49 ± 0.17 ab	3.80 ± 1.85 a
		Compost	0.020 ± 0.000 a	0.56 ± 0.07 a	7.95 ± 0.62 a	0.027 ± 0.011 a	1.38 ± 0.32 a	7.11 ± 3.46 a
		Mix	0.023 ± 0.004 a	1.16 ± 0.01 ab	8.25 ± 0.02 a	0.051 ± 0.019 a	1.50 ± 0.25 ab	5.25 ± 4.95 a
	CLL	Unamended	0.039 ± 0.007 b	0.89 ± 0.08 a	12.70 ± 0.16 a	0.055 ± 0.024 a	1.65 ± 0.49 ab	6.95 ± 3.43 a
		Biochar	0.040 ± 0.001 b	0.99 ± 0.20 ab	15.86 ± 3.79 a	0.038 ± 0.008 a	1.71 ± 0.24 ab	7.46 ± 4.77 a
		Compost	0.099 ± 0.065 b	2.24 ± 0.98 b	22.89 ± 8.76 a	0.036 ± 0.017 a	2.50 ± 1.11 b	15.37 ± 16.80 a
		Mix	0.041 ± 0.010 b	1.07 ± 0.09 ab	15.01 ± 5.22 a	0.042 ± 0.007 a	1.58 ± 0.51 ab	5.72 ± 2.61 a
BF	BB	Unamended	0.021 ± 0.002 ab	0.00 ± 0.000 a	0.271 ± 0.017 c	0.048 ± 0.021 b	0.006 ± 0.001 a	0.186 ± 0.021 b
		Biochar	0.015 ± 0.001 ab	0.003 ± 0.001 a	0.199 ± 0.050 bc	0.049 ± 0.021 b	0.007 ± 0.001 a	0.167 ± 0.032 b
		Compost	0.021 ± 0.001 ab	0.002 ± 0.000 a	0.161 ± 0.006 b	0.035 ± 0.011 b	0.006 ± 0.001 a	0.211 ± 0.037 b
		Mix	0.023 ± 0.003 b	0.005 ± 0.000 ab	0.171 ± 0.004 b	0.057 ± 0.003 b	0.006 ± 0.001 a	0.171 ± 0.036 b
	CLL	Unamended	0.008 ± 0.001 a	0.004 ± 0.000 a	0.055 ± 0.001 a	0.015 ± 0.004 a	0.007 ± 0.002 a	0.061 ± 0.007 a
		Biochar	0.007 ± 0.000 a	0.004 ± 0.001 a	0.058 ± 0.010 a	0.012 ± 0.003 a	0.007 ± 0.001 a	0.068 ± 0.010 a
		Compost	0.016 ± 0.008 ab	0.007 ± 0.002 b	0.072 ± 0.016 a	0.013 ± 0.003 a	0.010 ± 0.002 a	0.086 ± 0.036 a
		Mix	0.008 ± 0.001 a	0.005 ± 0.000 a	0.065 ± 0.009 a	0.012 ± 0.001 a	0.007 ± 0.002 a	0.055 ± 0.004 a

Exposure to soil amendment had significant effects in 2018 but not in 2019. In BB, addition of biochar significantly decreased Cd leaf concentration compared to the unamended block, while compost and biochar + compost had an opposite effect. Biochar + compost also increased Pb leaf concentration comparatively to the unamended block of BB. In CLL, the addition of biochar significantly decreased Cd leaf concentration, while compost increased Pb stem concentration comparatively to the unamended block.

In addition, some of the trends observed in 2018 in the amended blocks, comparatively to the unamended block of the site, were maintained in 2019: a higher Zn leaf concentration and a lower Zn stem concentration in BBbio treatment; a lower Pb leaf concentration and Cd stem concentration in BBcomp; and a higher Pb stem concentration in BBmix treatment. In CLL: a lower Pb leaf concentration and a higher Zn stem concentration in CLLbio and CLLcomp treatments.

Table 1.4: Hemp phytoextraction potential $\text{g} \cdot \text{ha}^{-1} \text{ year}^{-1}$. Plants were grown during 4 months (in 2018 and 2019) on HM-contaminated soil of Courcelles-lès-Lens (CLL) or on control soil of Bois-Bernard (BB) in the presence or in the absence of biochar, compost or biochar and compost (Mix).

		2018			2019			
Site	Block	Cd	Pb	Zn	Cd	Pb	Zn	
$\text{g ha}^{-1} \text{ year}^{-1}$	BB	Unamended	1.33	55	1241	1.81	59	582
		Biochar	0.80	39	772	1.05	46	377
		Compost	1.07	33	618	1.48	72	736
		Mix	1.50	78	812	1.72	53	468
	CLL	Unamended	2.05	58	991	2.38	61	665
		Biochar	2.12	65	1253	2.52	83	995
		Compost	4.98	126	1639	3.23	127	1415
		Mix	1.80	68	1076	2.25	70	731

To evaluate the capacity of hemp to extract HM from soil, the bioaccumulation factor (BF) was calculated, as well as the mass of exported-HM from soil ($\text{g ha}^{-1} \text{ year}^{-1}$). All the BF values obtained were below 0.06 for Cd, 0.01 for Pb and 0.3. for Zn (Table 1.3). BF values were significantly lower in CLL than in BB for Zn in 2018 and for Cd and Zn in 2019. Compared to the unamended block of BB, the addition of compost or biochar + compost led to a significant decrease of bioaccumulated Zn in 2018, while compost increased Zn bioaccumulation in 2018 in CLL (same trend for compost in 2019).

The average amount of HM extracted by hemp was approximately 2.22 g Cd; 59.81g Pb and 829 g Zn ha⁻¹ year⁻¹ in CLL (Table 1.4). In 2018 and 2019, exposure to compost was followed by a significant increase of Pb and Zn extraction ha⁻¹ in CLL and a non-significant increase of Cd extraction, compared to the unamended block. The same trends were observed for Pb and Zn after biochar exposure, and biochar + compost exposure.

3.3. Soil properties after hemp cultivation

At the end of the first and the second year of cultivation, variable effects were observed depending on the site, the nature of the amendments, and the agronomic parameters of the soils considered (Table S1.1, Figure 1.6). During the whole experiment the soil pH was significantly lower in BB than in CLL (Table S1.1). Compared to the unamended block of BB, the only significant effect of soil amendment was recorded in 2019 and consisted in an unexpected decrease of soil pH in the block amended with biochar. In CLL, compared to the unamended block, all the amendments applied increased pH and decreased CEC (significant in 2018, trend in 2019).

To evaluate the evolution of soil parameters over time under hemp cultivation, comparisons were done between: (a) soil samples collected after the first year of hemp cultivation (T1 hemp) and soil sampled before the beginning of the experiment (T0); (b) between soil samples collected after the second year of hemp cultivation (T2 hemp) and soil samples collected after the first year of wheat cultivation (T1 wheat), to take into account the crop rotation between the first and the second year of experiment. The results are reported in Table S1.1 and illustrated in Figure 1.6. In BB, CEC significantly decreased after the first year of hemp cultivation and increased the following year. In each block of CLL, hemp significantly reduced CEC after the first year and decreased pH during the second one. Besides, soil samples collected in the unamended block of CLL in T1 were unexpectedly more concentrated in Pb than in T0. However, hemp significantly reduced Cd concentration in CLL in T2 compared to T1. We also observed, in BB and CLL, an increase of bioavailable Zn in soil sampled in T2 in all the amended blocks, compared to the same blocks in T1.

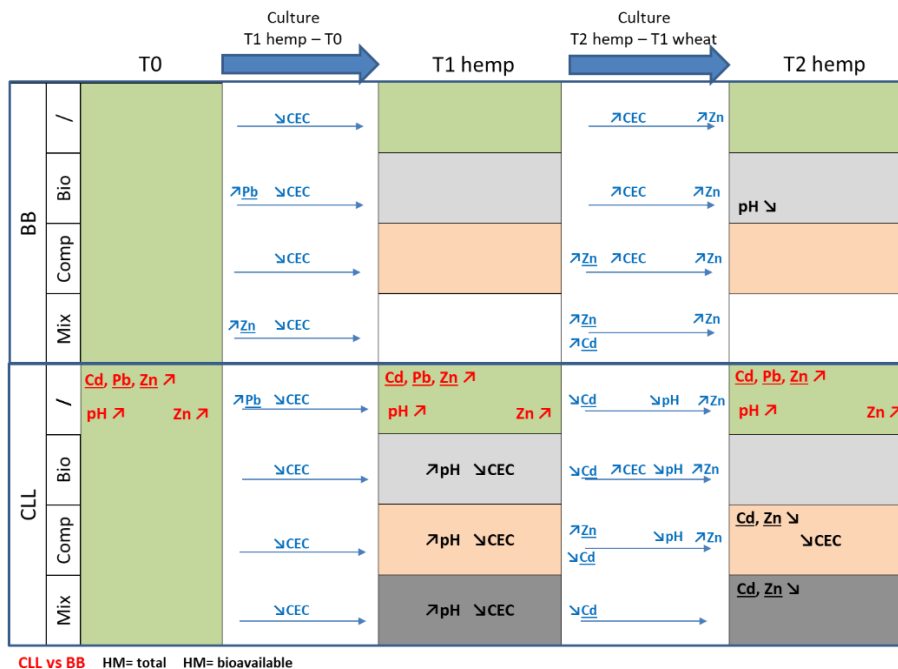


Figure 1.6: Heavy metal total concentration (\underline{Cd} , \underline{Pb} , \underline{Zn}), heavy metal bioavailability (\overline{Cd} , \overline{Pb} , \overline{Zn}), pH and cation exchange capacity (CEC) of soil samples collected before the beginning of the experiment (T0), after plant harvest in the area of each block under hemp cultivation in 2018 (T1 hemp), and after plant harvest in the area under hemp cultivation in 2019 (T2 hemp). The colors represent the experimental blocks set up in Bois-Bernard and Courcelles-lès-Lens: green: not amended, light grey: amended with biochar, orange: amended with compost, and dark grey: amended with biochar and compost. The columns below the arrows represent the impact over time of hemp cultivation on soil parameters, by comparisons of soil parameters between T1 hemp and T0, and T2 hemp and T1 wheat to consider the crop rotation between the first and the second year of experiment. Plants were grown 4 months on HM-contaminated soil of Courcelles-lès-Lens (CLL) or on control soil of Bois-Bernard (BB), in the presence or in the absence (/) of biochar (Bio), compost (Comp), or biochar and compost (Mix).

3.4. Influence of management methods on commercially utilizable hemp biomass

Heavy metal content in fibres, hurds and seeds

Soil contamination in CLL did not lead to a significant increase of Cd and Pb concentration in fibres, hurds and seeds comparatively to BB (Table 1.5).

Table 1.5: Cadmium, lead and zinc concentrations (in mg kg⁻¹ DW) in fibres, hurds and seeds of *C. sativa* (cv Futura 75). Plants were grown during 4 months on HM-contaminated soil of Courcelles-lès-Lens (CLL) or on control soil of Bois-Bernard (BB), in the presence or in the absence of biochar, compost, or biochar and compost (Mix). Data are means ± standard errors (*n*=3). For each element and plant part, values with different letters are significantly different at *P* < 0.05 according to the Tukey's HSD all-pairwise comparisons. Color code: significant impact of the site (CLL vs BB; blue) or, for each site, of the amendment (biochar, compost, mix) applied comparatively to the unamended block (green).

	Site	Block	Cd (mg kg ⁻¹ DM)	Pb (mg kg ⁻¹ DM)	Zn (mg kg ⁻¹ DM)
Fibres	BB	Unamended	0.050 ± 0.020 ac	0.74 ± 0.09 a	6.89 ± 1.39 bc
		Biochar	0.031 ± 0.006 a	1.01 ± 0.22 a	4.62 ± 1.35 ab
		Compost	0.044 ± 0.012 ac	0.87 ± 0.09 a	5.36 ± 1.03 ac
		Mix	0.030 ± 0.010 ab	0.99 ± 0.10 a	3.47 ± 1.00 a
	CLL	Unamended	0.061 ± 0.011 bc	0.91 ± 0.11 a	8.41 ± 1.78 c
		Biochar	0.046 ± 0.005 ac	1.05 ± 0.01 ab	5.62 ± 3.72 abc
		Compost	0.043 ± 0.009 ac	0.96 ± 0.15 a	2.42 ± 0.54 a
		Mix	0.065 ± 0.012 c	1.50 ± 0.34 b	4.55 ± 0.63 ab
Hurds	BB	Unamended	0.042 ± 0.006 a	1.41 ± 0.13 ab	6.63 ± 1.40 a
		Biochar	0.030 ± 0.005 b	1.73 ± 0.14 ac	5.85 ± 2.70 a
		Compost	0.032 ± 0.003 ab	1.30 ± 0.09 a	6.68 ± 2.53 a
		Mix	0.032 ± 0.001 b	1.80 ± 0.16 c	4.48 ± 0.95 a
	CLL	Unamended	0.048 ± 0.003 ab	1.85 ± 0.22 bc	3.18 ± 1.91 a
		Biochar	0.031 ± 0.005 ab	1.95 ± 0.18 c	6.52 ± 6.60 a
		Compost	0.046 ± 0.019 ab	1.77 ± 0.18 ac	5.45 ± 3.53 a
		Mix	0.044 ± 0.009 ab	1.74 ± 0.21 ac	5.22 ± 2.03 a
Seeds	BB	Unamended	0.057 ± 0.022 ac	0.21 ± 0.04 b	91.62 ± 5.67 b
		Biochar	0.041 ± 0.007 ab	0.35 ± 0.07 a	75.72 ± 5.78 a
		Compost	0.036 ± 0.005 a	0.30 ± 0.06 ab	87.03 ± 5.41 ab
		Mix	0.047 ± 0.008 ab	0.18 ± 0.04 b	88.88 ± 5.55 ab
	CLL	Unamended	0.079 ± 0.007 c	0.30 ± 0.13 ab	91.67 ± 7.61 ab
		Biochar	0.063 ± 0.006 bc	0.35 ± 0.21 ab	96.93 ± 10.97 ab
		Compost	0.044 ± 0.009 ab	0.27 ± 0.12 ab	92.64 ± 6.14 ab
		Mix	0.078 ± 0.010 c	0.21 ± 0.04 ab	90.85 ± 10.70 ab

Cd and Zn concentrations in fibres of plants grown on amended blocks tended to decrease compared to plants of unamended blocks in both BB and CLL, while Pb concentrations showed the opposite trend. These results were significant for Pb concentration in CLLmix treatment and Zn concentration in BBmix, CLLcomp and CLLmix treatments.

In hurds, the exposure to amendments also reduced Cd concentration (significant for BBbio and BBmix treatments) compare to plants of unamended blocks of BB and CLL. Exposure to biochar (in BB and CLL) tended to increase Pb concentration in hurds, while exposure to compost had the opposite effect on Pb concentration and tended to increase Zn concentration. In seeds, all the amendments used in both sites tended to decrease Cd concentration (significant for CLLcomp), exposure to biochar tended to increase Pb concentration (significant for BBbio) and finally exposure to biochar + compost tended to decrease Pb and Zn concentration in seeds compare to plants of unamended blocks.

Fibres' and hurds' mechanical properties

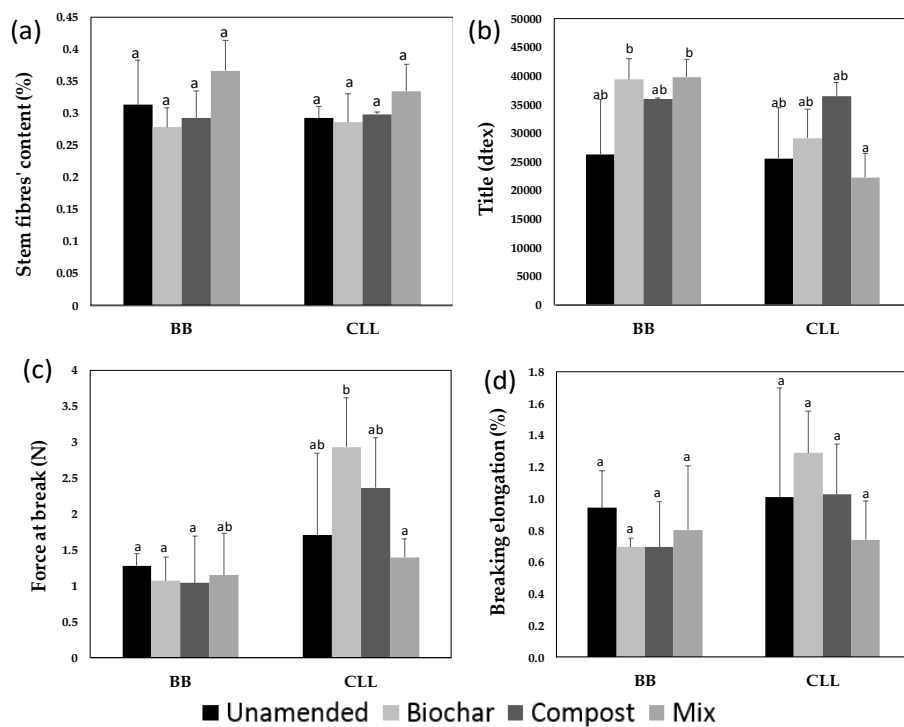


Figure 1.7: Characterisation of fibres. (a) stem fibres' content, (b) fibres bundles title (20-30 bundles, norm MO123, CELABOR), (c) force at break (N) and (d) breaking elongation (%) of fibres (10 fibres, norm XP T25-501-3, CELABOR). Plants were grown during 4 months on HM-contaminated soil of Courcelles-lès-Lens (CLL) or on control soil of Bois-Bernard (BB), in the presence or in the absence of biochar, compost, or biochar and compost (Mix). The different letters indicate that the values are significantly different from each other ($P < 0.05$; Tukey's HSD all-pairwise comparisons).

Soil contamination, as well as the amendments applied may also affect fibres' content and quality. The title of fibre bundles and fibre tensile strength are part of the parameters tested in industry to assess fibres quality. As illustrated in Figure 1.7, stem fibres content (%) and fibres mechanical properties were not significantly influenced by the site or the amendment applied. However, some trends can be observed. Force at break measured in the blocks of BB seemed to be lower than in CLL. In BB, exposure to amendments (biochar, compost, mix) tended to increase fibre bundles' title and decrease breaking elongation values (Figure 1.7b, d). In CLL, exposure to biochar or compost tended to increase force at break (Figure 1.7c), while biochar alone tended to increase breaking elongation values (Figure 1.7d). Moreover, in both sites, stem fibres' content tended to be higher in the presence of biochar + compost than in the absence of a soil amendment.

Analyses of the mechanical properties were supplemented by infra-red quantification of lignin, cellulose and hemicellulose contents in fibres and hurds (Figure 1.8). In fibres, only cellulose and hemicellulose were detected. The cellulose content in fibres (68.60%) was slightly lower, while hemicelluloses (18.47%) tended to increase in plants of unamended block in CLL compared to those grown in BB (70.95% and 17.18% respectively; Figure 1.8a). In CLL, exposure to biochar or compost tended to increase fibres' cellulose content (72.91% and 70.98% respectively), and biochar slightly decreased the hemicellulose content (15.97%). The same effects of amendments on cellulose and hemicellulose contents were observed in hurds of plants cultivated in CLL, while no differences were reported between the unamended blocks of BB and CLL (Figure 1.8b). Finally, hurds' lignin content was not significantly impacted by the site nor the amendment applied.

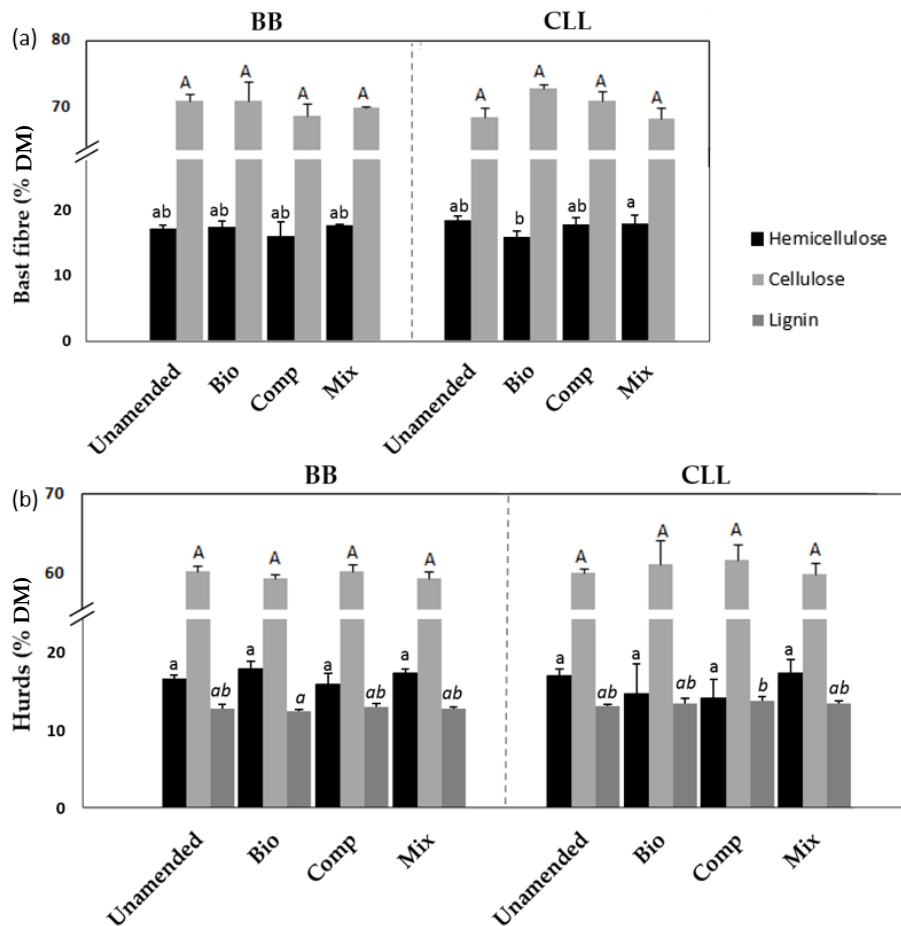


Figure 1.8: Infra-red prediction of the hemicellulose, cellulose and lignin contents within hemp fibres and hurds. Plants were grown 4 months (in 2019) on HM-contaminated soil of Courcelles-lès-Lens (CLL) or on control soil of Bois-Bernard (BB), in the presence or in the absence of biochar (Bio), compost (Comp), or biochar and compost (Mix). Statistical analysis were performed for the hemicellulose, cellulose (capital letters) and lignin (letters in italic) contents. The different letters indicate that the values are significantly different from each other ($P < 0.05$; Tukey's HSD all-pairwise comparisons).

4. Discussion

The contamination of agricultural soils with HM constitutes a major concern for human health and soil productivity in many regions across the world. The possibility to combine soil remediation with non-food production purposes,

thus providing incomes to farmers, is receiving more and more interest (Linger et al., 2002; Jaskulak et al., 2020). Hemp has already been mentioned as a good candidate for phytomanagement purposes, and non-food biomass produced offers multiple commercial applications (Baldini et al., 2018). Moreover, the use of amendments in order to improve crop behavior could help achieve this goal (Landi et al., 2019; Praspaliauskas et al., 2020; Zielonka et al., 2020).

Could hemp, grown on contaminated soil, be used for phytomanagement strategies?

Heavy metal tolerance is a key property that makes phytomanagement possible (Citterio et al., 2003; Luo et al., 2017; Saxena et al., 2019; Praspaliauskas et al., 2020). Hemp was shown to be tolerant to HM soil contamination: in this investigation, HM did not interfere significantly with photosynthesis and hemp growth, except a decrease of CO₂ concentration in intercellular spaces in 2019. Hemp ability to avoid cell damage by activating different molecular mechanisms, like increased phytochelatin synthesis, has already been reported in the literature (Citterio et al., 2003; Huang et al., 2019; Luyckx et al., 2021b; Xu et al., 2021). The low HM environmental availability recorded in our study also explains these results, since HM accumulation in shoot tissues remains compatible with the metabolic functions. Only a slight decrease of hemp yield was reported in 2018 and 2019 in the unamended block of CLL compared to the unamended block of BB, despite an obvious difference in Cd and Zn concentrations between the two sites. We may hypothesize the existence of a competition between HM and soil nutrients. This hypothesis is supported by the decrease of soil pH under hemp cultivation: plant roots have the ability to induce pH changes through specific processes, such as the excretion of organic acids to give organic salts in order to sustain ion uptake (Neina, 2019). Moreover, we observed a yield increase in CLL after biochar or compost exposure: biochar may have lowered HM bioavailability thus limiting competition with nutrients, while compost is known to contribute to the supply of essential nutrients (Beesley et al., 2010; Forján et al., 2016; Mudhoo et al., 2020). The maintenance of hemp yield in CLL was associated with a higher HM content in the leaves, thus confirming that this plant species is able to cope with internal accumulated toxic ions and not only to limit their absorption by the root system. Yield increase may also be explained by an increase of net photosynthesis values in CLLbio treatment.

The experimentation during 2 consecutive years has highlighted the variability of hemp behavior depending on microclimatic conditions. We might have expected a lower yield in 2018 due to drier and warmer conditions during the growth season than in 2019. However, we observed the opposite trend. Hemp is resistant to drought thanks to its deep root system (up to 3.5 m, *InterChanvre, 2017*), and the reduced yield in 2019 is more probably linked to competition between hemp and the weed *Chenopodium album* L.. In 2018, biochar and compost incorporation in soils before hemp sowing allowed to start the experiment without any weeds: soil treatment for amendments' incorporation indeed removed weed seedlings. In 2019, biochar and compost incorporation was not renewed and *Chenopodium album* L. was established before sowing. *Chenopodium album* is known to absorb nutrients very efficiently and is able to alter crop germination and growth: this weed may cause more than 90% loss in crop yields (Bajwa et al., 2019). Fortunately, due to hemp ability to grow rapidly (Bono et al., 2020), the yield decrease reported in our experiment was far less than 90%.

The low environmental availability of HM and the absence of a significant effect of soil contamination on hemp physiology suggest that plants accumulated very small and non-toxic concentrations of HM. Despite a low HM bioavailability in CLL, foliar concentrations of Cd, Pb and Zn (in 2018 and 2019) were significantly higher in plants (leaves, stems) sampled in this site compared to those harvested in BB. Interestingly, HM foliar concentrations tended to exceed stem concentrations, particularly during the second year of cultivation. We would expect the opposite in relation to the fixing property of fibres which is exploited in biosorption strategies (Pejic et al., 2011; Vukcevic et al., 2014; Vukčević et al., 2014) and the fact that the cell wall-mediated retention could also intervene *in planta*, during fibres' formation. Although unexpected, similar observations were also reported by Di Candito et al. (2004) in a field experiment and it suggests that HM transported by the xylem sap mainly accumulate in transpiring organs. The fact that HM were mainly accumulated in leaves highlight the importance to harvest hemp before natural leaf drop in order to maximize HM removal. Moreover, in case of higher HM accumulation in the stem, the retting process should be preferentially performed *ex-situ* in liquid medium rather than on the field to avoid HM transfer from the plant to the soil surface or from the soil surface to the valued parts of the harvested biomass.

To evaluate the hemp phytoextraction potential, the BF, as well as the mass of exported-HM $\text{ha}^{-1} \text{year}^{-1}$ were calculated. Cadmium, Pb and Zn

concentrations measured in above-ground biomass were considerably lower than soil concentrations, and the quantities of HM removed by the crop were modest, although not negligible. Similar BF and HM extraction values were obtained by Di Candito et al. (2004) in a field experiment with similar Cd soil concentration. It is nevertheless essential to keep in mind that, apart from the extraction capabilities of the plant, the bioavailability of HM in the soil is another crucial factor for phytoextraction efficiency (Di Candito et al., 2004). In our study, environmental bioavailability of HM estimated by classical CaCl_2 0.01 M procedure was extremely low. It is noteworthy, however, that phytoextraction potential and leaf HM concentrations of unamended sites were higher for plants growing on CLL than for those of BB, although the bioavailability did not strongly differ between the two sites. This prompted us to consider that a selective extraction procedure provides useful information but is not an exhaustive criteria of HM bioavailability, since the root-soil interaction is a dynamic process occurring during plant culture and that physiological activities of the root system could not be fully assessed by one single punctual estimation performed before the plant culture (Lambrechts et al., 2011). Besides, the unexpected increase of total Pb concentration in the unamended block of CLL in T1 probably results from hotspots of Pb contamination with the same origin as those detected at BB: CLL is close enough from BB (about 10 km from it) to be also impacted by the presence of some shrapnel issued from World War I.

Beside the above-mentioned distribution of HM in the shoot part, we may also expect that HM were only partially translocated from roots to shoots in order to preserve photosynthetically active parts of the plant. In an experiment conducted in nutrient solution contaminated with Cd, we demonstrated that this element was mainly accumulated in the roots (Luyckx, et al., 2021a) and similar results were obtained by Praspaliauskas et al., (2020). In our experimental conditions, hemp could therefore be used for phytostabilization rather than phytoextraction of HM: the vegetation cover can reduce the mobility and bioavailability of HM in the environment, the plant canopy reduces aeolian dispersion, while plant roots prevent water erosion, immobilize HM and prevent leaching (Wang et al., 2017). However, in conditions of higher HM bioavailability, various authors have shown hemp to be more efficient in removing HM (Citterio et al., 2003; Linger et al., 2005). Moreover, hemp is much better suited for phytomanagement than most other crops due to its higher biomass yield, deeper soil restoration through a well-developed root system and greater adaptability to different soil and climatic

conditions (Husain et al., 2019; Pietrini et al., 2019). HM bioavailability could be improved through the use of chelating agents (such as EDTA, EDDS or NTA) (Ferrarini et al., 2021). However, they should be used carefully to prevent seepage of the solubilized metals into deeper layers of the soil and groundwater (Di Candito et al., 2004). Moreover, if the purpose is to be able to exploit contaminated soils, the optimal balance between HM extraction, their concentration in the commercial parts of the plant, and sufficient plant development must be met. In this perspective, the use of amendments to better guarantee the establishment of a plant cover is of particular interest (Peralta-Videa et al., 2009; Chowdhury et al., 2016; Luo et al., 2017; Meena et al., 2018). In our study, the addition of biochar, compost or biochar and compost induced a significant decrease of CEC and an increase of soil pH. Neutralization of soil acidity is one of the well documented effect of biochar in soils (Biederman & Harpole, 2013; Rodríguez-Vila et al., 2016; El-Naggar et al., 2019), but the decrease of CEC constitutes an unexpected result. It is thus difficult to precisely determine the impact of these amendments on HM bioavailability, especially when the concentrations of Cd and Pb extracted with CaCl_2 are lower than the detection limits, as it was the case in this study.

HM concentrations in stems increased on the blocks amended with compost, as well as HM extraction ($\text{g ha}^{-1} \text{ year}^{-1}$). Biochar and compost may have favored the development of hemp roots in addition to yield increase, especially during the dry summer of 2018 and both amendments are known to improve water retention in soils (Mudhoo et al., 2020; Barquilha and Braga, 2021). However, compost did not significantly increased the transpiration rate which could have enhanced HM translocation from the root to the shoot (Table 1.3). Another hypothesis could be that xylem loading was influenced by amendments and that a more concentrated xylem sap afforded more HM, even in the absence of any transpiration increase.

We also observed a change in HM distribution in plants cultivated on the amended blocks of CLL: stem concentrations tended to increase while leaf concentrations followed the opposite trend, compared to the unamended block of CLL. Biochar and compost could thus improve plant behavior by limiting HM concentration in photosynthetically active parts of the plants while increasing HM extraction ha^{-1} via yield increase. Exposure to both biochar and compost did not affect hemp yield, but tended to increase HM extraction $\text{ha}^{-1} \text{ year}^{-1}$ in CLL but differences between mix and single treatments remained rather low.

Besides, HM concentrations in plants were higher in 2019 compared to 2018. In 2019, hemp was grown on the area of each block under wheat cultivation in 2018. Wheat could have affected HM bioavailability in 2018, thus making them more available in 2019.

Could hemp, grown on contaminated soil, be used as raw material for commercial applications?

The major factors that impact the possibility to use the biomass produced on HM-contaminated soil include the contaminant concentration in the biomass, the type of product used and regulatory standards/guidelines on acceptable product quality (Rheay et al., 2020).

Soil contamination had no significant influence on fibres' and hurds' properties, probably due to the low HM bioavailability. However, some trends emerged: fibres seemed to be stronger (increased tensile strength) in CLL, with lower cellulose content, but higher hemicellulose and HM contents compared to BB. Cadmium has already been reported to negatively affect cellulose biosynthesis in fibres (Luyckx, et al., 2021b). Metal ions are mainly adsorbed at carboxylic groups (mainly found in hemicelluloses and pectins), and to some extent hydroxyl and carbonyl groups (Pejic et al., 2009). It is therefore not surprising to detect higher hemicellulose and HM contents in fibres of plants issued from CLL. To be used in clothes production, HM concentrations in hemp fibres should not exceed the STANDARD 100 by OEKO-TEX, which are 0.1 mg kg^{-1} for Cd and $0.2\text{--}1.0 \text{ mg kg}^{-1}$ Pb. In the current study, this commercial applications are not recommended, but contaminated fibres and hurds could be safely used in biocomposites where HM could not be set free (insulating material and cement agglomerates in bioconstruction, as a sound absorbent material in the automotive industry, ...) or to produce energy in thermal power stations with controlled incineration (Linger et al., 2002; Di Candito et al., 2004; Evangelou et al., 2015). Moreover, hemp-derived biofuels can replace gasoline for diesel engines without any needed modifications, and they produce less greenhouse gas carbon monoxide, potentially helping relieve global warming (Crini et al., 2020). Exposure to biochar or compost slightly lowered HM contents in fibres, and this material could therefore make clothes' production possible on moderately contaminated soils. Besides, fibres produced on contaminated soil amended with biochar or compost tended to be thicker (higher fibre bundles' title values) and more resistant (tensile strength), with higher cellulose contents. The experiment should be conducted several years to confirm these

results, but the possibility to adapt hurds' and fibres' properties to the particular needs of industries through soil amendment is an exciting perspective.

When plants were harvested, seeds were also collected. Soil contamination did not significantly affect HM contents in seeds. Hemp seeds have a high nutraceutical potential (Frassinetti et al., 2018). However, the use of our harvested seeds for human food, although unlikely on this type of site, is excluded: in CLL, Pb concentrations in seeds exceeded the maximum limit allowed in cereals, vegetables and legumes (0.20 mg Pb kg⁻¹ fresh weight), even if Cd concentration was below the limit (0.1 mg Cd kg⁻¹; Commission Regulation (EC) No 1881/2006 of 19 December 2006). Hemp seeds could instead be used in animal feed (maximum content in feed materials of vegetable origin: 1 mg Cd kg⁻¹; 5-40 mg Pb kg⁻¹; Directive 2002/32/EC), in lacquer or industrial oil production, as well as in biodiesel production (Viswanathan et al., 2021). Interestingly, exposure to compost or both biochar and compost allowed to obtain seeds with lower Pb concentrations.

5. Conclusion

Hemp growth and yield were found to be marginally affected by soil contamination: only a slight yield decrease was reported in CLL and the plants exhibited the same photosynthetic fitness than in BB. Hemp phytoextraction potential was limited by the low HM environmental availability in CLL, but fibres and hurds quality was similar to those in BB thus not representing a limit to its multiple non-food uses and making this contaminated soil potentially productive. Biochar and compost applied separately were found to be an interesting option to improve yield, to obtain less contaminated biomass and to produce fibres and hurds with specific properties.

Acknowledgement

This work was financed by ADEME (French Agency for the Environment and Energy Management; Convention MisChar n°1672C0044). The authors are grateful to Aurélien Dubar and Arnaud Lefebvre (LGCgE) for fibre preparation and soil samples analysis, to Mr. X. Joppin (Celabor - Research and Testing Centre in Food, Packaging, Environmental and Textile Technologies) for his valuable help in fibre analysis, and Mrs. M. Quinet for her valuable help for statistical analysis.

Table S1.1: Soil characterization before crop set up (T0) and after the first and the second years of hemp/wheat culture on HM-contaminated soil of Courcelles-lès-Lens (CLL) or on control soil of Bois-Bernard (BB), in the presence or in the absence of biochar, compost, or biochar and compost (Mix). Data are means \pm standard errors ($n=3$). For a specific time (T0, T1, T2) and culture (hemp, wheat), values with different letters are significantly different at $P < 0.05$. Color code: significant impact of the site (CLL vs BB; blue) or, for each site, of the amendment (biochar, compost, mix) applied comparatively to the unamended block (green).

	Site	Block	Pseudo-total concentration (mg kg ⁻¹ DM)			CaCl ₂ (0.01 M) extraction (mg kg ⁻¹ DM)			pH (water)	Exchangeable cations	
			Cd	Pb	Zn	Cd	Pb	Zn	NF ISO 10390	NF X31-130	
									NF ISO 10390	CEC	
T0	B	Unamended	1.11 \pm 0.06 a	259 \pm 115 a	81 \pm 4 a	<0.05	<0.64	0.09 \pm 0.09 a	7.04 \pm 0.20 a	17.50 \pm 0.57 a	
	C	Unamended	5.54 \pm 0.25 b	298 \pm 21 a	396 \pm 32 b	<0.05	<0.64	0.18 \pm 0.08 a	7.91 \pm 0.11 b	17 \pm 1.89 a	
T1	Hemp	Unamended	0.94 \pm 0.03 a	310 \pm 0.79 a	80 \pm 2 a	<0.05	1.01 \pm 0.25 a	0.07 \pm 0.01 a	7.35 \pm 0.12 ab	13.72 \pm 0.41 ab	
		BB	Biochar	1.00 \pm 0.04 a	451 \pm 215 a	83 \pm 2 a	<0.05	<0.87	0.06 \pm 0.02 a	7.23 \pm 0.14 a	13.42 \pm 0.86 a
		BB	Compost	0.97 \pm 0.01 a	156 \pm 29 a	98 \pm 29 a	<0.05	<0.64	<0.02	7.62 \pm 0.11 b	13.13 \pm 0.32 a
		BB	Mix	0.90 \pm 0.06 a	271 \pm 48 a	94 \pm 4 a	<0.05	0.93 \pm 0.12 a	0.08 \pm 0.02 a	7.49 \pm 0.16 ab	13.58 \pm 0.18 a
		CLL	Unamended	5.86 \pm 0.54 b	442 \pm 178 a	354 \pm 21 b	<0.05	<0.64	0.26 \pm 0.05 b	7.65 \pm 0.11 b	14.80 \pm 0.28 b
		CLL	Biochar	5.79 \pm 0.46 b	322 \pm 43 a	365 \pm 310 b	<0.05	<0.64	0.22 \pm 0.02 b	8.00 \pm 0.08 c	12.82 \pm 0.25 a
	Wheat	BB	Compost	6.08 \pm 0.06 b	344 \pm 13 a	383 \pm 15 b	<0.05	<0.64	0.27 \pm 0.11 b	8.02 \pm 0.06 c	12.99 \pm 0.24 a
		BB	Mix	5.55 \pm 0.16 b	310 \pm 31 a	354 \pm 19 b	<0.05	<0.64	0.22 \pm 0.06 b	8.07 \pm 0.17 c	13.27 \pm 0.41 a
		CLL	Unamended	1.00 \pm 0.10 a	283 \pm 96 a	92 \pm 11 a	<0.05	<0.64	0.07 \pm 0.02 a	6.99 \pm 0.10 a	13.43 \pm 0.07 a
		CLL	Biochar	0.86 \pm 0.07 a	313 \pm 77 a	141 \pm 98 a	<0.05	1.00 \pm 0.34	<0.03	7.32 \pm 0.28 a	13.73 \pm 0.39 ab
		CLL	Compost	0.95 \pm 0.10 a	251 \pm 33 a	89 \pm 1 a	<0.05	<0.64	0.03 \pm 0.02 a	7.12 \pm 0.18 a	13.38 \pm 0.37 a
		CLL	Mix	0.77 \pm 0.03 a	276 \pm 123 a	95 \pm 2 a	<0.05	<0.64	<0.03	7.37 \pm 0.05 a	14.40 \pm 0.05 b
T2	Hemp (T1: wheat)	Unamended	5.90 \pm 0.48 b	342 \pm 31 a	404 \pm 43 b	0.07 \pm 0.01	<0.64	0.24 \pm 0.02 b	7.87 \pm 0.05 b	15.37 \pm 0.18 c	
		BB	Biochar	5.48 \pm 0.11 b	293 \pm 22 a	377 \pm 38 b	<0.06	<0.64	0.19 \pm 0.02 b	7.96 \pm 0.11 b	13.23 \pm 0.31 a
		BB	Compost	5.44 \pm 0.28 b	295 \pm 7 a	352 \pm 33 b	<0.05	<0.64	0.15 \pm 0.03 b	8.01 \pm 0.10 b	13.18 \pm 0.50 a
		BB	Mix	5.65 \pm 0.26 b	322 \pm 26 a	386 \pm 33 b	<0.07	<0.64	0.23 \pm 0.03 b	7.86 \pm 0.05 b	14.01 \pm 0.71 ab
		CLL	Unamended	1.18 \pm 0.07 a	392 \pm 299 a	106 \pm 5 a	<0.05	<0.64	0.13 \pm 0.01 a	7.40 \pm 0.17 bcd	14.56 \pm 0.58 ab
		CLL	Biochar	1.08 \pm 0.11 a	265 \pm 80 a	107 \pm 7 a	<0.05	<0.64	0.16 \pm 0.03 a	7.10 \pm 0.11 a	14.52 \pm 0.21 ab
	Wheat (T1: hemp)	BB	Compost	1.15 \pm 0.07 a	234 \pm 138 a	103 \pm 4 a	<0.05	<0.64	0.14 \pm 0.02 a	7.17 \pm 0.07 ab	14.68 \pm 0.32 b
		BB	Mix	1.04 \pm 0.06 a	463 \pm 88 a	126 \pm 16 a	<0.05	<0.64	0.13 \pm 0.01 a	7.35 \pm 0.11 ac	14.89 \pm 0.05 b
		CLL	Unamended	4.99 \pm 0.17 c	344 \pm 10 a	451 \pm 13 c	0.09 \pm 0.02 a	<0.64	0.30 \pm 0.02 b	7.63 \pm 0.04 e	15.31 \pm 0.40 b
		CLL	Biochar	4.81 \pm 0.04 bc	307 \pm 10 a	435 \pm 15 bc	0.08 \pm 0.02 a	<0.64	0.30 \pm 0.01 b	7.69 \pm 0.06 e	14.48 \pm 0.24 ab
		CLL	Compost	4.62 \pm 0.17 b	301 \pm 9 a	416 \pm 3 b	0.08 \pm 0.01 a	<0.64	0.27 \pm 0.03 b	7.72 \pm 0.04 e	13.62 \pm 0.41 a
		CLL	Mix	4.55 \pm 0.11 b	303 \pm 27 a	413 \pm 8 b	0.08 \pm 0.02 a	<0.64	0.25 \pm 0.02 b	7.66 \pm 0.12 de	14.89 \pm 0.22 b
Wheat (T1: hemp)	BB	Unamended	0.29 \pm 0.21 a	314 \pm 169 a	86 \pm 8 a	<0.05	<0.64	0.12 \pm 0.02 a	7.15 \pm 0.06 a	13.60 \pm 0.55 a	
	BB	Biochar	0.43 \pm 0.09 a	243 \pm 20 a	81 \pm 2 a	<0.05	<0.64	0.12 \pm 0.00 a	7.10 \pm 0.09 a	13.83 \pm 0.71 a	
	BB	Compost	0.25 \pm 0.11 a	250 \pm 203 a	79 \pm 1 a	<0.05	<0.64	0.08 \pm 0.01 a	7.39 \pm 0.23 ac	13.13 \pm 0.28 a	
	BB	Mix	0.48 \pm 0.19 a	261 \pm 85 a	83 \pm 5 a	<0.05	<0.64	0.13 \pm 0.02 a	7.30 \pm 0.19 ab	14.19 \pm 1.72 a	
	CLL	Unamended	5.46 \pm 0.50 b	308 \pm 27 a	407 \pm 35 b	0.09 \pm 0.00 a	<0.64	0.31 \pm 0.03 b	7.58 \pm 0.08 bc	15.05 \pm 1.08 a	
	CLL	Biochar	5.74 \pm 0.21 b	310 \pm 4 a	453 \pm 9 b	0.07 \pm 0.01 a	<0.64	0.31 \pm 0.03 b	7.70 \pm 0.02 c	12.80 \pm 0.88 a	
Wheat (T1: hemp)	CLL	Compost	6.9 \pm 2.98 b	349 \pm 138 a	559 \pm 160 b	0.08 \pm 0.01 a	<0.66	0.31 \pm 0.06 b	7.71 \pm 0.03 c	13.2 \pm 1.38 a	
	CLL	Mix	5.23 \pm 0.30 b	294 \pm 25 a	412 \pm 35 b	0.08 \pm 0.01 a	<0.64	0.30 \pm 0.04 b	7.61 \pm 0.05 bc	13.75 \pm 0.85 a	

Table S1.2: Physicochemical parameters of compost produced by Agriopale ($n=3$)

Compost (Agriopale)		
Organic C	g kg ⁻¹	187 ± 12
Total N	g kg ⁻¹	16.3 ± 1.0
C/N		11.1 ± 0.2
Organic matter	g kg ⁻¹	374 ± 25
N-NH4	g kg ⁻¹	<0.05
NNO3	g kg ⁻¹	0.31 ± 0.30
Organic N	g kg ⁻¹	15.9 ± 1.2
Ca	g kg ⁻¹	46.23 ± 12.22
Mg	g kg ⁻¹	2.57 ± 0.33
P₂O₃	g kg ⁻¹	5.53 ± 0.30
K	g kg ⁻¹	10.87 ± 1.30
Cd	mg kg ⁻¹	0.33 ± 0.06
Pb	mg kg ⁻¹	26.1 ± 7.2
Zn	mg kg ⁻¹	134 ± 5

Table S1.3: Physicochemical parameters of biochar produced by ETIA ($n=4$)

Biochar (VTGreen. LGCgE-JUNIA. SADEF)		
Parent material		Miscanthus
T	°C	500
Duration	min	15
pH		9.8 ± 0.2
Total CaCO₃	g kg ⁻¹	16.2 ± 5.5
Total C	%	79.7 ± 2.02
Total H	%	2.73 ± 0.23
Total N	%	0.49 ± 0.03
Total O	%	5.51 ± 3.70
Volatile matter	%	12.15 ± 2.34
Specific surface area	m ² g ⁻¹	127.65 ± 10.96
Density	g cm ⁻³	0.44 ± 0.006
Porosity	%	68.92 ± 0.4
Ash	%	11.6 ± 2.1
H/C (aromaticity)		0.034 ± 0.004
O/C (hydrophobicity)		0.070 ± 0.048
(O+N)/C (polarity)		0.076 ± 0.048
Cd	mg kg ⁻¹	0.55 ± 0.15
Pb	mg kg ⁻¹	28.52 ± 30.52
Zn	mg kg ⁻¹	212 ± 24

Table S1.4: Accumulated rainfall and average temperature over the period of physiological measurements, as well as over the entire vegetation period in 2018 and 2019.

Lille-Lesquin weather station								
2018		April (15-30)	May (1-31)	June (1-30)	July (1-31)	August (1-20)	Physiological measurement period	Vegetation period
		Accumulated rainfall (mm)	28.6	85.1	7.7	13.8	22.9	Total: 44.4
	Average temperature (°C)	14.75	16.06	18.00	22.40	20.96	Mean: 20.45	Mean: 23.04
2019		May (15-31)	June (1-30)	July (1-31)	August (1-31)	Septem ber (1- 20)	Physiological measurement period	Vegetation period
		Accumulated rainfall (mm)	15.3	78.8	26.6	36.5	10.4	Total: 77.1
	Average temperature (°C)	15.46	18.54	18.82	18.56	15.82	Mean: 17.73	Mean: 21.80

Table S1.5: Photosynthesis-related parameters of *C. sativa* (cv Futura 75), recorded 11, 15 and 17 weeks after plant sowing. Plants were grown on HM-contaminated soil of Courcelles-lès-Lens (CLL) or on control soil of Bois-Bernard (BB) in the presence or in the absence of biochar, compost or biochar and compost (Mix). Data are means \pm standard errors ($n=5$). For each column and year, values with different letters are significantly different at $P < 0.05$ according to the Tukey's HSD all-pairwise comparisons. Color code: significant impact of the site (CLL vs BB; blue), the week, or, for each site, of the amendment comparatively to the unamended block (green).

Year	Site	Block	Week	F_v/F_m	φ_{PS2}	qP	NPQ	C_i ($\mu\text{mol mol}^{-1}$)	E ($\text{mmol H}_2\text{O m}^{-2}\text{s}^{-1}$)	A ($\mu\text{mol CO}_2 \text{ m}^{-2}\text{s}^{-1}$)	SC ($\text{mmol m}^{-2}\text{s}^{-1}$)
	2018	BB	Unamended	11	0.85 \pm 0.03 a	0.76 \pm 0.05 a	0.93 \pm 0.04 a	0.24 \pm 0.03 a	235 \pm 35 ad	3.02 \pm 0.90 bd	10.83 \pm 4.78 df
15				0.87 \pm 0.00 a	0.76 \pm 0.03 a	0.91 \pm 0.04 a	0.30 \pm 0.06 a	235 \pm 42 ad	1.52 \pm 0.49 ab	3.13 \pm 1.58 ab	309 \pm 264 ac
17				0.86 \pm 0.02 a	0.77 \pm 0.03 a	0.93 \pm 0.03 a	0.30 \pm 0.20 a	333 \pm 24 cd	2.06 \pm 0.69 ad	3.28 \pm 1.23 abd	304 \pm 36 ac
Biochar			11	0.80 \pm 0.04 a	0.69 \pm 0.03 a	1.00 \pm 0.09 a	0.52 \pm 0.22 a	266 \pm 42 ad	3.64 \pm 0.39 cd	11.16 \pm 2.14 ef	223 \pm 68 ac
			15	0.81 \pm 0.05 a	0.70 \pm 0.05 a	0.95 \pm 0.02 a	0.33 \pm 0.17 a	222 \pm 32 ad	3.77 \pm 1.38 d	6.97 \pm 3.07 abf	145 \pm 76 ac
			17	0.79 \pm 0.03 a	0.77 \pm 0.03 a	0.96 \pm 0.03 a	0.27 \pm 0.09 a	281 \pm 18 ad	1.72 \pm 0.44 abc	4.63 \pm 2.04 abde	268 \pm 63 ac
Compost			11	0.88 \pm 0.01 a	0.79 \pm 0.04 a	0.94 \pm 0.04 a	0.37 \pm 0.05 a	255 \pm 42 ad	3.06 \pm 0.86 bd	8.98 \pm 2.98 bcf	219 \pm 135 ac
			15	0.84 \pm 0.04 a	0.76 \pm 0.02 a	0.95 \pm 0.09 a	0.29 \pm 0.15 a	237 \pm 49 ad	2.30 \pm 1.10 ad	5.09 \pm 2.80 abde	266 \pm 139 ac
			17	0.85 \pm 0.01 a	0.80 \pm 0.01 a	0.95 \pm 0.01 a	0.20 \pm 0.03 a	304 \pm 57 ad	2.19 \pm 0.22 ad	6.65 \pm 3.83 abf	393 \pm 217 ac
Mix			11	0.84 \pm 0.08 a	0.75 \pm 0.00 a	1.00 \pm 0.07 a	0.45 \pm 0.35 a	263 \pm 62 ad	3.14 \pm 0.42 bd	9.67 \pm 5.02 bf	241 \pm 202 ac
			15	0.85 \pm 0.01 a	0.74 \pm 0.04 a	0.91 \pm 0.05 a	0.29 \pm 0.11 a	238 \pm 30 ad	2.64 \pm 0.36 ad	4.82 \pm 1.57 abde	412 \pm 248 c
			17	0.83 \pm 0.02 a	0.78 \pm 0.02 a	0.95 \pm 0.02 a	0.19 \pm 0.05 a	330 \pm 37 cd	2.11 \pm 0.10 ad	3.76 \pm 2.87 abde	442 \pm 274 bc
CLL		Control	11	0.80 \pm 0.02 a	0.71 \pm 0.04 a	0.98 \pm 0.04 a	0.35 \pm 0.16 a	315 \pm 52 cd	1.95 \pm 1.33 abc	1.66 \pm 1.59 a	104 \pm 22 ac
			15	0.81 \pm 0.04 a	0.73 \pm 0.03 a	0.95 \pm 0.05 a	0.28 \pm 0.12 a	213 \pm 31 ac	1.99 \pm 1.05 abc	3.31 \pm 1.74 ab	37 \pm 12 a
			17	0.81 \pm 0.00 a	0.74 \pm 0.03 a	0.97 \pm 0.02 a	0.25 \pm 0.04 a	259 \pm 101 ad	1.55 \pm 0.34 ab	4.41 \pm 3.64 abde	375 \pm 152 ac
		Biochar	11	0.85 \pm 0.07 a	0.73 \pm 0.08 a	0.92 \pm 0.17 a	0.44 \pm 0.44 a	303 \pm 67 bcd	1.23 \pm 0.17 a	2.54 \pm 2.41 ac	140 \pm 104 ac
			15	0.83 \pm 0.03 a	0.72 \pm 0.05 a	0.93 \pm 0.05 a	0.27 \pm 0.17 a	229 \pm 62 ad	1.23 \pm 0.38 a	3.11 \pm 1.52 ab	93 \pm 45 ab
			17	0.84 \pm 0.03 a	0.67 \pm 0.13 a	0.91 \pm 0.10 a	0.25 \pm 0.14 a	311 \pm 21 bcd	1.62 \pm 0.37 ab	3.81 \pm 1.13 abde	236 \pm 60 ac
		Compost	11	0.80 \pm 0.08 a	0.76 \pm 0.02 a	0.93 \pm 0.03 a	0.10 \pm 0.08 a	248 \pm 54 ad	1.74 \pm 0.41 ab	6.70 \pm 2.95 abf	104 \pm 65 ac
			15	0.86 \pm 0.06 a	0.78 \pm 0.05 a	0.95 \pm 0.03 a	0.23 \pm 0.06 a	249 \pm 56 ad	2.10 \pm 0.92 ad	4.63 \pm 3.03 abde	54 \pm 20 a
			17	0.87 \pm 0.01 a	0.78 \pm 0.03 a	0.96 \pm 0.02 a	0.18 \pm 0.06 a	348 \pm 26 d	1.73 \pm 0.14 abc	2.26 \pm 1.97 ab	277 \pm 147 ac
		Mix	11	0.84 \pm 0.08 a	0.74 \pm 0.06 a	0.93 \pm 0.12 a	0.37 \pm 0.15 a	258 \pm 41 ad	2.39 \pm 0.77 ad	5.50 \pm 2.76 abde	92 \pm 48 ab
			15	0.82 \pm 0.02 a	0.71 \pm 0.07 a	0.92 \pm 0.04 a	0.31 \pm 0.19 a	198 \pm 21 ad	2.30 \pm 0.19 ad	5.22 \pm 1.36 abde	72 \pm 29 a
			17	0.85 \pm 0.01 a	0.76 \pm 0.01 a	0.95 \pm 0.02 a	0.20 \pm 0.17 a	278 \pm 45 ad	1.46 \pm 0.45 ab	4.39 \pm 3.01 abde	232 \pm 44 ac

2019	Site	Block	Week	F_w/F_m	φ_{PS2}	qP	NPQ	C_i ($\mu\text{mol mol}^{-1}$)	E ($\text{mmol H}_2\text{O m}^{-2}\text{s}^{-1}$)	A ($\mu\text{mol CO}_2 \text{ m}^{-2}\text{s}^{-1}$)	SC ($\text{mmol m}^{-2}\text{s}^{-1}$)
	BB	Unamended	11	0.87 ± 0.01 b	0.79 ± 0.05	0.94 ± 0.04 a	0.25 ± 0.07 a	330 ± 35	2.59 ± 0.36	4.89 ± 2.38	295 ± 99
0.84 ± 0.03				0.65 ± 0.13	0.92 ± 0.02 a	0.43 ± 0.05 a	349 ± 35	1.08 ± 0.37 ac	1.75 ± 0.93	202 ± 88	
0.82 ± 0.07				0.65 ± 0.17	0.89 ± 0.94	392 ± 26	0.82 ± 0.73	138 ±			
15			0.82 ± 0.07	0.65 ± 0.17	0.89 ± 0.94	392 ± 26	0.82 ± 0.73	138 ±			
			0.82 ± 0.07	0.65 ± 0.17	0.89 ± 0.94	392 ± 26	0.82 ± 0.73	138 ±			
			0.82 ± 0.07	0.65 ± 0.17	0.89 ± 0.94	392 ± 26	0.82 ± 0.73	138 ±			
17			0.82 ± 0.07	0.65 ± 0.17	0.89 ± 0.94	392 ± 26	0.82 ± 0.73	138 ±			
			0.82 ± 0.07	0.65 ± 0.17	0.89 ± 0.94	392 ± 26	0.82 ± 0.73	138 ±			
			0.82 ± 0.07	0.65 ± 0.17	0.89 ± 0.94	392 ± 26	0.82 ± 0.73	138 ±			
Biochar			11	0.86 ± 0.01 b	0.79 ± 0.02 b	0.95 ± 0.04 a	0.20 ± 0.08 a	273 ± 67	3.60 ± 0.61 hi	10.47 ± 7.34	304 ± 78
				0.86 ± 0.01 b	0.79 ± 0.02 b	0.95 ± 0.04 a	0.20 ± 0.08 a	273 ± 67	3.60 ± 0.61 hi	10.47 ± 7.34	304 ± 78
				0.86 ± 0.01 b	0.79 ± 0.02 b	0.95 ± 0.04 a	0.20 ± 0.08 a	273 ± 67	3.60 ± 0.61 hi	10.47 ± 7.34	304 ± 78
		15	0.77 ± 0.06 a	0.58 ± 0.16 a	0.99 ± 0.01 a	0.47 ± 0.15 a	318 ± 50	1.17 ± 0.55 ac	1.96 ± 0.79	142 ± 34	
			0.77 ± 0.06 a	0.58 ± 0.16 a	0.99 ± 0.01 a	0.47 ± 0.15 a	318 ± 50	1.17 ± 0.55 ac	1.96 ± 0.79	142 ± 34	
			0.77 ± 0.06 a	0.58 ± 0.16 a	0.99 ± 0.01 a	0.47 ± 0.15 a	318 ± 50	1.17 ± 0.55 ac	1.96 ± 0.79	142 ± 34	
17		0.82 ± 0.05	0.58 ± 0.14	0.98 ± 0.04 a	1.44 ± 0.62 b	333 ± 50	0.55 ± 0.22 ac	2.42 ± 1.60	70 ± 10		
		0.82 ± 0.05	0.58 ± 0.14	0.98 ± 0.04 a	1.44 ± 0.62 b	333 ± 50	0.55 ± 0.22 ac	2.42 ± 1.60	70 ± 10		
		0.82 ± 0.05	0.58 ± 0.14	0.98 ± 0.04 a	1.44 ± 0.62 b	333 ± 50	0.55 ± 0.22 ac	2.42 ± 1.60	70 ± 10		
Compost		11	0.87 ± 0.01 b	0.80 ± 0.02 b	0.95 ± 0.02 a	0.18 ± 0.05 a	312 ± 68	2.76 ± 0.73	8.77 ± 7.90	304 ± 75	
			0.84 ± 0.02	0.69 ± 0.12	0.96 ± 0.03 a	0.48 ± 0.26 a	330 ± 64	0.90 ± 0.18 ac	4.76 ± 3.75	440 ± 70	
			0.84 ± 0.02	0.69 ± 0.12	0.96 ± 0.03 a	0.48 ± 0.26 a	330 ± 64	0.90 ± 0.18 ac	4.76 ± 3.75	440 ± 70	
		15	0.86 ± 0.01 b	0.74 ± 0.03	0.95 ± 0.03 a	0.64 ± 0.07	396 ± 45 e	0.75 ± 0.30 ac	1.19 ± 0.81	42 ± 14 a	
			0.86 ± 0.01 b	0.74 ± 0.03	0.95 ± 0.03 a	0.64 ± 0.07	396 ± 45 e	0.75 ± 0.30 ac	1.19 ± 0.81	42 ± 14 a	
			0.86 ± 0.01 b	0.74 ± 0.03	0.95 ± 0.03 a	0.64 ± 0.07	396 ± 45 e	0.75 ± 0.30 ac	1.19 ± 0.81	42 ± 14 a	
17	0.86 ± 0.01 b	0.74 ± 0.03	0.95 ± 0.03 a	0.64 ± 0.07	396 ± 45 e	0.75 ± 0.30 ac	1.19 ± 0.81	42 ± 14 a			
	0.86 ± 0.01 b	0.74 ± 0.03	0.95 ± 0.03 a	0.64 ± 0.07	396 ± 45 e	0.75 ± 0.30 ac	1.19 ± 0.81	42 ± 14 a			
	0.86 ± 0.01 b	0.74 ± 0.03	0.95 ± 0.03 a	0.64 ± 0.07	396 ± 45 e	0.75 ± 0.30 ac	1.19 ± 0.81	42 ± 14 a			
Mix	11	0.86 ± 0.01 b	0.78 ± 0.03	0.93 ± 0.01 a	0.19 ± 0.13 a	316 ± 70	3.13 ± 0.39	5.75 ± 4.91	221 ± 39		
		0.82 ± 0.05	0.62 ± 0.16	0.91 ± 0.01 a	0.32 ± 0.16 a	322 ± 56	1.83 ± 0.53	4.79 ± 3.61	227 ± 76		
		0.82 ± 0.05	0.62 ± 0.16	0.91 ± 0.01 a	0.32 ± 0.16 a	322 ± 56	1.83 ± 0.53	4.79 ± 3.61	227 ± 76		
	15	0.82 ± 0.05	0.62 ± 0.16	0.91 ± 0.01 a	0.32 ± 0.16 a	322 ± 56	1.83 ± 0.53	4.79 ± 3.61	227 ± 76		
		0.82 ± 0.05	0.62 ± 0.16	0.91 ± 0.01 a	0.32 ± 0.16 a	322 ± 56	1.83 ± 0.53	4.79 ± 3.61	227 ± 76		
		0.82 ± 0.05	0.62 ± 0.16	0.91 ± 0.01 a	0.32 ± 0.16 a	322 ± 56	1.83 ± 0.53	4.79 ± 3.61	227 ± 76		
17	0.87 ± 0.02 b	0.67 ± 0.10	0.96 ± 0.04 a	1.22 ± 0.82 b	371 ± 39	0.65 ± 0.47 ac	2.33 ± 3.70	72 ± 44			
	0.87 ± 0.02 b	0.67 ± 0.10	0.96 ± 0.04 a	1.22 ± 0.82 b	371 ± 39	0.65 ± 0.47 ac	2.33 ± 3.70	72 ± 44			
	0.87 ± 0.02 b	0.67 ± 0.10	0.96 ± 0.04 a	1.22 ± 0.82 b	371 ± 39	0.65 ± 0.47 ac	2.33 ± 3.70	72 ± 44			
CLL	Control	11	0.84 ± 0.02 b	0.79 ± 0.02 b	0.97 ± 0.03 a	0.24 ± 0.07 a	252 ± 40	2.83 ± 0.43 fh	10.87 ± 3.76	396 ±	
			0.83 ± 0.04	0.73 ± 0.08	0.96 ± 0.03 a	0.34 ± 0.22 a	206 ± 67 a	1.78 ± 0.90	6.08 ± 3.65	190 ± 32	
			0.83 ± 0.04	0.73 ± 0.08	0.96 ± 0.03 a	0.34 ± 0.22 a	206 ± 67 a	1.78 ± 0.90	6.08 ± 3.65	190 ± 32	
		15	0.83 ± 0.07	0.75 ± 0.02	0.94 ± 0.06 a	0.32 ± 0.12 a	291 ± 76	0.86 ± 0.67 ac	2.97 ± 4.25	76 ± 59	
			0.83 ± 0.07	0.75 ± 0.02	0.94 ± 0.06 a	0.32 ± 0.12 a	291 ± 76	0.86 ± 0.67 ac	2.97 ± 4.25	76 ± 59	
			0.83 ± 0.07	0.75 ± 0.02	0.94 ± 0.06 a	0.32 ± 0.12 a	291 ± 76	0.86 ± 0.67 ac	2.97 ± 4.25	76 ± 59	
	17	0.83 ± 0.07	0.75 ± 0.02	0.94 ± 0.06 a	0.32 ± 0.12 a	291 ± 76	0.86 ± 0.67 ac	2.97 ± 4.25	76 ± 59		
		0.83 ± 0.07	0.75 ± 0.02	0.94 ± 0.06 a	0.32 ± 0.12 a	291 ± 76	0.86 ± 0.67 ac	2.97 ± 4.25	76 ± 59		
		0.83 ± 0.07	0.75 ± 0.02	0.94 ± 0.06 a	0.32 ± 0.12 a	291 ± 76	0.86 ± 0.67 ac	2.97 ± 4.25	76 ± 59		
	Biochar	11	0.84 ± 0.02	0.78 ± 0.03	0.97 ± 0.03 a	0.25 ± 0.08 a	253 ± 12	3.24 ± 0.69 hi	9.28 ± 2.79	394 ± 84	
			0.81 ± 0.04	0.70 ± 0.09	0.95 ± 0.04 a	0.33 ± 0.18 a	271 ± 79	1.38 ± 0.39	2.74 ± 2.62	204 ± 38	
			0.81 ± 0.04	0.70 ± 0.09	0.95 ± 0.04 a	0.33 ± 0.18 a	271 ± 79	1.38 ± 0.39	2.74 ± 2.62	204 ± 38	
15		0.83 ± 0.03	0.75 ± 0.10	0.96 ± 0.04 a	0.33 ± 0.21 a	280 ± 99	0.29 ± 0.12 a	1.67 ± 1.51	79 ± 24		
		0.83 ± 0.03	0.75 ± 0.10	0.96 ± 0.04 a	0.33 ± 0.21 a	280 ± 99	0.29 ± 0.12 a	1.67 ± 1.51	79 ± 24		
		0.83 ± 0.03	0.75 ± 0.10	0.96 ± 0.04 a	0.33 ± 0.21 a	280 ± 99	0.29 ± 0.12 a	1.67 ± 1.51	79 ± 24		
17	0.83 ± 0.03	0.75 ± 0.10	0.96 ± 0.04 a	0.33 ± 0.21 a	280 ± 99	0.29 ± 0.12 a	1.67 ± 1.51	79 ± 24			
	0.83 ± 0.03	0.75 ± 0.10	0.96 ± 0.04 a	0.33 ± 0.21 a	280 ± 99	0.29 ± 0.12 a	1.67 ± 1.51	79 ± 24			
	0.83 ± 0.03	0.75 ± 0.10	0.96 ± 0.04 a	0.33 ± 0.21 a	280 ± 99	0.29 ± 0.12 a	1.67 ± 1.51	79 ± 24			
Compost	11	0.85 ± 0.03	0.77 ± 0.03 b	0.96 ± 0.03 a	0.30 ± 0.24 a	262 ± 34	4.36 ± 0.83 i	11.96 ± 2.94	247 ± 82		
		0.82 ± 0.04	0.70 ± 0.07	0.92 ± 0.06 a	0.28 ± 0.16 a	258 ± 52	1.63 ± 0.59	3.62 ± 2.35	217 ± 57		
		0.82 ± 0.04	0.70 ± 0.07	0.92 ± 0.06 a	0.28 ± 0.16 a	258 ± 52	1.63 ± 0.59	3.62 ± 2.35	217 ± 57		
	15	0.86 ± 0.02	0.77 ± 0.03	0.93 ± 0.01 a	0.23 ± 0.05 a	321 ± 42	0.39 ± 0.09	2.10 ± 0.95	62 ± 21		
		0.86 ± 0.02	0.77 ± 0.03	0.93 ± 0.01 a	0.23 ± 0.05 a	321 ± 42	0.39 ± 0.09	2.10 ± 0.95	62 ± 21		
		0.86 ± 0.02	0.77 ± 0.03	0.93 ± 0.01 a	0.23 ± 0.05 a	321 ± 42	0.39 ± 0.09	2.10 ± 0.95	62 ± 21		
17	0.86 ± 0.02	0.77 ± 0.03	0.93 ± 0.01 a	0.23 ± 0.05 a	321 ± 42	0.39 ± 0.09	2.10 ± 0.95	62 ± 21			
	0.86 ± 0.02	0.77 ± 0.03	0.93 ± 0.01 a	0.23 ± 0.05 a	321 ± 42	0.39 ± 0.09	2.10 ± 0.95	62 ± 21			
	0.86 ± 0.02	0.77 ± 0.03	0.93 ± 0.01 a	0.23 ± 0.05 a	321 ± 42	0.39 ± 0.09	2.10 ± 0.95	62 ± 21			
Mix	11	0.85 ± 0.01 b	0.79 ± 0.03	0.96 ± 0.03 a	0.25 ± 0.08 a	338 ± 15	3.23 ± 0.98 hi	3.63 ± 0.73	361 ±		
		0.81 ± 0.04	0.70 ± 0.07	0.95 ± 0.05 a	0.40 ± 0.19 a	237 ± 68	1.51 ± 0.51	6.50 ± 5.50	218 ± 35		
		0.81 ± 0.04	0.70 ± 0.07	0.95 ± 0.05 a	0.40 ± 0.19 a	237 ± 68	1.51 ± 0.51	6.50 ± 5.50	218 ± 35		
	15	0.84 ± 0.03	0.73 ± 0.05	0.95 ± 0.02 a	0.39 ± 0.21 a	207 ± 25	0.38 ± 0.23	2.26 ± 1.42	130 ±		
		0.84 ± 0.03	0.73 ± 0.05	0.95 ± 0.02 a	0.39 ± 0.21 a	207 ± 25	0.38 ± 0.23	2.26 ± 1.42	130 ±		
		0.84 ± 0.03	0.73 ± 0.05	0.95 ± 0.02 a	0.39 ± 0.21 a	207 ± 25	0.38 ± 0.23	2.26 ± 1.42	130 ±		
17	0.84 ± 0.03	0.73 ± 0.05	0.95 ± 0.02 a	0.39 ± 0.21 a	207 ± 25	0.38 ± 0.23	2.26 ± 1.42	130 ±			
	0.84 ± 0.03	0.73 ± 0.05	0.95 ± 0.02 a	0.39 ± 0.21 a	207 ± 25	0.38 ± 0.23	2.26 ± 1.42	130 ±			
	0.84 ± 0.03	0.73 ± 0.05	0.95 ± 0.02 a	0.39 ± 0.21 a	207 ± 25	0.38 ± 0.23	2.26 ± 1.42	130 ±			

Chapter 1: Highlights and Perspectives

The contamination of agricultural soils with HM constitutes a major concern for human health and soil productivity. The possibility to combine soil management with plants (phytomanagement) for non-food production has emerged as a cost-efficient and eco-sustainable solution, but there is a lack of information regarding the possibility to conciliate both purposes. Besides, the field applicability of this strategy can be limited by the concentration of HM in the biomass, the type of product use, and the slower growth rate of cultivated plant. The use of soil amendments may consequently be recommended to better guarantee the establishment of a plant cover.

In this Chapter, hemp was therefore cultivated in natural field conditions on an agricultural soil formerly contaminated by Cd and Zn, and amended or not with compost, biochar and their combination. We investigated the phytomanagement potential of hemp, and the impact of these treatments on the plant growth potential, and on the fibres' HM contents and major mechanical properties considering for the first time industrial standards.

The present Chapter demonstrated that (Figure 1.9):

- Hemp phytoextraction capacity was limited by the low environmental availability of HM. However, hemp high biomass yield and its important root system may reduce the dispersion of HM in the environment suggesting that, in conditions of low environmental availability, hemp can be used as a suitable crop for phytostabilization rather than phytoextraction strategies.
- Except for a slight yield decrease, hemp was found to be statistically unaffected by soil contamination and showed the same photosynthetic fitness and fibres quality than control plants. Contaminated fibres containing immobilized HM, but with preserved properties, could thus be used for specific purposes such as inclusion in cement agglomerates.
- Biochar and compost applied individually were found to be interesting options to improve yield, to reduce Cd and Zn contents in bast fibres and to promote the production of thicker and more resistant fibres.

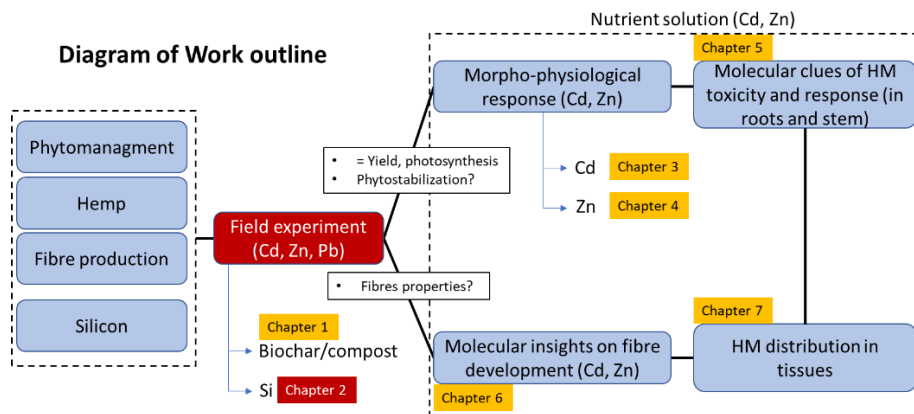
Chapter 2

Studying the influence of Silicon application on hemp physiological properties and the impact on fibres' final properties after harvest.

Marie Luyckx, Mathilde Blanquet, Arnaud Isenborghs, Gea Guerriero, Géraldine Bidar, Christophe Waterlot, Francis Douay, Stanley Lutts.
International Journal of Environmental Researches

Author's contributions

ML and SL designed the methodology; ML performed the whole experiment, treated, and analyzed the data; MB and AI contributed to mineral analysis; SL supervised the whole research process; ML and SL wrote the original draft. All authors reviewed the manuscript.



Abstract

Heavy metal (HM) pollution in agricultural fields reduces crop productivity and quality, and poses a risk for human health. On these areas, the cultivation of crops devoted to biomaterial and bioenergy production thus constitutes an attractive alternative to food crop production. To maintain the soil productivity and to obtain a biomass compatible with the requirements of industry, the use of the beneficial metalloid silicon, applied on leaves during plant growth, has been considered. A field study using *Cannabis sativa* L. (cv. Futura 75) was performed during two consecutive years on two sites (one soil parcel contaminated with Cd, Zn and Pb, and one taken as uncontaminated control) in the North of France. One half of the plants received weekly foliar spray of Si (2 mM). Photosynthesis-related parameters were analysed *in situ*, while mineral concentration and fibre properties were determined after 4 months of culture. Our results suggest that, in the absence of soil contamination, Si application improves and preserves the mechanical properties of fibres when plants are exposed to HM stress. Si was also shown to increase by 27% the Cd concentration in leaves and by 30% the Zn concentration in stems. Contaminated fibres and hurds containing immobilized HM could be used for specific purposes such as inclusion in cement agglomerates.

1. Introduction

In numerous areas in the world, activities, such as industrialization, urbanization and agricultural practices have resulted in the release of heavy metals (HM) in the environment. Heavy metals' pollution in agricultural fields frequently results in soil degradation, reduced crop productivity and poor quality of agricultural products. It induces significant hazards for human and animal health through food chain contamination (Peralta-Videa et al. 2009; Wang et al. 2016; Jaskulak et al. 2020). On these areas, the cultivation of crops devoted to biomaterial and bioenergy production may constitute an attractive alternative to food crops (Fernando et al. 2015). This implies that biomass production should not be compromised by HM from a quantitative point of view, and that the properties of the harvested biomass remain compatible with the requirements of industry from a qualitative point of view (Luyckx et al. 2019).

Fibre crops like textile hemp are important sources of raw materials for paper, textiles and composite production, as they provide, in a sustainable manner, a great amount of biomass in a relatively short time (Gorshkova et al. 2012; Guerriero et al. 2017a). Fibres' commercial applications are largely based on their mechanical properties: as a whole, the structure of the fibre cell wall is similar to a nanocomposite reinforced with cellulose microfibrils and is characterized by high anisotropy, high stiffness and strength in the direction of the fibre axis (reviewed by Gorshkova et al. 2012).

Several silicon (Si) derivatives (silane, siloxane, etc.) are used in industry to improve the mechanical properties and thermal stability of the harvested fibres (Abdelmouleh et al. 2004; Orue et al. 2016; Han et al. 2020). Silicon is known to interact with specific cell wall components, although the mechanisms involved in amorphous silica-SiO₂ precipitation remain elusive (Luyckx et al. 2017a). Besides, the presence of -SiO₂ in hemp woody fibres favour their valorisation in eco-construction. Indeed, the presence of SiO₂ strengthens the bonds between fibres and lime in the manufacture of a lightweight concrete-like material known as "hemcrete" (Luyckx et al. 2017a). Hemcrete is not only very light (6 times lighter than traditional concrete), but also more resistant to degradation. Moreover, the presence of SiO₂ protects it against the attack of chewing insects, termites, fungi and rodents (Luyckx et al. 2017b). SiO₂ is also commonly considered fire-retardant (Luyckx et al. 2017b; Piot et al. 2017).

As far as plant physiology is concerned, Si is known to have numerous beneficial effects on plants exposed to abiotic and biotic stresses (Pilon et al. 2013; Frew et al. 2018). Various authors reported that the addition of Si improved the growth of plants exposed to HM (Wu et al. 2013; Adrees et al. 2015; Imtiaz et al. 2016; Bhat et al. 2019). Silicon protective mechanisms in alleviating HM toxicity include improved expression of defense genes, increase in antioxidant enzymes' activities, changes in transpiration rates and CO₂ assimilation, osmotic adjustments leading to the maintenance of water content and turgor pressure, alterations in HM uptake and modifications in phytohormone concentrations (Frew et al. 2018). Given the positive effects of Si on plants, Si treatments during fibre development in plants cultivated on HM-contaminated soils could therefore represent an asset for biomass valorization: Si may not only increase fibre production but is also expected to provide improved mechanical properties to the fibres through SiO₂ precipitation in the cell walls (Luyckx et al. 2017a and 2019). Luyckx et al. (2021b; 2021c) recently demonstrated that exogenous Si modified gene

expression in Cd-treated *Cannabis sativa* L., including genes involved in secondary cell wall metabolism, which could thus influence fibre development. Khan and Roy (1964) reported increased cell elongation and fineness of the commercial fibre jute as a result of soil application of silicate. However, the availability of Si fertilizer applied into fields is quite low because this silicate slag is hard to dissolve and is easily adsorbed on organic matters and/or minerals in the soils (Wang et al. 2015a). In our present study, the foliar application of Si was therefore considered in order to avoid its immobilization in soil. Si foliar fertilizers with smaller particle size have already been used and were shown to easily penetrate the leaf but also to form a thick SiO₂ layer on the leaf surface (Wang et al. 2015a).

The aim of this study performed *in situ* was to evaluate i) the influence of Si application on hemp physiological properties when grown on HM-contaminated agricultural soils and ii) to determine the impact of Si applied during fibres' development on their final properties after harvest.

2. Material and methods

2.1. Growth conditions

Two agricultural sites (Courcelles-lès-Lens, CLL (50°24'58.2"N 3°01'40.0"E), and Bois-Bernard, BB (50°22'52.0"N 2°55'11.3"E); France), described in Chapter 1 (p.79-80) were selected: CLL is located near (about 1 km to the southeast) a former lead and zinc smelter (Metaleurop), while BB is far enough from it (about 9 km to the southwest) not to be influenced by contaminated dust fallout and was taken as a control.

Before the beginning of the experiment, 3 soil samples from ploughed layer (0 - 25 cm) from each site were characterized. Total HM concentrations in CLL soil were homogeneously distributed all over the sites (5.5 ± 0.2 mg Cd, 396.4 ± 31.8 mg Zn, 298 ± 21 mg Pb per kg of soil; MisChar program) and exceeded, for Zn and Pb, the permissible limits (PL) commonly recommended for agricultural use (10 mg Cd kg⁻¹, 250 mg Zn kg⁻¹, and 200 mg Pb kg⁻¹; Tóth et al., 2016), while in BB, Cd and Zn concentrations were 5 times lower than in CLL and below the PL for Cd and Zn (1.1 ± 0.1 mg Cd, 80.9 ± 3.9 mg Zn per kg of soil; MisChar program). The presence of Pb in the topsoil of BB (285 ± 95 mg kg⁻¹) is linked to the presence of some shrapnel issued from World War I. Detailed soil analyses for both sites are provided in Table S2.1 (supplemental data). In both BB and CLL, HM extraction with

CaCl₂ 0.01 M revealed very low environmental availability of Cd and Pb, since their extractable concentration was below the detection limits of the flame atomic absorption spectrometer (0.05 mg kg⁻¹ for Cd, 0.65 mg kg⁻¹ for Pb). In both sites, the Cation Exchange Capacity (CEC) was between 17.3 and 19.8 cmol kg⁻¹, and soil pH in CLL (7.9 ± 0.1) was slightly more alkaline than in BB (7.0 ± 0.2).

The field study was carried out in 2018 and 2019. Year 2018 was drier and warmer than 2019 (Lille-Lesquin weather station). The accumulated rainfall over the entire vegetation period in 2019 (167.6 mm) slightly exceeded those of 2018 (158.1 mm), while average temperatures were higher in 2018 (23.04°C) than in 2019 (21.80°C).

2.2. Soil characterization

Soils samples were collected before plant sowing in 2018 (T0), after plant harvest in 2018 (T1) and 2019 (T2). We analyzed total HM concentrations, HM concentrations after CaCl₂ 0.01 M extraction (HM environmental availability), CEC and pH (as detailed in Chapter 1, p.81-82).

2.3. Plant material

For each site, 2 contiguous blocks (9 m * 10 m) were set up, one for industrial hemp and the other for wheat, to establish a crop rotation. From year to year, hemp and wheat were alternate at the 2 joint blocks of each site, but only hemp will be considered in this study. Seeds of a monoecious hemp fibre variety (*C. sativa*, cv Futura 75) were sown at the end of April (2018) or at the beginning of May (2019), with a sowing density of 50 kg ha⁻¹. No additional fertilization nor weeding were applied. Foliar application of Si started six weeks after sowing, and was then repeated once a week until harvest. For Si application, areas of 1 m² were delimited within each block: one half without Si application, the other half with Si application. Si was applied as metasilicic acid (2 mM, the maximum solubility of H₂SiO₃ in solution) with a hand sprayer until the solution began to drip off leaves. Metasilicic acid was obtained from a pentahydrate sodium metasilicate (Na₂SiO₃, 5 H₂O) which was passed through an H⁺ ion exchanger resin IR 20 Amberlite type according to Dufey et al. (2014). Four treatments were thus defined, considering soil contamination (site) and the concomitant presence/absence of Si application, and will hereafter be referred to as BB (control), CLL (contaminated), BBSi (BB with Si application), and CLLSi.

In 2018 and 2019, plants were harvested 4 months after sowing. For each treatment, 10 plants were cut 5 cm above the ground, and all the leaves still present on the stem, and stems from a same treatment were then separated. Subsamples of each treatment and plant part were pooled and dried at 70 °C for 72 h before analyses.

2.4. Photosynthesis-related parameters

Before plant harvest, photosynthesis-related parameters were measured in 2018 and 2019 on 5 plants per treatment, on the middle portion of the leaf blades constituting the second fully formed leaves from the top.

Chlorophyll fluorescence parameters (maximum quantum yield of photosystem II (F_v/F_m), photochemical quenching (q_p), non-photochemical quenching (NPQ) and actual efficiency of photosystem II (Φ_{PSII})), leaf stomatal conductance (g_s), the instantaneous CO₂ assimilation under ambient conditions (400 ppm CO₂) (A) and instantaneous transpiration (E) were measured as described in Chapter 1 (p.83-84). All measurements were performed around midday (between 10 a.m. and 2 p.m).

2.5. Fibre's and hurds' characterization

The protocol used for fibre's and hurds' characterization is detailed in Chapter 1 (p.84).

2.6. Mineral concentration in stems, leaves, fibres and hurd

For Cd, Pb and Zn quantification, the protocol is described in Chapter 1 (p. 84).

For Si quantification, 1 g DM was placed in an oven and heated to 500 °C for 48 h. Ashes were then mixed with 0.4 g tetraborate and 1.6 g metaborate and heated to 1000 °C for 5 min. The obtained pellet was dissolved with 34% v/v HNO₃. Cations were quantified by Inductively Coupled Plasma-Optical Emission Spectroscopy (Varian, type MPX). The metal bioaccumulation factor (BF) was defined, for each element, as the ratio between the mean value of HM concentration recorded in the whole aerial part divided by the mean value of total concentration in the soil.

2.7. Statistical analysis

Five replicates were analyzed for each treatment. ANOVA analyses were performed separately for each year. Normality of the data was verified using Shapiro-Wilk tests and the data were log-transformed when required. Homogeneity of the data was verified using Levene's tests. Two-way ANOVA were performed at a significant level of P -value < 0.05 using R (version 3.3.1) considering the soil contamination (BB, CLL) and Si application as main factors. Means were compared using Tukey's HSD all-pairwise comparisons at 5% level as a post-hoc test.

3. Results

3.1. Yield

Table 2.1: Yield (t ha^{-1}) of *C. sativa* (cv Futura 75) grown during 4 months (in 2018 and 2019) on HM-contaminated soil of Courcelle-Lès-Lens (CLL) or on control soil of Bois-Bernard (BB), in the presence or in the absence of 2 mM H_2SiO_3 (Si). Data are means \pm standard errors ($n = 5$). For each column and year, values with different letters are significantly different at $P < 0.05$ according to the Tukey's HSD all-pairwise comparisons.

Year	Site	Si (mM)	Yield (t ha^{-1})
2018	BB	0	39.6 ± 4.22 a
		2	32.25 ± 4.10 a
	CLL	0	31.97 ± 9.26 a
		2	40.07 ± 7.32 a
2019	BB	0	25.47 ± 3.15 a
		2	20.73 ± 3.01 a
	CLL	0	18.93 ± 2.63 a
		2	23.73 ± 2.52 a

Table 2.2: Fibres and hurd yield (%) of *C. sativa* (cv Futura 75) grown during 4 months (in 2019) on HM contaminated soil of Courcelle-Lès-Lens (CLL) or on control soil of Bois-Bernard (BB), in the presence or in the absence of 2 mM H_2SiO_3 (Si). Data are means \pm standard errors ($n = 5$). For each column and year, values with different letters are significantly different at $P < 0.05$ according to the Tukey's HSD all-pairwise comparisons.

Year	Site	Si (mM)	Fibres yield (%)	Hurd yield (%)
2019	BB	0	31 ± 7 a	68 ± 7 a
		2	29 ± 2 a	70 ± 2 a
	CLL	0	31 ± 4 a	68 ± 7 a
		2	30 ± 1 a	69 ± 1 a

The aerial biomass yield of *C. sativa* was higher in 2018 than in 2019 (Table 2.1). However, for each considered year, neither the presence of pollutants nor the exogenous application of Si had any significant impact on biomass yield; even if Si exposure tended to decrease the yield in BB and to increase it in CLL. For year 2019, the proportions of fibres and hurds were not impacted by the treatments (Table 2.2).

3.2. Photosynthesis-related parameters

Table 2.3: Light-dependent parameters of photosynthesis. *C. sativa* (cv Futura 75) plants were grown during 4 months (in 2018 and 2019) on HM-contaminated soil of Courcelle-Lès-Lens (CLL) or on control soil of Bois-Bernard (BB), in the presence or in the absence of 2 mM H₂SiO₃ (Si). Maximum quantum yield of photosystem II (F_v/F_m), actual efficiency of photosystem II (Φ_{PSII}), photochemical quenching (qP), and non-photochemical quenching (NPQ). Data are means \pm standard errors ($n = 5$). For each column and year, values with different letters are significantly different at $P < 0.05$ according to the Tukey's HSD all-pairwise comparisons.

Year	Site	Si (mM)	F_v/F_m	Φ_{PSII}	qP	NPQ
2018	BB	0	0.861 \pm 0.015 b	0.767 \pm 0.030 ab	0.932 \pm 0.028 a	0.296 \pm 0.205 a
		2	0.792 \pm 0.052 ab	0.704 \pm 0.059 a	0.990 \pm 0.061 a	0.359 \pm 0.135 a
	CLL	0	0.815 \pm 0.002 a	0.744 \pm 0.019 a	0.969 \pm 0.014 a	0.252 \pm 0.029 a
		2	0.864 \pm 0.018 b	0.814 \pm 0.033 b	0.944 \pm 0.057 a	0.199 \pm 0.091 a
2019	BB	0	0.818 \pm 0.067 a	0.647 \pm 0.174 ab	0.958 \pm 0.037 a	0.894 \pm 0.944 a
		2	0.878 \pm 0.006 a	0.744 \pm 0.035 ab	0.933 \pm 0.038 a	0.663 \pm 0.547 a
	CLL	0	0.834 \pm 0.068 a	0.753 \pm 0.020 b	0.938 \pm 0.056 a	0.322 \pm 0.117 a
		2	0.813 \pm 0.002 a	0.671 \pm 0.032 a	0.964 \pm 0.048 a	0.702 \pm 0.489 a

Light-dependent parameters of photosynthesis (F_v/F_m , Φ_{PSII} , qP , NPQ , Table 2.3) were marginally influenced by soil contamination and Si application. In 2018, the F_v/F_m ratio was increased by exogenous Si in CLL. In the absence of Si application, the Φ_{PSII} value recorded in 2018 was similar in BB and CLL treatments, but Si application decreased Φ_{PSII} in BB and significantly increased it in CLL, while an opposite trend was recorded in 2019. Conversely, Si application slightly decreased NPQ in CLL treatments in 2018 but increased it in 2019. However, NPQ displayed a high level of variability and the recorded trends remained not significant. Photochemical quenching (qP) remained similar in all treatments, irrespective of the year considered.

In 2018 and in the absence of Si, CO₂ concentration in intercellular spaces (*C_i*) and *E* (Table 2.4) tended to be higher in BB than in CLL while *A* and *g_s* tended to be higher in the plants growing on the contaminated soil comparatively to the control one. Exogenous Si decreased *C_i* concentration but increased *A* values. The recorded increase was especially important for plants growing on CLL. Exogenous Si tended to decrease stomatal conductance on BB but to increase it in CLL. Plants cultivated in 2019 exhibited a different trend since *E* and *g_s* values were lower than in 2018. Moreover, exogenous Si tended to decrease *A* values for plants growing on both sites. Nevertheless, net photosynthesis still remained unexpectedly higher in plants cultivated in CLL than in those cultivated in BB, as previously observed in 2018, while *g_s* values were lower.

Table 2.4: Light-independent parameters of photosynthesis. *C. sativa* (cv Futura 75) plants were grown during 4 months (in 2018 and 2019) on HM-contaminated soil of Courcelle-Lès-Lens (CLL) or on control soil of Bois-Bernard (BB), in the presence or in the absence of 2 mM H₂SiO₃ (Si). Concentration of CO₂ in intercellular spaces (*C_i*), instantaneous transpiration (*E*), instantaneous CO₂ assimilation under ambient conditions (*A*) and leaf stomatal conductance (*g_s*). Data are means ± standard errors (*n* = 5). For each column and year, values with different letters are significantly different at *P* < 0.05 according to the Tukey's HSD all-pairwise comparisons.

Year	Site	Si (mM)	<i>C_i</i> (μmol mol ⁻¹)	<i>E</i> (mmol H ₂ O m ⁻² s ⁻¹)	<i>A</i> (μmol CO ₂ m ⁻² s ⁻¹)	<i>g_s</i> (mmol m ⁻² s ⁻¹)
2018	BB	0	332.67 ± 23.86 b	2.060 ± 0.691 a	3.277 ± 1.229 a	304.33 ± 36.00 ab
		2	285.66 ± 63.32 ab	1.363 ± 0.581 a	3.963 ± 3.547 a	225.00 ± 40.73 a
	CLL	0	258.68 ± 101.36 ab	1.550 ± 0.344 a	4.407 ± 3.640 a	375.33 ± 151.74 ab
		2	160.33 ± 21.94 a	2.707 ± 0.860 a	13.917 ± 3.478 b	442.50 ± 7.50 b
2019	BB	0	392.25 ± 25.99 a	0.878 ± 0.626 a	0.820 ± 0.7332 a	137.70 ± 121.329 a
		2	389.00 ± 32.92 a	0.687 ± 0.291 a	0.610 ± 0.711 a	134.37 ± 89.45 a
	CLL	0	291.50 ± 75.85 a	0.863 ± 0.667 a	2.968 ± 4.249 a	76.10 ± 58.75 a
		2	284.67 ± 42.44 a	0.883 ± 0.212 a	1.637 ± 1.294 a	58.12 ± 30.305 a

3.3.Si accumulation in hemp

Concentrations of Si in leaves, stems and mean values calculated for the whole aerial parts are reported in Table 2.5. Silicon content was always higher in the leaves than in the stems. In 2018, Si application unexpectedly decreased Si concentration in both leaves and stems of plants cultivated in the uncontaminated control BB, while it tended to increase Si content in the stem

of plants cultivated in CLL. In 2019, Si application significantly increased the leaf Si content in plants cultivated on CLL, resulting in a global significant increase of Si content in the whole aerial parts of plants cultivated on the contaminated site. In the absence of Si application, however, the mean Si concentration in the aerial part was higher in plants growing on BB than on CLL for both years.

Table 2.5: Silicon concentration (in mg kg⁻¹ DW) in leaves and stems of *C. sativa* (cv Futura 75) and mean value calculated for the whole vegetative aerial part. Plants were grown during 4 months (in 2018 and 2019) on HM-contaminated soil of Courcelle-Lès-Lens (CLL) or on control soil of Bois-Bernard (BB), in the presence or in the absence of 2 mM H₂SiO₃ (Si). Data are means ± standard errors (*n* = 5). For each organ and year, values with different letters are significantly different at *P* < 0.05 according to the Tukey's HSD all-pairwise comparisons.

		2018		2019	
		Site	Si (mM)	Si	Si
Leaves	BB	0		7269 ± 1155 b	7013 ± 235 b
		2		4420 ± 20 a	6661 ± 231 b
	CLL	0		6271 ± 428 b	5515 ± 359 a
		2		5646 ± 52 b	6975 ± 121 b
Stems	BB	0		861 ± 76 a	410 ± 193 ab
		2		364 ± 148 a	227 ± 16 b
	CLL	0		319 ± 33 a	157 ± 22 a
		2		988 ± 484 a	259 ± 9 b
Aerial parts	BB	0		2784 ± 293 b	2391 ± 206 b
		2		1581 ± 98 a	2157 ± 81 ab
	CLL	0		2104 ± 151 ab	1764 ± 123 a
		2		2385 ± 354 ab	2274 ± 30 ab

3.4. HM accumulation in hemp

Cadmium, Pb and Zn were detected in plants cultivated in BB and CLL (Table 2.6). In both sites, foliar concentrations of Cd, Pb and Zn tended to exceed stem concentrations. In the absence of Si application, the leaf Cd, Pb and Zn concentrations were always higher in plants growing in CLL than in BB. The difference was however less obvious for stems which even tended to present higher Pb and Zn concentrations in BB than in CLL in 2018. When mean concentration values were calculated for the whole aerial part, the accumulation was still higher in CLL than in BB.

Table 2.6: Cadmium, lead and zinc concentrations (in mg kg⁻¹ DW) in leaves and stems of *C. sativa* (cv Futura 75), and metal bioaccumulation factor (BF). Plants were grown during 4 months (in 2018 and 2019) on HM-contaminated soil of Courcelle-Lès-Lens (CLL) or on control soil of Bois-Bernard (BB), in the presence or in the absence of 2 mM H₂SiO₃ (Si). Data are means ± standard errors (*n* = 5). For each element, organ and year, values with different letters are significantly different at *P* < 0.05 according to the Tukey's HSD all-pairwise comparisons. Color code: significant impact of the site (CLL vs BB; blue) or, for each site, of foliar spraying of Si comparatively to the unsprayed plants (green).

		2018				2019		
	Site	Si (mM)	Cd	Pb	Zn	Cd	Pb	Zn
Leaves	BB	0	0.018 ± 0.003 a	1.099 ± 0.219 a	25.27 ± 4.10 a	0.075 ± 0.032 a	2.721 ± 1.026 a	41.74 ± 6.35 a
		2	0.032 ± 0.002 b	1.887 ± 0.044 b	34.76 ± 0.22 b	0.081 ± 0.009 ab	2.941 ± 0.205 a	36.27 ± 2.39 a
	CLL	0	0.058 ± 0.004 c	2.171 ± 0.074 c	42.69 ± 1.65 c	0.165 ± 0.040 bc	3.721 ± 0.387 a	65.67 ± 5.06 b
		2	0.076 ± 0.006 d	2.466 ± 0.163 c	37.99 ± 2.34 bc	0.204 ± 0.021 c	2.911 ± 0.225 a	62.61 ± 1.17 b
Stems	BB	0	0.026 ± 0.002 b	0.920 ± 0.005 b	20.47 ± 3.68 d	nd	1.103 ± 0.114 a	10.211 ± 0.879 a
		2	0.014 ± 0.001 a	0.858 ± 0.016 a	8.25 ± 0.02 a	nd	0.997 ± 0.063 a	12.098 ± 2.918 a
	CLL	0	0.039 ± 0.007 bc	0.887 ± 0.083 ab	12.70 ± 0.16 b	0.074 ± 0.015 a	1.193 ± 0.075 ab	12.148 ± 0.961 a
		2	0.040 ± 0.003 c	0.819 ± 0.127 ab	16.07 ± 1.90 c	0.145 ± 0.036 b	1.379 ± 0.068 b	16.333 ± 3.700 a
Aerial parts	BB	0	0.024 ± 0.003 a	0.974 ± 0.069 a	21.915 ± 1.350 a	0.025 ± 0.012 a	1.698 ± 0.272 ab	20.641 ± 1.305 a
		2	0.019 ± 0.004 a	1.167 ± 0.040 b	18.508 ± 3.289 a	0.024 ± 0.002 a	1.594 ± 0.036 a	20.087 ± 1.779 a
	CLL	0	0.045 ± 0.003 b	1.272 ± 0.036 c	21.696 ± 0.382 a	0.106 ± 0.019 b	1.893 ± 0.064 b	28.533 ± 1.379 b
		2	0.051 ± 0.004 b	1.313 ± 0.040 c	22.649 ± 0.629 a	0.164 ± 0.023 c	1.822 ± 0.071 b	31.196 ± 2.415 b
BF	BB	0	0.021 ± 0.002 b	0.003 ± 0.000 a	0.271 ± 0.017 b	0.022 ± 0.011 ab	0.006 ± 0.001 a	0.255 ± 0.016 b
		2	0.018 ± 0.000 b	0.004 ± 0.000 ab	0.229 ± 0.041 b	0.022 ± 0.002 a	0.006 ± 0.000 a	0.248 ± 0.022 b
	CLL	0	0.008 ± 0.001 a	0.004 ± 0.000 b	0.055 ± 0.001 a	0.019 ± 0.003 a	0.006 ± 0.000 a	0.072 ± 0.003 a
		2	0.009 ± 0.001 a	0.004 ± 0.000 b	0.057 ± 0.002 a	0.030 ± 0.004 b	0.006 ± 0.000 a	0.079 ± 0.006 a

In 2018, Si application significantly increased Cd, Pb and Zn concentrations in the leaves of plants cultivated in BB while an opposite trend was recorded for the stem. In CLL, Si increased Cd and Pb in the leaves but had no impact on the stem. In 2019, however, we noticed that Si application almost doubled the concentration of Cd in the stem of plants cultivated on the contaminated site CLL.

To evaluate the impact of Si on hemp HM bioaccumulation factor (BF), the ratio between concentrations of the individual metals in the above-ground biomass and in soil both expressed on a DW basis was calculated (Table 2.6). In the absence of Si, Cd and Zn BF were higher in BB than in CLL, while Pb BF remained similar for both sites. These results were significant in 2018 and the same trend was recorded in 2019. Exogenous Si had only small impacts on BF values in plants growing on BB. It however significantly increased Cd BF in 2019.

3.5. Fibres and hurds characterization

Fibre bundles title and fibre tensile strength (force at break and breaking elongation) are classical parameters tested in industry to assess the quality of fibres. Soil contamination induced a significant increase of fibres bundles title in the absence of Si treatment (Figure 2.1). Exogenous Si increased bundle title in fibres harvested on the BB site but decreased it in CLL, thus suppressing the recorded differences between the two sites (Figure 2.1). Fibres derived from plants harvested on the uncontaminated site BB presented significantly lower force break and breaking elongation than those issued from the contaminated site CLL (Figure 2.2). Si had no significant impact on these parameters.

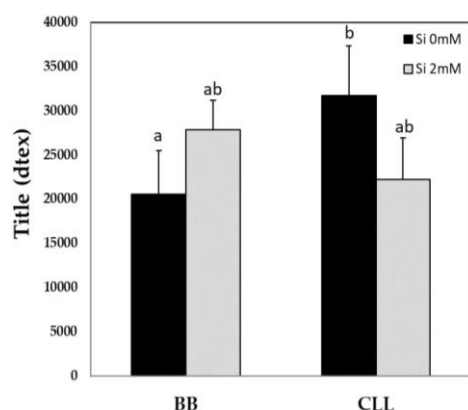


Figure 2.1: Fibre bundles' title (20-30 bundles, norm MO123, CELABOR). Plants were grown for 4 months on HM-contaminated soil of Courcelles-lès-Lens (CLL) or on control soil of Bois-Bernard (BB), in the presence or in the absence of 2 mM H_2SiO_3 (Si). The different letters indicate that the values are significantly different from each other ($P < 0.05$; Tukey's HSD all-pairwise comparisons).

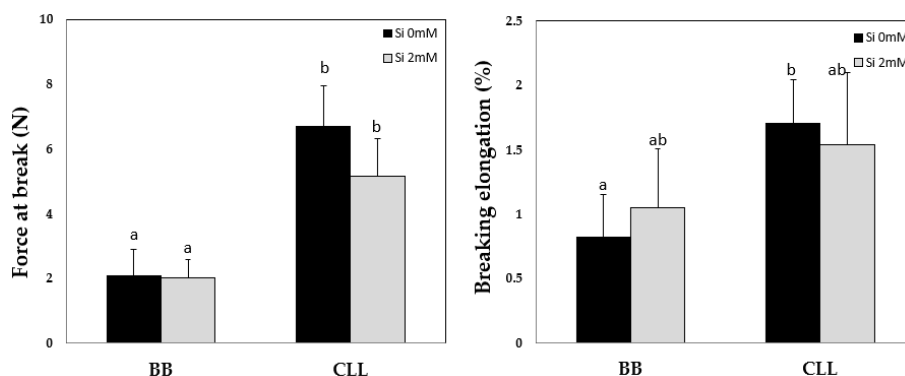


Figure 2.2: Force at break (N) and breaking elongation (%) of fibres (10 fibres, norm XP T25-501-3, CELABOR). Plants were grown for 4 months on HM-contaminated soil of Courcelles-lès-Lens (CLL) or on control soil of Bois-Bernard (BB), in the presence or in the absence of 2 mM H_2SiO_3 (Si). The different letters indicate that the values are significantly different from each other ($P < 0.05$; Tukey's HSD all-pairwise comparisons).

Heavy metal accumulation values in hurds and fibres of harvested plants are provided in Figure 2.3. Cadmium content in hurds was higher in plants collected from CLL than in those harvested on BB, and exogenous Si increased Cd accumulation in hurds in CLL. In contrast, Pb content in hurds was similar for the two considered sites without Si. Exogenous Si significantly decreased Pb content in hurds from BB but had no impact on CLL. Zn could not be accurately quantified in hurds. As far as fibres are concerned, Cd accumulation was similar in plants from BB and CLL, but exogenous Si increased Cd content in BB while it strongly reduced it in CLL. Lead content was similar in fibres derived from the two sites and, in both cases, Si significantly increased Pb content in the fibres. Exogenous Si reduced Zn concentration in the fibres issued from BB while the fibres harvested on CLL always exhibited a very low amount of Zn. Silicon concentration in hurds remained unaffected by Si treatment. In contrast, it strongly increased in fibres harvested from BB and to a lower extent in those harvested from CLL (Figure 2.4).

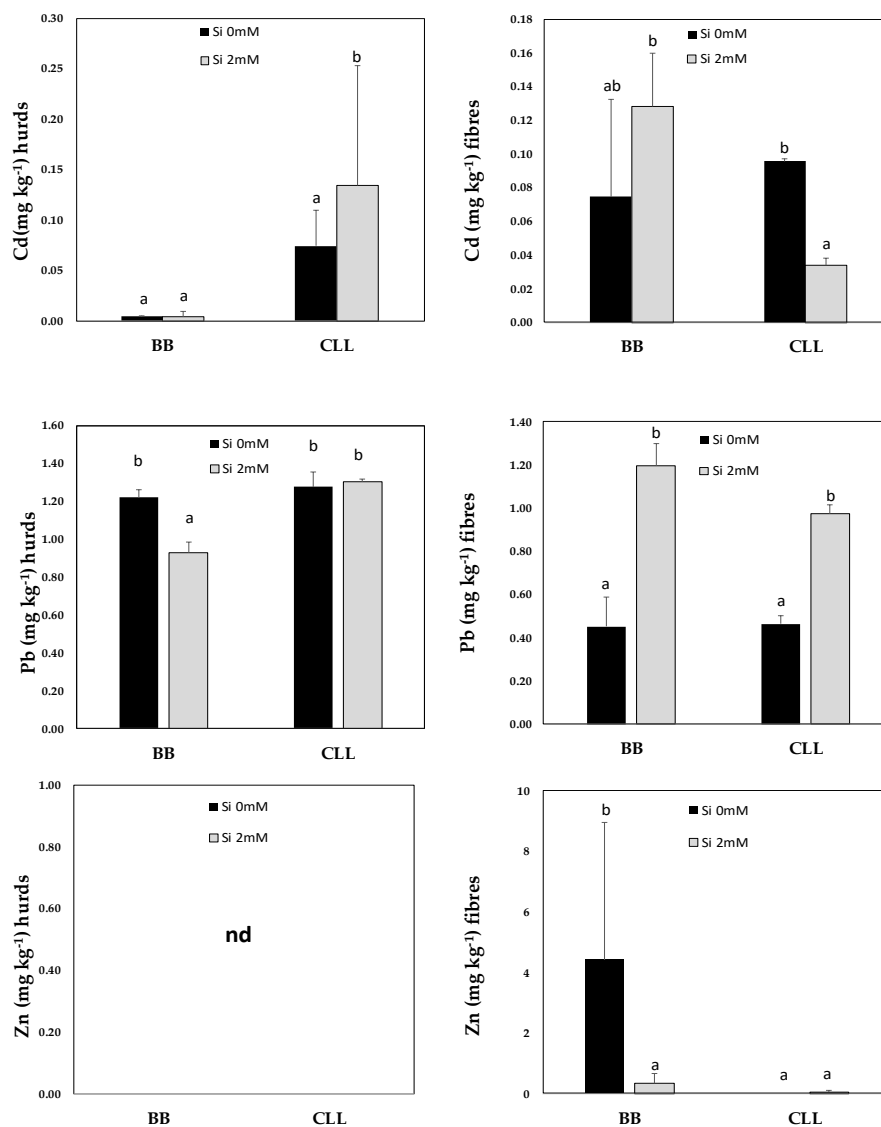


Figure 2.3: Cadmium, Pb and Zn concentrations (in mg kg⁻¹ DW) in hurds and fibres of *C. sativa* (cv Futura 75). Plants were grown for 4 months (in 2018 and 2019) on HM-contaminated soil of Courcelle-Lès-Lens (CLL) or on control soil of Bois-Bernard (BB), in the presence or in the absence of 2 mM H₂SiO₃ (Si). Data are means ± standard errors (*n* = 5). Nd= not detected (< LOD). Values with different letters are significantly different at *P* < 0.05 according to the Tukey's HSD all-pairwise comparisons.

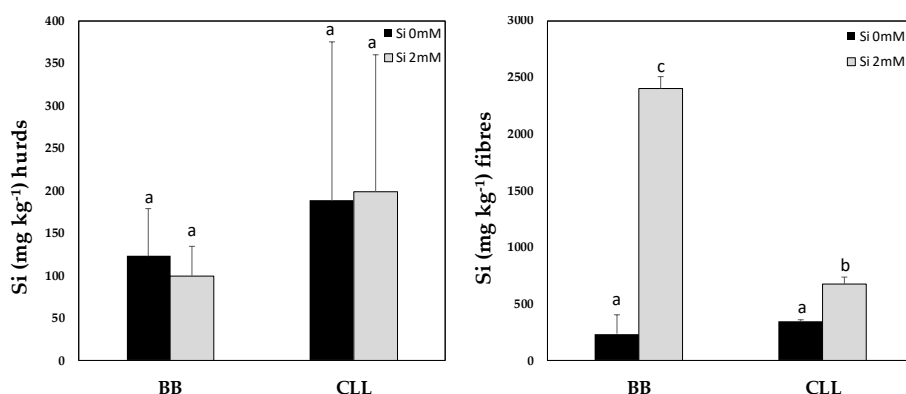


Figure 2.4: Silicon concentrations (in mg kg⁻¹ DW) in hurds and fibres of *C. sativa* (cv Futura 75). Plants were grown for 4 months (in 2018 and 2019) on HM contaminated soil of Courcelle-Lès-Lens (CLL) or on control soil of Bois-Bernard (BB), in the presence or in the absence of 2 mM H₂SiO₃ (Si). Data are means ± standard errors ($n = 5$). Values with different letters are significantly different at $P < 0.05$ according to the Tukey's HSD all-pairwise comparisons.

Table 2.7: Infra-red prediction of the hemicellulose, cellulose and lignin contents within hemp fibres and hurds. Plants were grown during 4 months (in 2019) on HM-contaminated soil of Courcelle-Lès-Lens (CLL) or on control soil of Bois-Bernard (BB), in the presence or in the absence of 2 mM H₂SiO₃ (Si). The different letters indicate that the values are significantly different from each other ($P < 0.05$; Tukey's HSD all-pairwise comparisons).

	Site	Si (mM)	Hemicellulose (% DW)	Cellulose (% DW)	Lignin (% DW)
Fibres	BB	0	19.13 ± 0.55 b	61.27 ± 1.05 a	nd
		2	16.91 ± 0.97 a	61.17 ± 0.82 a	nd
	CLL	0	17.12 ± 0.62 a	62.78 ± 1.35 ab	nd
		2	20.08 ± 0.86 b	63.15 ± 0.67 b	nd
Hurds	BB	0	14.21 ± 0.37 a	60.82 ± 0.70 a	12.94 ± 0.49 b
		2	14.15 ± 1.03 ab	61.38 ± 0.67 a	11.98 ± 0.20 a
	CLL	0	15.23 ± 0.87 ab	60.17 ± 0.44 a	13.48 ± 0.20 b
		2	16.21 ± 0.96 b	59.18 ± 1.50 a	13.36 ± 0.67 b

In the absence of Si treatment, fibres issued from BB had a higher percentage of hemicellulose (Table 2.7) than those derived from CLL plants. Silicon, however, inverted the trend since it significantly decreased hemicellulose in fibres from BB but increased it in fibres from CLL. No lignin could be accurately detected in fibres, and the cellulose concentration was slightly higher for fibres issued from CLL than those harvested on BB, the

difference being significant for Si-treated plants only. Hurds contained lower amount of hemicellulose than fibres in the absence of Si on BB site. The hemicellulose amount tended to be higher in plants cultivated on CLL than on BB. Lignin was also higher for hurds issued from CLL comparatively to BB. Silicon significantly decreased lignin content in hurds derived from BB but had no impact in CLL. Neither the sites nor Si treatment had any significant impact on cellulose percentage in hurds.

4. Discussion

Several Si derivatives (silane, siloxane, etc.) are used in industry to improve the mechanical properties of plant fibres and their thermal stability (Abdelmouleh et al. 2004; Orue et al. 2016). Moreover, through an enhanced tolerance to stress, Si application could improve hemp biomass production on agricultural soils contaminated with HM and where food production is prohibited. Foliar spraying of Si during hemp cultivation could therefore represent an asset for fibre production and valorization (Luyckx et al. 2017a).

In the current study, foliar application of Si had no significant impact on the photosynthetic activity of hemp, although its application tended to decrease C_i , E and g_s values in the absence of soil contamination issued from the former smelter activity. Silicon may have deposited as amorphous silica at the transpiration sites when the liquid fraction of the Si solution has evaporated, and caused partial occlusion of the stomata, resulting in a decrease in E and g_s (Zhu and Gong 2014) as we observed in 2018. Although stomatal conductance conditions the flow of water through the stomata, it also conditions gas exchange, including the entry of CO_2 . The potential obstruction of stomata by silica crystals could thus have limited the CO_2 input and explain the decrease in intercellular CO_2 observed. In the present study, however, such a decrease in g_s did not significantly affect net photosynthesis. In an experiment conducted on wheat cultivars, Maghsoudi et al. (2015) did not observe any significant effect of Si foliar application on photosynthesis, while increased photosynthesis and transpiration rates were reported by Pilon et al. (2013). For the majority of the studies available, the effects of Si under normal conditions are latent (Luyckx et al., 2017a). Under control conditions, Si probably activates the metabolic status of the plant, by making it more efficient in responding to exogenous stimuli (Luyckx et al., 2017a): a stimulation of the Calvin cycle might ensure net photosynthesis maintenance and also contributes to C_i decrease.

The present work demonstrates that HM soil contamination did not alter biomass yield and fibres/hurds proportion of *C. sativa* and that hemp could therefore be recommended for the valorization of moderately contaminated agricultural soils, as recently suggested by Rhey et al. (2020). Soil contamination slightly decreased NPQ and C_i , and slightly increased net photosynthesis, but Si application had not impact on these parameters. Decreased NPQ values under HM exposure have already been observed in one of our previous studies (Luyckx et al. 2021a). Non-photochemical-quenching is involved in energy dissipation through heat and is commonly reported to increase in response to abiotic stress (Maxwell and Johnson, 2000). The opposite trend observed in the present case suggests that PSII antenna and/or zeaxanthine concentration started to be affected by HM toxicity, leading to a drop in non-photochemical quenching (Stirbet et al. 2018). Despite this observation, our data confirm that the light-phase of photosynthesis is only marginally affected by HM, as previously reported by Shi et al. (2012) for numerous accessions of hemp.

Plant species strongly differ in their capacity to absorb and accumulate Si (Frew et al. 2018). Monocots usually accumulate more Si than dicots (Luyckx et al. 2017b). The present work demonstrated that hemp is able to accumulate Si in stems and to a higher extent in leaves in the presence as well as in the absence of foliar application of H_2SiO_3 , so that this species could be regarded as capable of absorbing and accumulating Si in its tissues. In the absence of soil contamination, however, application of H_2SiO_3 unexpectedly tended to decrease Si accumulation in leaves and stems (Table 2.5). Similar results were obtained in an experiment conducted in greenhouse conditions with soil samples from BB (Appendix 1). The highest Si concentrations in plants are found in the major transpiration sites (Zhu and Gong, 2014). Guntzer et al. (2012) suggested that Si concentration in a given plant organ reflects its transpiration rate. We may thus hypothesize that the decreased transpiration rate observed in controlled conditions after Si exposure reduced Si accumulation in above-ground biomass. Mineral nutrition is a highly regulated process. For essential elements such as iron, a shoot-to-root signal downregulates iron absorption when the concentration of this element in the roots is sufficient to cover the requirement for metabolism of photosynthetic leaves (Lucena and Hernandez-Apaolaza 2017). Silicon is not regarded as an essential element and it enters passively in plants with water. The channel-type membrane protein (Lsi1) mediates the passive entry of Si, and its expression level in rice was shown to be downregulated by Si (Ma and Yamaji,

2015). Such a downregulation of *Lsi1* under Si exposure in hemp could thus not be ruled out.

Plants grown in CLL accumulated higher Si concentrations in leaves and stem when exposed to Si compared to plants grown in CLL without Si application, and this suggests that the response of the plant to Si application is completely different when plants are exposed to pollutants. Pilon et al. (2013) also reported greatest Si concentration in leaves after foliar application of Si. If Si supplementation may be beneficial for the development of plants subjected to HM stress, it is not surprising to observe an increase in Si accumulation in plants of CLLSi treatment compared to CLL treatment. However, when we compare plants that did not receive Si foliar treatment, we found that Si accumulation was lower in plants cultivated on contaminated CLL than on BB soil and this is valid for both years. It may be hypothesized that Si absorption by roots is somewhat hampered in contaminated soil. Endoderm suberization is frequently increased in HM-treated plants (Pires-Lira et al. 2020). However, Si itself enhances suberization and lignification in root (Fleck et al. 2011). Silicon translocation in accumulators such as rice occurs through the cooperative action of aquaporins and efflux transporters (Ma and Yamaji, 2015), and the presence of HM may have an impact on the membrane proteins involved in Si translocation. We may also hypothesize that climatic conditions, and thus plant transpiration rate, rather than soil characteristics are the reason of the difference in the results obtained between BB and CLL. Soil analysis indeed revealed that, except for soil contamination, the two sites were quite similar.

Although considered as not contaminated, BB presented traces of Cd and Pb in soils samples and plants. Foliar application of H_2SiO_3 tended to decrease stem accumulation of Cd and Pb but it increased the leaf accumulation. This observation demonstrates that foliar application of Si may modify HM distribution in aerial parts of the plants, although the underlying mechanisms still remains elusive. Silicon sprayed onto leaves may have entered leaves and increased Cd and Zn sequestration to the cell wall and trichomes, decreasing the potential for further redistribution (Iwasaki and Matsumura 1999; Wang et al. 2016), but this hypothesis is not supported by the above-mentioned reported decrease in Si for plants cultivated on BB soil (Table 2.5). The fact that HM were mainly accumulated in leaves highlights the importance to harvest hemp before natural leaf drop in order to avoid recontamination of the soil (Di Candilo et al. 2004).

Soil contamination increased leaf and stem HM concentrations compared to plants grown in BB. Plants' exposure to Si increased Cd and Zn accumulation in stems and Cd accumulation in leaves. We suppose that to deal with higher toxic ions concentration in plant, Si increased HM compartmentalization in the stem apoplast, in addition to accumulation in leaf cell walls and trichomes. Liu et al. (2013b) suggested a mechanism of co-deposition of Si and Cd in the cell walls via a [Si-wall matrix]Cd co-complexation as a plausible explanation for the *in vivo* detoxification of Cd.

Bioaccumulation factor (BF) reflects the ability of plants to take up HM from soil and to accumulate it in the shoots. The results showed that Zn was most easily absorbed from soil, followed by Cd and then Pb, even if BF values remained rather low for these two elements. In the absence of Cd and Zn contamination in BB, Si tended to reduce Cd and Zn BF, which is in accordance with many results obtained using foliar application of Si (Wang et al. 2016). Decreased BF may be explained by Si decreased Cd and Zn uptake by roots, and/or by coprecipitation of Cd and Zn with Si in metabolically less active tissues, especially in the endodermis cell wall considering that Si reinforces the endoderm structure (Fleck et al. 2011; Wang et al. 2016). However, this implies that Si was able to translocate from the leaves to the roots. We may nevertheless hypothesize that after several weeks of foliar application of Si, part of the solution reaches the soil and may have reduce the phytoavailability of HM by changing their speciation in soil solution through the formation of silicate complexes (Bhat et al., 2019): in soil solution, soluble silicate can hydrolyze to generate gelatinous metasilicic acid (H_2SiO_3) which can absorb HM (Gu et al. 2011). However, this hypothesis is not supported by the Si-induced significant increase of Cd BF in the presence of soil contamination on the CLL site.

Interactions of hurds and fibres with HM depend on the chemical composition of the polymers. Although Arru et al. (2004) reported that primary bast fibres seem not to be involved in copper accumulation, the present study shows that both Pb and Cd may accumulate on the fibres and that this was the case for plants growing on BB and on CLL. The two sites contained more or less the same amounts of Pb. It is noteworthy, however, that CLL soil contained 5 times more Cd than BB soil, but that the Cd accumulated in the fibres is statistically equivalent. Moreover, the mean concentration of Cd in the fibres was higher than the mean stem concentration, suggesting that fibres constitute a preferential site for Cd sequestration. Metal ions are mainly absorbed at carboxylic groups (mainly found in hemicellulose

and pectin), and to some extent hydroxyl and carbonyl groups (Pejic et al. 2009). Surprisingly, exogenous Si had an opposite effect on Cd retention by fibres because it increased Cd retention in fibres for plants from BB, and decreased the retention of fibres issued from CLL. A modification in hemicellulose content is not responsible for this process: indeed, it presents an opposite trend since it decreased in response to Si in BB, while it increased in response to CLL (Table 2.6). Additional information regarding the precise composition of hemicellulose and the presence of pectic compounds could help to answer this question. Silicon was reported to bind to hemicellulose and the type of binding depends on the nature of polymers (He et al. 2015). If coprecipitation of silicate and Cd occurs, a different composition in hemicellulose polymers might explain a different impact of Si on Cd fixation on fibres from plants harvested on the two sites. In contrast Si similarly increased the Pb content on the fibre for both sites. Lead may also bind to the cell walls, but Xu et al. (2021) recently reported that it mainly exists in the form of insoluble oxalate precipitate.

As mentioned before, field application of Si could improve fibres' quality (Abdelmouleh et al. 2004; Orue et al. 2016; Han et al. 2020). In controlled conditions, fibres fineness (= bundles title), as well as fibres' breaking elongation increased after Si exposure. Similar results were obtained by Khan and Roy (1964) with the commercial fibre jute after soil application of silicate. Guerriero et al. (2019 and 2020) previously showed, via SIMS nano-analysis, that in hemp bast fibres Si accumulates in a specific region of the G-layer closest to the lumen and, preferentially, on the distal side facing the cortex. The presence of Si in the G-layer may account for the mechanical properties observed in the present study. Soil contamination significantly increased fibre bundles' title, as well as force at break and breaking elongation. Si application was shown to be beneficial in the presence of soil contamination by counteracting the effects of soil contamination. However, in the present case, the impact of Si during fibre development on final fibre quality requires additional information. Indeed, Si strongly decreased in fibres harvested on CLL comparatively to those harvested on BB (Figure 2.4), while despite such a decrease, force at break and breaking elongation were higher than for the fibres harvested on BB (Figure 2.2).

To be used in clothes production, heavy metal concentrations in hemp fibres should not exceed the STANDARD 100 established by OEKO-TEX, which is 0.1 mg kg⁻¹ for Cd and 0.2–1.0 mg kg⁻¹ Pb (Linger et al. 2002). In our study, these commercial applications are not recommended, but contaminated

fibres and hurds could be safely used in combined material where HM could not be set free (insulating material and cement agglomerates in bioconstruction, as a sound absorbent material in the automotive industry, ...) or to produce energy in thermal power stations with controlled incineration processes (Linger et al. 2002; Di Candilo et al. 2004; Rheay et al. 2020). If fibres need to be isolated from the stem, retting should be preferentially performed *ex-situ* in liquid medium rather than on the field to avoid HM transfer from the plant to the soil surface or from the soil surface to the valued parts of the harvested biomass.

5. Conclusion

The present work demonstrated that foliar application of Si had no significant impact on the photosynthetic activity of hemp. Nevertheless, our results suggest that Si treatments during fibre development could represent an asset for biomass valorization by providing improved mechanical properties in the absence of Cd and Zn contamination, and by preserving fibres properties when plants are exposed to HM stress. However, Si increased HM accumulation in above-ground biomass. Contaminated fibres and hurds should therefore be used in a way that HM could not be set free, like in cement agglomerates or for energy production with controlled incineration.

Acknowledgement

This work was financed by ADEME (French Agency for the Environment and Energy Management); Convention MisChar n°1672C0044), by FNRS (Fonds National pour la Recherche Scientifique, convention n°T.0147.21), and by the Luxembourg National Research Fund (INTER/FNRS/20/15045745). The authors are grateful to Aurélien Dubar and Arnaud Lefebvre (LGCgE) for fibre preparation and soil samples analysis, and to Mr. X. Joppin (Celabor - Research and Testing Centre in Food, Packaging, Environmental and Textile Technologies) for his valuable help in fibre analysis.

Table S2.1: Soil characterization before crop set up (T0) and after the first and the second years of hemp/wheat culture on HM-contaminated soil of Courcelles-lès-Lens (CLL) or on control soil of Bois-Bernard (BB). Data are means \pm standard errors ($n = 3$). For a specific time (T0, T1, T2) and culture (hemp, wheat), values with different letters are significantly different at $P < 0.05$.

	Site	Culture	Total concentration (mg kg ⁻¹ DM)			CaCl ₂ (0.01M) extractable-HM (mg kg ⁻¹ DM)			pH (water) NF ISO 10390	Exchangeable cations NF X31-130 (cmol kg ⁻¹) CEC
			Cd	Pb	Zn	Cd	Pb	Zn		
T0	BB		1.11 \pm 0.06 a	259 \pm 115 a	81 \pm 4 a	<0.05	<0.64	0.09 \pm 0.09 a	7.04 \pm 0.20 a	17.50 \pm 0.57 a
	CLL		5.54 \pm 0.25 b	298 \pm 21 a	396 \pm 32 b	<0.05	<0.64	0.18 \pm 0.08 a	7.91 \pm 0.11 b	17 \pm 1.89 a
T1	BB	Hemp	0.94 \pm 0.03 a	310 \pm 0.79 a	80 \pm 2 a	<0.05	1.01 \pm 0.25 a	0.07 \pm 0.01 a	7.35 \pm 0.12 a	13.72 \pm 0.41 a
	CLL		5.86 \pm 0.54 b	442 \pm 178 a	354 \pm 21 b	<0.05	<0.64	0.26 \pm 0.05 b	7.65 \pm 0.11 b	14.80 \pm 0.28 b
	BB	Wheat	1.00 \pm 0.10 a	283 \pm 96 a	92 \pm 11 a	<0.05	<0.64	0.07 \pm 0.02 a	6.99 \pm 0.10 a	13.43 \pm 0.07 a
	CLL		5.90 \pm 0.48 b	342 \pm 31 a	404 \pm 43 b	0.07 \pm 0.01	<0.64	0.24 \pm 0.02 b	7.87 \pm 0.05 b	15.37 \pm 0.18 b
T2	BB	Hemp (T1: wheat)	1.18 \pm 0.07 a	392 \pm 299 a	106 \pm 5 a	< 0.05	< 0.64	0.13 \pm 0.01 a	7.40 \pm 0.17 a	14.56 \pm 0.58 a
	CLL		4.99 \pm 0.17 b	344 \pm 10 a	451 \pm 13 b	0.09 \pm 0.02 a	< 0.64	0.30 \pm 0.02 b	7.63 \pm 0.04 b	15.31 \pm 0.40 a
	BB	Wheat (T1: hemp)	0.29 \pm 0.21 a	314 \pm 169 a	86 \pm 8 a	< 0.05	< 0.64	0.12 \pm 0.02 a	7.15 \pm 0.06 a	13.60 \pm 0.55 a
	CLL		5.46 \pm 0.50 b	308 \pm 27 a	407 \pm 35 b	0.09 \pm 0.00 a	< 0.64	0.31 \pm 0.03 b	7.58 \pm 0.08 b	15.05 \pm 1.08 a

Chapter 2: Highlights and Perspectives

Any sustainable strategy helping the plant to cope with heavy metal toxicity could be usefully integrated in a phytomanagement scheme and this is especially the case for Si application: this non-essentially beneficial element contributes to abiotic stress resistance in a wide range of plant species, and several Si derivatives (silane, siloxane, etc.) are used in industry to improve the mechanical properties of the harvested fibres. Foliar spraying of Si during hemp cultivation could therefore represent an asset for fibre production and valorization. In this Chapter, hemp was therefore cultivated in natural field conditions on an agricultural soil formerly contaminated by Cd and Zn, and one half of the plants received weekly foliar spray of Si (2 mM). We investigated the influence of Si application on hemp physiological properties and the impact on fibres' final properties after harvest.

The present Chapter demonstrated that (Figure 2.5):

- Hemp is capable of absorbing and accumulating Si in stems and to a higher extent in leaves in the presence as well as in the absence of foliar application of H_2SiO_3 .
- Plants grown in the presence of HM accumulated higher Si concentrations in leaves than unexposed plants, which might be regarded as an increased need of Si for the induction of adaptative response.
- Si had no significant impact on the photosynthetic activity of hemp, but tended to increase the yield.
- Si increased by 27% the Cd concentration in leaves and by 30% the Zn concentration in stems.
- Si application preserved fibre properties when plants were exposed to HM stress.

Si application can thus be beneficial in the presence of soil contamination by counteracting the effects of HM. However, the efficiency of Si foliar spraying is still a matter of debate: it partly depends on the capacity of Si to enter the plant through stomata and to translocate from the shoot to the roots by the phloem.

Besides, similar impacts of HM on fibres' HM content and properties were obtained in Chapter 1 and Chapter 2, except for hemicellulose content: it

increased in Chapter 1 but decreased in Chapter 2. We may hypothesize that the chemical composition of fibres polymers is highly sensitive to HM content in stems: fibres obtained in Chapter 1 were more concentrated in Pb (2x) and Zn than fibres obtained in Chapter 2. Moreover, in the current study, HM concentration in plants may not have reached a toxic level due to the low HM bioavailability, and we may hypothesize that climatic conditions, rather than soil characteristics, may be the reason of the difference in the results obtained.

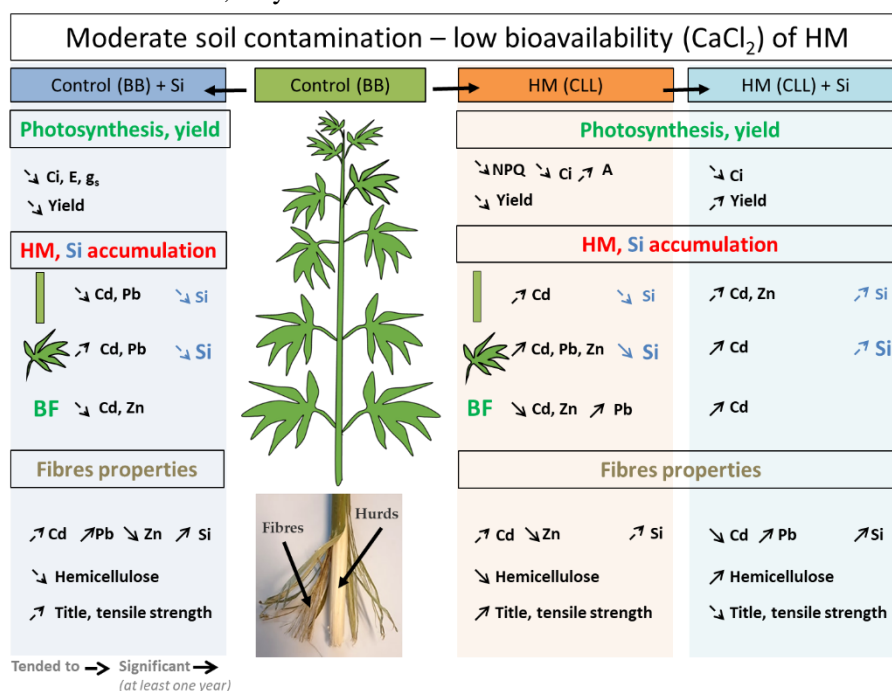


Figure 2.5: Summary of the results obtained in Chapter 2. CO₂ in intercellular spaces (C_i), instantaneous evapotranspiration (E), leaf stomatal conductance (g_s), net photosynthesis (A), bioaccumulation factor (BF). Arrows in dotted lines indicate a non-significant increase/decrease of values, while black arrows illustrate the significant results.

To obtain complementary valuable information regarding the interest of hemp in relation to environmental management, and to quantify the maximal capacities of the plant for bioaccumulation of pollutants independently of the adsorption process occurring in the soils, *C. sativa* was grown in nutrient solution in the presence or absence of Cd (Chapter 3) or Zn (Chapter 4), and in the presence or absence of 2mM Si. In nutrient solution Si is fully available and the control of the pH allows to maintain the bioavailability of HM. Moreover, to the best of our knowledge, no data are available regarding Si impact on HM-treated young plants of hemp.

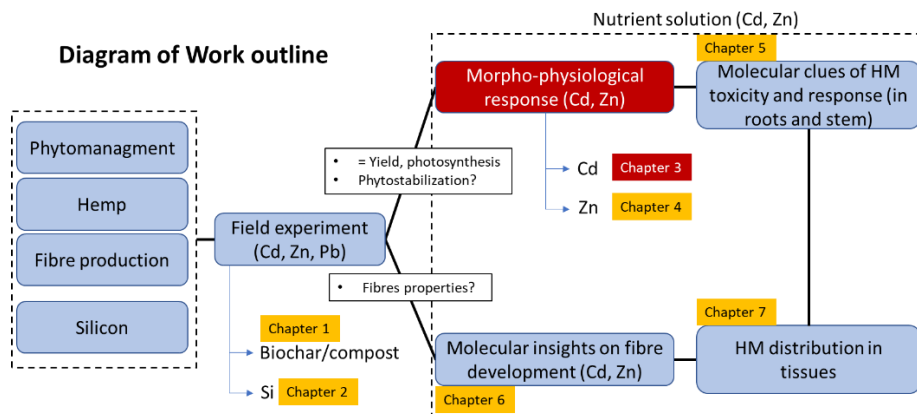
Chapter 3

Studying the impact of a high bioavailability of Cd, as well as the short-term impact of silicon (Si) on biomass production

Published article: Marie Luyckx, Jean-François Hausman, Mathilde Blanquet, Gea Guerriero, Stanley Lutts. Silicon reduces cadmium absorption and increases root-to-shoot translocation without impacting growth in young plants of hemp (*Cannabis sativa* L.) on a short-term basis. 2021. *Environmental Science and Pollution Research*, 1-15.

Author's contributions

ML, GG and SL designed the methodology; ML performed the whole experiment, treated, and analyzed the data; MB contributed to mineral analysis; JFH and SL supervised the whole research process; ML and SL wrote the original draft. All authors reviewed the manuscript.



Abstract

Textile hemp (*Cannabis sativa* L.) is a non-edible multipurpose crop suitable for fibre production and/or phytomanagement on moderately heavy metal-contaminated soils. Experiments were conducted in nutrient solution to assess the short-term impact of silicon (Si), a well-known beneficial element, on plants exposed to 20 μ M cadmium (Cd) in nutrient solution. Cd decreased plant growth and affected photosynthesis through non-stomatal effects. Cd translocation factor was higher than 1, confirming the interest of hemp for phytoextraction purposes. Additional Si did not improve plant growth after 1 week of treatment but decreased Cd accumulation in all organs and improved water use efficiency through a decrease in transpiration rate. Si had only marginal impact on Cd distribution among organs. It increased glutathione and phytochelatin synthesis allowing the plants to efficiently cope with oxidative stress through the improvement of Cd sequestration on thiol groups in the roots. Si may thus have a fast impact on the plant behavior before the occurrence of plant growth stimulation.

1. Introduction

Since the industrial revolution, the phenomenon of heavy metal pollution has been steadily increasing, leading to a rise in atmospheric concentrations and contamination of soil and water in many parts of the world (Barceló and Poschenrieder 2003; Ali et al. 2013; Mahar et al. 2016). Most polluted soils are multi-contaminated, and unlike organic pollutants, heavy metals cannot be degraded but only moved from one place to another (Kumpiene et al. 2008). From an economic point of view, this pollution limits the availability of soils for several uses (residential, commercial, industrial). This is particularly true for agriculture, as environmental legislation prohibits the production of food on contaminated soils considering obvious risks for human health (Grčman et al. 2001; Douay et al. 2013).

Cd is a widespread pollutant extremely toxic for all living organisms. It may accumulate in farmland soils as a result of the use of fertilizers (especially poor-quality phosphate fertilizer), sewage sludge, irrigation wastes, and dry or wet atmospheric deposition (Comnan et al. 2013; Kumarpondit et al. 2017). As a non-essential element, Cd is absorbed by other metal transporters and non-selective cation channels and Cd uptake may consequently compete with the absorption of other divalent cations (Ca, Mg,

Fe, Zn, Mn, and Cu). Numerous transporters from the IRT (iron-regulated transporter), YSL (yellow stripe-like), and NRAMP (natural resistance associated macrophage protein) families were shown to be involved, to various extent, in Cd absorption (Huang et al. 2020). Once it is accumulated within plant tissues, Cd induces a wide range of metabolic disorders, such as oxidative stress; damages to PSII; and decreases in photosynthetic pigments, water stress, leaf chlorosis, and necrosis leading to reduced growth and, ultimately, to plant death (Baryla et al. 2001; Lefèvre et al. 2014; He et al. 2017; Berni et al. 2018). Strategies adopted by the plants to cope with high Cd concentration involve reduction of Cd uptake and root-to-shoot translocation, activation of antioxidative systems, and synthesis of sulfur-containing ligands mainly phytochelatins (PC) allowing Cd vacuolar sequestration (Cobbett 2000; Huang et al. 2020).

Plants may be grown on Cd-contaminated substrate for two distinct purposes. The first one is phytomanagement where plants are cultivated to extract, degrade, or immobilize various contaminants from polluted soils (Barceló and Poschenrieder 2003; Ali et al. 2013). Phytoextraction consisting in pollutant accumulation in harvestable parts appears as an interesting cheap alternative to the physicochemical methods traditionally used, since the initial investment is lower although the immobilization of the site is quite longer than for classical engineering approaches (Mahar et al. 2016). The second application of plant culture concerns moderately contaminated substrates and consists in the use of non-edible crop of commercial interest to valorize these marginal farmland soils and provide incomes for the farmer (Tóth et al. 2016; Feng et al. 2020). It is commonly assumed that these two types of plant utilization are somewhat incompatible, since phytoextraction relies on heavy metal absorption by the plant while agricultural application is expected to produce non-contaminated plant products. This, however, partly depends on the nature of the harvested organs in relation to heavy metal distribution at the whole plant level. If the harvested organs are free of pollutant while the remaining part of the shoot contains high amounts of pollutant, it appears possible to combine an agricultural purpose and a phytomanagement process. Hence, determining pollutant distribution among plant organs, as well as bioaccumulation and root-to-shoot translocation factors, is of paramount importance.

Fibre crops are important plant species for bio-economy and are now receiving considerable attention (Guerriero et al. 2017b). Hemp (*Cannabis sativa* L.) is considered a rotation head in culture systems. It provides cortical

fibre mainly used in paper industries and for the manufacture of various products (composites, insulators, reinforced thermoplastics), and hurds used for the manufacture of animal litter and, in particular, in the composition of building materials (Duque- Schumacher et al. 2020; Vandepitte et al. 2020). Seeds may also be harvested and contain valuable essential oil (Ascrizzi et al. 2019). Many authors (Angelova et al. 2004; Shi et al. 2009, 2012; Ahmad et al. 2016a; Kumar et al. 2017; Zielonka et al. 2020) have considered using hemp in phytomanagement and believe that the plant is able, to a certain extent, to reduce Cu, Zn, Cd, and Pb contamination in soils. While heavy metals can accumulate within walls in plant tissues (Krzeslowska 2011), the influence of these metals on the growth and development of hemp remains poorly understood, particularly in relation to the kinetics of fibre development. Although seeds may accumulate Cd concentrations above the upper limit (Mihoc et al. 2012), preliminary data demonstrated that bast fibres remain free of heavy metals when plants were grown in heavy metal-rich solution (Arru et al. 2004) so that fibre production might appear compatible with phytoextraction.

Hemp cultivars differ for their average level of Cd resistance (Huang et al. 2019; Zielonka et al. 2020; Kalousek et al. 2020). Besides a breeding approach aiming to select the most appropriate cultivars, some technical strategies, such as the application of biodegradable chelators (Kos and Leštan 2004) or the inoculation with arbuscular mycorrhiza fungus (Citterio et al. 2005), also contribute to reinforce the capacity of *Cannabis sativa* to accumulate toxic heavy metals. Application of Si fertilizers is a promising option to mitigate the deleterious impact of heavy metal stress on various species (Neumann and Zur Nieden 2001; Doncheva et al. 2009; Wu et al. 2013; Bhat et al. 2019). The young plant stage is often considered the most sensitive one to heavy metals which is mainly due to an incomplete formation of suberized endoderm, thus allowing massive uncontrolled translocation of pollutant through by pass flow (Lefèvre et al. 2009). Si has been reported to deposit in the vicinity of the endodermis, thus contributing to reinforce the barrier against Cd translocation (Shi et al. 2005; Imtiaz et al. 2016) and similar finding were reported for other mineral constraints such as salinity (Yeo et al. 1999). Moreover, Si can accumulate within the parietal structures where it is present in the form of opaline silica (SiO₂) and contributes to reinforce the mechanical properties of the cell wall polymers (Kröger and Poulsen 2004). Adrees et al. (2015) also reported that Si is suspected to influence the root-to-shoot translocation of heavy metals.

The nature and the extent of Si-induced protection depend on the plant species and on the nature of the stressor. As far as hemp is concerned, Guerriero et al. (2019) recently identified aquaporins putatively involved in Si absorption. Berni et al. (2020) confirmed that exogenous Si may mitigate the deleterious effect of salt stress in *C. sativa*. However, to the best of our knowledge, no data are available regarding Si impact on Cd-treated young plants of hemp. The present work was therefore undertaken in order to determine the Si impact on Cd distribution in young hemp plants and the short-term physiological consequences of this impact on photosynthesis-related parameters, water status, and oxidative stress.

2. Material and methods

2.1. Plant material and growing conditions

Seeds of a monoecious hemp fibre variety (*C. sativa* cv. Santhica 27) were sown in loam substrate in greenhouse conditions. After 1 week, the obtained seedlings were transferred to nutrient Hoagland solution (in mM: 2.0 KNO₃, 1.7 Ca(NO₃)₂, 1.0 KH₂PO₄, 0.5 NH₄NO₃, 0.5 MgSO₄; in μM: 17.8 Na₂SO₄, 11.3H₃BO₃, 1.6 MnSO₄, 1 ZnSO₄, 0.3CuSO₄, 0.03 (NH₄), 6 Mo₇O₂₄, and 14.5 Fe-EDDHA) in 5-L tanks: for each tank, the seedling was adapted to plugged hole in a polystyrene plate floating at the top of the nutrient solution. Tanks were placed in a phytotron under fully controlled environmental conditions (permanent temperature of 24 ± 1 °C with a mean light intensity of 230 μmol m⁻² s⁻¹ provided by Phillips lamps (Phillips Lighting S.A., Brussels, Belgium) (HPI-T 400 W), with a photoperiod of 16 h under a relative humidity of 65%). After a week of acclimatization, half of the tanks received Si in the form of H₂SiO₃ to a final concentration of 2 mM Si (the maximum solubility of H₂SiO₃ in solution). Metasilicic acid was obtained from a pentahydrate sodium metasilicate (Na₂SiO₃ × 5 H₂O) which was passed through an H⁺ ion exchanger resin IR 20 Amberlite type according to Dufey et al. (2014). Tanks were randomly arranged in the phytotron, and the nutrient solution was permanently aerated by SuperFish Air Flow 4 pump. A week later, Cd was applied in the form of CdCl₂ (20 μM). The pH of the solution was maintained at 5.5. Four treatments were thus defined, considering the presence of Cd and the concomitant presence or absence of Si and will be designated as C (control: no heavy metals and no Si), CSi, Cd, and CdSi (7 tanks per treatment). The solubility of added heavy metal was confirmed by the

VisualMINTEQ09 software; speciation of Cd was Cd^{2+} (93.82%), CdHPO_4 (5.96%), CdCl^+ (0.129%), and CdNO_3^+ (0.04%) while speciation of Si indicated H_4SiO_4 (94.06%) and H_3SiO_4^- (5.93%). Si had no significant impact on Cd solubility and speciation. Cadmium and Si in the nutrient solution were analyzed at the beginning and at the end of treatment to ensure they remain soluble and available to the plants.

Harvests were performed after a week of Cd exposure. Stem length and diameter, number of leaves, and main root length were considered. Roots were quickly rinsed in deionized water for 30 s just before harvest to remove ions from the free spaces. Roots were then separated from shoots, and leaves were separated from the stem. Roots and leaves from the same treatment were pooled, quickly frozen in liquid nitrogen, and then stored at $-80\text{ }^\circ\text{C}$ until analysis, except for subsamples of 3 plants per treatment incubated in an oven at $70\text{ }^\circ\text{C}$ for 72 h to estimate dry weight and water content and to determine ion content.

2.2. Mineral concentration

Fifty mg DM (dry matter) of plant samples was dried at $70\text{ }^\circ\text{C}$ for 72 h, then digested in 68% HNO_3 and acid evaporated to dryness on a sand bath at $80\text{ }^\circ\text{C}$. Minerals were incubated with a mix of HCl 37%– HNO_3 68% (3:1) and the mixture was slightly evaporated and dissolved in distilled water. After filtration on Whatman no. 1 filter paper, cations were quantified by inductively coupled plasma-optical emission spectroscopy (Varian, type MPX). For Si quantification, 1-g DM was placed in an oven and heated to $500\text{ }^\circ\text{C}$ for 48 h. Ashes were then mixed with 0.4 g tetraborate and 1.6 g metaborate and heated to $1000\text{ }^\circ\text{C}$ for 5 min. The obtained pellet was dissolved with 34% HNO_3 . Cations were quantified by inductively coupled plasma-optical emission spectroscopy (Varian, type MPX).

Translocation factor reflects the capacity of the plant to translocate heavy metal from the root to the shoot and was estimated (1) on the basis of the concentration expressed on a dry weight basis in each plant part (TFc) and (2) on the basis of total amount of the considered element (TFa)

$\text{TFc} = \text{Cd concentration in the shoot} / \text{Cd concentration in the root}$

$\text{TFa} = \text{Total Cd amount accumulated in the shoot} / \text{Cd accumulated in the root}$

The bioaccumulation factor (BF) considers the capacity of the plant to store heavy metals in relation to external concentration. Since a nutrient

solution was used in the present work rather than a solid substrate, the internal concentration in the plant was estimated on a water content basis, considering the proportion of the different organs:

$BF = \text{Cd concentration in the plant (mg}\cdot\text{L}^{-1})/\text{Cd concentration in the solution (mg}\cdot\text{L}^{-1})$

2.3. Photosynthesis-related parameters

Before plant harvest, physiological measurements were performed on 5 plants per treatment, on the middle portion of the blades on the second fully expanded leaf from the top. Chlorophyll fluorescence parameters (maximum quantum yield of photosystem II (F_v/F_m), photochemical quenching (q_p), non-photochemical quenching (NPQ) and actual efficiency of photosystem II (Φ_{PSII})), leaf stomatal conductance (g_s), the instantaneous CO_2 assimilation under ambient conditions (400 ppm CO_2) (A) and instantaneous transpiration (E) were measured as detailed in Chapter 1 (p.83-84). All measurements were performed around midday (between 12 a.m. and 2 p.m).

Total chlorophyll (a + b) and carotenoid concentrations were measured according to Lichtenthaler (1987): 100-mg ground fresh samples were homogenized in 10 mL of cold acetone, then centrifuged at 936g for 10 min at 4 °C. Absorbance was measured on supernatant at 663.2 nm, 646.8 nm, and 470 nm.

For osmotic potential determination (Ψ_s), the middle portion of the leaf blades constituting the second fully formed leaves from the top was quickly collected from five plants, cut in small segments placed in Eppendorf tubes perforated with small holes, and immediately frozen in liquid nitrogen. Samples were then thawed 5 min at ambient temperature to rupture the membranes. Freeze-thawing cycles were repeated three times. Each tube was then encased in a second intact Eppendorf tube and centrifuged at 8000g for 15 min at 4 °C. The osmolarity of the collected sap was analyzed with a vapor pressure osmometer (VAPRO® Vapor Pressure Osmometer 5520).

2.4. Malondialdehyde content and total antioxidant activities

The level of lipid peroxidation in the control and Cd-treated plants was assessed from the concentration of malondialdehyde (MDA) as determined by the thiobarbituric acid (TBA) reaction (Heath and Packer 1968). To estimate

the total global antioxidant activity, ferric-reducing ability of plasma (FRAP) was assayed according to Benzie and Strain (1996), considering the ability of plant extract to reduce ferric to ferrous ion at low pH and to produce a colored ferrous-tripyridyltriazine complex which was spectrophotometrically detected at 593 nm. The hydrophilic (AOAM) and hydrophobic fractions (AOAD) were discriminated. The standard curve was established with Trolox (50–800 μM). The concentration is expressed in micromolars of trolox equivalents (TE) g^{-1} of fresh material.

2.5. Glutathione and total non-protein thiols

For reduced (GSH) and total (GSht) glutathione quantification, 200 mg of frozen samples was extracted and derivatized by orthophthalaldehyde (OPA) according to Cereser et al. (2001). GSht was quantified after a reduction step of oxidized glutathione (GSSG) by dithiothreitol. Five microliters of sample was injected into a Shimadzu HPLC system (Shimadzu, 's-Hertogenbosch, The Netherlands) equipped with a Nucleodur C18 Pyramid column (125×4.6 -mm internal diameter; 5- μm particle size) (Macherey-Nagel, Duren, Germany). Fluorimetric detection was performed with a spectra system Shimadzu RF-20A fluorescence detector at 420 nm after excitation at 340 nm.

The total non-protein thiol (NPT) concentration was determined according to De Vos et al. (1992) using Ellman's reagent. The NPT concentration was estimated spectrophotometrically at 412 nm using an extinction coefficient of $13,600 \text{ M}^{-1} \text{ cm}^{-1}$. Phytochelatin content was evaluated as the difference between NPT and GSH levels.

2.6. Statistical analysis

All analyses were performed on 5 replicates. Normality of the data was verified using Shapiro-Wilk tests, and the data were transformed when required. Homogeneity of the data was verified using Levene's tests. ANOVA 2 were performed at a significant level of P value < 0.05 using R (version 3.3.1) considering the type of heavy metal treatment, and the Si application as main factors. Means were compared using Tukey's HSD all-pairwise comparisons at 5% level as a post hoc test.

3. Results

3.1. Plant growth and morphological parameters



Figure 3.1: *C. sativa* (cv. Santhica 27) exposed for 1 week to Cd (20 μ M), in the presence or in the absence of 2 mM H_2SiO_3 .

As illustrated in Figure 3.1, the presence of Cd in the external nutrient solution strongly hampered plant development and compromised plant growth, inducing a decrease in shoot elongation, stem diameter, and number of leaves while the length of the root remained unaffected by the treatments (Figure 3.2). Cd-treated plants exhibited a stunted growth, leaf chlorosis, and leaf rolling behavior. Si had no impact on control plant, except a slight decrease in stem diameter, and it did not attenuate the impact of Cd on morphological parameters of heavy metal-treated plants considering the duration of the treatment (1 week) (Figure 3.2).

Cd decreased both fresh and dry weights of roots, stems, and leaves in *C. sativa* (Table 3.1). It had no impact on the water content of roots and stems but it decreased the leaf WC. Exogenous Si did not interfere with Cd-induced growth inhibition. Cd decreased the leaf osmotic potential, and this effect was even reinforced by the concomitant presence of Si exposure. Si also significantly decreased leaf Ψ_s in the absence of Cd.

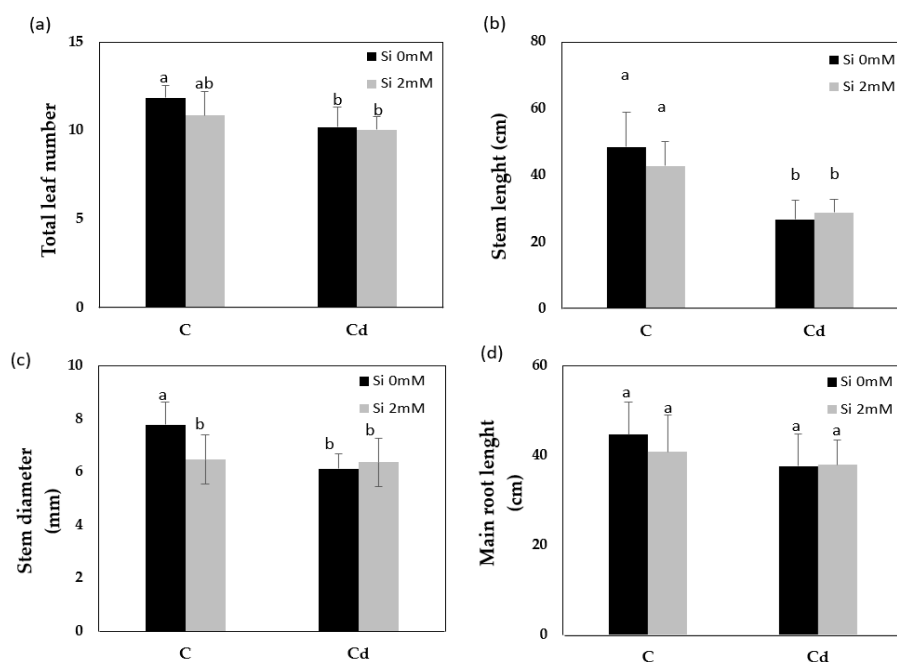


Figure 3.2: Total leaf number (a), stem length (b) and diameter (c), and root length (d) of *C. sativa* (cv. Santhica 27) exposed for 1 week to Cd (20 μ M), in the presence or in the absence of 2 mM H_2SiO_3 . Data are means \pm standard errors ($n = 5$). Values with different letters are significantly different ($P < 0.05$; Tukey's HSD all-pairwise comparisons).

Table 3.1: Fresh weight (FW), dry weight (DW), water content (WC), and osmotic potential (ψ_s) of *C. sativa* (cv. Santhica 27). Plants were exposed for 1 week to Cd (20 μ M) in the presence or in the absence of 2 mM H_2SiO_3 . For a given organ, different letters indicate significant differences at $P < 0.05$. Each value is the mean of 3 replicates (FW, DW, and WC) or 5 replicates (ψ_s).

	C	CSi	Cd	CdSi
FW (g)				
Roots	14.67 \pm 3.76 a	13.08 \pm 4.52 a	6.96 \pm 1.62 b	5.84 \pm 1.53 b
Stems	16.37 \pm 3.56 b	12.28 \pm 2.15 b	5.72 \pm 1.36 a	6.01 \pm 1.83 a
Leaves	40.88 \pm 2.09 b	30.24 \pm 8.43 b	8.20 \pm 3.26 a	11.01 \pm 0.12 a
DW (g)				
Roots	1.43 \pm 0.19 b	1.23 \pm 0.03 b	0.56 \pm 0.12 a	0.49 \pm 0.12 a
Stems	1.62 \pm 0.32 b	1.42 \pm 0.28 b	0.72 \pm 0.12 a	0.81 \pm 0.15 a
Leaves	6.34 \pm 0.54 b	5.62 \pm 0.72 b	2.31 \pm 0.50 a	2.18 \pm 0.60 a
WC (%)				
Roots	91 \pm 1.0 a	93 \pm 0.4 b	92 \pm 0.9 ab	91 \pm 0.7 a
Stems	90 \pm 2.3 b	90 \pm 1.0 b	88 \pm 0.8 ab	85 \pm 2.3 a
Leaves	84 \pm 0.2 b	85 \pm 1.0 b	78 \pm 3.3 a	77 \pm 2.9 a
ψ_s (Mpa)				
Leaves	-1.15 \pm 0.03 d	-1.21 \pm 0.04 c	-1.48 \pm 0.05 b	-1.56 \pm 0.04 a

3.2.Plant mineral content

Cd accumulated to higher concentration in the roots than in the shoot (Table 3.2). As far as shoot is concerned, Cd accumulation was higher in the stem than in the leaves. The additional presence of Si in the nutrient solution significantly reduced Cd accumulation in all organs, but it increased both TF_c and TF_a values comparatively to plants exposed to Cd in the absence of Si. In all cases, TF_a values were higher than TF_c values. The Cd bioaccumulation factor was as high as 89.1 in Cd-treated plants and Si only slightly reduced Cd BF. As expected, Si content increased in all plant parts when unstressed plants were exposed to Si treatment, reaching more than $2 \text{ g}\cdot\text{kg}^{-1}$ in roots and more than $3 \text{ g}\cdot\text{kg}^{-1}$ DM in leaves, while the minimal value was recorded in the stem. It is noteworthy that Cd treatment in CdSi-exposed plants significantly reduced Si accumulation in the roots and in the stems but strongly increased it in the leaves, where it reached almost $5 \text{ g}\cdot\text{kg}^{-1}$. Cd treatment induced a strong increase of TF_a and TF_c values recorded for Si (Table 3.2), and it also increased by more than 50% the Si bioaccumulation factor in *C. sativa*.

Table 3.2: Cadmium (Cd) and silicon (Si) concentrations (in mg kg^{-1} DW) and translocation factor (TF) in roots, stem, and leaves of *C. sativa* (cv. Santhica 27). Plants were exposed for 1 week to Cd ($20 \mu\text{M}$) in the presence or in the absence of $2 \text{ mM H}_2\text{SiO}_3$. TF_c : translocation factor estimated on a concentration basis. TF_a : translocation factor estimated on a total amount basis. BF: bioaccumulation factor. For a given parameter and a given organ, means ($n = 3$) followed by different letters are significantly different at $P < 0.05$. Nd, not detected ($< \text{LOD}$).

	C	CSi	Cd	CdSi
Cd (mg kg^{-1} DW)				
Roots	$5.59 \pm 1.56 \text{ a}$	nd	$2687 \pm 624 \text{ c}$	$1819 \pm 532 \text{ b}$
Stems	$0.04 \pm 0.08 \text{ a}$	$0.25 \pm 0.50 \text{ a}$	$1243 \pm 174 \text{ c}$	$978 \pm 141 \text{ b}$
Leaves	nd	nd	$717 \pm 88 \text{ b}$	$623 \pm 76 \text{ a}$
TF_c	$0.00 \pm 0.00 \text{ a}$	$0.00 \pm 0.00 \text{ a}$	$0.31 \pm 0.06 \text{ b}$	$0.40 \pm 0.12 \text{ b}$
TF_a	$0.01 \pm 0.002 \text{ a}$	$0.00 \pm 0.00 \text{ a}$	$1.68 \pm 0.27 \text{ b}$	$2.40 \pm 0.54 \text{ b}$
BF	$0.04 \pm 0.001 \text{ a}$	$0.00 \pm 0.00 \text{ a}$	$89.10 \pm 5.74 \text{ b}$	$81.18 \pm 2.38 \text{ b}$
Si (mg kg^{-1} DW)				
Roots	$212 \pm 39 \text{ a}$	$2002 \pm 212 \text{ b}$	$237 \pm 63 \text{ a}$	$1626 \pm 156 \text{ c}$
Stems	nd	$218 \pm 13 \text{ a}$	nd	$89 \pm 35 \text{ b}$
Leaves	$70 \pm 13 \text{ a}$	$3391 \pm 65 \text{ b}$	nd	$4852 \pm 102 \text{ c}$
TF_c	$0.26 \pm 0.04 \text{ b}$	$1.33 \pm 0.11 \text{ c}$	$0.00 \pm 0.00 \text{ a}$	$2.19 \pm 0.57 \text{ d}$
TF_a	$1.47 \pm 0.20 \text{ b}$	$8.64 \pm 1.25 \text{ c}$	$0.00 \pm 0.00 \text{ a}$	$13.31 \pm 3.25 \text{ d}$
BF	$0.22 \pm 0.01 \text{ b}$	$7.60 \pm 0.43 \text{ c}$	$0.06 \pm 0.01 \text{ a}$	$11.76 \pm 0.64 \text{ d}$

In the absence of Cd, Si induced an increase in Ca and Mg concentration in the root, an increase in stem Fe, and a decrease in leaf P (Table 3.3). Cd increased Ca, P, and S in the stems and in the leaves. It increased Fe concentration in the roots but decreased it in the leaves and also decreased K concentration in the leaves. The addition of Si to Cd-treated plants mitigated the impact of Cd: it strongly increased the leaf Fe content, suppressed the Cd-induced decrease in Ca in the roots and mitigated the Cd-induced P increase in the shoot parts. In contrast, Si had no significant impact on S accumulation in the shoot of Cd-treated plants.

Table 3.3: Calcium (Ca), iron (Fe), potassium (K), magnesium (Mg), phosphorus (P), and sulfur (S) concentrations and translocation factor (TF) in roots, stem, and leaves of *C. sativa* (cv. Santhica 27). Plants were exposed for 1 week to Cd (20 μ M) in the presence or in the absence of 2 mM H₂SiO₃. TF_c: translocation factor estimated on a concentration basis. TF_a: translocation factor estimated on a total amount basis. BF: bioaccumulation factor. For a given parameter and a given organ, means followed by different letters are significantly different at $P < 0.05$. Each value is the mean of 3 replicates.

	C	CSi	Cd	CdSi
Ca (mg kg⁻¹ DW)				
Roots	2709 ± 36 a	3050 ± 133 b	2385 ± 103 c	2685 ± 72 a
Stems	8712 ± 141 a	9889 ± 320 ab	10978 ± 479 b	9021 ± 602 a
Leaves	50539 ± 1061 a	48008 ± 919 a	55234 ± 1342 b	50344 ± 1427 a
Fe (mg kg⁻¹ DW)				
Roots	588 ± 39 a	660 ± 46 a	867 ± 55 b	847 ± 88 b
Stems	49 ± 1 ac	64 ± 5 b	56 ± 5 bc	45 ± 2 a
Leaves	133 ± 10 a	118 ± 9 abc	91 ± 3 c	207 ± 18 d
K (mg kg⁻¹ DW)				
Roots	40923 ± 972 a	44665 ± 2698 a	45837 ± 2942 a	40658 ± 1979 a
Stems	53487 ± 783 b	46209 ± 29 ac	46234 ± 864 a	40488 ± 3354 c
Leaves	43327 ± 694 a	42149 ± 1605 a	35444 ± 663 b	35736 ± 293 b
Mg (mg kg⁻¹ DW)				
Roots	2468 ± 64 a	3044 ± 169 b	2823 ± 151 ab	2862 ± 186 b
Stems	1660 ± 16 b	1664 ± 16 b	2100 ± 75 a	1776 ± 156 b
Leaves	5877 ± 87 a	5679 ± 80 a	5761 ± 89 a	5851 ± 240 a
P (mg kg⁻¹ DW)				
Roots	11430 ± 329 a	10356 ± 762 a	11683 ± 1057 a	10353 ± 835 a
Stems	6000 ± 35 ab	5188 ± 7 a	9368 ± 243 c	7064 ± 632 b
Leaves	7403 ± 106 a	6984 ± 117 b	10140 ± 104 c	8472 ± 230 d
S (mg kg⁻¹ DW)				
Roots	1871 ± 472 a	2477 ± 158 a	2255 ± 918 a	3348 ± 410 a
Stems	616 ± 158 a	412 ± 138 a	2029 ± 382 b	1793 ± 439 b
Leaves	1203 ± 117 a	967 ± 61 a	2254 ± 148 b	1908 ± 740 b

3.3. Photosynthesis-related parameters

Si applied in the absence of Cd significantly increased *Chla*, *Chlb*, and carotenoid concentration in the leaves of *C. sativa* (Figure 3.3). Conversely, Cd induced a strong decrease in all photosynthetic pigments and Si was unable to reduce the heavy metal impact on chlorophyll and carotenoid concentrations. Neither Si nor Cd had any impact on F_v/F_m , q_p , and Φ_{PSII} which remained constant in all treatments (Table 3.4). Cd unexpectedly reduced NPQ values: the recorded decrease was similar in Cd and CdSi-treated plants.

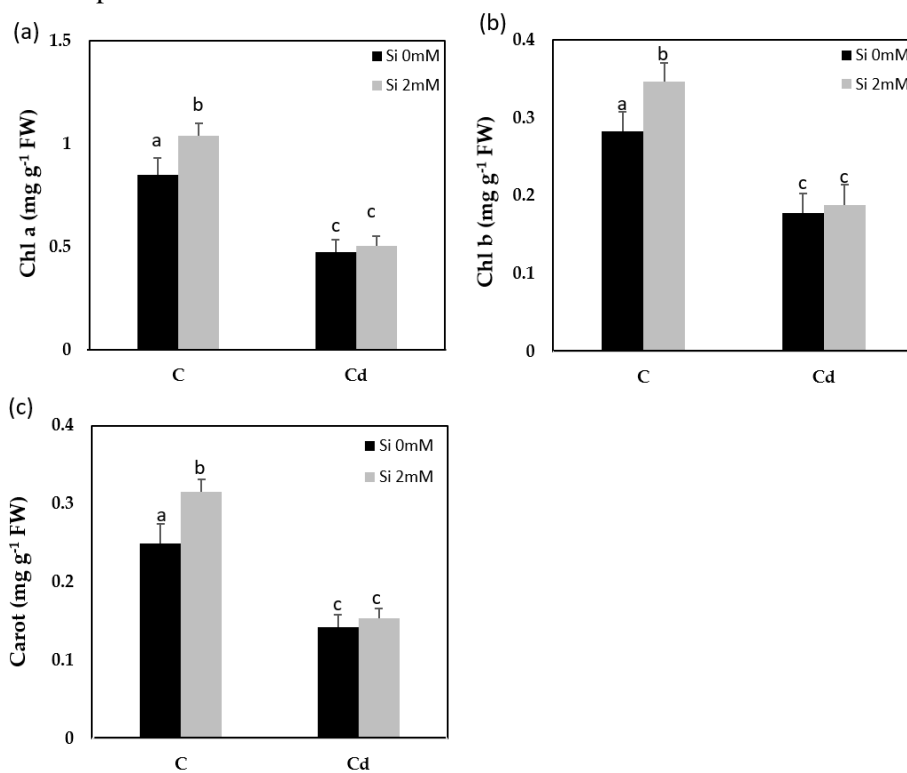


Figure 3.3: Chlorophyll a (a), chlorophyll b (b), and carotenoid (c) content of *C. sativa* (cv. Santhica 27) exposed for 1 week to Cd (20 μ M), in the presence or in the absence of 2 mM H₂SiO₃. Data are means \pm standard errors (n = 5). Values with different letters are significantly different (P < 0.05; Tukey's HSD all-pairwise comparisons).

Net photosynthesis (A ; Table 3.4) was not affected by Si in the absence of Cd. Cd decreased the A values, and Si had no mitigating impact on Cd effects. A high level of variability was observed for stomatal conductance: Si reduced g_s in Cd treated plants. Similarly, Si had no impact on instantaneous

transpiration (E) in the absence of Cd and Cd in the absence of Si also had no impact on transpiration. However, Si significantly decreased E values in the presence of Cd. Cd-treated plants exhibited higher C_i values than control ones, especially in the absence of Si.

Table 3.4: Photosynthesis-related parameters of *C. sativa* (cv. Santhica 27). Plants were exposed for 1 week to Cd (20 μM) in the presence or in the absence of 2 mM H_2SiO_3 . Maximum quantum yield of dark-acclimated leaves (F_v/F_m), the photochemical efficiency of photosystem II (ϕ_{PSII}), photochemical quenching (qP), non-photochemical quenching (NPQ), stomatal conductance (g_s), net photosynthesis (A), instantaneous evapotranspiration (E), CO_2 in intercellular spaces (C_i). For a given organ, different letters indicate significant differences at $P < 0.05$. Each value is the mean of 5 replicates.

	C	CSi	Cd	CdSi
F_v/F_m	0.91 \pm 0.01 <i>a</i>	0.91 \pm 0.01 <i>a</i>	0.89 \pm 0.03 <i>a</i>	0.91 \pm 0.01 <i>a</i>
ϕ_{PSII}	0.87 \pm 0.01 <i>a</i>	0.87 \pm 0.01 <i>a</i>	0.84 \pm 0.03 <i>a</i>	0.85 \pm 0.05 <i>a</i>
qP	0.98 \pm 0.01 <i>a</i>	0.97 \pm 0.02 <i>a</i>	0.98 \pm 0.02 <i>a</i>	0.95 \pm 0.04 <i>a</i>
NPQ	0.25 \pm 0.04 <i>b</i>	0.29 \pm 0.03 <i>b</i>	0.19 \pm 0.03 <i>a</i>	0.17 \pm 0.03 <i>a</i>
g_s ($\text{mmol m}^{-2} \text{s}^{-1}$)	478 \pm 252 <i>b</i>	435 \pm 441 <i>ab</i>	411 \pm 163 <i>b</i>	161 \pm 90 <i>a</i>
A ($\mu\text{mol m}^{-2} \text{s}^{-1}$)	4.21 \pm 0.37 <i>b</i>	3.43 \pm 0.63 <i>b</i>	1.79 \pm 0.42 <i>a</i>	1.66 \pm 0.84 <i>a</i>
E ($\text{mmol m}^{-2} \text{s}^{-1}$)	2.47 \pm 0.65 <i>b</i>	2.40 \pm 1.00 <i>b</i>	2.71 \pm 0.34 <i>b</i>	1.72 \pm 0.56 <i>a</i>
C_i ($\mu\text{mol mol}^{-1}$)	333 \pm 20 <i>a</i>	342 \pm 20 <i>ab</i>	371 \pm 8 <i>c</i>	355 \pm 8 <i>b</i>

3.4. Oxidative stress-related parameters and phytochelatin estimation

Malondialdehyde (MDA) as an indicator of oxidative stress increased in the leaves in response to Si in the absence of Cd (Figure 3.4a). The highest leaf MDA concentration was observed in response to Cd treatment: addition of Si slightly decreased Cd-induced MDA accumulation but the recorded decrease was not significant from a statistical point of view. At the root level (Figure 3.4b), the MDA concentration was the highest for the control plants, while Si and Cd applied separately decreased MDA content to similar extent. The impacts of Si and Cd were somewhat additive since the lowest MDA value was recorded for CdSi treatment.

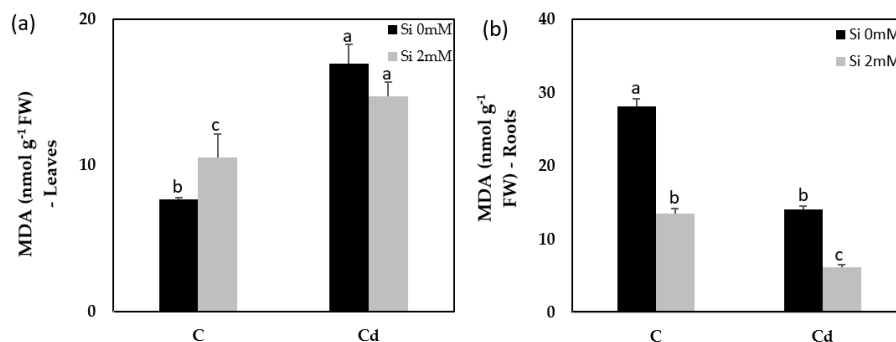


Figure 3.4: Malondialdehyde (MDA) content in leaves (a) and roots (b) of *C. sativa* (cv. Santhica 27) exposed for 1 week to Cd (20 μM), in the presence or in the absence of 2 mM H_2SiO_3 . Data are means \pm standard errors ($n = 5$). Values with different letters are significantly different ($P < 0.05$; Tukey's HSD all-pairwise comparisons).

The total antioxidant activity was determined for the leaves by using the FRAP index (Figure 3.5) and discriminating the AOAD (hydrophobic) and AOAM (hydrophilous) fractions. The FRAP index increased in response to Si for both fractions in control plants. In Cd- and in CdSi-treated plants, the AOAD fraction decreased to lower value than the control while the AOAM fraction was similar in those plants comparative to control.

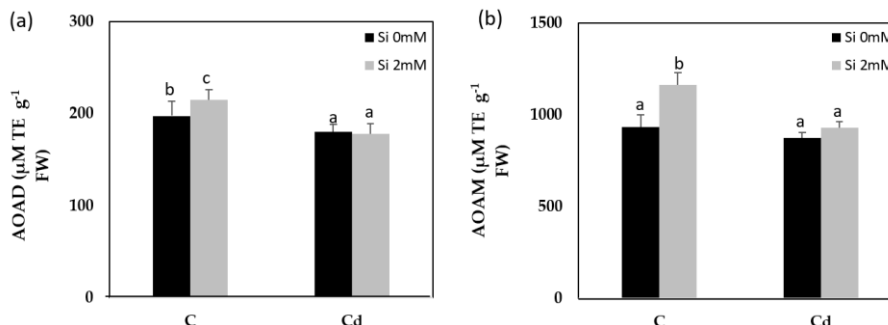


Figure 3.5: Total antioxidant activity in the hydrophobic fraction (AOAD; a) and the hydrophilic fraction (AOAM; b) of leaves of *C. sativa* (cv. Santhica 27). Plants were exposed for 1 week to Cd (20 μM), in the presence or in the absence of 2 mM H_2SiO_3 . Data are means \pm standard errors ($n = 5$). Values with different letters are significantly different ($P < 0.05$; Tukey's HSD all-pairwise comparisons)

The concentration of total glutathione in the roots (Table 3.5) was the highest for control plants and decreased in response to Cd, Si, and Cd + Si treatments. The ratio GSSG/GSH was also the highest for control and decreased in all other treatments, being the lowest for CdSi-exposed plants. The leaves displayed a different profile with similar values for total GSH in

control and Si-treated plants and a significant drop in plants exposed to Cd or CdSi. A strong increase in the leaf GSSG/GSH ratio was also observed in response to Cd. The non-protein phytochelatin (Table 3.5) strongly increased in the roots of plants exposed to Cd and reached more than 3000 $\mu\text{mol g}^{-1}$ FW in both Cd- and CdSi-treated plants. Phytochelatin concentration also increased in response to Cd in the leaves, although to a lower extent than in the roots and plants exposed to Cd and to CdSi once again exhibited similar behavior.

Table 3.5: Total glutathione (GSHt), oxidized (GSSG)/reduced (GSH) glutathione, and phytochelatin (PC) concentrations in roots and leaves of *C. sativa* (cv. Santhica 27). Plants were exposed for 1 week to Cd (20 μM) in the presence or in the absence of 2 mM H_2SiO_3 . For a given parameter and a given organ, means followed by different letters are significantly different at $P < 0.05$. Each value is the mean of 5 replicates

	C	CSi	Cd	CdSi
Roots				
GSHt (nmol g^{-1} FW)	116 \pm 9 c	72 \pm 5 a	67 \pm 2 a	92 \pm 31 b
GSSG/GSH	32.70 \pm 5.28 c	7.67 \pm 0.53 b	2.41 \pm 0.15 a	2.11 \pm 0.98 a
PC (nmol g^{-1} FW)	296 \pm 19 b	248 \pm 24 a	3473 \pm 181 c	3727 \pm 169 c
Leaves				
GSHt (nmol g^{-1} FW)	455 \pm 42 b	455 \pm 24 b	291 \pm 38 a	285 \pm 7 a
GSSG/GSH	2.34 \pm 0.73 a	7.41 \pm 1.21 ac	12.95 \pm 5.96 bc	15.00 \pm 6.00 b
PC (nmol g^{-1} FW)	362 \pm 84 a	464 \pm 24 b	1749 \pm 73 c	1613 \pm 120 c

4. Discussion

Cd impact on hemp behavior

Since a few years, hemp (*C. sativa*) receives considerable attention in relation to fibre production in the stem (Duque-Schumacher et al. 2020; Vandepitte et al. 2020), cannabinoid synthesis in the flowers (Hussain et al. 2019b; Yang et al. 2020), and oil in the grains (Mihoc et al. 2012; Ascrizzi et al. 2019) and as an interesting biomass-producing plant (Matassa et al. 2020; Zhao et al. 2020). This promising multipurpose crop was also recently recommended as a possible candidate for phytomanagement of heavy metal-contaminated soils (Ahmad et al. 2016a; Kumar et al. 2017; Pietrini et al. 2019; Zielonka et al. 2020).

The use of nutrient solution with high heavy metal bioavailability allows for the quantification of the maximal capacities of the plant for bioaccumulation of pollutants independently of the adsorption process occurring in the soils and which restricts heavy metal transfer from soil to the root system (Kos and Leštan 2004). The present work demonstrates that Cd mainly accumulated in the roots, as recently shown by Praspaliauskas et al. (2020). As far as the shoot is concerned, Cd accumulation was higher in the stem than in the leaves. Although Arru et al. (2004) demonstrated that accumulated Cu did not fix on hemp bast fibres, a different behavior might be expected for Cd which is able to interact with hemp bast fibres during biosorption processes (Pejic et al. 2009; Vukčević et al. 2014). One may therefore expect that Cd *in planta* could also strongly interact with cell wall polymers as recently demonstrated for *Medicago sativa* (Gutsch et al. 2019a) or *Kosteletzkya pentacarpos* (Zhou et al. 2018), and more especially during the process of bast fibres or hurds' formation. The resulting risks for users, as well as the consequence of this localization on fibres' quality, need to be determined. Even if Cd did not accumulate in bast fibres or hurds but in adjacent tissues, a risk of dissemination subsists as a consequence of retting process occurring in the field and which involves selective degradation of the parenchyma cells surrounding the fibres (Bleuze et al. 2018). A sound appraisal of the resulting environmental damages requires the precise determination of Cd distribution in the stem tissues using adapted histological imaging techniques (Lefèvre et al. 2014).

As far as the whole shoot is concerned, hemp accumulates Cd to concentrations quite higher than 100-mg kg⁻¹ DW commonly referenced as the minimal value for Cd-hyperaccumulating plants (Mahar et al. 2016). Despite such a high level of accumulation, hemp could not be considered as a hyperaccumulating species since Cd strongly impaired growth. Interestingly, however, the translocation factor calculated on the basis of the total amount of Cd was also clearly higher than 1, suggesting that hemp displays, to some extent, physiological attempts allowing the plant to cope with the high Cd content in photosynthetic tissues. Similarly, the recorded bioaccumulation factor was close to 90 in Cd-treated plants, an extremely high value comparative to most plant species used for phytoextraction purposes (Barceló and Poschenrieder 2003; Ali et al. 2013; Mahar et al. 2016; Yang et al. 2017; Feng et al. 2020).

Besides Cd content itself, the present work demonstrates that this heavy metal affected the distribution of other elements in young hemp plants:

Ca translocation was increased by Cd treatment, while Fe exhibited an opposite trend since it accumulated in the roots but decreased in the leaves. Even though Cd is a non-essential element, it competes with numerous Fe and Ca transporters. Some of these transporters are mainly present in the roots (IRT1, IRT2, NRAMP5), while others are more specifically present in vascular tissues (NRAMP3, NRAMP4, HMA2, HMA4) (Huang et al. 2020). According to the relative sensitivities of these transporters to Cd excess, long-distance transport of essential elements such as Ca and/or Fe may be strongly affected. Sulfur strongly increased in all organs, which could be related to the Cd induced oversynthesis of phytochelatin containing numerous thiol groups (Cobbett 2000). It has however to be mentioned that S mainly increased in the leaves while PC accumulated to a higher extent in the roots than in the shoots.

Photosynthesis is an important physiological process and was reported to be strongly impaired by Cd toxicity (Baryla et al. 2001; Lefèvre et al. 2014). Stress-induced inhibition of photosynthesis may be due to stomatal or to non-stomatal causes. Cadmium did not induce stomatal closure on the second fully expanded leaf in Cd-treated hemp, and a decrease in leaf WC was reported despite osmotic adjustment, reflecting an alteration in the plant water status. The fact that A strongly decreased while g_s remained unaffected supports the hypothesis that Cd mainly act on this precise leaf through non-stomatal targets.

Carotenoid content also decreased following Cd application. Carotenoids absorb light energy from chlorophyll and have the capability to act as antioxidants by scavenging singlet molecular oxygen (1O_2) and peroxy radicals (ROO^{\cdot}) in chloroplasts (Khalid et al. 2019). It is likely that stress conditions accelerated their degradation and disrupted their protective function (Mlinarić et al. 2016). Neither F_v/F_m , Φ_{PSII} , nor q_p was affected by Cd treatment. This suggests that the plant remained able to trigger protective mechanisms even if very high doses of Cd reduced pigment concentration. Lefèvre et al. (2014) showed that Cd exposure of Cd-resistant plants lead to the synthesis of chloroplastic proteins contributing to the protection of photosystems and stabilization of the thylakoid membranes. It has however to be mentioned that Cd also induced a decrease in NPQ: this is an unexpected observation since abiotic stresses commonly induce an increase rather than a decrease in NPQ values (Kalaji et al. 2016; Jonar et al. 2020). Non-photochemical quenching would protect against all mechanisms that depend on light absorbed by the PSII antenna. The drop in NPQ recorded in Cd-treated plants suggests that these antennas and/or other parameters influencing the

NPQ process started to be affected by Cd toxicity. At the time of photosynthesis measurement, the second fully expanded leaf was photosynthetically active and was therefore of crucial importance for whole plant survival. It did not necessarily reflect all leaf behavior, especially regarding the fact that the oldest leaves are encountering senescence which strongly impact photosynthetic processes at different levels (Mayta et al. 2019); cadmium-induced senescence may depend on Cd distribution among leaves of different ages, and a preferential accumulation of Cd in old leaves could not be ruled out.

Among the plethora of injuries induced by Cd toxicity, oxidative stress related to ROS oversynthesis is of paramount importance. In order to prevent oxidative burst, plant cells may increase the endogenous concentration of antioxidant and activities of antioxidative enzymes. Cd induced an obvious increase in leaf MDA, resulting from lipid peroxidation. Surprisingly, Cd induced a decrease in root MDA. Malondialdehyde is often considered a non-toxic end-product reflecting the rate of lipid peroxidation. In fact, it has to be noticed that MDA itself is a toxic molecule able to react with DNA and protein to form several different adducts. It has been referred to as a potentially mutagenic and atherogenic compound and is thought to generate unwanted DNA-protein cross-links (Del Rio et al. 2005). According to Yan et al. (2021), major damages induced by Cd on earthworms result from MDA toxicity rather than from primary ROS. Plants may decompose MDA through activation of aldehyde dehydrogenase or aldo-keto-reductases (AKR) (Sengupta et al. 2015). One hypothesis explaining the low level of root MDA in Cd-exposed plants is that this metabolic pathway was activated in roots to prevent damages induced by MDA.

Among the antioxidants involved in ROS detoxification, GSH plays a dual function since it acts also as a precursor of PC involved in vacuolar sequestration of Cd. Jozefczak et al. (2014) demonstrated that root GSH may be preferentially allocated to PC synthesis for Cd chelation leading to a transient decrease in free GSH. Our results corroborate this observation since we recorded a significant decrease in GSHt and a strong increase in root PC with no concomitant increase in MDA concentration suggesting that oxidative stress remained limited thanks to an efficient Cd sequestration. In the leaves, PC concentration was lower than in the roots and a proportion of free Cd may induce oxidative stress. The total antioxidant of our samples was only marginally affected by Cd, but the high GSSG/GSH ratio observed in Cd-treated leaves suggests that the activity of glutathione reductase may be

impaired to some extent by the heavy metal. Besides its role as antioxidant and metal chelator, glutathione also assumes crucial role in transcriptional activation of Cd-induced DNA damages response and an impact in cell cycle regulation so that even a transient depletion of GSHt may contribute to growth inhibition (Hendrix et al. 2020).

Si impact on plant response to Cd

It is now well-established that Si is a non-essentially beneficial element contributing to abiotic stress resistance in a wide range of plant species (Epstein 1994; Kim et al. 2017; Luyckx et al. 2017a; Berni et al. 2020). As far as heavy metal stress is concerned, Bhat et al. (2019) reported that the beneficial effects of Si are more evident in plants able to accumulate high level of Si. Recently, Guerriero et al. (2019) identified a gene coding for Si channel in hemp. The maximal level of Si accumulation in our material was around 0.5% DW for hemp leaves, suggesting that *C. sativa* is a low Si accumulator when compared with species such as rice or horsetail (Epstein 1994). This explains why Si had only a marginal impact on control plants that were not exposed to Cd stress. In our experimental approach, Si was applied before Cd, allowing the plants to already contain significant amounts of Si when Cd stress was applied. Numerous authors reported that the addition of Si improved growth of plants exposed to heavy metals (Wu et al. 2013; Adrees et al. 2015; Imtiaz et al. 2016; Bhat et al. 2019) but this is a long-term observation and the underlying reasons for this growth stimulation remain poorly documented. In order to unravel the putative first targets of Si, we thus analyzed plants' behavior on a short-term basis before growth stimulation occurred.

In some studies, Si was shown to co-precipitate with Cd in the external medium, leading to a decrease in stress intensity through a reduction in Cd bioavailability (Adrees et al. 2015). Cadmium may be fixed by the walls of the tanks while Cd and Si may be absorbed by microorganisms, thus reducing heavy metal toxicity for plants. At acidic pH, polymerization of the monosilicic acid and capsulation of Cd could not be excluded. If they occurred, these processes remained of limited importance in our work since both VisualMinteq software and nutrient solution analysis clearly indicated that Cd speciation was not affected by added Si and that both Cd and silicic acid remained soluble and fully available during the time course of the experiment. Numerous works also demonstrated that Si reduced root-to-shoot translocation of Cd by blocking the apoplastic bypass flow after Si deposits in the vicinity of the endodermis leading to Cd accumulation in the root (Shi et

al. 2005; Adrees et al. 2015; Bhat et al. 2019). In the present work, Si significantly reduced Cd accumulation in all organs including the roots and this suggests that Si impacted the Cd absorption process and not the translocation step. Indeed, the TF_a and TF_c values increased in CdSi-treated plants comparative to values recorded for Cd-treated ones (Table 3.2) and root retention was not the strategy adopted by the plant to cope with Cd in the presence of Si. As a consequence, the relative distribution of Cd in the CdSi-treated plants was almost similar to that of Cd-treated ones (Figure 3.6). Conversely, Cd reduced Si accumulation in the stem but strongly increased it in the leaves, resulting in an increase in TF_a and TF_c for Si, but also in a strong increase in BF values (Table 3.2; Figure 3.6). In the xylem sap, Si is mostly present in the form of monosilicic acid and aquaporins involved in Si xylem unloading and intervascular transport were identified in some species (Adrees et al. 2015). Our data suggest that Cd might have an impact on these aquaporins which may lead to a higher Si deposit as amorphous silica at the transpiration sites.

Besides distribution between organs of the plants, Si was shown to accumulate within cell walls and this is also the case for Cd (Krzyszowska 2011) so that co-precipitation might occur. Si concentration remained the lowest in the stem comparatively to roots and leaves but Guerriero et al. (2019) clearly demonstrated that Si is not evenly distributed among stem tissues and is specifically present in the wall of bast fibres. This may have a positive impact on the mechanical properties of the fibres since harvested fibres are frequently coated with silica during industrial processing to improve the quality (Branda et al. 2016; Jiang et al. 2018; Koushki et al. 2020). It has to be noticed that Cd reduced by more than 50% Si accumulation in the stem and may thus hamper the Si contact with mature thickened bast fibres.

Si application to Cd-treated plants strongly decreased the g_s and E values in relation to the abovementioned increase in Si content in the leaves, while this phenomenon was not observed in the plants exposed to Si alone. Once again, hemp displayed a specific behavior in this respect, since numerous studies performed on other species reported a Si-induced increase in g_s and transpiration rates of heavy metal-exposed plants (Wu et al. 2013; Adrees et al. 2015; Imtiaz et al. 2016). In our case, however, the fact that A was less impacted than E values by stomatal closure leads to an increase of WUE in CdSi-treated plants comparative to Cd-treated ones. Although a positive impact of Si on chlorophyll content was detected in control plants, this was not observed for plants exposed to Cd and Si was similarly unable to

restore the NPQ values of Cd-treated plants. Hence, the photosynthetic machinery did not appear as the first target of Si impact on Cd treated plants.

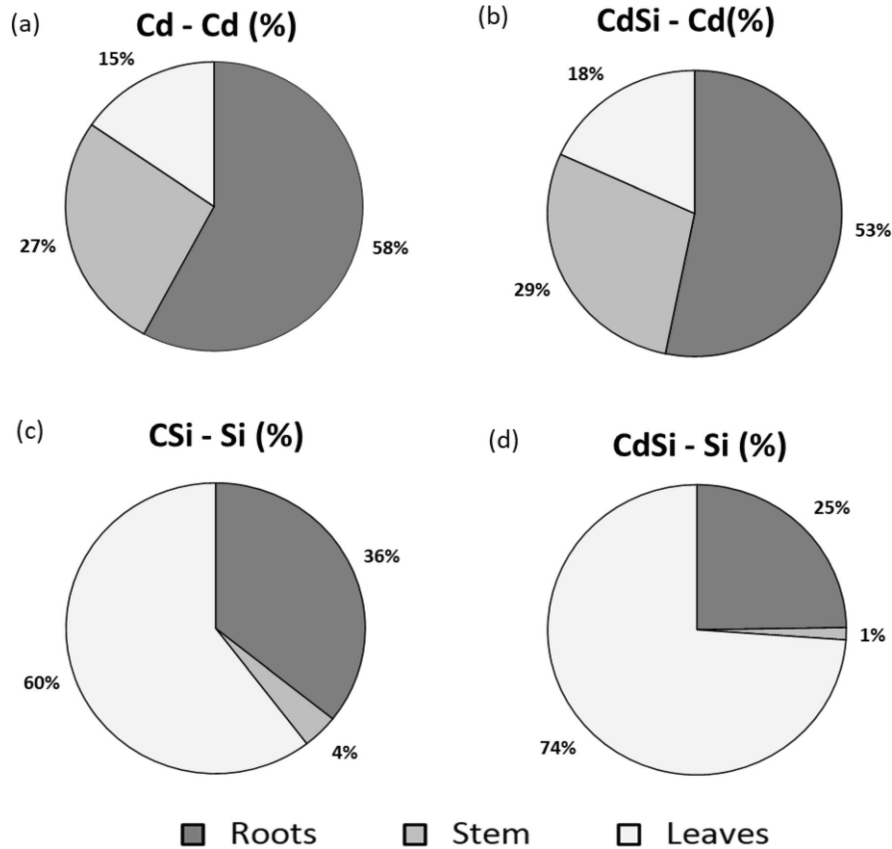


Figure 3.6: Distribution (%) of Cd in roots, stem, and leaves of Cd-exposed plants (Cd, CdSi; a and b), and distribution (%) of Si in roots, stem, and leaves of Si-exposed plants (CSi, CdSi; c and d). *Cannabis sativa* (cv. Santhica 27) plants were exposed for 1 week to Cd (20 μ M) in the presence or in the absence of 2 mM H_2SiO_3 .

Si was also reported to decrease the oxidative stress induced by heavy metals and thus decrease MDA content in various organs (Adrees et al. 2015; Kim et al. 2017). Si obviously decreased MDA content in the roots of hemp, but not in the leaves. It increased the total antioxidants in the leaves (for both AOAD and AOAM fractions), but only in control plants and not in Cd-exposed ones. At the root level, Si significantly increased the GSht concentration and slightly increased the PC concentration, allowing the plant to efficiently sequester Cd on thiol groups while maintaining at the same time its capacity to detoxify ROS with free available glutathione. According to Wu et al. (2013), Si is able to stimulate *PCSI* (the major phytochelatin synthase

gene) in *Arabidopsis thaliana* while Bhat et al. (2019) reported a Si-induced increase in the transcript levels of *MT2a* and *MT2b* corresponding to metallothionein also involved in Cd sequestration.

5. Conclusions

The present study indicates that *C. sativa* is able to accumulate high concentration of Cd and is therefore suitable for phytoextraction purposes. The use of produced fibres should however be considered with caution in relation to Cd accumulation in the stem and the resulting risks of Cd dispersion during the retting process. The addition of Si has numerous physiological impacts on the plant behavior occurring rapidly after Cd stress application and before any modification in terms of growth. Si reduced Cd accumulation in all organs but did not impact Cd distribution within the plant. It also improved water use efficiency in relation to stomatal closure and decrease in transpiration rates. Exogenous Si stimulated phytochelatin synthesis at the root level and thus improved Cd sequestration. It also mitigated the deleterious impact of Cd on leaf Fe and root Ca content but was unable to reduce Cd effect on chloroplastic PSII antenna. The Cd-induced increase in Si accumulation may be regarded as an attempt to absorb this beneficial element. Further experimentations are required to analyze the long-term effect of Si impact on plant growth and to precisely map Cd distribution in plant organs.

Funding

This work was financed by ADEME (Agence de la Transition écologique; Convention MisChar no. 1672C0044).

Chapter 3: Highlights and Perspectives

In field conditions hemp growth and yield were found to be marginally affected by HM and Si, while phytoextraction capacity was limited by the low environmental availability of HM (Chapters 1, 2).

In this Chapter, hemp was therefore cultivated in nutrient solution to assess the impact of a high bioavailability of Cd, as well as the short-term impact of silicon (Si) on biomass production. Plants were grown 4 weeks in Hoagland solution. In the solution, we applied Cd in the form of CdCl₂ (20 µM), and Si in the form of H₂SiO₃ (2 mM Si). The impact of a high bioavailability of Zn will be assessed in Chapter 4. We investigated the phytoextraction capacity of hemp, as well as the influence of Cd and Si application on hemp physiological properties.

The present Chapter demonstrated that (Figure 3.7):

- *C. sativa* is able to accumulate high concentration of Cd in roots (the main organ of accumulation) and shoots (BF = 90). The use of produced fibres should thus be considered with caution in relation to Cd accumulation in the stem and the resulting risks of Cd dispersion during the retting process.
- Cd decreased plant growth and affected photosynthesis through non-stomatal effects.
- The addition of Si had numerous physiological impacts on the plant behavior occurring rapidly after Cd stress application and before any modification in terms of growth:
 - Si reduced Cd accumulation in all organs but did not impact Cd distribution within the plant.
 - Si improved water use efficiency through a decrease in transpiration rate.
 - Si stimulated GSH and PC synthesis at the root level and thus improved Cd sequestration, allowing the plants to efficiently cope with oxidative stress.
- Si had only a marginal impact on control plants that were not exposed to HM stress. This suggests that the response of the plant to Si

application is completely different when plants are exposed to pollutants.

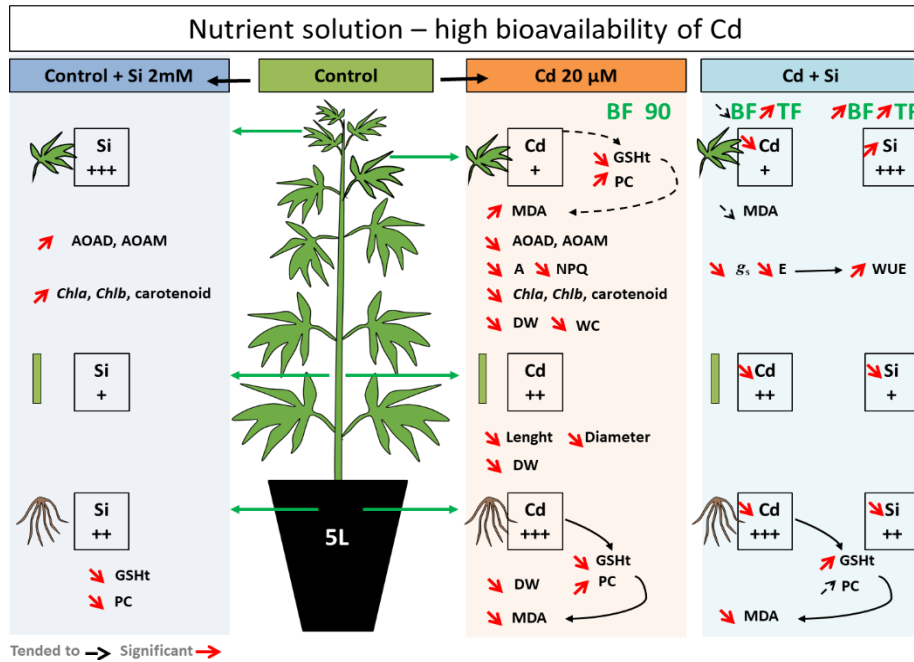


Figure 3.7: Summary of the results obtained in Chapter 3. Total global antioxidant activity (hydrophilic (AOAM), hydrophobic fractions (AOAD)), chlorophyll (*Chl*), total glutathione (GSHt), phytochelatin (PC), bioaccumulation factor (BF), malondialdehyde (MDA), net photosynthesis (*A*), non-photochemical quenching (NPQ), dry weight (DW), water content (WC), translocation factor (TF), leaf stomatal conductance (g_s), instantaneous evapotranspiration (*E*), water use efficiency (WUE). Black arrows indicate a non-significant increase/decrease of values, while red arrows illustrate the significant results.

Despite a high level of Cd accumulation, hemp could not be considered as a hyperaccumulating species since Cd strongly impaired growth. However, the recorded bioaccumulation factor confirms its interest for phytoextraction purposes. Besides, Cd accumulation was higher in the stem than in the leaves, while, under field conditions (Chapters 1,2), HM foliar concentrations tended to exceed stem concentrations. It clearly demonstrates that HM distribution is a function of the external dose. In Chapter 4, a similar experiment in nutrient solution, was conducted with Zn applied in excess, to assess whether the results obtained in this Chapter are element (Cd) dependent.

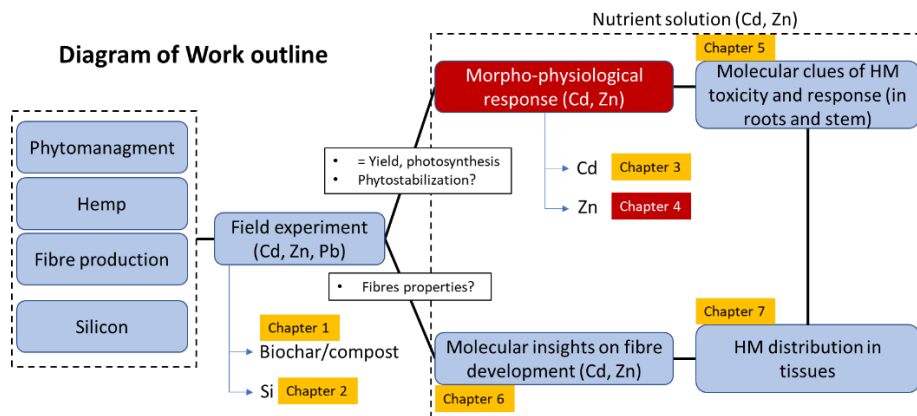
Chapter 4

Studying the impact of a high bioavailability of Zn, as well as the short-term impact of silicon (Si) on biomass production

Marie Luyckx, Jean-François Hausman, Gea Guerriero, Stanley Lutts.

Author's contributions

SL, JFH and GG coordinated the project. ML, SL and GG conceived and designed the experiment. ML performed all experimental analysis. ML and SL wrote the manuscript. All authors reviewed and approved the final manuscript.



Abstract

Hemp (*Cannabis sativa* L.) is a promising crop for non-food agricultural production on soils contaminated by moderate doses of heavy metals, while silicon, as a beneficial element, is frequently reported to improve stressed plants behavior. Using a hydroponic system, plants of *Cannabis sativa* (cv. Santhica 27) were exposed for one week to 100 μ M Zn in the presence or absence of 2 mM Si. Zinc accumulated in all plants organs but was mainly sequestered in the roots. Additional Si reduced Zn absorption but had no impact on Zn translocation. Zn accumulation had a negative impact on biomass and chlorophyll content but additional Si did not mitigate these symptoms. Exogenous Si reduced the Zn-induced membrane lipid peroxidation (assessed by MDA quantification) and increase the total antioxidant activities estimated by the FRAP index. In the absence of Si, leaf phytochelatin and total glutathione were the highest in Zn-treated plants and Si significantly decreased these parameters. Additional approaches using *omics* strategies and histological localization of element will provide interesting information regarding the interaction of Zn and Si in hemp.

Keywords : *Cannabis sativa* · Hemp · Phytomanagement · Silicon · Zinc

1. Introduction

Increasing numbers of agriculturally used areas are contaminated by anthropogenic-derived heavy metals (HM) (Linger et al. 2002; SPAQuE 2011; Ali et al. 2013). Management of these areas constitutes a major environmental challenge since toxic materials absorbed by plants may contaminate the food chain and represents a major risk for human health (Linger et al. 2002; Muthusaravanan et al. 2018). These areas are therefore no longer suitable for food crop production. Other crop species may be used for bioenergy production but the phytotoxicity of HM in plants and the resistance mechanisms plants have to set up to mitigate and repair toxic associated damages often lead to a decrease in biomass production (Kim et al. 2017; Shahid et al. 2019). Consequently the costs associated with environmental pollution are potentially enormous (Etesami et al. 2018).

Several approaches exist to reduce soil pollution. Phytomanagement, based on the ability of plants to extract, degrade or immobilize various contaminants from polluted soils, appears as an interesting and ecologically

alternative to the traditional remediation approaches (Kurade et al. 2021). However, it still faces some limitations: HM hyper-accumulator plants are able to accumulate high concentration of toxic elements, usually clean up only the soil surface because of their shallow root systems and produce low biomass, so that the amounts of elements extracted from the soil remain extremely low (Muthusaravanan et al. 2018; Khan et al. 2000). The possibility of combining phytomanagement and non-food production, with the view of achieving low price decontamination of soil by the production of a commercially usable resource arouses more and more interest (Vareda et al. 2019; Kanwar et al. 2020; Kurade et al. 2021). The implementation of this strategy requires the selection of fast-growing crops with HM uptake ability, rapid biomass gain and that can tolerate heavy metals. Among plants producing a high above ground biomass and a deep root system, *Cannabis sativa* is a multi-purpose promising crop widely employed in many types of non-food industries (Citterio et al. 2003; Schluttenhofer and Yuan 2017; Yang et al. 2020; Zhao et al. 2020; Charai et al. 2021). The plant indeed provides cortical fibre mainly used in paper and for the manufacture of various products (composites, insulators, reinforced thermoplastics), and hurds used for the manufacture of animal litter and, in particular, in the composition of building materials (Boutin et al. 2006; Deleuran and Flengmark 2006). Hemp would also be able, to a certain extent, to reduce Cu, Cd and Pb contamination in soils (Angelova et al. 2004; Bona et al. 2007; Shi et al. 2009 et 2012; Ahmad et al. 2016a; Kumar et al. 2017), making it a good candidate for soil phytomanagement, even in the case of organic pollution (Wu et al. 2021).

Zinc is an essential element for all living organisms and it assumes key biological functions during plant growth and development, acting as a cofactor for numerous enzymes and being integrated in the electron transport chain in mitochondria and chloroplasts (Zlobin 2021). An excess of Zn in the substrate, occurring as a result of anthropogenic activities, may however constitute a serious threat for ecosystem stability and plant development (Luo et al. 2022). Zinc contamination has a detrimental impact on plant growth and reduces yield in several cultivated plants. It affects the plant water status and compromises photosynthesis through a decrease in pigment concentration and stomatal regulation, as well as respiration and nitrogen metabolism. It was also reported to affect absorption and translocation of essential elements. Zn toxicity damages the membranes, proteins but also genetic material through association with phosphate group of DNA (Pilon et al. 2013; Bokor et al. 2014; Andrejić et al. 2018; Kaur and Garg 2021). Although Zn is a non-redox

heavy metal, overgeneration of reactive oxygen species (ROS) may be possible due to metabolic disturbance in numerous metabolic pathways. In order to cope with oxidative stress, plants may produce antioxidant molecules among which glutathione plays a key role (Goodarzi et al. 2020). Moreover, glutathione acts as a precursor of phytochelatins which are cysteine rich peptides able to bind heavy metals and sequester those toxic compounds in the vacuole avoiding the toxic effects of free heavy metals on cytosol and organelles (Tennstedt et al. 2009; Fan et al. 2018).

To enhance crop growth and help the plant to cope with HM toxicity, the use of silicon (Si)-fertilizer is predicted to become a sustainable strategy and an emerging trend in agriculture (Etesami et al., 2018). Si is a non-essential element that can contribute to improve the behavior of plant exposed to wide range of environmental constraints, including HM (Doncheva et al. 2009; Adrees et al. 2015; Imtiaz et al. 2016; Etesami et al. 2018). As far as hemp is concerned, Si was shown to mitigate the deleterious effect of salt (Berni et al. 2021; Guerriero et al. 2021) and Cd (Luyckx et al. 2021a) toxicities, but Si impact on Zn-exposed plants requires additional experiments. Si can also accumulate within the parietal structures where it is present in the form of orthosilicic acid and contribute to reinforce the mechanical properties of the parietal polymers (Kröger and Poulsen, 2004). As far as hemp fibres are concerned, silica treatments after harvest also provides technical advantages such as moisture buffering properties or acting as a fire retardant (Branda et al. 2016; Jiang et al. 2018).

The present work was therefore undertaken in order to evaluate the impact of a toxic dose of Zn on *Cannabis sativa* cultivated in the presence or absence of exogenous Si. Zn accumulation was quantified in different plant organs and the impact of toxic ions on mineral nutrition, photosynthesis and oxidative stress were recorded.

2. Material and methods

2.1. Plant material and growing conditions

Seeds of a monoecious hemp fibre variety (*Cannabis sativa* cv. Santhica 27) were sown in loam substrate in greenhouse conditions. After one week, the obtained seedlings were transferred to nutrient Hoagland solution in 5 L tanks, as described in Chapter 3 (p. 141). Tanks were placed in a phytotron under fully controlled environmental conditions (constant temperature of $24 \pm 1^\circ\text{C}$

with a mean light intensity of $230 \mu\text{moles m}^{-2}\text{s}^{-1}$ provided by Phillips lamps (Phillips Lighting S.A., Brussels, Belgium) (HPI-T 400 W), a photoperiod of 16h under a relative humidity of 65%). After a week of acclimatization, half of the tank received Si in the form of H_2SiO_3 to a final concentration of 2 mM Si. Metasilicic acid was obtained from a pentahydrate sodium metasilicate ($\text{Na}_2\text{SiO}_3 \times 5 \text{H}_2\text{O}$) which was passed through an H^+ ion exchanger resin IR 20 Amberlite type according to Dufey et al. (2014). Tanks were randomly arranged in the phytotron and nutrient solution was permanently aerated by SuperFish Air Flow 4 pump. A week later, Zn was applied in the form of ZnCl_2 (100 μM). The pH of the solution was maintained at 5.5. Solubility of added heavy metal was confirmed by the Visual MINTEQ09 software. Four treatments were thus defined, considering the presence of Zn and the concomitant presence or absence of Si and will be designed as C (control: no heavy metals and no Si), CSi, Zn and ZnSi (7 tanks per treatment).

Harvests were performed after a week of Zn exposure. Stem length and diameter, number of leaves and main root length were considered. Roots were quickly rinsed in deionized water for 30 s under gentle agitation just before harvest to remove ions from the free spaces: roots, stems and leaves were then separated. Roots and leaves from a same treatment were pooled, quickly frozen in liquid nitrogen and then stored at $-80 \text{ }^\circ\text{C}$ until analysis, except subsamples of 3 plants per treatment incubated in an oven at $70 \text{ }^\circ\text{C}$ for 72 h to estimate dry weight and water content and to determine ion content.

2.2. Physiological measurements

Before plant harvest physiological measurements were performed on 5 plants per treatment, on the middle portion of the leaf blades constituting the second fully formed leaves from the top. Chlorophyll fluorescence parameters (maximum quantum yield of photosystem II (F_v/F_m), photochemical quenching (q_p), non-photochemical quenching (NPQ) and actual efficiency of photosystem II (Φ_{PSII}), leaf stomatal conductance (g_s), the instantaneous CO_2 assimilation under ambient conditions (400 ppm CO_2) (A) and instantaneous transpiration (E) were measured as detailed in Chapter 1 (p.83-84). All measurements were performed around midday (between 12 a.m. and 2 p.m).

Total chlorophyll (a+b) and carotenoid concentrations, as well as osmotic potential (Ψ_s), were measured according to the protocole described in Chapter 3 (p. 143).

2.3. Mineral concentration

The protocols used for Zn and Si quantification are described in Chapter 3 (p. 142-143).

Translocation factor reflects the capacity of the plant to translocate HM from the root to the shoot and was estimated according to Luyckx et al. (2021a) 1) on the basis of the concentration expressed on a dry weight basis in each plant part (TF_c) and 2) on the basis of total amount of the considered element (TF_a)

$TF_c = \text{Zn concentration in the shoot} / \text{Zn concentration in the root}$

$TF_a = \text{Total Zn amount accumulated in the shoot} / \text{Zn accumulated in the root}$

The bioaccumulation factor (BF) considers the capacity of the plant to store heavy metals in relation to external concentration. Since a nutrient solution was used in the present work rather than a solid substrate, the internal concentration in the plant was estimated on a water content basis, considering the proportion of the different organs:

$BF = \text{Zn concentration in the plant (mg}\cdot\text{L}^{-1}) / \text{Zn concentration in the solution (mg}\cdot\text{L}^{-1})$

2.4. Malondialdehyde (MDA) content and total antioxidant activities

The concentration of malondialdehyde (MDA) and the total global antioxidant activity, ferric reducing ability of plasma (FRAP) were assessed, as detailed in Chapter 3 (p. 143-144).

2.5. Glutathione and total non-protein thiols

Reduced (GSH) and total (GSht) glutathione were quantified, as described in Chapter 3 (p. 144).

2.6. Statistical analysis

All analysis were performed on 5 replicates. Normality of the data was verified using Shapiro-Wilk tests and the data were transformed when required. Two-way ANOVA were performed at a significant level of P -value < 0.05 using R (version 3.3.1) considering the Zn and the silicon application

as main factors. Means were compared using Tukey's HSD all-pairwise comparisons at 5% level as a post-hoc test.

3. Results

3.1. Plant growth



Figure 4.1: *Cannabis sativa* plants cultivated in hydroponic conditions; C: control plants; Zn: plants exposed for one week to 100 μ M Zn.

Zinc excess induced leaf chlorosis and early senescence marked by a wilting process, especially in the youngest leaves (Figure 4.1). Zinc excess also reduced leaf and stem fresh and dry weights, total leaf number, and stem length compared to control plants (Table 4.1, Figure 4.2), although these trends were not statistically confirmed for roots and leaves dry weight, considering the high level of variability. Zinc excess in the absence of Si did not impact stem diameter or main root length (Figure 4.2).

Silicon addition to control nutrient did not impact plant behaviour in terms of growth or morphological properties. Silicon did not afford obvious protection against Zn toxicity and ZnSi was even the most deleterious treatment for root growth (Table 4.1).

Table 4.1: Fresh weight (FW), dry weight (DW), water content (WC) and osmotic potential (Ψ_s) of *C. sativa* (cv. Santhica 27). Plants were exposed for one week to Zn (100 μ M) in the presence or in the absence of 2 mM H_2SiO_3 . For a given organ, different letters indicate significant differences at $P < 0.05$ according to Tukey's HSD all-pairwise comparisons. Each value is mean of 3 replicates (FW, DW and WC) or 5 replicates (Ψ_s).

	C	CSi	Zn	ZnSi
FW (g)				
Roots	11.88 \pm 11.31 <i>a</i>	8.93 \pm 7.54 <i>ab</i>	6.04 \pm 3.59 <i>ab</i>	3.97 \pm 3.02 <i>b</i>
Stems	10.03 \pm 3.49 <i>a</i>	9.09 \pm 5.00 <i>a</i>	4.19 \pm 3.04 <i>b</i>	4.83 \pm 2.94 <i>b</i>
Leaves	19.67 \pm 9.37 <i>a</i>	18.20 \pm 10.66 <i>ab</i>	10.59 \pm 4.96 <i>bc</i>	9.45 \pm 4.10 <i>c</i>
DW (g)				
Roots	0.87 \pm 0.19 <i>ab</i>	0.95 \pm 0.25 <i>a</i>	0.57 \pm 0.20 <i>bc</i>	0.48 \pm 0.16 <i>c</i>
Stems	1.22 \pm 0.28 <i>a</i>	1.27 \pm 0.23 <i>a</i>	0.71 \pm 0.41 <i>a</i>	1.00 \pm 0.47 <i>a</i>
Leaves	3.40 \pm 1.58 <i>ab</i>	3.97 \pm 0.83 <i>a</i>	2.40 \pm 1.03 <i>ab</i>	2.09 \pm 0.65 <i>b</i>
WC (%)				
Roots	88.05 \pm 8.00 <i>a</i>	94.28 \pm 0.58 <i>a</i>	92.54 \pm 1.26 <i>a</i>	91.53 \pm 1.68 <i>a</i>
Stems	86.17 \pm 3.16 <i>ab</i>	90.92 \pm 0.58 <i>a</i>	89.22 \pm 2.01 <i>ab</i>	86.18 \pm 2.42 <i>b</i>
Leaves	82.12 \pm 2.36 <i>a</i>	85.54 \pm 1.38 <i>a</i>	82.49 \pm 2.33 <i>a</i>	82.01 \pm 3.45 <i>a</i>
Ψ_s (Mpa)				
Leaves	-1.21 \pm 0.06 <i>a</i>	-1.18 \pm 0.04 <i>a</i>	-1.34 \pm 0.04 <i>b</i>	-1.19 \pm 0.04 <i>a</i>

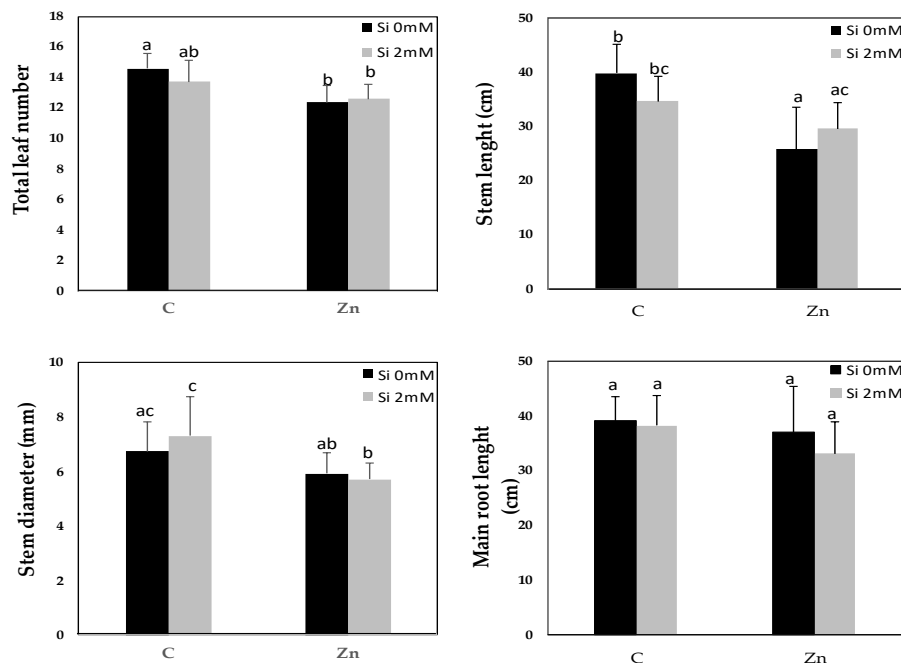


Figure 4.2: Total leaf number, stem length and diameter, and root length of *C. sativa* exposed for one week to Zn (100 μ M), in the presence or in the absence of 2 mM H_2SiO_3 . Data are means \pm standard errors (n = 5). Values with different letters are significantly different ($P < 0.05$; Tukey's HSD all-pairwise comparisons).

3.2. Mineral concentrations

Zinc significantly accumulated in response to 100 μM ZnCl_2 in all plant organs. Zn was mainly accumulated in roots followed by stems and leaves (Table 4.2). In the absence of Zn stress, H_2SiO_3 application had no impact on Zn content. In the presence of Zn excess, however, exogenous Si significantly reduced Zn accumulation in all organs. Both TF_c and TF_a for Zn increased in response to exogenous Si in the absence of Zn excess, while BF values significantly decreased. Zn excess reduced TF_c and TF_a values and in this case, Si had no impact anymore on translocation factors or BF values.

Table 4.2: Zinc (Zn), and silicon (Si) concentrations and translocation factor (TF) in roots, stem and leaves of *C. sativa* (cv. Santhica 27). Plants were exposed for one week to Zn (100 μM) in the presence or in the absence of 2 mM H_2SiO_3 . TF_c : translocation factor estimated on a concentration basis, TF_a : translocation factor estimated on a total amount basis. For a given parameter and a given organ, means followed by different letters are significantly different at $P < 0.05$ according to Tukey's HSD all-pairwise comparisons. Each value is mean of 3 replicates.

	C	CSi	Zn	ZnSi
Zn (mg kg⁻¹ DW)				
Roots	464 ± 172 a	280 ± 14 a	13231 ± 236 c	11110 ± 619 b
Stems	41 ± 2 a	52 ± 9 a	1362 ± 95 c	1035 ± 36 b
Leaves	57 ± 6 a	62 ± 4 a	1003 ± 31 c	904 ± 41 b
TF_c	0.11 ± 0.02 a	0.21 ± 0.05 b	0.08 ± 0.03 a	0.09 ± 0.06 a
TF_a	0.60 ± 0.12 a	1.17 ± 0.18 b	0.45 ± 0.15 a	0.55 ± 0.31 a
BF	294 ± 24.98 c	157 ± 6.59 b	49.95 ± 13.28 a	44.45 ± 9.42 a
Si (mg kg⁻¹ DW)				
Roots	827 ± 38 a	3017 ± 101 c	945 ± 8 b	6948 ± 596 d
Stems	103 ± 34 ab	174 ± 4 b	55 ± 3 a	136 ± 21 b
Leaves	260 ± 4 b	3006 ± 116 d	162 ± 5 a	1941 ± 100 c
TF_c	0.26 ± 0.04 b	0.77 ± 0.19 c	0.15 ± 0.06 a	0.20 ± 0.04 ab
TF_a	1.41 ± 0.30 b	4.22 ± 0.77 c	0.79 ± 0.28 a	1.24 ± 0.42 ab
BF	0	6.20 ± 0.38 a	0	6.03 ± 0.61 a

Although not intentionally added to the nutrient solution, Si was detected in control plants probably as a consequence of the presence of Si traces in the salt used for nutrient solution preparation. Root Si increased in response to H_2SiO_3 application and the recorded increase was by far higher in Zn-treated plants than in control ones. In contrast, only a slight effect of exogenous Si on Si content was recorded in the stem which remained low comparatively to other organs. In response to H_2SiO_3 application, the leaves

displayed a higher concentration than the stem, and the leaf Si concentration was higher in the absence of Zn excess than in the presence of high Zn concentration. In the absence of Si, the Si concentration in the roots and in the leaves were in the same range. TF values for Si increased in response to exogenous application of Si but the recorded increase was significant in the absence of Zn excess only. The addition of Zn excess had no impact on BF values for Si.

Zn excess increased Fe concentration in the roots but decreased it in the leaves (Table 4.3). Exogenous Si in the presence of Zn excess did not mitigate this trend and even decreased Fe concentration in the stem. Zn excess also increased Mg concentration in the roots and in the stem and slightly decreased it in the leaves. The highest leaf Mg content was recorded for CSi-treated plants and the lowest for ZnSi-exposed ones. Exogenous Si in the absence of Zn excess increased S concentration in all organs. A similar effect was observed when plants were exposed to Zn excess in the absence of Si and was even more marked. In ZnSi-treated plants, S concentration increased in the roots and to a lower extent in the leaves but remained unmodified in the stem comparatively to control plants.

Table 4.3: Iron (Fe), magnesium (Mg) and sulfur (S) concentrations in roots, stem and leaves of *C. sativa* (cv. Santhica 27). Plants were exposed for one week to Zn (100 μ M) in the presence or in the absence of 2 mM H₂SiO₃. For a given parameter and a given organ, means followed by different letters are significantly different at $P < 0.05$ according to Tukey's HSD all-pairwise comparisons. Each value is mean of 3 replicates.

	C	CSi	Zn	ZnSi
Fe (mg kg⁻¹ DW)				
Roots	1526 ± 37 <i>b</i>	922 ± 11 <i>a</i>	2281 ± 12 <i>c</i>	2298 ± 36 <i>c</i>
Stems	55 ± 4 <i>b</i>	42 ± 14 <i>ab</i>	58 ± 1 <i>b</i>	22 ± 4 <i>a</i>
Leaves	109 ± 4 <i>b</i>	115 ± 1 <i>b</i>	64 ± 2 <i>a</i>	55 ± 3 <i>a</i>
Mg (mg kg⁻¹ DW)				
Roots	3537 ± 193 <i>a</i>	3346 ± 11 <i>a</i>	6631 ± 24 <i>c</i>	4754 ± 3 <i>b</i>
Stems	1295 ± 58 <i>a</i>	1639 ± 4 <i>b</i>	1599 ± 5 <i>b</i>	1419 ± 55 <i>a</i>
Leaves	4441 ± 12 <i>c</i>	5572 ± 5 <i>d</i>	4209 ± 31 <i>b</i>	3637 ± 83 <i>a</i>
S (mg kg⁻¹ DW)				
Roots	2145 ± 205 <i>a</i>	2420 ± 107 <i>ab</i>	3963 ± 47 <i>c</i>	2897 ± 7 <i>b</i>
Stems	729 ± 12 <i>a</i>	1028 ± 77 <i>b</i>	1330 ± 52 <i>c</i>	746 ± 11 <i>a</i>
Leaves	1016 ± 126 <i>a</i>	1721 ± 1 <i>d</i>	1597 ± 115 <i>c</i>	1242 ± 14 <i>b</i>

3.3. Photosynthesis-related parameters

Zn exposure had no significant impact on photosynthesis-related parameters but tended to decrease stomatal conductance (g_s), net photosynthesis (A) and instantaneous evapotranspiration (E) (Table 4.4). Although no significant difference was recorded following H_2SiO_3 application, Si slightly increased gas exchange parameters and stomatal conductance in the absence of Zn excess. In Zn-exposed plants, additional Si tended to decrease the photochemical efficiency of photosystem II (Φ_{PSII}), photochemical quenching (qP), stomatal conductance (g_s) and concentration of CO_2 in intercellular spaces (C_i) of Zn exposed plants while it non-significantly increased the NPQ values.

Table 4.4: Photosynthesis-related parameters of *Cannabis sativa* (cv. Santhica 27). Plants were exposed for one week to Zn (100 μM) in the presence or in the absence of 2 mM H_2SiO_3 . Maximum quantum yield of dark acclimated leaves (F_v/F_m), the photochemical efficiency of photosystem II (Φ_{PSII}), photochemical quenching (qP), non-photochemical quenching (NPQ), stomatal conductance (g_s), net photosynthesis (A), instantaneous evapotranspiration (E), CO_2 in intercellular spaces (C_i). For a given organ, different letters indicate significant differences at $P < 0.05$. Each value is mean of 5 replicates.

	C	CSi	Zn	ZnSi
F_v/F_m	0.88 ± 0.01 <i>ab</i>	0.88 ± 0.01 <i>b</i>	0.85 ± 0.03 <i>a</i>	0.86 ± 0.01 <i>ab</i>
Φ_{PSII}	0.83 ± 0.01 <i>a</i>	0.83 ± 0.03 <i>a</i>	0.80 ± 0.04 <i>ab</i>	0.74 ± 0.08 <i>b</i>
qP	0.96 ± 0.02 <i>a</i>	0.97 ± 0.01 <i>a</i>	0.96 ± 0.02 <i>ab</i>	0.89 ± 0.08 <i>b</i>
NPQ	0.16 ± 0.04 <i>a</i>	0.16 ± 0.03 <i>a</i>	0.15 ± 0.03 <i>a</i>	0.24 ± 0.11 <i>a</i>
g_s (mmol m ⁻² s ⁻¹)	745 ± 565 <i>ac</i>	1012 ± 729 <i>c</i>	301 ± 186 <i>ab</i>	205 ± 163 <i>b</i>
A (μ mol m ⁻² s ⁻¹)	2.44 ± 2.07 <i>a</i>	2.67 ± 1.35 <i>a</i>	1.57 ± 1.49 <i>a</i>	2.23 ± 1.09 <i>a</i>
E (mmol m ⁻² s ⁻¹)	2.95 ± 0.80 <i>ac</i>	3.22 ± 0.56 <i>c</i>	1.72 ± 1.01 <i>ab</i>	1.62 ± 1.16 <i>b</i>
C_i (μ mol mol ⁻¹)	402 ± 24 <i>a</i>	406 ± 16 <i>a</i>	415 ± 15 <i>a</i>	385 ± 32 <i>a</i>

In the absence of Zn excess, exogenous Si surprisingly decreased Chl a, Chl b and carotenoids content (Figure 4.3). In the absence of Si, Zn excess decreased Chl a and carotenoids but had no impact on Chl b. Exogenous Si did not significantly mitigate the deleterious effect of Zn on this parameter.

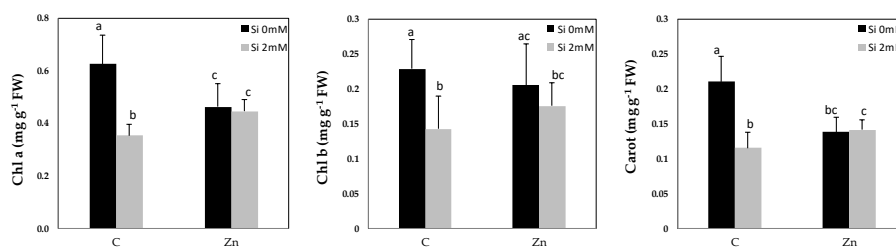


Figure 4.3: Chlorophyll (a, b) and carotenoid content of *C. sativa* (cv. Santhica 27) exposed for one week to Zn (100 μ M), in the presence or in the absence of 2 mM H_2SiO_3 . Data are means \pm standard errors ($n = 5$). Values with different letters are significantly different ($P < 0.05$; Tukey's HSD all-pairwise comparisons).

3.4. Plant water and oxidative status

Water status was assessed using the osmotic potential (Ψ_s) and the water content (WC) of the leaves. As shown in Table 4.1, Zn in the absence of H_2SiO_3 significantly lowered Ψ_s values in leaves, while plants of the ZnSi treatment have similar values than control ones. WC was not affected by the treatments applied.

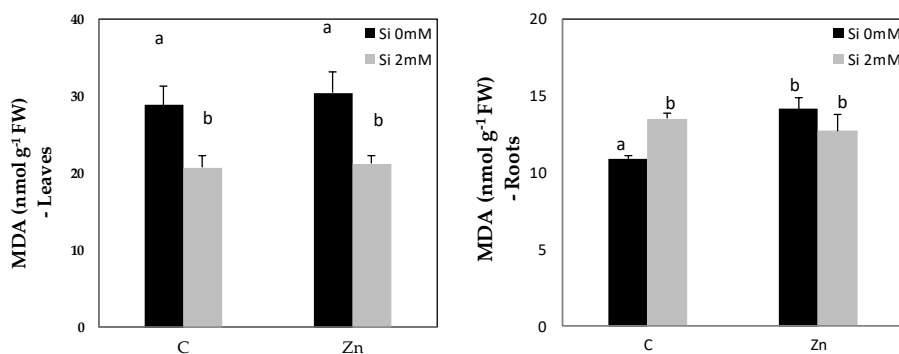


Figure 4.4: Malondialdehyde (MDA) content in leaves and roots of *C. sativa* (cv. Santhica 27) exposed for one week to Zn (100 μ M), in the presence or in the absence of 2 mM H_2SiO_3 . Data are means \pm standard errors ($n = 5$). Values with different letters are significantly different ($P < 0.05$; Tukey's HSD all-pairwise comparisons).

Malondialdehyde (MDA) is a cytotoxic product resulting from lipid peroxidation and commonly considered as an indicator of oxidative stress. Its concentration increased in roots but remained unaffected in leaves of Zn-exposed plants compared to the controls (Figure 4.4). The addition of Si significantly decreased MDA concentration in leaves of all treatments. In roots, Si application increased MDA concentration of plants cultivated in the absence of Zn excess.

Data for total antioxidant capacity for the hydrophobic (AOAD) and hydrophilic (AOAM) fractions are provided in Figure 4.5. AOAD and AOAM fractions were reduced in plants exposed to Zn, but increased when exposed to Si in the presence or absence of Zn excess.

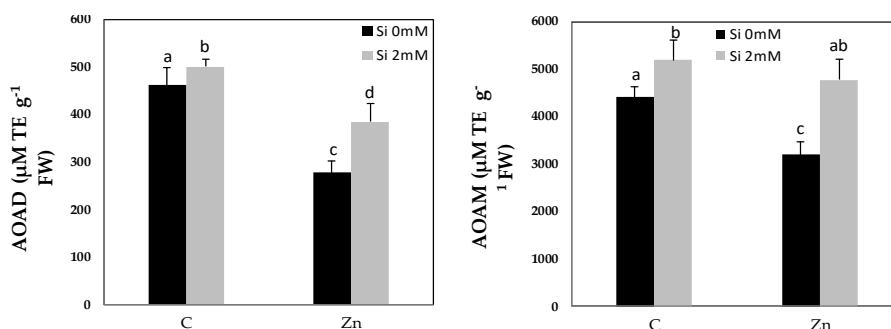


Figure 4.5: Total antioxidant activity in the hydrophobic fraction (AOAD) and the hydrophilic fraction (AOAM) of leaves of *Cannabis sativa* (cv. Santhica 27). Plants were exposed for one week to Zn (100 μM), in the presence or in the absence of 2 mM H_2SiO_3 . Data are means \pm standard errors ($n = 5$). Values with different letters are significantly different ($P < 0.05$; Tukey's HSD all-pairwise comparisons).

Table 4.5: Total glutathione (GSHt), oxidize (GSSG)/reduced (GSH) glutathione, and phytochelatine (PC) concentrations in roots and leaves of *Cannabis sativa* (cv. Santhica 27). Plants were exposed for one week to Zn (100 μM) in the presence or in the absence of 2 mM H_2SiO_3 . For a given parameter and a given organ, means followed by different letters are significantly different at $P < 0.05$. Each value is mean of 5 replicates.

	C	CSi	Zn	ZnSi
Roots				
GSHt (nmol g^{-1} FW)	176 \pm 20 a	82 \pm 34 b	1622 \pm 171 c	762 \pm 37 d
GSSG/GSH	14.38 \pm 6.85 a	5.89 \pm 5.84 b	3.61 \pm 0.73 b	8.43 \pm 4.27 ab
PC (nmol g^{-1} FW)	241 \pm 28 ab	209 \pm 20 a	222 \pm 37 ab	275 \pm 55 b
Leaves				
GSHt (nmol g^{-1} FW)	412 \pm 19 a	294 \pm 33 b	824 \pm 161 c	564 \pm 48 d
GSSG/GSH	6.03 \pm 0.27 a	7.07 \pm 0.76 a	11.12 \pm 2.28 b	14.56 \pm 1.70 c
PC (nmol g^{-1} FW)	821 \pm 84 a	658 \pm 24 b	1243 \pm 73 c	974 \pm 121 d

Zn exposure strongly increased total glutathione (GSHt, Table 4.5) content in roots and leaves. The addition of silicon significantly decreased GSHt in roots and leaves of plants exposed to Zn, but also in leaves of plants cultivated in the absence of Zn excess. The ratio between oxidize glutathione (GSSG) and reduced glutathione (GSH) is an indicator of the oxidative stress undergone. GSSG/GSH ratio was significantly lower in roots and higher in

leaves of HM treated plants compare to controls (Table 4.5). H_2SiO_3 application decreased GSSG/GSH in roots in the absence of Zn excess, and increased this ratio in leaves of plants exposed to Zn.

As far as roots are concerned, PC concentration was significantly higher in ZnSi-treated plants than in CSi-exposed ones. Zn in the absence of Si had no effect on PC concentration of control plants. PC was higher in the leaves than in the roots for all treatments: the highest value was recorded for plants exposed to Zn in the absence of Si, since exogenous Si significantly reduced the PC concentration of Zn-treated plants.

4. Discussion

The possibility of combining non-food production and phytomanagement arouses more and more interest. The implementation of this strategy requires the selection of fast-growing crops that can accumulate and tolerate HM. Hemp is a multi-uses plants providing cortical fibres used in the manufacture of various products, and hurds that enter in the composition of building materials (Boutin et al. 2006; Deleuran and Flengmark 2006), and is thought to be able to reduce HM contamination in soils thus contributing to the remediation of contaminated sites (Angelova et al. 2004; Bona et al. 2007; Shi et al. 2009 and 2012; Ahmad et al. 2016a; Kumar et al. 2017).

The present study confirmed that Zn significantly accumulated in *C. sativa* cultivated in nutrient solution under Zn excess. Growth properties were only marginally affected by Zn excess: the recorded reduction in fresh and dry weight remained not significant from a statistical point of view. It has however to be mentioned that we used a short-term exposure of one week and it can therefore not be excluded that a longer duration would lead to a significant yield decrease.

In plants exposed to Zn excess, Zn concentration in stem was higher than in the leaves. This could be linked to the fixing properties of the fibres which are exploited for biosorption purposes by numerous authors (Pejic et al. 2011; Vukcevic et al. 2014a, 2014b). Zinc is able to bind to carboxyl and hydroxyl groups of cell wall polymers such as those occurring in bast fibres and Loiacono et al. (2018) recently demonstrated that hemp fibres may be efficiently used to clean up waste water contaminated by numerous HM. Wall retention could also occur *in planta*, during the formation of the fibres, although this implies that HM need to be in close contact with the fibre and

bast fibres are located in the phloem rather than in the xylem where transpiration stream occurs. More accurate techniques of histological localization would allow us to precise the location of Zn *in situ*.

Zn translocation from roots to shoots, estimated on a concentration basis (TF_c), was however limited (TF_c ~ 0.1). Growth inhibition could have lowered TF values by altering the concentrations measured. It was therefore interesting to estimate TF on a total amount basis (TF_a, Table 4.3) based on the quantities actually exported from the substrate (Ali et al. 2013). For all treatments, translocation factor estimated on a total amount basis (TF_a) was higher than translocation factor estimated on a concentration basis (TF_c) but remained always lower than 1. This suggests that, despite a good level of tolerance, hemp adopted an excluding strategy. A similar observation has already been reported by Angelova et al. (2004), Löser et al. (2002) and Shi et al. (2009) in hemp exposed to HM. Root sequestration is a strategy widely developed by non-hyperaccumulating plants to avoid the accumulation of toxic elements in photosynthetic tissues. Hence, the use of *Cannabis sativa* cv *Santhica 27* in phytomanagement should be restricted to phytostabilization but not phytoextraction of Zn from contaminated soils. This implies that hemp is also able to display tolerance mechanisms.

We demonstrated that metallic stress had a slight negative impact on biomass production (FW, DW, total leaf number, stem length) and pigment concentration, although we did not observe any mortality in plants nor a significant impact on photosynthesis-related parameters. According to Piotrowska-Cyplik and Czarnecki (2003) and Linger et al. (2005) a reduction of pigments content, and therefore the availability of photoassimilats, as well as the energy cost of tolerance mechanisms, may explain the reduced biomass production (Ghnaya et al., 2009). According to Küpper et al. (1998), Zn may substitute to Mg within chlorophyll and this could explain both an alteration in the efficiency of light phase, and a decrease in unstable chlorophyll prone to a degradation by chlorophyllase. This, however, mainly occurred in response to Mg deficiency and we demonstrated in the present study that presence of Zn excess reduced the Mg content in the leaves by only 5.2% (Table 4.3). Accordingly, data provided by chlorophyll fluorescence indicate that the light phase by itself is only marginally affected by Zn excess.

We also paid attention to plant water and antioxidative status. Water content was not affected by the treatments applied but Zn excess significantly lowered Ψ_s values in leaves, which is a clear indication that adaptations were required for Zn-treated plants to maintain internal water potential and turgor.

Such accumulation of osmotic compounds contributes to turgor maintenance and CO₂ diffusion within the mesophyll. This probably explain stable C_i values in plants exposed to Zn excess compare to controls while gas exchange parameters tended to decrease. Beside CO₂ diffusion within the mesophyll, the highest resistance encountered by CO₂ to reach the sites of carboxylation is located at the stomatal level. Zinc tended to decrease the g_s value but this had no impact on mean C_i which suggest that the carboxylation efficiency might be hampered by Zn excess. Indeed, Zn-treated plants exhibited the lowest A value: Cambrollé et al. (2013) mentioned that Zn may also substitute to Mg in Rubisco itself, leading to under-utilization of ATP and NADPH in CO₂ fixation. Nevertheless, this hypothesis might be invalid in our case since no important Mg decrease was recorded in the leaves. Data are still missing regarding the impact of Zn on activity of other enzymes involved in the Calvin cycle.

The present study also showed that hemp exposed to Zn excess encountered a moderate oxidative stress: MDA content in leaves remained similar to controls, but increased in roots. Zinc accumulated to higher amounts in the roots than in the leaves; hence, a higher oxidative stress in the below part of the plant was not unexpected. This suggests that, in leaves, oxygen species were quickly scavenged. Reduced glutathione (GSH) is involved in the reduction of an important part of ROS generated due to stress (Shao et al. 2007). In our study, HM exposure led to higher GSHt concentration in leaves and elevated GSSG/GSH ratio, suggesting that GSH helped to withstand oxidative stress in leaves. This may also explain the decrease of total antioxidant capacity, GSH being part of the AOAM fraction. Besides its role as an antioxidant, GSH acts as a precursor of phytochelatin (PC) synthesis. In our study, HM exposure led to higher PC content in leaves. Chelating metals by forming PCs or metallothioneins (MTs) metal complex at the intra- and intercellular level are part of the mechanisms used by plants to counteract HM toxicity (Alloway et al., 2013; Citterio et al., 2003; Tennstedt et al. 2009; Emamverdian et al., 2015). Nevertheless, a higher PC concentration in the leaves than in the roots is rare in plants exposed to HM. Wogkaew et al. (2019) suggested that glutathione may be involved in the translocation of Zn from the root to the shoot: the underlying mechanisms however, remains unknown and this observation did not explain why, in the present case, Zn remained sequestered in the roots while glutathione accumulated in the leaves. Besides, oversynthesis of glutathione requires large quantities of S. Hemp increased the S accumulation in roots, stems and leaves in the presence of Zn excess

confirming that hemp is able to trigger this protective mechanism. However, it is important to keep in mind that to combine phytostabilization with non-food production, the properties of the harvested biomass have to remain compatible with the requirements of industry from a qualitative point of view (Luyckx et al., 2019). Additional work is therefore needed to precise the impact of Zn excess on valuable plant parts.

Although Si is not considered as essential for plants, it intervenes as a beneficial element in their defence and growth. As such, it is used in agriculture as a biostimulant. Hemp is not considered as an Si accumulator under normal conditions. However, in this study, Si significantly increased root and leaf Si concentration in the absence and in the presence of Zn excess. In roots, plants of CSi treatment accumulated 3.6x more Si than plants of C treatment; while ZnSi treated plants accumulated 7.4x more Si than plants of Zn treatment. This suggests that plants stimulated Si uptake to cope with Zn stress. In rice exposed to heavy metals and Si, Kim et al. (2017) and Ma et al. (2015) reported an increase in the expression of genes involved in the transport of Si (*OsLSi1* and *OsLSi2*) to improve resistance to metal stress. In the present case, however, high Si accumulation in the root of ZnSi-treated plants did not protect the roots from oxidative stress since MDA concentration was similar to Zn-treated plants.

H₂SiO₃ application under Zn exposure interfered with HM absorption. Zn concentration was clearly lower in roots, stems and leaves of plants in the presence of Zn excess than in plants exposed to Zn in the absence of Si. A first hypothesis is that the presence of Si in the nutrient solution reduces Zn availability through the precipitation of Zn silicate. Bokor et al. (2014) indeed mentioned that Zn₂SiO₄ may occur in water experiments but this is not confirmed by the speciation program VISUAL MinTEQ which clearly indicated that, for the range of concentration and pH of the solution, Zn remained fully soluble in the solution. The decrease of Zn concentration cannot be attributed to a decrease in transpiration rate since no significant difference for *E* values was observed between ZnSi and Zn treatments. It has already been observed in rice plants treated with Cu/Cd a decrease in the expression of HM transporters in the presence of Si (Kim et al. 2017; Ma et al. 2015). Huang and Ma (2020) recently demonstrated that Si supply decreased Zn concentration in both the root and the shoots: according to these authors Si acts on Zn uptake by down-regulating *OsZIP1* implicated in Zn uptake. The comparison should however be established with caution considering that rice is a specific plant species for Si hyperaccumulation and

that data obtained with rice are not necessarily valid for other plant species, especially dicots. Beside Zn absorption, some authors reported that Si may reduce Zn translocation from the root to the shoot (Zajackowska et al. 2020; Naeem et al. 2015) but this was not observed in our experiment since TF value for Zn were hardly modified by Si. This implies that as far as hemp is concerned, Si may impact transporters involved in Zn uptake (especially those encoded by *ZIP* genes) but had no impact on transporters involved in Zn xylem loading and long-distance transport (HMA2 and HMA4) (Zlobin 2021).

It is also interesting to notice that the recorded Zn-induced increase of Zn accumulation was higher than the Si-induced decrease of Zn accumulation in plants of ZnSi treatment. Hence, if Si contributes to defence and growth, silicon could be compatible with phytostabilization purposes. Zn accumulation in control plants was not significantly affected by Si. Although no significant difference was recorded following H_2SiO_3 application, Si slightly improved gas exchange (g_s , A , E) in controls and net photosynthesis under Zn exposure. In the same treatment (ZnSi), the fact that NPQ was always higher than in Zn treatment may indicate that plants quickly dissipate an excess of energy in order to maintain an adequate balance between photosynthetic electron transport and carbon metabolism (Gharbi et al., 2017). Si paradoxically decreased pigments content in control plants which was an unexpected result.

Exogenous application of Si under Zn excess increased total antioxidant capacity (AOAM and AOAD fractions) and decreased MDA content mainly in the leaves, as already observed by Kim et al. (2017). This suggests that Si may trigger oxidative tolerance processes in hemp. The same beneficial effect of Si was noticed in leaves of control plants. Increased antioxidant capacity under Si exposure suggested a higher GSHt content. However, in the present study, under Zn excess GSHt content decreased following Si application. The increased antioxidant capacity while GSHt content decreased may be due to activation of other antioxidants by Si: the fact that both AOAD and AOAM antioxidant activities increased in response to Si suggests indeed that other compounds, such as ascorbate and α -tocopherol, which were not quantified in the present study, may increase in response to exogenous Si. Moreover, the lower Zn accumulation induced by Si probably decreased ROS production and the need of GSH as an antioxidant and a precursor of PC synthesis. PC content in leaves was indeed decreased in plants of ZnSi treatment comparatively to Zn-treated plants, while we

observed an opposite trend in roots. We may suppose that Si supply improved Zn sequestration through PC synthesis in the organ where Zn was the most accumulated. In the absence of Zn excess, Si application reduced membrane damage (decrease in MDA), which may explain the decrease of GSht and GSSG/GSH ratio contents. It is not surprising that PC content also decreased given the lower GSht content and the absence of Zn excess.

As a matter of fact, exogenous Si provides some metabolic advantages to hemp exposed to Zn excess, especially in relation to a decrease in Zn accumulation in the different parts of the plant. However, this was not sufficient to significantly increase plant growth on a short-term basis. Bokor et al. (2014) found similar data regarding specific maize cultivars simultaneously exposed to Zn and Si. According to these authors, increasing concentration of Si in combination with Zn treatment even increased physiological stress in comparison to Zn treatment. Similar results were observed by Masarovic et al. (2012) in sorghum who observed no positive effect of Si on high Zn in the medium.

5. Conclusion

Results obtained in nutrient solution indicated that *Cannabis sativa* cv Santhica 27 is able to significantly accumulate Zn when exposed to Zn excess, Zn being mainly accumulated in roots. Hemp can thus not be considered as an hyperaccumulator. In order to be used in phytostabilization strategies, the plant has to be able to tolerate heavy metals. In our study, hemp activated antioxidant defences and coped with the significant accumulation of Zn by limiting its transfer to the aerial parts. However, Zn excess negatively affected biomass production even though we did not observe any mortality in plants. Our experiment was carried out in nutrient solution where Zn bioavailability was high. It could be assumed that in field conditions Zn impact on biomass production would be more limited. Moreover, the use of Si to improve hemp growth on HM contaminated soils should be considered: in our experiment, Si decreased the proportion of Zn removed by the plants and improved the antioxidant response of control and Zn-exposed plants. Silicon however did not significantly improve growth of hemp exposed to Zn excess. In order to combine phytostabilization with non-food production, the properties of the harvested biomass have to remain compatible with the requirements of industry from a qualitative point of view (Luyckx et al., 2019). It would be

therefore appropriate to link morphophysiological observations with the distribution of HM in hemp tissues.

Acknowledgement

This work was financed by ADEME (Agence de la Transition écologique; Convention MisChar n°1672C0044), by FNRS (Fonds National pour la Recherche Scientifique, convention n°T.0147.21) and by the Luxembourg National Research Fund (20/15045745).

Chapter 4: Highlights and Perspectives

In this Chapter, hemp was cultivated in nutrient solution to assess the impact of a high bioavailability of Zn, as well as the short-term impact of silicon (Si) on hemp biomass production. Plants were grown 4 weeks in Hoagland solution. In the solution, we applied Zn in the form of ZnCl₂ (100 µM), and Si was added in the form of H₂SiO₃ (2 mM Si). We investigated the phytoextraction capacity of hemp, as well as the influence of Zn and Si application on hemp physiological properties.

The present Chapter demonstrated that (figure 4.6):

- *C. sativa* is able to significantly accumulate Zn in roots (the main organ of accumulation) and shoots (BF = 50). The use of produced fibres should thus be considered with caution in relation to Zn accumulation in the stem and the resulting risks of Zn dispersion during the retting process.
- Zn excess negatively affected biomass production and chlorophyll content.
- Hemp activated antioxidant defences and coped with the significant accumulation of Zn by limiting its transfer to the aerial parts.
- The addition of Si had numerous physiological impacts on the plant behavior occurring rapidly after Zn stress application and before any modification in terms of growth:
 - Si reduced Zn absorption but had no impact on Zn translocation
 - Si improved the antioxidant response of control and Zn-exposed plants.

Despite a BF of Zn close to 50, hemp could not be considered as a hyperaccumulating species since the translocation factor was lower than 1. This suggests that, despite a good level of tolerance, hemp exposed to Zn excess adopted an excluding strategy. Zn did not strongly impaired growth as observed with Cd in Chapter 3, but its accumulation was also higher in the stem than in the leaves. It reinforces the idea mentioned in interchapter 3 that HM distribution is a function of the external dose. In any cases, HM accumulation in leaves and stems point the importance to harvest hemp before natural leaf drop in order to maximize HM removal, and to consider with

caution the use of produced fibres in relation to the risks of HM dispersion during the retting process.

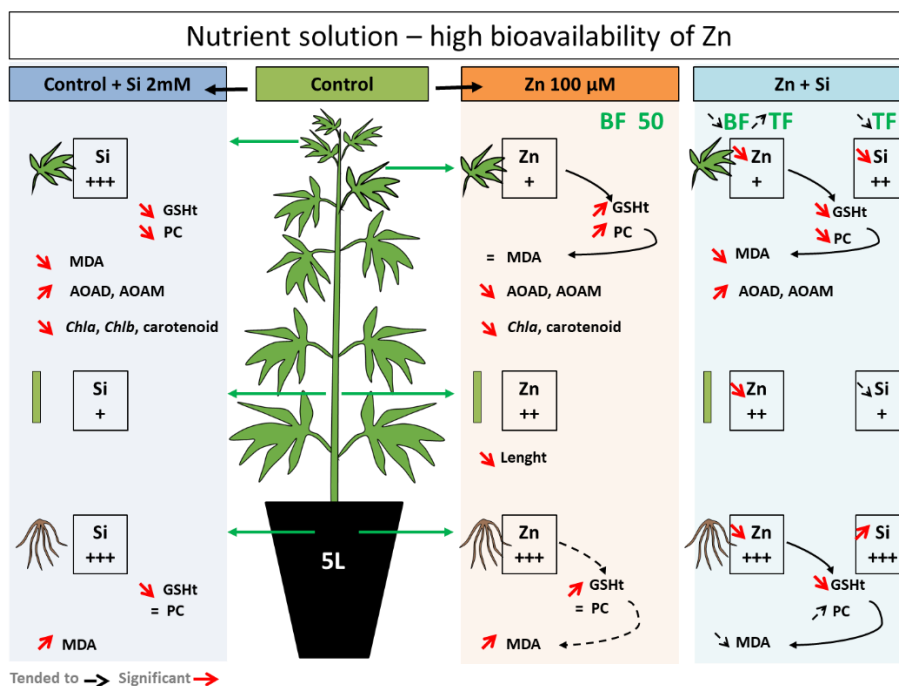


Figure 4.6: Summary of the results obtained in Chapter 4. Total glutathione (GSht), phytochelatin (PC), malondialdehyde (MDA), total global antioxidant activity (hydrophilic (AOAM) and hydrophobic fractions (AOAD)), chlorophyll (*Chl*), bioaccumulation factor (BF), translocation factor (TF). Black arrows indicate a non-significant increase/decrease of values, while red arrows illustrate the significant results.

To link morphophysiological observations with molecular responses, we evaluated in Chapter 5 the impact of Cd and Zn on the expression of key genes and the abundance of proteins in roots and leaves of *C. sativa*, and the impact of Si on those in stressed and unstressed plants.

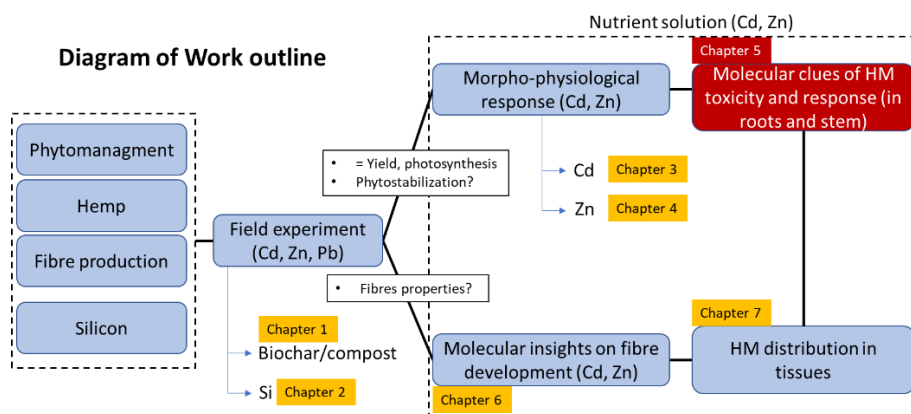
Chapter 5

Molecular and biochemical clues of Cd and Zn toxicity and response in hemp' roots and stems, and the potential effect of Si on stress response

Published article : Marie Luyckx, Jean-François Hausman, Kjell Sergeant, Gea Guerriero, Stanley Lutts. Molecular insights into hemp early responses to Cd and Zn exposure and the potential effect of Si on stress response. 2021. *Frontiers in plant science*, 12.

Author's contributions

SL, JFH and GG coordinated the project. ML, SL and GG conceived and designed the experiment. ML performed all experimental analysis. GG contributed to transcriptomic data analysis. KS contributed to proteomic data analysis. ML and SL wrote the manuscript. All authors reviewed and approved the final manuscript.



Abstract

With the intensification of human activities, plants are more frequently exposed to heavy metals. Zinc and cadmium are frequently simultaneously found in contaminated soils, including agronomic soils contaminated by atmospheric fallout near smelters. The fibre crop *Cannabis sativa* L. is a suitable alternative to food crops for cultivation on these soils. In the present study Cd (20 μ M) and Zn (100 μ M) were shown to induce a comparable growth inhibition in *Cannabis sativa*. To devise agricultural strategies aimed at improving crop yield, the effect of silicon (2 mM Si) on plants' stress tolerance was considered. Targeted gene expression and proteomic analysis were performed on leaves and roots after one week of treatment. Both Cd and Zn stimulated genes involved in proline biosynthesis (*P5CR*) and phenylpropanoid pathway (*PAL*) but Cd also specifically increased the expression of *PCS1-1* involved in phytochelatin synthesis. Si exposure influence the expression of numerous genes in a contrasting way in Cd- and Zn-exposed plants. At the leaf level, the accumulation of 122 proteins was affected by Cd while 47 proteins were affected by Zn: only 16 proteins were affected by both Cd and Zn. The number of proteins affected by Si exposure (27) alone was by far lower and 12 of them were not modified by heavy-metal treatment while no common protein appeared to be modified by both CdSi and ZnSi treatment. It is concluded that Cd and Zn had a clear different impact on plant metabolism and that Si confers a specific physiological status to stressed plants with quite distinct impacts on hemp proteome depending on the considered heavy metal.

1. Introduction

Plants often experience various biotic and abiotic stresses during their life cycle. The abiotic stresses include mainly drought, salt, temperature (low/high), flooding and element deficiency/excess (Ahmad et al., 2016b). Among the naturally occurring elements, 53 are classified as heavy metals (HM), the majority of which does not play an essential role in plants, although some of them such as Zn and Cu are essential elements for eukaryotic cells (Bhat et al., 2019). With the intensification of human activities, such as mining and industrial activities and the excessive utilization of poor-quality phosphate fertilizer, plants are more and more exposed to HM, which hamper crop growth and yield to a great extent

(Ahmad et al., 2016b; Jian et al., 2020). HM-induced stress represents, therefore, a critical challenge for agricultural productivity (Ghosh et al., 2017; Kosova et al., 2018).

In numerous areas of the world, HM-polluted agricultural soils cannot be safely used anymore for edible crop production due to risks for human health and only non-edible plant production remains possible (Feng et al., 2020). HM affect crop growth and yield through a negative impact on photosynthesis, root growth which alters the water balance and nutrient assimilation, thereby affecting their translocation to above ground plant parts and biomass production (Singh et al., 2016). At the molecular levels HM exposure can affect protein synthesis and structure, block functional groups of metabolically important molecules, supersede functionality of essential metals in biomolecules, affect the integrity of membranes, and increase the generation of reactive oxygen species (ROS) (reviewed by Emamverdian et al., 2015 and Singh et al., 2016).

The initial step of plant cells behavior towards any environmental constraint is stress sensing (Hossain and Komatsu, 2013): changes in ambient conditions are sensed by receptors at the plasma membrane inducing signaling pathways transferring stress signal from the plasma membrane to nucleus and leading to changes in gene expression (Kosova et al., 2018; Singh et al., 2016). Sequestration of HM in the cell wall (CW) is probably the first strategy to limit the entry of heavy metals in plant cells (Ye et al., 2012; Fernandez et al., 2014; Parrotta et al., 2015; Nawaz et al., 2019). Pectins can adsorb HM via their carboxylic groups and lignification of the cell wall could be a strategy to limit HM entry into the cell by making the CW less permeable (Pejic et al., 2009; Vukcevic et al., 2014; Gutsch et al., 2019a). Once inside cells, regulation of plasmodesmatal aperture through callose synthesis and deposition may limit the transfer of metal ions from one cell to another (Singh et al., 2016; O'Leary et al., 2018). To limit their toxicity, HM have to be delivered to the appropriate subcellular compartment (Singh et al., 2016; O'Leary et al., 2018). This can be achieved through ion chelation (phytochelatin, metallothionein): the complex formed between metal ion and chelating agent is transported into the vacuoles where metal ions can no longer affect cells' functioning (Cobbett, 2000; Fernandez et al., 2014; Jost and Jost-Tse, 2018). Using these mechanisms, many plant species have the ability to grow on contaminated sites and some of them are able to accumulate high concentrations of HM in their tissues.

Cannabis sativa L. (hemp) is a multipurpose crop, considered as a potential crop for cleaning the soil from HM because of its high biomass production, its long root system and its capability to absorb and accumulate HM (Ahmad et al., 2016a; Kumar et al., 2017). It is a promising species for fibre production on low HM-contaminated substrates (Hussain et al., 2019a, 2019b; Pietrini et al., 2019). Both woody fibres (shivs) and cellulosic bast fibres are produced in the stem and this organ therefore receives considerable attention in order to decipher the major molecular cues controlling the biogenesis of these two types of fibre (Guerriero et al. 2017c; 2017b; Behr, 2018; Luyckx et al., 2021a). Luyckx et al. (2021a) reported that Cd and high concentrations of Zn reduced the diameter of primary bast fibres and that Cd negatively affected cellulose and lignin biosynthesis while high concentrations of Zn had an opposite effect. According to this study, only a minor proportion of proteins was affected by both Cd and Zn. Cadmium increased the abundance of enzymes from the TCA cycle and negatively affected proteins involved in cell wall deposition, while Zn had an opposite effect. According to Pietrini et al. (2019), *Cannabis sativa* can grow on soil containing 150 mg.Kg⁻¹ Zn but other studies revealed that this species is still able to cope, to some extent, with 500 mg.Kg⁻¹ Zn (Angelova et al., 2004; Meers et al., 2005). Considering mean values of Zn bioavailability in polluted soils (Kos and Leštan, 2004), it may be considered that doses ranging from 50 to 150 µM Zn in nutrient solution correspond to a realistic moderate stress for *C. sativa* (Zlobin, 2021).

To devise agricultural strategies aimed at improving crop yield, the effect of silicon (Si) on plants' stress tolerance should be considered as a promising strategy (Luyckx et al., 2017b). This element is not considered as essential for plant growth and development, but the beneficial effects of Si fertilizers on plant growth and crop yields are now well documented in the literature (Keeping and Reynolds, 2009; Bhat et al., 2019). The commonly considered mechanisms contributing to Si-induced stress tolerance include toxic metal immobilization in the soil, stimulation of antioxidants, coprecipitation of metals within plant tissues, metal ions' chelation, compartmentation, structural alterations of plant tissues and biochemical response triggering metabolic changes (Luyckx et al., 2017a; Bhat et al., 2019). However, the precise molecular parameters involved in Si-induced adaptive processes have not been clearly identified (Luyckx et al., 2017a).

Besides the stems, which constitute the site of fibres' differentiation, the behaviors of roots and leaves are of paramount importance for whole

stressed plants' survival. Roots are indeed the first organs in direct contact with HM and regulate pollutant absorption and transfer to the shoot parts. Leaves provide energy for plant growth and control ion translocation through regulation of transpiration. Lefèvre et al. (2014) demonstrated that Cd and Zn may exhibit distinct distribution in leaf tissues and bind to different ligands in *Zygophyllum fabago* (Syrian bean-caper). Leaf proteomics evidenced a protection of photosynthetically active tissues and maintenance of cell turgor through synthesis of proteins involved in the photosynthetic apparatus, C-metabolism and osmoprotectants' synthesis. As far as hemp is concerned, Luyckx et al. (2021b) recently demonstrated that Cd affects photosynthesis through non-stomatal effects and increased glutathione and phytochelatin synthesis in the roots while exogenous Si decreased Cd accumulation in all organs and improved water use efficiency. Hemp leaves accumulate Si in the form of silica precipitating in epidermal cells and the basal cells and shafts of non-secreting trichomes (Guerriero et al., 2019; Berni et al., 2020), but the molecular link between Si accumulation and physiological protection remains unknown.

The aims of the present study are i) to determine the impact of Cd and Zn on the expression of key genes in roots and leaves of *C. sativa*, ii) to assess the effect of these conditions on the leaf proteome and iii) to analyze the impact of Si on those molecular responses in stressed and unstressed plants.

2. Material and methods

2.1. Plant material and growth conditions

Seeds of a monoecious hemp fibre variety (*C. sativa* cv. Santhica 27) were sown in loam substrate in greenhouse conditions. After one week, the obtained seedlings were transferred to nutrient Hoagland solution (described in Chapter 3, p. 140) in 25 L tanks: for each tank, 10 seedlings were adapted to plugged holes in a polystyrene plate floating at the top of the solution. Tanks (24) were placed in a phytotron under fully controlled environmental conditions (permanent temperature of $24 \pm 1^\circ\text{C}$ with a mean light intensity of $230 \mu\text{moles m}^{-2}\text{s}^{-1}$ provided by Phillips lamps (Philips Lighting S.A., Brussels, Belgium) (HPI-T 400 W), with a photoperiod of 16h under a relative humidity of 65%). Half of the tanks received 2 mM Si in the form of metasilicic acid (H_2SiO_3)

obtained from a pentahydrate sodium metasilicate ($\text{Na}_2\text{SiO}_3 \cdot 5 \text{H}_2\text{O}$) which was passed through an H^+ ion exchanger resin IR 20 Amberlite type according to Dufey et al. (2014). Tanks were randomly arranged in the phytotron and nutrient solution was permanently aerated by SuperFish Air Flow 4 pump. After two weeks of acclimatization, HM were then applied in the form of CdCl_2 (final concentration of 20 μM) and ZnCl_2 (100 μM). The pH of the solution was maintained at 5.5. Solubility of added HM was confirmed by the Visual MINTEQ09 software. Six treatments were thus defined, considering the presence of HM and the concomitant presence or absence of Si i.e. C (control: no HM and no Si), CSi, Cd, CdSi, Zn and ZnSi (4 tanks per treatment). Plants were harvested after one week of treatment. Plants from the same tank were pooled: hence, four pools containing 6 plants each were obtained for each treatment. Roots, leaves and stems were separated and weighed. Some samples were incubated in an oven (70 °C) for analysis of ion content while the remaining samples were frozen in liquid nitrogen and then stored at -80 °C until subsequent biochemical, gene expression analysis and proteomics.

2.2. Ion content, glutathione, phytochelatin and proline concentration

The protocols used for Cd, Zn and Si quantification are described in Chapter 3 (p. 142-143).

Glutathione (GSH and GSSG) was determined by HPLC on frozen samples after derivatization by orthophthalaldehyde according to Cereser et al. (2001). Total non-protein thiol (NPT) concentration was determined using Ellman's reagent according to De Vos et al. (1992). Phytochelatin content was evaluated as the difference between NPT and GSH levels. Proline was spectrophotometrically quantified at 520 nm using the acid ninhydrin method (Bates et al. 1973).

2.3. Targeted gene expression analysis

Total RNA was extracted from leaves and roots according to Guerriero et al. (2017c) and Mangeot-Peter et al. (2016) using the RNeasy Plant Mini Kit (Qiagen) treated on-column with DNase I. The RNA concentration and quality were measured for each sample by using a Nanodrop ND-1000 (Thermo Scientific) and a 2100 Bioanalyzer (Agilent Life Sciences), respectively. The

RNA integrity number (RIN) of all samples was higher than 7, and the ratios A260/280 and A260/230 were between 1.7 and 2.4. The extracted RNA was retrotranscribed into cDNA using the SuperScript II reverse transcriptase (Invitrogen) and random primers, according to the manufacturer's instructions. The synthesized cDNA was diluted to 2 ng/ μ L and used for the RT-qPCR analysis in 384-well plates. An automated liquid handling robot (epMotion 5073, Eppendorf) was used to prepare the 384-well plates. To check the specificity of the amplified products, a melt curve analysis was performed. The relative gene expression was calculated with qBase^{PLUS} (version 2.5, Biogazelle) by using the reference genes (*eTIF4E*, *TIP41*, *F-box* and *RAN*, Mangeot-Peter et al., 2016). Statistics (ANOVA2) was performed using R (version 3.3.1).

The target genes belong to candidates involved in photosynthesis [(RuBisCO activase, *RCA*), (RuBisCO, *RBCS*), (chlorophyllases, *CLH*), aquaporin mediating silicon passage (*Lsi*), *NIP2-1* (silicon channel) and *NIP2-2*, HM transport and sequestration (metallothionein, *MT2B*; phytochelatin synthase, *PCS2*), signaling (ethylene-responsive factor, *ERF1*; gibberellin receptor *Gibbrec*), proline biosynthesis (pyrroline-5-carboxylate reductase, *P5CR*; pyrroline-5-carboxylate synthetase, *P5CS*), stress response (iron superoxide dismutase, *FSD*; ascorbate peroxidase, *APX*; heat shock protein, *HSP*), and phenylpropanoid pathway (cinnamyl alcohol dehydrogenase, *CAD*; phenylalanine ammonia lyase, *PAL*). Those genes were selected on the basis of previous studies (Berni et al., 2020; Guerriero et al., 2017c, 2017d; Guerriero et al., 2019; Luyckx et al., 2021a) and were analyzed in the appropriate organ according to these works.

The corresponding primers were designed using Primer3Plus (<http://www.bioinformatics.nl/cgi-bin/primer3plus/primer3plus.cgi/>) and verified with the OligoAnalyzer 3.1 tool (Integrated DNA technologies, <http://eu.idtdna.com/calc/analyzer>). Primer efficiencies were checked via qPCR using 6 serial dilutions of cDNA (10, 2, 0.4, 0.08, 0.016, 0.0032 ng/ μ L).

2.4. Proteomic analysis

For each sample, 500 mg fresh matter of *C. sativa* leaves were homogenized in a Potter (Wheaton) homogenizer in 2 mL of homogenization buffer (50 mM Tris, pH 7.5 (HCl), 2 mM EDTA, 5 mM dithiothreitol (DTT), protease inhibitor mix (1 mM phenylmethylsulfonyl fluoride (PMSF), 2 μ g/mL each of leupeptin, aprotinin, antipain, pepstatin, and chymostatin, 0.6% w/v

polyvinylpyrrolidone, 30 mM spermine). The homogenate was centrifuged for 5 min at 2,000 rpm and 4 °C. Protein extracts were centrifuged at 2 °C for 30 minutes at 54,000 rpms (TLA55, Optima-Beckman-Coulter) to obtain a pellet of crude membranes and supernatant.

Twenty µg of each sample were transferred to 0.5 mL polypropylene Protein LoBind Eppendorf tubes and precipitated with chloroform-methanol method (Wessel and Flügge, 1984); 20 µL of 100 mM TEAB (triethylammonium bicarbonate) were then added to reach pH 8.5. Proteins were reduced by 5 mM DTT (dithiothreitol) and alkylated by 15 mM iodoacetamide. Proteolysis was performed with 0.5 µg of trypsin and allowed to continue overnight at 37 °C. Each sample was dried under vacuum with a Savant Speed Vac Concentrator.

Before peptide separation, the samples were dissolved in 20 µL of 0.1 % (v/v) formic acid and 2% (v/v) acetonitrile (ACN). Peptide mixture was separated by reverse phase chromatography on a NanoACQUITY UPLC MClass system (Waters) working with MassLynx V4.1 (Waters) software; 200 ng of digested proteins were injected on a trap C18, 100Å 5 µm, 180 mm x 20 mm column (Waters) and desalted using isocratic conditions with a flow rate of 15 µL/min using a 99% formic acid and 1% (v/v) ACN buffer for 3 min. The peptide mixture was subjected to reverse phase chromatography on a C18, 100Å 1.8 mm, 75 µm x 150 mm column (Waters) PepMap for 120 min at 35 °C at a flow rate of 300 nL/min using a two parts linear gradient from 1% (v/v) ACN, 0.1 % formic acid to 35 % (v/v) ACN, 0.1 % formic acid and from 35% (v/v) ACN, 0.1 % formic acid to 85 % (v/v) ACN, 0.1 % formic acid. The column was re-equilibrated at initial conditions after washing 10 min at 85% (v/v) ACN, 0.1 % formic acid at a flow rate of 300 nL/min. For online LC-MS analysis, the nanoUPLC was coupled to the mass spectrometer through a nano-electrospray ionization (nanoESI) source emitter.

IMS-HDMSE (Ion Mobility Separation-High Definition Enhanced) analysis was performed on an SYNAPT G2-Si high-definition mass spectrometer (Waters) equipped with a NanoLockSpray dual electrospray ion source (Waters). Precut fused silica PicoTipR Emitters for nanoelectrospray, outer diameters: 360 µm; inner diameter: 20 µm; 10 µm tip; 2.5" length (Waters) were used for samples and Precut fused silica TicoTipR Emitters for nanoelectrospray, outer diameters: 360 µm; inner diameter: 20 mm; 2.5" length (Waters) were used for the lock mass solution. The eluent was sprayed at a spray voltage of 2.4 kV with a sampling cone voltage of 25 V and a source offset of 30 V. The source temperature was set to 80 °C. HDMSE method in

resolution mode was used to collect data from 15 min after injection to 106 min. This method acquires MSE in positive and resolution mode over the m/z range from 50 to 2000 with a scan time of 1 sec. with a collision energy ramp starting from ion mobility bin 20 (20 eV) to 110 (45 eV). The collision energy in the transfer cell for low-energy MS mode was set to 4 eV. For the post-acquisition lock mass correction of the data in the MS method, the doubly charged monoisotopic ion of [Glu1]-fibrinopeptide B was used at 100 fmol/mL using the reference sprayer of the nanoESI source with a frequency of 30 s at 0.5 mL/min into the mass spectrometer.

HDMSE data were processed with Progenesis Q1 (Nonlinear DYNAMICS, Waters) software using *C. sativa* NCBI database downloaded October 8, 2019. Carbamidomethylation as the fixed cysteine modification, oxidation as the variable methionine modification, trypsin as the digestion enzyme were selected and one miscleavage allowed.

2.5. Microscopic determination of lignification and Cd deposition in leaves and roots

Pieces of leaf tissue were rapidly excised from fresh leaves (n^o2; acropetal numbering) with a scalpel and dipped into tissue freezing media (O.C.T., Tissue Tek, Jung etc.), and into propane cooled by liquid nitrogen. The plant pieces were next sectioned at 60 µm thickness with a Leica CM3050 cryotome (Leica), placed in Al holders and transferred to an Alpha 2-4 Christ freeze dryer (-50 °C, 0.04 mbar, 3 days). Freeze-dried cross-sections were photographed using a digital camera (AxioCam) mounted on a Zeiss Axioscope 2 fluorescence microscope (wave length: 405nm). Cross-sections were also studied using X-ray fluorescence at beamline ID21 (ESRF).

2.6. Statistical analysis

Except for proteomic, four independent biological replicates and three technical replicates were analyzed for each condition. Normality of the data was verified using Shapiro-Wilk tests and the data were transformed when required. Homogeneity of the data was verified using the Levene's test. ANOVA 2 were performed at a significant level of *p*-value < 0.05 using R (version 3.3.1) considering the type of HM treatment, and the Si application as main factors. Means were compared using Tukey's HSD all-pairwise comparisons at 5% level as a post-hoc test.

Proteomic analysis was performed two times and provided similar trends. Non-conflicting method was used as relative quantification method. To identify statistically significant differentially expressed proteins, combined criteria of a minimum of three or greater unique peptides, a 1.5-fold change ratio or greater and a p -value < 0.05 in the Student's t -test were adopted.

3. Results

3.1. Heavy metal impacts on plant growth

Cadmium decreased the dry weight of roots, stems and leaves by 53, 62 and 71%, respectively, while Zn decreased the dry weight of roots, stems and leaves by 34, 42 and 29%, respectively. Silicon mitigated growth inhibition induced by Zn (+12% in roots and +13% in shoots) and Cd (+21% in roots and +18% in shoots) comparatively to plants exposed to heavy metals in the absence of Si (detailed in Figure S5.1).

3.2. Ion accumulation, glutathione, phytochelatin and proline content

Cadmium was detected in Cd-treated plants only and accumulated to higher concentrations in the roots than in the leaves (Figure 5.1 a and b). Silicon had no significant impact on Cd accumulation. In Zn-treated plants, Zn also accumulated to a higher extent in the roots (Figure 5.1c) than in the leaves (Figure 5.1d): Si tended to reduce Zn accumulation in both organs, although the recorded decrease was not significant. A similar root Si accumulation was recorded for control and Cd-treated plants (Figure 5.1e), while the Si accumulation in roots was clearly the highest for Zn-treated plants. As far as the leaves are concerned (Figure 5.1f), the highest Si accumulation was recorded for Cd-treated plants. Glutathione accumulated in the roots of Zn-treated plants and additional Si strongly reduced such accumulation (Figure 5.2a). In the leaves, Cd decreased GSH content in the absence, as well as in the presence of Si (Figure 5.2b), while leaf GSH content increased in response to Zn and to a higher extent in the absence than in the presence of Si. Phytochelatin accumulated mainly in the roots of Cd-treated plants (Figure 5.2c) and Si had no impact on this parameter. Phytochelatin concentration was lower in the leaves than in the roots: the highest leaf PC concentration was recorded in Cd-treated plants (Figure 5.2d) and the lowest in control ones. Treatments had no significant impact on root proline content (Figure 5.2e). In the leaves, however, Si increased proline concentration in

control plants (Figure 5.2f). Both Cd and Zn increased leaf proline concentration but Si had contrasting impacts since it increased leaf proline concentration in Cd-treated plants, but drastically reduced it in Zn-exposed ones.

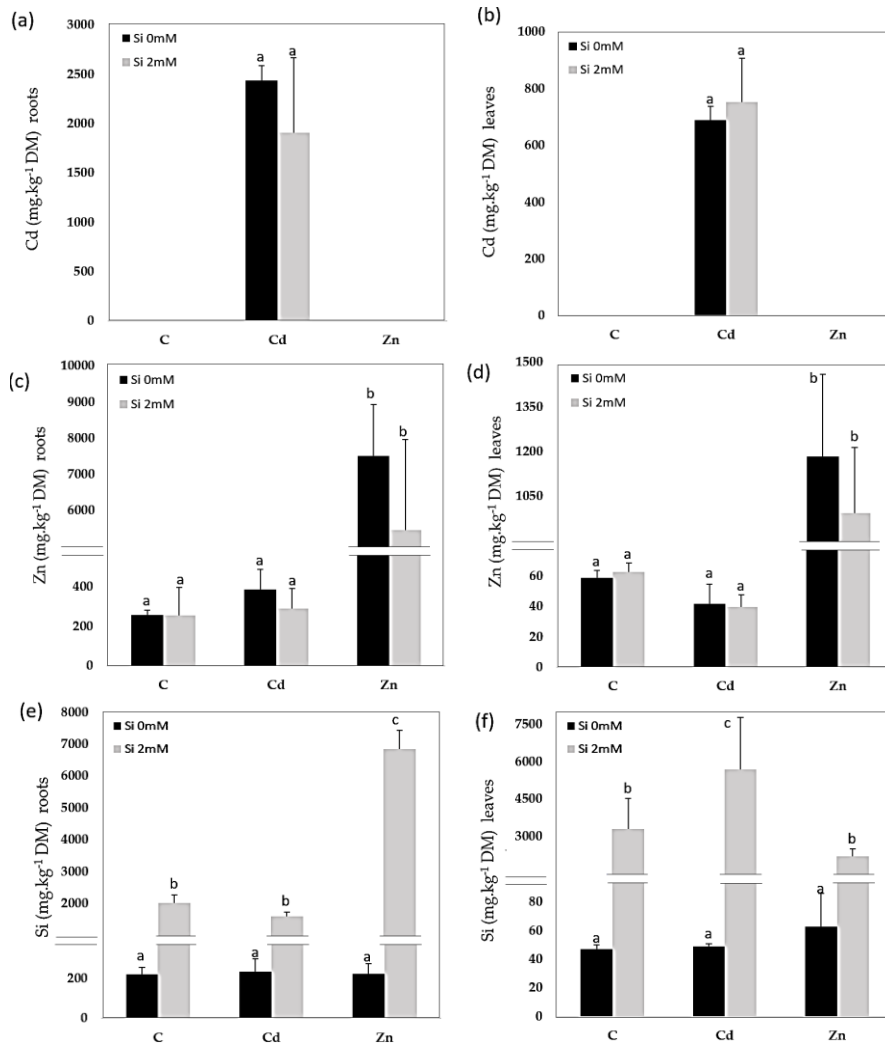


Figure 5.1: Cadmium (Cd), zinc (Zn) and silicon (Si) in roots (a, c, e) and leaves (b, d, f) of *C. sativa* (cv. Santhica 27). Plants were exposed for one week to Cd (20 μ M) or Zn (100 μ M) in the presence or absence of Si (2mM) (C: control plants not exposed to heavy metals). The different letters indicate that the values are significantly different from each other ($P < 0.05$; Tukey's HSD all-pairwise comparisons).

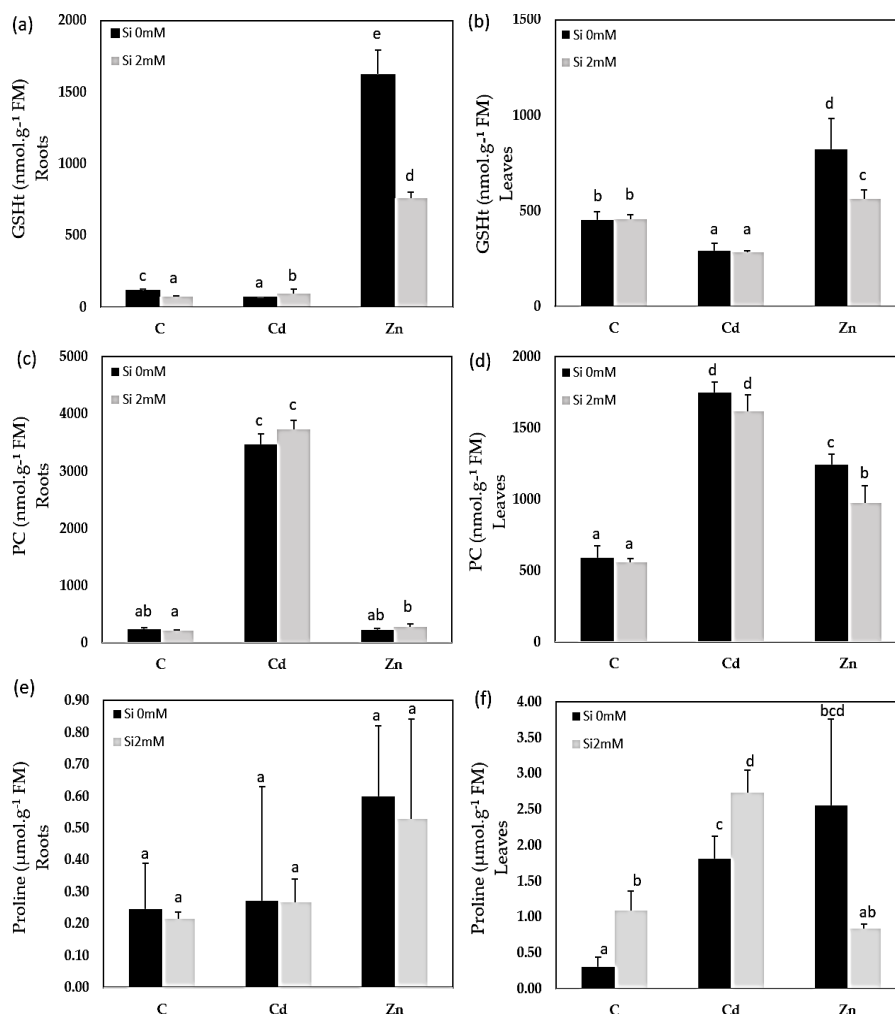


Figure 5.2: Glutathione (GSHt), phytochelatin (PC) and proline contents in roots (a, c, e) and leaves (b, d, f) of *C. sativa* (cv. Santhica 27). Plants were exposed for one week to Cd (20 μ M) or Zn (100 μ M) in the presence or absence of Si (2mM) (C: control plants not exposed to heavy metals). The different letters indicate that the values are significantly different from each other ($P < 0.05$; Tukey's HSD all-pairwise comparisons).

3.3. Gene expression in leaves and roots

The hierarchical clustering of the expression profiles (represented as a heatmap; Figure 5.3 (leaves) and Figure 5.4 (roots)) for the various treatments was performed using a Euclidean distance matrix in complete linkage. The clustering resulted in a separation between control plants (C, CSi), Cd exposed plants (Cd, CdSi) and Zn exposed plants (Zn, ZnSi).

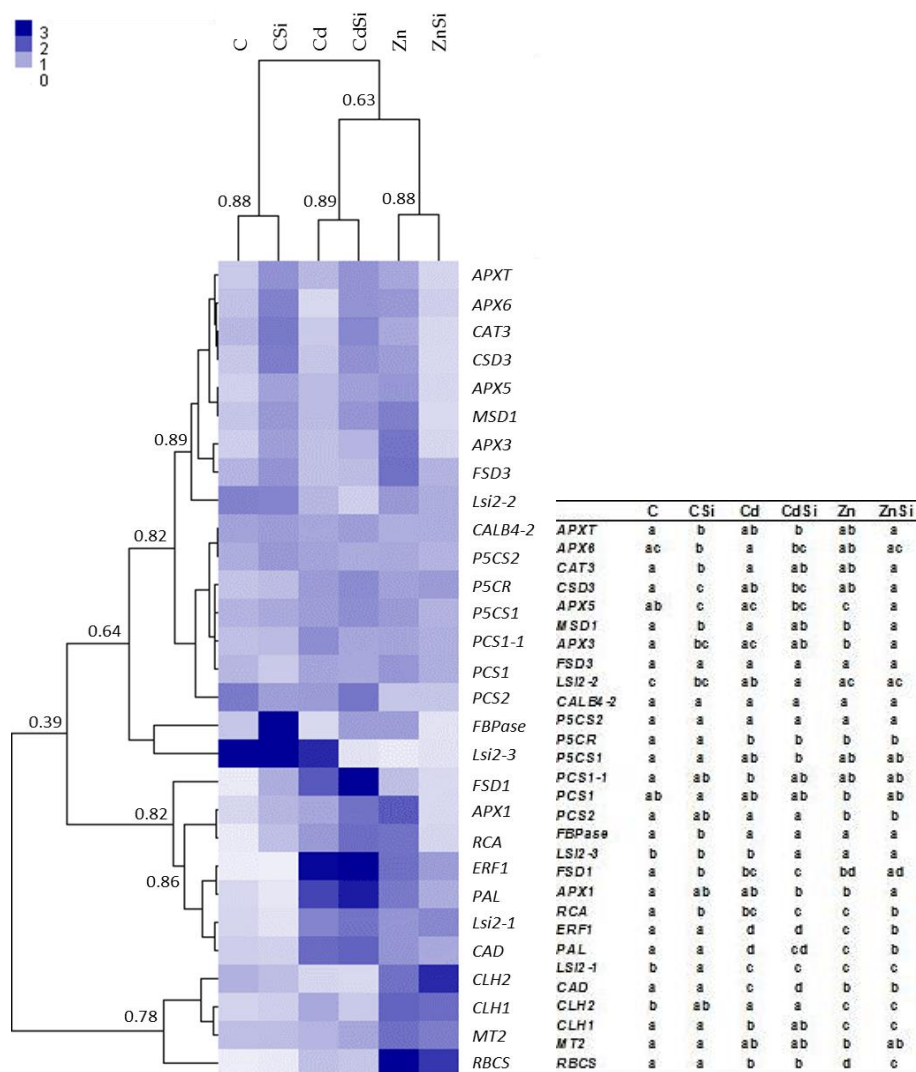


Figure 5.3: Heatmap hierarchical clustering showing the expression of genes assessed by RT-qPCR in leaves of hemp plants. Plants were exposed for one week to Cd (20 μ M) or Zn (100 μ M) in the presence or absence of Si (2mM) (C: control plants not exposed to heavy metals). Values represent Normalized Relative Quantities (NRQs). For each group, the Pearson coefficient is provided. The table represents statistical analyses of the heatmap hierarchical clustering. The different letters indicate that the values are significantly different from each other ($P < 0.05$; Tukey's HSD all-pairwise comparisons).

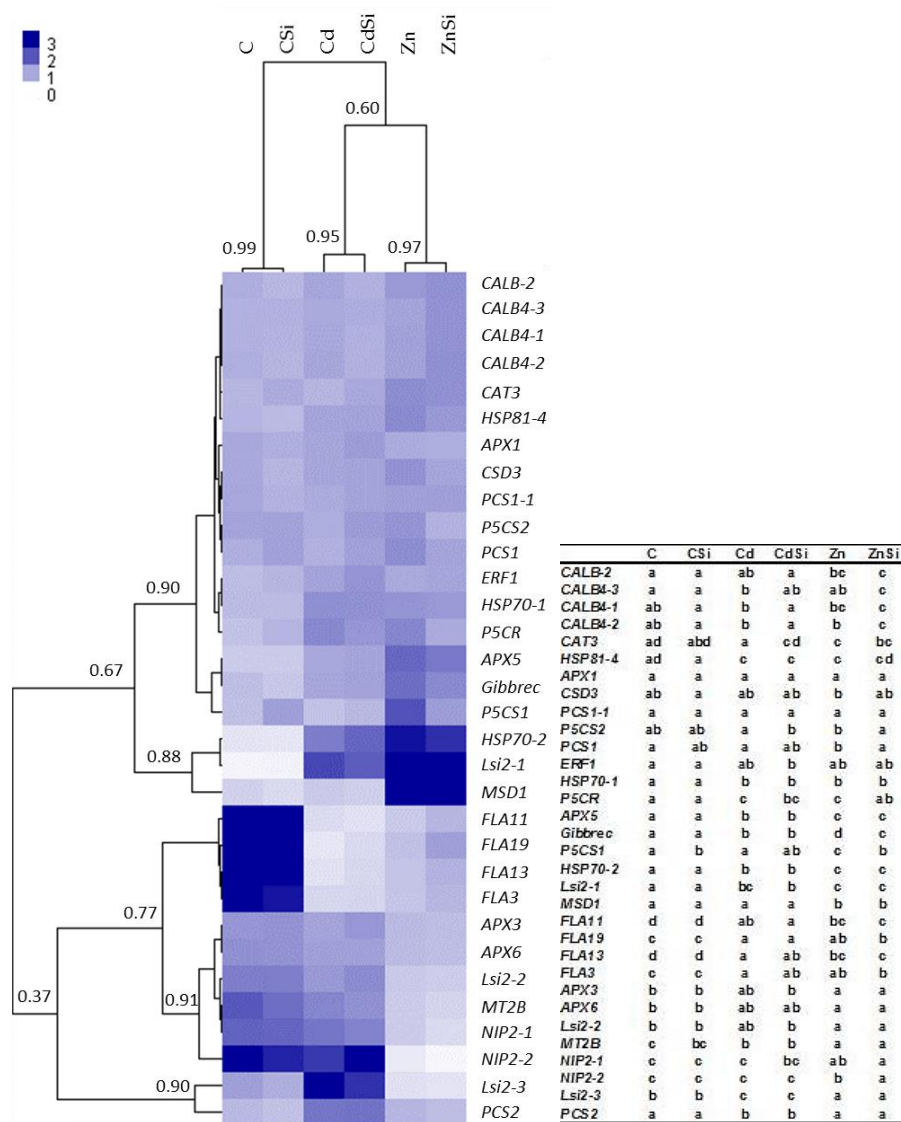


Figure 5.4: Heatmap hierarchical clustering showing the expression of genes assessed by RT-qPCR in roots of hemp plants. Plants were exposed for one week to Cd (20 μ M) or Zn (100 μ M) in the presence or absence of Si (2mM) (C: control plants not exposed to heavy metals). Values represent Normalized Relative Quantities (NRQs). For each group, the Pearson coefficient is provided. The table represents statistical analyses of the heatmap hierarchical clustering. The different letters indicate that the values are significantly different from each other ($P < 0.05$; Tukey's HSD all-pairwise comparisons).

In leaves of HM-stressed plants several transcripts were more abundant as compared to controls. Notably *RCA*, *RBCS* and *CLH1* (genes involved in photosynthesis), *CAD* (involved in lignin synthesis), *P5CR* (involved in proline biosynthesis), *ERF1* (involved in signal transduction), *FSD1* (involved in cell rescue), *PAL* (involved in phenylpropanoid pathway) and *Lsi2-1* (involved in Si accumulation). In addition, Cd exposure increased the expression of *PCS1-1* (involved in phytochelatin synthesis) and decreased the expression of *CLH2* and *Lsi2-2* compared to control plants. A higher expression of *MSD1*, *APX1*, *APX3*, *APX5*, *MT2* (genes involved in cell rescue), *CLH2*, and a decreased expression of *PCS2* and *Lsi2-3* was observed in Zn-treated plants compared to control plants. A significant effect of Si application on the expression of genes of HM-stressed plants was detected: Si exposure increased the expression of a gene involved in cell rescue (*APX6*) and decreased the expression of *Lsi2-3* in Cd-treated plants, while the abundances of transcripts coding for *RCA*, *RBCS*, *ERF1*, *APX1*, *APX3*, *APX5* and *MSD1* were lower in Zn-Si treated plants than in those exposed to Zn in the absence of Si. In control plants, Si application stimulated the expression of genes involved in photosynthesis (*FBPase*, *RCA*) and cell rescue (*CAT3*, *APX3*, *APX5*, *APX6*, *APXT*, *CSD3*, *FSD1*, *MSD1*), while the abundance of *Lsi2-1* transcript decreased.

In roots, HM exposure increased the expression of HSPs (*HSP81-4*, *HSP70-1*, *HSP70-2*), *P5CR* (proline biosynthetic gene), *APX5*, *Gibbrec*, *Lsi2-1* (silicon transport), and decreased the expression of *FLAs* (*FLA3*, *FLA11*, *FLA13*, *FLA19*; cell wall-related) and *MT2B* (metallothionein). In addition, Cd exposure also increased the expression of *CALB4-3* (intracellular signaling), *Lsi2-3* and *PCS2* (phytochelatin synthase) compared to control plants. A pronounced expression of *CALB-2*, *PCS1*, *MSD1*, and a decreased expression of *APX3*, *APX6*, *Lsi2-2*, *Lsi2-3*, *NIP2-1* (silicon channel) and *NIP2-2* was observed in plants when exposed to Zn. In control plants, Si exposure significantly stimulated the expression of a gene involved in proline biosynthesis (*P5CS1*). In plants exposed to Cd, Si decreased the expression of *CABLA-1* and *CABLA-2*, and increased those of *CAT3* and *P5CS2*. Genes involved in intracellular signaling (*CABLA-3*, *CABLA-2*) were more expressed and *P5CS2*, *PCS1*, *P5CR*, *Gibbrec*, *P5CS1*, and *NIP2-2* were less expressed in ZnSi-treated plants than in Zn exposed ones.

3.4. Proteomics

The data relative to the impact of the treatments on protein regulation are provided in Table 5.1 which simultaneously considers soluble and membrane-bound protein fractions. The accumulation of 122 proteins was affected by Cd while 47 were affected by Zn (Figure 5.5). Only a minor proportion of proteins (16) was affected by both Cd and Zn, suggesting a different impact of these HM on plant metabolism. The number of proteins affected by Si (27) exposure was by far lower than the number of proteins affected by HM. Detailed results are presented below.

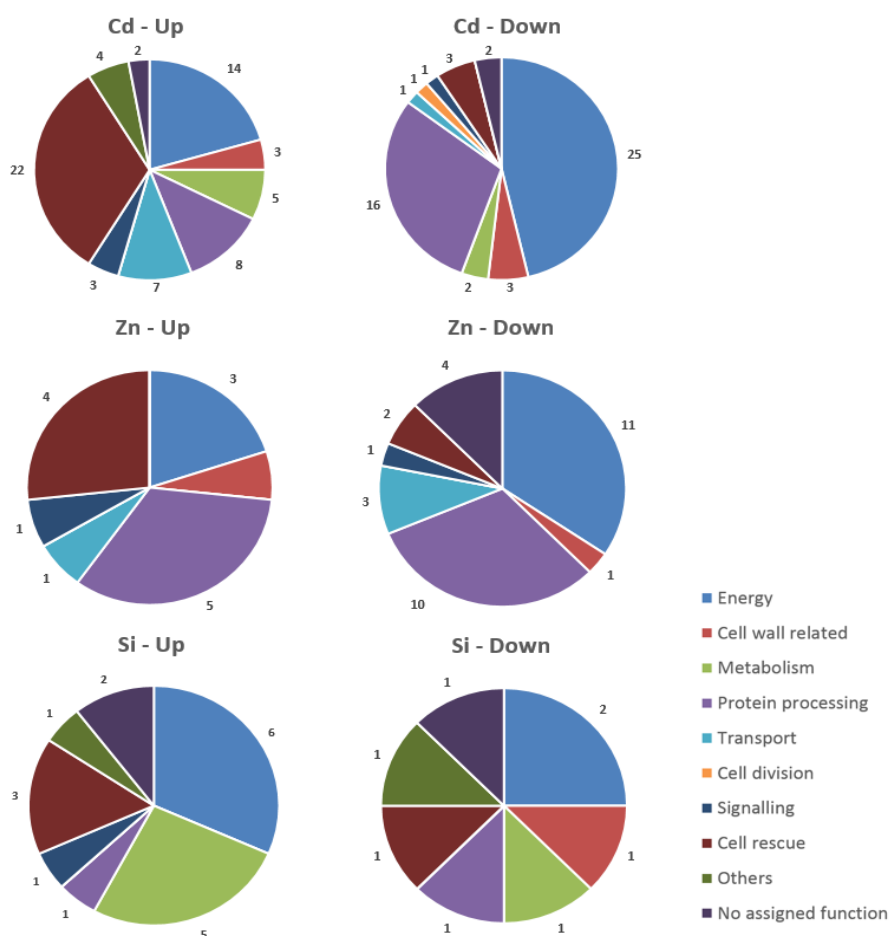


Figure 5.5: Functional classification of proteins with significant quantitative changes in abundance in hemp leaves in response to Cd, Zn and Si. Seedlings were exposed for one week either to Cd 20 μ M, Zn 100 μ M or Si 2 mM and proteins were extracted from leaves. Mixed treatment (CSi, CdSi, ZnSi) are not indicated for the sake of clarity.

Photosynthesis/ CO₂ assimilation

Most of the identified proteins involved in light-dependent and light-independent reactions of photosynthesis, as well as chlorophyll biosynthesis related-proteins showed reduced abundance under HM exposure.

Hemp response to Cd resulted in a significant decrease in the abundance of oxygen-evolving enhancer protein (OEE), plastocyanin (Pc), photosystem I reaction center (subunits N, VI), ferredoxin (Fd) and Fd-NADP⁺ reductase (NADP⁺ reductase), RuBisCO activase (RCA), RuBisCO large subunit-binding protein (rbcL), CBBY and ribulose-phosphate 3-epimerase (PPE), protochlorophyllide reductase (POR), hydroxymethylbilane synthase and coproporphyrinogen III oxidase (CPOX). Only 2 proteins (Fd and rbcS) were significantly upregulated in CdSi-exposed plants comparatively to Cd-treated ones.

Under Zn exposure, NADH-plastoquinone oxidoreductase subunit I (Ndh), cytochrome b6f (cytb6f), Pc, Fd, RCA, phosphoglycerate kinase (PGK), Calvin cycle protein CP12-1 (CP12-1), protochlorophyllide reductase, geranylgeranyl diphosphate reductase and magnesium-protoporphyrin IX monomethyl ester cyclase were found to be less abundant comparatively to controls. Photosynthesis-related proteins were not affected by Si in ZnSi-exposed plants comparatively to Zn-treated ones.

In the absence of HM stress, Si exposure was shown to increase the abundance of glycerate dehydrogenase (GlyDH), a protein involved in photorespiration.

Carbohydrate metabolism and TCA cycle

Proteins involved in carbohydrate metabolism and TCA cycle undergo the greatest change in accumulation under conditions of Cd stress: a phosphoglucomutase (PGM), 2 phosphoenolpyruvate carboxylase (PEPC) and a glyceraldehyde-3-phosphate dehydrogenase (G3PDH) had a lower abundance while an NADP-dependent malic enzyme (MDH), 3 components of pyruvate dehydrogenase (PDH) complex, an aconitate hydratase (AH) and an isocitrate dehydrogenase (IDH) were more abundant compare to unstressed plants. The application of 2 mM H₂SiO₃ under Cd exposure decreased the abundance of a PEPC (PEPC2), while the levels of PEPC1, a G3PDH and an IDH increased comparatively to Cd treatment. With the exception of G3PDH, proteins involved in carbohydrate metabolism were reduced by Cd, while enzymes involved in tricarboxylic acid pathway increased.

Zn exposure decreased the abundance of a MDH. The addition of Si to Zn-treated plants had no impact on the abundance of proteins involved in carbohydrate metabolism.

In the absence of an HM stress, Si application decreased the abundance of a PDH compared to control plants.

GABA shunt and ATP synthesis

Two enzymes involved in γ -aminobutyrate (GABA) shunt were induced under Cd exposure: glutamate decarboxylase (GluDC) which catalyzes the conversion of glutamate to GABA, and γ -aminobutyrate transaminase (GABA-T) responsible of GABA conversion to succinic semialdehyde. ATP synthesis is induced under HM stress as observed for Cd and Zn-treated plants compared to control ones.

In both unstressed and HM-stressed plants no significant effect of Si application on the abundance of proteins involved in GABA shunt and ATP synthesis was detected.

Cell wall-related

HM exposure had an impact on several enzymes involved in cell wall formation. Cell wall components whose biosynthesis/assembly/degradation are affected by Cd exposure are pectin and hemicellulose (UDP-glucose 6-dehydrogenase, UGDH; pectinesterase inhibitor, PME), cellulose (glycosyltransferase STELLO1), and lignin (caffeic acid 3-*O*-methyltransferase, COMT; caffeoyl-CoA *O*-methyltransferase, CCOMT; lignin-forming anionic peroxidase). Among them, lignin associated enzymes were more abundant in Cd-treated plants, the others were less abundant. In the same treatment, Si exposure induced a decreased abundance of GroES-like zinc-binding alcohol dehydrogenase family protein (CAD).

Plants under Zn stress exhibited a lower abundance of fasciclin-like arabinogalactan protein 10 (FLA10) involved in SCW synthesis and a higher abundance of a xylose isomerase (xylan metabolism). Si application had no effect on these proteins.

Amino acids, nitrogen and glutathione metabolism

Cd exposure had an impact on proteins involved in amino acids, nitrogen and glutathione metabolism. Enzymes of methionine metabolism (methionine synthase, MS), alanine metabolism (alanine aminotransferase, AlaAT), a spermidine synthase (SPDS) and a glutamine synthetase (GLN) were

upregulated, two isoforms of glutamate dehydrogenase (GluDH) had altered abundance and a hydroxyphenylpyruvate reductase (HPPR) constitute a biosynthetic pathway from tyrosine to 4-hydroxyphenyllactic acid (pHPL) was down-regulated. In this treatment, Si application increased the abundance of a protein involved in the pathway of L-valine degradation (probable 3-hydroxyisobutyrate dehydrogenase-like) and an aminomethyltransferase.

Zn exposure had no impact on this part of the metabolism. However, plants of ZnSi treatment exhibited an increased abundance of a methyltetrahydropteroyltriglutamate-homocysteine methyltransferase (MS) involved in methionine metabolism and a ferredoxin-nitrite reductase (NiR) involved in nitrogen assimilation comparatively to plants of Zn treatment.

In the absence of HM stress, the abundance of an S-adenosylmethionine synthase (SAM) was increased after Si exposure.

Protein synthesis, processing, modification

HM exposure affected enzymes involved in protein synthesis, processing and modification. In both Cd and Zn treatments, the abundance of proteins involved in synthesis is significantly decreased while most of the proteases identified were more abundant. Two proteins involved in folding and stabilization showed the same variation of abundance under Cd or Zn stress: the 20kDa chaperonin was less abundant and luminal-binding protein 5 was more abundant. Cd treatment also increased the abundance of heat shock proteins (HSP81, HSP80), a protein disulfide-isomerase, and decreased abundance of HSP93. Zn exposed plants had a lower abundance of a chaperonin 60 beta. Si application only impacted abundance of a HSP80 in Cd-treated plants and an oligo-ubiquitin involved in proteolysis (UBQ8) in control plants.

Aquaporin, Transport facilitation, transport mechanism, membrane modification

In Cd treatment, plants exhibited higher levels of an exportin (protein export from nucleus), a patatin-like protein 2 (PLP2, phospholipase activity), a porin, and two proteins involved in vesicular trafficking (alpha-soluble NSF attachment protein 2; clathrin light chain 1, CLC1).

Zn exposure also affected vesicular trafficking by lowering the abundance of a putative clathrin assembly protein and a voltage-dependent cation-selective channel (TIC), and by increasing the abundance of an aquaporin (PIP1-2).

Si had no effect on this class of proteins.

Ionic homeostasis

Cd and Zn had a different impact on V-type proton ATPase's subunits. In Cd-treated plants, the abundance of the A subunit increased while in Zn treatment B subunit was less abundant. Cd exposure also increased the abundance of another plasma membrane ATPase and decreased abundance of a ferritin (ferritin 3), involved in iron buffering.

Si had no effect on this class of proteins.

Signal transduction and metabolism regulation

Most of the proteins with a function in signal transduction and metabolism regulation were upregulated under Cd stress: a 1-aminocyclopropane-1-carboxylate oxidase (ACC oxidase), involved in ethylene synthesis; a calcium-dependent protein kinase (CDPK) and an allene oxide synthase (AOS, involved in jasmonate synthesis, Farmer and Goossens, 2019) were more abundant. In these plants, thiamine thiazole synthase (THI) was less abundant. In *Arabidopsis*, THI1 interacts with Ca²⁺-dependent protein kinase CPK33 and modulates the S-type anion channels and stomatal closure (Li et al., 2016). Compared to plants of Cd treatment, plants of CdSi treatment exhibited a higher abundance of a protein identified as general regulatory factor 2.

In Zn treatment, two proteins had a different abundance compared to control ones: AOS was more abundant while guanosine nucleotide diphosphate dissociation inhibitor (GDI) which regulate the activity of ROP (Rho of Plants) proteins. Si exposure had no impact on Zn-treated plants for this class of proteins.

Cell rescue, defense

Most of cell rescue proteins induced by Cd are part of two functional classes: pathogenesis-related proteins (PR) and oxidative stress response. Cd exposure up-regulated PR1, a PR-related protein (PRR), 2 thaumatin-like proteins (TLP), 2 endochitinases (ECH2) and 3 callose-associated enzymes (glucan endo-1,3-beta-glucosidases, BG). Oxidative stress response-related proteins with higher abundance in Cd-treated plants were: peroxidases (PRX2, PRX12, PRX15, protein P21-like), 2 probable nucleoredoxins (Trx), a probable aldoketo reductase (AKR), 2 aldehyde dehydrogenases (ALDH) a probable NAD(P)H dehydrogenase (quinone) FQR1-like1, and a GDP-D-mannose 3'-5'-epimerase (GME) which regulates ascorbate synthesis under stress

conditions, and adjusts the balance between ascorbate and cell-wall monosaccharide biosynthesis. The abundance of a formate dehydrogenase (FDH) was also increased under Cd exposure while a probable mannitol dehydrogenase (MTD), a peroxiredoxin (PRN) and a glucan synthase-like 11 (GSL11) were less abundant compared to control. In the same treatment, Si application increased the abundance of an FDH and a BG.

Zn exposure increased the abundance of proteins involved in oxidative stress response (PRX2, PRX12, Trx), but also that of a probable plastid-lipid-associated protein. Zn-treated plants also exhibited a decreased abundance of a callose synthase (CALS) and a PRN. Si application under Zn stress induced higher abundance of a macrophage migration inhibitory factor homolog (MDL, involved in stress response pathways), and decreased the abundance of a PRX2 comparatively to Zn-treated plants in the absence of Si.

Others

Cd-stressed plants exhibited a higher abundance of a secoisolariciresinol dehydrogenase-like (SDH) protein, involved in lignan biosynthesis. Another SDH was more abundant in CdSi treatments comparatively to Cd treatment.

In the absence of HM stress, Si had an impact on the phenylpropanoid pathway: phenylalanine ammonia-lyase (PAL) was less abundant.

Table 5.1 (below): List of proteins with significant quantitative changes of hemp leaves in response to Cd, Zn and Si. Seedlings were exposed for one week either to Cd 20 μ M, Zn 100 μ M or Si 2 mM and proteins were extracted from leaves. MFC: Max Fold Change. Abr.: abbreviation; sol: soluble; mbr: membrane-located.

Accession	Soluble protein name	C-Cd		C-Zn		C-CSi		Cd-CdSi		Zn-ZnSi		Abr.
		Anova	MFC	Anova	MFC	Anova	MFC	Anova	MFC	Anova	MFC	
ENERGY												
Photosynthesis/CO2 assimilation												
XP_030507415.1	plastocyanin	↘	4.32E-02	4.0								Pc
XP_030507415.1	plastocyanin	↘	8.10E-06	4.4	↘	1.27E-04	2.2					Pc
XP_030510336.1	ferredoxin-like				↘	1.30E-04	1.7					Fd
XP_030510578.1	ferredoxin-like	↘	4.28E-02	3.5				↗	3.16E-02	2.4		Fd
XP_030491053.1	oxygen-evolving enhancer protein 3-2_ chloroplastic-like	↘	1.45E-03	1.8								OEE
XP_030496367.1	oxygen-evolving enhancer protein 1_ chloroplastic	↘	2.42E-04	1.5								OEE
XP_030496723.1	photosystem I reaction center subunit N_ chloroplastic	↘	1.82E-03	1.6								CR
XP_030491785.1	photosystem I reaction center subunit VI_ chloroplastic-like	↘	1.11E-04	1.5								CR
XP_030486101.1	ferredoxin-NADP reductase_ leaf-type isozyme_ chloroplastic-like	↘	1.07E-03	1.5								NADP reducta
XP_030498930.1	protein HHL1_ chloroplastic	↘	5.51E-05	1.6								HHL1
XP_030492156.1	ribulose biphosphate carboxylase/oxygenase activase_ chloroplastic isoform X2	↘	8.16E-03	2.2								RCA
XP_030492156.1	ribulose biphosphate carboxylase/oxygenase activase_ chloroplastic isoform X2	↘	3.99E-04	1.7								RCA
XP_030504809.1	ribulose biphosphate carboxylase/oxygenase activase 2_ chloroplastic-like	↘	4.65E-03	1.5								RCA
XP_030504809.1	ribulose biphosphate carboxylase/oxygenase activase 2_ chloroplastic-like	↘	3.26E-04	1.6	↘	6.95E-04	1.6					RCA
XP_030501759.1	ribulose biphosphate carboxylase small chain_ chloroplastic-like							↗	5.28E-02	1.7		rbcs
XP_030478872.1	ruBisCO large subunit-binding protein subunit beta_ chloroplastic	↘	5.53E-03	1.5								rbcl
XP_030478872.1	ruBisCO large subunit-binding protein subunit beta_ chloroplastic	↘	3.32E-05	1.5								rbcl
XP_030495826.1	CBBY-like protein	↘	2.64E-03	1.5								CBBY
XP_030494025.1	ribulose-phosphate 3-epimerase_ chloroplastic	↘	1.50E-03	1.5								PPE
XP_030489666.1	protochlorophyllide reductase_ chloroplastic	↘	1.44E-05	2.2	↘	3.77E-05	2.0					POR
XP_030502075.1	glycine cleavage system H protein_ mitochondrial-like	↘	3.48E-03	1.5								GCS-H
XP_030487982.1	glycerate dehydrogenase							↗	2.01E-02	1.5		GlyDH
AT5G08280.1	hydroxymethylbilane synthase	↘	3.95E-04	1.6								CPOX
AT1G03475.1	Coproporphyrinogen III oxidase	↘	4.11E-02	1.6								CPOX
XP_030479749.1	chlorophyll a-b binding protein of LHClI type 1				↗	3.90E-04	2.3					
AIK91475.1	NADH-plastoquinone oxidoreductase subunit I (chloroplast)				↘	8.47E-03	1.6					Ndh
YP_009143583.1	cytochrome b6 (chloroplast)				↘	9.38E-04	1.5					cytb6f
AT1G56190.1	phosphoglycerate kinase family protein chr1:21028403-21030454 FORWARD LENGTH=478				↘	9.72E-04	1.5					PGK
XP_030492934.1	geranylgeranyl diphosphate reductase_ chloroplastic				↘	5.50E-04	1.5					

Accession	Soluble protein name	C-Cd		C-Zn		C-CSi		Cd-CdSi		Zn-ZnSi		Abr.
		Anova	MFC	Anova	MFC	Anova	MFC	Anova	MFC	Anova	MFC	
XP_030509499.1	magnesium-protoporphyrin IX monomethyl ester [oxidative] cyclase_chloroplast			↘	5.68E-05	1.6						
XP_030489172.1	calvin cycle protein CP12-1_chloroplast-like			↘	3.02E-03	1.5						CP12-1
Carbohydrate metabolism, glycolysis and gluconeogenesis												
XP_030496986.1	phosphoglucomutase_cytoplasmic	↘	1.56E-02	1.9								PGMc
AT1G53310.1	phosphoenolpyruvate carboxylase 1							↗	2.36E-02	2.1		PEPC1
AT2G42600.2	phosphoenolpyruvate carboxylase 2	↘	4.30E-02	1.6				↘	7.72E-03	1.5		PEPC2
XP_030484584.1	phosphoenolpyruvate carboxylase_housekeeping isozyme-like	↘	8.96E-03	1.5								PEPC
XP_030496981.1	glyceraldehyde-3-phosphate dehydrogenase_cytosolic	↗	1.41E-03	1.6								G3PD
AT1G42970.1	glyceraldehyde-3-phosphate dehydrogenase B subunit	↘	8.86E-03	1.6								G3PD
XP_030510057.1	NADP-dependent glyceraldehyde-3-phosphate dehydrogenase							↗	3.92E-02	1.5		G3PD
Tricarboxylic-acid pathway												
XP_030491388.1	NADP-dependent malic enzyme	↗	2.74E-05	1.6								MDH
XP_030508797.1	malate dehydrogenase			↘	2.66E-04	2.1						MDH
XP_030496791.1	pyruvate dehydrogenase E1 component subunit alpha-1_mitochondrial-like	↗	1.49E-04	2.1			↘	8.91E-03	1.7			PDH
XP_030490683.1	dihydrolipoilysine-residue acetyltransferase component 2 of pyruvate dehydrogenase complex_mitochondrial isoform X11	↗	2.13E-04	2.3								PDH
XP_030497354.1	dihydrolipoilysine-residue succinyltransferase component of 2-oxoglutarate dehydrogenase complex 1_mitochondrial-like	↗	7.13E-05	2.0								PDH
XP_030483075.1	aconitate hydratase_cytoplasmic	↗	1.83E-04	1.7								AH
XP_030485874.1	isocitrate dehydrogenase [NAD] regulatory subunit 1_mitochondrial							↗	1.04E-02	1.6		IDH
XP_030507063.1	isocitrate dehydrogenase [NADP]	↗	6.14E-04	1.8								IDH
Respiration												
XP_030480140.1	cytochrome c1-2_heme protein_mitochondrial	↗	1.11E-04	1.5								CYC1
γ-aminobutyrate (GABA) shunt												
XP_030507263.1	glutamate decarboxylase 1	↗	3.92E-04	1.5								GluDC
XP_030482659.1	gamma aminobutyrate transaminase 3_chloroplast-like	↗	1.26E-02	2.6								GABA
ATP synthesis												
XP_030498910.1	ATP synthase subunit beta_mitochondrial	↗	9.28E-05	1.6	↗	5.19E-05	1.6					
XP_030491925.1	ATP synthase subunit delta'_mitochondrial	↗	4.40E-06	1.5								
ANC49115.1	ATPase subunit 1 (mitochondrion)	↗	1.72E-04	1.5	↗	2.72E-05	1.6					
Pentose-phosphate pathway												
XP_030484850.1	6-phosphogluconate dehydrogenase_decarboxylating 2	↗	3.14E-04	2.2								6PGD
CELL WALL RELATED												
AT3G29360.1	UDP-glucose 6-dehydrogenase family protein	↘	3.75E-05	1.6								UGDH
XP_030498194.1	pectinesterase inhibitor-like	↘	8.11E-03	2.4								PMEI
XP_030493991.1	probable glycosyltransferase STELLO1	↘	1.09E-03	1.5								STELLO
XP_030489949.1	caffeic acid 3-O-methyltransferase-like isoform X2	↗	4.61E-03	2.2								COMT
XP_030486279.1	caffeoyl-CoA O-methyltransferase	↗	4.81E-03	1.5								CCOM

Accession	Soluble protein name	C-Cd		C-Zn		C-CSi		Cd-CdSi		Zn-ZnSi		Abr.	
		Anova	MFC	Anova	MFC	Anova	MFC	Anova	MFC	Anova	MFC		
XP_030508514.1	lignin-forming anionic peroxidase-like	↗	8.04E-03	1.5									
AT5G51970.1	GroES-like zinc-binding alcohol dehydrogenase family protein							↘	5.00E-02	2.1		CADI	
XP_030489850.1	fascidin-like arabinogalactan protein 10			↘	7.10E-05	1.5						FLA10	
XP_030510845.1	xylose isomerase	↗	4.69E-02	1.7									
METABOLISM													
Amino acids, nitrogen and glutathione metabolism													
XP_030504084.1	S-adenosylmethionine synthase 1-like					↗	3.89E-02	1.6				SAMS	
AT5G20980.1	methionine synthase 3	↗	3.20E-02	1.7								MS	
XP_030490921.1	alanine aminotransferase 2-like	↗	1.27E-03	1.5								AlaAT	
XP_030492265.1	probable 3-hydroxyisobutyrate dehydrogenase-like 1_mitochondrial							↗	1.19E-04	2.0			
XP_030480326.1	hydroxyphenylpyruvate reductase-like	↘	3.64E-02	1.6								HPPR	
XP_030491636.1	aminomethyltransferase_mitochondrial							↗	5.35E-02	1.6			
AT3G03910.1	glutamate dehydrogenase 3	↘	6.43E-03	1.9								GluDH	
XP_030507269.1	glutamate dehydrogenase 1	↗	3.15E-04	2.0								GluDH	
XP_030500358.1	glutamine synthetase nodule isozyme	↗	8.02E-04	2.3								GLN	
XP_030497088.1	spermidine synthase 1	↗	2.72E-02	1.6								SPDS	
XP_030507612.1	S-methyltetrahydropteroylglutamate--homocysteine methyltransferase 1-like									↗	3.90E-02	1.51	MS
XP_030486263.1	LOW QUALITY PROTEIN: ferredoxin--nitrite reductase_chloroplastic-like									↗	3.27E-02	2.2	NIR
Purine, pyrimidine, ribonucleotide and deoxyribonucleotide metabolism													
AT3G09820.1	adenosine kinase 1 chr3:3012122-3014624 FORWARD LENGTH=344									↘	4.36E-02	1.94	ADK
PROTEIN SYNTHESIS, PROCESSING, MODIFICATION													
Transcription													
XP_030497012.1	basic transcription factor 3	↘	2.19E-03	2.8								BTF3	
AT1G72730.1	DEAD(D/H)-box RNA helicase family protein	↘	1.13E-03	1.8									
XP_030503291.1	DEAD-box ATP-dependent RNA helicase 3_chloroplastic-like	↘	1.49E-04	1.7									
XP_030481652.1	histone H4	↗	3.91E-02	1.5								H4	
Protein synthesis (ribosomal proteins, translation, translational control, amino-acyl tRNA synthetases)													
XP_030493873.1	RNA-binding protein CP29B_chloroplastic	↘	3.06E-02	2.1								CP29B	
XP_030499617.1	glycine-rich RNA-binding protein-like	↘	2.37E-03	1.8									
XP_030510025.1	glycine--tRNA ligase_mitochondrial 1-like	↘	5.82E-03	1.5									
XP_030484196.1	S05 ribosomal protein L12-3_chloroplastic-like	↘	9.11E-05	2.0	↘	1.69E-04	1.7					L12	
XP_030502076.1	S05 ribosomal protein L11_chloroplastic	↘	1.09E-04	1.8	↘	2.97E-04	1.5					L11	
AT2G40010.1	Ribosomal protein L10 family protein	↘	8.85E-04	1.6								L10	
XP_030484291.1	LOW QUALITY PROTEIN: S05 ribosomal protein L9_chloroplastic	↘	1.02E-04	1.6								L9	
XP_030504362.1	S05 ribosomal protein L4_chloroplastic isoform X2	↘	4.03E-04	1.5								L4	
XP_030480118.1	S05 ribosomal protein L3_chloroplastic	↘	7.25E-05	1.5	↘	5.34E-05	1.5					L3	
XP_030491783.1	S05 ribosomal protein S17_chloroplastic				↘	1.82E-03	1.9					S17	
XP_030478586.1	S05 ribosomal protein S10_chloroplastic	↘	4.89E-03	1.6	↘	4.53E-04	1.8					S10	
YP_009143588.1	ribosomal protein S8 (chloroplast)				↘	7.45E-05	1.5					S8	

Accession	Soluble protein name	C-Cd		C-Zn		C-CSi		Cd-CdSi		Zn-ZnSi		Abr.
		Anova	MFC	Anova	MFC	Anova	MFC	Anova	MFC	Anova	MFC	
AT2G33800.1	Ribosomal protein S5 family protein	↘	9.73E-06	1.6								S5
XP_030483051.1	30S ribosomal protein 3_chloroplastic-like				↘	5.65E-04	1.6					
Protein folding and stabilization												
AT3G48870.1	ATCLPC ATHSP93-III_HSP93-III Clp ATPase	↘	1.41E-02	1.8								HSP93
AT5G56030.1	heat shock protein 81-2	↗	1.40E-04	2.7								HSP81
XP_030509817.1	heat shock cognate protein 80	↗	1.71E-03	1.7				↗	1.30E-02	1.7		HSP80
XP_030488797.1	LOW QUALITY PROTEIN: 20 kDa chaperonin_chloroplastic	↘	9.28E-05	1.6	↘	1.31E-03	1.6					
XP_030487791.1	protein disulfide-isomerase-like	↗	3.12E-05	1.5								PDIL
XP_030501851.1	luminal-binding protein 5 isoform X1	↗	1.96E-05	1.8	↗	2.77E-04	1.5					LBP5
AT1G55490.1	Symbols: CPN60B_LEN1 chaperonin 60 beta chr1:20715717-20718673 REVERSE LENGTH=600				↘	2.70E-04	1.5					
Proteases												
AT3G09790.1	ubiquitin 8 chr3:3004111-3006006 REVERSE LENGTH=631							↘	1.44E-02	1.6		UBQ8
XP_030485940.1	26S proteasome non-ATPase regulatory subunit 4 homolog	↗	1.84E-04	1.8	↗	1.36E-03	1.5					26SP
XP_030491129.1	kunitz trypsin inhibitor 5-like	↗	2.30E-06	4.1								KTI
XP_030481504.1	probable mitochondrial-processing peptidase subunit beta_mitochondrial isoform X2	↗	4.58E-04	1.5								
XP_030488931.1	LOW QUALITY PROTEIN: ATP-dependent Clp protease ATP-binding subunit ClpA homolog CD48_chloroplastic-like				↘	3.38E-02	1.6					ClpA
XP_030480662.1	ATP-dependent Clp protease proteolytic subunit 4_chloroplastic				↗	4.61E-03	1.6					Clp4
XP_030490013.1	cucumislin-like				↗	2.36E-05	1.9					Cucumislin
XP_030477762.1	aspartic proteinase A1-like				↗	1.38E-05	1.6					AP
TRANSPORT FACILITATION. TRANSPORT MECHANISM. MEMBRANE MODIFICATION												
XP_030488902.1	exportin-2-like	↗	5.23E-03	2.2								
XP_030510010.1	patatin-like protein 2 isoform X1	↗	4.50E-05	4.5								PLP2
XP_030481475.1	LOW QUALITY PROTEIN: mitochondrial outer membrane protein porin of 34 kDa-like	↗	1.01E-03	1.9								
XP_030489156.1	alpha-soluble NSF attachment protein 2	↗	9.79E-03	1.5								
XP_030507565.1	clathrin light chain 1	↗	2.58E-04	2.0								CLC1
XP_030509812.1	putative clathrin assembly protein At5g57200				↘	1.37E-02	1.5					
XP_030487862.1	LOW QUALITY PROTEIN: aquaporin PIP1-2-like				↗	7.61E-04	1.5					
XP_030506023.1	protein TIC110_chloroplastic				↘	9.97E-05	2.0					TIC
Ionic homeostasis												
XP_030490597.1	ferritin-3_chloroplastic-like	↘	3.10E-06	1.5								
XP_030496049.1	V-type proton ATPase catalytic subunit A	↗	2.79E-05	1.6								
XP_030486210.1	V-type proton ATPase subunit B 1				↘	2.42E-05	1.8					
XP_030483484.1	plasma membrane ATPase 4	↗	6.86E-05	2.3								
CELL DIVISION												
XP_030493617.1	cell division control protein 48 homolog D	↘	4.31E-03	1.6								
SIGNAL TRANSDUCTION AND METABOLISM REGULATION												
XP_030482663.1	1-aminocyclopropane-1-carboxylate oxidase	↗	2.40E-02	1.5								ACC oxidase

Accession	Soluble protein name	C-Cd		C-Zn		C-CSi		Cd-CdSi		Zn-ZnSi		Abr.	
		Anova	MFC	Anova	MFC	Anova	MFC	Anova	MFC	Anova	MFC		
XP_030502265.1	thiamine thiazole synthase_chloroplastic	↘	4.96E-02	2.4								THI	
AT1G78300.1	general regulatory factor 2							↗	1.17E-02	1.5			
XP_030510026.1	calcium-dependent protein kinase 2-like	↗	5.53E-06	5.8								CDPK2	
XP_030508471.1	allene oxide synthase 1_chloroplastic-like	↗	1.75E-02	1.5	↗	1.75E-04	1.5					AOS	
XP_030492117.1	guanosine nucleotide diphosphate dissociation inhibitor 1				↘	2.56E-03	1.5					GD11	
CELL RESCUE. DEFENSE													
XP_030489118.1	pathogenesis-related protein 1-like	↗	4.01E-05	10.9								PR1	
XP_030501451.1	pathogenesis-related protein R major form-like	↗	2.77E-04	6.3								PRR	
AT3G59100.1	glucan synthase-like 11	↘	1.42E-03	1.5								GSL11	
XP_030508841.1	glucan endo-1_3-beta-glucosidase_basic vacuolar isoform-like	↗	5.24E-04	2.7				↗	4.41E-02	1.6		BG	
XP_030494289.1	glucan endo-1_3-beta-glucosidase_basic isoform-like	↗	1.68E-02	2.0								BG	
XP_030494289.1	glucan endo-1_3-beta-glucosidase_basic isoform-like isoform X1	↗	2.27E-03	1.6								BG	
XP_030510675.1	callose synthase 1-like isoform X2				↘	7.57E-05	2.0					CALS	
XP_030492842.1	thaumatin-like protein 1b	↗	1.56E-03	6.2								TLP	
XP_030502231.1	thaumatin-like protein 1	↗	3.45E-06	2.2								TLP	
XP_030485657.1	endochitinase 2	↗	2.42E-04	4.7								ECH2	
XP_030485657.1	endochitinase 2	↗	6.86E-06	7.1								ECH2	
XP_030501453.1	protein P21-like	↗	2.74E-05	4.2								PRX	
XP_030479401.1	peroxidase 15-like	↗	3.14E-06	14.9								PRX15	
XP_030492321.1	peroxidase 12-like	↗	2.52E-05	3.7	↗	7.40E-03	1.5					PRX12	
XP_030510658.1	cationic peroxidase 2-like	↗	8.43E-03	1.5								PRX	
XP_030510658.1	cationic peroxidase 2-like	↗	1.11E-05	2.3	↗	1.20E-07	3.1			↘	5.09E-04	1.7	PRX2
XP_030496794.1	probable nucleoredoxin 1	↗	4.05E-04	1.8								Trx	
XP_030496794.1	probable nucleoredoxin 1	↗	2.80E-05	1.9	↗	1.67E-05	2.2					Trx	
XP_030507761.1	probable aldo-keto reductase 2	↗	2.68E-04	1.5								AKR	
XP_030489998.1	aldehyde dehydrogenase family 7 member A1	↗	8.80E-05	1.7								ALDH	
XP_030493646.1	aldehyde dehydrogenase family 2 member B4_mitochondrial-like	↗	1.43E-03	1.5								ALDH	
XP_030485469.1	peroxiredoxin-2B-like	↘	1.42E-02	1.5								PRN	
XP_030493857.1	peroxiredoxin-2E-2_chloroplastic				↘	1.08E-03	1.5					PRN	
AT5G28840.1	GDP-D-mannose 3'_5'-epimerase	↗	1.46E-03	1.7								GME	
XP_030491240.1	probable NAD(P)H dehydrogenase (quinone) FQR1-like 1	↗	6.81E-03	1.5									
XP_030481542.1	formate dehydrogenase_mitochondrial	↗	9.59E-03	1.6				↗	3.77E-02	1.5		FDH	
XP_030497100.1	probable mannitol dehydrogenase	↘	1.52E-02	1.7								MTD	
XP_030481127.1	macrophage migration inhibitory factor homolog isoform X1									↗	2.70E-02	1.63	MDL
XP_030501195.1	probable plastid-lipid-associated protein 3_chloroplastic				↗	8.18E-04	1.6						
OTHERS													
XP_030487929.1	S-norcochlorine synthase-like	↗	5.86E-05	3.7								NCS1	
XP_030478816.1	alpha-humulene synthase-like	↗	2.78E-03	3.1								α-HS	
XP_030491464.1	polyphenol oxidase_chloroplastic-like	↗	1.74E-04	2.0								PPO	
Phenylpropanoid pathway													
XP_030494389.1	phenylalanine ammonia-lyase-like							↘	2.48E-02	1.9		PAL	

Accession	Soluble protein name	C-Cd		C-Zn		C-CdSi		Cd-CdSi		Zn-ZnSi		Abr.
		Anova	MFC	Anova	MFC	Anova	MFC	Anova	MFC	Anova	MFC	
Lignan biosynthesis												
XP_030482060.1	secoisolaricresinol dehydrogenase-like	↗	3.48E-04	2.0								SDH
XP_030481758.1	secoisolaricresinol dehydrogenase-like							↗	1.28E-02	1.5		SDH
NO ASSIGNED FUNCTION												
XP_030496730.1	uncharacterized protein LOC115712571	↗	1.46E-03	1.6								
XP_030478572.1	uncharacterized protein LOC115695655					↘	4.57E-02	1.5				
XP_030500211.1	uncharacterized protein LOC115715691					↗	3.08E-02	1.5				
XP_030489475.1	uncharacterized protein LOC115706092 isoform X2								↗	4.23E-02	1.7	
XP_030505388.1	uncharacterized protein LOC115720376	↘	6.17E-04	1.7								
XP_030503597.1	uncharacterized protein LOC115718918	↘	3.96E-04	1.5								
XP_030507137.1	uncharacterized protein LOC115722147	↗	1.19E-05	2.1								
XP_030506176.1	uncharacterized protein LOC115721071				↘	4.49E-03	3.3					
XP_030487836.1	uncharacterized protein LOC115704770				↘	1.21E-04	1.6					
XP_030482857.1	uncharacterized protein LOC115699532				↘	1.07E-03	1.5					
AT1G78150.1	Symbols: unknown protein				↘	3.72E-03	1.5					

3.5. Microscopic determination of lignification and Cd deposition in leaves and roots

Confocal microscopy images (Figure 5.6) pointed out an increase of lignified areas in leaves of Cd treatment compared to control ones. Pictures obtained in ESRF showed that Cd is mostly localized in these lignified areas of Cd-treated plants (Figure 5.7). In CdSi treatments, Cd was also detected in leaf trichomes, while it was absent from trichomes in leaves of Cd treatment. In roots, confocal microscopy images (Figure 5.8) showed increased lignification of the stele in Cd treatment, and increased lignification of the exodermis in Zn treatment, compared to control ones.

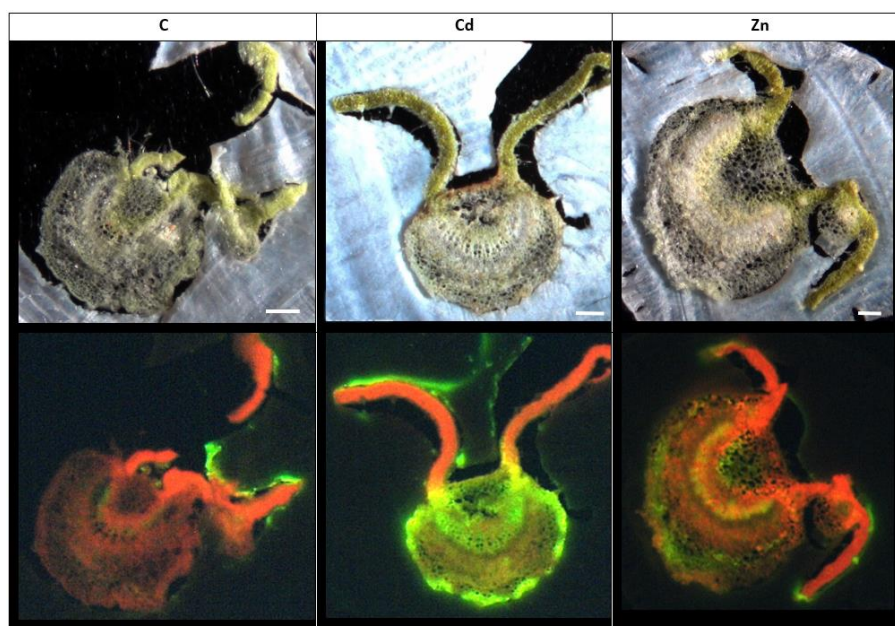


Figure 5.6: Confocal microscope observation of hemp leaf sections (60 μm) (Axioscope 2 MOT, 405 nm). Plants were exposed for one week to Cd (20 μM) or Zn (100 μM) (C: control plants not exposed to heavy metals). Fluorescence highlights lignified areas (yellow), and areas containing chlorophyll (orange-red color). Scale bar: 200 μm .

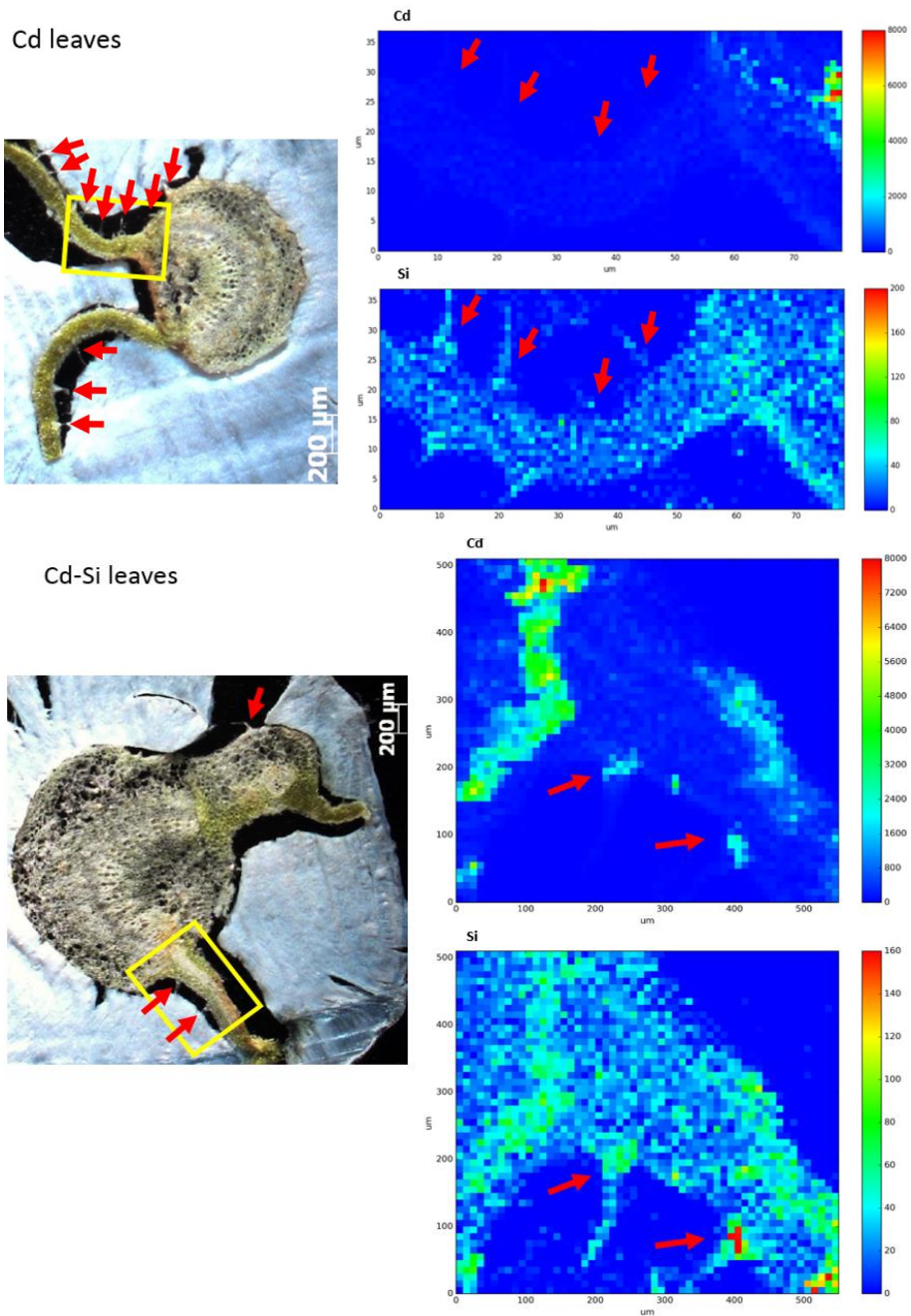


Figure 5.7: Synchrotron-ID21. Cd and Si distribution in hemp leaf sections ($60\ \mu\text{m}$) of Cd and CdSi exposed plants. Plants were exposed for one week to Cd ($20\ \mu\text{M}$) (C: control plants not exposed to heavy metals). Red arrows: trichomes.

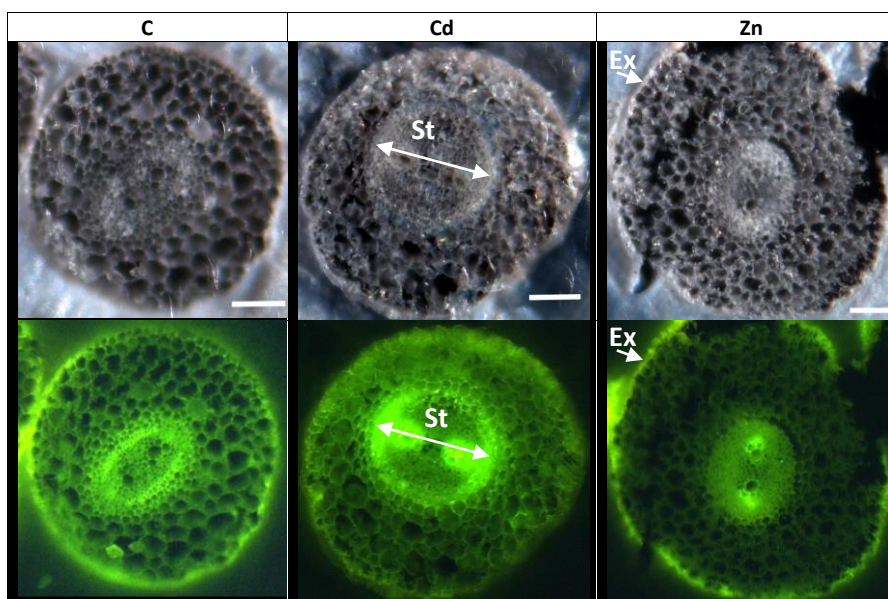


Figure 5.8: Confocal microscope observation of hemp root sections (60 μm) (Axioscope 2 MOT, 405 nm). Plants were exposed for one week to Cd (20 μM) or Zn (100 μM) (C: control plants not exposed to heavy metals). Fluorescence highlights lignified areas (yellow). Scale bar: 100 μm . Stele (St), exodermis (Ex).

4. Discussion

Zinc and cadmium are frequently simultaneously found in HM-contaminated soils (Feng et al., 2020). Those elements share numerous chemical properties and in the present study induce a comparable range of growth inhibition in *C. sativa*. However, we also demonstrated that Cd and Zn clearly acted on distinct cellular targets and this is valid for both gene expression and protein abundance.

Stress sensing and ROS management

Stress sensing constitutes the first step of plant response to deleterious environmental conditions. Proteins/genes involved in signal perception were found to be higher in abundance upon HM exposure. These include Ca^{++} signaling related proteins/genes in leaves of Cd treatment (calcium-dependent protein kinase, CDPK), and roots of Cd and Zn treatments (calcium-dependent lipid binding proteins *CALB*); and allene oxide synthase (AOS) in both HM metal treated plants. *CALB* proteins have been proposed to partake in intracellular signaling upon stress (de Silva et al., 2011) and many AOSs

generate precursors of the defense hormone jasmonate (Farmer and Goossens, 2019).

Ethylene has dual functions in plants since it acts as a major determinant of plant senescence but also as a key mediator of biotic and abiotic stress response (Müller & Munné-Bosch, 2015). *S*-adenosylmethionine (SAM) is the precursor of ethylene, and MS catalyzes the conversion of homocysteine to methionine, which is further converted into SAM by *S*-adenosylmethionine synthetase (Hossain et al., 2012). The increased abundance of ethylene biosynthesis-related proteins (MS and 1-aminocyclopropane-1-carboxylate oxidase) has been observed in plants exposed to Cd but not in response to Zn (Table 5.1). In contrast, we observed a similar increased expression of *ERF1* in the leaves of plants exposed to Cd or Zn. *ERF1* is involved in both ethylene and jasmonic acid signaling pathways (Müller and Munné-Bosch, 2015). Furthermore Müller & Munné-Bosch (2015) suggest that *ERFs* might regulate ROS-responsive gene expression, thereby conferring stress tolerance. Several cell rescue proteins that accumulated in Cd and Zn-exposed plants were indeed found to be oxidoreductases, indicating detoxification-mediated tolerance in the plant. Peroxidases and a probable nucleoredoxin (Trx), involved in regulation of antioxidant enzymes (Kneeshaw et al., 2017) were more abundant in stressed plants compared to control ones, as well as leaves' transcript abundances of *SODs* (*FSD*) and *APXs*.

Cadmium obviously had a stronger impact than Zn on proteins involved in cell rescue and defense (Figure 5.5). However, Zn exposure had a stronger impact on *APX*, *SOD* and *CAT* gene expression than Cd: in roots, it decreased gene expression of *APX3* and *APX6*, while *APX5*, *MSD1* and *CAT3* were more expressed. In leaves of Zn-exposed plants *APX1*, *APX3*, *APX5*, *MSD1* and *FSD1* were more expressed compared to controls. Cd exposure only affected root expression of *APX5* (increased) and expression of *FSD1* in the leaves (increased). To cope with ROS-induced reactive aldehydes, plants under Cd stress also exhibited increased leaf content of aldo-keto reductase (AKR) and aldehyde dehydrogenase (ALDH) (Table 5.1), catalyzing reactions leading to less toxic alcohols and carboxylic acids, respectively (Sengupta et al., 2015; Vemanna et al., 2017; Ahmad et al., 2019), while this type of strategy was not involved in the response to Zn. Cd-exposed plants also increased the abundance of a patatin-like protein 2 (PLP2) with phospholipase activity in plants exposed to Cd. The patatin-related phospholipase A (pPLA) might be involved in the removal of oxidatively

modified fatty acids from membranes in membrane remodeling and repair (Yang et al., 2012).

Cell wall retention and intracellular compartmentation

Retention of HM in the cell wall constitutes an efficient strategy to limit their accumulation in the symplasm and lignification may contribute to make the CW less permeable for toxic ions (Pejic et al., 2009; Ye et al., 2012; Fernández et al., 2014; Vukcevic et al., 2014; Nawaz et al., 2019; Gutsch et al., 2019a). In this study, hemp plants subjected to an excess of Zn or Cd showed increased expression of *PAL* and *CAD* involved in lignin biosynthesis in the leaves (Figure 5.3). Lignin monomers are synthesized through the phenylpropanoid pathway, of which phenylalanine ammonia lyase (*PAL*) catalyzes the initial step (Gutsch et al., 2019a). However, as far as protein abundances are concerned, only Cd had a detectable impact on enzymes involved in lignin synthesis (caffeic acid 3-*O*-methyltransferase, *COMT*; caffeoyl-CoA *O*-methyltransferase, *CCOMT*; lignin-forming anionic peroxidase; GroES-like zinc-binding alcohol dehydrogenase family protein, *CADI*). These results correlate with the rise of lignified areas observed on confocal microscopy images (Figure 5.6 and 5.8) and which clearly indicate lignification zones in Cd-treated roots and leaves, but not in Zn-exposed plants.

Once inside the symplasm, regulation of plasmodesmatal aperture through callose synthesis and deposition may limit the transfer of metal ions from one cell to another (Singh et al., 2016; O'Leary et al., 2018). While a decrease in plasmodesmata permeability may be considered as an attempt to ion sequestration in some cells, the opposite reaction consisting to increase permeability should be regarded as an attempt of dilution at the whole tissue level. Interestingly, alterations in the abundance of callose-associated enzymes (glucan synthase-like 11, *GSL11*; glucan endo-1,3-beta-glucosidase, *BG*; callose synthase, *CALS*) was observed under HM exposure and we suspect Cd and Zn to decrease callose content and increase plasmodesmatal permeability by acting on two distinct targets. Glucan endo-1,3- β -D-glucosidases or β -1,3-glucanase (*BG*) are often referred to as *PR* because of their ability to hydrolyze β -1,3-glucan chains of fungal cell walls (Hong et al., 2002) but the one identified in the present case is lysosomal and so not involved in the degradation of fungi cell wall. In our work, isoforms corresponding to these enzymes were strongly increased in response to Cd stress but not in response to Zn. Conversely, Zn reduced callose synthase, thus

suggesting that Zn reduces the synthesis of callose while Cd increased its degradation.

Chelating metals by forming phytochelatin (PCs) or metallothioneins (MTs) metal complex at the intra- and intercellular level are part of the mechanisms used by plants to counteract HM toxicity (Alloway, 2012; Emamverdian et al., 2015). At the root level, the gene coding for MT2 was not induced in response to Cd, and it was even slightly repressed by Zn, suggesting that this metallothionein did not afford key protection in roots of HM-treated plants. It has to be noticed, however, that *MT2* was induced at the leaf level in plants exposed to Zn in the presence and in the absence of Si. Conversely, we detected a strong accumulation of PC in Cd-treated roots (Figure 5.2c), which could be related to an induction of *PCS2* expression in Cd-treated roots, while *PCS1-1* expression remained unmodified comparatively to control plants. As far as leaves are concerned, an increase in *PCS1* was observed in Zn-treated plants which could explain PC accumulation; however, Cd-treated plants still accumulated PC at the leaf level and for this treatment, only *PCS1-1* was overexpressed comparatively to control. The fact that PC may translocate from the root to the shoot may to some extent modify the relationship between PC synthase gene expression at a given organ and PC concentration recorded in this precise organ.

The complex formed between metal ion and chelatant is transported to the vacuoles where the ion will be released and fixed to organic acids (Cobbett, 2000; Jost, 2018). Other transporters may also directly transfer free HM to the vacuole. This study also revealed the accumulation of cation/proton exchanger in Cd-treated plants (V-type proton ATPase catalytic subunit A and plasma membrane ATPase 4), while the opposite trend was observed under Zn exposure (decreased abundance of V-type proton ATPase subunit B1). Induction of vacuolar pumps (V-ATPase and V-PPase), together with a set of tonoplast transporters and primary ATP-dependent pumps allow vacuolar compartmentalization of HM (Sharma et al., 2016). Besides direct transport over the tonoplast membrane, vesicular transport may play a role in vacuolar sequestration or in efflux from the cell (Leitenmaier and Küpper, 2011). In Cd treatment, plants exhibited higher levels of two proteins involved in vesicular trafficking: CLC1 and alpha-soluble NSF attachment protein 2. Clathrin is composed of two heavy chain subunits (CHC1 and CHC2) and two light chain subunits (CLC1 and CLC2). The subunits assemble a cage-like scaffold around developing vesicles to support vesicle formation. Once the vesicle is fully formed, this scaffolding dissociates and detached from the initial

membrane by dynamin, allowing the vesicle to traffic to its destination (reviewed by Larson et al., 2017). At destination, vesicle fusion to membranes is mediated by Soluble NSF Attachment Protein Receptor (SNARE) complexes that assemble from subunits present at both the plasma membrane and the surface of the docking vesicles (Larson et al., 2017): NSF is associated with membranes by binding soluble NSF attachment protein (Lee et al., 2009). Stimulation of vesicular trafficking under Cd exposure may be linked to HM sequestration or efflux from the cell, but could also reflect a strategy to regulate the internalization of critical plasma membrane proteins involved in hormone signaling, stress responses, and nutrient uptake (Wan and Zhang, 2012; Wang et al., 2013). Surprisingly Zn had the opposite effect by lowering the abundance of a putative clathrin assembly protein.

Photosynthetic processes, TCA cycle and carbohydrate metabolism

A recent study demonstrated that Cd induced a decrease in all photosynthetic pigments leading to a decrease in net photosynthesis (Luyckx et al., 2021b). Zinc is also known to have a deleterious effect on leaf photosynthesis (Lefèvre et al., 2014). The present study, once again, demonstrated that Cd and Zn acted on distinct photosynthetic-related proteins since only 3 recorded proteins were affected by both Cd and Zn.

Cadmium reduced the light-absorbing efficiency of photosystems (PS) by decreasing the abundance of enzymes involved in steps 4, 7 and 13 (hydroxymethylbilane synthase, CPOX and POR respectively) of chlorophyll synthesis (Beale, 2005); and by decreasing the abundance of OEE complex (the donor side of PSII) and PSI reaction center-related proteins. Zn also affected the abundance of photosynthetic pigments by decreasing abundance of enzymes involved in steps 10 (magnesium-protoporphyrin IX monomethyl ester cyclase) and 13, but no impact on PS reaction center was detected. Moreover, in Zn-treated plants, the increased expression of two chlorophyllases (*CLH1* and *CLH2*) was observed while Cd had a contrasting effect on *CLH* expression. Both Cd and Zn altered the accumulation of protein involved in electron transport (Fd and Pc) with a specific impact of Zn on Cytb6f complex and Pq abundances. It can be assumed that stress impairment of the light reactions will decrease ATP and NADPH production, necessary for the CO₂ reduction process. Cd and Zn also limited the abundance of proteins involved in the Calvin cycle. Cadmium negatively affected the abundance of protein involved in carbon fixation (RCA, *rbcL*), G3PDH abundance and ribulose 1,5-bisphosphate (RuBP) regeneration (PPE and

CBBY), while Zn mostly affected enzymes involved in the fixation of CO₂ (RCA, PGK) and CP12-1. In leaves, the increased expression of Calvin cycle-linked transcripts (*RCA*, *RBCS*) was observed under HM stress, probably to counteract the negative effect of HM on RuBisCO activity, Zn having a higher impact than Cd on *RBCS* expression

The toxic effects of Cd and Zn can be linked to the ability of HM to bind –SH groups of pigment biosynthetic enzymes, their ability of superseding the functionality of essential metal ions and indirectly to ROS-induced oxidation and degradation of proteins (Bashir et al., 2015). HM toxicity also entails impairment of protein biosynthesis: Cd or Zn exposure had a negative impact on transcription and protein biosynthesis, and most of the proteins detected had a chloroplastic localisation (Cd: 62%; Zn: 100%). Zn exposure also decreased the abundance of a voltage-dependent cation-selective channel (TIC). The translocon at the inner envelope membrane of chloroplasts (TIC) plays a central role in plastid biogenesis by coordinating the sorting of nucleus-encoded preproteins across the inner membrane and coordinating the interactions of preproteins with the processing and folding machineries of the stroma (Inaba et al., 2005). Downregulation of TIC upon Zn stress probably reduced the accumulation of a variety of plastid proteins. Taken together, these results suggest a reduction of the overall photosynthetic capacity of hemp plants exposed to HM. When photosynthesis is not well operating, plants need to upregulate metabolic pathways such as glycolysis and tricarboxylic acid (TCA) cycle in order to maintain the normal growth and development and sustain defenses strategies (Ghnaya et al., 2009; Ashraf and Harris, 2013; Ben Hossain and Komatsu, 2013; Smirnova et al., 2017). In our study, Cd-treated plants exhibited a higher abundance of TCA cycle proteins. ATP synthases were also found to be of higher abundance under stress conditions. Up-regulation of glycolysis and the TCA cycle might help the stressed plant to produce more reducing power to compensate the high-energy demand of Cd-challenged cell (Hossain and Komatsu, 2013).

Many defense strategies also depend on N metabolism. Accumulation of soluble N compounds (such as glycinebetaine, spermidine, and proline) in plants facing adverse environmental constraints may help regulate osmotic potential in cells, and protect and stabilize the membranes, thus improving HM stress tolerance (Hussain et al., 2020). Our work demonstrates that proline accumulated in leaves but not in roots of HM-exposed plants. Besides a role in regulation of cell osmotic potential, proline can act as metal chelator, antioxidative defense molecule, and signaling molecule during stress (Kaur

and Asthir, 2015; Siddique et al., 2018). The last step of proline synthesis from pyrroline-5-carboxylate is catalyzed by P5CR, and the corresponding gene was upregulated in HM-treated plants. *P5CS1* was specifically up-regulated in roots of Zn-exposed plants, but the resulting increase in proline content remained insignificant considering the high level of variability.

HM exposure can severely hamper nitrogen metabolism by reducing NO_3^- uptake (alteration of membrane permeability) and altering the activity of various N assimilatory enzymes by binding to the vital -SH groups (Ashan et al., 2009; Hussain et al., 2020). It is therefore crucial for plants to be able to maintain N assimilation under stress. Glutamine synthetase (GLN)/glutamate synthase (GOGAT) is the main pathway of NH_4^+ assimilation into nontoxic glutamine and glutamate under normal conditions (Ashan et al., 2009; Hussain et al., 2020). GLN plays also a role in the re-assimilation of ammonium released during photorespiration. Photorespiratory N cycling may be 10 times higher than primary N assimilation (Kaminski et al., 2015). When the endogenous NH_4^+ concentration increases, i.e. in response to Cd toxicity, an alternative pathway, controlled by glutamate dehydrogenase (GluDH), contributes in lowering this internal NH_4^+ concentration (Hussain et al., 2020). GluDH is also involved in the recycling of carbon molecules by supplying 2-oxoglutarate to tissues becoming carbon limited (Dubois et al., 2003). The higher abundance of GLN and an isoform of GluDH under Cd exposure (Table 5.1) may indicate a rise of photorespiration and the ability of hemp plants to elevate nitrogen and carbon use efficiency to deal with stress conditions. Additionally, Cd was able to trigger activation of the GABA shunt through increased abundance of glutamate decarboxylase while Zn had no impact (Table 5.1). Synthesis of GABA could contribute to the dissipation of excess of energy and release CO_2 allowing the Calvin cycle to function. According to Carillo (2018), GABA shunt can supply NADH to the mitochondrial transport chain under conditions in which TCA cycle is impaired, but in Cd-treated plants numerous proteins involved in TCA cycle increased suggesting that this pathway may adequately react to Cd toxicity.

It has to be mentioned that an increase in gene expression did not necessarily lead to a recorded increase in the corresponding protein abundances. This was the case for enzymes involved in phytochelatin synthesis (see above) and for enzymes involved in proline synthesis, whose abundance did not increase. Discrepancies between transcriptomic and proteomic data have already been discussed by Kubala et al. (2015). In the

present study, it was demonstrated that Cd stress, and to a lesser extent Zn toxicity, decreased the abundance of a wide range of proteins regulating protein synthesis, while increasing numerous proteases' abundance and this could add an additional level of complexity which hamper correlation between gene expression and abundance of corresponding gene products.

Impact of Si supply on gene expression and protein abundance in hemp facing or not HM stress

Si is considered as beneficial to plants under stress condition (Ma et al., 2001). In a previous study we showed that hemp is able to absorb Si from nutrient solution and translocate this element to the aerial parts of the plant (Guerriero et al., 2019; Luyckx et al., 2021a; 2021b). In the present study, we demonstrate that Zn-treated plants exposed to Si accumulated higher amounts of Si in their roots than plants exposed to Si alone. Similarly, Cd-treated plants exposed to Si exhibited higher concentration of Si in their leaves than plants exposed to Si alone. Moreover, Si induced Cd accumulation in leaf trichomes (Fig. 5.7). According to Ma et al. (2015) and to Kim et al. (2017), such a behavior suggests that increasing Si content may be regarded as an attempt to improve stress tolerance. An increased accumulation of the well-known osmoprotectant proline in the leaves of CdSi-treated plants comparatively to Cd-exposed ones supports this hypothesis.

Si accumulation in plants is well described in rice and ortholog genes to rice Si channels and efflux transporters have been found in hemp (Guerriero et al., 2019). In the present study, *C. sativa* genes corresponding to the rice efflux transporter *OsLsi2* on the one hand and *NIP2-1* and *NIP2-2* corresponding to the rice silicon channel *OsLsi* mediating silicic acid passage (Guerriero et al., 2019), were analyzed. At the root level, *CsaLsi2-1* expression was increased by HM treatment. *CsaLsi2-3* was increased in Cd-treated plants but was surprisingly reduced in Zn-treated plants as it was the case for *CsaLsi2-2*. It is tempting to speculate that *CsaLsi2-1* mainly contributes to Si accumulation in roots of Zn-treated plants, although it has to be explained how this could occur considering the *NIP2-1* and *NIP2-2* expressions were also decreased by Zn treatments. As far as leaves are concerned, *CsaLsi2-1* was also increased by HM exposure. When supplemented with Si, control plants and plants exposed to Cd or Zn globally exhibited a decreased gene expression of Si channels and efflux transporter. Plants were exposed to Si a week before HM exposure. We may assume that

when a protective concentration of Si is reached in plants, increased transcription of Si channels/efflux transporters is no longer needed.

The idea of a protecting effect of Si is supported by the number of proteins (27) affected by Si exposure comparatively to plants grown in the absence of Si. Moreover, out of the 27 proteins with an altered abundance after Si exposure: 7 were modified in control plants and 20 were found in plants exposed to HM treatments. It is noteworthy that among these 20 proteins, 12 were not modified by HM treatment in the absence of Si, suggesting that Si does not only counteract the impact of heavy metals but also confer a specific physiological status to stressed plants. This is supported by the fact that none of these proteins were modified by Si in the absence of heavy metals. Moreover, Cd and Zn had quite distinct impact on hemp proteome (see above) and it is therefore not unexpected that no common protein appeared to be modified by both CdSi and ZnSi treatments.

In control plants Si supplementation stimulated the Calvin cycle by increasing the expression of *FBPase* and *RCA* but it also increases the abundance of glycerate dehydrogenase (GlyDH), a protein involved in photorespiration. It has already been suggested that Si-enhanced stress tolerance is linked to the accumulation of photorespiratory enzymes (Frew et al., 2018). Even if plants were not exposed to HM, basic metabolic processes can impart stress on plants (Frew et al., 2018). Supplementing plants with Si also tended to stimulate proline synthesis in leaves (*P5CS1*, *P5CS2*) and roots (*P5CR*) and plant oxidative response capacity (increased expression of *CAT*, *APX* and *SOD (FSD)*). This underlines the potential importance of Si for basic metabolic processes and not only for plant response to external stresses (Frew et al., 2018).

In plants exposed to HM, energy metabolism is of crucial importance to sustain cost of metabolic adaptations the plant needs to set up. A beneficial effect of Si on energy metabolism was observed under Cd exposure only: light-dependent reactions (Fd), light-independent reactions (*FBPase* and *RCA* expression, *rbcS* abundance), glycolysis (G3PDH) and TCA cycle (IDH) were stimulated in plants of CdSi treatment comparatively to plants of Cd treatment in the absence of Si.

As discussed earlier, N metabolism represents another important component of defense strategies. Si supply was associated with an increased NiR (N assimilation) abundance under Zn exposure, and increased expression of *P5CS2* in roots of Cd- treated plants. Proline, as well as PC and MT are

associated with metal chelation. While the expression of MT and PCS isoforms tended to increase in Cd-treated plants supplemented with Si, the opposite trend occurred in plants of ZnSi treatment compare to plants of Zn treatment. It has already been suggested that retention of HM in the cell wall is probably the first strategy in response to metal entry in plants and that lignin-bound silica in cell-walls improves metal binding and reduces the transfer of metal ions (Ye et al., 2012; Fernández et al., 2014; Nawaz et al., 2019). Once inside the cells, non-protein thiols and organic acids might also participate in HM tolerance (Fernández et al., 2014). We can assume that Si-mediated compartmentation is sufficient to lower excess ions concentration of Zn and do not require another sequestration strategy given that, unlike Cd, Zn is an essential element for plants and was also shown to be preferentially bound to O/N ligands rather than to PC (Lefèvre et al., 2014). HM exposure is usually followed by ROS accumulation. Si application was shown to improve the oxidative response capacity in leaves and roots of plants exposed to Cd (*APX6*, *CAT3*) but decreased root expression of APXs (*APX1,3,5*) and SOD (*MSD1*), and PRX2 abundance in leaves of plants exposed to Zn.

Si had an impact on signal transduction: supplementing plants with Si induced a decreased root expression of CALBs in plants of Cd treatment and *Gibbrec* in plants of Zn treatment, but increased expression of CALBs in roots of Zn treatment. Surprisingly Si decreased expression of *ERF1* in leaves of Zn-treated plants.

5. Conclusion

Zinc and cadmium are frequently simultaneously found in HM-contaminated soils. HM exposure had a negative impact on photosynthesis and protein synthesis and induced a comparable range of reactions in *C. sativa*: stimulation of antioxidants, metal ions' chelation and compartmentation, and up-regulation of glycolysis and TCA cycle. However, we demonstrated that Cd and Zn clearly acted on distinct cellular targets and this is valid for both gene expression and protein abundance.

To devise agricultural strategies aimed at improving crop yield, the effect of silicon (Si) on plants' stress tolerance was considered. In the present study, we demonstrate that HM-treated plants exposed to Si accumulated higher amounts of Si than controls. Si was shown to counteract the impact of heavy metals but also to have confer a specific physiological status to stressed plants, with quite distinct impact on hemp proteome of CdSi and ZnSi

treatments. The main beneficial effects of Si application involved HM sequestration, improved oxidative response, and stimulation of energy metabolism

Funding

This work was financed by ADEME (Agence de la Transition écologique; Convention MisChar n°1672C0044) and by FNRS (Fonds National pour la Recherche Scientifique, convention n°T.0147.21).

Acknowledgments

The authors are grateful to Pr. C. Hachez and Mrs M.C. Eloy for assistance in using confocal microscope, to Dr P. Morsomme and Mr. H. Degand for their valuable help in proteomic analysis and to Mr. B. Capelle, Mrs M.E. Renard and B. Vanpee for their technical assistance during plant culture and samples analysis.

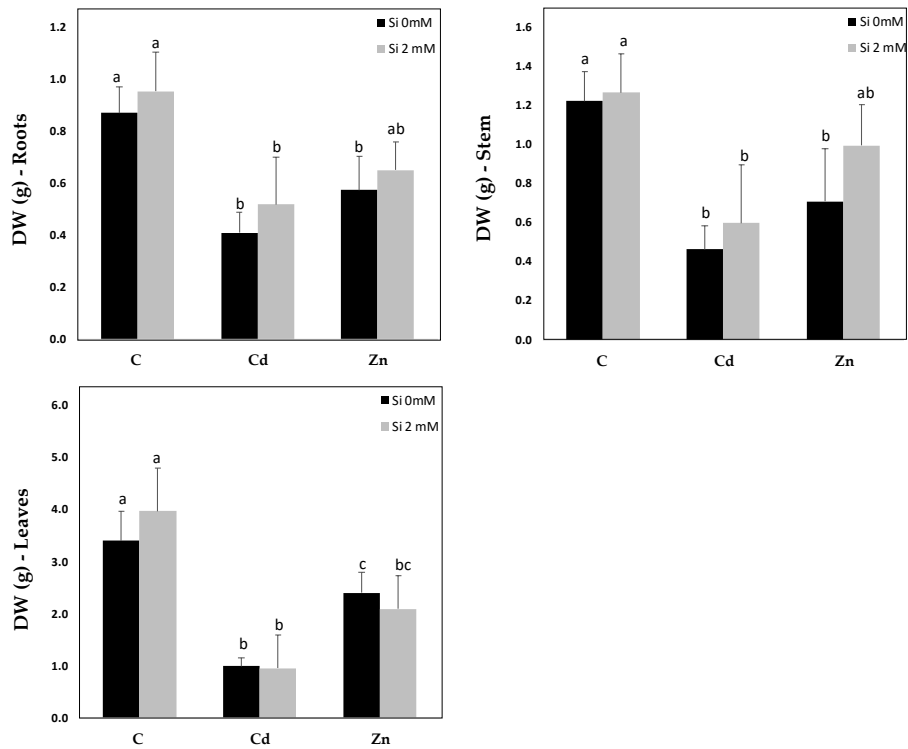


Figure S5.1 : Dry weight (g) of roots, stems and leaves of *Cannabis sativa* (cv. Santhica 27). Plants were exposed for one week to Cd (20 μM) or Zn (100 μM) in the presence or absence of Si (2mM) (C: control plants not exposed to heavy metals). The different letters indicate that the values are significantly different from each other ($P < 0.05$; Tukey's HSD all-pairwise comparisons).

Chapter 5: Highlights and Perspectives

The behaviors of roots and leaves are of paramount importance for whole stressed plants' survival. Roots are the first organs in direct contact with HM and regulate pollutant absorption and transfer to the shoot parts, while leaves provide energy for plant growth and control ion translocation through regulation of transpiration. In this Chapter, the effect of 20 μ M Cd, 100 μ M Zn and 2 mM Si on plants' stress tolerance was considered. Targeted gene expression and proteomic analysis were performed on leaves and roots after one week of treatment.

We demonstrated that (Figure 5.9):

- Cd and Zn had a negative impact on photosynthesis and protein synthesis.
- HM exposure induced a comparable range of reactions in *C. sativa*: stimulation of antioxidants, metal ions' chelation and compartmentation, and up-regulation of glycolysis and TCA cycle.
- Cd and Zn clearly acted on distinct cellular targets and this is valid for both gene expression and protein abundance.
- HM-treated plants exposed to Si:
 - accumulated higher amounts of Si than controls.
 - Si was shown to counteract the impact of heavy metals.
 - Si had quite distinct impact on hemp proteome and the expression of numerous genes of CdSi and ZnSi treatments.

Besides the roots and leaves, the stems constitute the site of fibres' differentiation. *C. sativa* L. is a promising species for fibre production on moderately HM-contaminated substrates. As we intend to combine phytomanagement with non-food production, data regarding the precise impact of element such as Cd and Zn on genes involved in fibres development *in planta* are of crucial importance. In Chapter 6, we therefore analysed the impact of Cd and Zn, in the presence or absence of Si, on the expression of genes regulating fibre development fibre and characterized the proteome of hypocotyls. This innovative approach should help us to more deeply understand the relationship between plant molecular adaptation and subsequent plant production.

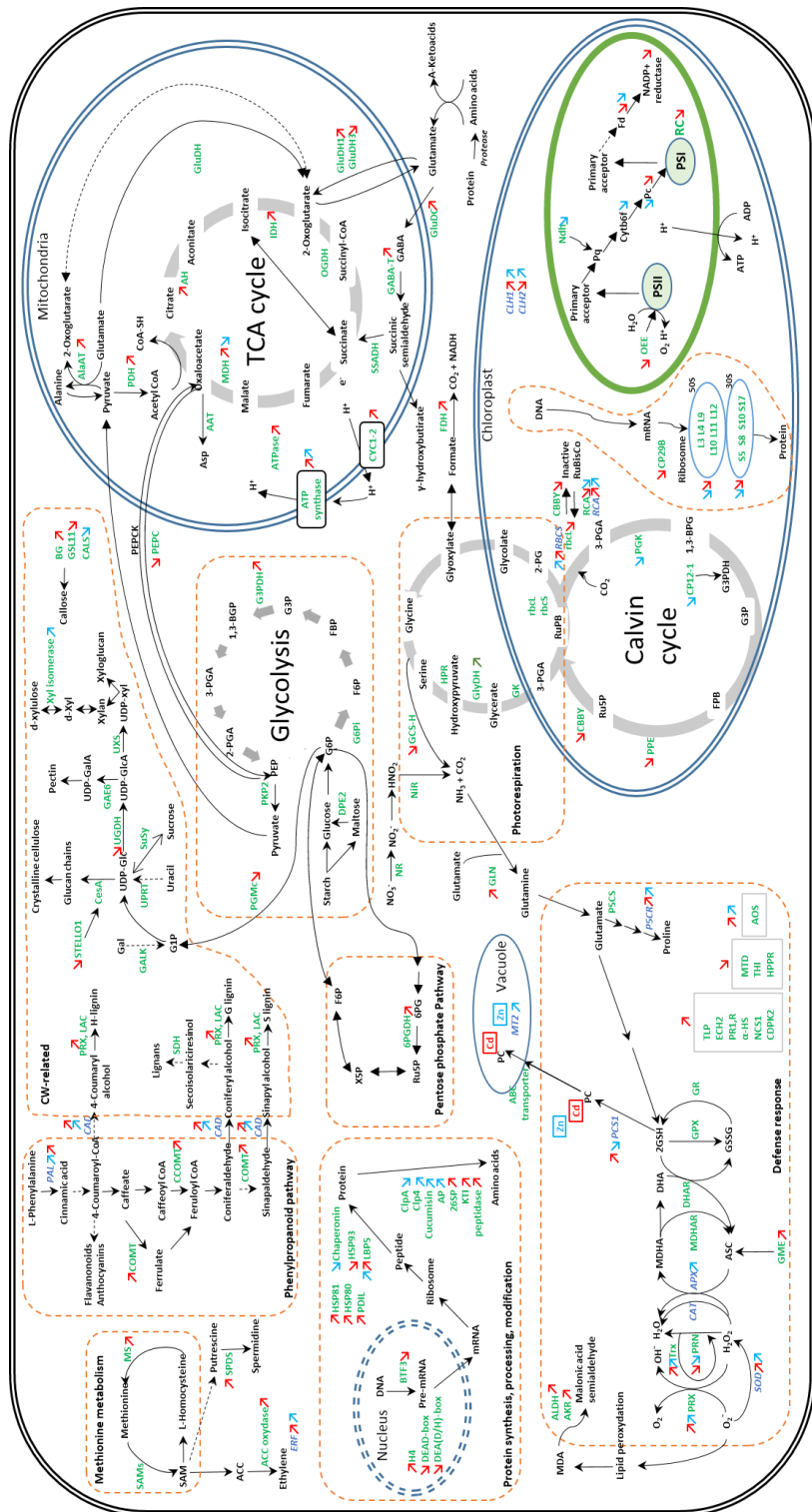


Figure 5.9: Summary of the results obtained in Chapter 5. Red arrows indicate a significant increase/decrease of gene expression/protein abundance following Cd exposure, while significant effects of Zn exposure are illustrated by blue arrow.

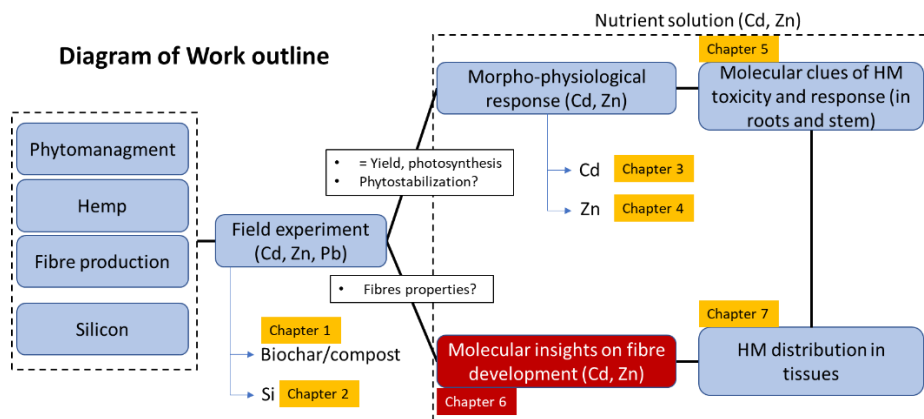
Chapter 6

Proteins and cell wall-related gene expression in young stems of hemp in relation to Cd, Zn and/or Si exposure

Published article: Marie Luyckx, Jean-François Hausman, Arnaud Isenborghs, Gea Guerriero, Stanley Lutts. Impact of cadmium and zinc on proteins and cell wall-related gene expression in young stems of hemp (*Cannabis sativa* L.) and influence of exogenous silicon. 2021. *Environmental and Experimental Botany* 183:104363

Author's contributions

ML, GG and SL designed methodology; ML performed the whole experiment, treated and analyzed the data; AI contributed to mineral analysis and confocal microscopy; JFH and SL supervised the whole research process; ML and SL wrote the original draft; All authors reviewed the manuscript.



Abstract

The study aims to determine the impact of Cd (20 μ M) and Zn (100 μ M) in the presence or absence of Si (2 mM) on plant development and fibre differentiation in young stem of hemp (*Cannabis sativa* L.). Gene expression and proteome involved in fibre development were analyzed. Both elements reduced the diameter of primary bast fibres. Cadmium negatively affected cellulose and lignin biosynthesis and decreased substitution of xylan in fibres, while Zn had an opposite impact on cellulose metabolism. Only a minor proportion of proteins were affected by both Cd and Zn, suggesting that the two heavy metals have a quite different impact on protein regulation in *C. sativa*. Silicon had a specific impact on some proteins observed in CdSi treatment comparatively to plants exposed to Cd in the absence of Si: 55 % of those proteins (10 among 18) were specifically regulated by this treatment and remained unaffected by Cd or Si applied alone. Six proteins were significantly regulated in ZnSi-exposed plants comparatively to Zn-treated ones and none of them was specifically regulated by Si in the absence of Zn. Diameter of bast fibre increased in response to Si in Cd-treated plants. This confirms that the presence of protecting Si confers a specific physiological status in relation to cell wall differentiation to heavy metal-treated plants.

1. Introduction

Human activities related to urbanization, industrialization and agriculture practices have resulted in the accumulation of heavy metals in soils and water in numerous areas of the world. Management of these contaminated sites constitutes a major environmental challenge since heavy metals may affect human health and environment stability. Conventional treatments for heavy metals removal from the soils include surface capping, soil flushing, air sparging, electrokinetic extraction, or vitrification, while chemical precipitation, coagulation, flocculation, and membrane filtration may be used to clean up contaminated water (Vareda et al., 2019). However, the use of plants to remove or stabilize pollutants has also been proposed as a promising alternative to those expensive remediation methods, but requires the availability of heavy metal-resistant species (Ali et al., 2013; Jaskulak et al., 2020).

Toxic effects of heavy metals on plants include alteration of mineral nutrition, photosynthesis modification in relation to reduced chlorophyll and

carotenoid content, induction of oxidative stress or alteration of the plant water and hormonal status resulting in growth reduction and thus biomass production (Chandra and Kang 2016; Berni et al., 2018; Luyckx et al., 2019). Besides former industrial and mining areas which are frequently polluted by very high concentrations of toxic elements, agricultural soils may also be impacted by moderate pollution as a result of atmospheric contamination from surrounding areas and use of low-quality fertilisers or pesticides. Since food crops cannot be cultivated in those areas as they represent a major risk for human health, non-food alternatives need to be proposed to producers (Pogrzeba et al., 2019; Feng et al., 2020).

Cannabis sativa L. is an annual high yielding industrial crop grown for its fibres and seeds (Pejic et al., 2009; Morin-Crini et al., 2019). As a multipurpose crop, *C. sativa* is receiving an increasing attention for the production of a wide range of bioactive molecules, but also as a source of feed in relation to the presence of oil, flour and protein and as a bioenergy crop (Andre et al., 2016; García-Tejero et al., 2019). Hemp can be used as potential crop for cleaning the soil from heavy metals (Citterio et al., 2003; Angelova et al., 2004; Candilo et al., 2004; Meers et al., 2005; Kumar et al., 2017) but could also be recommended as a good candidate for plant production on low contaminated substrates (Arru et al., 2004; Pietrini et al., 2019; Hussain et al., 2019a, 2019b). This implies that the non-edible parts of the plant need to be harvested and that hemp culture on marginal contaminated soil should focus on fibre cultivars (Linger et al., 2002), even if the seeds were recently reported to have a rather low metal content when plants were grown on slightly polluted substrates (Mihoc et al., 2012). Short hemp fibres, obtained as a waste from textile industry, can also be used as biosorbent for the removal of metal ions from polluted water (Vukcevic et al., 2014). Coating of harvested fibres with maltodextrin-1,2,3, 4-butanetetracarboxylic polymer was reported to provide ion-exchange properties improving heavy metal retention by a hemp-based felt (Loiacono et al., 2017). Besides such post-harvest treatments, heavy metals are also suspected to influence the pre-harvest development of hemp fibres, but data regarding the precise impact of element such as Cd and Zn on genes involved in this development in planta remain scant.

The stem of *Cannabis sativa* L. differentiates two types of fibres: (i) primary and secondary bast fibres associated with the conductive elements of phloem and bundles held together by pectins and lignin, and (ii) woody core fibres, called hurds or shivs, located in the xylem (Angelova et al., 2004; Guerriero et al., 2013; Behr, 2018; Morin-Crini et al., 2019). The hemp stem

contains approximately 20–40 % of bast fibres and 60–80 % of hurds (Stevulova et al., 2014). The bast fibres initially elongate through intrusive growth, then cease elongation and start to thicken by secondary cell wall (SCW) deposition (Guerriero et al., 2017c; Behr, 2018). Plant fibre primary cell wall (PCW) consists mainly of cellulose, hemicelluloses and pectin (Pejic et al., 2009). They have the ability to bind heavy metal compounds (Vukcevic et al., 2014): metal ions indeed adsorb mainly to carboxylic (primarily present in hemicelluloses and pectin) and to some extent to hydroxylic (cellulose, hemicelluloses, and pectin) groups (Pejic et al., 2009; Hu et al., 2010; Vukcevic et al., 2014).

Secondary xylem, primary and secondary bast fibres undergo SCW deposition after the beginning of secondary growth (Behr, 2018). The composition of SCW is not similar for xylem- and phloem-located fibres. Xylem fibres differentiate a xylan-type SCW, while in the phloem fibres, SCW is of gelatinous (G-layer) type (Gorshkova et al., 2012). The CW of xylan-type fibres are lignified, contain predominantly xylan as hemicellulose constituent and show a typical layered structure (S1–S3) because of the different orientation of the cellulose microfibrils (Neutelings, 2011). The SCW of gelatinous fibres is also deposited in three layers, S1 and S2 compositions being similar to xylan-type wall while the G-layer has a very different organization: the major part of the G-layer is characterized by a high abundance of crystalline cellulose embedded in a rhamnogalacturonan-I (RG-I) matrix and a low content of xylan and lignin (Guerriero et al., 2013, 2017a; Behr, 2018; Chernova et al., 2018). The transition from bast fibre elongation via intrusive growth to SCW deposition occurs at a specific area called the “snap point” (SP) (Gorshkova et al., 2003). The formation of SCW in hemp phloem fibres begins with the deposition of the Gn-layer (“gelatinous-new”) (Chernova et al., 2018). During further CW development, the Gn-layer is transformed to a “solid” G-layer: enzymatic digestion of the pectic matrix leads to the compaction of cellulose microfibrils and final organization of the G-layer (Chernova et al., 2018). It was also recently reported that in the young hemp hypocotyl, the G-layer has a loose structure (Gf) and that it gets compacted at later stages of development (Behr et al., 2019).

Guerriero et al. (2017c, d) and Behr et al. (2018) have highlighted key genes coding for proteins involved in hemp fibre development, from bast fibre early growth stage (protodermal factor, PDF1), to SCW deposition (cellulose synthases *CESA4*, *CESA7*, *CESA8*), fasciclin-like arabinogalactan protein (*FLAs*), class III peroxidases; methyltransferase (*MET1*), S-

adenosylmethionine synthetase (*SAMS*), including genes controlling the transition from elongation to thickening (acid phosphatase, AT1G04040). These molecular players are good candidates to evaluate the impact of heavy metal toxicity on plant fibre development. Besides transcriptomics, a proteomic analysis may also provide a useful set of information, but most of those analysis performed on *C. sativa* focused on cannabinoid synthesis rather than fibre CW formation (Aiello et al., 2016; Behr et al., 2018; Vincent et al., 2019; Jenkins and Orsburn, 2020). As far as exposure to heavy metal stress is concerned, data are only available for roots exposed to copper excess (Bona et al., 2007).

Any sustainable strategy helping the plant to cope with heavy metal toxicity could be usefully integrated in a phytomanagement scheme and this is especially the case for Si application (Wu et al., 2013; Adrees et al., 2015; Imtiaz et al., 2016; Etesami and Jeong, 2018; Bhat et al., 2019). Si is not considered essential for plant growth and development. However, increasing evidence in the literature show that this metalloid is beneficial to plants, especially under stress conditions (see Luyckx et al., 2017a for review). In hemp, the positive effects of Si on biomass production may be explained, among others, by an action on phytohormone balance regulating important stages of bast fibre development (Luyckx et al., 2017b). Si was recently shown to mitigate the impact of salt stress on hemp leaves (Berni et al., 2020). Guerriero et al. (2019) identified in hemp two NOD26-like intrinsic proteins exhibiting typical features reported to be associated with Si transport and revealed the presence of Si in isolated trichomes from the leaves, but also in the distal CW of bast fibres.

Silica hydrophobic coating is frequently used during processing of harvested fibres to reduce their water absorption (Jiang et al., 2018) or as a fire retardant (Branda et al., 2016). According to Hussain et al. (2019b), silica matrix used for composite with hemp shive may assume multifunctional purposes which suggest that Si may, to some extent, directly interact with hemp fibres. However, the impact of Si on hemp fibre during their development process remains poorly documented, especially in the case of heavy metal-exposed plants.

The present work was therefore undertaken in order to determine the impact of Cd and Zn in the presence or absence of Si on plant development and fibre differentiation in relation to heavy metal accumulation in young stem of *C. sativa*. The expression of genes regulating fibre development was analyzed and the proteome of hypocotyls was characterized.

2. Material and Methods

2.1. Plant material and growing conditions

Seeds of a monoecious hemp fibre variety (*Cannabis sativa* cv. Santhica 27) were sown in loam substrate in greenhouse conditions. After one week, the obtained seedlings were transferred to nutrient Hoagland solution (described in Chapter 3, p. 141) in 25 L tanks. For each tank, 10 seedlings were adapted to plugged holes in a polystyrene plate floating at the top of the solution. Tanks (24) were placed in a phytotron under fully controlled environmental conditions (permanent temperature of 24 ± 1 °C with a mean light intensity of $230 \mu\text{moles m}^{-2}\text{s}^{-1}$ provided by Phillips lamps (Philips Lighting S.A., Brussels, Belgium) (HPI-T 400 W), with a photoperiod of 16 h under a relative humidity of 65 %).

After one week, half of the tanks received Si in the form of H_2SiO_3 to a final concentration of 2 mM Si. Metasilicic acid was obtained from a pentahydrate sodium metasilicate ($\text{Na}_2\text{SiO}_3 \times 5 \text{H}_2\text{O}$) which was passed through an H^+ ion exchanger resin IR 20 Amberlite type according to Dufey et al. (2014). Tanks were randomly arranged in the phytotron and nutrient solution was permanently aerated by SuperFish Air Flow 4 pump. After an additional week of acclimatization, heavy metals were applied in the form of CdCl_2 (final concentration of 20 μM) and ZnCl_2 (100 μM) as previously stated (Luyckx et al., 2017b). The pH of the solution was maintained at 5.5. Solubility of added heavy metals was confirmed by the Visual MINTEQ09 software. Six treatments were thus defined, considering the presence of heavy metals and the concomitant presence or absence of Si and will be designed as C (control: no heavy metals and no Si), CSi, Cd, CdSi, Zn and ZnSi (4 tanks per treatment). Plants were harvested after one week of treatment and roots were thoroughly rinsed in deionized water: 4 plants per tank were selected to measure stem length and diameter, number of leaves, root length, fresh and dry weight (obtained after 72 h of incubation in an oven at 70 °C) and heavy metal concentration in roots, leaves and stems. The remaining plants from the same tank were pooled: roots, leaves and stems were separated. Hypocotyl parts of the stem were separated from epicotyls, frozen in liquid nitrogen and then stored at - 80 °C until subsequent transcriptomic and proteomic analysis. Segments of stem in the internode containing the SP were rapidly excised for confocal microscope observation.

2.2. Mineral concentration

The protocols used for Cd, Zn and Si quantification are described in Chapter 3 (p. 142-143).

2.3. Gene expression analysis

Total RNA was extracted from hypocotyls according to Guerriero et al. (2017c) and Mangeot-Peter et al. (2016) using the RNeasy Plant Mini Kit (Qiagen) treated on-column with DNase I. The RNA concentration and quality were measured for each sample by using a Nanodrop ND-1000 (Thermo Scientific) and a 2100 Bioanalyzer (Agilent Life Sciences), respectively. The RNA integrity number (RIN) of all samples was higher than 7, and the ratios A260/280 and A260/230 were between 1.7 and 2.4. The extracted RNA was retrotranscribed into cDNA using the SuperScript II reverse transcriptase (Invitrogen) and random primers, according to the manufacturer's instructions. The synthesized cDNA was diluted to 2 ng/μL and used for the RT-qPCR analysis in 384-well plates. An automated liquid handling robot (epMotion 5073, Eppendorf) was used to prepare the 384-well plates. To check the specificity of the amplified products, a melt curve analysis was performed. The relative gene expression was calculated with qBasePLUS (version 2.5, Biogazelle) by using the reference genes (*eTIF4E*, *TIP41*, *F-box* and *RAN*, Mangeot-Peter et al., 2016). Statistics (ANOVA2) were performed using R (version 3.3.1).

The target genes were chosen on the basis of preliminary results (Guerriero et al., 2017c, 2017d) and belong to genes regulating the lignification process [methyltransferase (*MET1*), S-adenosylmethionine synthase (*SAMS*), class-III peroxidases (*PRX49*, *PRX 52*, *PRX 72*), genes coding for SCW cellulose synthases (*CesA4*, *CesA7*, *CesA8*) and fasciclin-like arabinogalactan protein (*FLA3*, *FLA11*, *FLA13*, *FLA19*).

The corresponding primers were designed using Primer3Plus (<http://www.bioinformatics.nl/cgi-bin/primer3plus/primer3plus.cgi/>) and verified with the OligoAnalyzer 3.1 tool (Integrated DNA technologies, <http://eu.idtdna.com/calc/analyzer>). Primer efficiencies were checked via qPCR using 6 serial dilutions of cDNA (10, 2, 0.4, 0.08, 0.016, 0.0032 ng/μL). For each considered gene, selected primers are listed in Table S6.1.

2.4. Proteomic analysis

The protocol used for proteomic analysis is detailed in Chapter 5 (p. 191-193).

2.5. Confocal microscope observation

Segments of stem tissue in the internode containing the SP were rapidly excised from fresh plants with a scalpel and dipped into tissue freezing media (O.C.T., Tissue Tek, Jung etc.), and into propane cooled by liquid nitrogen. The plant pieces were next sectioned at 60 µm thickness with a Leica CM3050 cryotome (Leica), placed in Al holders and transferred to an Alpha 2–4 Christ freeze dryer (- 50 °C, 0.04 mbar, 3 days). Freeze-dried cross-sections were photographed using a digital camera (AxioCam) mounted on a Zeiss Axioscope 2 fluorescence microscope (wavelength: 405 nm).

2.6. Immunohistochemistry

Hemp stems sections of 5 mm in the internode containing the SP were fixed in FAA (90 mL ethanol 70 %/5 mL glacial acetic acid/5 mL formaldehyde 35 %) for 24 h at room temperature, dehydrated in ethanol series (70 %–80 %–100 %) and ethanol:butanol series (2/3:1/ 3–1/3:2/3 – butanol 100 %), impregnated in paraffin 12 h at 37 °C and 24 h at 60 °C, and finally included. The plant pieces were next sectioned at 10 µm thickness with a microtome (Leica), and used for immunohistochemistry (IHC). Image acquisition was performed with a confocal microscope LSM 710 (Zeiss).

The protocol used for immunohistochemistry is described by Behr et al. (2016): LM10 (xylan, Plant Probes) antibody was diluted 10-fold in milk protein (MP)/PBS (5 % w/v). Sections were then incubated for 1.5 h, rinsed three times in PBS and incubated for 1.5 h with the anti-rat IgG coupled to FITC (Sigma) diluted 100-fold in MP/PBS. Before observation, three washings with PBS were performed. CBM3a (crystalline cellulose, Plant Probes) was diluted to 10 µg/mL in MP/PBS, incubated in mouse anti-His monoclonal antibody (1 % in MP/PBS, Sigma) and finally incubated in 50-fold diluted anti-mouse IgG coupled to FITC (Sigma). Each incubation lasted for 1.5 h. Between each step, three washes with PBS were performed. The slides were observed with the following settings: excitation at 488 nm, filter HFT 493/564 and emission recorded with LP 505. The microscope settings were kept rigorously constant between the different observations for a given

epitope. Negative controls where either the primary or secondary antibody was omitted resulted in a very weak and negligible signal.

Images were imported into ImageJ to get quantitative data and were calibrated with the “Set Scale” command. Fluorescence intensity in the different stem tissues was measured using the “Freehand selections” command the, and the “Straight line” was used to measure both the diameter and the CW thickness of bast fibres (primary and secondary bast fibres). Three plants per treatment were analyzed and 6–10 measurements were made for each one.

2.7. Statistical analysis

Four independent biological replicates and three technical replicates were analyzed for each condition. Normality of the data was verified using Shapiro-Wilk tests and the data were transformed when required. Homogeneity of the data was verified using Levene’s tests. ANOVA 2 were performed at a significant level of p-value <0.05 using R (version 3.3.1) considering the type of heavy metal treatment, and the Si application as main factors. Means were compared using Tukey’s HSD all-pairwise comparisons at 5 % level as a post-hoc test.

For proteomic analysis, non-conflicting method was used as relative quantification method. To identify statistically significant differentially expressed proteins, combined criteria of a minimum of three or greater unique peptides, a two-fold change ratio or greater and a p-value <0.05 in the Student’s t-tests were adopted.

3. Results

3.1. Impact of Cd and Zn on plant physiological parameters

Phenotypes of plant cultivated in the different conditions are illustrated in Fig. S6.1. In the absence of heavy metals, Si had no impact on root and stem length, stem diameter and total leaf number (Table 6.1). In contrast, both Cd and Zn in the absence of H₂SiO₃ significantly reduced root length, stem diameter and total leaf number while only Cd had a significant impact on stem length.

Table 6.1: Root length, stem length and diameter, and total leaf number of *C. sativa* (cv. Santhica 27) exposed for one week to Cd (20 μ M) or Zn (100 μ M), in the presence or in the absence of 2 mM H₂SiO₃. Data are means \pm standard errors ($n = 4$). Values with different letters are significantly different ($P < 0.05$; Tukey's HSD all-pairwise comparisons).

Treatment	Root length (cm)	Stem length (cm)	Stem diameter (mm)	Total leaf number
C	42.60 \pm 2.21 <i>b</i>	27.12 \pm 5.91 <i>b</i>	7.13 \pm 0.77 <i>c</i>	10.20 \pm 0.45 <i>b</i>
CSi	40.92 \pm 8.49 <i>b</i>	29.78 \pm 7.49 <i>b</i>	6.68 \pm 0.50 <i>bc</i>	10.20 \pm 0.45 <i>b</i>
Cd	31.22 \pm 3.99 <i>a</i>	12.66 \pm 2.64 <i>a</i>	4.58 \pm 0.48 <i>a</i>	7.80 \pm 0.84 <i>a</i>
CdSi	36.18 \pm 3.26 <i>ab</i>	14.90 \pm 4.79 <i>a</i>	5.16 \pm 0.52 <i>ab</i>	8.40 \pm 0.55 <i>a</i>
Zn	30.10 \pm 5.96 <i>a</i>	20.20 \pm 4.37 <i>ab</i>	4.65 \pm 1.05 <i>a</i>	9.40 \pm 1.14 <i>a</i>
ZnSi	34.20 \pm 1.09 <i>ab</i>	21.78 \pm 2.68 <i>ab</i>	4.97 \pm 1.20 <i>a</i>	9.20 \pm 0.84 <i>a</i>

The application of 2 mM H₂SiO₃ tended to slightly mitigate the deleterious impact of heavy metal stress on root length and stem diameter, although no significant difference was recorded for the mean values. Heavy metals also significantly reduced root, stem and leaf dry weight (DW) (Table 6.2), Cd being more toxic than Zn for root and leaves. Heavy metals reduced the water content in stems, only. Si tended to slightly increase the mean DW of roots in Cd-treated plants and of both stem and leaves in Zn-treated ones, although the difference was not significant considering the high variability occurring among replicates.

Table 6.2: Roots, stems and leaves dry weight and water content of *C. sativa* (cv. Santhica 27) exposed for one week to Cd (20 μ M) or Zn (100 μ M), in the presence or in the absence of 2 mM H₂SiO₃. Data are means \pm standard errors ($n = 4$). Values with different letters are significantly different ($P < 0.05$; Tukey's HSD all-pairwise comparisons).

Treatment	Dry weight (g)			Water content (%)		
	Roots	Stems	Leaves	Roots	Stems	Leaves
C	8.80 \pm 1.04 <i>c</i>	7.90 \pm 0.30 <i>b</i>	18.07 \pm 1.62 <i>b</i>	93 \pm 1.3 <i>a</i>	92 \pm 1.3 <i>b</i>	86 \pm 2.1 <i>a</i>
CSi	7.93 \pm 0.50 <i>c</i>	6.77 \pm 1.18 <i>b</i>	14.73 \pm 3.85 <i>b</i>	93 \pm 1.1 <i>a</i>	92 \pm 0.4 <i>b</i>	82 \pm 1.2 <i>a</i>
Cd	3.07 \pm 1.51 <i>a</i>	2.23 \pm 1.02 <i>a</i>	3.33 \pm 0.71 <i>a</i>	93 \pm 1.1 <i>a</i>	89 \pm 1.6 <i>a</i>	81 \pm 5.5 <i>a</i>
CdSi	3.87 \pm 0.76 <i>ab</i>	2.10 \pm 0.62 <i>a</i>	3.60 \pm 0.26 <i>a</i>	92 \pm 3.0 <i>a</i>	82 \pm 1.6 <i>a</i>	86 \pm 13.1 <i>a</i>
Zn	3.97 \pm 1.27 <i>b</i>	2.87 \pm 1.19 <i>a</i>	6.20 \pm 2.51 <i>c</i>	92 \pm 1.1 <i>a</i>	77 \pm 7.9 <i>a</i>	79 \pm 5.2 <i>a</i>
ZnSi	3.77 \pm 1.47 <i>ab</i>	3.67 \pm 1.53 <i>a</i>	8.07 \pm 3.71 <i>ac</i>	91 \pm 1.1 <i>a</i>	86 \pm 2.1 <i>a</i>	78 \pm 1.9 <i>a</i>

3.2. Mineral content

Cd (Table 6.3) was detected in Cd- and CdSi-treated plants only (detection limit: 0.013 mg/L). The root Cd concentration was significantly higher than

in leaves (p -values < 0.01) while the stem showed an intermediate value. H_2SiO_3 application slightly decreased Cd content in roots and stems. Zn excess strongly increased root, stem and leaf Zn concentration (Table 6.3), with higher values in roots than in stems and leaves (p -value < 0.01). Exposure to H_2SiO_3 increased root and leaf Si concentration in the absence and in the presence of heavy metals but the recorded increase in Si was not significant in the stem (Table 6.3). Si concentration was higher in the roots and leaves of ZnSi treated plants than in those of CdSi-treated ones while an opposite trend was recorded for the stem.

Table 6.3: Cadmium, zinc and silicon concentration (in $mg\ kg^{-1}$ DW) in roots, stems and leaves of *C. sativa* (cv Santhica 27) exposed for one week to Cd (20 μM) or Zn (100 μM), in the presence or in the absence of 2 mM H_2SiO_3 . Data are means \pm standard errors ($n = 4$). For each organ and element, values with different letters are significantly different at $P < 0.05$ according to the Tukey's HSD all-pairwise comparisons (nd = not detected).

		Treatment					
		C	CSi	Cd	CdSi	Zn	ZnSi
Cd ($mg\ kg^{-1}$ DW)	Roots	nd	nd	2441 \pm 151 a	1910 \pm 759 a	nd	nd
	Stems	nd	nd	1246 \pm 439 a	1036 \pm 42 a	nd	nd
	Leaves	nd	nd	689 \pm 49 a	753 \pm 155 a	nd	nd
Zn ($mg\ kg^{-1}$ DW)	Roots	259 \pm 25 a	255 \pm 143 a	388 \pm 102 a	292 \pm 100 a	7518 \pm 1422 b	5458 \pm 2511 b
	Stems	52 \pm 14 a	38 \pm 2 a	111 \pm 25 a	103 \pm 13 a	1169 \pm 225 b	1393 \pm 438 b
	Leaves	59 \pm 5 a	63 \pm 6 a	42 \pm 13 a	40 \pm 8 a	1185 \pm 275 b	994 \pm 221 b
Si ($mg\ kg^{-1}$ DW)	Roots	220 \pm 36 a	2030 \pm 240 b	236 \pm 63 a	1598 \pm 147 b	225 \pm 49 a	6854 \pm 578 c
	Stems	98 \pm 27 ab	160 \pm 4 b	nd	83 \pm 31 a	48 \pm 3 b	129 \pm 19 ab
	Leaves	47 \pm 3 c	3297 \pm 1223 b	49 \pm 2 c	5691 \pm 2098 a	63 \pm 23 c	2210 \pm 287 b

3.3. Gene expression in the stem

The hierarchical clustering of the expression profiles (represented as a heatmap; Figure 6.1) for the various treatments was performed using a Euclidean distance matrix in complete linkage. The clustering resulted in a separation between control plants (C, CSi), Cd exposed plants (Cd, CdSi) and Zn exposed plants (Zn, ZnSi). In plants that were not exposed to heavy metals, exposure to Si stimulated the expression of *CesA4*, *CesA8*, *FLA11*, and *MET1*, the difference being significant for *CesA4*, only.

In Cd-stressed plants, several transcripts related to SCW formation were less abundant as compared to the control, notably *CesA7*,

CesA8, *FLA3*, *FLA11*, *FLA13*, and *FLA19* involved in cellulose deposition (Behr et al., 2016; Guerriero et al., 2017d). In the same plant samples, some genes controlling several biochemical pathways, including the regulation of lignification, displayed a different expression pattern: *MET1* and *SAMS* (generation of methyl donors) were down-regulated by Cd, whereas *PRX49*, *PRX52* and *PRX72* (genes controlling lignification; Herrero et al. (2013) and previously shown to be upregulated in hypocotyls aged 15 and 20 days; Behr (2018) were more expressed in Cd-treated plants than in controls. No significant effect of Si application on the expression of genes in Cd-stressed plants was detected but, once again, trends may be observed: *PDF1*, a gene shown to be upregulated in the young hemp internode (Guerriero et al., 2017c) and maybe involved in fibre initiation, *CesA4*, *FLA13*, *FLA19*, *FLA3*, *MET1*, *PRX49*, *PRX52* seem to be more expressed in CdSi-treated plants than in Cd exposed ones, while a gene encoding an acid phosphatase influencing CW-related processes in bast fibres during the transition from elongation to thickening (Guerriero et al., 2017c), *SAMS* and *PRX72* showed an inverse trend.

In Zn-treated plants, *CesA4*, *FLA19*, *PRX49*, *PRX52* and the gene coding for the acid phosphatase were upregulated compared to control plants. A higher expression of *PDF1*, *CesA8* and *CesA7* was observed in Zn-treated plants when exposed to Si comparatively to Zn-treated plants cultivated in the absence of Si. The abundance of transcripts coding for the acid phosphatase, *PDF1*, *FLA19*, *CESA7* and *PRX49* were higher in ZnSi-treated plants than in those exposed to Si in the absence of heavy metals (CSi).

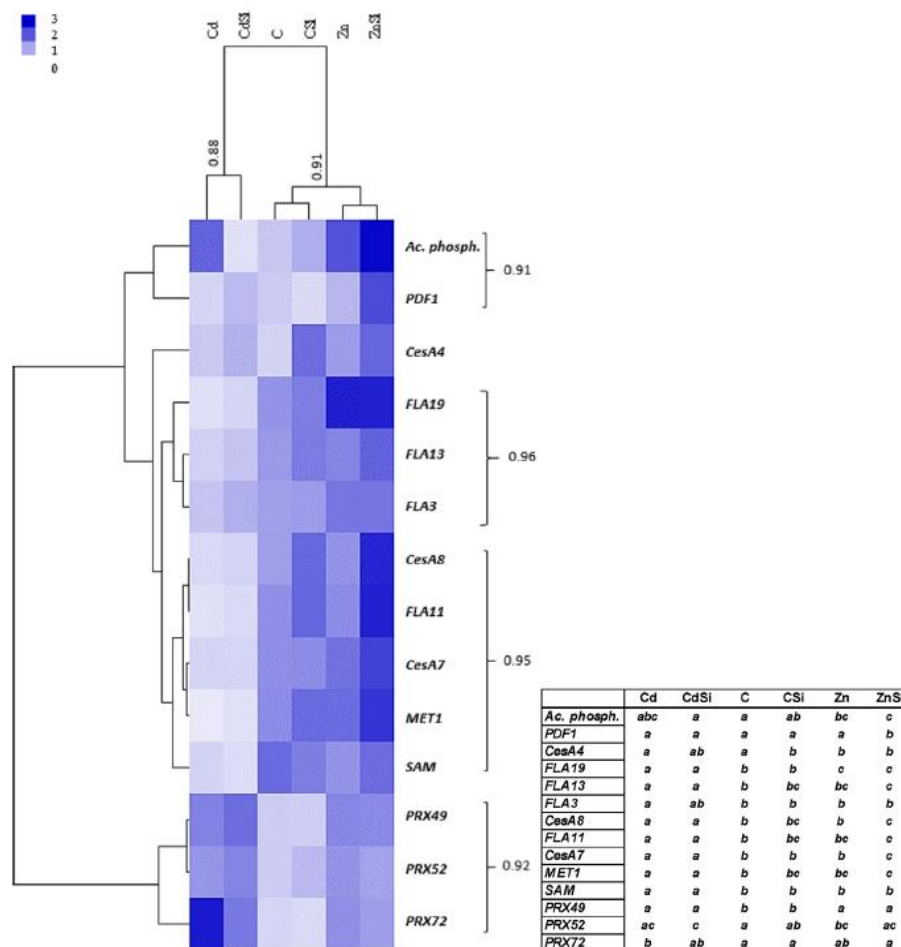


Figure 6.1: Heatmap hierarchical clustering showing the expression of genes assessed by RT-qPCR in hypocotyls of hemp plants. Plants were exposed for one week to Cd (20 μ M) or Zn (100 μ M) in the presence or absence of Si (2 mM) (C: control plants not exposed to heavy metals). Values represent Normalized Relative Quantities (NRQs). For each group, the Pearson coefficient is provided. The table represents statistical analyses of the heatmap hierarchical clustering. The different letters indicate that the values are significantly different from each other ($P < 0.05$; Tukey's HSD all-pairwise comparisons).

3.4. Proteomics

The data relative to the impact of the treatments on protein regulation are provided in Table 6.4 which simultaneously considers soluble and membrane-bound protein fractions.

Hemp response to Cd resulted in a significant increase in the abundance of 2 proteins involved in tricarboxylic acid (TCA) pathway, one controlling callose remodelling (glucan endo-1_3-beta-glucosidase, BG), one protein regulating lignin biosynthesis (cytochrome P450 CYP73A100-like, CYP73A100), a protein regulating proline biosynthesis (Δ -1-pyrroline-5-carboxylate synthase-like, P5CS), a protein responsible for glutamate metabolism (glutamate dehydrogenase, GluDH), a protein involved in sulphate assimilation (sulfite reductase, SIR), 3 protein involved in protein synthesis and 3 involved in proteolysis, 3 proteins controlling transport, 4 involved in ionic homeostasis, a protein managing cell organization, 4 proteins involved in signal transduction and metabolism regulation and 5 in cell rescue. Conversely, Cd treatment negatively impacted the abundance of a protein involved in photosynthesis (ribulose-1,5-bisphosphate carboxylase/oxygenase, RuBisCO small subunit), 2 proteins regulating carbohydrate metabolism, one in TCA cycle, one protein involved in fermentation, a protein controlling γ -aminobutyrate (GABA) shunt, proteins controlling cellulose biosynthesis (sucrose synthase, SuSy; cellulose synthase; CESA7, CESA8), lignin biosynthesis (caffeic acid 3-O-methyltransferase, COMT; laccase 4, LAC4; CYP736A12), lignin monomer methylation (methylenetetrahydrofolate reductase, MTHFR) and pectin synthesis (UDP-glucuronate 4-epimerase 6, GAE6), 2 proteins involved in amino acid metabolism, 6 proteins regulating protein synthesis and one involved in protein folding, 2 proteins involved in transport, 4 proteins managing cellular organization, 6 proteins involved in signal transduction and metabolism regulation and a protein controlling cell rescue (class V chitinase-like, CH5) (Table 6.4). Cd had no direct impact on proteins regulating cell division but it nevertheless affected the cytoskeleton through a decrease in tubulin alpha-1 chain. As shown in Fig. 6.2, the most important category of proteins up-regulated by Cd was related to cell rescue and defence and includes protein dealing with oxidative stress such as catalase and peroxidases. Conversely, most down-regulated proteins were related to SCW synthesis, as it was the case for cellulose synthase CESA7 and CESA8 or for caffeic acid 3-O-methyltransferase which catalyses the multi-step methylation reactions of hydroxylated monomeric lignin precursor.

Table 6.4 (next pages): List of proteins with significant quantitative changes of hemp stems in response to Cd, Zn and Si. Seedlings were exposed for one week either to Cd 20 μ M, Zn 100 μ M or Si 2 mM and proteins were extracted from hypocotyls. MFC: Max Fold Change. Proteins which abundance increased were indicated in green while those which abundance decreased are indicated in brown.

Accession	Soluble protein name	C-Cd		C-Zn		C-Cd		Cd-Cd		Zn-Zn	
		Anova	MFC	Anova	MFC	Anova	MFC	Anova	MFC	Anova	MFC
Energy											
Photosynthesis/CO2 assimilation											
XP_030478704.1; XP_030510713.1	ribulose biphosphate carboxylase small chain clone S12-like	↘	8.44E-03	4.1	↘	4.62E-02	2.2				rbcS
XP_030501759.1; XP_030499118.1	ribulose biphosphate carboxylase small chain_ chloroplastic-like							↘	1.32E-02	2.3	rbcS
XP_030508755.1	dihydropyridyl dehydrogenase_ mitochondrial-like					↘	2.39E-02	2.0			
Carbohydrate metabolism, glycolysis and gluconeogenesis											
KAA8710862.1;KP W80790.1	phosphoenolpyruvate carboxylase [Pseudomonas cannabina]	↘	6.32E-03	2.6							PEPC
XP_030484584.1	phosphoenolpyruvate carboxylase_ housekeeping isozyme- like			↗	1.45E-03	2.0					PEPC
XP_030496786.1	phosphoenolpyruvate carboxylase (ATP)-like			↗	1.11E-03	3.9					PEPCK
XP_030506683.1; XP_030506682.1	pyruvate kinase_ cytosolic isozyme							↘	2.70E-03	1.6	
XP_030508612.1; XP_030502051.1; XP_030502053.1; XP_030502054.1; XP_030502055.1	galactokinase-like			↗	1.22E-02	3.1					GALK
XP_030484068.1	probable alpha- mannosidase At5g13980							↘	7.53E-03	2.7	
XP_030500791.1; XP_030500475.1	plastidial pyruvate kinase 2	↘	3.35E-03	4.7							PKP2
XP_030484115.1; XP_030484116.1	4-alpha- glucanotransferase DPE2			↗	5.44E-03	2.4					
XP_030501231.1; XP_030484128.1	glucose-6-phosphate isomerase_ cytosolic					↗	5.51E-03	2.6			G6PI
Tricarboxylic acid pathway											
XP_030482299.1	dihydropyridylsine- residue acetyltransferase component 4 of pyruvate dehydrogenase complex_ chloroplastic	↘	4.83E-02	2.0							PDH
XP_030496961.1	aconitate hydratase 1	↗	3.20E-02	2.2							AH1
XP_030488149.1	NADP-dependent malic enzyme	↗	2.61E-02	2.0							MDH
Fermentation											
XP_030479792.1	pyruvate decarboxylase 2	↘	4.84E-03	2.1							PDC2
γ-aminobutyrate (GABA) shunt											
XP_030506646.1	glutamate decarboxylase 4-like	↘	6.19E-03	3.0							GluDC4
XP_030488867.1; XP_030488649.1	LOW QUALITY PROTEIN: succinate-semialdehyde dehydrogenase_ mitochondrial-like							↗	2.53E-03	2.2	SSADH
Cell wall related											
XP_030500584.1	monocopper oxidase-like protein SKU5			↗	1.96E-03	4.4					SKU5
XP_030491523.1; XP_030488795.1; XP_030488796.1; XP_030491522.1	UDP-glucuronic acid decarboxylase 6-like			↗	2.31E-03	3.3					UXS
XP_030505523.1	fascilin-like arabinogalactan protein 12	↘	1.40E-02	2.0	↘	8.51E-03	2.3				FLA12
XP_030506444.1; XP_030503116.1	fascilin-like arabinogalactan protein 12			↗	2.31E-03	3.6					FLA12
XP_030478954.1	glycerophosphodiester phosphodiesterase GDPDL3-like	↘	3.18E-02	6.0							GDPDL3
XP_030489949.1; XP_030489948.1; XP_030487755.1 XP_030501009.1	caffeic acid 3-O- methyltransferase-like isoform X2	↘	2.98E-03	3.0				↗	1.65E-02	2.2	COMT
XP_030486346.1; XP_030486319.1	cinnamyl alcohol dehydrogenase 1-like			↗	3.60E-02	2.5					CAD
XP_030508841.1; XP_030507959.1	glucan endo-1,3-beta- glucosidase_ basic vacuolar isoform-like	↗	1.28E-03	3.7				↘	4.06E-03	1.5	BG
XP_030508841.1; XP_030507959.1	glucan endo-1,3-beta- glucosidase_ basic vacuolar isoform-like	↗	9.35E-05	5.6	↗	3.91E-03	2.1				BG

Accession	Soluble protein name	C-Cd		C-Zn		C-CsI		Cd-CdSI		Zn-ZnSI		
		Anova	MFC	Anova	MFC	Anova	MFC	Anova	MFC	Anova	MFC	
XP_030509516.1	putative beta-D-xylosidase							7.60E-03	2.0			BXL
XP_030485245.1	protein TPLATE			4.52E-02	2.1							TPLATE
XP_030488625.1;	sucrose synthase-like	2.82E-04	2.3									SuSy
XP_030488624.1												
XP_030507721.1	sucrose synthase 7-like			5.92E-05	2.9							SuSy7
XP_030510687.1	cellulose synthase A catalytic subunit 7 [UDP-forming]	4.66E-02	6.4							3.68E-03	6.3	CesA7
XP_030494583.1;	cellulose synthase A catalytic subunit 8 [UDP-forming]-like	2.88E-03	2.2									CesA8
XP_030480065.1												
XP_030492130.1	methylenetetrahydrofolate reductase 2-like	2.16E-02	2.0									MTHFR
XP_030480227.1	laccase-4-like	5.15E-05	8.1	5.52E-06	6.7	6.79E-04	4.0					LAC4
XP_030496050.1	cytochrome P450 71B34-like	4.19E-05	2.3									CYP71
XP_030506964.1	cytochrome P450 CYP73A12-like	5.17E-03	2.3	6.25E-04	4.3							CYP73
XP_030493605.1	cytochrome P450 CYP73A100-like	4.84E-03	3.7	1.10E-04	2.4							CYP73
XP_030499477.1;	pectin acetyltransferase 3-like isoform X2			6.68E-04	2.8							PAE
XP_030499405.1												
XP_030507468.1	UDP-glucuronate 4-epimerase 6	2.49E-04	3.1									GA6E
XP_030500851.1	bifunctional dTDP-4-dehydrorhamnose 3_5-epimerase/dTDP-4-dehydrorhamnose reductase							3.50E-03	2.2			
METABOLISM												
Amino acids, nitrogen, sulphur and glutathione metabolism												
XP_030488276.1	LOW QUALITY PROTEIN: delta-1-pyrroline-5-carboxylate synthase-like	3.58E-02	2.2	5.12E-04	3.1							P5CS
XP_030486258.1	ferredoxin-nitrite reductase_chloroplastic-like			3.21E-02	2.6							NIR
XP_030495540.1	S-adenosylmethionine synthase 3	2.65E-04	2.7									SAMs
XP_030503589.1	5-methyltetrahydropteroyltylglutamate-homocysteine methyltransferase 2					1.48E-02	2.8					M5
XP_030483244.1	aspartate aminotransferase P2_mitochondrial	1.75E-02	2.3	8.03E-04	3.5							AAT
XP_030507269.1;	glutamate dehydrogenase 1	3.99E-04	3.6									GluDH
XP_030507270.1;												
XP_030501899.1;												
XP_030501900.1												
XP_030503475.1	sulfite reductase [ferredoxin]_chloroplastic	3.36E-05	3.2	1.98E-02	2.2							SIR
Purine, pyrimidine, ribonucleotide and deoxyribonucleotide metabolism												
XP_030481118.1;	uracil phosphoribosyltransferase-like			4.38E-02	3.2							UPRT
XP_030479601.1												
Protein synthesis, processing, modification												
Transcription												
XP_030505854.1	protein argonaute 4-like			1.00E-02	2.2							
Protein synthesis (ribosomal proteins, translation, translational control, amino-acyl tRNA synthetases)												
XP_030500635.1;	60S ribosomal protein L15-2			2.38E-02	2.8							L15
XP_030489438.1												
XP_030480012.1;	60S acidic ribosomal protein P2-2-like	2.00E-02	4.2	3.15E-02	2.5							P2
XP_030480011.1												
XP_030503144.1;	60S ribosomal protein L10-like			5.46E-03	2.3							L10
XP_030488761.1												
XP_030483002.1	60S-ribosomal protein L10a			2.55E-02	2.2	4.03E-03	3.0					L10
XP_030507532.1;	60S ribosomal protein L13a-4			6.34E-04	2.2							L13
XP_030499844.1												
XP_030491361.1;	60S ribosomal protein L14-2-like					3.93E-02	4.0					L14
XP_030489954.1												
XP_030480081.1;	60S ribosomal protein L18a-2-like isoform X1	4.52E-02	26.8	9.77E-03	192.6							L18
XP_030494264.1;												
XP_030501207.1												
XP_030506326.1;	60S ribosomal protein L23a					4.72E-02	23.0					L23
XP_030488101.1;												
XP_030488102.1;												
XP_0304895139.1												
XP_030484025.1;	60S ribosomal protein L31	1.54E-02	2.4	7.49E-07	14.1			3.55E-02	3.7			L31
XP_030488290.1;												
XP_030489190.1												
XP_030477674.1	60S acidic ribosomal protein P3			1.70E-04	2.6							P3
XP_030480009.1	60S acidic ribosomal protein P2A-like			3.70E-02	2.2							P2
XP_030510107.1;	40S ribosomal protein S7-like			8.14E-03	2.2	1.67E-02	2.5					S7
XP_030494538.1;												
XP_030507235.1												
XP_030510106.1												

Accession	Soluble protein name	C-Cd		C-Zn		C-CSI		Cd-CdSI		Zn-ZnSI		
		Anova	MFC	Anova	MFC	Anova	MFC	Anova	MFC	Anova	MFC	
XP_030504232.1	40S ribosomal protein S4-3							↗	2.40E-02	2.2		S4
XP_030480754.1;	40S ribosomal protein S11-like			↘	4.00E-04	6.1		↘	9.32E-03	2.8		S11
XP_030477635.1	40S ribosomal protein S3-3			↘	4.50E-05	2.4						S3
XP_030488957.1	leucine-tRNA ligase, cytoplasmic	↘	3.75E-02	2.1	↘	6.81E-03	2.4	↘	2.52E-02	2.1		
XP_030504382.1	elongation factor 1-beta 2	↘	9.98E-05	2.0	↘	1.17E-03	2.2					EF1
XP_030503776.1;	elongation factor 1-alpha							↗	5.62E-03	2.6		EF1
XP_030503775.1	aspartate-tRNA ligase 2, cytoplasmic	↗	2.07E-02	2.3								
XP_030507726.1	ketol-acid reductoisomerase, chloroplastic	↗	5.81E-03	2.2								
XP_030481816.1	eukaryotic translation initiation factor 5A-2	↘	1.13E-02	40.9	↘	5.77E-03	123.3					EIF5A2
XP_030491241.1;	eukaryotic translation initiation factor 3 subunit K-like			↘	1.70E-05	5.2						
XP_030490754.1	probable N-acetyl-gamma-glutamyl-phosphate reductase, chloroplastic			↗	7.32E-04	3.3						
XP_030486602.1	signal recognition particle receptor subunit beta	↗	1.65E-02	3.4	↗	5.41E-04	7.9	↗	4.23E-03	7.4		SRPRB
Protein folding and stabilization												
XP_030478962.1	heat shock 70 kDa protein-like			↘	4.41E-05	3.6						
XP_030498755.1	chaperonin CPN60-2, mitochondrial-like			↘	1.06E-02	2.1						CPN60
XP_030490603.1	chaperonin CPN60-like 2, mitochondrial			↗	1.17E-02	2.4						CPN60
XP_030488166.1	BAG family molecular chaperone regulator 7	↘	8.64E-04	2.2								BAG7
Proteases												
XP_030484572.1;	proteasome subunit alpha type 1-A-like			↗	1.38E-03	2.3						
XP_030501354.1;	ubiquitin-40S ribosomal protein S27a	↗	1.28E-02	2.1	↗	5.88E-03	2.3					UBQ
XP_030497408.1;												
XP_030486007.1;												
XP_030491754.1;												
XP_030493197.1;												
XP_030493346.1;	ubiquitin carboxyl-terminal hydrolase 6-like			↘	5.93E-04	5.0						UCH6
XP_030491503.1	cullin-1	↗	2.78E-03	2.9	↗	6.76E-03	2.2					CUL1
XP_030508051.1;	F-box/kelch-repeat protein SKIP4								↘	4.30E-03	2.8	SKIP4
XP_030490048.1;												
XP_030490049.1	subtilisin-like protease SBT1.7	↗	5.23E-03	3.4	↗	3.85E-03	4.4					SBT1
XP_030509608.1;	subtilisin-like protease SBT5.3 isoform X1							↗	1.95E-03	3.4		SBT5
XP_030509609.1	probable cysteine protease RD19B			↗	2.84E-05	2.8						
XP_030485032.1												
Transport facilitation, transport mechanism, membrane modification												
XP_030507209.1	importin subunit alpha-1-like			↘	1.46E-02	2.1						
XP_030505754.1	ras-related protein RABA2a			↗	4.21E-02	2.4						RABA2
XP_030488383.1	pleiotropic drug resistance protein 1-like	↗	2.37E-02	2.4	↗	2.73E-02	2.6					PDR1
XP_030489689.1;	protein FATTY ACID EXPORT 3, chloroplastic isoform X1	↗	1.17E-02	2.1								FAX1
XP_030489690.1;												
XP_030489691.1;												
XP_030489692.1;												
XP_030489693.1	pyrophosphate-energized vacuolar membrane proton pump-like	↘	6.08E-03	2.5	↘	4.87E-04	2.9					
XP_030495608.1	ras-related protein RABC2a-like			↘	1.31E-02	2.2						RABC2
XP_030505782.1	guanosine nucleotide diphosphate dissociation inhibitor AT5g09550			↘	2.38E-02	2.2						
XP_030502238.1	dynamine-related protein 1E-like							↗	2.41E-02	2.0		DRP1
XP_030480160.1	gamma-soluble NSF attachment protein			↘	1.83E-02	4.3						
XP_030480614.1	vesicle-associated membrane protein 711	↗	1.21E-03	3.0								VAMP7
XP_030507156.1;	vesicle-associated protein 2-1-like isoform X2							↗	2.80E-02	2.1		VAMP2
XP_030507155.1;	LOW QUALITY PROTEIN: coatamer subunit beta'-1-like			↗	2.80E-02	2.3						
XP_030488587.1;												
XP_030488355.1	clathrin light chain 2-like			↗	2.73E-02	2.0						CLC2
XP_030479858.1	putative clathrin assembly protein			↗	9.82E-07	2.7						
XP_030496965.1;												
XP_030496964.1	At2g01600 isoform X2											
XP_030499077.1	AP-1 complex subunit gamma-2-like							↗	1.08E-02	2.5		
XP_030477745.1	transmembrane 9 superfamily member 11	↘	3.85E-02	4.6								TMN11
Ionic homeostasis												

Accession	Soluble protein name	C-Cd		C-Zn		C-CsI		Cd-CdSI		Zn-ZnSI	
		Anova	MFC	Anova	MFC	Anova	MFC	Anova	MFC	Anova	MFC
XP_030489388.1	copper transporter 5.1-like			7.07E-04	2.9						COPT
XP_030489759.1	proton pump-interactor 1	9.59E-04	2.1	1.75E-05	3.1						PPI1
XP_030483484.1	plasma membrane ATPase 4	3.39E-03	2.2								
XP_030477717.1	plasma membrane ATPase 4-like			2.50E-04	3.6						
XP_030495866.1	ABC transporter C family member 3-like	9.93E-03	4.2								
XP_030493045.1	ABC transporter E family member 2			2.09E-02	10.3			6.58E-03	8.0		
XP_030493046.1	oligopeptide transporter 3	5.26E-05	3.6	3.82E-05	6.6						OPT3
Cell division, cell organisation											
Cell division											
XP_030501768.1	protein FIZZY-RELATED 2-like			3.66E-03	3.0						
Cellular organization (organization of cytoskeleton)											
XP_030482459.1	tubulin alpha-1 chain	4.15E-02	2.6								
XP_030481404.1	tubulin beta-1 chain	9.78E-04	2.6								
XP_030496340.1	tubulin alpha-3 chain	8.25E-03	2.1								
XP_030499509.1	actin-7	3.16E-02	2.2	1.94E-04	5.7	2.22E-02	2.3	1.11E-02	2.6		
XP_030499508.1	LOW QUALITY PROTEIN: villin-3-like	1.39E-02	3.0					2.00E-02	2.6		VLN3
Signal transduction and metabolism regulation											
XP_030496860.1	14-3-3 protein 1 isoform X1			5.93E-03	2.3						14-3-3
XP_030484623.1	14-3-3-like protein B isoform X2	4.00E-02	2.9	2.93E-02	2.6						14-3-3
XP_030484622.1	calreticulin					4.66E-02	2.6				CRT
XP_030485891.1	phosphoinositide phosphatase SAC7-like	2.77E-02	4.1								SAC7
XP_030504426.1	G-type lectin S-receptor-like serine/threonine-protein kinase RLK1			2.84E-02	5.0						LecRLK1
XP_030498105.1	probable serine/threonine-protein kinase PBL21			2.09E-05	4.7			3.36E-02	2.7		
XP_030496318.1	leucine-rich repeat receptor-like serine/threonine-protein kinase BAM1			1.82E-03	9.9						BAM1
XP_030486886.1	annexin-like protein RJ4	1.32E-02	3.8	1.92E-02	2.6						
XP_030487730.1	spermidine synthase 1	1.91E-02	3.3	1.78E-02	3.5						SPD5
XP_030500392.1	RGG repeats nuclear RNA binding protein A	1.95E-02	10.8	4.58E-02	5.2	1.63E-02	7.4				RGGA
XP_030504790.1	probable AUXIN RESPONSE 4	2.65E-02	8.3								
XP_030486567.1	allene oxide synthase 3-like			1.13E-03	2.3						AOS3
XP_030480062.1	WD repeat-containing protein 44	1.71E-03	3.1	3.05E-02	2.0	3.60E-03	2.6				WD-44
XP_030483053.1	protein TRANSPARENT	2.56E-02	2.0								TT9
XP_030502571.1	TESTA 9-like										
XP_030503439.1	mitochondrial Rho	6.02E-03	2.6	4.98E-04	5.1						MIRO1
XP_030503440.1	GTPase 1-like										
XP_030507175.1	GTP-binding protein SAR1A-like	1.22E-02	3.2	2.40E-02	2.1						SAR1A
XP_030507283.1	apyrase 2-like	1.74E-04	5.1								APY2
Cell rescue, defense											
XP_030501451.1	pathogenesis-related protein R major form-like	4.57E-03	4.5								PRR
XP_030487534.1	pathogenesis-related protein 1-like	3.63E-05	26.5	1.25E-04	8.4						PR1
XP_030502231.1	thaumatin-like protein 1	6.83E-03	2.6								TLP
XP_030485657.1	endochitinase 2	1.04E-03	4.8	3.35E-02	2.1						ECH2
XP_030485657.1	endochitinase 2	3.80E-03	11.9								ECH2
XP_030510068.1	class V chitinase-like	6.86E-04	2.2								CH5
XP_030506215.1	barwin-like	3.24E-02	7.1								
XP_030503115.1	probable aldo-keto reductase 2							3.36E-02	2.4		AKR
XP_030507759.1	probable aldo-keto reductase 2	1.99E-03	3.6	5.57E-05	5.5	2.49E-02	2.7				AKR
XP_030507759.1	probable aldo-keto reductase 2										
XP_030507758.1	universal stress protein PHO532							6.27E-03	2.1		
XP_030508067.1	universal stress protein PHO532	1.43E-04	2.7								
XP_030486303.1	cyclase-like protein 2	2.42E-02	3.5	2.26E-02	4.3						CYCL2
XP_030498132.1	catalase-2			3.78E-02	2.9						CAT
XP_030493815.1	catalase isozyme 2-like	4.49E-02	2.2								CAT

Accession	Soluble protein name	C-Cd		C-Zn		C-CSI		Cd-CdSI		Zn-ZnSI				
		Anova	MFC	Anova	MFC	Anova	MFC	Anova	MFC	Anova	MFC			
XP_030499793.1	peroxidase 72			↗	2.62E-02	2.7						PRX		
XP_030479401.1	peroxidase 15-like	↗	4.02E-02	2.5								PRX		
XP_030485526.1	peroxidase 4-like	↗	5.44E-05	2.2								PRX		
XP_030501341.1	monodehydroascorbate reductase_chloroplastic/mitochondrial				↗	1.17E-02	4.9	↗	3.80E-02	3.2		MDHAR		
XP_030504138.1	CBS domain-containing protein CBSX3_mitochondrial	↗	6.63E-04	2.2								CBSX3		
XP_030507868.1	aldehyde dehydrogenase 22A1				↘	1.39E-02	10.5	↘	1.87E-02	9.3		ALDH		
XP_030481542.1	formate dehydrogenase_mitochondrial	↗	2.64E-05	3.6								FDH		
XP_030494341.1; XP_030494342.1; XP_030495485.1	L-galactono-1,4-lactone dehydrogenase_mitochondrial-like				↗	1.04E-02	17.2					GLDH		
XP_030498417.1	phosphoprotein ECPP44-like	↗	1.69E-02	3.1										
Others														
XP_030508375.1	probable monoterpene synthase MTS1_chloroplastic									↘	1.58E-02	1.9	MTS1	
XP_030510929.1	farnesyl pyrophosphate synthase-like				↘	3.58E-02	2.4						FPPS	
XP_030508570.1	gamma conglutin 1-like	↗	9.39E-03	2.5									TM9SF9	
XP_030478866.1	transmembrane 9 superfamily member 9-like				↘	1.51E-02	2.0							
XP_030480855.1; XP_030480856.1 XP_030507618.1	prosaposin-like 3-ketoacyl-CoA thiolase 2_peroxisomal				↗	1.50E-04	3.5						KAT2	
XP_030485010.1; XP_030485011.1	DEXH-box ATP-dependent RNA helicase DEXH17 isoform X1	↘	4.28E-02	3.7	↘	5.14E-07	24.3	↘	4.45E-02	2.8				
XP_030489288.1	serine carboxypeptidase-like										↗	2.10E-02	2.2	SCPL
XP_030507087.1	probable methyltransferase PMT3	↘	1.13E-03	11.4	↘	4.96E-03	3.4						PMT3	
XP_030490122.1	probable methyltransferase PMT13				↗	6.74E-03	6.0	↗	3.87E-02	2.3			PMT13	
XP_030501398.1	probable methyltransferase PMT14	↘	3.53E-03	2.6									PMT14	
XP_030499403.1	stemmadenine O-acetyltransferase-like	↗	1.10E-03	2.5	↗	1.60E-06	5.7							
XP_030484735.1; XP_030484734.1	peroxisomal and mitochondrial division factor 1	↗	3.60E-03	4.6									PMD1	
XP_030508261.1	gamma conglutin 1-like	↗	3.83E-04	8.4	↗	2.30E-03	3.5							
No assigned function														
XP_030492112.1	uncharacterized protein LOC115708075	↗	4.91E-02	2.2										
XP_030505388.1	uncharacterized protein LOC115720376				↘	3.12E-02	2.6							
XP_030485083.1	uncharacterized protein At5g39570				↗	1.87E-02	2.0							
XP_030488475.1; XP_030488483.1	protein unc-13 homolog isoform X1	↘	6.29E-03	5.9	↘	4.95E-02	2.7							
XP_030503417.1	probable inactive receptor kinase At5g58300				↘	1.33E-02	2.0							
XP_030487712.1	uncharacterized protein LOC115704652	↗	6.44E-05	28.6	↗	2.30E-03	4.8							
XP_030479238.1; XP_030497626.1; XP_030502429.1; XP_030502664.1	uncharacterized protein LOC115696478	↗	3.62E-03	5.9	↗	1.02E-02	2.4	↗	2.30E-02	2.3	↘	2.40E-02	3.2	
XP_030485083.1	uncharacterized protein At5g39570				↘	3.27E-03	2.1							
XP_030508867.1	LOW QUALITY PROTEIN: uncharacterized protein LOC115723511_partial				↗	3.78E-02	4.2							
XP_030481950.1	uncharacterized protein At1g08160-like				↗	1.21E-02	2.5							
ARE72265.1	IDI_partial									↘	4.44E-02	2.3		

Among proteins up-regulated by Zn exposure (Table 6.4; Figure 6.2), 4 are involved in carbohydrate metabolism, one in callose remodelling (BG), one in CW expansion (monocopper oxidase-like protein SKU5), one in cellulose biosynthesis (SuSy), one in xylan biosynthesis (UDP-glucuronic acid decarboxylase 6-like, UXS), on in SCW synthesis (fasciclin-like

arabinogalactan protein 12, FLA12), 2 in lignin biosynthesis (cinnamyl alcohol dehydrogenase 1-like, CAD1; and CYP73A100), one in pectin acetylation (pectin acetyltransferase 3-like isoform X2, PAE), one in proline biosynthesis (P5CS), 2 in nitrate and sulphur assimilation (NiR, SIR), one in pyrimidine metabolism, 4 in protein synthesis and 1 in protein folding, 5 in proteolysis, 5 are involved in transport, 3 in ionic homeostasis, one in cell division, 7 in signal transduction and metabolism regulation, and 7 assume key functions in cell rescue. Zn exposure also reduced the abundances of a protein involved in photosynthesis (RuBisCO small subunit), a protein controlling in SCW synthesis (FLA12), a protein controlling the accumulation of crystalline cellulose (glycerophosphodiester phosphodiesterase GDPDL3-like), 2 involved in lignin biosynthesis (LAC4 and CYP736A12), one is involved in amino acid synthesis (aspartate aminotransferase, AAT), one regulating transcription, 16 involved in protein synthesis and folding, one managing in proteolysis, 5 controlling transport, 2 in ionic homeostasis, one in cell organization (actin), 5 playing role in signal transduction and metabolism regulation and 2 involved in cell rescue (catalase, CAT; probable aldo-keto reductase, AKR). The most important category of proteins down-regulated by Zn toxicity were involved in protein processing. It has to be noticed that only a minor proportion of proteins (40) were affected by both Cd and Zn, suggesting that the two heavy metals have a quite different impact on protein regulation in *C. sativa*, despite the fact that they share numerous chemical properties (Jaskulak et al., 2020). When a same protein was affected by both heavy metals, Cd and Zn had similar impacts in terms of up- or down-regulation and no opposite effect was recorded. This was especially the case for LAC4 whose abundance was reduced by both heavy metals, and for glucan endo-1, 3- β -glucosidase (BG) involved in callose degradation which was increased by Cd and by Zn.

The number of proteins affected by Si exposure was by far lower than the number of proteins affected by heavy metals (Table 6.4 and Fig. 6.2). Exposure of hemp plants to Si in the absence of heavy metal stress up-regulated proteins involved in photosynthesis (1), amino acid metabolism (MS1), protein synthesis (3), transport (2) and cell rescue (especially MDHAR involved in Asada-Halliwel cycle). Si significantly decreased the accumulation of some proteins involved in photosynthesis (1), SCW formation (FLA12), protein synthesis (4), cell organization (1), signal transduction and metabolism regulation (3) and cell rescue (2). Si had contrasting impact on proteins involved in lignin biosynthesis since it

increased the abundance of caffeic acid 3-O-methyltransferase (COMT), while it decreased the abundance of a laccase (LAC4).

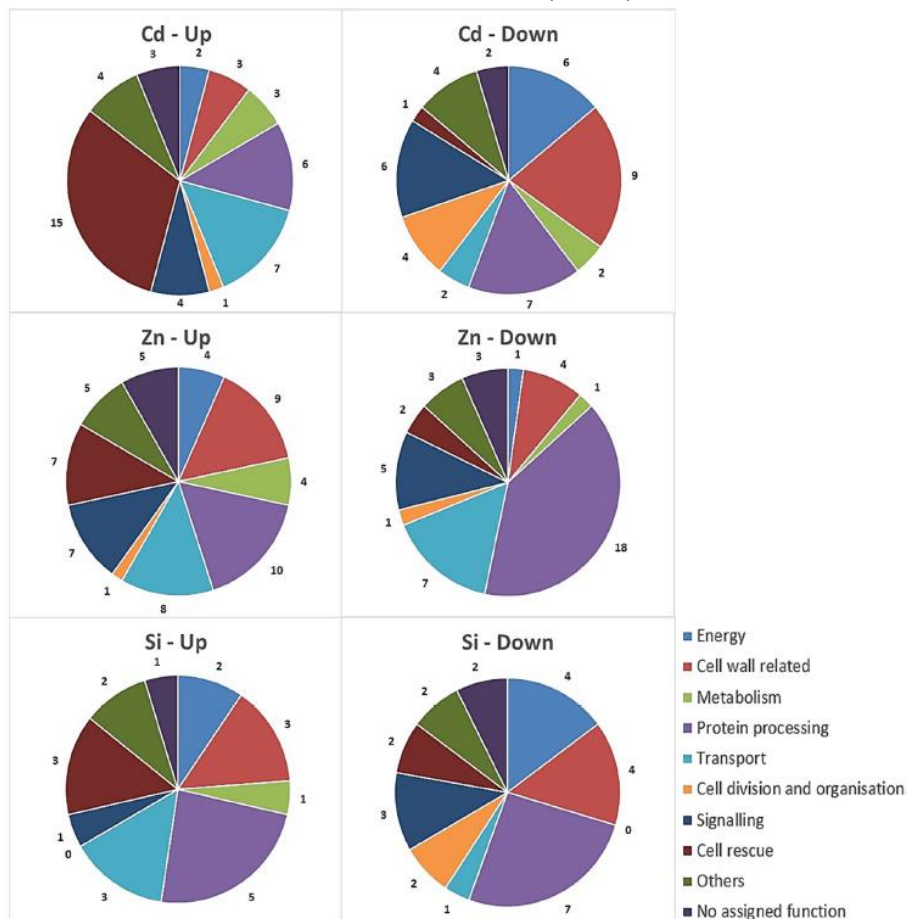


Figure 6.2: Functional classification of proteins with significant quantitative changes in abundance in hemp hypocotyls in response to Cd, Zn and Si. Seedlings were exposed for one week either to Cd 20 μ M, Zn 100 μ M or Si 2 mM and proteins were extracted from hypocotyls. Mixed treatment (CSi, CdSi, ZnSi) are not indicated for the sake of clarity.

Si had a specific impact on some proteins observed in CdSi treatment comparatively to plants exposed to Cd in the absence of Si: 55 % of those proteins (10 among 18) were specifically regulated by this treatment and remained unaffected by Cd or Si applied alone. This was the case for β -D-xylosidase and dehydrorahmnose reductase. Additional Si to Cd- treated plants had no impact on other CW-related proteins previously mentioned to be affected by Cd treatment. Only 6 proteins were significantly regulated in ZnSi-exposed plants comparatively to Zn-treated ones and none of them were

specifically regulated by Si in the absence of Zn. Similarly, one glucan endo 1,3- β -glucosidase and cellulose synthase A were respectively down- and up-regulated in response to ZnSi while these proteins were not affected by Si or by Zn applied separately.

3.5. Confocal microscopy and immunohistochemistry

Confocal microscope observation of stem sections (Figure 6.3) revealed that Cd-treated plants displayed a lower level of lignin than controls and Zn-treated plants displayed the highest proportion of lignin comparatively to control (C) or Cd-treated plants.

Confocal microscope observations were also carried out on 3 plants per treatment for immunochemistry. A monoclonal antibody recognizing xylan (LM10) and His-tagged recombinant protein recognizing crystalline cellulose (CBM3a) were used to study the impact of heavy metals on bast fibre development.

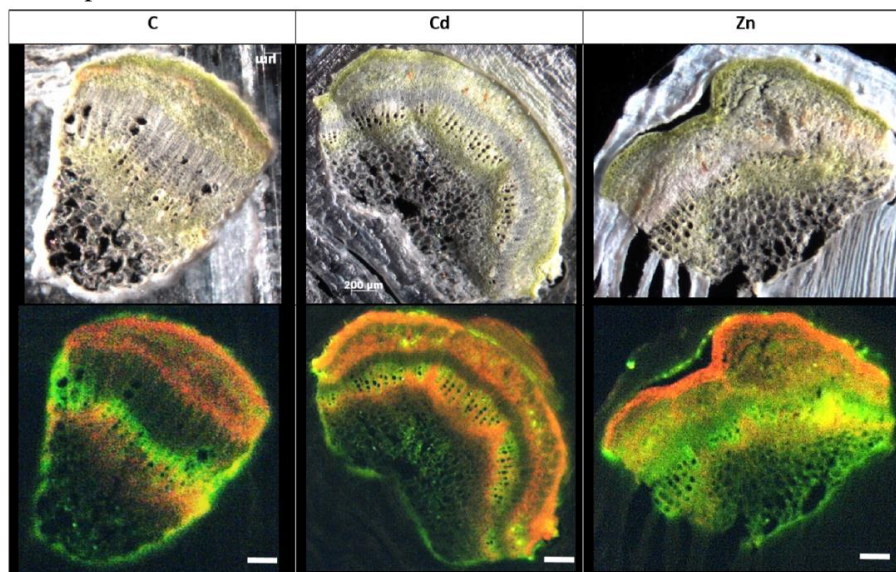


Figure 6.3: Confocal microscope observation of hemp stem sections (60 μm) (Axioscope 2 MOT, 405 nm). Plants were exposed for one week to Cd (20 μM) or Zn (100 μM) (C: control plants not exposed to heavy metals). Fluorescence highlights lignified areas (yellow), areas containing chlorophyll (orange-red color), and simple phenols compounds (green). Scale bar: 200 μm .

Figures 6.4 and 6.5 allowed us to observe the histological modifications induced by heavy metals in the stem, as well as the impact of Si. In all plant sections, secondary growth can be observed by the presence of

cambial cells and the typical radial organization of secondary xylem vessels. This radial organization was less marked for plants of Cd treatment without Si supply. Primary and secondary bast fibres were easily distinguishable in the stems of all treatments, except in stems of Cd-treated plants. The diameter of primary and secondary bast fibres was measured for each treatment. In plants of Cd treatment, the differentiation stage of secondary bast fibres was not compatible with an analysis. The diameter decreased in both types of bast fibres when plants were exposed to heavy metals (Cd and Zn, Fig. 6.6). Interestingly, the diameter increased in Cd-stressed plants when they were simultaneously exposed to Si, but this was not observed for Zn-treated plants. Both diameter and thickness of xylem vessels (Figure 6.7) were smaller in plants exposed to Cd or Zn, with a contrasting effect of Si on the diameter of Cd and Zn treatments since it increased in Cd-stressed plants and decreased in plants treated with Zn.

On sections observed at the confocal microscope (Figure 6.4), the xylan epitope was detected mainly in xylem cells (x) and in the C of primary bast fibres (pf). In Cd, CdSi and Zn-treated plants a clear signal was also detected in collenchyma cells (c) (Table 6.5). The walls of primary bast fibres were more strongly labelled by this antibody in Cd-treated plants as compared to control ones. Si decreased the signal intensity in the collenchyma of Zn-treated plants. Using the ImageJ program, we measured the thickness of the signal distribution in bast fibres. The results presented in Table 6.5 show that in plants exposed to Cd or Zn, the thickness significantly decreased as compared to control plants. The same observation can be made when control plants are treated with Si (Table 6.5).

Crystalline cellulose was visualized with CBM3a. It was observed in all tissues, especially in collenchyma, xylem cells and in both primary and secondary bast fibres (Figure 6.5). In the case of Cd-treated plants, the signal from secondary bast fibres was not detected but we saw an effect of Si in the case of Cd-treated plants: the differentiation stage of secondary bast fibres was sufficient to detect a signal. (Figure 6.5). In Cd and Zn-treated plants, primary bast fibres displayed a more intense signal than the one detected in control plants. On the contrary, the signal was less intense in secondary fibres for the same plants (Figure 6.5, Table 6.6). The thickness of the fibres as detected with the CBM3a signal, was influenced by the heavy metal treatment: it decreased in primary bast fibres of Cd-exposed plants and in secondary fibres of Zn-treated plants (Table 6.6).

Table 6.5: Immunodetection of the LM10 epitope specific for xylan in stem sections of *Cannabis sativa* (cv. Santhica 27). Plants were exposed for one week to Cd (20 μ M) or Zn (100 μ M) in the presence or in the absence of Si 2 mM. Mean \pm Standard Deviation (SD). The different letters indicate that the values are significantly different from each other ($P < 0.05$; Tukey's HSD all-pairwise comparisons). Signal thickness (in μ m) specify the thickness of the area wher signal was detected in the cell wall.

LM10							
Treatment	Signal intensity					Signal thickness in cell wall (μ m)	
	Epidermis	Collenchy ma	Primary fibres	Secondary fibres	Xylem	Primary fibres	Secondary fibres
C	195 \pm 57 <i>a</i>	123 \pm 41 <i>ab</i>	411 \pm 169 <i>a</i>	nd	27.12 \pm 5.91 <i>b</i>	4.30 \pm 2.47 <i>b</i>	nd
CSi	410 \pm 93 <i>b</i>	172 \pm 73 <i>bc</i>	313 \pm 56 <i>a</i>	nd	29.78 \pm 7.49 <i>b</i>	1.76 \pm 0.23 <i>a</i>	nd
Cd	490 \pm 159 <i>bc</i>	442 \pm 181 <i>d</i>	717 \pm 212 <i>b</i>	nd	12.66 \pm 2.64 <i>a</i>	2.03 \pm 0.56 <i>a</i>	nd
CdSi	666 \pm 183 <i>c</i>	490 \pm 192 <i>d</i>	715 \pm 106 <i>b</i>	nd	14.90 \pm 4.79 <i>a</i>	1.97 \pm 0.48 <i>a</i>	nd
Zn	594 \pm 258 <i>bc</i>	252 \pm 76 <i>c</i>	411 \pm 150 <i>a</i>	nd	20.20 \pm 4.37 <i>ab</i>	2.10 \pm 0.51 <i>a</i>	nd
ZnSi	258 \pm 182 <i>a</i>	100 \pm 71 <i>a</i>	345 \pm 85 <i>a</i>	nd	21.78 \pm 2.68 <i>ab</i>	1.80 \pm 0.33 <i>a</i>	nd

Table 6.6: Immunodetection of the CBM3a epitope specific for crystalline cellulose in stem sections of *Cannabis sativa* (cv. Santhica 27). Plants were exposed for one week to Cd (20 μ M) or Zn (100 μ M) in the presence or in the absence of Si 2 mM. Mean ($n = 3$) \pm Standard Deviation (SD). The different letters indicate that the values are significantly different from each other ($P < 0.05$; Tukey's HSD all-pairwise comparisons). Signal thickness (in μ m) specify the thickness of the area wher signal was detected in the cell wall.

CBM3a							
Treatment	Signal intensity					Signal thickness in cell wall (μ m)	
	Epidermis	Collenchy ma	Primary fibres	Secondar y fibres	Xylem	Primary fibres	Secondary fibres
C	1009 \pm 326 <i>a</i>	873 \pm 370 <i>bc</i>	846 \pm 280 <i>b</i>	862 \pm 288 <i>b</i>	632 \pm 136 <i>b</i>	2.54 \pm 0.50 <i>b</i>	2.62 \pm 0.66 <i>b</i>
CSi	778 \pm 145 <i>a</i>	508 \pm 72 <i>a</i>	507 \pm 118 <i>a</i>	521 \pm 96 <i>c</i>	449 \pm 54 <i>a</i>	2.47 \pm 0.41 <i>b</i>	2.37 \pm 0.50 <i>ab</i>
Cd	753 \pm 174 <i>a</i>	938 \pm 149 <i>c</i>	1088 \pm 263 <i>c</i>	nd	773 \pm 132 <i>c</i>	1.95 \pm 0.39 <i>a</i>	nd
CdSi	800 \pm 196 <i>a</i>	859 \pm 222 <i>bc</i>	1141 \pm 196 <i>c</i>	669 \pm 138 <i>a</i>	790 \pm 150 <i>c</i>	2.49 \pm 2.66 <i>a</i>	2.19 \pm 0.40 <i>a</i>
Zn	786 \pm 178 <i>a</i>	642 \pm 153 <i>a</i>	915 \pm 265 <i>bc</i>	720 \pm 148 <i>ab</i>	653 \pm 62 <i>b</i>	2.56 \pm 0.38 <i>b</i>	2.21 \pm 0.73 <i>a</i>
ZnSi	849 \pm 130 <i>a</i>	678 \pm 114 <i>ab</i>	1135 \pm 267 <i>c</i>	724 \pm 237 <i>ab</i>	717 \pm 80 <i>bc</i>	2.49 \pm 0.79 <i>b</i>	2.31 \pm 0.51 <i>ab</i>

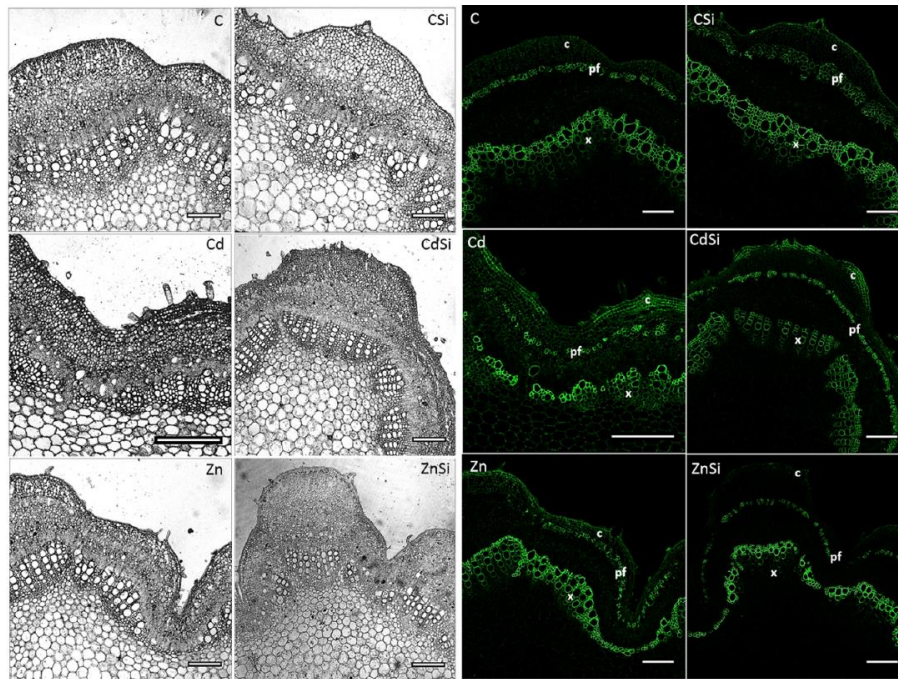


Figure 6.4: Confocal microscope observation and immunodetection of the LM10 epitope specific for xylan in stem sections of *C. sativa* (cv. Santhica 27). Plants were exposed for one week to Cd (20 μ M) or Zn (100 μ M) in the presence or in the absence of Si 2 mM. Control plants (C), Cd (Cd-treated plants), Zn (Zn-treated plants), with or without silicon (Si). Primary bast fibre (pf), secondary bast fibre (sf), xylem (x). Scale bar: 200 μ m.

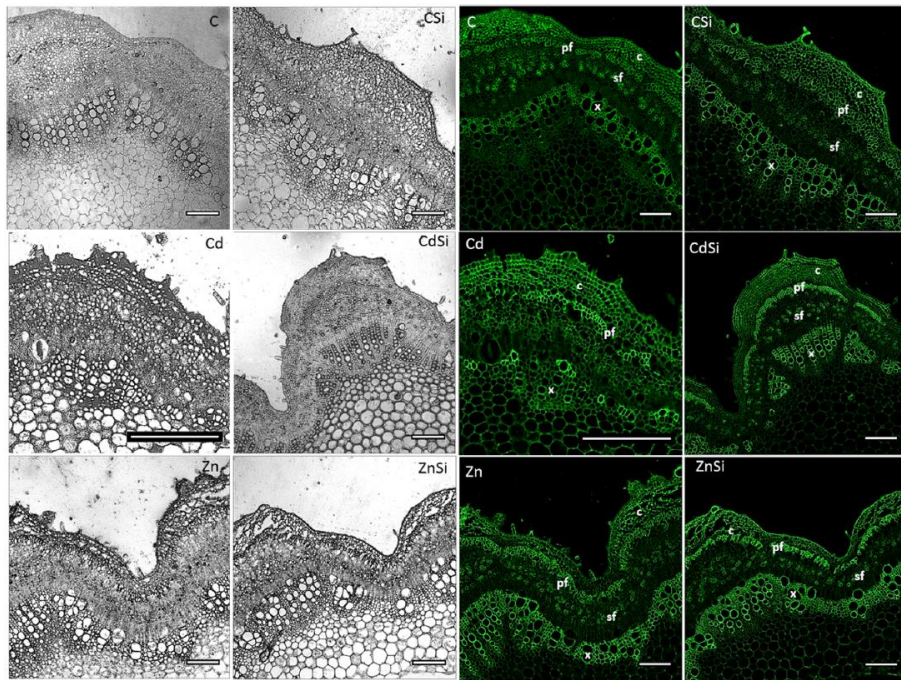


Figure 6.5: Confocal microscope observation and immunodetection of the CBM3a epitope specific for crystalline cellulose in stem sections of *C. sativa* (cv. Santhica 27). Plants were exposed for one week to Cd (20 μM) or Zn (100 μM) in the presence or in the absence of Si 2 mM. Control plants (C), Cd (cadmium treated plants), Zn (zinc treated plants), with or without silicon (Si). Primary bast fibre (pf), secondary bast fibre (sf), xylem (x). Scale bar: 200 μm .

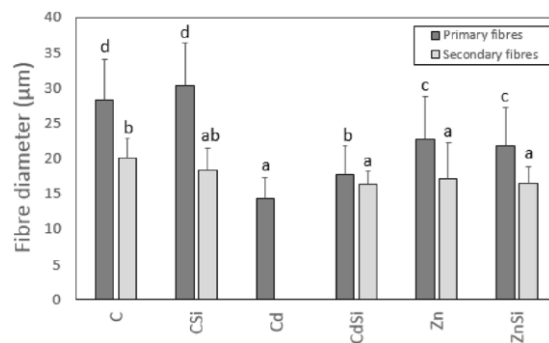


Figure 6.6: Diameter of primary (FI) and secondary (FII) bast fibres in stems of *C. sativa* (cv. Santhica 27). Plants were exposed for one week to Cd (20 μM) or Zn (100 μM) in the presence or in the absence of Si 2 mM. FII were not detected in Cd treated plants. The different letters indicate that the values are significantly different from each other ($P < 0.05$; Tukey's HSD all-pairwise comparisons). $n = 15$ (3 plants/treatment, 5 fibres/plant).

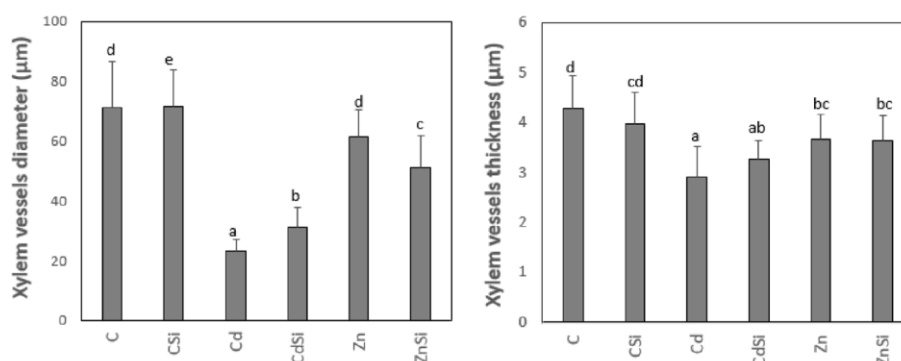


Figure 6.7: Diameter and thickness of the xylem vessels cell walls in stems of *Cannabis sativa* (cv. Santhica 27). Plants were exposed for one week to Cd (20 µM) or Zn (100 µM) in the presence or in the absence of Si 2 mM. The different letters indicate that the values are significantly different from each other ($P < 0.05$; Tukey's HSD all-pairwise comparisons). $n = 30$ (3 plants/treatment, 10 vessels/plant).

4. Discussion

Cd and Zn are well known environmental pollutants which negatively affect plant growth and biomass production. Si has frequently been reported to protect plants from heavy metal toxicity (Neumann and zur Nieden, 2001; Wu et al., 2013; Adrees et al., 2015; Imtiaz et al., 2016). The present work confirms the deleterious impact of Cd and Zn on root and shoot growth in hemp and also highlights that both elements reduced the diameter of primary bast fibres, suggesting that these pollutants may have a negative impact on fibre yield in *C. sativa*. Although exogenous Si tended to improve the behaviour of plants exposed to heavy metals, such a positive impact remained insignificant which could be partly explained by the high level of intraspecific variability still present in most hemp cultivars (Mihoc et al., 2012; García-Tejero et al., 2019; Jenkins and Orsburn, 2020), but also by the short duration of the simultaneous exposure to Si and heavy metals: it might indeed be argued that one week was not sufficient to detect the significant advantage conferred by Si to the growth of Cd- and Zn-treated plants, even if it allowed us to detect the impact of Si on some gene expression and specific protein abundances (see below).

A high concentration of Cd was recorded in roots and shoots of *C. sativa* after one week of treatment, reflecting the capacity of hemp to absorb and accumulate this toxic element. The recorded values were higher than those mentioned in the literature (Citterio et al., 2003; Angelova et al., 2004; Meers

et al., 2005) which could be due to the fact that the present experiment was conducted in nutrient solution rather than in soils where Cd bioavailability constitutes a limiting factor for Cd absorption. Cd and Zn accumulations in stems and leaves of heavy-metal treated plants (expressed relative to the corresponding organ DW basis) were in the same order of magnitude, while Si accumulation in the stem of the Si-treated plants was clearly lower than in roots which are in close contact with the Si-containing nutrient solution, and in leaves which represent evaporative organs where accumulation of passively translocated elements may occur. The low level of Si accumulation in stems, however, does not preclude a significant effect of Si on stem metabolism and mechanical properties. Indeed, Si is not uniformly distributed in plant tissues and accumulates at specific sites (Guerriero et al., 2020). As far as hemp stem is concerned, SIMS nano-analysis revealed the presence of Si in the distal CW of bast fibres (Guerriero et al., 2019).

Heavy metals also accumulate within the CW and this represents an efficient strategy preventing heavy metal accumulation in the cytosol. Vacuolar compartmentation of toxic elements is also considered as a valuable option for improving cell resistance (Sharma et al., 2016) and a positive effect of Cd on ABC transporters and oligopeptides transporters recorded in our study may be regarded as an attempt to limit Cd accumulation in the cytosol. Additional Si had a dual impact on these processes since it reduced the abundance of ABC transporters, but obviously increased the abundance of a protein involved in vesicular trafficking. Neumann and zur Nieden (2001) demonstrated in the Zn-resistant plant *Arabidopsis halleri* that Zn transiently accumulates as silicate in vacuolar vesicles and to a lower extent in the cytosol before being translocated to vacuoles where Zn-silicates are slowly degraded to SiO₂. This clearly suggests that Si distribution is not limited to the apoplasm.

Besides vacuolar sequestration, cell to cell trafficking constitutes a strategy to dilute heavy metals in the symplasm avoiding these ions to reach toxic levels. Callose (β -1,3-glucan) regulates plasmodesmatal permeability since an increase in plasmodesmata-localized callose is associated with a decrease in plasmodesmatal aperture (O'Leary et al., 2018). In *A. thaliana*, O'Leary et al. (2018) reported that Cd reduced plasmodesmatal permeability but our data on hemp stem provide a different picture since Cd and Zn increased the abundance of β -1, 3-glucosidase (BG) involved in callose breakdown. In contrast, Si reduced BG abundance in heavy-metal treated plants which may limit Cd and Zn mobility between cells. Silica precipitation

may indeed be induced by callose which was shown to play a key role in silification of Si-accumulating species like *Equisetum arvense* and *Oryza sativa* (Guerriero et al., 2018a, 2018b, 2020).

After one week of treatment, heavy metals affected numerous proteins playing important roles in cell metabolism. Heavy metal toxicity is known to disturb photosynthesis and the fact that Cd and Zn decreased RuBisCO subunit was not unexpected. It is interesting to note, however, that in our study heavy metals mainly act on the chloroplastic small subunit confirming that this organelle is particularly sensitive to the deleterious effect of Cd and Zn (Lefevre et al., 2014; Chandra and Kang, 2016). Cd also affected numerous enzymes involved in TCA cycle which could be related to an increase in the requirement of energy to cope with stress. In contrast, Zn excess did not directly impact TCA cycle but affected carbohydrate metabolism through an increase in DPE2 involved in maltose breakdown to glucose and by affecting the abundance of GALK which contributes to the synthesis of glucose-1-phosphate.

The non-protein amino-acid γ -aminobutyric acid (GABA) is assuming important functions in stress metabolism and signaling in plants and is synthesized via calcium/calmodulin-dependent glutamate decarboxylase activity (GluDC) (Seifikalhor et al., 2019). GluDC was strongly reduced in Cd-treated plants, but this should not be necessarily regarded as a symptom of injury and could be explained by the crucial role of glutamate as a precursor of other important molecules for stressed plants: glutamate is indeed converted to 2-oxoglutarate by glutamate dehydrogenase to fuel the TCA cycle and it is a precursor of proline which is a valuable protecting compound frequently overproduced in various stress conditions and which is suspected to directly chelate heavy metals (Lefèvre et al., 2014; Seifikalhor et al., 2019). The recorded increased abundance of P5CS (catalyzing the rate-limiting step of proline synthesis) in Cd- and in Zn-treated plants, supports the hypothesis that glutamate should remain available for the synthesis of this osmoprotectant. Glutamate is also an important precursor of the endogenous antioxidant glutathione (GSH) which is itself involved in the synthesis of phytochelatins (PC) directly implicated in heavy metal binding to cysteine, the complex being subsequently sequestered in vacuoles. Such a protecting process is especially efficient in response to Cd toxicity which triggers PC overproduction (Lefevre et al., 2016).

A specific attention was paid to SCW deposition and a global overview of the impact of Cd and Zn on the synthesis of CW precursor is

provided in Fig. 6.8. We studied gene expression and protein abundance in the hypocotyls of 28 days-old plants. At this stage, secondary xylem and secondary bast fibres, together with primary bast fibres, undergo SCW deposition (Behr, 2018). We analysed genes coding for bast fibre early growth stage (*PDF1*), genes involved in the transition from elongation to thickening (acid phosphatase, *AT1G04040*) and genes involved in SCW deposition (*CesA4*, *CesA7* and *CesA8*, class III peroxidases, *MET1* and *SAMS*).

Protodermal factor 1 (*PDF1*) is likely regulating hemp bast fibre early growth (Guerriero et al., 2017c). In 28-days hemp hypocotyls, fibres have completed their elongation and have started SCW deposition. Si application induced an increased expression level of *PDF1* for plants exposed to Zn and to a lower extent to Cd (not significant) treatments. Similarly, acid phosphatase is controlling CW-related processes in bast fibres during the transition from elongation to thickening (Guerriero et al., 2017c) and appears to be more expressed in Cd- and Zn-stressed plants compared to control ones. These data suggest that the timing of fibre elongation and transition from elongation to thickening may be affected by heavy metals and that Si may have an influence on this process.

Cd and Zn had contrasting effects on genes and proteins involved in SCW deposition. While Cd negatively affected gene expression and protein abundance involved in CW deposition, Zn had an opposite impact although it did not act on the same target. Indeed, plants exposed to Cd showed a lower expression of two genes coding for the cellulose synthases *CesA7* and *CesA8*, while in Zn-stressed plant *CesA4* expression level increased. *CesA4*, *CesA7* and *CesA8* are usually associated with SCW biogenesis in both xylan-type and gelatinous-type SCW (Taylor et al., 2003; Gorshkova et al., 2012). They are therefore regulating the deposition of the SCW in both tissues (Behr, 2018). Our sample contained both bast fibres in the cortical part of the stem and xylem tissues in the core. It is therefore difficult to attribute the expression of these genes to xylan-type or gelatinous-type SCW. However, a recent study performed on flax has highlighted that both PCW- and SCW-related *CesAs* have a higher expression in phloem fibres depositing their G-layer (Mokshina et al., 2017). Our proteomic data corroborated transcriptomic results since Cd clearly decreased the abundance of *CESA7* and *CESA8* (Figure 6.8).

To visualize Cd and Zn effect on cellulose deposition in stems, we performed confocal microscope observations of His-tagged recombinant protein recognizing crystalline cellulose (CBM3a). In Cd and Zn treated plants, primary bast fibres displayed a signal that was more intense than the

one detected in control plants, while abundance of CESA7 and CESA8 was shown to increase in Cd treated plants. Secondary bast fibres were not detected under Cd treatment. In Zn- and CdSi-treated plants, the signal was less intense than in control plants. It may therefore be hypothesized that heavy metals could modify bast fibres properties in relation to the decrease in cellulose abundance and to affect cellulose crystallinity detected by the recombinant protein used, although CBM3a is not fully specific to crystalline cellulose since it may also recognize xyloglucan present in PCW (Hernandez-Gomez et al., 2015). A Zn-induced decrease in GDPDL3 controlling cellulose crystallisation (Fig. 6.8) as well as a decrease in the thickness of distribution of the CBM3a signal in primary (and secondary for CdSi-exposed plants) bast fibres of Cd-exposed plants and in secondary fibres of Zn-treated plants support this hypothesis. It could not be excluded, however, that cell wall modification possibly induced by heavy metals can also modify epitope accessibility, thus accounting for reduction of labelling. Cd (but not Zn!) also decreased the abundance of sucrose synthase (SuSy; Fig. 6.8) isoforms which provide UDP-glucose to cellulose synthase (Granot and Stein, 2019) and this may also contribute to alter cellulose synthesis in Cd-treated plants. The addition of Si to Cd-treated plants did not counteract the impact of Cd on gene expression or protein abundance, which clearly shows that Si may act on specific cues and must not be regarded as a Cd antagonist.

Fasciclin-like arabinogalactan proteins are cell surface proteins linked to CW deposition and stem development in many species, from herbaceous to woody (Behr, 2018). In hemp, Guerriero et al. (2017d) identified specific *FLAs* likely involved in SCW deposition during the thickening stage (*CsaFLA3-12-13-15-16-18-19*; Guerriero et al., 2017d). In our hemp hypocotyls, the number of transcripts of *FLA3*, *FLA13*, *FLA11* and *FLA19* was lower for Cd-stressed plants and *FLA19* expression was higher for Zn stressed plants compared to controls, confirming once again a differential impact of the two considered heavy metals. *CsFLA13* and *CsFLA19* are highly expressed at the snap point as well as in older stem region (Guerriero et al., 2017b) and this might indicate a specific role in secondary growth. The concerted action of specific *FLAs* and chitinases may be involved in the transition from elongation to G-layer formation in hemp via the cleavage of the GlcNAc oligosaccharides part of *FLA* (Guerriero et al., 2017d): two endochitinase were increased in Cd-treated plants but their involvement in interaction with *FLA* is not demonstrated at this stage and requires further investigations

The present work demonstrates that Cd reduced the abundance of enzymes regulating lignin biosynthesis (decrease in COMT, CytP450, MTHFR, LAC4, CYP736A12; Fig. 6.8), while the situation was less clear for Zn which increased CAD1 but decreased LAC4 and CYP736A12. This contrasts with the results obtained in *Medicago sativa* where Cd exposure increased numerous proteins involved in the promotion of lignification (Gutsch et al., 2018). Hence, plant response may differ according to the species but also depending on stress duration: Gutsch et al. (2018) applied a long-term Cd treatment while we recorded the data after one week only. Lignin is mainly present in shivs while bast fibres contain between 2–7 % lignin only (Guerrero et al., 2017c). Despite being a minor component in bast fibres, lignin is deposited in the S1-layer for mechanical reasons as the hypocotyl ages (Behr et al., 2019) and lignin in hemp bast fibres is rich in S-units as the hypocotyl ages, because of the high abundances of enzymes regulating monolignol methylation (Behr et al., 2018). It is well established that apoplastic H₂O₂ is important for lignification processes and it functions as a signaling molecule triggering enzymatic activities like those of CW-localized peroxidases (Cosio and Dunand, 2008; Gutsch et al., 2019a). A role of peroxidases in fibre elongation and lignification through H₂O₂ production modulation has been recently reviewed (Berni et al., 2018): in cotton, Guo et al. (2016) observed that plants with downregulation of an ascorbate peroxidase (*GhAPXIAT*) are characterized by a significant increase in the number of fibres and by oxidative stress, which significantly reduces fibre elongation. During gene overexpression, cells show enhanced tolerance to oxidative stress suggesting that optimal levels of hydrogen peroxide are key mechanisms regulating fibre elongation (Guo et al., 2016). A high concentration of H₂O₂ would thus act as a signal for initiation of secondary wall thickening (Tang et al., 2014; Guo et al., 2016).

Peroxidases are necessary to initiate the polymerization of monolignols (Berthet et al., 2011; Chernova et al., 2018; Novo-Uzal et al., 2013). Our data show that in hemp stems, the expressions of PRX49 and PRX72, were higher under Cd/Zn treatment than in controls. Similarly, the abundance of PRX proteins increased (Figure 6.8; PRX4 and PRX15 for Cd, PRX72 for Zn). Lignification occurs during normal growth but also during defense responses: in hemp stems, the increased lignin-related transcripts could be a strategy to reduce HM entry into the cell by making the CW less permeable. Besides their role in lignification, PRXs may have a role in gelatinous CW modification. In experiments conducted by Behr et al. (2018),

S lignin staining and peroxidase activity were overlapping in bast fibres, and they observed higher abundances of both transcripts (orthologs of *AtPRX49*, *AtPRX52* and *AtPRX72*) and proteins (orthologs of *AtPRX3*, *AtPRX52* and *AtPRX54*) at older stages of hemp development. Behr et al. (2019) also observed that in hemp, most of the signal of a peroxidase detected by the *CsaPRX64* antibody had a distribution in the G-layer, with a scarcity or absence of signal in the S1-layer. The developing G-layer of phloem fibres from the tree *Mallotus japonicus* also shows a peroxidase activity, despite the absence of lignin (Nakagawa et al., 2014). The peroxidase activity detected in the G-layer may thus be involved in gelatinous CW modification, or in cellular defense mechanisms, and could be affected by plant exposure to Cd or Zn. Moreover, *PRX72* participates in the biosynthesis of lignans, monolignol-derived molecules which may contribute to the hypolignification of bast fibres by subtracting monolignols from the lignin polymerization process (Behr, 2018). In lettuce and ryegrass, stem and root elongation is regulated by specific lignans, such as syringaresinol and sesamin (Yamauchi et al., 2015) and further experiments are thus required to precise the impact of Cd and Zn on lignan synthesis in hemp in relation to the observed root and shoot elongation decrease.

METS and *SAMS* are enzymes involved in the generation of methyl donors, required for G and S monolignol methylation (Shen et al., 2002; Behr et al., 2017; Tang et al., 2014). Their expression level decreased in the presence of Cd while a number of *SAMS* transcripts only slightly decreased in response to Zn excess. These genes are in general more expressed in the core tissue than in the cortical tissue (Guerriero et al., 2017d). Guerriero et al. (2017d) showed that the higher lignin content of the xylem tissues is correlated with an upregulation of the genes of the phenylpropanoid/monolignol pathway (*CAD*, *METS*, *SAMS*, *PAL*). We thus hypothesize that Cd-induced decrease in diameter and thickness of xylem vessels might be a consequence of *METS* and *SAMS* inhibition.

Xylan, the main hemicellulose of the SCW, was detected by LM10 antibody in xylem cells and the CW of primary bast fibres. In xylem cells, xylan is largely present in the lignifying SCW while in the bast fibres the G-layer is almost completely depleted in lignin and xylan (Behr, 2018). The chemical composition of xylan in these two tissues may be regulated to fulfil distinct functions, such as water conduction in xylem vessels and mechanical resistance in phloem fibres (Behr et al., 2019). The CW of primary bast fibres was more strongly labelled by the antibody in Cd-treated plants compared to

control ones. In xylem vessels, only Zn exposure affected the signal intensity (higher). Considering that LM10 recognizes unsubstituted or low substituted xylan (McCartney et al., 2005), the results obtained suggest a decreased substitution of xylan in these CW, which may contribute to a higher CW stiffness caused by the HM (Shrestha et al., 2019). Chemical analyses will validate this hypothesis.

Pectin is considered as the main binding site for Cd. Structural changes frequently appear in the composition of pectic polysaccharide in plants exposed to Cd (Gutsch et al., 2019b). A variety of enzymes, including pectinesterase, β -like galactosidase, α -galactosidase are acting on the pectin network. This is especially the case for enhancement of pectin methylesterases (PME) which allow demethylesterification of homogalacturonan thus creating binding sites for Cd and avoiding its entry in cytosol (Hu et al., 2010; Gutsch et al., 2018). In Cd-treated plants, compared to control ones, the abundance of glucuronate 4-epimerase 6 (GAE6), involved in pectin synthesis, was decreased. We did not record any impact of heavy metals or Si treatment on PME abundance in our hemp samples. It has however to be mentioned that Zn excess triggered pectin acetylerase accumulation. Pectin acetylerase (E.C. 3.1.1.6; PAE) cleaves the acetyler bond from pectin, especially in homogalacturonan where GalA residues can be acetylated at positions O-2 or O-3, also creating available binding sites for divalent cation binding.

5. Conclusion

It is concluded that Cd and Zn reduced bast fibre diameter in hemp and that Cd negatively affected lignin and cellulose synthesis while Zn had an opposite effect on cellulose. The two considered heavy metals had distinct effects on gene expression and specific protein synthesis. Silicon did not significantly improve plant growth on a short-term basis but slightly decreased Cd content in roots and stems and had a specific impact on protein regulation in plants exposed to Cd stress. Moreover, Si increased bast fibre diameter in Cd-treated plants, and its application in Cd and Zn-treated plants was shown to have an influence on the timing of fibre elongation and transition from elongation to thickening. Silicon application may thus have a beneficial impact on the properties of the harvested fibres

Table S6.1: Primers used for gene expression designed using Primer3Plus (<http://www.bioinformatics.nl/cgi-bin/primer3plus/primer3plus.cgi/>) and verified with the OligoAnalyzer 3.1 tool (Integrated DNA technologies, <http://eu.idtdna.com/calc/analyzer>). Genes correspond to cell wall cellulose synthase (synthases (*CesA4*, *CesA7*, *CesA8*), Protodermal factor 1 (*PDF1*) fasciclin-like arabinogalactan protein (*FLA3*, *FLA11*, *FLA13*, *FLA19*) methyltransferase (*MET1*), S-adenosylmethionine synthase (*SAMS*) and class-III peroxidases (*PRX49*, *PRX 52*, *PRX 72*).

Targeted genes	Contig	Primer forward	Primer reverse	Amplicon length	Reference
acid phosphatase, <i>ATIG04040</i>		TTATTGGGATGG TGGGGAAC	GTCTTCAAGT TGGCGTTGG		
<i>CesA4</i>	contig 804	GGGGTGAATGC TAAGACTG	GGCTCCATTT CCCCAAAC	130	
<i>CesA7</i>	contig 6418	CCTGATGTCAAG CAATGTGG	TGATCTTGTG GGGATGCAC	91	Behr et al., 2016
<i>CesA8</i>	contig 9355	GGGAGCCAAAGG AACCTG	GAGCTGTTAC CACAAGTGTTA C	74	Behr et al., 2016
<i>FLA3</i>	Genomic scaffold82789	GCCCAAGCACCA ATTACATC	TTTTGAGGAGG TGGACGAAG	136	Guerriero et al., 2017d
<i>FLA11</i>		TTTTGGAACGGC TACAGCTC	GCACCAGAATC GTCATCATC	129	Guerriero et al., 2017d
<i>FLA13</i>		TACAACGGAGGG AAACTTCG	CGCTTTCGAGC CAAAGATAC	142	Guerriero et al., 2017d
<i>FLA19</i>		ACATCATCATCG TCGCCAAC	GCAACAAGAAT GGAGATCGTG	127	Guerriero et al., 2017d
<i>MET1</i>	EST00122 Hemp Uni-ZAP XR cDNA library	TGCCACTGTTCT GCTATGG	TTGCACTGCCT TGTGTGATG		Behr et al., 2018
<i>PDF1</i>		TTTGGGGTATTGT TGGTGAC	TGGTACATTGG GTTGGGAAG		
<i>PRX49</i>	<i>csa_locus_510_iso_2_len_1175_ver_2</i>	GACTTGGGAATT CGTTGACC	CAACCCCAAC ACTTTTGAC		Behr et al., 2018
<i>PRX52</i>	<i>csa_locus_2704_iso_2_len_1193_ver_2</i>	TAAGGCCAGGT TGAGAAAG	TTCCAATCAGG TCCTCCAAG		Behr et al., 2018
<i>PRX72</i>	<i>csa_locus_10948_iso_2_len_1210_ver_2</i>	CACAGCTTAGAA ACCGATGC	CCTTTGAGGCC AACAAGTTC	96	Behr et al., 2018
<i>SAM</i>	<i>csa_locus_10479_iso_4_len_1500_ver_2</i>	TGGTTTACATCG AGCAGCAG	TCACCAGTCC AATTTCCTC	88	

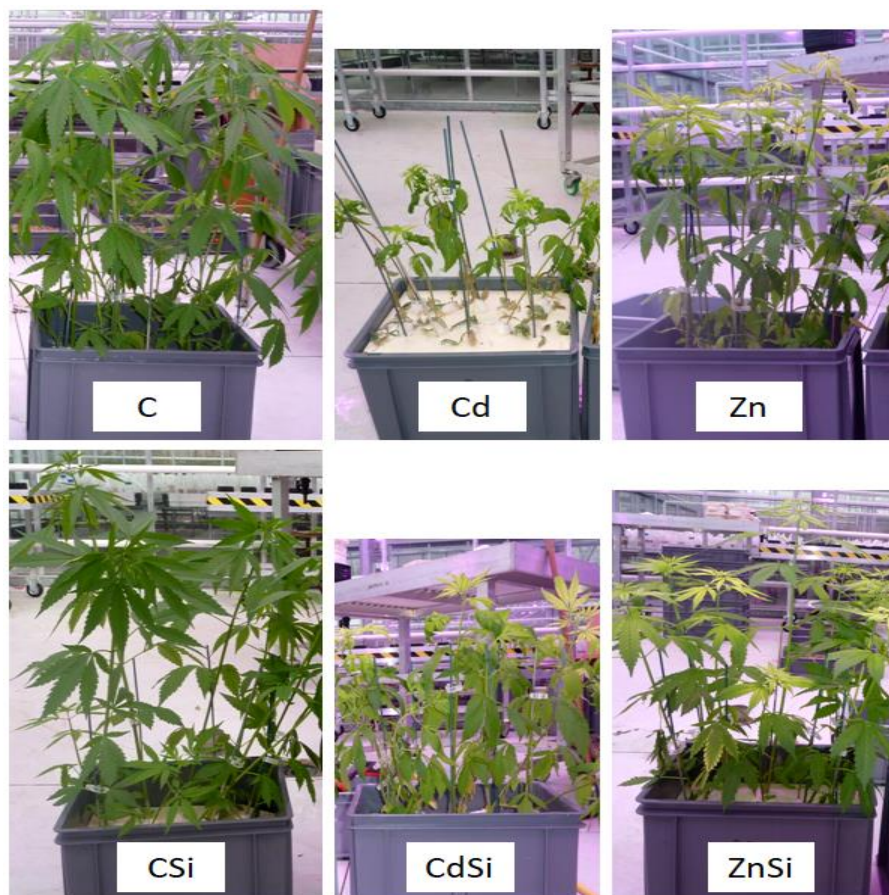


Figure S6.1. Plants of *Cannabis sativa* (cv. Santhixa 27) exposed for one week to Cd (20 μM) or Zn (100 μM) in the presence or absence of Si (2mM) (C: control plants not exposed to heavy metals). Plants exposed to Cd appeared partially wilted and their behavior was improved in response to additional Si.

Chapter 6: Highlights and Perspectives

In this Chapter we used nutrient solution to discriminate between the impact of Cd (20 μM), Zn (100 μM) and Si (2 mM) on fibre differentiation in relation to HM accumulation in young stem of *C. sativa*. The expression of genes regulating fibre development was analysed and the proteome of hypocotyls was characterized.

We demonstrated that (Figure 6.9):

- Both Cd and Zn reduced the diameter of primary bast fibres.
- Cd negatively affected cellulose and lignin biosynthesis and decreased substitution of xylan in fibres, while Zn had an opposite impact on cellulose metabolism.
- Only a minor proportion of proteins were affected by both Cd and Zn, suggesting that the two heavy metals have a quite different impact on protein regulation in *C. sativa*.
- Si
 - Had a specific impact on some proteins observed in CSi, CdSi or ZnSi treatments comparatively to C, Cd or Zn treatments respectively.
 - Increased the diameter of bast fibre in Cd-treated plants.

It has to be mentioned that, in this Chapter, our approach was performed on whole stem segments and not on isolated bast fibers. Our sample contained both bast fibres in the cortical part of the stem and xylem tissues in the core. A part of the gene expressed under HM exposure may therefore regulate the deposition of the SCW in both tissues

Besides, determining pollutant distribution in stems is of paramount importance to determine applicative value of combined phytomanagement and fibre production and the resulting risks for users, but only data regarding total ion concentration in plant organs are available in the literature. In Chapter 7, we therefore analyzed the impact of 20 μM Cd or 100 μM Zn and/or 2mM Si treatments on ions distribution in stems of *C. sativa* at tissue and cell level.

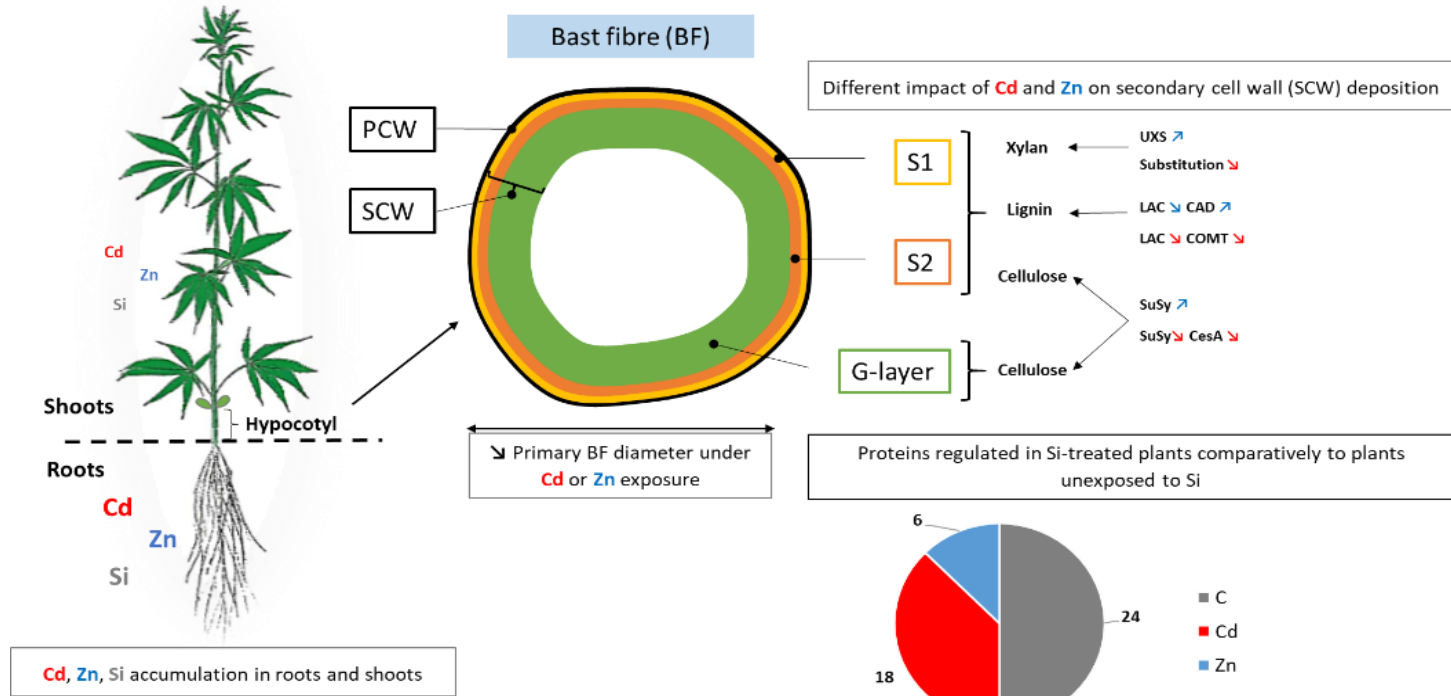


Figure 6.9: Summary of the results obtained in Chapter 6. Primary cell wall (PCW), secondary cell wall (SCW), bast fibres (BF). Blue arrows indicate a significant increase/decrease of protein abundance following Zn exposure, while red arrows illustrate the significant results induced by Cd exposure.

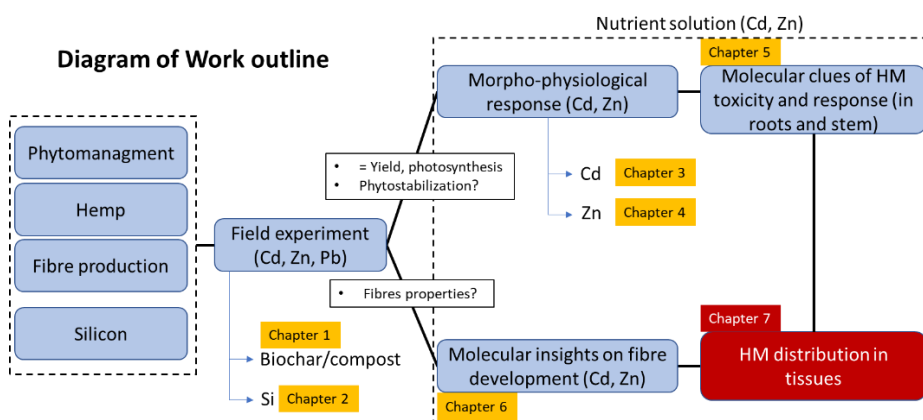
Chapter 7

Impact of Silicon and Heavy Metals on Hemp (*Cannabis sativa* L.) ions distribution in roots, stems and leaves at tissue and cell level

Marie Luyckx, Gea Guerriero, Stanley Lutts, Katarina Vogel-Mikuš.

Author's contributions

ML, KV and SL designed methodology; ML performed the whole experiment, treated and ML and KV analyzed the data; KV and SL supervised the whole research process; ML and SL wrote the original draft; All authors reviewed the manuscript.



Abstract

The impact of 20 μM Cd or 100 μM Zn and/or 2mM Si treatments on ions distribution in roots, stems and leaves of *Cannabis sativa* at tissue and cell level was addressed. Micro-proton-induced X-ray emission imaging indicated that heavy metals preferentially accumulated in CW of cortex cells in roots, while in stems hotspots of Cd concentrations were found in trichomes. In leaves, Cd was preferentially accumulated in collenchyma cells while Zn accumulated in trichomes and within spongy mesophyll cells, indicating a mechanism of protecting sensitive and metabolically more active tissues from metal toxicity. Silicon application increased Cd retention in root endodermis and increased Cd sequestration in leaf trichomes. Within hemp roots, stems and leaves, elemental distribution also showed clear alterations after HM exposure, especially after Cd stress.

1. Introduction

Heavy metal (HM) pollution is a major environmental problem faced by the modern world (Mishra et al., 2019). Heavy metals can cause phytotoxicity by strongly impacting plant physiology and development, and is a serious threat to animal/human health, once plants enter the trophic chain (Khan et al., 2015; Berni et al., 2019).

Zinc and cadmium are frequently simultaneously found in contaminated soils, including agronomic soils contaminated by atmospheric fallout near smelters (Luyckx et al., 2021a). Zinc and Cd share many similar physiochemical properties, but their compartmentation, complexation and impact on other mineral element distribution in plant tissues may drastically differ (Lefèvre et al., 2014). Cadmium belongs to the category of non-essential trace elements, and is absorbed by other metal transporters and non-selective cation channels (Zeng et al., 2017; Luyckx et al., 2021b). In plants, Cd toxicity may consequently result from a disturbance in uptake and translocation of other divalent cations (Ca, Mg, Fe, Zn, Mn, and Cu), and disturbance in plant metabolism, inhibiting plant growth and development (Shiyu et al., 2020; Luyckx et al., 2021b). As an essential element, Zn plays essential metabolic roles in plants. This element is notably a structural component of a variety of metalloenzymes like carbonic anhydrase, alcohol dehydrogenase, Cu-Zn superoxide dismutase and RNA polymerase (Reviewed by Lefèvre et al., 2014). Zinc thus plays an important role in regulating nitrogen metabolism,

cell multiplication, photosynthesis and in the synthesis of nucleic acid, carbohydrates, proteins and auxins. However, above the plant requirements, this element becomes toxic (Lefèvre et al., 2014).

In order to avoid toxicity and to maintain homeostasis and consequent optimal cell functioning and integrity, proper allocation of elements at organ, tissue, cellular and subcellular level is needed (Vogel-Mikus et al., 2014). In addition, element/metal speciation and ligand environment present a key to bioavailability and homeostasis in organisms (Vogel-Mikus et al., 2014). Several mechanisms coordinate to help a plant to withstand HM stress, such as the reduction of HM uptake, the decrease of HM root-to-shoot translocation, and the stimulation of antioxidant enzyme activities, and production of phytochelatin (Nawaz et al., 2019; Shiyu et al., 2020). In this respect, silicon (Si) has been found associated with amelioration of HM stresses in plants (Nawaz et al., 2019). Silicon can deposit in the vicinity of the endodermis, thus contributing to reinforce the barrier against Cd translocation (Shi et al. 2005; Imtiaz et al. 2016). Adrees et al. (2015) also reported that Si is suspected to influence the root-to-shoot translocation of HM. Moreover, Si can accumulate within the parietal structures where it is present in the form of opaline silica (SiO_2) (Kröger and Poulsen 2004). Lignin-bound silica in cell-walls may create complexes with metal ions and thus reduces the transfer of metal ions. Ma, et al. (2015) reported that hemicellulose-bound silica with a net negative charge inhibits cadmium uptake in rice by Cd complexation and subsequent co-deposition.

Hemp is an annual high yielding industrial crop grown for its fibres and seeds (Pejic et al., 2009; Morin-Crini et al., 2019). The stem differentiates primary and secondary bast fibres associated with the conductive elements of phloem, and woody core fibres, called hurds or shivs, located in the xylem (Angelova et al., 2004; Guerriero et al., 2013; Behr, 2018; Morin-Crini et al., 2019). The plant has already been considered as a good candidate for fibre production and/or phytomanagement on moderately heavy metal-contaminated soils (Luyckx et al., 2021b). Phytomanagement is a soil management strategy where plants are cultivated to extract, degrade, or immobilize various contaminants from polluted soils (Barceló and Poschenrieder 2003; Ali et al. 2013). The use of hemp to valorise these marginal farmland soils and provide incomes for the farmer partly depends on the HM distribution at the whole plant level. Besides, hemp fibres are one of the most promising materials for biosorption of metal ions from diluted waste streams (Morin-Crini et al., 2019). Heavy metals could therefore strongly

interact with cell wall polymers *in planta*, as recently demonstrated for *Medicago sativa* (Gutsch et al. 2019a) or *Kosteletzkya pentacarpos* (Zhou et al. 2018), and affect fibres' quality.

Studies of element localization, as well as speciation and ligand environment, are therefore crucial to reveal the mechanisms of element trafficking and also tolerance and toxicity (Vogel-Mikus et al., 2014). Moreover, determining pollutant distribution in stems is of paramount importance to determine applicative value of combined phytomanagement and fibre production and the resulting risks for users. The present work was therefore undertaken in order to determine the impact of 20 μM Cd or 100 μM Zn and/or 2mM Si treatments on ions distribution in roots, stems and leaves of *Cannabis sativa* at tissue and cell level.

2. Material and Methods

2.1. Plant material and growing conditions

Seeds of a monoecious hemp fibre variety (*C. sativa* cv. Santhica 27) were sown in loam substrate in greenhouse conditions. After one week, the obtained seedlings were transferred to nutrient Hoagland solution in 5 L tanks, as described in Chapter 3 (p. 141). Tanks were placed in a phytotron under fully controlled environmental conditions (permanent temperature of $24 \pm 1^\circ\text{C}$ with a mean light intensity of $230 \mu\text{moles m}^{-2}\text{s}^{-1}$ provided by Phillips lamps (Philips Lighting S.A., Brussels, Belgium) (HPI-T 400 W), with a photoperiod of 16h under a relative humidity of 65%). After a week of acclimatization, half of the tanks received 2 mM Si in the form of metasilicic acid (H_2SiO_3) obtained from a pentahydrate sodium metasilicate ($\text{Na}_2\text{SiO}_3 \cdot 5 \text{H}_2\text{O}$) which was passed through an H^+ ion exchanger resin IR 20 Amberlite type according to Dufey et al. (2014). Tanks were randomly arranged in the phytotron and nutrient solution was permanently aerated by SuperFish Air Flow 4 pump. A week later, HM were then applied in the form of CdCl_2 (final concentration of 20 μM) and ZnCl_2 (100 μM). The pH of the solution was maintained at 5.5. Solubility of added HM was confirmed by the Visual MINTEQ09 software. Six treatments were thus defined, considering the presence of HM and the concomitant presence or absence of Si i.e. C (control: no HM and no Si), CSi, Cd, CdSi, Zn and ZnSi (4 tanks per treatment). Plants were harvested after one week of treatment. Roots were separated from shoots, and leaves were separated from the stem. Leaves from the second node from the bottom, will

be hereafter designated as L2. L2 were formed before stress application. Element distribution and EXAFS were investigated in roots, stem and leaves (L2).

2.2. Sample preparation for micro-PIXE analysis

Segments of stem in the internode containing the SP, of roots, and of L2 (sectioned to smaller pieces of ca. 2 mm x 5 mm) were rapidly excised with a scalpel from fresh plants (Figure 7.1). The pieces were immediately inserted into a 2 mm stainless steel needle and dipped into tissue freezing media (Jung, Leica, Germany), and rapidly frozen in liquid propane cooled by liquid nitrogen (Vogel-Mikuš et al. 2008b). The plant pieces were next sectioned at 60 μm thickness with a Leica CM3050 cryotome (Leica, Bensheim, Germany), placed in Al holders and transferred to an Alpha 2–4 Christ freeze dryer (- 50 $^{\circ}\text{C}$, 0.04 mbar, 3 days). The frozen-hydrated sections were mounted on the Al sample holder between two thin layers of Pioloform foil (SPI Chem).



Figure 7.1: Segments of leaf (L2, a), stem in the internode containing the SP (b), and root (c). CT: transversal cutting.

2.3. Micro-PIXE analysis

The measurements by micro-PIXE and data evaluation for the biological samples of intermediate thickness were performed at the micro-PIXE set-up at Jožef Stefan Institute (Slovenia) as previously described in detail (Vogel-Mikuš et al. 2008b; Lefèvre et al., 2014). An on-off axis scanning transmission ion microscopy (STIM) was performed to determine beam exit energy from the sample, related to the sample local areal density

(Pallon *et al.* 2004). The proton dose was determined by a rotating in-beam chopper (Vogel-Mikuš *et al.* 2008b).

For the generation of the elemental images, dynamic analysis methods were used (Ryan 2000), which are an essential part of GeoPIXE II software package. For the evaluation of Cd concentrations, the Cd K α line at 23.17 keV was used, as the Cd L lines overlaps with the pronounced K α line of potassium (Vogel-Mikuš *et al.* 2008b). The calibration of the PIXE method was verified by the analysis of the multi-elemental standard reference materials NIST SRM 1573a (tomato leaves, homogenized powder, analysed in the form of a pressed pellet), NIST SRM 1107 (Naval Brass B, alloy) and NIST SRM 620 (Soda-Lime Flat Glass), as well as in the intercomparison with ICP-MS, neutron activation and Roentgen fluorescence method (Nečemer *et al.* 2008). The inter-calibration of PIXE and STIM was verified by thin mono-elemental metallic foils.

Using GEOPIXEII software for quantitative analysis, fully quantitative images were generated and exported in ASCII code in order to generate numerical matrices separately for each element of interest (Vogel-Mikuš *et al.* 2008b). ASCII files generated by GEOPIXEII were imported to ImageJ programme (<http://www.macbiophotonics.ca/imagej/>) as text files, generating 32-bit gray-scale images where the information of concentration of particular element is retained in each pixel. With brush selection tool, we extracted the mean concentrations from selected regions, representing for example particular tissue (Vogel-Mikuš *et al.* 2008b).

Freeze-dried leaf cross-sections were photographed using a digital camera (AxioCam) mounted on a Stem SV 11 (Carl Zeiss, Göttingen, Germany) stereomicroscope.

2.4. Scanning electron microscopy (SEM-EDX)

Simultaneous with the micro-PIXE mapping, SEM-EDX was carried out to determine Si distribution in our plant samples. For the evaluation of Si concentrations, a gold coating of 10 nm was used. The accelerating voltage was of 15kV. Three detectors were used: Secondary Superior Electron Imaging (SEI), Low Angle Backscattered Electron Imaging (LBE) and Lower Secondary Electron Imaging (LEI). For Si mapping, the parameters used are 10kV, Probe current of 15, dead time = 15% and 1500 counts per seconds.

2.5. Microscopic determination of lignification in stems

Hemp stems sections of 5 mm in the internode containing the SP were collected, fixed in FAA (70% ethanol:acetic acid: formaldehyde, 18:1:1 by vol.), dehydrated in a graded ethanol series, embedded in paraffin, and sectioned at 10 μm . Serial transversal sections were stained with safranin-fast green and observed with a light microscope.

3. Results

3.1. Histological description of root, stem and leaf in hemp

To ensure a good understanding of the element distribution maps, the main tissues of roots, stems and leaves are captioned in Figure 7.2.

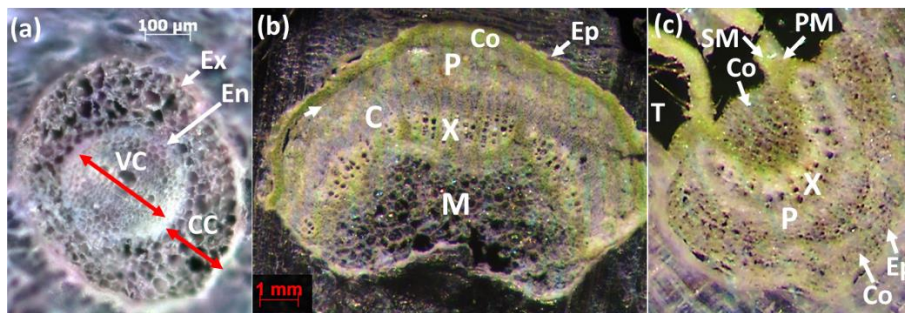


Figure 7.2: Photographs of a representative (a) root, (b) stem, and (c) leaf cross sections of *C. sativa* as analysed by light microscopy. Exodermis (Ex), endodermis (En), cortex cells (CC), vascular cylinder (VC), epidermis (Ep), collenchyma cells (Co), phloem (P), cambium (C), xylem (X), pith (M), palisade mesophyll (PM), spongy mesophyll (SM), trichome (T).

3.2.Element concentration and distribution within root tissues

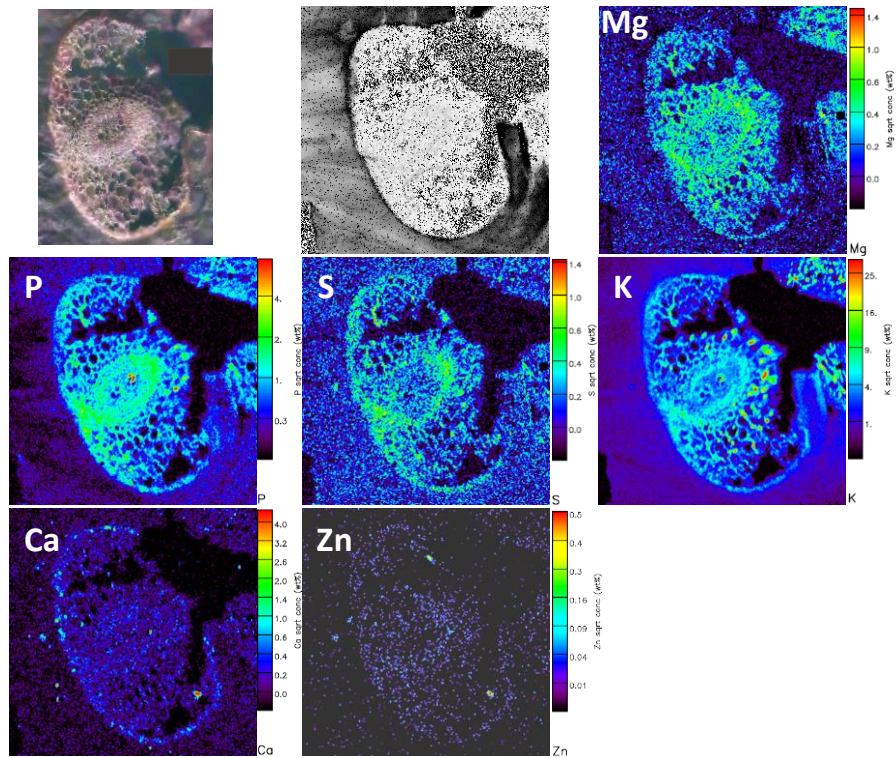


Figure 7.3: Photographs of a representative root cross section of *C. sativa* as analysed by light microscopy (upper left), and the associated quantitative elemental maps of Mg, P, S, K, Ca and Zn generated with GEOPIXE II software package after microPIXE analysis. Colored bars are not of the same order of magnitude among the elements. Scan size, $850 \mu\text{m} \times 850 \mu\text{m}$.

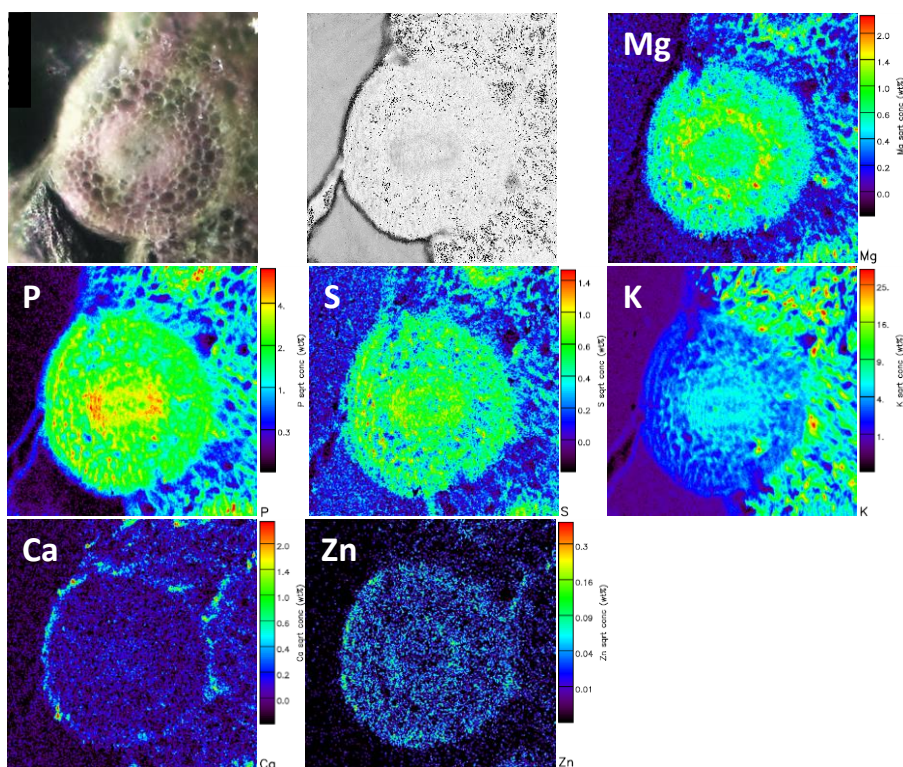


Figure 7.4: Photographs of a representative root cross section of *C. sativa* treated with 2 mM Si during 2 weeks as analysed by light microscopy (upper left), and the associated quantitative elemental maps of Mg, P, S, K, Ca and Zn generated with GEOPIXE II software package after micro-PIXE analysis. Colored bars are not of the same order of magnitude among the elements. Scan size, $400\ \mu\text{m} \times 400\ \mu\text{m}$.

Figure 7.3 obtained by micro-PIXE analysis, shows a representative example of element distribution in a root cross section of *C. sativa*, while Figure 7.4. shows controls treated with 2 mm Si. In both controls and Si-treated plants, Ca was mainly located in epidermis, Mg was mainly found in endodermis, P was mainly found in the vascular cylinder, while Zn, K and S were more homogeneously distributed in the root section. In control, S seemed to be mainly located in cell walls (CW), while it was more homogeneously distributed in CSi treatment.

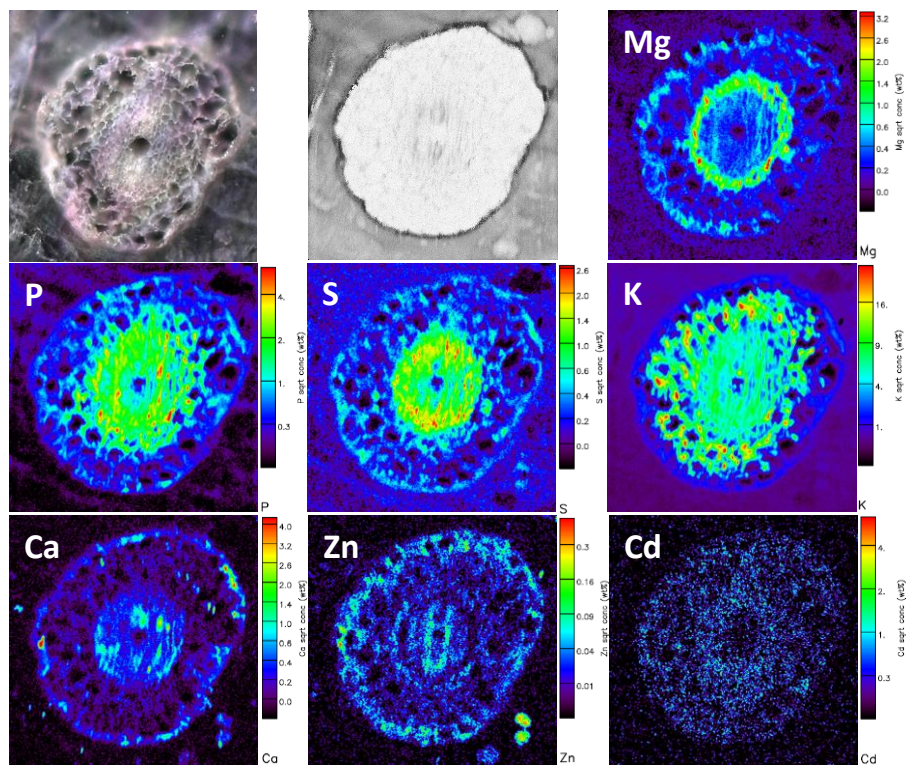


Figure 7.5: Photographs of a representative root cross section of *C. sativa* treated with $20\ \mu\text{M}$ Cd during 1 weeks as analysed by light microscopy (upper left), and the associated quantitative elemental maps of Mg, P, S, K, Ca, Zn and Cd generated with GEOPIXE II software package after micro-PIXE analysis. Colored bars are not of the same order of magnitude among the elements. Scan size, $450\ \mu\text{m} \times 450\ \mu\text{m}$.

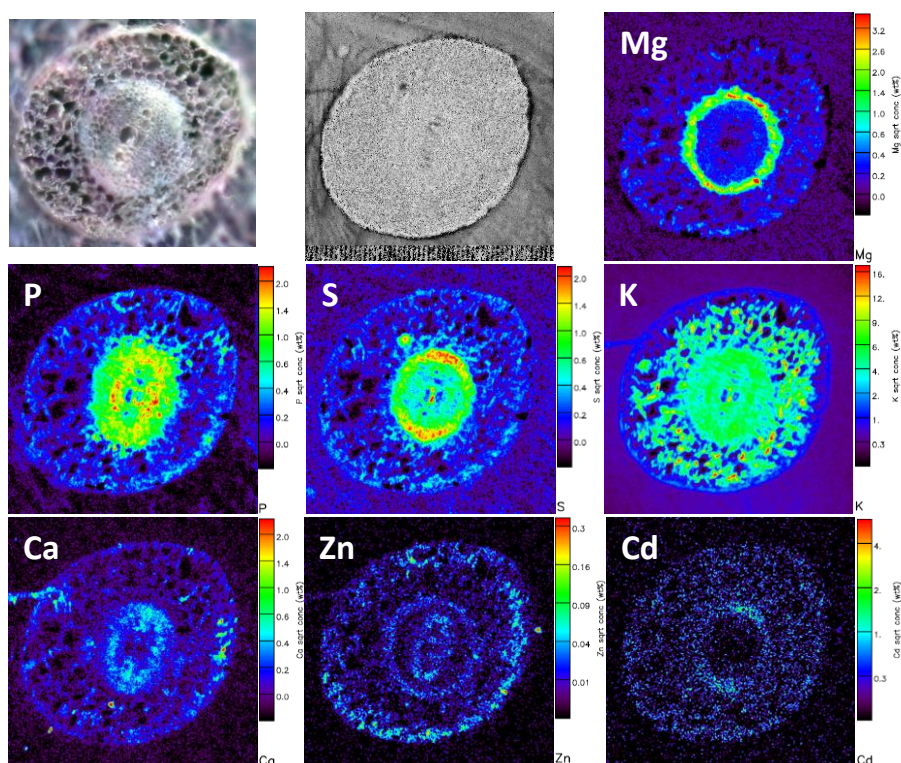


Figure 7.6: Photographs of a representative root cross section of *C. sativa* treated with 2mM Si during 2 weeks and 20 μ M Cd during 1 weeks as analysed by light microscopy (upper left), and the associated quantitative elemental maps of Mg, P, S, K, Ca, Zn and Cd generated with GEOPIXE II software package after micro-PIXE analysis. Colored bars are not of the same order of magnitude among the elements. Scan size, 650 μ m \times 650 μ m.

In Cd treatment, Cd was found to be quite homogeneously distributed in CW of cortex cells, with lower concentration in the vascular cylinder (Figure 7.5). Besides, hemp exposure to Cd (Cd and CdSi treatments) induced an increase of: Mg accumulation in endodermis, S accumulation in vascular cylinder, and Zn accumulation in epidermis. Moreover, in Cd treated plants, Si exposure increased Cd accumulation in endodermis (Figure 7.6).

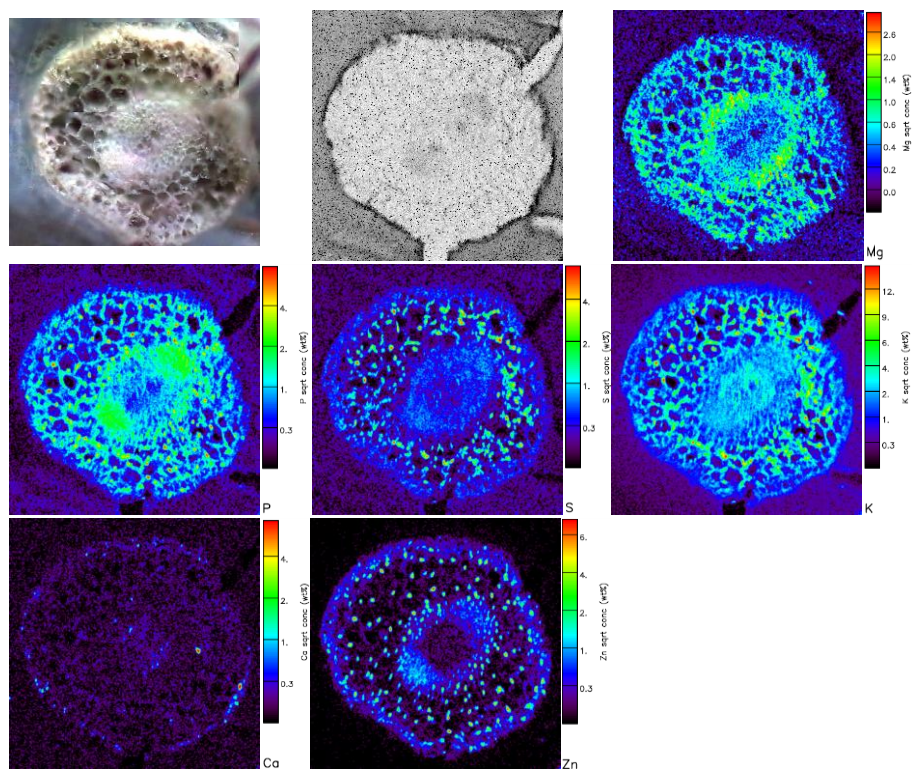


Figure 7.7: Photographs of a representative root cross section of *C. sativa* treated with $100\ \mu\text{M}$ Zn during 1 weeks as analysed by light microscopy (upper left), and the associated quantitative elemental maps of Mg, P, S, K, Ca and Zn generated with GEOPIXE II software package after micro-PIXE analysis. Colored bars are not of the same order of magnitude among the elements. Scan size, $700\ \mu\text{m} \times 700\ \mu\text{m}$.

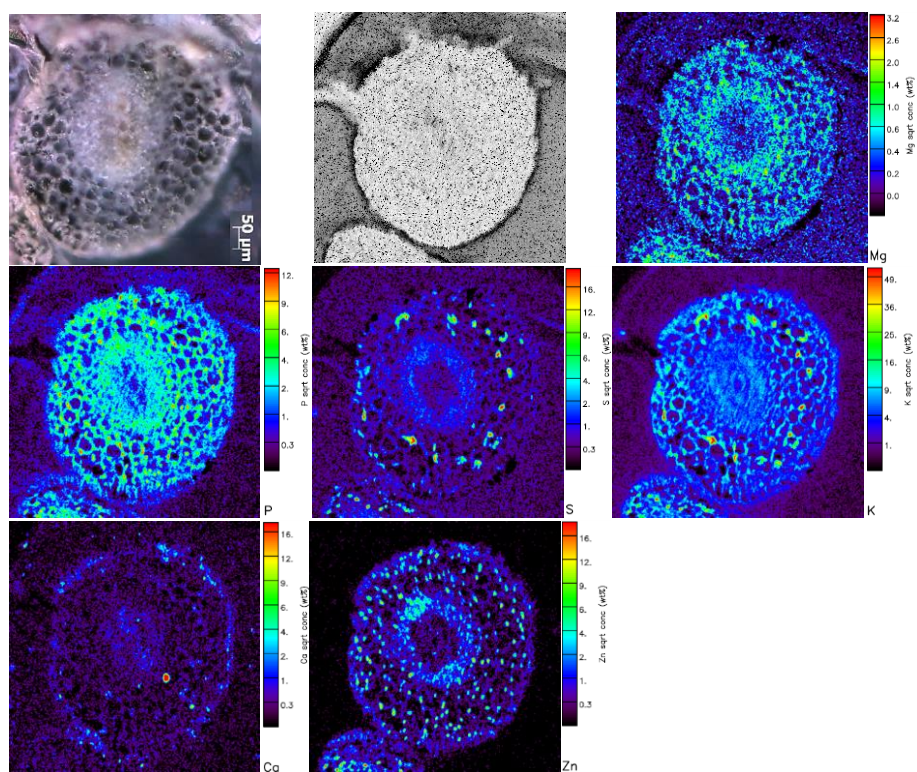


Figure 7.8: Photographs of a representative root cross section of *C. sativa* treated with 2mM Si during 2 weeks and 100 μ M Zn during 1 weeks as analysed by light microscopy (upper left), and the associated quantitative elemental maps of Mg, P, S, K, Ca and Zn generated with GEOPIXE II software package after micro-PIXE analysis. Colored bars are not of the same order of magnitude among the elements. Scan size, 650 μ m \times 650 μ m.

In roots exposed to 100 μ M Zn, Zn was mainly concentrated in CW of cortex cells (hotspots), as well as in epidermis and endodermis (Figure 7.7). In this treatment, Zn exposure induced an increased accumulation of S in CW of cortex cells (hotspots). Moreover, distributions of P and Zn seemed to be similar. Si exposure had not impact on elements distribution in Zn-treated plants, but decreased the number of S hotspots in the cortex (Figure 7.8).

3.3. Element concentration and distribution within stem tissues

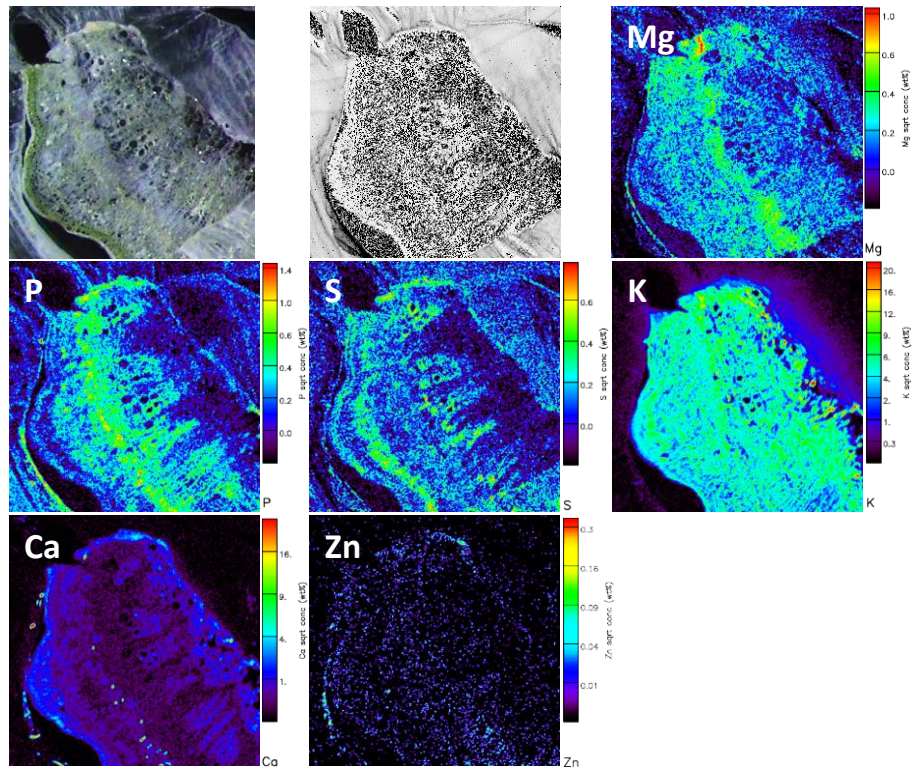


Figure 7.9: Photographs of a representative stem cross section of *C. sativa* as analysed by light microscopy (upper left), and the associated quantitative elemental maps of Mg, P, S, K, Ca and Zn generated with GEOPIXE II software package after microPIXE analysis. Colored bars are not of the same order of magnitude among the elements. Scan size, $1800\ \mu\text{m} \times 1800\ \mu\text{m}$.

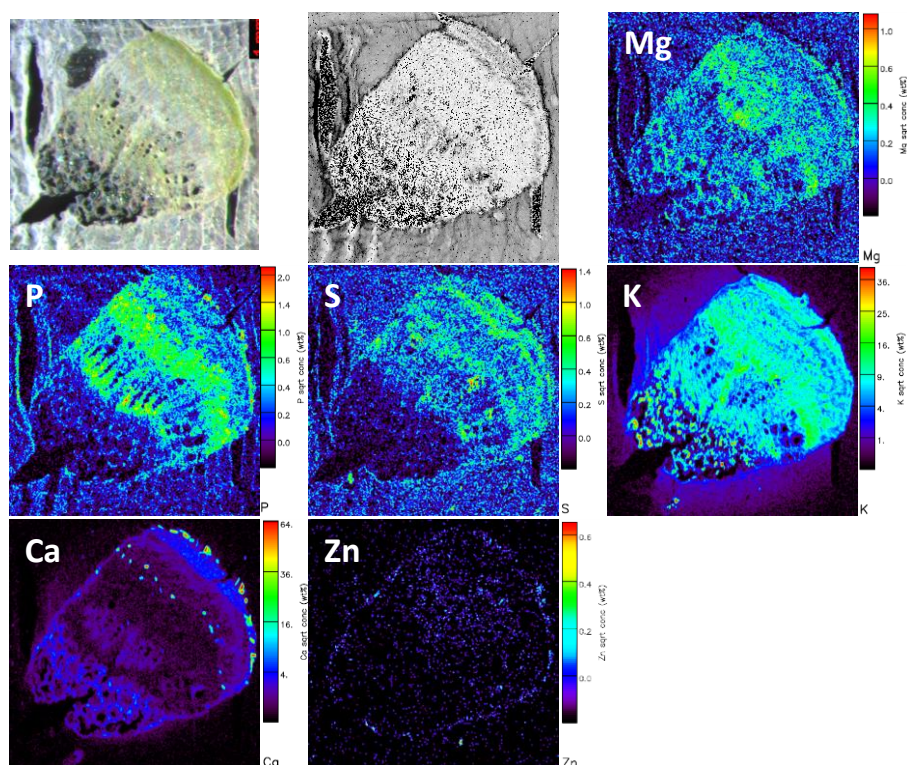


Figure 7.10: Photographs of a representative stem cross section of *C. sativa* treated with 2 mM Si during 2 weeks as analysed by light microscopy (upper left), and the associated quantitative elemental maps of Mg, P, S, K, Ca and Zn generated with GEOPIXE II software package after micro-PIXE analysis. Colored bars are not of the same order of magnitude among the elements. Scan size, $1800\ \mu\text{m} \times 1800\ \mu\text{m}$.

Figure 7.9 obtained by micro-PIXE analysis, shows a representative example of element distribution in a stem cross section of *C. sativa*, while Figure 7.10 shows plants treated with 2 mM Si. In both controls and Si-treated plants, S was mainly located in vascular tissues, Ca was mainly found in epidermis (trichomes) and as concentrated spots in phloem, while other elements were more homogeneously distributed. Si exposure in controls had no impact of elements distribution in stems.

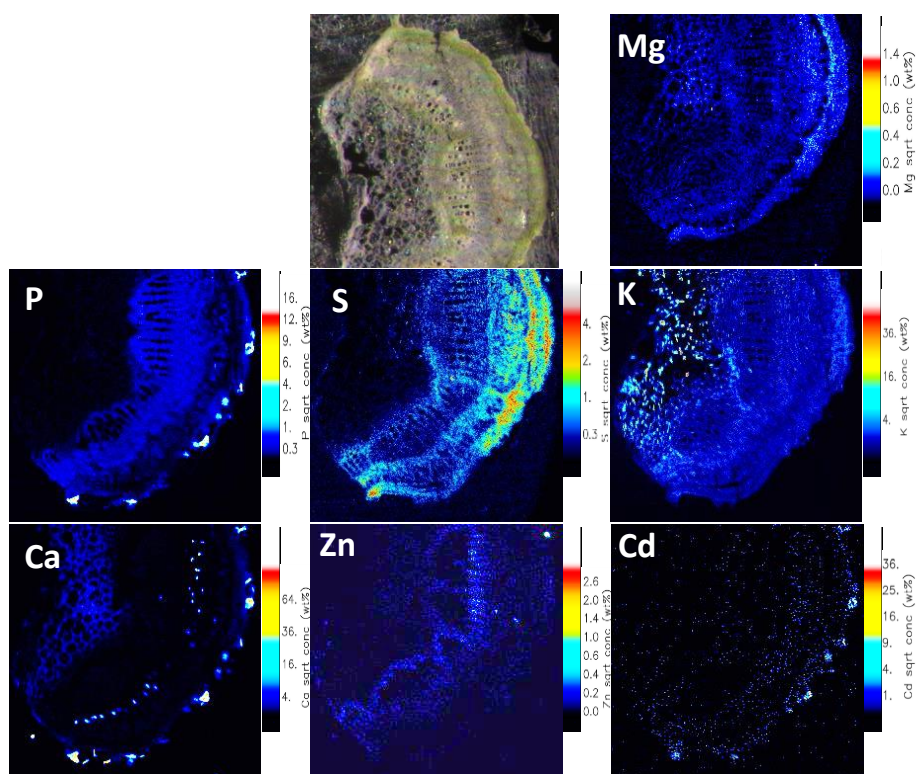


Figure 7.11: Photographs of a representative stem cross section of *C. sativa* treated with $20\ \mu\text{M}$ Cd during 1 weeks as analysed by light microscopy (upper left), and the associated quantitative elemental maps of Mg, P, S, K, Ca, Zn and Cd generated with GEOPIXE II software package after micro-PIXE analysis. Colored bars are not of the same order of magnitude among the elements. Scan size, $\mu\text{m} \times \mu\text{m}$.

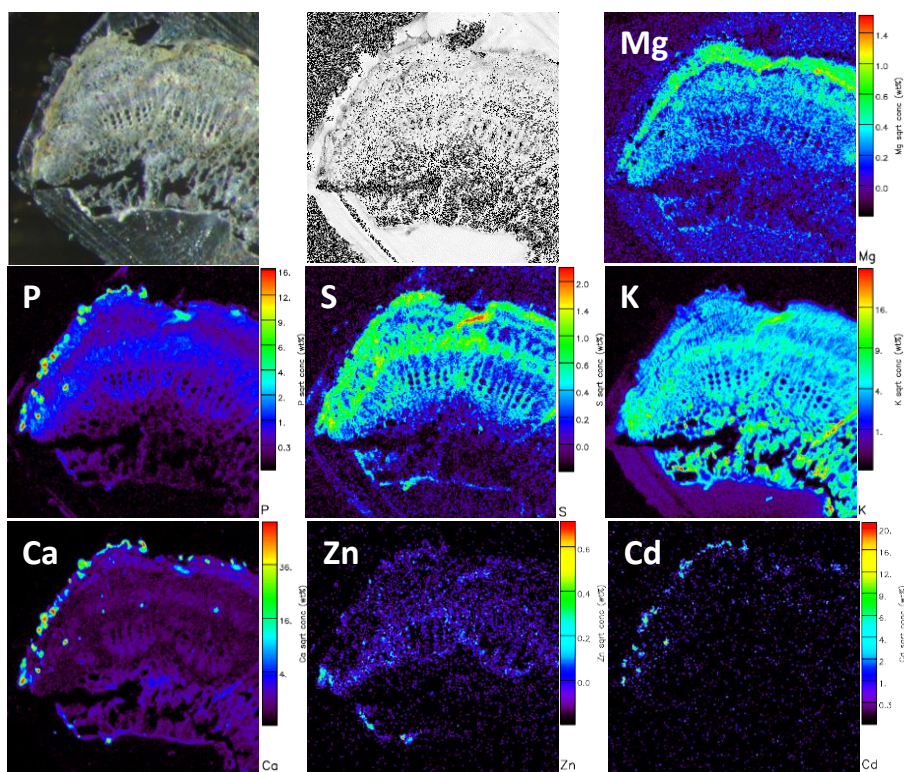


Figure 7.12: Photographs of a representative stem cross section of *C. sativa* treated with 2mM Si during 2 weeks and 20 μ M Cd during 1 weeks as analysed by light microscopy (upper left), and the associated quantitative elemental maps of Mg, P, S, K, Ca, Zn and Cd generated with GEOPIXE II software package after micro-PIXE analysis. Colored bars are not of the same order of magnitude among the elements. Scan size, 1700 μ m \times 1700 μ m.

In stems, the addition of Cd induced changes in Mg, P, S distributions: P was mainly distributed in epidermis (trichomes) and Mg and S distribution in collenchyma cells increased compared to controls (Figure 7.11). In both Cd and CdSi treatments, Cd was mainly found in trichomes, co-localised with P and Ca, and no differences in elements distribution between Cd and CdSi treatments were noticed (Figure 7.12).

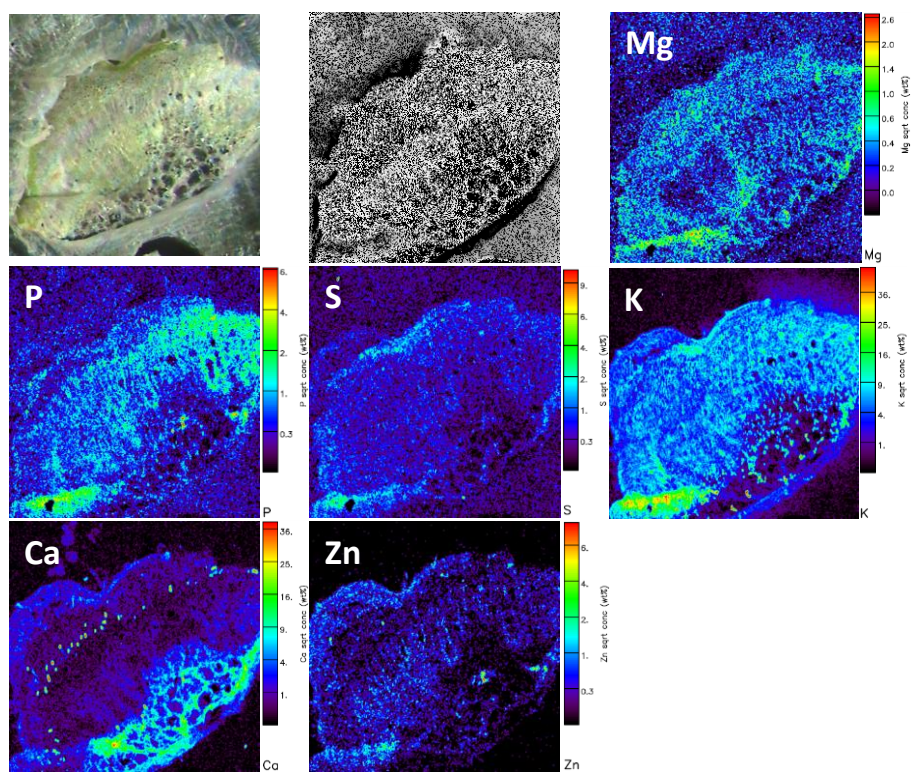


Figure 7.13: Photographs of a representative stem cross section of *C. sativa* treated with $100\ \mu\text{M}$ Zn during 1 weeks as analysed by light microscopy (upper left), and the associated quantitative elemental maps of Mg, P, S, K, Ca and Zn generated with GEOPIXE II software package after micro-PIXE analysis. Colored bars are not of the same order of magnitude among the elements. Scan size, $1600\ \mu\text{m} \times 1600\ \mu\text{m}$.

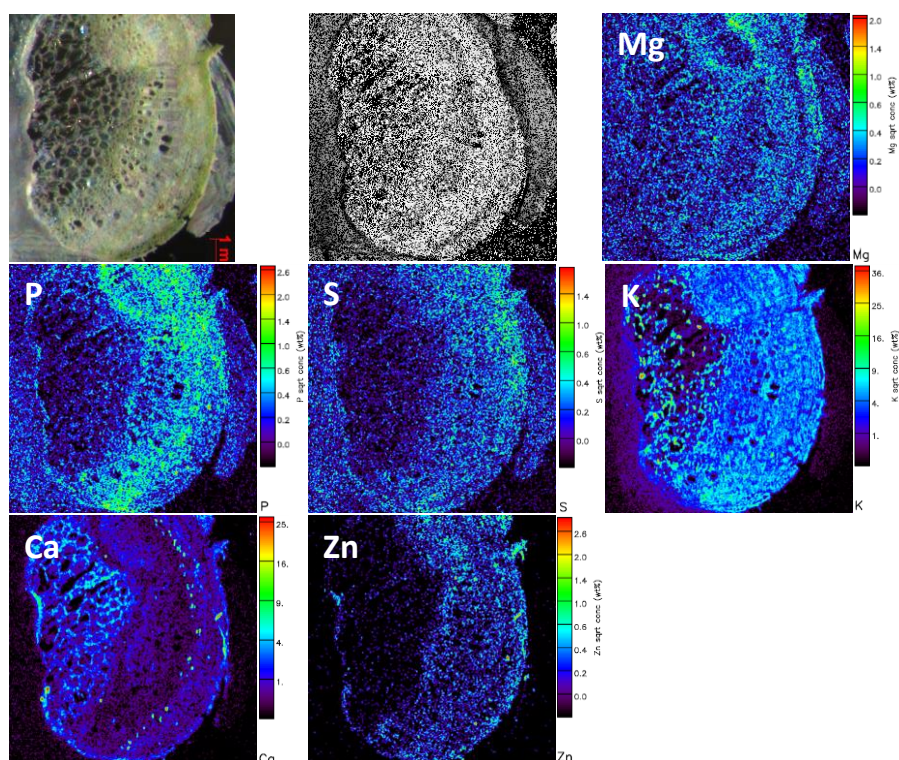


Figure 7.14: Photographs of a representative stem cross section of *C. sativa* treated with 2mM Si during 2 weeks and 100 μm Zn during 1 weeks as analysed by light microscopy (upper left), and the associated quantitative elemental maps of Mg, P, S, K, Ca and Zn generated with GEOPIXE II software package after micro-PIXE analysis. Colored bars are not of the same order of magnitude among the elements. Scan size, 1800 μm \times 1800 μm .

In plants exposed to Zn (Zn and ZnSi treatments), Mg and S were more homogeneously distributed than in controls, and Ca was found in the form of concentrated spots in phloem (as observed in controls), but also in CW of pith (Figures 7.13, 7.14). Zn was homogeneously distributed in all the stem section, with lower concentration in pith. No differences in elements distribution were noticed between Zn and ZnSi treatments.

3.4. Element concentration and distribution within leaf tissues

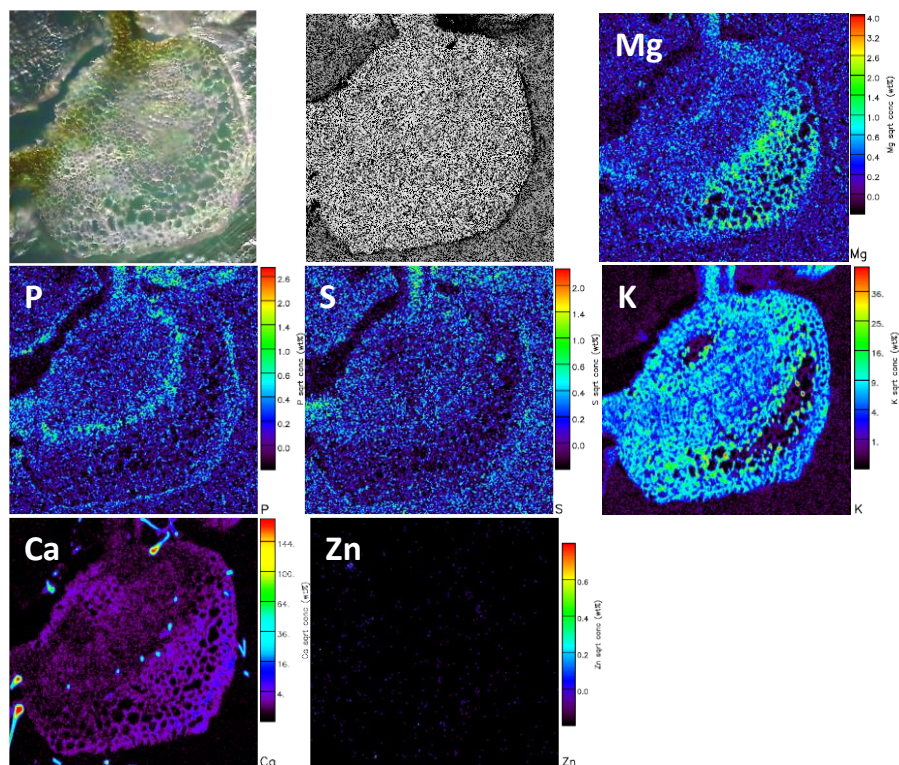


Figure 7.15: Photographs of a representative leaf cross section of *C. sativa* as analysed by light microscopy (upper left), and the associated quantitative elemental maps of Mg, P, S, K, Ca and Zn generated with GEOPIXE II software package after microPIXE analysis. Colored bars are not of the same order of magnitude among the elements. Scan size, $1100\ \mu\text{m} \times 1100\ \mu\text{m}$.

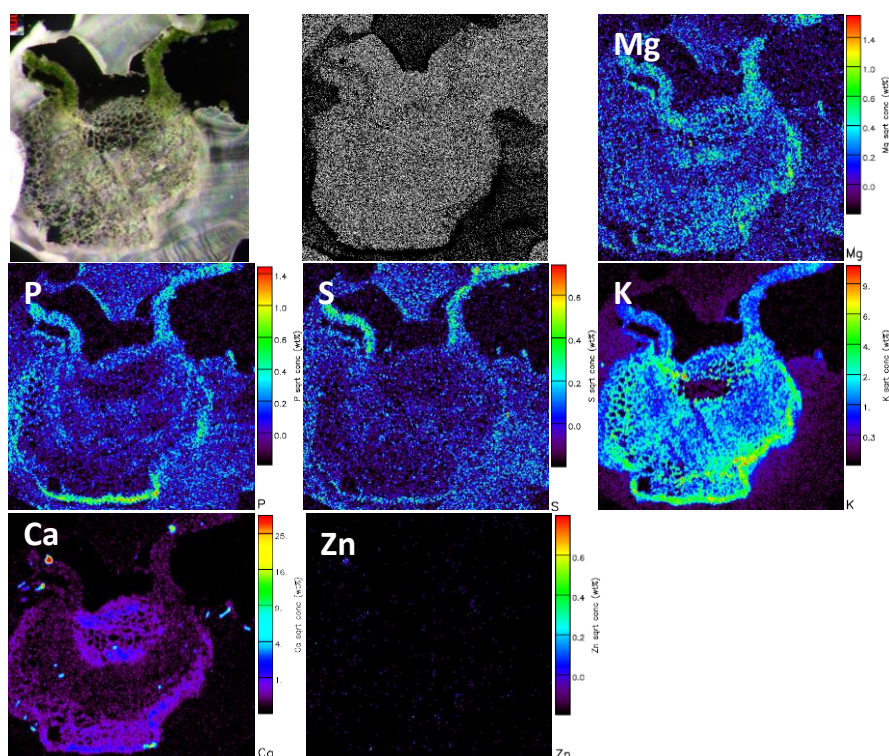


Figure 7.16: Photographs of a representative leaf cross section of *C. sativa* treated with 2 mM Si during 2 weeks as analysed by light microscopy (upper left), and the associated quantitative elemental maps of Mg, P, S, K, Ca and Zn generated with GEOPIXE II software package after micro-PIXE analysis. Colored bars are not of the same order of magnitude among the elements. Scan size, $1800\ \mu\text{m} \times 1800\ \mu\text{m}$.

In the leaf cross sections of *Cannabis sativa* (Figure 7.15), Mg was mainly found in parenchyma cells below the vascular bundle, P was mainly distributed in the phloem region and in palisade mesophyll in mesophyll, S was mainly found in palisade mesophyll, while K and Zn were homogeneously distributed within leaf tissues. Ca was distributed in the form of concentrated spots lining the phloem, and in trichomes. When exposed to Si, control plants exhibited lower P distribution in vascular bundle and a more homogeneous distribution of Mg (Figure 7.16).

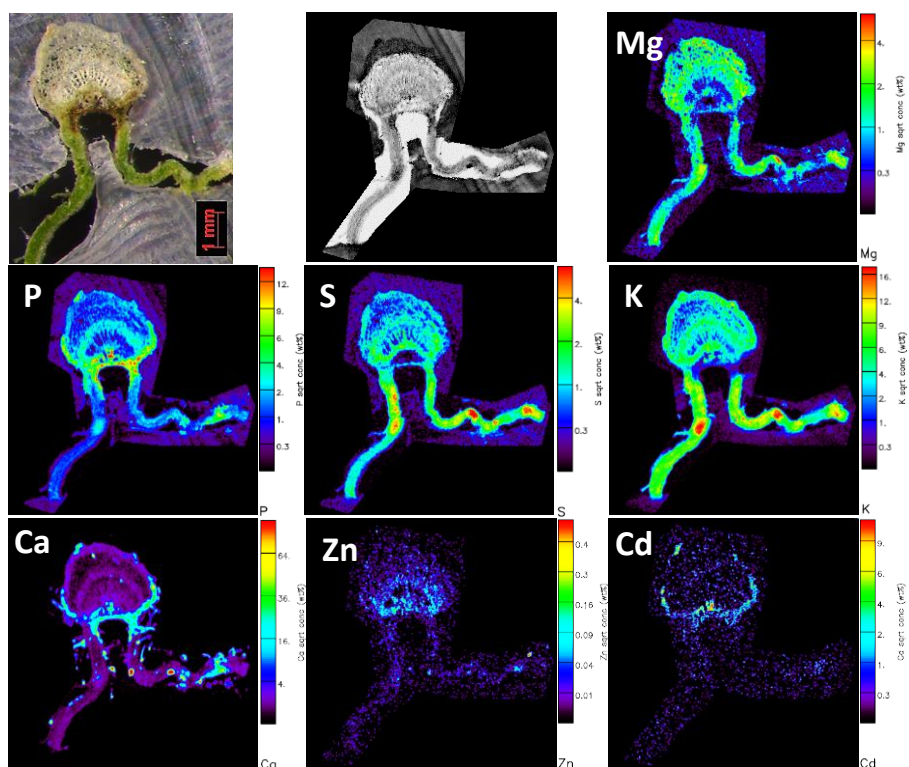


Figure 7.17: Photographs of a representative leaf cross section of *C. sativa* treated with $20 \mu\text{M}$ Cd during 1 weeks as analysed by light microscopy (upper left), and the associated quantitative elemental maps of Mg, P, S, K, Ca, Zn and Cd generated with GEOPIXE II software package after micro-PIXE analysis. Colored bars are not of the same order of magnitude among the elements. Scan size, $2000 \mu\text{m} \times 2000 \mu\text{m}$.

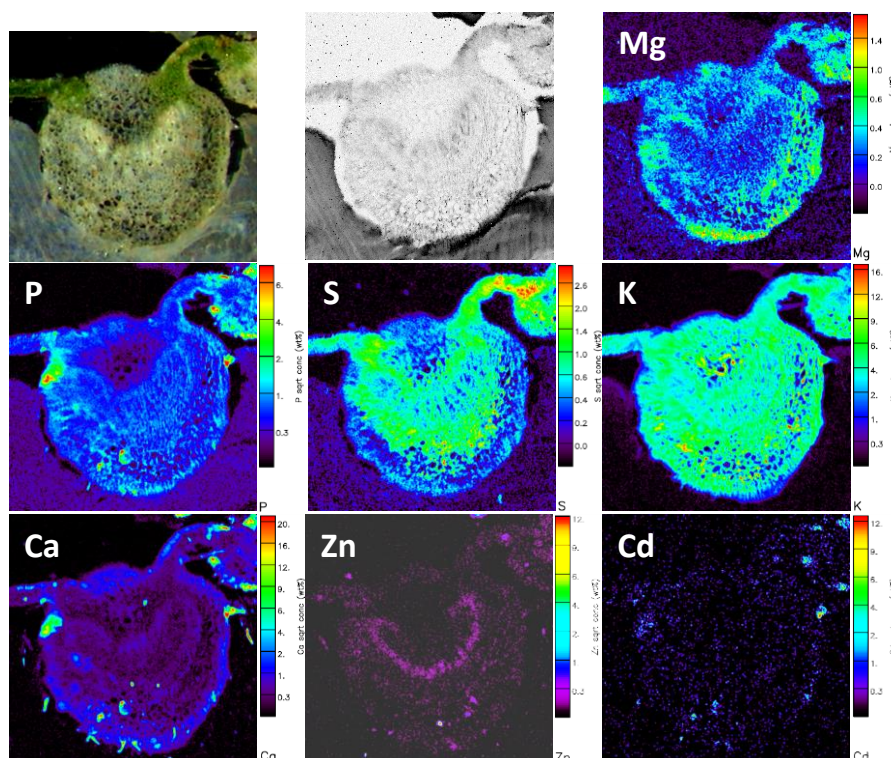


Figure 7.18: Photographs of a representative leaf cross section of *C. sativa* treated with 2mM Si during 2 weeks and 20 μ M Cd during 1 weeks as analysed by light microscopy (upper left), and the associated quantitative elemental maps of Mg, P, S, K, Ca, Zn and Cd generated with GEOPIXE II software package after micro-PIXE analysis. Colored bars are not of the same order of magnitude among the elements. Scan size, 1500 μ m \times 1500 μ m.

In leaves, the addition of Cd induced changes in Mg, P, Ca and Zn distributions: Mg was more uniformly distributed in the leaf section (except in the xylem), P is still concentrated in the phloem region but also in upper midrib epidermis and collenchyma located near the vascular bundle, Ca was not only located in trichomes but also in upper epidermis and collenchyma of the midrib, and Zn in the upper part of the midrib (Figure 7.17). In Cd treatment, Cd followed the same distribution than Ca in the midrib, but not in trichomes. However, plants exposed to both Cd and Si were found to accumulate Cd in trichomes. In CdSi treatment, P was also found to be more homogeneously distributed in the leaf section than in Cd treatment, and Zn was mainly distributed in phloem (Figure 7.18).

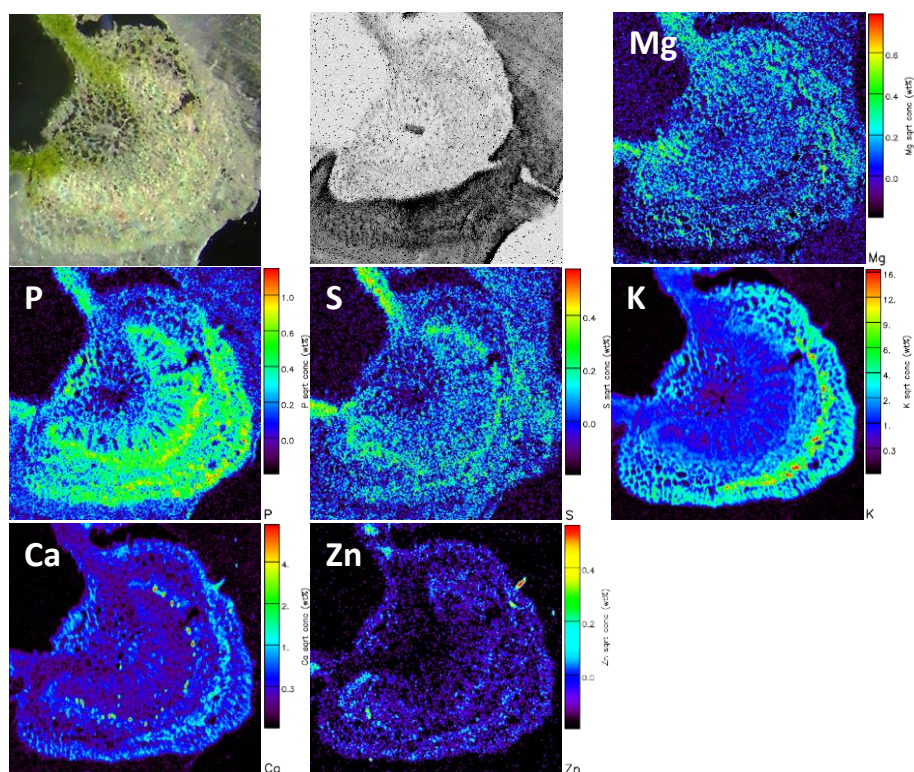


Figure 7.19: Photographs of a representative leaf cross section of *C. sativa* treated with $100\ \mu\text{M}$ Zn during 1 weeks as analysed by light microscopy (upper left), and the associated quantitative elemental maps of Mg, P, S, K, Ca and Zn generated with GEOPIXE II software package after micro-PIXE analysis. Colored bars are not of the same order of magnitude among the elements. Scan size, $1600\ \mu\text{m} \times 1600\ \mu\text{m}$.

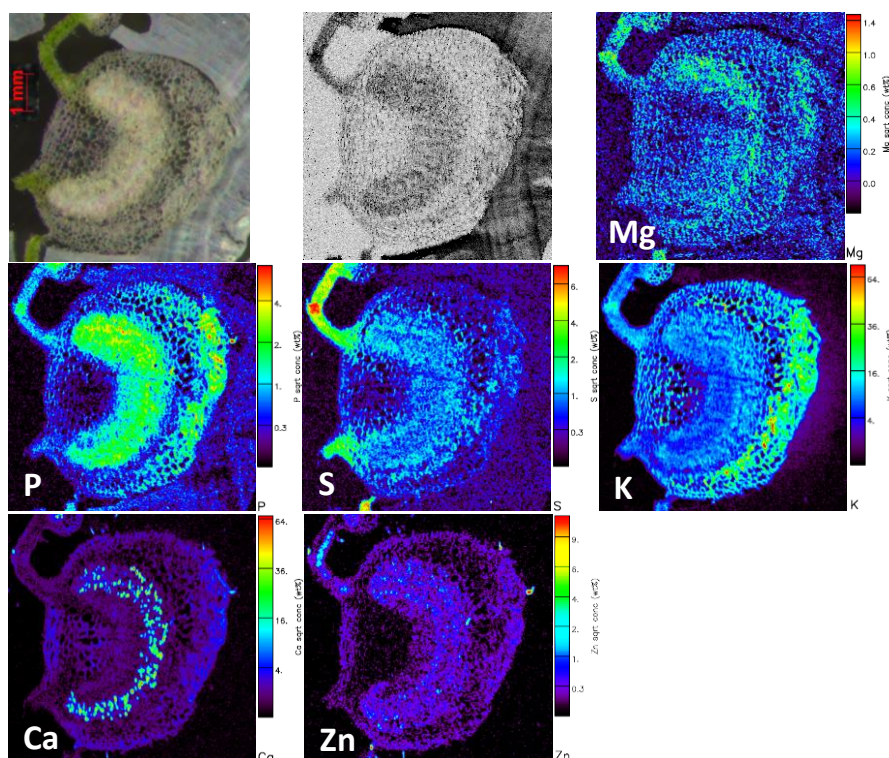


Figure 7.20: Photographs of a representative leaf cross section of *C. sativa* treated with 2mM Si during 2 weeks and 100 μm Zn during 1 weeks as analysed by light microscopy (upper left), and the associated quantitative elemental maps of Mg, P, S, K, Ca and Zn generated with GEOPIXE II software package after micro-PIXE analysis. Colored bars are not of the same order of magnitude among the elements. Scan size, 2000 μm \times 2000 μm .

In leaves, the addition of Zn induced changes in Mg, P, S and Zn distributions: Mg was more uniformly distributed in the leaf section, P is still concentrated in the phloem region but also in xylem and parenchyma and collenchyma cells in lower part of the midrib, S was found in mesophyll but also in phloem, and Zn was mainly distributed in trichomes and inside the cells of spongy mesophyll (Figure 7.19). In Zn treatment, addition of Si seemed to increase Ca concentrated spots in the vascular bundle (Figure 7.20).

3.5. EDX analysis of Si distribution in roots, stems and leaves

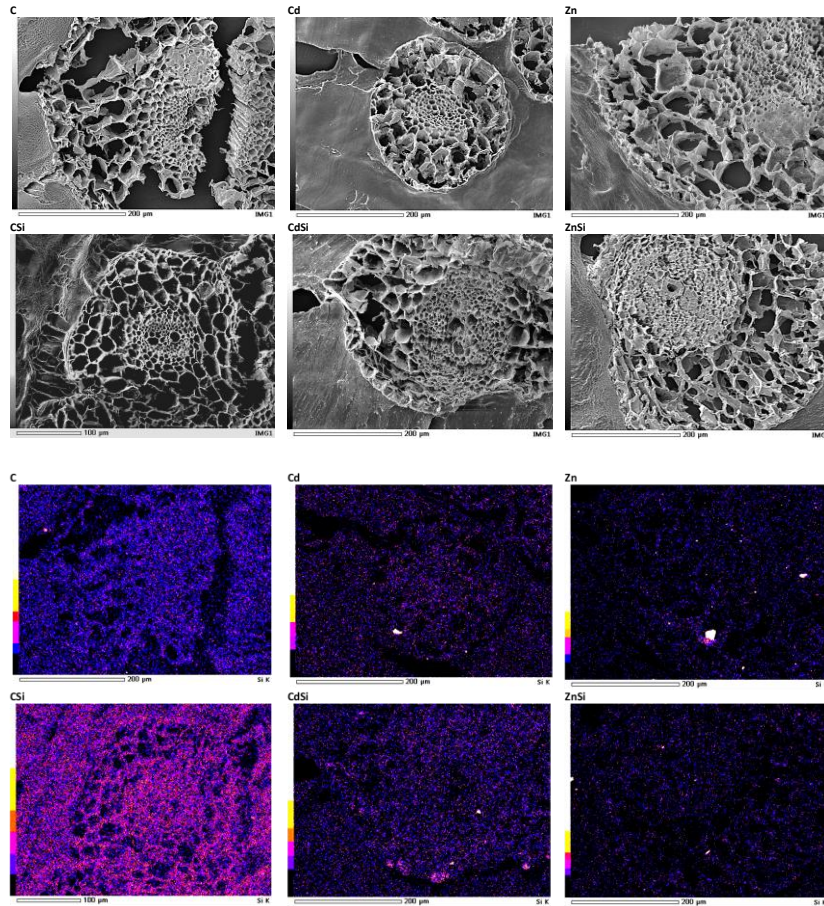


Figure 7.21: Photographs of a representative root cross section of *C. sativa* treated or not with 20 μM Cd, 100 μM Zn with or without 2mM Si, and the associated quantitative elemental maps of Si generated with EDX.

In all the treatments, Si was found to be distributed homogeneously in roots, except hotspots detected in root epidermis of CdSi treatment (Figure 7.21).

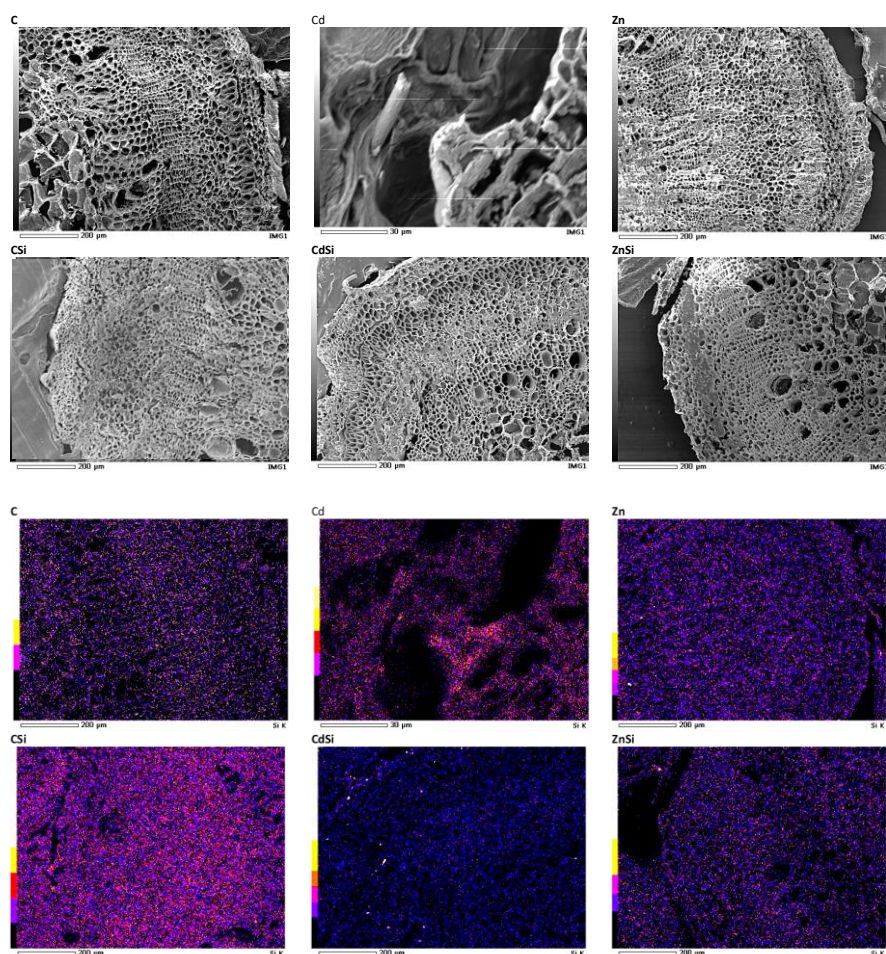


Figure 7.22: Photographs of a representative stem cross section of *C. sativa* treated or not with 20 μM Cd, 100 μM Zn with or without 2mM Si, and the associated quantitative elemental maps of Si generated with EDX.

In controls, controls treated with Si, as well as in plants exposed to Zn (Zn, ZnSi), Si was found to be distributed homogeneously in stems (Figure 7.22). In plants exposed to Cd, Si was mainly concentrated in trichomes (Figure 7.22).

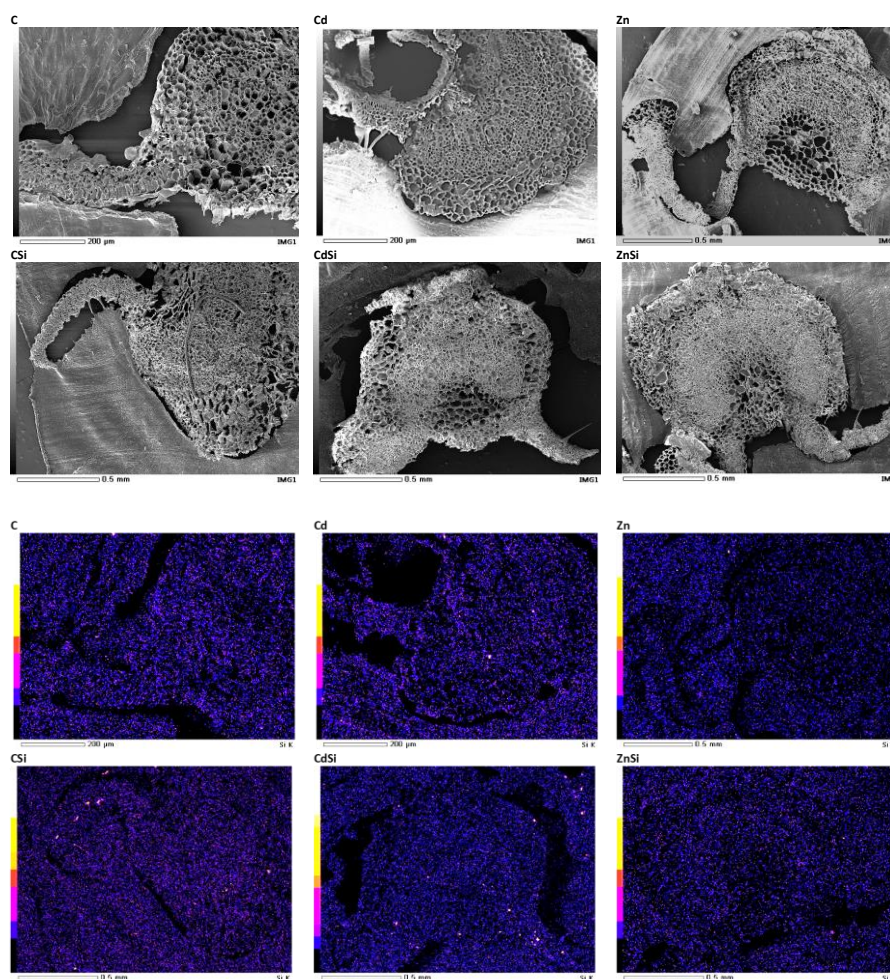
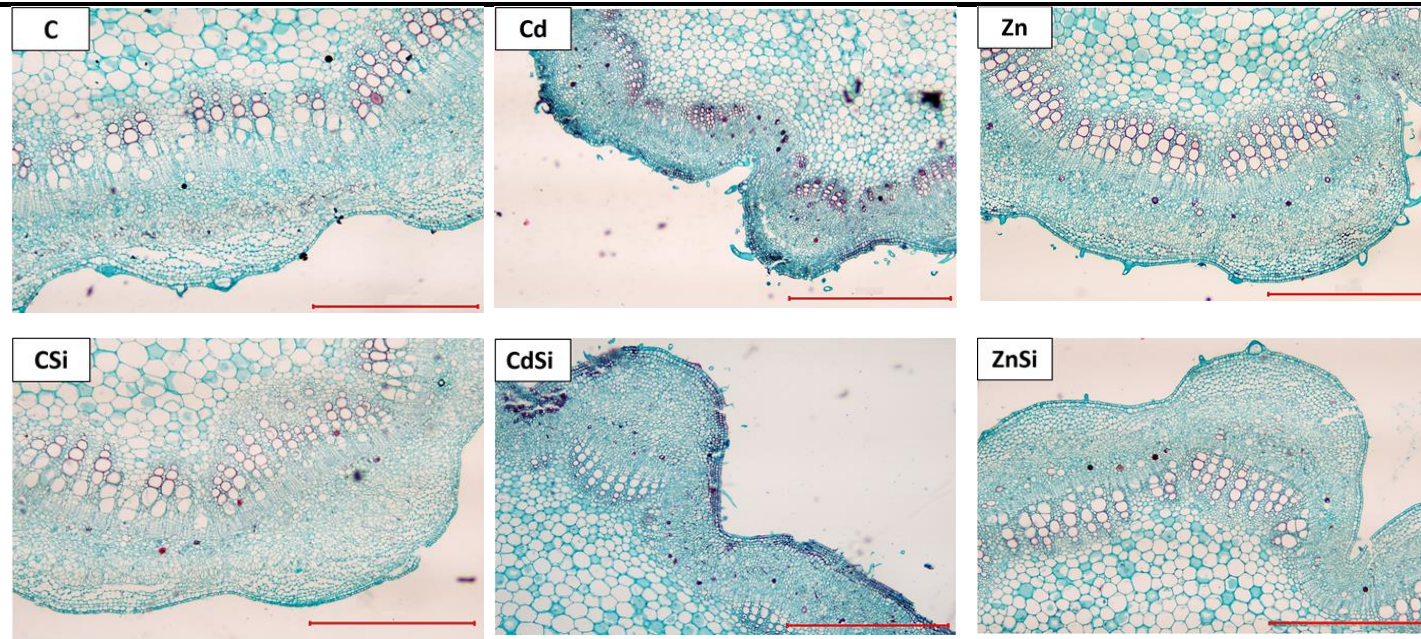


Figure 7.23: Photographs of a representative leaf cross section of *C. sativa* treated or not with 20 μM Cd, 100 μM Zn with or without 2mM Si, and the associated quantitative elemental maps of Si generated with EDX.

In controls and plants exposed to Cd or Zn but not treated with Si, Si is uniformly distributed in the leaf section (Figure 7.23). When exposed to Si, both controls and Cd/Zn-treated plants were shown to mainly accumulate Si in trichomes (Figure 7.23).

3.6. Cellulose and lignin detection in stems



297

Figure 7.24: Photographs of stem cross section of *C. sativa* cultivated in the presence or in the absence of 2mM H₂SiO₃ (Si) during 2 weeks and exposed to 20μM CdCl₂ (Cd) or ZnCl₂ (Zn) during 1 week, as analysed by light microscopy. Scale bar: 800 μm. Coloration: safranin and fast green.

Figure 7.24 illustrates stem cross section of *C. sativa* colored with safranin and fast green. Lignified tissues are colored in red by lignin, while cellulosic CW are colored in blue by fast green. Plants exposed to Cd exhibited a sclerified collenchyma compared to controls. Zn exposure also induced sclerification of collenchyma, but to a lesser extent than Cd. In Zn treatment, Si exposure appeared to cancel collenchyma sclerification.

4. Discussion

Heavy metal pollution is a major environmental problem and a serious threat to plant growth and development (Berni et al., 2019). For their mineral nutrition, plants need to satisfy their minimal nutrient requirements on the one side, and to control the surplus on the other (Lyubenova et al., 2013). Maintenance of this narrow optimum is extremely important, and accordingly, it is greatly demanding (Lyubenova et al., 2013). Understanding how plants cope with extreme concentrations of essential elements, and with elements that are toxic at very low concentrations will significantly help to design effective phytomanagement strategies (Lyubenova et al., 2013).

Strategies adopted by the plants to cope with HM toxicity involve reduction of HM uptake and root-to-shoot translocation, activation of antioxidative systems, and synthesis of sulfur-containing ligands mainly phytochelatins (PC) allowing HM vacuolar sequestration (Cobbett 2000; Huang et al. 2020). Studies of the distribution of metals within plant tissues are thus crucial for understanding the physiology of HM accumulation and tolerance (Koren et al., 2013), and are required for the management of harvested products if phytomanagement is combined with an agricultural purpose.

Besides, Si is known to have numerous beneficial effects on plants exposed to abiotic and biotic stresses (Frew et al. 2018; Pilon et al. 2013). In a previous study we showed that hemp is able to absorb Si from nutrient solution and translocate this element to the aerial parts of the plant (Guerriero et al., 2019; Luyckx et al., 2021a; 2021b).

4.1. Roots

Comparison of the element distribution between the root samples from controls and plants exposed to HM using the element distribution maps showed that Cd (Cd and CdSi treatments) and Zn (Zn and ZnSi treatments)

were mainly accumulated in CW of cortex cells, and only small amounts of HM were detected in the vascular cylinder. Moreover, Zn was also found to accumulate in epidermis and endodermis. To restrict HM transport in plants, three major processes regulating root to shoot translocation are frequently increased in HM-treated plants: (i) transport from the extracellular space (apoplast) to symplast within the root cortex, (ii) translocation from root cortex to vascular cylinder across the endodermis, and (iii) further transport into xylem (Schneider et al., 1999). Increased Zn accumulation in epidermis under Zn exposure may be regarded as an attempt to limit Zn absorption, while CW sequestration represents an efficient strategy to reduce Cd and Zn translocation to vascular cylinder and exclude them from metabolic pathways (Shiyu et al., 2020). Retention of HM in the cell wall may be achieved through HM fixation on carboxylic (primarily present in hemicelluloses and pectin) and to some extent to hydroxylic (cellulose, hemicelluloses, and pectin) groups, or through lignification to make the CW less permeable for toxic ions (Pejic et al., 2009; Hu et al., 2010; Ye et al., 2012; Fernández et al., 2014; Vukcevic et al., 2014; Gutsch et al., 2019a; Nawaz et al., 2019). Besides, endoderm suberization is frequently increased in HM-treated plants to limit HM transfer to the above-ground parts (Pires-Lira et al. 2020; Shiyu et al., 2020), and seemed to be involved in the response to Zn toxicity.

Heavy metal exposure also induced changes in elements distribution, but Cd and Zn were shown to have a different impact. Cd exposure increased accumulation of S in vascular cylinder, while Zn exposure increased S accumulation in CW of cortex cells. Sulfur accumulation is frequently increased in all organs of plants exposed to HM, which is usually related to the HM-induced oversynthesis of thiol compounds (phytochelatins and metallothioneins) followed by chelation and the sequestration of HM chelates in the vacuoles (Cobbett 2000; Lux et al., 2011; Mendoza-Cózatl et al., 2011). This strategy may have been involved in Zn sequestration in hemp roots, however Zn appeared to be mainly accumulated in CW and chelation to PC or MT would have implied Zn and S co-localisation and further HM transfer in vacuoles. It is more likely that Zn co-precipitated with P: their distributions seemed to be similar and precipitation of Zn with phosphate, and binding with pectate or histidyl groups may contribute to reduce Zn mobility and toxicity (Wang P et al., 2015). Such a similarity of P localisation with Cd was not observed in Cd-treated plants. In plants exposed to Cd and Zn, CW compartmentalization may thus represent the main sequestration strategy in roots. The percentage of Cd accumulation in cell walls has already be reported

to be more than 95% of total Cd content, which indicates that the cell wall may play an important role in preventing Cd uptake (Reviewed by Shiyu et al., 2020). Cd, being non-essential for plants may require the transport of S to aerial parts, where HM may induce a wide range of toxic effects (on photosynthesis, ...), for effective Cd sequestration through PC synthesis.

Besides, Cd increased Zn accumulation in epidermis and vascular cylinder comparatively to controls. Interestingly, both Cd and Zn enhanced Mg concentration in endodermis comparatively to controls. The mechanisms involved in HM retention in CW may have induced Mg sequestration in the endodermis, and Zn accumulation in epidermis under Cd exposure.

In roots, Si application appeared to increased Cd retention in endodermis. Endoderm suberization is frequently increased in HM-treated plants, and Si was found to enhance suberization and lignification in root (Fleck et al. 2011; Pires-Lira et al. 2020). Numerous works also demonstrated that Si reduced root-to-shoot translocation of Cd by blocking the apoplastic bypass flow after Si deposits in the vicinity of the endodermis leading to Cd accumulation in the root (Shi et al. 2005; Adrees et al. 2015; Bhat et al. 2019). However, Si accumulation in endodermis was not demonstrated in the current study.

4.2. Stems

Hemp is an annual high yielding industrial crop grown for its fibres and seeds (Pejic et al., 2009; Morin-Crini et al., 2019). The use of hemp to valorise HM-contaminated farmland soils and provide incomes for the farmer partly depends on HM distribution in stems. Hemp fibre primary cell wall (PCW) consisting mainly of cellulose, hemicelluloses and pectin, have the ability to bind HM compounds (Pejic et al., 2009; Vukcevic et al., 2014). In this study, Zn was homogeneously distributed in the whole stem section, while Cd was mainly found in trichomes, together with P and Ca. Trichomes are supposed to be a pathway that plants use to actively exclude toxic metals by forming and excreting Ca-containing crystals, like Cd in tobacco plants and Zn in *Arabidopsis* (reviewed by Zeng et al., 2017). Arru et al. (2004) also demonstrated that accumulated HM did not fix on hemp bast fibres. Even if Cd and Zn did not accumulate in bast fibres but in adjacent tissues, they may have impacted hemp fibre during their development process. Moreover, a risk of Cd dissemination subsists as a consequence of retting process occurring in the field and which involves selective degradation of the epidermal,

collenchyma and parenchyma cells surrounding the fibres (Bleuze et al. 2018).

As observed in roots, Zn and Cd exposure had a different impact on elemental distributions in stems: in plants exposed to Zn, Mg and S were more homogeneously distributed than in controls, while Cd treatment increased their accumulation in collenchyma cells. Histological observations of stems cross sections coloured with safranin and fast green showed that collenchyma CW of Cd-treated plants get lignified comparatively to controls. It has already been observed that collenchyma may become more rigid due to changes in CW composition or may undergo sclerification through lignification of newly deposited cell wall material (Leroux, 2012). As discussed earlier, lignification makes the CW less permeable for toxic ions, but probably also for essential elements like Mg and S. Increased S accumulation in tissues where Cd was found to be accumulated is also probably linked to PC synthesis: Cd-treated plants were found to increase S transport to root vascular cylinder.

Besides, no differences in elements distribution between Cd and CdSi treatments or between Zn and ZnSi treatments were noticed. In one of our previous study, Si was shown to mainly accumulate in leaves (Luyckx et al., 2021b), which could explain its limited impact in stems. However, in plants exposed to Cd, Si was mainly concentrated in CW of trichomes, and could be involved in Cd sequestration in this structure. It has already been suggested that co-precipitation between Si accumulated within cell walls and Cd may occur (Krzeslowska, 2011). Liu et al. (2013b) suggested a mechanism of co-deposition of Si and Cd in the cell walls via a [Si-wall matrix]Cd co-complexation as a plausible explanation for the *in vivo* detoxification of Cd.

4.3. Leaves

In Cd treatment, Cd followed the same distribution than Ca and P in collenchyma cells of the midrib. In Cd-tolerant *S. viminalis*, Cd sequestration in the pectin-rich CW of collenchyma was proposed to be an active detoxification process protecting the sensitive and metabolically more active areas inside vascular bundles (Vollenweider *et al.* 2006). Cadmium could also be coprecipitated with Ca oxalate crystals. Moreover, in stems we observed that collenchyma cells were lignified after Cd exposure, and Cd tended to accumulate in lignified collenchyma cells. In one of our study, hemp plants subjected to an excess of Zn or Cd showed increased expression of PAL and CAD involved in lignin biosynthesis in the leaves (Luyckx et al., 2021c). We

may hypothesise that CW lignification is involved in Cd sequestration in hemp leaves. Interestingly, in Cd-treatment, Si exposure induced Cd accumulation in trichomes, which could help the plant to improved toxic ion management.

Once more, plant's response to Cd differed from response to Zn: Zn was mainly accumulated in trichomes, even in the absence of Si application. It was also co-localised with S within the cells of spongy mesophyll. We may assume that, unlike the sequestration of Zn in CW of cortex in roots, in leaves Zn is chelated to thiols groups in vacuoles of spongy mesophyll cells. The involvement of the leaf mesophyll in metal accumulation and tolerance is reasonable, as mesophyll cells represent almost 75% of the leaf weight, and are positioned between the vascular bundles (representing a source of metals in the leaves after xylem loading) and the epidermal cells (Vogel-Mikuš et al., 2008; Koren et al., 2013). These observations indicate that these metabolically less active cells represent another storage place for Zn in leaves of *C. sativa*. In Zn-treated plants, the addition of Si seemed to increase Ca hotspots in the vascular bundle. Si may favour the coprecipitation of Zn with Ca oxalate crystals.

5. Conclusion

The impact of 20 μM Cd or 100 μM Zn and/or 2mM Si treatments on ions distribution in roots, stems and leaves of *Cannabis sativa* at tissue and cell level was addressed. According to the element localization patterns, the main HM detoxification mechanism in roots was HM sequestration in the apoplast of cortex cells. In stems, HM preferentially accumulated in trichomes. A different pattern of HM accumulation was shown in leaves: Zn was mainly sequestered in trichomes and within spongy mesophylls cells, while Cd was preferentially accumulated in collenchyma cells, indicating a mechanism of protecting sensitive and metabolically more active tissues from metal toxicity. Si was shown to improve toxic ion retention in root endodermis and in leaf trichomes. Within hemp roots, stems and leaves, elemental distribution also showed clear alterations after HM exposure, especially after Cd stress

References (Chapter 1 to 7)

- Abdelmouleh, M., Boufi, S., Belgacem, M. N., Duarte, A. P., Salah, A. B., & Gandini, A. (2004). Modification of cellulosic fibres with functionalised silanes: development of surface properties. *International Journal of Adhesion and Adhesives*, 24, 43-54.
- Abot, A., Bonnafous, C., Touchard, F., Thibault, F., Chocinski-Arnault, L., Lemoine, R., & Dedaldechamp, F. (2013). Effects of cultural conditions on the hemp (*Cannabis sativa*) phloem fibres: Biological development and mechanical properties. *Journal of Composite Materials*, 47, 1067-1077.
- Adrees, M., Ali, S., Rizwan, M., Zia-ur-Rehman, M., Ibrahim, M., Abbas, F., ... & Irshad, M. K. (2015). Mechanisms of silicon-mediated alleviation of heavy metal toxicity in plants: a review. *Ecotoxicology and Environmental Safety*, 119, 186-197.
- Ager, F. J., Ynsa, M. D., Dominguez-Solis, J. R., Gotor, C., Respaldiza, M. A., & Romero, L. C. (2002). Cadmium localization and quantification in the plant *Arabidopsis thaliana* using micro-PIXE. *Nuclear Instruments and Methods in Physics Research Section B: Beam Interactions with Materials and Atoms*, 189, 494-498.
- Ahmad, R., Tehsin, Z., Malik, S. T., Asad, S. A., Shahzad, M., Bilal, M., ... & Khan, S. A. (2016a). Phytoremediation potential of hemp (*Cannabis sativa* L.): identification and characterization of heavy metals responsive genes. *CLEAN–Soil, Air, Water*, 44, 195-201.
- Ahmad, P., Abdel Latef, A. A., Rasool, S., Akram, N. A., Ashraf, M., and Gucel, S. (2016b). Role of proteomics in crop stress tolerance. *Front. Plant Sci.* 7, 1336.
- Ahmad, J., Baig, M. A., Amna, Ali, A., A., and Qureshi, M., I. (2019). Proteomics of Cadmium Tolerance in Plants. *Cadmium Tolerance in Plants*, 143–175.
- Ahsan, N., Renaut, J., and Komatsu, S. (2009). Recent developments in the application of proteomics to the analysis of plant responses to heavy metals. *Proteomics* 9, 2602-2621.
- Ai, Y. J., Li, F. P., Gu, H. H., Chi, X. J., Yuan, X. T., & Han, D. Y. (2020). Combined effects of green manure returning and addition of sewage sludge compost on plant growth and microorganism communities in gold tailings. *Environmental Science and Pollution Research*, 27, 31686-31698.
- Aiello, G., Fasoli, E., Boschini, G., Lammi, C., Zanoni, C., Citterio, A., & Arnoldi, A. (2016). Proteomic characterization of hempseed (*Cannabis sativa* L.). *Journal of proteomics*, 147, 187-196.
- Ali, H., Khan, E., & Sajad, M. A. (2013). Phytoremediation of heavy metals— Concepts and applications. *Chemosphere*, 91, 869-881.
- Alloway, B. J. (Ed.). (2012). *Heavy metals in soils: trace metals and metalloids in soils and their bioavailability* (Vol. 22). Springer Science & Business Media.

- Andre, C. M., Hausman, J. F., & Guerriero, G. (2016). *Cannabis sativa*: the plant of the thousand and one molecules. *Frontiers in plant science*, 7, 19.
- Andrejić, G., Gajić, G., Prica, M., Dželetović, Ž., & Rakić, T. (2018). Zinc accumulation, photosynthetic gas exchange, and chlorophyll a fluorescence in Zn-stressed *Miscanthus × giganteus* plants. *Photosynthetica*, 56, 1249-1258.
- Angelova, V., Ivanova, R., Delibaltova, V., & Ivanov, K. (2004). Bio-accumulation and distribution of heavy metals in fibre crops (flax, cotton and hemp). *Industrial crops and products*, 19, 197-205.
- Arru, L., Rognoni, S., Baroncini, M., Bonatti, P. M., & Perata, P. (2004). Copper localization in *Cannabis sativa* L. grown in a copper-rich solution. *Euphytica*, 140, 33-38.
- Ascrizzi, R., Ceccarini, L., Tavarini, S., Flamini, G., & Angelini, L. G. (2019). Valorisation of hemp inflorescence after seed harvest: Cultivation site and harvest time influence agronomic characteristics and essential oil yield and composition. *Industrial Crops and Products*, 139, 111541.
- Ashraf, M., H., P., J., C., and Harris, P., J., C. (2013). Photosynthesis under stressful environments: an overview. *Photosynthetica*, 51, 163-190.
- Bajwa, A. A., Zulfiqar, U., Sadia, S., Bhowmik, P., & Chauhan, B. S. (2019). A global perspective on the biology, impact and management of *Chenopodium album* and *Chenopodium murale* : Two troublesome agricultural and environmental weeds. *Environmental Science and Pollution Research*, 26, 5357-5371.
- Baldini, M., Ferfua, C., Piani, B., Sepulcri, A., Dorigo, G., Zuliani, F., ... & Cattivello, C. (2018). The performance and potentiality of monoecious hemp (*Cannabis sativa* L.) cultivars as a multipurpose crop. *Agronomy*, 8, 162.
- Barquilha C.E.R., & Braga, M.C.B. (2021). Adsorption of organic and inorganic pollutants onto biochars: Challenges, operating conditions, and mechanisms. *Bioresource Technology Reports* 15, 100728.
- Baryla, A., Carrier, P., Franck, F., Coulomb, C., Sahut, C., & Havaux, M. (2001). Leaf chlorosis in oilseed rape plants (*Brassica napus*) grown on cadmium-polluted soil: causes and consequences for photosynthesis and growth. *Planta*, 212, 696-709.
- Bashir, H., Qureshi, M., I., Ibrahim, M., M., and Iqbal, M. (2015). Chloroplast and photosystems: Impact of cadmium and iron deficiency. *Photosynthetica*, 53, 321-335.
- Bates, L.S., Waldren, R.P. and Teare, I.D. (1973) Rapid determination of free proline for water-stress studies. *Plant Soil* 39, 205-207.
- Beale, S., I. (2005). Green genes gleaned. *Trends in Plant Science*, 10, 309-312.
- Beesley, L., Moreno-Jiménez, E., & Gomez-Eyles, J. L. (2010). Effects of biochar and greenwaste compost amendments on mobility, bioavailability and toxicity of inorganic and organic contaminants in a multi-element polluted soil. *Environmental pollution*, 158, 2282-2287.

- Beesley, L., Moreno-Jiménez, E., Gomez-Eyles, J. L., Harris, E., Robinson, B., & Sizmur, T. (2011). A review of biochars' potential role in the remediation, revegetation and restoration of contaminated soils. *Environmental Pollution*, *159*, 3269-3282. <https://doi.org/10.1016/j.envpol.2011.07.023>
- Behr, M., Legay, S., Žižková, E., Motyka, V., Dobrev, P. I., Hausman, J. F., ... & Guerriero, G. (2016). Studying secondary growth and bast fiber development: the hemp hypocotyl peeks behind the wall. *Frontiers in plant science*, *7*, 1733.
- Behr, M., Legay, S., Hausman, J. F., Lutts, S., & Guerriero, G. (2017). Molecular investigation of the stem snap point in textile hemp. *Genes*, *8*, 363.
- Behr, M. (2018). Molecular investigation of cell wall formation in hemp stem tissues (Doctoral dissertation, UCL-Université Catholique de Louvain).
- Behr, M., Sergeant, K., Leclercq, C. C., Planchon, S., Guignard, C., Lenouvel, A., ... & Guerriero, G. (2018). Insights into the molecular regulation of monolignol-derived product biosynthesis in the growing hemp hypocotyl. *BMC plant biology*, *18*, 1-18.
- Behr, M., Faleri, C., Hausman, J. F., Planchon, S., Renaut, J., Cai, G., & Guerriero, G. (2019). Distribution of cell-wall polysaccharides and proteins during growth of the hemp hypocotyl. *Planta*, *250*, 1539-1556.
- Békésiová, B., Hraška, Š., Libantová, J., Moravčíková, J., and Matušíková, I. (2008). Heavy-metal stress induced accumulation of chitinase isoforms in plants. *Molecular Biology Reports*, *35*, 579-588.
- Ben Ghnaya, A., Charles, G., Hourmant, A., Ben Hamida, J., Branchard, M. (2009). Physiological behaviour of four rapeseed cultivar (*Brassica napus* L.) submitted to metal stress. *Comptes Rendus Biologies* *332*, 363-370.
- Benzie, I. F., & Strain, J. J. (1996). The ferric reducing ability of plasma (FRAP) as a measure of "antioxidant power": the FRAP assay. *Analytical biochemistry*, *239*, 70-76.
- Berni, R., Luyckx, M., Xu, X., Legay, S., Sergeant, K., Hausman, J. F., ... & Guerriero, G. (2019). Reactive oxygen species and heavy metal stress in plants: Impact on the cell wall and secondary metabolism. *Environmental and Experimental Botany*, *161*, 98-106.
- Berni, R., Mandlik, R., Hausman, J. F., & Guerriero, G. (2021). Silicon-induced mitigatory effects in salt-stressed hemp leaves. *Physiologia Plantarum*, *171*, 476-482.
- Berthet, S., Demont-Caulet, N., Pollet, B., Bidzinski, P., Cézard, L., Le Bris, P., ... & Jouanin, L. (2011). Disruption of LACCASE4 and 17 results in tissue-specific alterations to lignification of *Arabidopsis thaliana* stems. *The Plant Cell*, *23*, 1124-1137.
- Bhat, J. A., Shivaraj, S. M., Singh, P., Navadagi, D. B., Tripathi, D. K., Dash, P. K., ... & Deshmukh, R. (2019). Role of silicon in mitigation of heavy metal stresses in crop plants. *Plants*, *8*, 71.

- Biederman, L. A., & Harpole, W. S. (2013). Biochar and its effects on plant productivity and nutrient cycling: A meta-analysis. *GCB Bioenergy*, 5, 202-214. <https://doi.org/10.1111/gcbb.12037>
- Bleuze, L., Lashermes, G., Alavoine, G., Recous, S., & Chabbert, B. (2018). Tracking the dynamics of hemp dew retting under controlled environmental conditions. *Industrial crops and products*, 123, 55-63.
- Bokor, B., Vaculík, M., Slovák, L., Masarovič, D., & Lux, A. (2014). Silicon does not always mitigate zinc toxicity in maize. *Acta Physiologiae Plantarum*, 36, 733-743.
- Bona, E., Marsano, F., Cavaletto, M., & Berta, G. (2007). Proteomic characterization of copper stress response in *Cannabis sativa* roots. *Proteomics*, 7, 1121-1130.
- Bono et al. (2020). *Memento 2020 – Panorama des marchés « Fibres végétales techniques en matériaux (hors bois) en France—Recherche Google*. (s. d.). [https://www.google.com/search?q=Bono+et+al.+2020+Memento+2020+%E2%80%93+Panorama+des+march%C3%A9s+%C2%AB+Fibres+v%C3%A9g%C3%A9tales+techniques+en+mat%C3%A9riaux+\(hors+bois\)+en+France&rlz=1C1PNJJ_frBE929BE929&oq=Bono+et+al.+2020+Memento+2020+%E2%80%93+Panorama+des+march%C3%A9s+%C2%AB+Fibres+v%C3%A9g%C3%A9tales+techniques+en+mat%C3%A9riaux+\(hors+bois\)+en+France&aqs=chrome..69i57j69i60.1050j0j1&sourceid=chrome&ie=UTF-8](https://www.google.com/search?q=Bono+et+al.+2020+Memento+2020+%E2%80%93+Panorama+des+march%C3%A9s+%C2%AB+Fibres+v%C3%A9g%C3%A9tales+techniques+en+mat%C3%A9riaux+(hors+bois)+en+France&rlz=1C1PNJJ_frBE929BE929&oq=Bono+et+al.+2020+Memento+2020+%E2%80%93+Panorama+des+march%C3%A9s+%C2%AB+Fibres+v%C3%A9g%C3%A9tales+techniques+en+mat%C3%A9riaux+(hors+bois)+en+France&aqs=chrome..69i57j69i60.1050j0j1&sourceid=chrome&ie=UTF-8) (Accessed 30 April 2021).
- Boutin, M.P., Flamin C, Quinton S, Gosse G (2006) Etude des caractéristiques environnementales du chanvre par leur analyse de cycle de vie, Rapport du Ministère de l’agriculture et de la pêche.
- Branda, F., Malucelli, G., Durante, M., Piccolo, A., Mazzei, P., Costantini, A., ... & Bifulco, A. (2016). Silica treatments: A fire retardant strategy for hemp fabric/epoxy composites. *Polymers*, 8, 313.
- Cambrollé, J., Mancilla-Leytón, J. M., Muñoz-Vallés, S., Figueroa-Luque, E., Luque, T., & Figueroa, M. E. (2013). Evaluation of zinc tolerance and accumulation potential of the coastal shrub *Limoniastrum monopetalum* (L.) Boiss. *Environmental and experimental botany*, 85, 50-57.
- Carillo, P. (2018). GABA shunt in durum wheat. *Frontiers in Plant Science*, 9, 100.
- Cereser, C., Guichard, J., Draï, J., Bannier, E., Garcia, I., Boget, S., ... & Revol, A. (2001). Quantitation of reduced and total glutathione at the femtomole level by high-performance liquid chromatography with fluorescence detection: application to red blood cells and cultured fibroblasts. *Journal of Chromatography B: Biomedical Sciences and Applications*, 752, 123-132.
- Chandra, R., & Kang, H. (2016). Mixed heavy metal stress on photosynthesis, transpiration rate, and chlorophyll content in poplar hybrids. *Forest Science and Technology*, 12, 55-61.
- Charai, M., Sghiouri, H., Mezrhab, A., & Karkri, M. (2021). Thermal insulation potential of non-industrial hemp (*Moroccan cannabis sativa* L.) fibers for

- green plaster-based building materials. *Journal of Cleaner Production*, 292, 126064.
- Chernova, T. E., Mikshina, P. V., Salnikov, V. V., Ibragimova, N. N., Sautkina, O. V., & Gorshkova, T. A. (2018). Development of distinct cell wall layers both in primary and secondary phloem fibers of hemp (*Cannabis sativa* L.). *Industrial Crops and Products*, 117, 97-109.
- Chowdhury, S., Mazumder, M. J., Al-Attas, O., & Husain, T. (2016). Heavy metals in drinking water : Occurrences, implications, and future needs in developing countries. *Science of the Total Environment*, 569, 476-488.
- Citterio, S., Santagostino, A., Fumagalli, P., Prato, N., Ranalli, P., & Sgorbati, S. (2003). Heavy metal tolerance and accumulation of Cd, Cr and Ni by *Cannabis sativa* L. *Plant and Soil*, 256, 243-252.
- Citterio, S., Prato, N., Fumagalli, P., Aina, R., Massa, N., Santagostino, A., ... & Berta, G. (2005). The arbuscular mycorrhizal fungus *Glomus mosseae* induces growth and metal accumulation changes in *Cannabis sativa* L. *Chemosphere*, 59, 21-29.
- Cobbett, C. S. (2000). Phytochelatins and their roles in heavy metal detoxification. *Plant physiology*, 123, 825-832.
- Connan, O., Maro, D., Hébert, D., Rroupsard, P., Goujon, R., Letellier, B., & Le Cavelier, S. (2013). Wet and dry deposition of particles associated metals (Cd, Pb, Zn, Ni, Hg) in a rural wetland site, Marais Vernier, France. *Atmospheric Environment*, 67, 394-403.
- Cosio, C., & Dunand, C. (2009). Specific functions of individual class III peroxidase genes. *Journal of experimental botany*, 60, 391-408.
- Crini, G., Lichtfouse, E., Chanet, G., & Morin-Crini, N. (2020). Traditional and new applications of hemp. In *Sustainable Agriculture Reviews 42* (p. 37-87). Springer.
- Daud, M., K., Quiling, H., Lei, M., Ali, B., and Zhu, S., J. (2015). Ultrastructural, metabolic and proteomic changes in leaves of upland cotton in response to cadmium stress. *Chemosphere*, 120, 309-320.
- Décret Wallon du 1er mars 2018 relatif à la gestion et à l'assainissement des sols—Recherche* Google. (s. d).
https://www.google.com/search?q=D%C3%A9cret+Wallon+du+1er+mars+2018+relatif+%C3%A0+la+gestion+et+%C3%A0+l%27assainissement+des+sols+&rlz=1C1PNJJ_frBE929BE929&sxsrf=ALeKk02-NPpAdo9Q8fIB-lrONgxdNdJ4w%3A1619788687173&ei=jwOMYJqCCsTqkgWooLO4Dg&oq=D%C3%A9cret+Wallon+du+1er+mars+2018+relatif+%C3%A0+la+gestion+et+%C3%A0+l%27assainissement+des+sols+&gs_lcp=Cgnd3Mtd2l6EANQ5d8GWOXfBmCH5gZoAHAAeACAAWSIAWSSAQMWLjGYAQGgAQKGAQGqAQdnd3Mtd2l6wAEB&scient=gws-wiz&ved=0ahUKEwjahb2Kh6bwAhVEtaQKHSjQDOcQ4dUDCA4&uact=5 (Accessed 30 April 2021).

- Degryse, F., Broos, K., Smolders, E., & Merckx, R. (2003). Soil solution concentration of Cd and Zn can be predicted with a CaCl₂ soil extract. *European Journal of Soil Science*, 54, 149-158.
- Deleuran, L. C., & Flengmark, P. K. (2006). Yield potential of hemp (*Cannabis sativa* L.) cultivars in Denmark. *Journal of Industrial Hemp*, 10, 19-31.
- Del Rio, D., Stewart, A. J., & Pellegrini, N. (2005). A review of recent studies on malondialdehyde as toxic molecule and biological marker of oxidative stress. *Nutrition, metabolism and cardiovascular diseases*, 15, 316-328.
- de Silva, K., Laska, B., Brown, C., Sederoff, H. W., & Khodakovskaya, M. (2011). *Arabidopsis thaliana* calcium-dependent lipid-binding protein (AtCLB): a novel repressor of abiotic stress response. *Journal of experimental botany*, 62, 2679-2689.
- De Vos, C. R., Vonk, M. J., Vooijs, R., & Schat, H. (1992). Glutathione depletion due to copper-induced phytochelatin synthesis causes oxidative stress in *Silene cucubalus*. *Plant physiology*, 98, 853-858.
- Di Candito, M., Ranalli, P., & Dal Re, L. (2004). Heavy metal tolerance and uptake of Cd, Pb and Tl by hemp. *Advances in Horticultural Science*, 138-144.
- Doncheva, S. N., Poschenrieder, C., Stoyanova, Z., Georgieva, K., Velichkova, M., & Barceló, J. (2009). Silicon amelioration of manganese toxicity in Mn-sensitive and Mn-tolerant maize varieties. *Environmental and Experimental Botany*, 65, 189-197.
- Douay, F., Pelfrène, A., Planque, J., Fourier, H., Richard, A., Roussel, H., & Girondelot, B. (2013). Assessment of potential health risk for inhabitants living near a former lead smelter. Part 1: metal concentrations in soils, agricultural crops, and homegrown vegetables. *Environmental monitoring and assessment*, 185, 3665-3680.
- Dubois, F., Tercé-Laforgue, T., Gonzalez-Moro, M. B., Estavillo, J. M., Sangwan, R., Gallais, A., & Hirel, B. (2003). Glutamate dehydrogenase in plants: is there a new story for an old enzyme?. *Plant Physiology and Biochemistry*, 41, 565-576.
- Dufey, I., Gheysens, S., Ingabire, A., Lutts, S., & Bertin, P. (2014). Silicon application in cultivated rices (*Oryza sativa* L and *Oryza glaberrima* Steud) alleviates iron toxicity symptoms through the reduction in iron concentration in the leaf tissue. *Journal of agronomy and crop science*, 200, 132-142.
- Duque-Schumacher, A. G. D., Pequito, S., & Pazour, J. (2020). Industrial hemp fiber: A sustainable and economical alternative to cotton. *Journal of Cleaner Production*, 268, 122180.
- EIHA (2019). *Hemp Cultivation Area in the European Union 1993 to 2017*. *European Industrial Hemp Association*. - Recherche Google. (s. d.). https://www.google.com/search?q=EIHA+%282019%29.+Hemp+Cultivation+Area+in+the+European+Union+1993+to+2017.+European+Industrial+Hemp+Association.&rlz=1C1PNJJ_frBE929BE929&sxsrf=ALeKk00X0CkCskCrsHf63X7s9-

7NgZDGXw%3A1619788950822&ei=lgSMYKPCMc3kgXSxKKoAQ&oq=EIHA+%282019%29.+Hemp+Cultivation+Area+in+the+European+Union+1993+to+2017.+European+Industrial+Hemp+Association.&gs_lcp=Cg dnd3Mtd2l6EANQp8UCWKfFAMDrygJoAHACeACAAQCIQAQCSAQCY AQQgAQKgAQGqAQdnd3Mtd2l6wAEB&sclient=gws-wiz&ved=0ahUKEwuj5ZiliKbwAhXKu6QKHVKiCBUQ4dUDCA4&uact=5 (Accessed 30 April 2021).

- El-Naggar, A., Lee, S. S., Rinklebe, J., Farooq, M., Song, H., Sarmah, A. K., Zimmerman, A. R., Ahmad, M., Shaheen, S. M., & Ok, Y. S. (2019). Biochar application to low fertility soils: A review of current status, and future prospects. *Geoderma*, 337, 536-554.
- Emamverdian, A., Ding, Y., Mokhberdoran, F., & Xie, Y. (2015). Heavy metal stress and some mechanisms of plant defense response. *The Scientific World Journal*, 2015.
- Epstein, E. (1994). The anomaly of silicon in plant biology. *Proceedings of the National Academy of Sciences*, 91, 11-17.
- Etesami, H., & Jeong, B.R. (2018) Silicon (Si): Review and future prospects on the action mechanisms in alleviating biotic and abiotic stresses in plants. *Ecotoxicology and Environmental Safety* 147, 881-896.
- Fan, W., Guo, Q., Liu, C., Liu, X., Zhang, M., Long, D., ... & Zhao, A. (2018). Two mulberry phytochelatin synthase genes confer zinc/cadmium tolerance and accumulation in transgenic *Arabidopsis* and tobacco. *Gene*, 645, 95-104.
- Farmer, E., E., and Goossens, A. (2019). Jasmonates: What ALLENE OXIDE SYNTHASE does for plants. *Journal of Experimental Botany*, 70, 3373-3378.
- Feng, W., Guo, Z., Xiao, X., Peng, C., Shi, L., Ran, H., & Xu, W. (2020). A dynamic model to evaluate the critical loads of heavy metals in agricultural soil. *Ecotoxicology and environmental safety*, 197, 110607.
- Fernández, R., Fernández-Fuego, D., Bertrand, A., and González, A. (2014). Strategies for Cd accumulation in *Dittrichia viscosa* (L.) Greuter: role of the cell wall, non-protein thiols and organic acids. *Plant Physiology and Biochemistry*, 78, 63-70.
- Fernando, A. L., Duarte, M. P., Vatsanidou, A., & Alexopoulou, E. (2015). Environmental aspects of fiber crops cultivation and use. *Industrial Crops and Products*, 68, 105-115.
- Ferrarini, A., Fracasso, A., Spini, G., Fornasier, F., Taskin, E., Fontanella, M.C., Beone, G.M., Amaducci, S. & Puglisi, E. (2021) Bioaugmented phytoremediation of metal-contaminated soils and sediments by hemp and giant reed. *Frontiers in Microbiology* 12, 645893.
- Filiberto, D. M., & Gaunt, J. L. (2013). Practicality of Biochar Additions to Enhance Soil and Crop Productivity. *Agriculture*, 3, 715-725.

- Fleck, A. T., Nye, T., Repenning, C., Stahl, F., Zahn, M., & Schenk, M. K. (2011). Silicon enhances suberization and lignification in roots of rice (*Oryza sativa*). *Journal of Experimental Botany*, 62, 2001-2011.
- Fleck, A. T., Schulze, S., Hinrichs, M., Specht, A., Waßmann, F., Schreiber, L., & Schenk, M. K. (2015). Silicon promotes exodermal Casparian band formation in Si-accumulating and Si-excluding species by forming phenol complexes. *PLoS One*, 10(9), e0138555.
- Forján, R., Asensio, V., Vila, A. R., & Covelo, E. F. (2016). Contributions of a compost-biochar mixture to the metal sorption capacity of a mine tailing. *Environmental Science and Pollution Research*, 23, 2595-2602.
- Franić, M., and Galić, V. (2019). As, Cd, Cr, Cu, Hg: Physiological Implications and Toxicity in Plants. In *Plant metallomics and functional omics*. Springer, Cham.
- Frassinetti, S., Moccia, E., Caltavuturo, L., Gabriele, M., Longo, V., Bellani, L., Giorgi, G., & Giorgetti, L. (2018) Nutraceutical potential of hemp (*Cannabis sativa* L.) seeds and sprouts. *Food Chemistry* 262, 56-66.
- Frew, A., Weston, L. A., Reynolds, O. L., & Gurr, G. M. (2018). The role of silicon in plant biology: a paradigm shift in research approach. *Annals of botany*, 121, 1265-1273.
- García-Tejero, I. F., Zuazo, V. D., Sánchez-Carnenero, C., Hernández, A., Ferreiro-Vera, C., & Casano, S. (2019). Seeking suitable agronomical practices for industrial hemp (*Cannabis sativa* L.) cultivation for biomedical applications. *Industrial crops and products*, 139, 111524.
- Gharbi, E., Martínez, J. P., Benahmed, H., Hichri, I., Dobrev, P. I., Motyka, V., ... & Lutts, S. (2017). Phytohormone profiling in relation to osmotic adjustment in NaCl-treated plants of the halophyte tomato wild relative species *Solanum chilense* comparatively to the cultivated glycophyte *Solanum lycopersicum*. *Plant Science*, 258, 77-89.
- Ghnaya, A. B., Charles, G., Hourmant, A., Hamida, J. B., & Branchard, M. (2009). Physiological behaviour of four rapeseed cultivar (*Brassica napus* L.) submitted to metal stress. *Comptes Rendus Biologies*, 332, 363-370.
- Ghosh, D., and Xu, J. (2014). Abiotic stress responses in plant roots: a proteomics perspective. *Frontiers in Plant Science*, 5, 6.
- Ghosh, D., Lin, Q., Xu, J., and Hellmann, H. A. (2017). How plants deal with stress: exploration through proteome investigation. *Frontiers in Plant Science*, 8, 1176.
- Goodarzi, A., Namdjoyan, S., & Soorki, A. A. (2020). Effects of exogenous melatonin and glutathione on zinc toxicity in safflower (*Carthamus tinctorius* L.) seedlings. *Ecotoxicology and environmental safety*, 201, 110853.
- Gorshkova, T. A., Sal'nikov, V. V., Chemikosova, S. B., Ageeva, M. V., Pavlencheva, N. V., & van Dam, J. E. (2003). The snap point: a transition point in *Linum usitatissimum* bast fiber development. *Industrial Crops and Products*, 18, 213-221.

- Gorshkova, T., Brutch, N., Chabbert, B., Deyholos, M., Hayashi, T., Lev-Yadun, S., ... & Pilate, G. (2012). Plant fiber formation: state of the art, recent and expected progress, and open questions. *Critical Reviews in Plant Sciences*, 31, 201-228.
- Granot, D., Stein, O., (2019). An overview of sucrose synthases in plants. *Frontiers in plant science*, 10, 95.
- Grčman, H., Velikonja-Bolta, Š., Vodnik, D., Kos, B., & Leštan, D. (2001). EDTA enhanced heavy metal phytoextraction: metal accumulation, leaching and toxicity. *Plant and Soil*, 235, 105-114.
- Griga, M., & Bjelková, M. (2013). Flax (*Linum usitatissimum* L.) and Hemp (*Cannabis sativa* L.) as fibre crops for phytoextraction of heavy metals: Biological, agro-technological and economical point of view. In *Plant-based remediation processes* (p. 199-237). Springer.
- Gu, H. H., Qiu, H., Tian, T., Zhan, S. S., Chaney, R. L., Wang, S. Z., ... & Qiu, R. L. (2011). Mitigation effects of silicon rich amendments on heavy metal accumulation in rice (*Oryza sativa* L.) planted on multi-metal contaminated acidic soil. *Chemosphere*, 83, 1234-1240.
- Guerriero, G., Sergeant, K., & Hausman, J. F. (2013). Integrated-omics: a powerful approach to understanding the heterogeneous lignification of fibre crops. *International Journal of Molecular Sciences*, 14, 10958-10978.
- Guerriero, G., Behr, M., Hausman, J. F., & Legay, S. (2017a). Textile hemp vs. salinity: Insights from a targeted gene expression analysis. *Genes*, 8, 242.
- Guerriero, G., Behr, M., Backes, A., Faleri, C., Hausman, J. F., Lutts, S., & Cai, G. (2017b). Bast fibre formation: insights from next-generation sequencing. *Procedia engineering*, 200, 229-235.
- Guerriero, G., Behr, M., Legay, S., Mangeot-Peter, L., Zorzan, S., Ghoniem, M., and Hausman, J.F. (2017c). Transcriptomic profiling of hemp bast fibres at different developmental stages. *Scientific Reports*, 7, 4961.
- Guerriero, G., Mangeot-Peter, L., Legay, S., Behr, M., Lutts, S., Siddiqui, K. S., and Hausman, J.F. (2017d). Identification of fasciclin-like arabinogalactan proteins in textile hemp (*Cannabis sativa* L.): In silico analyses and gene expression patterns in different tissues. *BMC Genomics* 18, 741.
- Guerriero, G., Law, C., Stokes, I., Moore, K. L., & Exley, C. (2018a). Rough and tough. How does silicic acid protect horsetail from fungal infection?. *Journal of Trace Elements in Medicine and Biology*, 47, 45-52.
- Guerriero, G., Stokes, I., & Exley, C. (2018b). Is callose required for silicification in plants?. *Biology letters*, 14, 20180338.
- Guerriero, G., Deshmukh, R., Sonah, H., Sergeant, K., Hausman, J. F., Lentzen, E., ... & Exley, C. (2019). Identification of the aquaporin gene family in *Cannabis sativa* and evidence for the accumulation of silicon in its tissues. *Plant Science*, 287, 110167.

- Guerriero, G., Stokes, I., Valle, N., Hausman, J. F., & Exley, C. (2020) Visualising silicon in plants: histochemistry, silica sculptures and elemental imaging. *Cells*, 9,1066.
- Guerriero, G., Sutura, F. M., Torabi-Pour, N., Renaut, J., Hausman, J. F., Berni, R., ... & Saffie-Siebert, S. (2021). Phyto-Courier, a Silicon Particle-Based Nanobio-stimulant: Evidence from *Cannabis sativa* Exposed to Salinity. *ACS nano*, 15, 3061-3069.
- Guntzer, F., Keller, C., & Meunier, J. D. (2012). Benefits of plant silicon for crops: a review. *Agronomy for Sustainable Development*, 32, 201-213.
- Guo, K., Du, X., Tu, L., Tang, W., Wang, P., Wang, M., ... & Zhang, X. (2016). Fibre elongation requires normal redox homeostasis modulated by cytosolic ascorbate peroxidase in cotton (*Gossypium hirsutum*). *Journal of experimental botany*, 67, 3289-3301.
- Gutsch, A., Keunen, E., Guerriero, G., Renaut, J., Cuypers, A., Hausman, J. F., & Sergeant, K. (2018). Long-term cadmium exposure influences the abundance of proteins that impact the cell wall structure in *Medicago sativa* stems. *Plant Biology*, 20, 1023-1035.
- Gutsch, A., Vandionant, S., Sergeant, K., Jozefczak, M., Vangronsveld, J., Hausman, J. F., & Cuypers, A. (2019a). Systems Biology of Metal Tolerance in Plants: A Case Study on the Effects of Cd Exposure on Two Model Plants. In *Plant Metallomics and Functional Omics* (pp. 23-37). Springer, Cham.
- Gutsch, A., Sergeant, K., Keunen, E., Prinsen, E., Guerriero, G., Renaut, J., ... & Cuypers, A. (2019b). Does long-term cadmium exposure influence the composition of pectic polysaccharides in the cell wall of *Medicago sativa* stems?. *BMC plant biology*, 19, 1-17.
- Han, R. M., Lefèvre, I., Albacete, A., Pérez-Alfocea, F., Barba-Espín, G., Díaz-Vivancos, P., ... & Lutts, S. (2013). Antioxidant enzyme activities and hormonal status in response to Cd stress in the wetland halophyte *Kosteletzkya virginica* under saline conditions. *Physiologia Plantarum*, 147, 352-368.
- Han, H. C., Gong, X. L., Zhou, M., Li, C., & Yang, H. B. (2021). A study about silane modification and interfacial ultraviolet aging of hemp fiber reinforced polypropylene composites. *Polymer Composites*, 42, 2544-2555.
- He, C., Ma, J., & Wang, L. (2015). A hemicellulose-bound form of silicon with potential to improve the mechanical properties and regeneration of the cell wall of rice. *New Phytologist*, 206, 1051-1062.
- Heath, R. L., & Packer, L. (1968). Photoperoxidation in isolated chloroplasts: I. Kinetics and stoichiometry of fatty acid peroxidation. *Archives of biochemistry and biophysics*, 125, 189-198.
- Hendrix, S., Jozefczak, M., Wójcik, M., Deckers, J., Vangronsveld, J., & Cuypers, A. (2020). Glutathione: A key player in metal chelation, nutrient homeostasis, cell cycle regulation and the DNA damage response in cadmium-exposed *Arabidopsis thaliana*. *Plant Physiology and Biochemistry*, 154, 498-507.

- Hernandez-Gomez, M. C., Rydahl, M. G., Rogowski, A., Morland, C., Cartmell, A., Crouch, L., ... & Knox, J. P. (2015). Recognition of xyloglucan by the crystalline cellulose-binding site of a family 3a carbohydrate-binding module. *FEBS letters*, 589, 2297-2303.
- Herrero, J., Esteban-Carrasco, A., & Zapata, J. M. (2013). Looking for *Arabidopsis thaliana* peroxidases involved in lignin biosynthesis. *Plant Physiology and Biochemistry*, 67, 77-86.
- Hong, T., Y., Cheng, C., W., Huang, J., W., and Meng, M. (2002). Isolation and biochemical characterization of an endo-1, 3- β -glucanase from *Streptomyces sioyaensis* containing a C-terminal family 6 carbohydrate-binding module that binds to 1, 3- β -glucan. *Microbiology*, 148, 1151-1159.
- Hossain, Z., Makino, T., and Komatsu, S. (2012). Proteomic study of β -aminobutyric acid-mediated cadmium stress alleviation in soybean. *Journal of Proteomics*, 75, 4151-4164.
- Hossain, Z., and Komatsu, S. (2013). Contribution of proteomic studies towards understanding plant heavy metal stress response. *Frontiers in Plant Science*, 3, 310.
- Houben, D., Sonnet, P., & Cornelis, J.-T. (2014). Biochar from *Miscanthus*: A potential silicon fertilizer. *Plant and soil*, 374, 871-882.
- Hu, G., Huang, S., Chen, H., & Wang, F. (2010). Binding of four heavy metals to hemicelluloses from rice bran. *Food research international*, 43, 203-206.
- Huang, Y., Li, D., Zhao, L., Chen, A., Li, J., Tang, H., Pan, G., Chang, L., Deng, Y., Huang, S. (2019). Comparative transcriptome combined with physiological analyses revealed key factors for differential cadmium tolerance in two contrasting hemp (*Cannabis sativa* L.) cultivars. *Industrial Crops and Products* 140, 111638.
- Huang, X., Duan, S., Wu, Q., Yu, M., & Shabala, S. (2020). Reducing cadmium accumulation in plants: structure–function relations and tissue-specific operation of transporters in the spotlight. *Plants*, 9, 223.
- Huang, S., & Ma, J. F. (2020). Silicon suppresses zinc uptake through down-regulating zinc transporter gene in rice. *Physiologia Plantarum*, 170, 580-591.
- Hussain, R., Weeden, H., Bogush, D., Deguchi, M., Soliman, M., Potlakayala, S., Katam, R., Goldman, S., and Rudrabhatta, S. (2019a). Enhanced tolerance of industrial hemp (*Cannabis sativa* L.) plants on abandoned mine land soil leads to overexpression of cannabinoids. *PloS ONE* 14, e0221570
- Hussain, A., Calabria-Holley, J., Lawrence, M., Ansell, M.P., Jiang, Y., Schorr, D., and Blanchet, P. (2019b). Development of novel building composites based on hemp and multi-functional silica matrix. *Composites B*, 156, 266-273.
- Hussain, S., Khaliq, A., Noor, M., A., Tanveer, M., Hussain, H., A., Hussain, S., et al. (2020). Metal Toxicity and Nitrogen Metabolism in Plants: An Overview. In *Carbon and Nitrogen Cycling in Soil* (221-248). Springer, Singapore.

- Imtiaz, M., Rizwan, M. S., Mushtaq, M. A., Ashraf, M., Shahzad, S. M., Yousaf, B., ... & Tu, S. (2016). Silicon occurrence, uptake, transport and mechanisms of heavy metals, minerals and salinity enhanced tolerance in plants with future prospects: a review. *Journal of environmental management*, 183, 521-529.
- Inaba, T., Alvarez-Huerta, M., Li, M., Bauer, J., Ewers, C., Kessler, F., and Schnell, D., J. (2005). *Arabidopsis* tic110 is essential for the assembly and function of the protein import machinery of plastids. *Plant Cell*, 17, 1482-1496.
- InterChanvre (2017) : Plan filière de l'interprofession du chanvre, Plan submitted to the French Ministry of Agriculture—Recherche Google. (s. d.). https://www.google.com/search?q=InterChanvre+%282017%29%3A+Plan+fili%C3%A8re+de+l%E2%80%99interprofession+du+chanvre%2C+Plan+submitted+to+the+French+Ministry+of+Agriculture&rlz=1C1PNJJ_frBE929BE929&sxsrf=ALeKk01BLuwSuiUo0zWTxFLDQ844QTXuRw%3A1619788994105&ei=wgSMYJr1BcicsAeyhZTgBA&oq=InterChanvre+%282017%29%3A+Plan+fili%C3%A8re+de+l%E2%80%99interprofession+du+chanvre%2C+Plan+submitted+to+the+French+Ministry+of+Agriculture&gs_lcp=Cgdnd3Mtd2l6EANQgqYKWIKmCmC_rApoAHACeACAAQCI AQCSAQCYAQQgAQKgAQGqAQdnd3Mtd2l6wAEB&scclient=gws-wiz&ved=0ahUKEwia3uqciKbwAhVIDuwKHbICBUwQ4dUDCA4&uact=5 (Accessed 29 April 2021)
- Iwasaki, K., & Matsumura, A. (1999). Effect of silicon on alleviation of manganese toxicity in pumpkin (*Cucurbita moschata* Duch cv. Shintosa). *Soil Science and Plant Nutrition*, 45, 909-920.
- Janus, A., Pelfrène, A., Heymans, S., Deboffe, C., Douay, F., & Waterlot, C. (2015). Elaboration, characteristics and advantages of biochars for the management of contaminated soils with a specific overview on *Miscanthus* biochars. *Journal of environmental management*, 162, 275-289.
- Janus, A., Pelfrène, A., Sahmer, K., Heymans, S., Deboffe, C., Douay, F., Waterlot, C. (2017) Value of biochars from *Miscanthus x giganteus* cultivated on contaminated soils to decrease the availability of metals in multicontaminated aqueous solutions. *Environmental Science and Pollution Reserach* 24, 18204-18217.
- Jaskulak, M., Grobelak, A., & Vandenbulcke, F. (2020). Modelling assisted phytoremediation of soils contaminated with heavy metals—Main opportunities, limitations, decision making and future prospects. *Chemosphere*, 249, 126196.
- Jenkins, C., & Orsburn, B. (2020). The *Cannabis* proteome draft map project. *International journal of molecular sciences*, 21, 965.
- Jian, M., Zhang, D., Wang, X., Wei, S., Zhao, Y., Ding, Q., et al. (2020). Differential expression pattern of the proteome in response to cadmium stress based on proteomics analysis of wheat roots. *BMC Genomics*, 21, 1-13.
- Jiang, Y., Bourebrab, M. A., Sid, N., Taylor, A., Collet, F., Pretot, S., ... & Lawrence, M. (2018). Improvement of water resistance of hemp woody substrates

- through deposition of functionalized silica hydrophobic coating, while retaining excellent moisture buffering properties. *ACS Sustainable Chemistry & Engineering*, 6, 10151-10161.
- Jia-Wen, W. U., Yu, S. H. I., Yong-Xing, Z. H. U., Yi-Chao, W. A. N. G., & Hai-Jun, G. O. N. G. (2013). Mechanisms of enhanced heavy metal tolerance in plants by silicon: a review. *Pedosphere*, 23, 815-825.
- Jonard, F., De Canniere, S., Brüggemann, N., Gentine, P., Gianotti, D. S., Lobet, G., ... & Vereecken, H. (2020). Value of sun-induced chlorophyll fluorescence for quantifying hydrological states and fluxes: Current status and challenges. *Agricultural and Forest Meteorology*, 291, 108088.
- Jost, J., P., and Jost-Tse, Y., C. (2018). Les plantes hyperaccumulatrices de métaux lourds: Une solution à la pollution des sols et de l'eau? Editions Publibook.
- Jozefczak, M., Keunen, E., Schat, H., Blik, M., Hernández, L. E., Carleer, R., ... & Cuypers, A. (2014). Differential response of *Arabidopsis* leaves and roots to cadmium: glutathione-related chelating capacity vs antioxidant capacity. *Plant Physiology and Biochemistry*, 83, 1-9.
- Kalaji, H. M., Jajoo, A., Oukarroum, A., Brestic, M., Zivcak, M., Samborska, I. A., ... & Ladle, R. J. (2016). Chlorophyll a fluorescence as a tool to monitor physiological status of plants under abiotic stress conditions. *Acta physiologiae plantarum*, 38, 102.
- Kalousek, P., Schreiber, P., Vyhnánek, T., Trojan, V., Adamcová, D., & Vaverková, M. D. (2020). Effect of landfill leachate on the growth parameters in two selected varieties of fiber hemp. *International Journal of Environmental Research*, 14, 155-163.
- Kaminski, K. P., Kørup, K., Andersen, M., N., Sønderkær, M., Andersen, M., S., Kirk, H., G., and Nielsen, K., L. (2015). Cytosolic glutamine synthetase is important for photosynthetic efficiency and water use efficiency in potato as revealed by high-throughput sequencing QTL analysis. *Theoretical and Applied Genetics*, 128, 2143-2153.
- Kanwar, V. S., Sharma, A., Srivastav, A. L., & Rani, L. (2020). Phytoremediation of toxic metals present in soil and water environment: a critical review. *Environmental Science and Pollution Research*, 1-26.
- Kaur, G., and Asthir, B. (2015). Proline: a key player in plant abiotic stress tolerance. *Biologia Plantarum*, 59, 609-619.
- Keeping, M., G., and Reynolds, O., L. (2009). Silicon in agriculture: new insights, new significance and growing application. *Annals of Applied Biology*, 155, 153.
- Khalid, N., Aqeel, M., & Noman, A. (2019). System biology of metal tolerance in plants: An integrated view of genomics, transcriptomics, metabolomics, and phenomics. *Plant Metallomics and Functional Omics*, 107-144.
- Khan, D. H., & Roy, A. C. (1964). Growth, p-uptake, and fibre cell dimensions of jute plant as affected by silicate treatment. *Plant and Soil*, 331-336.

- Khan, A. G., Kuek, C., Chaudhry, T. M., Khoo, C. S., & Hayes, W. J. (2000). Role of plants, mycorrhizae and phytochelators in heavy metal contaminated land remediation. *Chemosphere*, *41*, 197-207.
- Kim, Y. H., Khan, A. L., Waqas, M., & Lee, I. J. (2017). Silicon regulates antioxidant activities of crop plants under abiotic-induced oxidative stress: a review. *Frontiers in Plant Science*, *8*, 510.
- Kneeshaw, S., Keyani, R., Delorme-Hinoux, V., Imrie, L., Loake, G. J., Le Bihan, T., et al. (2017). Nucleoredoxin guards against oxidative stress by protecting antioxidant enzymes. *Proceedings of the National Academy of Sciences*, *114*, 8414-8419.
- Koren, Š., Arčon, I., Kump, P., Nečemer, M., & Vogel-Mikuš, K. (2013). Influence of CdCl₂ and CdSO₄ supplementation on Cd distribution and ligand environment in leaves of the Cd hyperaccumulator *Noccaea (Thlaspi) praecox*. *Plant and Soil*, *370*, 125-148.
- Kos, B., & Leštan, D. (2004). Soil washing of Pb, Zn and Cd using biodegradable chelator and permeable barriers and induced phytoextraction by *Cannabis sativa*. *Plant and soil*, *263*, 43-51.
- Kosová, K., Vítámvás, P., Urban, M. O., Prášil, I., T., and Renaut, J. (2018). Plant abiotic stress proteomics: the major factors determining alterations in cellular proteome. *Frontiers in Plant Science*, *9*, 122.
- Koushki, P., Kwok, T. H., Hof, L., & Wuthrich, R. (2020). Reinforcing silicone with hemp fiber for additive manufacturing. *Composites Science and Technology*, *194*, 108139.
- Kröger, N., & Poulsen, N. (2008). Diatoms—from cell wall biogenesis to nanotechnology. *Annual review of genetics*, *42*, 83-107.
- Krzyszowska, M. (2011). The cell wall in plant cell response to trace metals: polysaccharide remodeling and its role in defense strategy. *Acta physiologiae plantarum*, *33*, 35-51.
- Kubala, S., Gzarnczarska, M., Wojtyła, L., Clippe, A., Kosmala, A., Żmieńko, A., Lutts S., and Quinet, M. (2015). Deciphering priming-induced improvement of rapeseed (*Brassica napus* L.) germination through an integrated transcriptomic and proteomic approach. *Plant Science*, *231*, 94-113.
- Kumar, S., Singh, R., Kumar, V., Rani, A., & Jain, R. (2017). *Cannabis sativa*: A plant suitable for phytoremediation and bioenergy production. In *Phytoremediation potential of bioenergy plants* (pp. 269-285). Springer, Singapore.
- Kumarpandit, T., Kumarnaik, S., Patra, P. K., Dey, N., Patra, P. K., & Das, D. K. (2017). Influence of organic manure and lime on cadmium mobility in soil and uptake by spinach (*Spinacia oleracea* L.). *Communications in soil science and plant analysis*, *48*, 357-369.
- Kumpiene, J., Lagerkvist, A., & Maurice, C. (2008). Stabilization of As, Cr, Cu, Pb and Zn in soil using amendments—a review. *Waste management*, *28*, 215-225.

- Küpper, H., Küpper, F., & Spiller, M. (1998). In situ detection of heavy metal substituted chlorophylls in water plants. *Photosynthesis Research*, 58, 123-133.
- Kurade, M. B., Ha, Y. H., Xiong, J. Q., Govindwar, S. P., Jang, M., & Jeon, B. H. (2021). Phytoremediation as a green biotechnology tool for emerging environmental pollution: A step forward towards sustainable rehabilitation of the environment. *Chemical Engineering Journal*, 129040.
- Laird, J. S., Ryan, C. G., Kirkham, R. A., van der Ent, A., & Jamieson, D. N. (2019). PIXE imaging of hyperaccumulator plants using the Maia detector array. *Nuclear Instruments and Methods in Physics Research Section B: Beam Interactions with Materials and Atoms*, 451, 73-78.
- Lambrechts, T., Couder, E., Pilar Bernal M., Faz, A., Iserentant, A., & Lutts, Z. (2011). Assessment of heavy metal bioavailability in contaminated soils from a former mining area (La Union, Spain) using a rhizospheric test. *Water, Air, Soil and Pollution*, 217, 333-346.
- Landi, S., Berni, R., Capasso, G., Hausman, J. F., Guerriero, G., & Esposito, S. (2019). Impact of nitrogen nutrition on *Cannabis sativa*: an update on the current knowledge and future prospects. *International journal of molecular sciences*, 20, 5803.
- Larson, E., R., Van Zelm, E., Roux, C., Marion-Poll, A., and Blatt, M., R. (2017). Clathrin heavy chain subunits coordinate endo- and exocytic traffic and affect stomatal movement. *Plant Physiology*, 175, 708-720.
- Lee, D., G., Ahsan, N., Lee, S., H., Lee, J., J., Bahk, J., D., Kang, K., Y., and Lee, B., H. (2009). Chilling stress-induced proteomic changes in rice roots. *Journal of Plant Physiology*, 166, 1-11.
- Lefevre, I., Marchal, G., Corréal, E., Zanuzzi, A., & Lutts, S. (2009). Variation in response to heavy metals during vegetative growth in *Dorycnium pentaphyllum* Scop. *Plant Growth Regulation*, 59, 1-11.
- Lefèvre, I., Vogel-Mikus, J., Jeromel, J., Vavpetic, P., Planchon S., Arcon, I., van Elteren, J., Lepoint, G., Gobert, S., Renaut, J., Pelicon, P., and Lutts, S. (2014). Cadmium and zinc distribution in relation to their physiological impact in the leaves of the accumulating *Zygophyllum fabago* L. *Plant, Cell & Environment*, 37, 1299-1320.
- Lefèvre, I., Vogel-Mikuš, K., Arçon, I., & Lutts, S. (2016). How do roots of the metal-resistant perennial bush *Zygophyllum fabago* cope with cadmium and zinc toxicities?. *Plant and Soil*, 404, 193-207.
- Leitenmaier, B., and Küpper, H. (2011). Cadmium uptake and sequestration kinetics in individual leaf cell protoplasts of the Cd/Zn hyperaccumulator *Thlaspi caerulescens*. *Plant, Cell & Environment*, 34, 208-219.
- Leroux, O. (2012). Collenchyma: a versatile mechanical tissue with dynamic cell walls. *Annals of botany*, 110, 1083-1098.
- Li, C., L., Wang, M., Wu, X., M., Chen, D., H., Lv, H., J., Shen, J., L., et al. (2016). TH11, a thiamine thiazole synthase, interacts with Ca²⁺-dependent protein

kinase CPK33 and modulates the S-type anion channels and stomatal closure in *Arabidopsis*. *Plant Physiology*, 170, 1090-1104.

- Lichtenthaler, H. K. (1987). [34] Chlorophylls and carotenoids: pigments of photosynthetic biomembranes. *Methods in enzymology*, 148, 350-382.
- Linger, P., Müssig, J., Fischer, H., & Kobert, J. (2002). Industrial hemp (*Cannabis sativa* L.) growing on heavy metal contaminated soil: Fibre quality and phytoremediation potential. *Industrial Crops and Products*, 16, 33-42.
- Linger, P., Ostwald, A., & Haensler, J. (2005). *Cannabis sativa* L. growing on heavy metal contaminated soil: Growth, cadmium uptake and photosynthesis. *Biologia plantarum*, 49, 567-576.
- Liu, X., Zhang, A., Ji, C., Joseph, S., Bian, R., Li, L., Pan, G., & Paz-Ferreiro, J. (2013a). Biochar's effect on crop productivity and the dependence on experimental conditions—A meta-analysis of literature data. *Plant and Soil*, 373, 583-594.
- Liu, J., Ma, J., He, C., Li, X., Zhang, W., Xu, F., ... & Wang, L. (2013b). Inhibition of cadmium ion uptake in rice (*Oryza sativa*) cells by a wall-bound form of silicon. *New Phytologist*, 200, 691-699.
- Liu, N., Sun, Y., Pei, Y., Zhang, X., Wang, P., Li, X., et al. (2018). A pectin methylesterase inhibitor enhances resistance to *Verticillium* wilt. *Plant Physiology*, 176, 2202-2220.
- Loiacono, S., Crini, G., Martel, B., Chanet, G., Cosentino, C., Raschetti, M., ... & Morin-Crini, N. (2017). Simultaneous removal of Cd, Co, Cu, Mn, Ni, and Zn from synthetic solutions on a hemp-based felt. II. Chemical modification. *Journal of Applied Polymer Science*, 134, 45138.
- Loiacono, S., Morin-Crini, N., Martel, B., Chanet, G., Bradu, C., Torri, G., & Crini, G. (2018). Complexation du zinc, du cuivre et du manganèse par du chanvre: efficacité chimique et impact écotoxicologique. *Environnement, Risques & Santé*, 17, 240-252.
- Löser, C., Zehnsdorf, A., Fussy, M., & Stärk, H. J. (2002). Conditioning of heavy metal-polluted river sediment by *Cannabis sativa* L. *International Journal of Phytoremediation*, 4, 27-45.
- Lucena, J.J., Hernandez-Apaolaza, L. (2017). Iron nutrition in plants: an overview. *Plant Soil*, 41, 1-4
- Luo, R., Li, J., Zhao, Y., Fan, X., Zhao, P., & Chai, L. (2017). A critical review on the research topic system of soil heavy metal pollution bioremediation based on dynamic co-words network measures. *Geoderma*, 305, 281-292.
- Luo, Y., Zheng, Z., Wu, P., & Wu, Y. (2022). Effect of different direct revegetation strategies on the mobility of heavy metals in artificial zinc smelting waste slag: Implications for phytoremediation. *Chemosphere*, 286, 131678.
- Lux, A., Martinka, M., Vaculík, M., & White, P. J. (2011). Root responses to cadmium in the rhizosphere: a review. *Journal of experimental botany*, 62, 21-37.

- Luyckx, M., Hausman, J. F., Lutts, S., & Guerriero, G. (2017a). Silicon and plants: current knowledge and technological perspectives. *Frontiers in plant science*, 8, 411.
- Luyckx, M., Hausman, J. F., Lutts, S., & Guerriero, G. (2017b). Impact of silicon in plant biomass production: focus on bast fibres, hypotheses, and perspectives. *Plants*, 6, 37.
- Luyckx, M., Berni, R., Cai, G., Lutts, S., & Guerriero, G. (2019). Impact of heavy metals on non-food herbaceous crops and prophylactic role of Si. In *Plant Metallomics and Functional Omics* (pp. 303-321). Springer, Cham.
- Luyckx, M., Hausman, J.-F., Blanquet, M., Guerriero, G., & Lutts, S. (2021a). Silicon reduces cadmium absorption and increases root-to-shoot translocation without impacting growth in young plants of hemp (*Cannabis sativa* L.) on a short-term basis. *Environmental Science and Pollution Research*, 1-15.
- Luyckx, M., Hausman, J.-F., Isenborghs, A., Guerriero, G., & Lutts, S. (2021b). Impact of cadmium and zinc on proteins and cell wall-related gene expression in young stems of hemp (*Cannabis sativa* L.) and influence of exogenous silicon. *Environmental and Experimental Botany*, 183, 104363.
- Luyckx, M., Hausman, J. F., Sergeant, K., Guerriero, G., & Lutts, S. (2021c). Molecular and Biochemical Insights Into Early Responses of Hemp to Cd and Zn Exposure and the Potential Effect of Si on Stress Response. *Frontiers in Plant Science*, 12.
- Lyubenova, L., Pongrac, P., Vogel-Mikuš, K., Mezek, G. K., Vavpetič, P., Grlj, N., ... & Schröder, P. (2013). The fate of arsenic, cadmium and lead in *Typha latifolia*: a case study on the applicability of micro-PIXE in plant ionomics. *Journal of hazardous materials*, 248, 371-378.
- Ma, J. F., Miyake, Y., and Takahashi, E. (2001). Chapter 2 Silicon as a beneficial element for crop plants. In L. E. Datnoff, G. H. Snyder, & G. H. Korndörfer (Éds.), *Studies in Plant Science* (Vol. 8, p. 17-39). Elsevier.
- Ma, J., Cai, H., He, C., Zhang, W., and Wang, L. (2015). A hemicellulose-bound form of silicon inhibits cadmium ion uptake in rice (*Oryza sativa*) cells. *New Phytologist*, 206, 1063-1074.
- Ma, J. F., & Yamaji, N. (2015). A cooperative system of silicon transport in plants. *Trends in Plant Science*, 20, 435-442.
- Maghsoudi, K., Emam, Y., & Ashraf, M. (2015). Influence of foliar application of silicon on chlorophyll fluorescence, photosynthetic pigments, and growth in water-stressed wheat cultivars differing in drought tolerance. *Turkish Journal of Botany*, 39, 625-634.
- Mahar, A., Wang, P., Ali, A., Awasthi, M. K., Lahori, A. H., Wang, Q., ... & Zhang, Z. (2016). Challenges and opportunities in the phytoremediation of heavy metals contaminated soils: a review. *Ecotoxicology and environmental safety*, 126, 111-121.
- Mangeot-Peter, L., Legay, S., Hausman, J. F., Esposito, S., and Guerriero, G. (2016). Identification of reference genes for RT-qPCR data normalization in

- Cannabis sativa* stem tissues. *International Journal of Molecular Sciences*, 17, 1556.
- Masarovič, D., Slováková, E., Bokor, B., Bujdoš, M., & Lux, A. (2012). Effect of silicon application on *Sorghum bicolor* exposed to toxic concentration of zinc. *Biologia*, 67, 706-712.
- Matassa, S., Esposito, G., Pirozzi, F., & Papirio, S. (2020). Exploring the biomethane potential of different industrial hemp (*Cannabis sativa* L.) biomass residues. *Energies*, 13, 3361.
- Maxwell, K., Johnson, G. N. (2000). Chlorophyll fluorescence – A practical guide. *Journal of experimental botany*, 51, 659-668.
- Mayta, M. L., Hajirezaei, M. R., Carrillo, N., & Lodeyro, A. F. (2019). Leaf senescence: The chloroplast connection comes of age. *Plants*, 8, 495.
- McCartney, L., Marcus, S. E., & Knox, J. P. (2005). Monoclonal antibodies to plant cell wall xylans and arabinoxylans. *Journal of Histochemistry & Cytochemistry*, 53, 543-546.
- Meena, R. A. A., Sathishkumar, P., Ameen, F., Yusoff, A. R. M., & Gu, F. L. (2018). Heavy metal pollution in immobile and mobile components of lentic ecosystems—A review. *Environmental Science and Pollution Research*, 25, 4134-4148.
- Meers, E., Ruttens, A., Hopgood, M., Lesage, E., Tack, F.M.G. (2005) Potential of *Brassica rapa*, *Cannabis sativa*, *Helianthus annuus* and *Zea mays* for phytoextraction of heavy metals from calcareous dredged sediment derived soils. *Chemosphere*, 61, 561-572.
- Mendoza-Cózatl, D. G., Jobe, T. O., Hauser, F., & Schroeder, J. I. (2011). Long-distance transport, vacuolar sequestration, tolerance, and transcriptional responses induced by cadmium and arsenic. *Current opinion in plant biology*, 14, 554-562.
- Mihoc, M., Pop, G., Alexa, E., & Radulov, I. (2012). Nutritive quality of romanian hemp varieties (*Cannabis sativa* L.) with special focus on oil and metal contents of seeds. *Chemistry Central Journal*, 6, 1-12.
- MisChar program. Data were acquired as part of the MisChar program (Convention MisChar n°1672C0044) financed by ADEME (French Agency for the Environment and Energy Management, and aimed at "re-qualifying areas degraded by past industrial activities"
- Mishra, S., Bharagava, R. N., More, N., Yadav, A., Zainith, S., Mani, S., & Chowdhary, P. (2019). Heavy metal contamination: an alarming threat to environment and human health. In *Environmental biotechnology: For sustainable future* (pp. 103-125). Springer, Singapore.
- Mlinarić, S., Dunić, J. A., Štolfa, I., Cesar, V., & Lepeduš, H. (2016). High irradiation and increased temperature induce different strategies for competent photosynthesis in young and mature fig leaves. *South African Journal of Botany*, 103, 25-31.

- Mokshina, N., Gorshkov, O., Ibragimova, N., Chernova, T., & Gorshkova, T. (2017). Cellulosic fibres of flax recruit both primary and secondary cell wall cellulose synthases during deposition of thick tertiary cell walls and in the course of graviresponse. *Functional Plant Biology*, *44*, 820-831.
- Morin-Crini, N., Loiacono, S., Placet, V., Torri, G., Bradu, C., Kostić, M., ... & Crini, G. (2019). Hemp-based adsorbents for sequestration of metals: a review. *Environmental Chemistry Letters*, *17*, 393-408.
- Mudhoo, A., Ramasamy, D.L., Bhatnagar, A., Usman, M., Sillanpää M. (2020) An analysis of the versatility and effectiveness of compost for sequestering metal ions, dyes and xenobiotics from soils and aqueous milieu. *Ecotoxicology and Environmental Safety* *197*, 110587.
- Müller, M., and Munné-Bosch, S. (2015). Ethylene response factors: a key regulatory hub in hormone and stress signaling. *Plant Physiology*, *169*, 32-41.
- Muthusaravanan, S., Sivarajasekar, N., Vivek, J. S., Paramasivan, T., Naushad, M., Prakashmaran, J., ... & Al-Duaij, O. K. (2018). Phytoremediation of heavy metals: mechanisms, methods and enhancements. *Environmental chemistry letters*, *16*, 1339-1359.
- Nakagawa, K., Yoshinaga, A., & Takabe, K. (2014). Xylan deposition and lignification in the multi-layered cell walls of phloem fibres in *Mallotus japonicus* (Euphorbiaceae). *Tree physiology*, *34*, 1018-1029.
- Nawaz, M., A., Zakharenko, A., M., Zemchenko, I., V., Haider, M., S., Ali, M., A., Imtiaz, M., et al. (2019). Phytolith formation in plants: From soil to cell. *Plants*, *8*, 249.
- Neina, D. (2019). The Role of Soil pH in Plant Nutrition and Soil Remediation. *Applied and Environmental Soil Science*, *2019*, e5794869. <https://doi.org/10.1155/2019/5794869>
- Neumann, D., & Zur Nieden, U. (2001). Silicon and heavy metal tolerance of higher plants. *Phytochemistry*, *56*, 685-692.
- Neutelings, G. (2011). Lignin variability in plant cell walls: contribution of new models. *Plant Science*, *181*, 379-386.
- Novo-Uzal, E., Fernández-Pérez, F., Herrero, J., Gutiérrez, J., Gómez-Ros, L. V., Bernal, M. Á., ... & Pedreño, M. Á. (2013). From *Zinnia* to *Arabidopsis*: approaching the involvement of peroxidases in lignification. *Journal of experimental botany*, *64*, 3499-3518.
- O'Leary, R., Kasai, K., Clark, N., Fujiwara, T., Sozzani, R., and Gallagher, K., L. (2018). Exposure to heavy metal stress triggers changes in plasmodesmatal permeability via deposition and breakdown of callose. *Journal of Experimental Botany*, *69*, 3715-3728.
- Orue, A., Jauregi, A., Unsuain, U., Labidi, J., Eceiza, A., & Arbelaz, A. (2016). The effect of alkaline and silane treatments on mechanical properties and breakage of sisal fibers and poly (lactic acid)/sisal fiber composites. *Composites Part A: Applied Science and Manufacturing*, *84*, 186-195.

- Parrotta, L., Guerriero, G., Sergeant, K., Cai, G., and Hausman, J., F. (2015). Target or barrier? The cell wall of early-and later-diverging plants vs cadmium toxicity: differences in the response mechanisms. *Frontiers in Plant Science*, 6, 133.
- Parvez, A.M., Lewis, J.D. (2021) Potential of industrial hemp (*Cannabis sativa* L.) for bioenergy production in Canada: Status, challenges and outlook. *Renewable and Sustainable Energy Reviews* 141, 110784.
- Pejic, B., Vukcevic, M., Kostic, M., & Skundric, P. (2009). Biosorption of heavy metal ions from aqueous solutions by short hemp fibers : Effect of chemical composition. *Journal of Hazardous Materials*, 164, 146-153.
- Pejic, B. M., Vukcevic, M. M., Pajic-Lijakovic, I. D., Lausevic, M. D., & Kostic, M. M. (2011). Mathematical modeling of heavy metal ions (Cd^{2+} , Zn^{2+} and Pb^{2+}) biosorption by chemically modified short hemp fibers. *Chemical engineering journal*, 172, 354-360.
- Peralta-Videa, J. R., Lopez, M. L., Narayan, M., Saupe, G., & Gardea-Torresdey, J. (2009). The biochemistry of environmental heavy metal uptake by plants : Implications for the food chain. *The international journal of biochemistry & cell biology*, 41, 1665-1677.
- Pidlisnyuk, V., Newton, R. A., & Mamirova, A. (2021). Miscanthus biochar value chain-A review. *Journal of Environmental Management*, 290, 112611.
- Pietrini, F., Passatore, L., Patti, V., Francocci, F., Giovannozzi, A., & Zacchini, M. (2019). Morpho-physiological and metal accumulation responses of hemp plants (*Cannabis Sativa* L.) grown on soil from an agro-industrial contaminated area. *Water*, 11, 808.
- Pilon, C., Soratto, R. P., & Moreno, L. A. (2013). Effects of soil and foliar application of soluble silicon on mineral nutrition, gas exchange, and growth of potato plants. *Crop Science*, 53, 1605-1614.
- Piot, A., Béjat, T., Jay, A., Bessette, L., Wurtz, E., & Barnes-Davin, L. (2017). Study of a hempcrete wall exposed to outdoor climate: Effects of the coating. *Construction and Building Materials*, 139, 540-550.
- Piotrowska-Cyplik, A., & Czarnecki, Z. (2003). Phytoextraction of Heavy Metals by Hemp during Anaerobic Sewage Sludge Management in the Non-Industrial Sites. *Polish Journal of Environmental Studies*, 12.
- Pires-Lira, M. F., de Castro, E. M., Lira, J. M. S., de Oliveira, C., Pereira, F. J., & Pereira, M. P. (2020). Potential of *Panicum aquaticum* Poir. (Poaceae) for the phytoremediation of aquatic environments contaminated by lead. *Ecotoxicology and environmental safety*, 193, 110336.
- Pogrzeba, M., Krzyżak, J., Rusinowski, S., McCalmont, J. P., & Jensen, E. (2019). Energy crop at heavy metal-contaminated arable land as an alternative for food and feed production: biomass quantity and quality. In *Plant metallomics and functional omics* (pp. 1-21). Springer, Cham.
- Pós, V., Hunyadi-Gulyás, É., Caiazzo, R., Jócsák, I., Medzihradzsky, K., and Lukács, N. (2011). Induction of pathogenesis-related proteins in intercellular fluid by

cadmium stress in barley (*Hordeum vulgare* L.)—a proteomic analysis. *Acta Alimentaria*, 40, 164-175.

- Poschenrieder, C., & Coll, J. B. (2003). Phytoremediation: principles and perspectives. *Contributions to science*, 333-344.
- Poulsen, N., & Kroger, N. (2004). Silica morphogenesis by alternative processing of silaffins in the diatom *Thalassiosira pseudonana*. *Journal of Biological Chemistry*, 279, 42993-42999.
- Praspaliauskas, M., Žaltauskaitė, J., Pedišius, N., & Striūgas, N. (2020). Comprehensive evaluation of sewage sludge and sewage sludge char soil amendment impact on the industrial hemp growth performance and heavy metal accumulation. *Industrial Crops and Products*, 150, 112396.
- Rai, R., Agrawal, M., and Agrawal, S., B. (2016). Impact of heavy metals on physiological processes of plants: with special reference to photosynthetic system. In *Plant Responses to Xenobiotics*. Springer, Singapore.
- Réquilé S., Le Duigou, A., Bourmaud, A., Baley, C. (2018) Peeling experiments for hemp retting characterization targeting biocomposites. *Industrial Crops and Products* 123, 573-580.
- Rheay, H. T., Omondi, E. C., & Brewer, C. E. (2020). Potential of hemp (*Cannabis sativa* L.) for paired phytoremediation and bioenergy production. *GCB Bioenergy*, 13, 525-536.
- Rodríguez-Vila, A., Forján, R., Guedes, R. S., & Covelo, E. F. (2016). Changes on the Phytoavailability of Nutrients in a Mine Soil Reclaimed with Compost and Biochar. *Water, Air, & Soil Pollution*, 227, 453. <https://doi.org/10.1007/s11270-016-3155-x>
- Saxena, G., Purchase, D., Mulla, S. I., Saratale, G. D., & Bharagava, R. N. (2019). Phytoremediation of heavy metal-contaminated sites : Eco-environmental concerns, field studies, sustainability issues, and future prospects. *Reviews of Environmental Contamination and Toxicology Volume 249*, 71-131.
- Schäfer, H. J., Greiner, S., Rausch, T., & Haag-Kerwer, A. (1997). In seedlings of the heavy metal accumulator *Brassica juncea* Cu²⁺ differentially affects transcript amounts for γ -glutamylcysteine synthetase (γ -ECS) and metallothionein (MT2). *FEBS letters*, 404, 216-220.
- Schluttenhofer, C., & Yuan, L. (2017). Challenges towards revitalizing hemp: A multifaceted crop. *Trends in plant science*, 22, 917-929.
- Schneider, T., Haag-Kerwer, A., Maetz, M., Niecke, M., Povh, B., Rausch, T., & Schübler, A. (1999). Micro-PIXE studies of elemental distribution in Cd-accumulating *Brassica juncea* L. *Nuclear Instruments And Methods In Physics Research Section B: Beam Interactions With Materials And Atoms*, 158, 329-334.
- Seifikalhor, M., Aliniaiefard, S., Hassani, B., Niknam, V., & Lastochkina, O. (2019). Diverse role of γ -aminobutyric acid in dynamic plant cell responses. *Plant cell reports*, 1-21.

- Sengupta, D., Naik, D., & Reddy, A. R. (2015). Plant aldo-keto reductases (AKRs) as multi-tasking soldiers involved in diverse plant metabolic processes and stress defense: A structure-function update. *Journal of plant physiology*, *179*, 40-55.
- Shahid, M., Khalid, S., Abbas, G., Niazi, N. K., Murtaza, B., Rashid, M. I., & Bibi, I. (2019). Redox Mechanisms and Plant Tolerance Under Heavy Metal Stress: Genes and Regulatory Networks. In *Plant Metallomics and Functional Omics* (pp. 71-105). Springer, Cham.
- Shanying, H. E., Xiaoe, Y. A. N. G., Zhenli, H. E., & Baligar, V. C. (2017). Morphological and physiological responses of plants to cadmium toxicity: a review. *Pedosphere*, *27*, 421-438.
- Shao, H. B., Chu, L. Y., Lu, Z. H., & Kang, C. M. (2008). Primary antioxidant free radical scavenging and redox signaling pathways in higher plant cells. *International Journal of Biological Sciences*, *4*, 8.
- Sharma, S., S., Dietz, K. J., and Mimura, T. (2016). Vacuolar compartmentalization as indispensable component of heavy metal detoxification in plants. *Plant Cell and Environment*, *39*, 1112-1126.
- Shen, B., Li, C., & Tarczynski, M. C. (2002). High free-methionine and decreased lignin content result from a mutation in the *Arabidopsis* S-adenosyl-L-methionine synthetase 3 gene. *The Plant Journal*, *29*, 371-380.
- Shi, X., Zhang, C., Wang, H., & Zhang, F. (2005). Effect of Si on the distribution of Cd in rice seedlings. *Plant and Soil*, *272*, 53-60.
- Shi, G. R., Cai, Q. S., Liu, Q. Q., & Wu, L. (2009). Salicylic acid-mediated alleviation of cadmium toxicity in hemp plants in relation to cadmium uptake, photosynthesis, and antioxidant enzymes. *Acta physiologiae plantarum*, *31*, 969-977.
- Shi, G., Liu, C., Cui, M., Ma, Y., & Cai, Q. (2012). Cadmium tolerance and bioaccumulation of 18 hemp accessions. *Applied biochemistry and biotechnology*, *168*, 163-173.
- Shiyu, Q. I. N., Hongen, L. I. U., Zhaojun, N. I. E., Rengel, Z., Wei, G. A. O., Chang, L. I., & Peng, Z. H. A. O. (2020). Toxicity of cadmium and its competition with mineral nutrients for uptake by plants: A review. *Pedosphere*, *30*, 168-180.
- Shrestha, U. R., Smith, S., Pingali, S. V., Yang, H., Zahran, M., Breunig, L., ... & Petridis, L. (2019). Arabinose substitution effect on xylan rigidity and self-aggregation. *Cellulose*, *26*, 2267-2278.
- Siddique, A., Kandpal, G., and Kumar, P. (2018). Proline Accumulation and its Defensive Role Under Diverse Stress Condition in Plants: An Overview. *Journal of Pure and Applied Microbiology*, *12*, 1655-1659.
- Singh, S., Parihar, P., Singh, R., Singh, V., P., and Prasad, S., M. (2016). Heavy metal tolerance in plants: role of transcriptomics, proteomics, metabolomics, and ionomics. *Frontiers in Plant Science*, *6*, 1143.

- Smirnova, J., Fernie, A., R., Spahn, C., M., and Steup, M. (2017). Photometric assay of maltose and maltose-forming enzyme activity by using 4-alpha-glucanotransferase (DPE2) from higher plants. *Analytical Biochemistry*, 532, 72-82.
- SPAQuE (2011). Accueil > Publications > Métaux lourds. Consulté en ligne le 16/04/14, disponible à l'adresse <http://www.spaque.be/0125/fr/Publications>
- Stevulova, N., Cigasova, J., Estokova, A., Terpakova, E., Geffert, A., Kacik, F., ... & Holub, M. (2014). Properties characterization of chemically modified hemp hurds. *Materials*, 7, 8131-8150.
- Stirbet, A., Lazár, D., & Kromdijk, J. (2018). Chlorophyll a fluorescence induction: can just a one-second measurement be used to quantify abiotic stress responses? *Photosynthetica*, 56, 86-104.
- Tang, H. M., Liu, S., Hill-Skinner, S., Wu, W., Reed, D., Yeh, C. T., ... & Schnable, P. S. (2014). The maize *brown midrib2 (bm2)* gene encodes a methylenetetrahydrofolate reductase that contributes to lignin accumulation. *The Plant Journal*, 77, 380-392.
- Taylor, N. G., Howells, R. M., Huttly, A. K., Vickers, K., & Turner, S. R. (2003). Interactions among three distinct CesA proteins essential for cellulose synthesis. *Proceedings of the National Academy of Sciences*, 100, 1450-1455.
- Tennstedt, P., Peisker, D., Bottcher, C., Trampczynska, A., & Clemens, S. (2009). Phytochelatin synthesis is essential for the detoxification of excess zinc and contributes significantly to the accumulation of zinc. *Plant Physiology*, 149, 938-948.
- Tóth, G., Hermann, T., Da Silva, M. R., & Montanarella, L. (2016). Heavy metals in agricultural soils of the European Union with implications for food safety. *Environment international*, 88, 299-309.
- Vandepitte, K., Vasile, S., Vermeire, S., Vanderhoeven, M., Van der Borght, W., Latré, J., ... & Troch, V. (2020). Hemp (*Cannabis sativa* L.) for high-value textile applications: the effective long fiber yield and quality of different hemp varieties, processed using industrial flax equipment. *Industrial Crops and Products*, 158, 112969.
- Vareda, J. P., Valente, A. J., & Durães, L. (2019). Assessment of heavy metal pollution from anthropogenic activities and remediation strategies: A review. *Journal of environmental management*, 246, 101-118.
- Vemanna, R., S., Babitha, K., C., Solanki, J., K., Reddy, V., A., Sarangi, S., K., and Udayakumar, M. (2017). Aldo-keto reductase-1 (AKR1) protect cellular enzymes from salt stress by detoxifying reactive cytotoxic compounds. *Plant Physiology and Biochemistry*, 113, 177-186.
- Vincent, D., Binos, S., Rochfort, S., & Spangenberg, G. (2019). Top-down proteomics of medicinal cannabis. *Proteomes*, 7, 33.

- Viswanathan, M. B., Cheng, M. H., Clemente, T. E., Dweikat, I., & Singh, V. (2021). Economic perspective of ethanol and biodiesel coproduction from industrial hemp. *Journal of Cleaner Production*, 299, 126875.
- Vogel-Mikuš, K., SIMČIĆ, J., PELICON, P., BUDNAR, M., Kump, P., NEČEMER, M., ... & Regvar, M. (2008). Comparison of essential and non-essential element distribution in leaves of the Cd/Zn hyperaccumulator *Thlaspi praecox* as revealed by micro-PIXE. *Plant, cell & environment*, 31, 1484-1496.
- Vogel-Mikuš, K., Pongrac, P., & Pelicon, P. (2014). Micro-PIXE elemental mapping for ionome studies of crop plants. *International Journal of PIXE*, 24(03n04), 217-233.
- Vollenweider, P., Cosio, C., Günthardt-Goerg, M. S., & Keller, C. (2006). Localization and effects of cadmium in leaves of a cadmium-tolerant willow (*Salix viminalis* L.): Part II Microlocalization and cellular effects of cadmium. *Environmental and Experimental Botany*, 58, 25-40.
- Vukčević, M., Pejić, B., Kalijadis, A., Pajić-Lijaković, I., Kostić, M., Laušević, Z., & Laušević, M. (2014). Carbon materials from waste short hemp fibers as a sorbent for heavy metal ions—Mathematical modeling of sorbent structure and ions transport. *Chemical Engineering Journal*, 235, 284-292.
- Vukcevic, M., Pejic, B., Lausevic, M., Pajic-Lijakovic, I., & Kostic, M. (2014). Influence of chemically modified short hemp fiber structure on biosorption process of Zn²⁺ ions from waste water. *Fibers and Polymers*, 15, 687-697.
- Wan, L., and Zhang, H. (2012). Cadmium toxicity. *Plant Sign. Behav.* 7, 345-348.
- Wang, C., Yan, X., Chen, Q., Jiang, N., Fu, W., Ma, B., et al. (2013). Clathrin light chains regulate clathrin-mediated trafficking, auxin signaling, and development in *Arabidopsis*. *Plant Cell*, 25, 499-516.
- Wang, S., Wang, F., & Gao, S. (2015a). Foliar application with nano-silicon alleviates Cd toxicity in rice seedlings. *Environmental Science and Pollution Research*, 22, 2837-2845.
- Wang, P., Deng, X. J., Huang, Y. A., Fang, X. L., Zhang, J., Wan, H. B., Yang, C. Y. (2015b). Comparison of subcellular distribution and chemical forms of 180 S. Y. QIN et al. cadmium among four soybean cultivars at young seedlings. *Environmental Science and Pollution Research*, 22: 19584–19595.
- Wang, S., Wang, F., Gao, S., & Wang, X. (2016). Heavy metal accumulation in different rice cultivars as influenced by foliar application of nano-silicon. *Water, Air, & Soil Pollution*, 227, 1-13.
- Wang, L., Ji, B., Hu, Y., Liu, R., & Sun, W. (2017). A review on in situ phytoremediation of mine tailings. *Chemosphere*, 184, 594-600.
- Wang, W., Wang, Z., Yang, K., Wang, P., Wang, H., Guo, L., ... & He, X. (2020). Biochar application alleviated negative plant-soil feedback by modifying soil microbiome. *Frontiers in microbiology*, 11, 799.

- Waterlot C., Hechelski M. (2019). Benefits of ryegrass on multicontaminated soils. Part 1: Effects of fertilizers on bioavailability and accumulation of metals. *Sustainability*, 11, 5093-6013.
- Wessel, D., and Flügge, U.I. (1984). A method for the quantitative recovery of protein in dilute solution in the presence of detergents and lipids. *Analytical Biochemistry*, 138, 141-143.
- Wongkaew, A., Nakamura, S. I., Suzui, N., Yin, Y. G., Ishii, S., Kawachi, N., ... & Ohkama-Ohtsu, N. (2019). Elevated glutathione synthesis in leaves contributes to zinc transport from roots to shoots in Arabidopsis. *Plant Science*, 283, 416-423.
- Wu, J.W., Shi Y, Zhu Y.X., Wang Y.C., Gong H.J. (2013) Mechanisms of enhanced heavy metal tolerance in plants by silicon: a review. *Pedosphere*, 23, 815–825
- Wu, Y., Trejo, H. X., Chen, G., & Li, S. (2021). Phytoremediation of contaminants of emerging concern from soil with industrial hemp (*Cannabis sativa* L.): a review. *Environment, Development and Sustainability*, 1-31.
- Xu, Y., Geng, D., Guo, H., ang, M., Yang, Q. (2021) Accumulation and sub cellular distribution of lead (Pb) in industrial hemp grown in Pb contaminated soil. *Industrial Crops and Products* 161, 113220.
- Yamauchi, S., Ichikawa, H., Nishiwaki, H., & Shuto, Y. (2015). Evaluation of plant growth regulatory activity of furofuran lignan bearing a 7, 9': 7', 9-Diepoxy structure using optically pure (+)-and (–)-Enantiomers. *Journal of agricultural and food chemistry*, 63, 5224-5228.
- Yan, X., Wang, J., Zhu, L., Wang, J., Li, S., & Kim, Y. M. (2021). Oxidative stress, growth inhibition, and DNA damage in earthworms induced by the combined pollution of typical neonicotinoid insecticides and heavy metals. *Science of The Total Environment*, 754, 141873.
- Yang, W., Y., Zheng, Y., Bahn, S., C., Pan, X., Q., Li, M., Y., Vu, H., S., et al. (2012). The patatin-containing phospholipase A pPLAII α modulates oxylipin formation and water loss in *Arabidopsis thaliana*. *Molecular Plant*, 5, 452-460.
- Yang, Y., Zhou, X., Tie, B., Peng, L., Li, H., Wang, K., & Zeng, Q. (2017). Comparison of three types of oil crop rotation systems for effective use and remediation of heavy metal contaminated agricultural soil. *Chemosphere*, 188, 148-156.
- Yang, R., Berthold, E. C., McCurdy, C. R., da Silva Benevenuto, S., Brym, Z. T., & Freeman, J. H. (2020). Development of cannabinoids in flowers of industrial hemp (*Cannabis sativa* L.): a pilot study. *Journal of agricultural and food chemistry*, 68, 6058-6064.
- Ye, J., Yan, C., Liu, J., Lu, H., Liu, T., and Song, Z. (2012). Effects of silicon on the distribution of cadmium compartmentation in root tips of *Kandelia obovata* (S., L.) Yong. *Environmental Pollution*, 162, 369-373.

- Yeo, A. R., Flowers, S. A., Rao, G., Welfare, K., Senanayake, N., & Flowers, T. J. (1999). Silicon reduces sodium uptake in rice (*Oryza sativa* L.) in saline conditions and this is accounted for by a reduction in the transpirational bypass flow. *Plant, Cell & Environment*, 22, 559-565.
- Zajaczkowska, A., Korzeniowska, J., & Sienkiewicz-Cholewa, U. (2020). Effect of soil and foliar silicon application on the reduction of zinc toxicity in wheat. *Agriculture*, 10, 522.
- Zeng, L., Zhu, T., Gao, Y., Wang, Y., Ning, C., Björn, L. O., ... & Li, S. (2017). Effects of Ca addition on the uptake, translocation, and distribution of Cd in *Arabidopsis thaliana*. *Ecotoxicology and environmental safety*, 139, 228-237.
- Zhao, J., Xu, Y., Wang, W., Griffin, J., Roozeboom, K., & Wang, D. (2020). Bioconversion of industrial hemp biomass for bioethanol production: A review. *Fuel*, 281, 118725.
- Zhou, M. X., Dailly, H., Renard, M. E., Han, R. M., & Lutts, S. (2018). NaCl impact on *Kosteletzkya pentacarpos* seedlings simultaneously exposed to cadmium and zinc toxicities. *Environmental Science and Pollution Research*, 25, 17444-17456.
- Zhu, Y., Gong, H. (2014). Beneficial effects of silicon on salt and drought tolerance in plants. *Agronomy for Sustainable Development*, 34, 455–472.
- Zielonka, D., Szulc, W., Skowrońska, M., Rutkowska, B., & Russel, S. (2020). Hemp-Based Phytoaccumulation of Heavy Metals from Municipal Sewage Sludge and *Phosphogypsum* Under Field Conditions. *Agronomy*, 10, 907.
- Zlobin, I. E. (2021). Current understanding of plant zinc homeostasis regulation mechanisms. *Plant Physiology and Biochemistry*.

General Discussion

Human activities related to urbanization, industrialization and agriculture practices have resulted in the accumulation of heavy metals in soils and water in numerous areas of the world. Zinc and cadmium are frequently simultaneously found in contaminated soils, including agronomic soils contaminated by atmospheric fallout near smelters. Management of these contaminated soils constitutes a major environmental challenge since toxic metals are not biodegradable, and their accumulation in soils can affect the soil physicochemical and biological properties, thereby representing a threat to plants and animals and ultimately constitute a major risk for human health (Linger et al., 2005; Saxena et al., 2019; Jaskulak et al., 2020).

Many plant species have the ability to grow on these contaminated sites and some of them are able to accumulate high concentrations of heavy metals in their tissues. Plants may thus be grown on heavy metal-contaminated substrate for two distinct purposes. The first one is phytomanagement where plants are cultivated to extract, degrade, or immobilize various contaminants from polluted soils (Barceló and Poschenrieder 2003; Ali et al. 2013). The second application consists in the use of non-edible crop of commercial interest to valorise marginal farmland soils and provide incomes for the farmer (Tóth et al. 2016; Feng et al. 2020). If the harvested organs are free of pollutant while the remaining part of the shoot contains high amounts of pollutant, it appears possible to combine an agricultural purpose and a phytomanagement process. However, “soil remediation” is usually considered independently of “soil production” and there is an obvious lack of information regarding the possibility to conciliate phytomanagement and obtaining valuable marketable products.

Cannabis sativa L. (hemp) is a promising species for fibre production on moderately heavy metal-contaminated substrates (Hussain et al., 2019b; Pietrini et al., 2019) and considered as a potential crop for cleaning the soil from heavy metals because of its high biomass production, its long root system and its capability to absorb and accumulate heavy metals (Ahmad et al., 2016c; Kumar et al., 2017). The major factors that will impact the possibility to combine soil management with hemp plants for fibres production include: the contaminant concentration and distribution in hemp raw material, hemp HM tolerance, and the impact of HM on fibre yield and quality, although there is still a paucity of information regarding the last aspects.

Besides, the young plant stage is often considered the most sensitive one to heavy metals. To devise agricultural strategies aimed at improving crop yield, the effect of silicon (Si) on plants' stress resistance should be considered as a promising strategy (Luyckx et al., 2017a, b). The beneficial effects of Si fertilizers on plant growth and crop yields are well documented in the literature (Keeping and Reynolds, 2009; Bhat et al., 2019). However, to the best of our knowledge, no data are available regarding silicon impact on heavy metal-treated young plants of hemp.

This thesis thus aims at determining i) the capability of hemp to absorb and accumulate heavy metals from a soil management perspective; ii) its ability to adapt to heavy metals stress conditions; iii) the impact of heavy metals on fibre differentiation and properties in relation to heavy metal accumulation in young stem; iv) and the short-term impact of Si on hemp responses and fibre development in stressed and unstressed plants.

Hemp capability to absorb and accumulate heavy metals from a soil management perspective

To combine an agricultural purpose and a phytomanagement process, determining bioaccumulation and root-to-shoot translocation factors, as well as pollutant distribution among plant organs, is of paramount importance.

For this purpose, we used two different strategies: the first one consist to analyze the behaviour of hemp growing on a moderately contaminated agricultural soil for the whole growing period and to apply Si by foliar spraying. The second one implies to expose young plants for a short period on nutrient solution containing high concentrations of pollutants and to apply Si through the root system. Although these two approaches may appear somewhat contradictory, they are in fact complementary and allow us to obtain valuable information regarding the interest of hemp in relation to environmental management.

The use of nutrient solution with high heavy metals bioavailability allowed the quantification of the maximal capacities of the plant for bioaccumulation of pollutants independently of the adsorption process occurring in the soils and which restricts heavy metals transfer from soil to the root system (Kos and Leštan 2004; Ferrarini et al., 2021). It is well known that heavy metals cations may be adsorbed on clay particle and organic matter, strongly reducing their bioavailability for root absorption while nutrient

solution may be more adequately controlled regarding this aspect (Lambrechts et al., 2011).

We have evidenced in Chapters 3 and 4 the capability of *C. sativa* to accumulate high Cd and Zn concentrations in roots (the main organ of accumulation) and shoots, with Cd shoot concentrations quite higher than 100 mg kg⁻¹ dry weight, the commonly referenced as the minimum value for Cd hyperaccumulating plants (Mahar et al., 2016). Despite such a high level of accumulation, hemp could not be considered as a hyperaccumulating species since both metals strongly impaired growth. However, the recorded bioaccumulation factors, close to 90 for Cd and close to 50 for Zn, confirm its interest for phytoextraction purposes. These values should be regarded as “artificial” since they are established with very high doses rarely found in contaminated areas (Vareda et al., 2019). Moreover, the duration of exposure remained rather short (one week) and is not relevant from the long-term impact of accumulated heavy metals on plant metabolism.

Hence, it is essential to keep in mind that, apart from the extraction capabilities of the plant, the bioavailability of heavy metals in the soil is another crucial element of phytoextraction (Di Candito et al., 2004). For realistic results, an experiment was performed under field conditions on an agricultural soil previously contaminated by atmospheric fallout from a lead and zinc smelter closed in 2003 (Chapter 1). We demonstrated that hemp phytoextraction capacity was limited by the low environmental availability of heavy metals (estimated by classical CaCl₂ procedure), although, heavy metals were probably only partially translocated from roots to shoots in order to preserve photosynthetically active parts of the plant as demonstrated in controlled conditions. However, hemp high biomass yield and its important root system may reduce the dispersion of heavy metals in the environment suggesting that, in conditions of low environmental availability, hemp could be used as a suitable crop for phytostabilization rather than phytoextraction strategies, as previously suggested (Angelova et al., 2004; Pietrini et al., 2019; Wu et al., 2021).

As demonstrated in this thesis, the bioavailability of heavy metals in the soil is of paramount importance to decide whether hemp should be used for phytostabilization of phytoextraction strategies. A study performed on hemp cultivars cultivated on alkaline or acidic soils concluded that, based on bioaccumulation values, the potential ability for phytostabilization was observed in alkaline soil in order: Cu>Cr>Cd>Mo>Hg>Zn> Ni>Co>As>Pb, while in acid soil in order: Zn>Cd>Cr>Ni>Hg>Cu>Mo>As>Co>Pb. On

alkaline soil, Futura 75, and Santhica 27 proved to be hyperaccumulators of Zn and Mo; and Santhica 27 of Hg. On acid soil, Santhica 27 was hyperaccumulators of Cd and Zn; and Futura 75 and Santhica 27 hyperaccumulated Mo (Galić et al., 2019).

Besides, heavy metals bioavailability could be improved through the use of chelating agents (such as EDTA, EDDS or NTA) (Ferrarini et al., 2021), but they should be used carefully to prevent seepage of the solubilized metals into deeper layers of the soil and groundwater (Di Candito et al., 2004). Moreover, if the purpose is to be able to exploit contaminated soil, the optimal balance between heavy metals extraction, their concentration in the commercial parts of the plant, and sufficient plant development must be met. Kos and Lestan (2004) consider that the use of chelating agent may constitute an interesting strategy of so-called “induced phytotextraction”, but the aim of this strategy is only to remove pollutant from the soil, the harvested plants having no economic interest despite being incinerated to reduce volume of toxic metals. For this purpose, plants may even be dead at the time of harvest, the only important criteria being the amount of pollutant removed from the soil which is a function of plant biomass and heavy metals accumulation.

Our purpose is completely different: we intend to produce hemp in order to provide incomes for the farmer who are not allowed to grow food crop on contaminated soil. Therefore, the agricultural soils we are targeting are low- or moderately-contaminated soils. Thus, it is also crucial to perform a sound analysis of heavy metals distribution within the harvested aerial part. As far as the shoot is concerned, Cd and Zn accumulation was higher in the stem than in the leaves when the bioavailability of heavy metals was high (Chapters 3, 4), while, under field conditions, heavy metals foliar concentrations tended to exceed stem concentrations suggesting that heavy metals transported by the xylem sap mainly accumulate in transpiring organs (Chapter 1). To the best of our knowledge, this is an innovative information because it clearly demonstrates that heavy metals distribution is a function of the external dose. These findings are confirmed by the results obtained in greenhouses conditions and presented in Appendix 1: plants obtained were 2 to 10 times more concentrated in Cd and Cd preferentially accumulated in stems rather than in leaves (independently from the cultivar used). As discussed below, when heavy metals concentration in plants reach a toxic level, plants have to trigger protective mechanisms that include free ions’ redistribution in plant. In any cases, heavy metals accumulation in leaves and stems point the importance to harvest hemp before natural leaf drop in order to maximize

heavy metals removal, and to consider with caution the use of produced fibres in relation to the risks of heavy metals dispersion during the retting process.

Ability of hemp to adapt to heavy metals stress conditions: roots and leaves

The crop sensitivity to heavy metals constitutes one of the major limitations of phytomanagement techniques and a critical challenge for agricultural productivity (Ghosh et al., 2017; Kosová et al., 2018). Heavy metals toxicity is a function of the total heavy metals' concentration in the growth medium, but also of their bioavailability and the exposure duration. It is also highly variable depending on the considered species, and within a species, even between cultivars. As far as hemp is concerned, Shi et al. (2012) already pointed out a high variability in the level of Cd bioaccumulation between 18 hemp accessions.

As demonstrated in Chapter 1 in natural field conditions with low environmental availability of heavy metals, hemp accumulated heavy metals but was unaffected (yield, photosynthesis) by the long-term exposure to soil contamination. However, one week of highly bioavailable (nutrient solution Cd (20 μM) or Zn (100 μM) exposure (Chapters 3, 4) induced, especially under Cd exposure, a range of morphological changes associated with altered water status, absorption of essential elements, as well as photosynthesis, resulting in a comparable range of growth inhibition and thus biomass production. However, in both cases, neither the maximal efficiency of photosystem II (F_v/F_m), the actual photosystem II efficiency (Φ_{PSII}), nor the photochemical quenching coefficient (qP) of the second fully expanded leaf were affected by Cd or Zn treatment, although at the biochemical level, Cd is thought to negatively affect photosystem reaction center II, while both Cd and Zn alter electron transport in other species (Rusinowski et al., 2019; Zhang et al., 2020). This suggests that hemp has a fascinating capacity to trigger protective mechanisms even if very high doses of heavy metals reduced photosynthetic pigments and proteins abundance. The underlying cause of this high level of resistance still has to be determined

The production of reactive oxygen species was also hastened by heavy metals, leading to lipid peroxidation, as illustrated by the increase in leaf malondialdehyde content in Cd treatment and the root malondialdehyde content with Zn. It is often (and erroneously) considered that malondialdehyde is a stable non-toxic product accumulating in plant tissue as a reliable indicator

of lipid peroxidation. This is an oversimplification because malondialdehyde is easy to quantify and thus used in a wide range of studies. malondialdehyde itself is a toxic molecule able to react with DNA and protein to form several different adducts. Cd stress, and to a lesser extent Zn toxicity, also decreased the abundance of a wide range of proteins regulating protein synthesis, while increasing numerous proteases' (Del Rio et al., 2005). Other indicators of oxidative stress may be recommended, such as carbonyl residues issued from protein oxidation (Altomare et al., 2021)

Roots and stems are of paramount importance for the whole survival of stressed plants. Roots are the first organ to have direct contact with heavy metals, regulate pollutant absorption, and transfer them to the shoot parts, while leaves provide energy for plant growth and control ion translocation through the regulation of transpiration. To minimize the detrimental effects of heavy metals, *C. sativa* activated a comparable range of reactions under Cd and Zn exposure, but the cellular targets involved were distinct and this is valid for both gene expression and protein abundance (Chapter 5). Furthermore, Cd obviously had a stronger impact than Zn on proteins involved in cell rescue and defense. Subsequently to heavy metal uptake, the main strategies activated by hemp to minimize the detrimental effects of heavy metals can be summarized as (a) free metal ions' management, (b) up-regulation of glycolysis and tricarboxylic acid cycles, and (c) cellular detoxification and repair.

Roots were found to be the major organ of Cd and Zn accumulation in hemp. According to the element localization patterns (Chapter 7), the main heavy metals detoxification mechanism in roots was heavy metals sequestration in the apoplast of cortex cells. Cell wall sequestration represents an efficient strategy to reduce Cd and Zn translocation to vascular cylinder and further transport into xylem, and it contributes to exclude heavy metals from metabolic pathways (Shiyu et al., 2020). In the current study, heavy metals sequestration in roots efficiently limited their translocation to aerial parts. Retention of heavy metals in the cell wall in Cd-treated plant was notably linked to increased lignification of cell wall making it less permeable for toxic ions (Pejic et al., 2009; Hu et al., 2010; Ye et al., 2012; Fernández et al., 2014; Vukcevic et al., 2014; Gutsch et al., 2019a; Nawaz et al., 2019), while in Zn-treated plants we hypothesized a precipitation of Zn with phosphate (co-localised, Chapter 7), and binding with pectate or histidyl groups (Wang et al., 2015b). Besides, endoderm suberization, which is frequently increased in heavy metals-treated plants to limit heavy metals

transfer to the above-ground parts (Pires-Lira et al. 2020; Shiyu et al., 2020), also appeared to be involved in the response to Zn toxicity (Zn accumulation in endodermis). It still has to be determined if plant exposure during heavy metals stress could modify cell wall composition in such a way that toxic ions could more efficiently be retained by the cell wall. Doudiche et al. (2010) showed that processes of methyl-esterification/de-esterification of homogalacturonan play a key role in heavy metals fixation to pectin and could be strongly influenced by the presence of Cd. Specific antibodies may constitute useful tools to identify specific targets that may be used for divalent cation fixation (Clausen et al., 2003).

These mechanisms, together with an increased abundance of several transcripts involved in cell rescue (proline biosynthesis, reactive oxygen species management) seemed to be effective to maintain oxidative stress in normal range (no increase in malondialdehyde content) in Cd-exposed plants, but not in Zn-exposed ones, in which glutathion produced in roots was probably allocated to reactive oxygen species detoxification rather than phytochelatin synthesis. It is noteworthy to notice that heavy metals chelation to phytochelatins may have been involved in hemp early response to Cd (increased synthesis and phytochelatin content), but in roots of Cd-treated plants S was mainly distributed in the vascular cylinder: this does not necessarily indicate that newly synthesized phytochelatins are translocated from the root to the shoot, and it is hard to explain the reasons for such translocation. At the root level, Cd- phytochelatin complexes are stored in root cell vacuoles, allowing to keep toxic Cd away from cytosolic enzyme, but to the best of our knowledge, a root-to-shoot translocation of phytochelatin has never been reported. In contrast, free cysteine or glutathion were frequently identified in the xylem sap and may account for the S signal detected in the root vascular structure (Verbruggen et al., 2009).

The situation appears somewhat different for Zn comparatively to Cd. In Zn-treated plants, the phytochelatin content indeed appeared lower in roots and higher in leaves. Previous studies performed on the Syrian beancaper *Zygophyllum fabago* demonstrated using K-edge extended X-ray absorption fine structure (EXAFS) that in Zn-treated roots, the Zn-O/C-C coordination was predominant and that only 14% of Zn was fixed to thiol groups (Lefèvre et al., 2016) while 77% of Cd was bound to thiol. The higher Zn- phytochelatin complex in leaves of our Zn-treated plants may result from phytochelatin synthesis occurring *de novo* at the leaf level: an increase in *PCSI* was observed in leaves (but also in roots) of Zn-treated plants and the used

precursor glutathion may be produced at this level, or translocated from the root but phytochelatins translocation itself remains unprobable since no identified PC transporter are identified at the root xylem loading site.

In leaves, free ions' management was also achieved via a decrease of CW permeability through an increase of the expression of genes involved in lignin biosynthesis (Cd: increased lignified areas) and heavy metals compartmentalization in vacuoles (increased phytochelatins synthesis (Zn) and content (Cd and Zn)). But heavy metals were also redistributed between cells through increased plasmodesmata permeability (via a decrease callose content), and, under Cd exposure, activation of vesicular trafficking. Distribution maps of heavy metals (ID21, PIXE) revealed that Cd was mainly accumulated in lignified collenchyma cells, while Zn was directed to spongy mesophyll and trichomes, which are metabolically less active parts of the plants. However, a proportion of heavy metals remained free to induce oxidative stress: while in roots only Zn was found to induce an increase of malondialdehyde production, malondialdehyde content in leaves increased following Cd exposure. Cd is a non-essential element whose BF reach 90 while Zn BF was around 50. This was thus not surprising that both treatments induced an increase of transcripts and proteins involved in reactive oxygen species detoxification, and that Cd also increased the abundance of aldo-keto reductase and aldehyde dehydrogenase for malondialdehyde decomposition. Moreover, since the overall photosynthetic capacity of hemp exposed to heavy metals was reduced, to maintain the growth and development and sustain defenses strategies, heavy metals-treated plants up-regulated glycolysis (Zn treatment) and tricarboxylic acid cycle (Cd treatment) (Chapters 5, 6). This might help the stressed plant produce more reducing power to compensate the high-energy demand of heavy metals-challenged cell (Hossain and Komatsu, 2013). Moreover, expression of Calvin cycle-linked transcripts (*RCA*, *RBCS*) increased under heavy metals stress, probably to counteract the negative effect of heavy metals on RuBisCO activity.

We can thus conclude that hemp exposure to highly bioavailable concentrations of heavy metals may strongly affect biomass production, although hemp was shown to be able to counteract many toxic effects of Cd and Zn. Such bioavailability in the field is unlikely to be encountered, but slower growth rate and decreased yield of cultivated plant could limit field applicability of combined phytomanagement and non-food production. The use of amendments to better guarantee the installation of a plant cover and improve crop yield can be advantageous. Biochars and compost can improve

soil properties while limiting the bioavailability of heavy metals (Forján et al., 2016; Mudloo et al., 2020). In our study, biochar and compost, applied separately were found to be an interesting option to reduce heavy metals content in valuable biomass, while increasing heavy metals extraction ($\text{g}\cdot\text{ha}^{-1}\cdot\text{year}^{-1}$) via yield increase.

Impact of heavy metals on fibre differentiation and characteristics in relation to heavy metal accumulation in stem

In addition to the restoration of soil quality and functions, phytotechnologies can produce valuable biomass that may integrate, under the conditions set by the regulations, industrial products with added value (Di Candito et al., 2004; Griga & Bjelková, 2013; Rhey et al., 2020). After hemp straw processing, different plant fractions are obtained: fibres (27-30% of above-ground biomass), hurds (45-55%) and powder (15-24%). In this thesis, a specific attention has been paid to the most economically valuable part of the plant: fibres (50% of the plant economic value; InterChanvre, 2017). The major factors that will impact the usability of the hemp fibres produced in the presence of soil contamination, include: the contaminant concentration and distribution in hemp raw material, and the impact of heavy metals on fibre yield and quality.

As discussed earlier, heavy metals accumulation depends on their bioavailability in the growth medium. When phytoavailability is low, as it was the case in field trials, heavy metals accumulation is commonly higher in the leaves than in the stem. In contrast, when bioavailability is high and in response to important heavy metals concentrations, these pollutants were found to be accumulated in stems and leaves and to a higher proportion in stems than in leaves. These results are not a consequence of the cultivar used (Santhica 27 in controlled conditions, Futura 75 in field experiments), as demonstrated in Appendix 2. Our results pointed out that in stems, an increase of pectin binding sites following Zn exposure could have led to an increased Zn accumulation in cell walls. Moreover, Cd is able to interact with hemp bast fibres during biosorption processes (Pejic et al. 2009; Vukčević et al. 2014). Zn distribution in stem (Chapter 7) was quite homogeneous, while Cd was mainly distributed in stem epidermis, and more specifically in trichomes. The contaminant concentration in fibres and hurds, assessed during field experiment also indicated that soil contamination did not lead to a significant

increase of heavy metals concentration in fibres comparatively to control, while stems Cd content was higher than control. This implies that the improvement of fibre quality recorded in material harvested in CLL comparatively to BB, mainly consisting in an increase of the force at break, and to an increase in breaking elongation, should not be regarded as directly linked to the presence of Cd in the fibre, but rather as a heavy metals-induced modification in fibre composition and structure occurring during fibre development as an indirect consequence of the presence of heavy metals.

However, although hemp fibres do not represent the main accumulation site of heavy metals, heavy metals content in fibres may exceed the requirements for clothes productions and thus represent a risk for human health. To safely use fibres obtained from a phytomanagement strategy, it is better to consider not to use them in clothes production but in combine material where heavy metals could not be set free such as insulating material and cement agglomerates in bioconstruction, as a sound absorbent material in the automotive industry (Ranalli and Venturi 2004; Panaitescu et al., 2016; Novakova 2018; Mazzanti et al., 2019; Moonart and Utara 2019; Abdellatef and Kavagic 2020). Besides, Cd accumulation in stem epidermis represent a risk of dissemination as a consequence of retting process occurring in the field (Bleuze et al., 2018; Réquillé et al., 2018). But considering heavy metals content in soil comparatively to heavy metals content in stems, it is more likely that it is rather the soil that may constitute a risk of contamination of the biomass produced during the retting process. Fortunately, some companies (EXIE) use the unretted stem for the production of insulating materials, thus avoiding the risks mentioned above. Interestingly, soil amendments, notably biochar or compost, used to improve yield on heavy metals contaminated soils (Chapter 1) may have a positive impact on fibre mechanical strength and thus respond to particular needs of industries. Nevertheless, this exciting perspective requires field assay conducted on several years to confirm the results obtained in this work. Other types of amendments such as the use of plant-growth-promoting bacteria (Pagnani et al., 2018) or mycorrhizal fungus (Citterio et al., 2005) also need to be tested in order to precise their impact on fibre development and heavy metal accumulation in hemp stem.

Besides, heavy metals accumulation in stem could also interact *in planta* with cell wall polymers during the process of bast fibres or hurds formation (Zhou et al. 2018; Gutsch et al. 2019a). In contrast to field trials, where both heavy metals are simultaneously present, the use of nutrient

solution allowed us to discriminate between the impact of Cd and Zn on molecular targets influencing secondary cell walls formation.

Cd and high concentrations of Zn reduced the diameter of primary bast fibres, suggesting that these pollutants may have a negative impact on fibre yield in *C. sativa*. This observation, however, was made at the young plant stage and field trials showed that, from a quantitative point of view, fibre yield was not drastically affected by heavy metals in moderately-contaminated site CLL. Moreover, Cd and Zn had an effect on bast fibres properties: we studied gene expression and protein abundance in the hypocotyls of 28 days-old plants. At this stage, secondary xylem and secondary bast fibres, together with primary bast fibres, undergo secondary cell walls deposition (Behr, 2018). Only a minor proportion of proteins was affected by both Cd and Zn. The data obtained suggest that the timing of fibre elongation and transition from elongation to thickening (*PDF1*, acid phosphatase, *AT1G04040*, *FLAs*) may be affected by heavy metals. Moreover, Cd negatively affected cellulose (*CesA4*, *CesA7* and *CesA8*) and lignin biosynthesis (class III peroxidases, *MET1* and *SAMS*, *COMT*, *CytP450*, *MTHFR*, *LAC4*, *CYP736A12*) and decreased substitution of xylan, the main hemicellulose of the SCW, which may contribute to a higher cell walls stiffness in fibres, while high concentrations of Zn had an opposite impact on cellulose metabolism. In the field experiment with plants grown four months on the heavy metal contaminated soil of CLL, the chemical composition of polymers was also found to be sensitive to heavy metals content in stems: fibres obtained in Chapter 1 were more concentrated in Pb (2x) than fibres obtained in Chapter 2, and were indeed found to have a slightly lower cellulose content (infra-red prediction) and higher force at break than control (Chapter 1). Beside the fact that molecular approach was performed at the young plant stage and considered very high doses of pollutants, it has to be mentioned that this approach was performed on whole stem segments and not on isolated bast fibres. A clear example is that Cd strongly reduced the abundance of enzymes involved in lignin biosynthesis (*COMT*, *CytP450*, *LAC4*,...) while it is well established that bast fibre contain very low lignin concentration, so that these modification should affect other cell types that the final product that will be harvest in the field.

Textile hemp has been cultivated for centuries for fibre production. However, *Cannabis sativa* is a multipurpose crop and other use may be considered, beside textile. From an economical point of view, identifying the end-use of the crop constitutes an essential element to be considered in the

implementation of combined phytomanagement and non-food production strategy. A cost-benefit-analysis of the economical efficiency of hemp crop grown on contaminated agricultural soil was performed as part as the project MisChar. As a whole, it suggested that, considering the limited agricultural surface to implement a phytomanagement strategy (usually about a dozen hectares), and the year-to-year variability in fibre production, it is preferable to harvest the fibres at seed maturity to benefit from the income derived from the sale of seeds and fibres. Current research shows that fibres harvested at seed maturity are less stiff and strong than fibres harvested at full-flowering. However, fibres harvested at a later stage still have an acceptable reinforcement potential, and it often makes little economic sense to not harvest the seeds (Jörg et al., 2020). Moreover, considering the heavy metals accumulation in leaves, and the negative impact that the presence of leaves may have on drying of the mown stems, the use of leaf/flower blower system mounted on the back side of the combine, just prior to mowing, could be of great interest for such a site. Leaf removal is also likely to increase the in-swath drying rate of the stems, thus minimizing the time for which the hemp crop occupies the field. In addition, the removal of the leaf also reduces the amount of material to be baled, stored, transported and processed, resulting in lower costs (Bruce et al., 2001). The flowers of the top parts could be used for nutraceuticals (CBD products) (HempFlax), while the seeds and leaves could be used for the production of energy. Indeed, the species has recently been recommended for the production of bioenergy with high capacity of production of ethanol and biodiesel (Parvez et al., 2021). Interestingly, biomass residues such as mixed leaves are an interesting source of biomethane (Matassa et al., 2020). According to Viswanathan et al. (2021), hemp is an ideal lignocellulosic plant for biofuel production and that its excellent properties allowed to produce energy at a low cost. Hemp could thus integrate a crop rotation with other non-food crops, such as rapeseed, soybean or cotton, used for biodiesel production on moderately contaminated substrates.

From an environmental point of view, however, we should always keep in mind that heavy metals are not degradable: we can just move them from one place to another place. Whatever the use of hemp material, the main question is still to determine the velocity of the heavy metal's displacement. If heavy metals are stored on fibre and hempcrete, we need to determine the stability of these material and to gain addition knowledge regarding the erosion of the final product since there is an obvious lack of information regarding this specific point.

Impact of Si on hemp responses and fibre development in stressed and unstressed plants

Any sustainable strategy helping the plant to cope with heavy metal toxicity could be usefully integrated in a phytomanagement scheme and this is especially the case for silicon application (Wu et al., 2013; Adrees et al., 2015; Imtiaz et al., 2016; Etesami and Jeong, 2018; Bhat et al., 2019). It is now well-established that Si is a non-essentially beneficial element contributing to abiotic stress resistance in a wide range of plant species (Epstein 1994; Kim et al. 2017; Luyckx et al. 2017a; Berni et al. 2020). Moreover, several Si derivatives (silane, siloxane, etc.) are used in industry to improve the mechanical properties and thermal stability of the harvested fibres (Abdelmouleh et al. 2004; Orue et al. 2016; Han et al. 2020). For example, the presence of SiO₂ in hemp woody fibres strengthens the bonds between fibres and lime in the manufacture of a lightweight and durable concrete-like material known as “hemcrete” (Luyckx et al. 2017a).

The present work was therefore undertaken in order to determine the impact of Si in the presence or absence of Cd and Zn on plant development and fibre differentiation in relation to heavy metal accumulation in young stem of *C. sativa*. The expression of genes regulating fibre development was analysed and the proteome of hypocotyls was characterized. Moreover, a field experiment was carried out to determine the impact of Si on hemp fibres mechanical properties.

These two strategies however strongly differ: in one case, Si was added to the nutrient solution and consequently absorbed by the roots while in the other case, Si was applied by spraying the leaf system. Most studies available in the literature consider Si application to the root system. Results may however be different regarding the type of substrate: in nutrient solution Si is fully available and the control of the pH allowed to maintain the bioavailability of heavy metals. In soil, however, due to the ability of silicate ions (SiO₃²⁻) to protonate, most of the silicate amendments are leaning alkalinity which may influence heavy metals availability (Rijkenberg and Depree 2010). Additionally, Si speciation in soil could promote polymerisation of SiO₃-slag that is a potential metal chelating agent (Naeem et al., 2018). Liang et al. 2005 clearly showed an increase in soil pH due to application of Si in the form of Na₂SiO₃ to the soil contaminated by Cd so that the beneficial effect of Si might be regarded as a decrease in Cd bioavailability rather than an improvement in plant tolerance to absorbed Cd.

The efficiency of Si foliar spraying is still a matter of debate. It partly depends on the capacity of Si to enter the plant through stomata, but also to the mobility of Si within the plant, especially in relation to the shoot-to-root translocation by the phloem. There is a crucial lack of information regarding these points. Zajackowska et al. (2021) compared soil and foliar application of Si in relation to reduction of Zn toxicity in wheat and concluded that foliar spraying is quite less efficient than soil application. Teixeira et al. (2021) also compared the two modes of application and found that although foliar Si absorption was quite low in comparison to root application, the physiological effect in relieving stress was equal in both cases: it has however to be mentioned that these authors focused on water deficit and not heavy metals stress, and that Si decreases water loss through the formation of a physical barrier of silica associated with cellulose in the leaf epidermis below the cuticula or precipitate near guard cells, which decreases transpiration. In a recent work, however, Zhou et al. (2021) reported a positive effect of Si spraying on Cd accumulation by plants, which could not be regarded as a consequence of a decrease in transpiration but rather to an effect of applied Si on transporters involved in Cd absorption.

The initial response to Si under nutritional stress is the uptake of supplied Si (Ali et al., 2020). The present work demonstrated that hemp is able to absorb Si from nutrient solution (Chapters 3,4) or soil substrate (Chapter 2) and passively translocate this element in stems and to a higher extent in leaves, even in the absence of Si application as observed in the field experiment. Hemp could thus be regarded as capable of absorbing and accumulating Si in its tissues, even if it is considered as a low Si accumulator in regards to the maximal level of Si accumulated in plant (around 0.5%). Moreover, when exposed to Si, plants grown in the presence of heavy metals accumulated higher Si concentrations in leaves than unexposed plants (Chapters 2, 3, 4) which might be regarded as an increase the need of Si for the induction of adaptative response. Heavy metals might thus have an impact on aquaporins involved in Si xylem (un)loading and intervascular transport, which may lead to a higher Si deposit as amorphous silica at the transpiration sites. Moreover, According to Ma et al. (2015) and to Kim et al. (2017), such a behavior suggests that increasing Si content may be regarded as an attempt to improve stress resistance.

The addition of Si had numerous beneficial impacts on hemp behaviour occurring rapidly after Cd or Zn stress application and before any modification in terms of growth. The main beneficial effects involved heavy

metals sequestration, improved oxidative response, and stimulation of energy metabolism. Besides, Si had only a marginal impact on control plants that were not exposed to heavy metals stress. This suggests that the response of the plant to Si application is completely different when plants are exposed to pollutants. It is well established that beneficial effects of Si are more evident in plants exposed to an (a)biotic stress, or able to accumulate high level of Si (Imtiaz et al., 2016; Guerriero et al., 2018)

In our study, accumulated Si mitigates metal toxicity by increasing heavy metals compartmentalization, especially under Cd exposure. In roots, Si increased Cd retention in the vicinity of the endodermis (Chapter 7), but distribution maps did not evidence co-localization with Si. We might thus expect that Si blocked the apoplastic bypass by enhancing suberization and lignification in root (Fleck et al. 2011; Pires-Lira et al. 2020). However, Si significantly reduced Cd and Zn accumulation in all organs including roots suggesting that Si impacted the heavy metals absorption process and not the translocation step. Besides, a co-precipitation of Si with Cd or Zn in the external medium is to be ruled out in our controlled conditions as Cd and Zn speciation were not affected by added Si, and remained soluble during the time course of the experiment (Chapters 3, 4). In leaves, Si induced Cd accumulation in non-secreting leaf trichomes, thus protecting the photosynthetic active parts of the plant. In stems Si was mainly concentrated in cell walls of trichomes, and could also be involved in Cd sequestration in this structure. Co-precipitation between Si accumulated within cell walls and Cd via a [Si-wall matrix]Cd co-complexation may occur (Krzeslowska, 2011) has already been suggested as a plausible explanation for the *in vivo* detoxification of Cd. Ma et al. (2015) already reported that a hemicellulose-bound form of silicon inhibits cadmium ion uptake in rice cells through increasing cell wall fixation.

But Si beneficial effect on toxic ion management is not only limited to the apoplasm. Our results highlighted a positive effect of Si on protein involved in vesicular trafficking. Neumann and zur Nieden (2001) demonstrated in the Zn-resistant plant *Arabidopsis halleri* that Zn transiently accumulates as silicate in vacuolar vesicles and to a lower extent in the cytosol before being translocated to vacuoles where Zn-silicates are slowly degraded to SiO₂.

Si also reduced lipid peroxidation by lowering malondialdehyde levels in roots, stimulated the antioxidant enzymes in leaves and roots of plants exposed to Cd (Chapter 5), and improved Cd and Zn sequestration on

thiol groups via stimulation of phytochelatin synthesis in the roots, thus decreasing oxidative stress. Moreover, a beneficial effect of Si on energy metabolism was observed under Cd exposure: light-dependent reactions (Fd), light-independent reactions (*FBPase* and *RCA* expression, *rbcS* abundance), glycolysis (G3PDH) and tricarboxylic acid cycle (IDH) were stimulated. In plants exposed to heavy metals, energy metabolism is of crucial importance to sustain cost of metabolic adaptations the plant needs to set up. Nevertheless, additional informations are urgently required to have a comprehensive approach regarding the impact of Si on gene expression and enzyme activities. Indeed, most of the Si recorded in plants appears as a precipitate: this could be the case at the endodermis levels, in the cell walls in various tissues, or at the transpiration sites and the most obvious illustration of this process consists in phytolith formation. Hence, the question still remains open “how can a solid precipitate could contribute to transduction pathways leading to obvious modification of cellular metabolism”. The fact that “solid Si” had so many effects on a plethora of metabolic functions remain puzzling. According to Katz (2014) however, there are indications that a small part of Si remains in the soluble form, as monosilicic acid that this low proportion is sufficient to trigger metabolic responses. In contrast to the environment, solubility of Si inside the tissues is difficult to determine (Khandekar and Leisner, 2011).

As mentioned before, field application of Si could improve fibres' quality (Abdelmouleh et al. 2004; Orue et al. 2016; Han et al. 2020). Si distribution mapping in stems of CdSi treatment indicated an accumulation of Si in bast fibres. Guerriero et al. (2019) clearly demonstrated that Si specifically present in the wall of bast fibres, and more precisely in the G-layer (Guerriero et al., 2019 and 2020). This specific distribution of Si in fibres may explain, in controlled conditions, the increase of fibres fineness (= bundles title) as well as fibres' breaking elongation after Si exposure. The same observations were reported with the commercial fibre jute after soil application of silicate (Khan and Roy, 1964). Under heavy metals exposure, Si application was also shown to have an impact on fibres mechanical properties, by counteracting the effects of soil contamination on fibre fineness and resistance. Diameter of bast fibre were also affected by Si exposure: both parameters increased in response to Si in Cd-treated plants. Moreover, Si application in Cd and Zn-treated plants was shown to have an influence on the timing of fibre elongation and transition from elongation to thickening (*PDF1*, *acid phosphatase*). This confirms that the presence of protecting Si confers a specific physiological status in relation to cell wall differentiation to heavy

metal-treated plants. Field trials (Chapter 2), however, demonstrated that Si by itself is probably not the only responsible for the improvement of fibre quality: indeed, force at break and breaking elongation increased to similar extent in Si and non-Si treated plants of CLL sites. Moreover, Si present on those fibres were only c.a. 25% of Si accumulated in fibres of plants from BB while these fibres exhibited lower quality for the considered parameter.

Conclusion and perspectives

The present study indicates that *C. sativa* is suited for fibre production associated with heavy metals (HM) management due to its extraction potential. However, this strategy should be limited to soils with a moderate content of HM. Indeed, high HM bioavailability had a negative impact on plant growth and development. Heavy metal exposure impacted fibre elongation and thickening, but not affected the mechanical properties of the fibre produced, and were mainly accumulated in trichomes rather than in fibres. Fibres may thus integrate, under the conditions set by the regulations, special products like insulating material and cements.

To devise agricultural strategies aimed at improving crop yield, the effect of silicon (Si) on plants' stress resistance was considered. Overall, we demonstrated that the addition of Si promoted tolerance against HM stress, through improved HM sequestration, oxidative response, and stimulation of energy metabolism. The beneficial effects of Si application were more pronounced when Si was applied to the root rather than to the foliar system. Further investigations are required to specify the advantages and disadvantages of both Si application methods, notably by comparing the two mode of application in similar plant growth conditions. Besides, Si accumulated in bast fibres and impacted cell wall differentiation in HM-treated plants. The application of Si during fibres' development could thus provide fibres with improved mechanical properties and thermal stability.

If this thesis demonstrated that hemp can be grown for fibre production on moderately contaminated agricultural soils, there remain a number of questions and challenges that still need to be considered for putting the strategy into practice. For instance, the potential risks associated with retting and the processing of harvested biomass: the soil may constitute a source of HM contamination of the biomass produced during the retting process, and the defibration of stems leads to dust formation that may contain HM and represent a risk for workers. Moreover, the stability of hemp material and the erosion of the final product need to be determined.

Besides, if this thesis focused on fibre production, the impact of HM on the production of other compounds of industrial (biofuels, ...) or pharmaceutical value (CBD) should be addressed to create new opportunities for the valorization of hemp and make phytoremediation of contaminated agricultural soils more attractive against traditional remediation techniques.

References

- Abdellatef Y. and M. Kavgić 2020. *Appl Thermal Eng.* 178 : 115-220.
- Abdelmouleh, M., Boufi, S., Belgacem, M. N., Duarte, A. P., Salah, A. B., & Gandini, A. (2004). Modification of cellulosic fibres with functionalised silanes: development of surface properties. *International Journal of Adhesion and Adhesives*, 24, 43-54.
- Adrees, M., Ali, S., Rizwan, M., Zia-ur-Rehman, M., Ibrahim, M., Abbas, F., ... & Irshad, M. K. (2015). Mechanisms of silicon-mediated alleviation of heavy metal toxicity in plants: a review. *Ecotoxicology and Environmental Safety*, 119, 186-197.
- Ahmad, P., & Prasad, M. N. V. (Eds.). (2011). *Environmental adaptations and stress tolerance of plants in the era of climate change*. Springer Science & Business Media.
- Ahmad, R., Tehsin, Z., Malik, S., T., Asad, S., A., Shahzad, M., Bilal, M., et al. (2016). Phytoremediation potential of hemp (*Cannabis sativa* L.): identification and characterization of heavy metals responsive genes. *CLEAN–Soil, Air, Water*, 44, 195-201.
- Ali, H., Khan, E., & Sajad, M. A. (2013). Phytoremediation of heavy metals—concepts and applications. *Chemosphere*, 91, 869-881.
- Ali, N., Réthoré, E., Yvin, J. C., & Hosseini, S. A. (2020). The regulatory role of silicon in mitigating plant nutritional stresses. *Plants*, 9, 1779.
- Altomare, A., Baron, G., Gianazza, E., Banfi, C., Carini, M., & Aldini, G. (2021). Lipid peroxidation derived reactive carbonyl species in free and conjugated forms as an index of lipid peroxidation: limits and perspectives. *Redox Biology*, 42, 101899.
- Angelova, V., Ivanova, R., Delibaltova, V., & Ivanov, K. (2004). Bio-accumulation and distribution of heavy metals in fibre crops (flax, cotton and hemp). *Industrial crops and products*, 19, 197-205.
- Poschenrieder, C., & Coll, J. B. (2003). Phytoremediation: principles and perspectives. *Contributions to science*, 333-344.
- Behr, M. (2018). *Molecular investigation of cell wall formation in hemp stem tissues* (Doctoral dissertation, UCL-Université Catholique de Louvain).
- Berni, R., Mandlik, R., Hausman, J. F., & Guerriero, G. (2021). Silicon-induced mitigatory effects in salt-stressed hemp leaves. *Physiologia Plantarum*, 171, 476-482.
- Bhat, J.A., Shivaraj, S.M., Singh, P., Navadagi, D.B., Tripathi, D.K., Dash, P.K., Solanke, A.U., Sonah, H., Deshmukh, R., (2019). Role of silicon in mitigation of heavy metal stresses in crop plants. *Plants*, 8, 71.
- Bleuze, L., Lashermes, G., Alavoine, G., Recous, S., & Chabbert, B. (2018). Tracking the dynamics of hemp dew retting under controlled environmental conditions. *Industrial crops and products*, 123, 55-63.

- Bokor, B., Vaculík, M., Slovák, L., Masarovič, D., & Lux, A. (2014). Silicon does not always mitigate zinc toxicity in maize. *Acta Physiologiae Plantarum*, *36*, 733-743.
- Bonatti, P. M., Ferrari, C., Focher, B., Grippo, C., Torri, G., & Cosentino, C. (2004). Histochemical and supramolecular studies in determining quality of hemp fibres for textile applications. *Euphytica*, *140*, 55-64.
- Bruce, D. M., Hobson, R. N., White, R. P., & Hobson, J. (2001). PM—Power and Machinery: Stripping of Leaves and Flower Heads to improve the Harvesting of Fibre Hemp. *Journal of agricultural engineering research*, *78*, 43-50.
- Chen, Y. E., Wu, N., Zhang, Z. W., Yuan, M., & Yuan, S. (2019). Perspective of monitoring heavy metals by moss visible chlorophyll fluorescence parameters. *Frontiers in plant science*, *10*, 35.
- Citterio, S., Prato, N., Fumagalli, P., Aina, R., Massa, N., Santagostino, A., ... & Berta, G. (2005). The arbuscular mycorrhizal fungus *Glomus mosseae* induces growth and metal accumulation changes in *Cannabis sativa* L. *Chemosphere*, *59*, 21-29.
- Clausen, M. H., Willats, W. G., & Knox, J. P. (2003). Synthetic methyl hexagalacturonate hapten inhibitors of anti-homogalacturonan monoclonal antibodies LM7, JIM5 and JIM7. *Carbohydrate Research*, *338*, 1797-1800.
- Del Rio, D., Stewart, A. J., & Pellegrini, N. (2005). A review of recent studies on malondialdehyde as toxic molecule and biological marker of oxidative stress. *Nutrition, metabolism and cardiovascular diseases*, *15*, 316-328.
- Di Candito, M., Ranalli, P., & Dal Re, L. (2004). Heavy metal tolerance and uptake of Cd, Pb and Tl by hemp. *Advances in Horticultural Science*, 138-144.
- Douchiche, O., Driouich, A., & Morvan, C. (2010). Spatial regulation of cell-wall structure in response to heavy metal stress: cadmium-induced alteration of the methyl-esterification pattern of homogalacturonans. *Annals of Botany*, *105*, 481-491.
- Epstein, E. (1994) The anomaly of silicon in plant biology. *PNAS*, *91*, 11-17.
- Etesami, H., & Jeong, B.R. (2018) Silicon (Si): Review and future prospects on the action mechanisms in alleviating biotic and abiotic stresses in plants. *Ecotoxicology and Environmental Safety* *147*, 881-896.
- Feng, W., Guo, Z., Xiao, X., Peng, C., Shi, L., Ran, H., & Xu, W. (2020). A dynamic model to evaluate the critical loads of heavy metals in agricultural soil. *Ecotoxicology and environmental safety*, *197*, 110607.
- Fernández, R., Fernández-Fuego, D., Bertrand, A., and González, A. (2014). Strategies for Cd accumulation in *Dittrichia viscosa* (L.) Greuter: role of the cell wall, non-protein thiols and organic acids. *Plant Physiol. Biochem.* *78*, 63-70.
- Ferrarini, A., Fracasso, A., Spini, G., Fornasier, F., Taskin, E., Fontanella, M.C., Beone, G.M., Amaducci, S. & Puglisi, E. (2021) Bioaugmented phytoremediation of metal-contaminated soils and sediments by hemp and giant reed. *Frontiers in Microbiology* *12*, 645893.

- Fleck, A. T., Nye, T., Repenning, C., Stahl, F., Zahn, M., & Schenk, M. K. (2011). Silicon enhances suberization and lignification in roots of rice (*Oryza sativa*). *Journal of Experimental Botany*, *62*, 2001-2011.
- Forján, R., Asensio, V., Vila, A. R., & Covelo, E. F. (2016). Contributions of a compost-biochar mixture to the metal sorption capacity of a mine tailing. *Environmental Science and Pollution Research*, *23*, 2595-2602.
- Ghosh, D., Lin, Q., Xu, J., & Hellmann, H. A. (2017). How plants deal with stress: exploration through proteome investigation. *Frontiers in plant science*, *8*, 1176.
- Griga, M., & Bjelková, M. (2013). Flax (*Linum usitatissimum* L.) and Hemp (*Cannabis sativa* L.) as fibre crops for phytoextraction of heavy metals: Biological, agro-technological and economical point of view. In *Plant-based remediation processes* (p. 199-237). Springer.
- Guerriero, G., Law, C., Stokes, I., Moore, K. L., & Exley, C. (2018). Rough and tough. How does silicic acid protect horsetail from fungal infection? *Journal of Trace Elements in Medicine and Biology*, *47*, 45-52.
- Guerriero, G., Deshmukh, R., Sonah, H., Sergeant, K., Hausman, J. F., Lentzen, E., et al. (2019). Identification of the aquaporin gene family in *Cannabis sativa* and evidence for the accumulation of silicon in its tissues. *Plant Science*, 110167.
- Guerriero, G., Stokes, I., Valle, N., Hausman, J.F., Exley, C., (2020). Visualising silicon in plants: histochemistry silica sculptures and elemental imaging. *Cells*, *9*, 1066.
- Gutsch, A., Vandionant, S., Sergeant, K., Jozefczak, M., Vangronsveld, J., Hausman, J. F., and Cuypers, A. (2019). Systems Biology of Metal Tolerance in Plants: A Case Study on the Effects of Cd Exposure on Two Model Plants. In *Plant Metallomics and Functional Omics*. Springer, Cham.
- Han, H. C., Gong, X. L., Zhou, M., Li, C., & Yang, H. B. (2021). A study about silane modification and interfacial ultraviolet aging of hemp fiber reinforced polypropylene composites. *Polymer Composites*, *42*, 2544-2555.
- HempFlax - Solutions from nature! « Discover the Hemp Plant ». Consulté le 10 novembre 2021. <https://www.hempflax.com/en/hempplant/>.
- Hossain, Z., & Komatsu, S. (2013). Contribution of proteomic studies towards understanding plant heavy metal stress response. *Frontiers in Plant Science*, *3*, 310.
- Hu, G., Huang, S., Chen, H., & Wang, F. (2010). Binding of four heavy metals to hemicelluloses from rice bran. *Food research international*, *43*, 203-206.
- Husain, R., Weeden, H., Bogush, D., Deguchi, M., Soliman, M., Potlakayala, S., ... & Rudrabhatla, S. (2019). Enhanced tolerance of industrial hemp (*Cannabis sativa* L.) plants on abandoned mine land soil leads to overexpression of cannabinoids. *PloS one*, *14*, e0221570.
- Imtiaz, M., Rizwan, M. S., Mushtaq, M. A., Ashraf, M., Shahzad, S. M., Yousaf, B., ... & Tu, S. (2016). Silicon occurrence, uptake, transport and mechanisms of

- heavy metals, minerals and salinity enhanced tolerance in plants with future prospects: a review. *Journal of environmental management*, 183, 521-529.
- InterChanvre (2017) : Plan filière de l'interprofession du chanvre, Plan submitted to the French Ministry of Agriculture—Recherche Google.* (s. d.). https://www.google.com/search?q=InterChanvre+%282017%29%3A+Plan+fili%C3%A8re+de+l%E2%80%99interprofession+du+chanvre%2C+Plan+submitted+to+the+French+Ministry+of+Agriculture&rlz=1C1PNJJ_frBE929BE929&sxsrf=ALeKk01BLuwSuiUo0zWTxFLDQ844QTXuRw%3A1619788994105&ei=wgSMYJr1BcicsAeyhZTgBA&oq=InterChanvre+%282017%29%3A+Plan+fili%C3%A8re+de+l%E2%80%99interprofession+du+chanvre%2C+Plan+submitted+to+the+French+Ministry+of+Agriculture&gs_lcp=Cgdnd3Mtd2l6EANQgqYKWIKmCmC_rApoAHACeACAAQCI AQCSAQCYAQQgAQKgAQGqAQdnd3Mtd2l6wAEB&sclient=gws-wiz&ved=0ahUKEwia3uqciKbwAhVIDuwKHbICBUwQ4dUDCA4&uact=5 (Accessed 29 April 2021)
- Jaskulak, M., Grobelak, A., & Vandenbulcke, F. (2020). Modelling assisted phytoremediation of soils contaminated with heavy metals—main opportunities, limitations, decision making and future prospects. *Chemosphere*, 249, 126196.
- Jörg, M., Amaducci, S., Alain, B., Johnny, B., & Shah, D. U. (2020). Transdisciplinary top-down review of hemp fibre composites: From an advanced product design to crop variety selection.
- Katz, O. (2014). Beyond grasses: the potential benefits of studying silicon accumulation in non-grass species. *Frontiers in Plant Science*, 5, 376.
- Keeping, M. G., & Reynolds, O. L. (2009). Silicon in agriculture: new insights, new significance and growing application. *Annals of Applied Biology*, 155, 153.
- Khan, D. H., & Roy, A. C. (1964). Growth, p-uptake, and fibre cell dimensions of jute plant as affected by silicate treatment. *Plant and Soil*, 331-336.
- Khandekar, S., & Leisner, S. (2011). Soluble silicon modulates expression of *Arabidopsis thaliana* genes involved in copper stress. *Journal of Plant Physiology*, 168, 699-705.
- Kim, Y. H., Khan, A. L., Waqas, M., & Lee, I. J. (2017). Silicon regulates antioxidant activities of crop plants under abiotic-induced oxidative stress: a review. *Frontiers in Plant Science*, 8, 510.
- Kos, B., Leštan, D. (2004) Soil washing of Pb, Zn and C using biodegradable chelator and permeable barriers and induced phytoextraction by *Cannabis sativa*. *Plant Soil*, 263:43–51
- Kosová, K., Vítámvás, P., Urban, M. O., Prášil, I. T., & Renaut, J. (2018). Plant abiotic stress proteomics: the major factors determining alterations in cellular proteome. *Frontiers in plant science*, 9, 122.
- Krzyszowska, M. (2011). The cell wall in plant cell response to trace metals: polysaccharide remodeling and its role in defense strategy. *Acta physiologiae plantarum*, 33, 35-51.

- Kumar S, Singh R, Kumar V, Rani A, Jain R (2017) *Cannabis sativa*: A Plant Suitable for Phytoremediation and Bioenergy Production. In: Baudh K, Singh B, Korstad J (eds) *Phytoremediation Potential of Bioenergy Plants*. Springer, Singapore, pp 269–285
- Lambrechts, T., Couder, E., Bernal, M. P., Faz, Á., Iserentant, A., & Lutts, S. (2011). Assessment of heavy metal bioavailability in contaminated soils from a former mining area (La Union, Spain) using a rhizospheric test. *Water, Air, & Soil Pollution*, 217, 333-346.
- Lefèvre, I., Vogel-Mikuš, K., Arčon, I., & Lutts, S. (2016). How do roots of the metal-resistant perennial bush *Zygophyllum fabago* cope with cadmium and zinc toxicities? *Plant and Soil*, 404, 193-207.
- Liang, Y., Wong, J. W. C., & Wei, L. (2005). Silicon-mediated enhancement of cadmium tolerance in maize (*Zea mays* L.) grown in cadmium contaminated soil. *Chemosphere*, 58, 475-483.
- Linger, P., Ostwald, A., & Haensler, J. (2005). *Cannabis sativa* L. growing on heavy metal contaminated soil: growth, cadmium uptake and photosynthesis. *Biologia plantarum*, 49, 567-576.
- Luyckx, M., Hausman, J. F., Lutts, S., & Guerriero, G. (2017a). Silicon and plants: current knowledge and technological perspectives. *Frontiers in plant science*, 8, 411.
- Luyckx, M., Hausman, J. F., Lutts, S., & Guerriero, G. (2017b). Impact of silicon in plant biomass production: focus on bast fibres, hypotheses, and perspectives. *Plants*, 6, 37.
- Ma, J. F., & Yamaji, N. (2015). A cooperative system of silicon transport in plants. *Trends in Plant Science*, 20, 435-442.
- Mahar, A., Wang, P., Ali, A., Awasthi, M. K., Lahori, A. H., Wang, Q., ... & Zhang, Z. (2016). Challenges and opportunities in the phytoremediation of heavy metals contaminated soils: a review. *Ecotoxicology and environmental safety*, 126, 111-121.
- Matassa, S., Esposito, G., Pirozzi, F., & Papirio, S. (2020). Exploring the biomethane potential of different industrial hemp (*Cannabis sativa* L.) biomass residues. *Energies*, 13, 3361.
- Mazzanti, V., Pariante, R., Bonanno, A., de Ballesteros, O. R., Mollica, F., & Filippone, G. (2019). Reinforcing mechanisms of natural fibers in green composites: Role of fibers morphology in a PLA/hemp model system. *Composites Science and Technology*, 180, 51-59.
- Moonart, U., & Utara, S. (2019). Effect of surface treatments and filler loading on the properties of hemp fiber/natural rubber composites. *Cellulose*, 26, 7271-7295.
- Mudhoo, A., Ramasamy, D.L., Bhatnagar, A., Usman, M., Sillanpää M. (2020) An analysis of the versatility and effectiveness of compost for sequestering metal ions, dyes and xenobiotics from soils and aqueous milieus. *Ecotoxicology and Environmental Safety*, 197, 110587.

- Naeem, A., Zia-ur-Rehman, M., Akhtar, T., Zia, M. H., & Aslam, M. (2018). Silicon nutrition lowers cadmium content of wheat cultivars by regulating transpiration rate and activity of antioxidant enzymes. *Environmental pollution*, 242, 126-135.
- Nawaz, M., A., Zakharenko, A., M., Zemchenko, I., V., Haider, M., S., Ali, M., A., Imtiaz, M., et al. (2019). Phytolith formation in plants: From soil to cell. *Plants* 8, 249.
- Neumann, D., & Zur Nieden, U. (2001). Silicon and heavy metal tolerance of higher plants. *Phytochemistry*, 56, 685-692.
- Nováková, P. (2018). Use of technical hemp in the construction industry. In *MATEC Web of Conferences* (Vol. 146, p. 03011). EDP Sciences.
- Orue, A., Jauregi, A., Unsuain, U., Labidi, J., Eceiza, A., & Arbelaiz, A. (2016). The effect of alkaline and silane treatments on mechanical properties and breakage of sisal fibers and poly (lactic acid)/sisal fiber composites. *Composites Part A: Applied Science and Manufacturing*, 84, 186-195.
- Pagnani, G., Pellegrini, M., Galieni, A., D'Egidio, S., Matteucci, F., Ricci, A., ... & Del Gallo, M. (2018). Plant growth-promoting rhizobacteria (PGPR) in *Cannabis sativa* 'Finola' cultivation: An alternative fertilization strategy to improve plant growth and quality characteristics. *Industrial crops and products*, 123, 75-83.
- Panaitecu, D. M., Nicolae, C. A., Vuluga, Z., Vitelaru, C., Sanporean, C. G., Zaharia, C., ... & Vasilevici, G. (2016). Influence of hemp fibers with modified surface on polypropylene composites. *Journal of Industrial and Engineering Chemistry*, 37, 137-146.
- Parvez, A. M., Lewis, J. D., & Afzal, M. T. (2021). Potential of industrial hemp (*Cannabis sativa* L.) for bioenergy production in Canada: Status, challenges and outlook. *Renewable and Sustainable Energy Reviews*, 141, 110784.
- Pejic, B., Vukcevic, M., Kostic, M., & Skundric, P. (2009). Biosorption of heavy metal ions from aqueous solutions by short hemp fibers: effect of chemical composition. *Journal of Hazardous Materials*, 164, 146-153.
- Pietrini, F., Passatore, L., Patti, V., Francocci, F., Giovannozzi, A., and Zacchini, M. (2019). Morpho-Physiological and metal accumulation responses of hemp plants (*Cannabis sativa* L.) grown on soil from an agro-industrial contaminated area. *Water*, 11, 808.
- Pires-Lira, M. F., de Castro, E. M., Lira, J. M. S., de Oliveira, C., Pereira, F. J., & Pereira, M. P. (2020). Potential of *Panicum aquaticum* Poir.(Poaceae) for the phytoremediation of aquatic environments contaminated by lead. *Ecotoxicology and environmental safety*, 193, 110336.
- Ranalli, P., & Venturi, G. (2004). Hemp as a raw material for industrial applications. *Euphytica*, 140, 1-6.

- Réquilé, S., Le Duigou, A., Bourmaud, A., & Baley, C. (2018). Peeling experiments for hemp retting characterization targeting biocomposites. *Industrial Crops and Products*, *123*, 573-580.
- Rheay, H. T., Omondi, E. C., & Brewer, C. E. (2020). Potential of hemp (*Cannabis sativa* L.) for paired phytoremediation and bioenergy production. *GCB Bioenergy*.
- Rijkenberg, M. J., & Depree, C. V. (2010). Heavy metal stabilization in contaminated road-derived sediments. *Science of the Total Environment*, *408*, 1212-1220.
- Rusinowski, S., Krzyżak, J., Sitko, K., Kalaji, H. M., Jensen, E., & Pogrzeba, M. (2019). Cultivation of C4 perennial energy grasses on heavy metal contaminated arable land: impact on soil, biomass, and photosynthetic traits. *Environmental Pollution*, *250*, 300-311.
- Saxena, G., Purchase, D., Mulla, S. I., Saratale, G. D., & Bharagava, R. N. (2019). Phytoremediation of heavy metal-contaminated sites : Eco-environmental concerns, field studies, sustainability issues, and future prospects. *Reviews of Environmental Contamination and Toxicology Volume 249*, 71-131.
- Shi, G., Liu, C., Cui, M., Ma, Y., & Cai, Q. (2012). Cadmium tolerance and bioaccumulation of 18 hemp accessions. *Applied biochemistry and biotechnology*, *168*, 163-173.
- Shiyu, Q. I. N., Hongen, L. I. U., Zhaojun, N. I. E., Rengel, Z., Wei, G. A. O., Chang, L. I., & Peng, Z. H. A. O. (2020). Toxicity of cadmium and its competition with mineral nutrients for uptake by plants: A review. *Pedosphere*, *30*, 168-180.
- Teixeira G.C.M., 2021. *Journal of Agronomy and Crop Science* (in press)
- Tóth, G., Hermann, T., Da Silva, M. R., & Montanarella, L. (2016). Heavy metals in agricultural soils of the European Union with implications for food safety. *Environment international*, *88*, 299-309.
- Vareda, J. P., Valente, A. J., & Durães, L. (2019). Assessment of heavy metal pollution from anthropogenic activities and remediation strategies: A review. *Journal of environmental management*, *246*, 101-118.
- Verbruggen, N., Hermans, C., & Schat, H. (2009). Molecular mechanisms of metal hyperaccumulation in plants. *New phytologist*, *181*, 759-776.
- Viswanathan, M. B., Cheng, M. H., Clemente, T. E., Dweikat, I., & Singh, V. (2021). Economic perspective of ethanol and biodiesel coproduction from industrial hemp. *Journal of Cleaner Production*, *299*, 126875.
- Vukčević, M., Pejić, B., Kalijadis, A., Pajić-Lijaković, I., Kostić, M., Laušević, Z., & Laušević, M. (2014). Carbon materials from waste short hemp fibers as a sorbent for heavy metal ions—Mathematical modeling of sorbent structure and ions transport. *Chemical Engineering Journal*, *235*, 284-292.
- Wang, P., Deng, X. J., Huang, Y. A., Fang, X. L., Zhang, J., Wan, H. B., Yang, C. Y. (2015). Comparison of subcellular distribution and chemical forms of 180 S. Y. QIN et al. cadmium among four soybean cultivars at young seedlings. *Environmental Science and Pollution Research*, *22*: 19584–19595.

- Wu, Y., Trejo, H. X., Chen, G., & Li, S. (2021). Phytoremediation of contaminants of emerging concern from soil with industrial hemp (*Cannabis sativa* L.): a review. *Environment, Development and Sustainability*, 1-31.
- Ye, J., Yan, C., Liu, J., Lu, H., Liu, T., & Song, Z. (2012). Effects of silicon on the distribution of cadmium compartmentation in root tips of *Kandelia obovata* (S., L.) Yong. *Environmental Pollution*, 162, 369-373.
- Zajaczkowska, A., Korzeniowska, J., & Sienkiewicz-Cholewa, U. (2020). Effect of soil and foliar silicon application on the reduction of zinc toxicity in wheat. *Agriculture*, 10, 522.
- Zhang, H., Xu, Z., Guo, K., Huo, Y., He, G., Sun, H., ... & Sun, G. (2020). Toxic effects of heavy metal Cd and Zn on chlorophyll, carotenoid metabolism and photosynthetic function in tobacco leaves revealed by physiological and proteomics analysis. *Ecotoxicology and Environmental Safety*, 202, 110856.
- Zhou, J., Zhang, C., Du, B., Cui, H., Fan, X., Zhou, D., & Zhou, J. (2021). Soil and foliar applications of silicon and selenium effects on cadmium accumulation and plant growth by modulation of antioxidant system and Cd translocation: Comparison of soft vs. durum wheat varieties. *Journal of Hazardous Materials*, 402, 123546.

Appendix

Appendix 1: Futura 75 grown in controlled conditions, in 5L pots filled with soil samples (BB, CLL) from the *in situ* experiment, and with or without foliar application of Si

The experimentation in field conditions during 2 consecutive years (Chapters 1, 2) has highlighted the variability of hemp behaviour depending on microclimatic conditions. Some trends observed in the results obtained during the first year were reversed during the second year of hemp cultivation. To precise the impact of the soil contamination and silicon application on hemp behaviour, we cultivated hemp in 5L pots (randomly distributed) filled with contaminated soil or control soil, in greenhouse conditions.

1. Material and Methods

1.1. Growing conditions

Soil samples from ploughed layer (0 - 25 cm) of two agricultural sites (Courcelles-lès-Lens, CLL (50°38'13" LN; 2°92'01"E), and Bois-Bernard, BB (50°41'62" LN; 3°02'78" E); France) were selected: CLL is located near (about 1 km to the southeast) a former lead and zinc smelter (Metaleurop), while BB is far enough from it (about 9 km southwest) not to be influenced by contaminated dust fallout and was taken as a control. The lead and zinc smelter Metaleurop closed in 2003 but previously released in the environment during decades dust particles responsible for HM contamination (mainly Cd, Zn and Pb) in the surroundings.

Before the beginning of the experiment the soils sampled from each site were characterized (detailed protocol in Chapter 2, section "Material and methods"). Total HM concentrations in CLL soil (5.5 ± 0.2 mg Cd, 396 ± 32 mg Zn, 298 ± 21 mg Pb kg^{-1} soil) exceeded, for Zn and Pb, the permissible limits (PL) recommended for agricultural use (10 mg Cd kg^{-1} , 250 mg Zn kg^{-1} , and 200 mg Pb kg^{-1} ; Tóth et al., 2016), while in BB soil, Cd and Zn concentrations were 5 times lower than in CLL and below the PL for Cd and Zn (1.1 ± 0.1 mg Cd, 80.9 ± 3.9 mg Zn per kg of soil). The presence of Pb in the topsoil of BB (285 ± 95 mg kg^{-1}) are linked to the presence of some shrapnel issued from World War I. Detailed soil analyses for both sites are provided in Table S2.1 of Chapter 2. In both BB and CLL, HM extraction with CaCl_2 0.01 M revealed very low environmental availability of Cd and Pb,

since their extractable concentration were below the detection limits of the flame atomic absorption spectrometer (0.05 mg kg⁻¹ for Cd, 0.65 mg kg⁻¹ for Pb). In both sites, the CEC was between 17.3 and 19.8 cmol kg⁻¹, and soil pH in CLL (7.9 ± 0.1) was slightly more alkaline than in BB (7.0 ± 0.2).

1.2. Plant material

Seeds of a monoecious hemp fibre variety (*Cannabis sativa* cv. Futura 75) were sown in 5L pots (arranged randomly) filled with soil of BB or CLL, in greenhouse conditions (22°C ± 2°C day and night, 60% ± 10% relative humidity and 16h photoperiod). Two weeks after sowing, 2 plants per pot were selected. Six weeks after sowing, half of the plants were sprayed with a solution of metasillicic acid (2 mM) once a week until harvest. Metasillicic acid was obtained from a pentahydrate sodium metasilicate (Na₂SiO₃ × 5 H₂O) which was passed through an H⁺ ion exchanger resin IR 20 Amberlite type according to Dufey et al. (2014). Four treatments were thus defined: BB (control soil sampled in Bois-Bernard), CLL (contaminated soil sampled in Courcelles-lès-Lens), BBSi (BB with Si exposure), CLLSi. Plants were harvested 4 months after sowing. On these plants, we evaluated morphological parameters (stem length and diameter, and fresh and dry weight of the leaves and stems), photosynthesis-related parameters, and harvested the leaves and stems in order to determine ion content.

1.3. Photosynthesis-related parameters

Before plant harvest photosynthesis-related parameters were measured on 5 plants per treatment, on the middle portion of the leaf blades constituting the second fully formed leaves from the top. fluorimeter (FMS II, Hansatech Instruments, Norfolk, UK) as detailed in Han et al. (2013). Chlorophyll fluorescence parameters (maximum quantum yield of photosystem II (F_v/F_m), photochemical quenching (q_p), non-photochemical quenching (NPQ) and actual efficiency of photosystem II (Φ_{PSII})) were considered.

Leaf stomatal conductance (g_s) was measured using an AP4 diffusion porometer (Delta-TDevices Ltd., Cambridge, UK). The instantaneous CO₂ assimilation under ambient conditions (400 ppm CO₂) (A) and instantaneous transpiration (E) were measured using an infrared gas analyzer (LCA4 8.7 ADC, Bioscience, Hertfordshire, UK). Gas exchanges were measured using a Parkinson leaf cuvette on intact leaves for 1 min (20 records min⁻¹) with an air flow of 300 mL min⁻¹. All measurements were performed around midday (between 12 a.m. and 2 p.m).

1.4. Mineral concentration in stems and leaves

For Cd, Pb and Zn quantification, 500 mg dry material (DM) were placed in an oven and heated to 500 °C for 48 h. The ashes were then digested in 68% HNO₃ and acid evaporated to dryness on a sand bath at 80°C. Minerals were incubated with a mix of HCl 37%-HNO₃ 68% (3:1; v/v) and the mixture was slightly evaporated and dissolved in distilled water, and filtered on Whatmann n°1 filter papers. For Si quantification, 1 g DM was placed in an oven and heated to 500 °C for 48 h. Ashes were then mixed with 0.4 g tetraborate and 1.6 g metaborate and heated to 1000 °C for 5 min. The obtained pellet was dissolved with 34% HNO₃. Cations were quantified by Inductively Coupled Plasma-Optical Emission Spectroscopy (Varian, type MPX). The metal bioaccumulation factor (BF) was defined, for each element, as the ratio between the mean value of HM concentration recorded in the whole aerial part divided by the mean value of total concentration in the soil.

1.5. Statistical analysis

Five replicates were analyzed for each condition. Normality of the data was verified using Shapiro-Wilk tests and the data were log-transformed when required. Homogeneity of the data was verified using Levene's tests. Two-way ANOVA were performed at a significant level of *P*-value < 0.05 using R (version 3.3.1) considering the soil contamination (BB, CLL) and Si application as main factors. Means were compared using Tukey's HSD all-pairwise comparisons at 5% level as a post-hoc test.

2. Results

2.1. Plant growth and morphological parameters

Table 1: Leaves and stems dry weight and water content of *C. sativa* (cv Futura 75). Plants were grown 4 months in 5L pots filled with HM contaminated soil of Courcelles-lès-Lens (CLL) or control soil of Bois-Bernard (BB), in the presence or in the absence of 2 mM H₂SiO₃ (Si). Data are means ± standard errors (n = 5). For each parameter and organ, values with different letters are significantly different at *P* < 0.05 according to the Tukey's HSD all-pairwise comparisons.

		BB	BBSi	CLL	CLLSi
Dry weight (g)	Leaves	1.68 ± 0.94 a	1.50 ± 0.55 a	1.50 ± 0.30 a	1.85 ± 0.30 a
	Stems	4.61 ± 1.00 a	3.76 ± 0.73 a	3.11 ± 0.64 a	4.02 ± 1.20 a
Water content (%)	Leaves	75 ± 2 a	74 ± 2 a	74 ± 2 a	72 ± 2 a
	Stems	62 ± 3 a	63 ± 1 a	63 ± 3 a	62 ± 1 a

Soil contamination tended to decrease both leaves and stem dry weight in *C. sativa*, but had no impact on the water content of leaves and stem (Table 1). Although not significant, a contrasting effect of exogenous Si was recorded in BB and CLL treatments: in BB treatment, Si tended to decrease leaves and stem dry weight while the opposite trend was observed in CLL treatment (Table 1). Plant exposure to Si had no impact on water content.

Soil contamination did not lead to a decrease of stem length but it slightly decreased stem diameter (Figure 1). Silicon had no impact on stem diameter but it slightly increased stem length in both BB and CLL treatments (Figure 1).

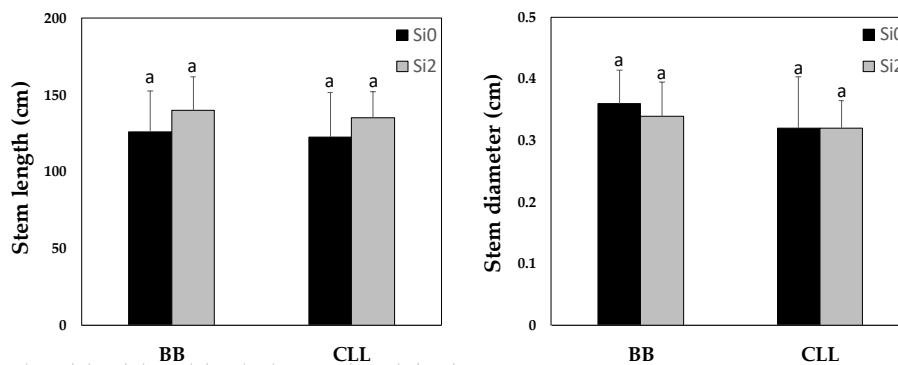


Figure 1: Stem length and diameter of *C. sativa* (cv Futura 75). Plants were grown 4 months in 5L pots filled with HM contaminated soil of Courcelles-lès-Lens (CLL) or control soil of Bois-Bernard (BB), in the presence or in the absence of 2 mM H_2SiO_3 (Si). Data are means \pm standard errors ($n = 5$). Values with different letters are significantly different at $P < 0.05$ according to the Tukey's HSD all-pairwise comparisons.

2.1. Photosynthesis-related parameters

Plant photosynthesis was not negatively influenced by soil contamination (Table 2). F_v/F_m , Φ_{PSII} , qP , C_i , E , A and SC remained constant in all treatments. Only a slight decrease of NPQ was recorded in CLL treatment comparatively to BB treatment (Table 2).

Table 2: Photosynthesis-related parameters of *C. sativa* (cv Futura 75). Plants were grown 4 months in 5L pots filled with HM contaminated soil of Courcelles-lès-Lens (CLL) or control soil of Bois-Bernard (BB), in the presence or in the absence of 2 mM H₂SiO₃ (Si). Data are means \pm standard errors (n = 5). Maximal efficiency of PSII photochemistry in the dark-adapted state (F_v/F_m), actual PSII efficiency (Φ_{PS2}), photochemical quenching coefficient (q_P), non-photochemical quenching (NPQ), CO₂ in intercellular spaces (C_i), instantaneous evapotranspiration (E), net photosynthesis (A), stomatal conductance (g_s). For each parameter, values with different letters are significantly different at $P < 0.05$ according to the Tukey's HSD all-pairwise comparisons.

	BB	BBSi	CLL	CLLSi
F_v/F_m	0.84 \pm 0.02 a	0.81 \pm 0.02 a	0.84 \pm 0.03 a	0.82 \pm 0.03 a
ϕ_{ps2}	0.73 \pm 0.05 a	0.68 \pm 0.04 a	0.72 \pm 0.08 a	0.73 \pm 0.02 a
q_P	0.94 \pm 0.03 a	0.92 \pm 0.03 a	0.92 \pm 0.05 a	0.94 \pm 0.01 a
NPQ	0.44 \pm 0.30 a	0.47 \pm 0.26 a	0.36 \pm 0.28 a	0.27 \pm 0.14 a
C_i ($\mu\text{mol mol}^{-1}$)	316 \pm 30 a	264 \pm 34 ab	293 \pm 20 ab	207 \pm 48 b
E ($\text{mmol H}_2\text{O m}^{-2}\text{s}^{-1}$)	0.95 \pm 0.50 a	1.07 \pm 0.50 a	1.03 \pm 0.40 a	0.93 \pm 0.50 a
A ($\mu\text{mol CO}_2 \text{m}^{-2} \text{s}^{-1}$)	1.28 \pm 0.40 a	2.25 \pm 0.50 a	1.92 \pm 0.50 a	2.79 \pm 0.80 a
g_s ($\text{mmol m}^{-2} \text{s}^{-1}$)	110 \pm 86 a	81 \pm 69 a	101 \pm 57 a	55 \pm 35 a

Similarly, Si had no significant impact on light-dependent reactions of photosynthesis, but it tended to increase net photosynthesis (A , Table 1) and to decrease CO₂ in intercellular spaces (C_i) and stomatal conductance (g_s , Table 1) in both BB and CLL treatments.

2.2. Plant mineral content

Cadmium, Pb and Zn were detected in plants of BB and CLL treatments (Table 3). In both treatments, Cd accumulated to higher concentration in the stem than in the leaves, while leaves were more concentrated in Pb and Zn. As expected, Cd and Pb leaves and stem concentrations in CLL treatment were significantly higher than in BB treatment. The additional presence of Si in CLL treatment significantly decreased Cd and Pb leaves and stem concentrations (Table 3). In BB treatment, Si exposure significantly decreased leaves Pb and Zn concentrations. Cadmium, Pb and Zn bioaccumulation factors were below 0.5 and Si significantly decreased Cd BF in CLL treatment (Table 3).

Table 3: Cadmium, lead and zinc concentration (in mg kg⁻¹ DW) in leaves and stems of *C. sativa* (cv Futura 75), and bioaccumulation factor (BF). Plants were grown 4 months in 5L pots filled with HM contaminated soil of Courcelles-lès-Lens (CLL) or control soil of Bois-Bernard (BB), in the presence or in the absence of 2 mM H₂SiO₃ (Si). Data are means ± standard errors (n = 5). For each element and organ, values with different letters are significantly different at *P* < 0.05 according to the Tukey's HSD all-pairwise comparisons.

		BB	BBSi	CLL	CLLSi
Cd (mg kg ⁻¹ DW)	Leaves	0.108 ± 0.012 <i>ab</i>	0.071 ± 0.008 <i>a</i>	0.272 ± 0.004 <i>c</i>	0.115 ± 0.011 <i>b</i>
	Stems	0.133 ± 0.000 <i>a</i>	0.150 ± 0.010 <i>a</i>	0.312 ± 0.046 <i>b</i>	0.179 ± 0.006 <i>a</i>
	BF	0.115 ± 0.003 <i>c</i>	0.116 ± 0.009 <i>c</i>	0.054 ± 0.005 <i>b</i>	0.029 ± 0.000 <i>a</i>
Pb (mg kg ⁻¹ DW)	Leaves	1.097 ± 0.039 <i>b</i>	0.889 ± 0.015 <i>a</i>	2.795 ± 0.040 <i>d</i>	2.101 ± 0.071 <i>c</i>
	Stems	0.914 ± 0.133 <i>a</i>	0.844 ± 0.004 <i>a</i>	2.115 ± 0.271 <i>b</i>	1.846 ± 0.071 <i>b</i>
	BF	0.003 ± 0.000 <i>a</i>	0.003 ± 0.000 <i>a</i>	0.008 ± 0.001 <i>b</i>	0.006 ± 0.000 <i>b</i>
Zn (mg kg ⁻¹ DW)	Leaves	62.63 ± 2.55 <i>b</i>	52.12 ± 0.21 <i>a</i>	63.91 ± 0.08 <i>b</i>	62.93 ± 1.23 <i>b</i>
	Stems	11.47 ± 3.06 <i>a</i>	13.88 ± 4.47 <i>a</i>	15.26 ± 7.92 <i>a</i>	14.04 ± 2.94 <i>a</i>
	BF	0.311 ± 0.019 <i>b</i>	0.306 ± 0.040 <i>b</i>	0.079 ± 0.013 <i>a</i>	0.074 ± 0.004 <i>a</i>

Silicon was detected in plants exposed to Si but also in unexposed plants. Silicon accumulated mainly in leaves. Unexpectedly, Si content tended to decrease in leaves and stem when unstressed and stressed plants were exposed to Si (Figure 2). It is noteworthy that soil contamination increased Si accumulation in the leaves and in the stem (Figure 2).

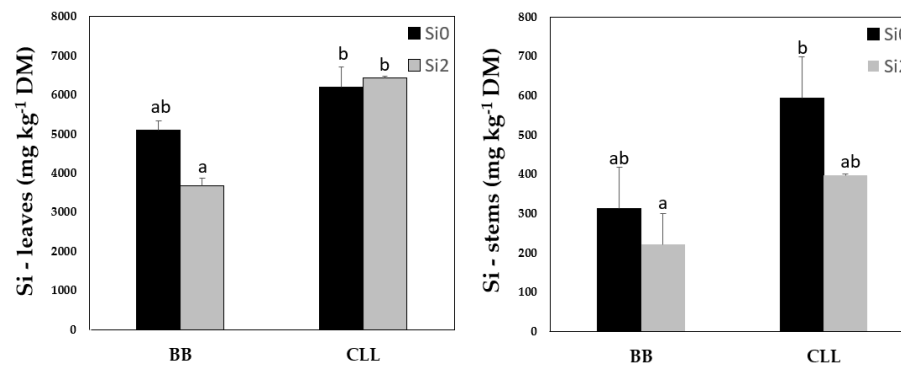


Figure 2: Silicon concentration (in mg kg⁻¹ DW) in leaves and stems of *C. sativa* (cv Futura 75). Plants were grown 4 months in 5L pots filled with HM contaminated soil of Courcelles-lès-Lens (CLL) or control soil of Bois-Bernard (BB), in the presence or in the absence of 2 mM H₂SiO₃ (Si). Data are means ± standard errors (n = 5). Values with different letters are significantly different at *P* < 0.05 according to the Tukey's HSD all-pairwise comparisons.

3. Discussion

Cd, Pb and Zn are well known environmental pollutants which negatively affect plant photosynthesis and biomass production. Si has frequently been reported to protect plants from various environmental stresses, including HM toxicity.

3.1. Plant growth and HM accumulation on contaminated soil

The present work in semi-controlled conditions on the soil samples from the *in situ* experiment (Chapter 2), confirmed that soil contamination in CLL had a limited impact on plant photosynthesis and biomass production. Soil contamination slightly reduced stem diameter, and in Chapter 2, a slight yield decrease was detected in CLL, suggesting that when hemp is exposed to high soil contamination, pollutants may have a negative impact on fibres and hurds yield. However, in the current study the impact of HM on photosynthesis and growth parameters were insignificant probably because of the low HM bioavailability: it is actually the accumulated HM that potentially alters the plant metabolism.

The present work indeed demonstrated a reduced HM transfer from soil to plants. Although not very bioavailable, the leaves of the plants obtained in CLL treatment contained more HM compared to those from the control treatment. Cd was mainly accumulated in the stem, while Pb and Zn were mainly accumulated in the leaves. We obtained a similar Cd distribution in Chapter 3 with plants grown in nutrient solution and exposed to 20 μM CdCl_2 . Cd is able to interact with hemp bast fibres during biosorption processes (Pejic et al. 2009; Vukcevic et al. 2014a, b) and may have a different accumulation behavior than Pb and Zn. But with such low HM contents in the plant, it is difficult to express an opinion on this hypothesis. Besides, in the *in situ* experiment (Chapter 2), Cd, Pb and Zn were mainly accumulated in leaves. The difference in Cd distribution between the two experiment is unexpected. However, plants obtained in the present study (for all treatments) were approximately 30% smaller, but exhibited foliar and stem Cd concentrations 2 to 10 times greater than those harvested *in situ* in 2018 (before any impact of wheat on HM bioavailability in 2019). They were also more concentrated in Pb (stems) and Zn (leaves) than plants harvested *in situ*, but to a lesser extent than with Cd (1,5 to 3 times more concentrated in Pb and Zn). We may hypothesize that the higher HM concentrations detected in plants grown in greenhouses conditions may be explained by the limited volume of soil (5L)

the roots had access to, comparatively to plants grown in the field whose roots may have reached, during the growing season, less contaminated layers of the soil. In any event, our results demonstrate that HM distribution in as function of the HM concentration in plants: when it starts to reach a toxic level, plants have to trigger protective mechanisms that include free ion's redistribution in plants.

3.2. Impact of Si on plant growth and HM accumulation

In the current study, foliar application of Si had no significant impact on the photosynthetic activity of hemp, although its application tended to increase net photosynthesis and to decrease C_i and g_s values in both BB and CLL treatments. In the *in situ* experiment (Chapter 2), similar results for C_i and g_s were obtained when plants exposed to Si were cultivated in the absence of soil contamination. We hypothesised in Chapter 2 that Si may have deposited as amorphous silica at the transpiration sites when the liquid fraction of the Si solution has evaporated, and caused partial occlusion of the stomata, resulting in a decrease of g_s (Zhu and Gong, 2004). However, such a decrease in g_s did not affect net photosynthesis since A values tended to increase. Pilon et al., (2013) also reported an increase photosynthesis after Si foliar application. A stimulation of Calvin cycle following Si exposure might have ensured net photosynthesis maintenance and also contributed to C_i decrease.

Besides, we demonstrated that, in control plants, Si slightly increased stem length, while it tended to decrease stem yield in the field experiment (Chapter 2). It has already been observed that in some plants, Si has a latent effect in the absence of an external stimulus (Fauteux et al., 2005). However, Si tended to have a beneficial effect on *C. sativa* growth parameters (leaves dry weight, stem dry weight and diameter) when plants were exposed to soil contamination. Moreover, in the *in situ* experiment, Si tended to increase yield of *C. sativa* grown on HM-contaminated soil of CLL. These results thus confirm that Si could be beneficial in the presence of soil contamination by counteracting the negative effects of HM on hemp yield. The increased biomass production under Si supplementation could be explained by an Si-mediated action on biosynthesis of phytohormone involved in plant growth (Luyckx et al., 2017a), or a decrease of HM accumulation in plants.

In the present work, foliar application of H_2SiO_3 significantly decreased Cd and Pb accumulation in leaves and stems of plants grown in CLL treatment, while it has an opposite effect in the field experiment. We mentioned above that HM concentration in plants grown in greenhouse

conditions was higher than those of plants grown *in situ*. We may suppose that, to deal with higher toxic ions exposure, Si decreased HM accumulation in plants. This idea is supported by the data obtained with plants grown in nutrient solution contaminated by 20 μM CdCl_2 (Chapter 3) or 100 μM ZnCl_2 (Chapter 4): we demonstrated that Si applied in the solution significantly reduced Cd and Zn accumulation in all organs including roots, suggesting that Si impacted the HM absorption process. In a recent work, Zhou et al., (2021) reported a positive effect of Si spraying on Cd accumulation by plants, which may result from an effect of applied Si on transporters involved in Cd absorption.

Furthermore, when exposed to Si, plants of CLL treatment accumulated higher Si concentrations in leaves and stems than controls, as already observed in the field experiment. In a previous experiment conducted in nutrient solution containing 2mM Si, plants exposed to Cd (Chapter 3) or Zn (Chapter 4) also accumulated higher Si concentrations in leaves than unexposed plants. If Si supplementation is beneficial for the development of plants subjected to HM stress, it is not surprising to observe an increase of Si accumulation in plants of CLL treatment compared to BB treatment. But surprisingly, foliar spraying of Si did not lead to increased Si contents in above-ground biomass, and even tended to decrease Si concentration in stems (BB and CLL). Silicon enters passively in plants with water, and we demonstrated that Si spraying tended to decrease g_s values in both BB and CLL: decreased stomatal conductance may have reduced Si accumulation in plants of BBSi and CLLSi treatments.

4. Conclusion

The present work in semi-controlled conditions on the soil samples from the *in situ* experiment, confirmed that soil contamination had a limited impact on plant photosynthesis and biomass production, probably because of the low HM bioavailability. As a consequence, plants accumulated limited amounts of HM. However, the concentrations detected were higher than those obtained *in situ*, resulting in a change of Cd distribution in aerial parts.

Besides, we demonstrated that the response of hemp to Si application is really sensitive to HM exposure. Indeed, beneficial effects of Si on plant growth and HM accumulation were more pronounced in plants grown *ex situ* (soil/nutrient solution contaminated with HM) than in plants grown *in situ*. The application of Si during cultivation to improve hemp behavior on

contaminated soils should therefore be investigated on a larger scale, comparing Si supply through soil amendment and foliar spraying.

Acknowledgement

This work was financed by ADEME (French Agency for the Environment and Energy Management); Convention MisChar n°1672C0044).

References

- Dufey, I., Gheysens, S., Ingabire, A., Lutts, S., & Bertin, P. (2014). Silicon application in cultivated rices (*Oryza sativa* L and *Oryza glaberrima* Steud) alleviates iron toxicity symptoms through the reduction in iron concentration in the leaf tissue. *Journal of agronomy and crop science*, 200, 132-142.
- Fauteux, F., Remus-Borel, W., Menzies, J. G., and Belanger, R. R. (2005). Silicon and plant disease resistance against pathogenic fungi. *FEMS Microbiology Letters*, 249, 1–6.
- Luyckx, M., Hausman, J. F., Lutts, S., & Guerriero, G. (2017). Impact of silicon in plant biomass production: focus on bast fibres, hypotheses, and perspectives. *Plants*, 6, 37.
- Pejic, B., Vukcevic, M., Kostic, M., & Skundric, P. (2009). Biosorption of heavy metal ions from aqueous solutions by short hemp fibers: effect of chemical composition. *Journal of Hazardous Materials*, 164, 146-153.
- Pilon, C., Soratto, R. P., & Moreno, L. A. (2013). Effects of soil and foliar application of soluble silicon on mineral nutrition, gas exchange, and growth of potato plants. *Crop Science*, 53, 1605-1614.
- Vukcevic, M., Pejic, B., Kaliajadis, A., Pajic-Lijakovic, I., Kostic, M., Lausevic, Z., Lausevic, M. (2014a). Carbon material from waste short hemp fibers as a sorbent for heavy metal ions – Mathematical modeling of sorbent structure and ions transport. *Chemical Engineering Journal*, 233, 284-292.
- Vukcevic, M., Pejic, B., Lausevic, M., Pajic-Lijaovic, I., Kostic, M., (2014b). Influence of chemically modified short hemp fiber structure on biosorption process of Zn²⁺ ions from waste water. *Fibers and Polymers*, 15, 687-697.
- Zhu, Y., Gong, H. (2014). Beneficial effects of silicon on salt and drought tolerance in plants. *Agronomy for Sustainable Development*, 34, 455–472.
- Zhou, J., Zhang, C., Du, B., Cui, H., Fan, X., Zhou, D., & Zhou, J. (2021). Soil and foliar applications of silicon and selenium effects on cadmium accumulation and plant growth by modulation of antioxidant system and Cd translocation: Comparison of soft vs. durum wheat varieties. *Journal of Hazardous Materials*, 402, 123546.

Appendix 2: Comparison of Santhica 27 and Futura 75 cultivars

Two different cultivars were used in this thesis: Santhica 27, in nutrient solution, and Futura 75, on an agricultural soil contaminated by atmospheric fallout from a smelter in Lille. Santhica 27 is the most used cultivar in Belgium for fibre production, while Futura 75 is most commonly used in the North of France (in recent years), and its integration into the MisChar project was part of the specifications.

The question therefore arises whether both cultivars behave in a comparable way when exposed to heavy metals (HM) and/or silicon (Si). Analysis of the technical documentation indeed shows that Santhica 27 and Futura 75 differ both in terms of early flowering, composition, production potential (fibres, straw) or fibre richness (Figures 1, 2; HEMP-it, catalogue variétal 2021).

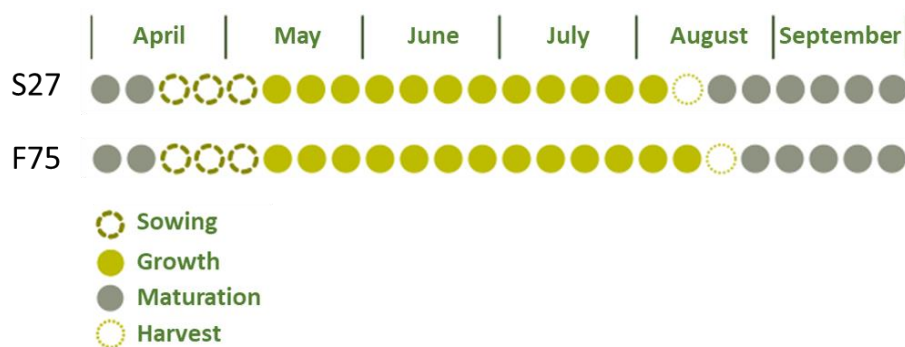


Figure 1: Comparison of cropping cycle of *Cannabis sativa* cv Santhica 27 and Futura 75 cultivars (HEMP-it, Catalogue variétal 2021 (<https://fr.calameo.com/read/0047134055d7ac7fd2049>)).

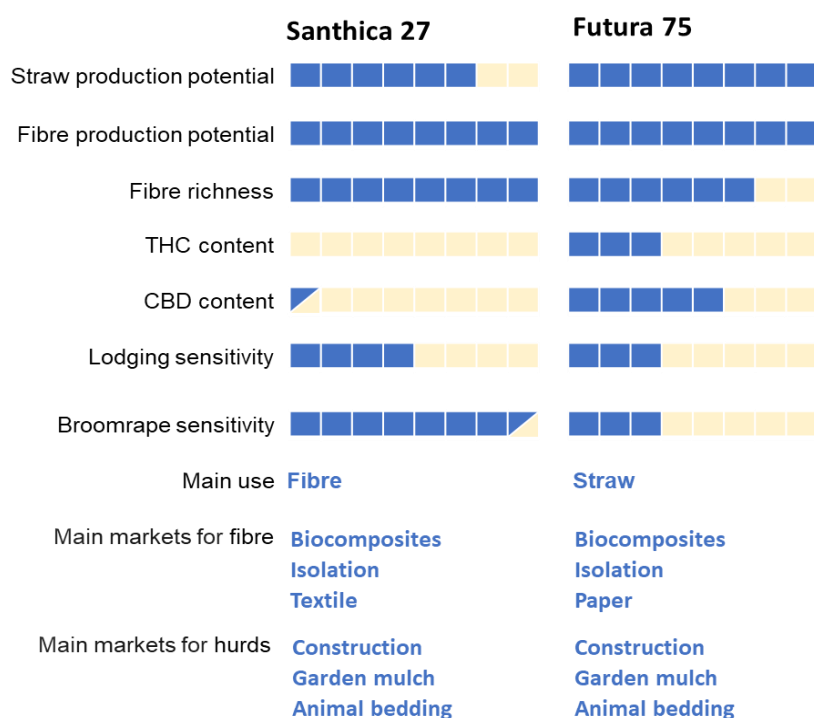


Figure 2: List of characteristics of *C. sativa* cv Santhica 27 and Futura 75 cultivars (HEMP-it, Catalogue variétal 2021 (<https://fr.calameo.com/read/0047134055d7ac7fd2049>)).

Hence, we analysed the behaviour of both cultivars growing in 5L pots (arranged randomly) filled with contaminated soil, in greenhouse conditions.

1. Material and Methods

1.1. Growing conditions

Soil samples from ploughed layer (0 - 25 cm) of two agricultural sites (Courcelles-lès-Lens, CLL (50°38'13" LN; 2°92'01"E), and Bois-Bernard, BB (50°41'62" LN; 3°02'78" E); France) were selected: CLL is located near (about 1 km to the southeast) a former lead and zinc smelter (Metaleurop), while BB is far enough from it (about 9 km southwest) not to be influenced by contaminated dust fallout and was taken as a control. The lead and zinc smelter Metaleurop closed in 2003 but previously released in the environment during decades dust particles responsible for HM contamination (mainly Cd, Zn and Pb) in the surroundings.

Before the beginning of the experiment the soils sampled from each site were characterized (detailed protocol in Chapter 2, section "Material and

methods”). Total HM concentrations in CLL soil (5.5 ± 0.2 mg Cd, 396 ± 32 mg Zn, 298 ± 21 mg Pb kg^{-1} soil) exceeded, for Zn and Pb, the permissible limits (PL) recommended for agricultural use (10 mg Cd kg^{-1} , 250 mg Zn kg^{-1} , and 200 mg Pb kg^{-1} ; Tóth et al., 2016), while in BB soil, Cd and Zn concentrations were 5 times lower than in CLL and below the PL for Cd and Zn (1.1 ± 0.1 mg Cd, 80.9 ± 3.9 mg Zn per kg of soil). The presence of Pb in the topsoil of BB (285 ± 95 mg kg^{-1}) are linked to the presence of some shrapnel issued from World War I. Detailed soil analyses for both sites are provided in Table S2.1 of Chapter 2. In both BB and CLL, HM extraction with CaCl_2 0.01 M revealed very low environmental availability of Cd and Pb, since their extractable concentration were below the detection limits of the flame atomic absorption spectrometer (0.05 mg kg^{-1} for Cd, 0.65 mg kg^{-1} for Pb). In both sites, the CEC was between 17.3 and 19.8 cmol kg^{-1} , and soil pH in CLL (7.9 ± 0.1) was slightly more alkaline than in BB (7.0 ± 0.2).

1.2. Plant material

Seeds of two monoecious hemp fibre varieties (*Cannabis sativa* cv. Santhica 27 and Futura 75) were sown in in 5L pots (arranged randomly) filled with soil of BB or CLL, in greenhouse conditions ($22^\circ\text{C} \pm 2^\circ\text{C}$ day and night, $60\% \pm 10\%$ relative humidity and 16h photoperiod). Two weeks after sowing, 2 plants per pot were selected. Six weeks after sowing, half of the plants were sprayed with a solution of metasillicic acid (2 mM) once a week until harvest. Metasillicic acid was obtained from a pentahydrate sodium metasilicate ($\text{Na}_2\text{SiO}_3 \times 5 \text{H}_2\text{O}$) which was passed through an H^+ ion exchanger resin IR 20 Amberlite type according to Dufey et al. (2014). Four treatments were thus defined: BB (control soil sampled in Bois-Bernard), CLL (contaminated soil sampled in Courcelles-lès-Lens), BBSi (BB with Si exposure), CLLSi. Plants were harvested 4 months after sowing. On these plants, we evaluated morphological parameters (stem length and diameter, and fresh and dry weight of the leaves and stems), photosynthesis-related parameters, and harvested the leaves and stems in order to determine ion content.

1.3. Photosynthesis-related parameters

Before plant harvest photosynthesis-related parameters were measured on 5 plants per treatment, on the middle portion of the leaf blades constituting the second fully formed leaves from the top. fluorimeter (FMS II, Hansatech Instruments, Norfolk, UK) as detailed in Han et al. (2013). Chlorophyll fluorescence parameters (maximum quantum yield of photosystem II (F_v/F_m),

photochemical quenching (q_p), non-photochemical quenching (NPQ) and actual efficiency of photosystem II (Φ_{PSII}) were considered.

Leaf stomatal conductance (g_s) was measured using an AP4 diffusion porometer (Delta-TDevices Ltd., Cambridge, UK). The instantaneous CO_2 assimilation under ambient conditions (400 ppm CO_2) (A) and instantaneous transpiration (E) were measured using an infrared gas analyzer (LCA4 8.7 ADC, Bioscience, Hertfordshire, UK). Gas exchanges were measured using a Parkinson leaf cuvette on intact leaves for 1 min (20 records min^{-1}) with an air flow of 300 $mL\ min^{-1}$. All measurements were performed around midday (between 12 a.m. and 2 p.m).

1.4. Mineral concentration

For Cd and Zn quantification, 50-100 mg dry material (DM) were placed in an oven and heated to 500 °C for 48 h. The ashes were then digested in 4 mL of 35% HNO_3 and acid evaporated to dryness on a sand bath at 80°C. The residue was redissolved with aqua regia (HCl 37%: HNO_3 65% 3:1) and filtered on Whatmann n°1 filter papers. Cations were quantified by flame atomic absorption spectrophotometry (ICE 3300; Thermo Scientific; Waltham, MA).

1.5. Statistical analysis

Five replicates were analyzed for each condition. Normality of the data was verified using Shapiro-Wilk tests and the data were log-transformed when required. Homogeneity of the data was verified using Levene's tests. Two-way ANOVA were performed at a significant level of P -value < 0.05 using R (version 3.3.1) considering the soil contamination (BB, CLL) and Si application as main factors. Means were compared using Tukey's HSD all-pairwise comparisons at 5% level as a post-hoc test.

2. Results

2.1. Plant growth and morphological parameters

Growth parameters of Santhica 27 were not statistically different from those of Futura 75, but some trends emerged. For a similar stem length, the DW of stems and leaves, measured (in BB and CLL) for Futura 75 was systematically higher than the DW of Santhica 27, while the WC followed the opposite trends.

Soil contamination had no significant impact on stem length, nor leaves and stems dry weight (DW) and water content (WC), and this is valid for both hemp cultivars (Figures 3,4). However, it tended to increase stems WC of Santhica 27, and to decrease stem DW of Futura 75.

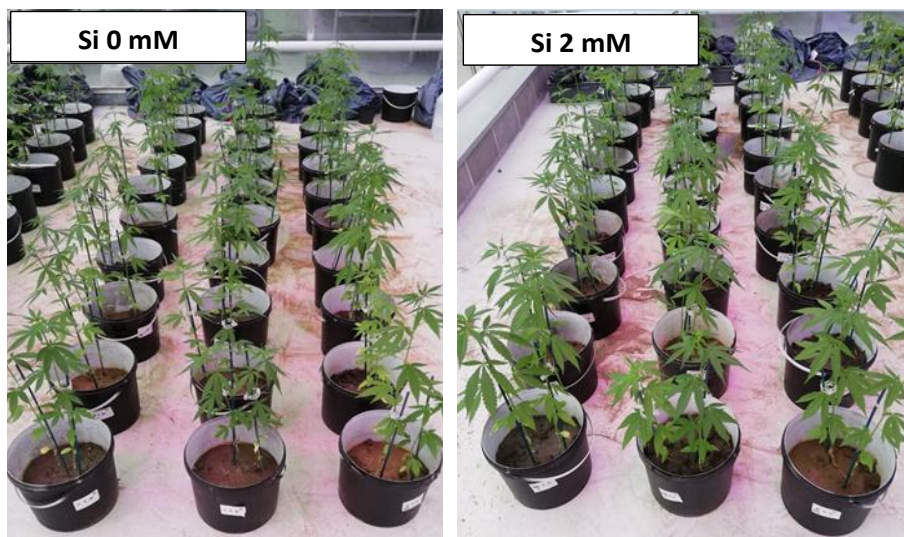


Figure 3: *C. sativa* cv Santhica 27 and Futura 75 grown in 5L pots (arranged randomly) filled with contaminated soil of Courcelles-lès-Lens or control soil of Bois-Bernard, in the presence or in the absence of 2 mM H_2SiO_3 (Si).

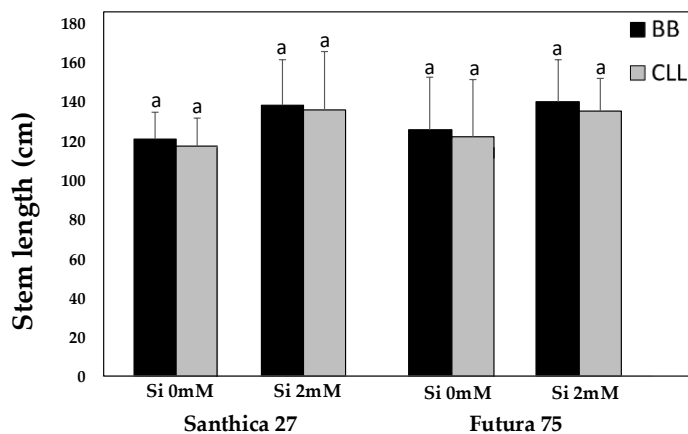


Figure 4: Stem length of *C. sativa* cv Santhica 27 and Futura 75. Plants were grown 4 months in 5L pots filled with HM contaminated soil of Courcelles-lès-Lens (CLL) or control soil of Bois-Bernard (BB), in the presence or in the absence of 2 mM H_2SiO_3 (Si). Data are means \pm standard errors ($n = 5$). Values with different letters are significantly different at $P < 0.05$ according to the Tukey's HSD all-pairwise comparisons.

In the absence of soil contamination, Si tended to increase stem length of both cultivars, and to decrease the leaves' DW of Santhica 27 and stems' DW of Futura 75. In the presence of soil contamination, Si slightly increased stem length of both cultivars. It also tended to decrease leaves' DW and stems WC of Santhica 27, while it increased leaves and stems' DW in Futura 75. Moreover, leaves WC seemed to be lower in Futura 75 exposed to Si, in the presence of soil contamination, comparatively to plants unexposed to Si.

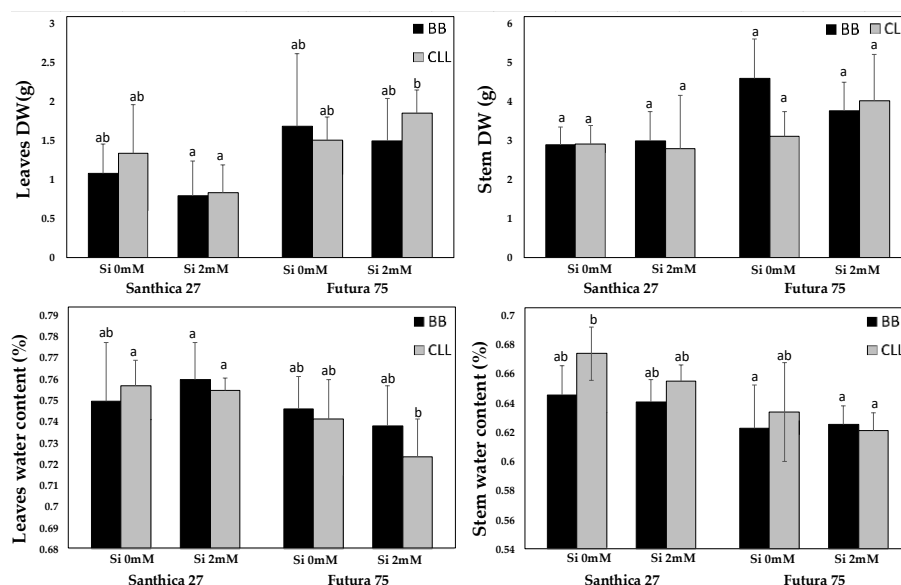


Figure 5: Leaves and stems dry weight (DW) and water content of *C. sativa* cv Santhica 27 and Futura 75. Plants were grown 4 months in 5L pots filled with HM contaminated soil of Courcelles-lès-Lens (CLL) or control soil of Bois-Bernard (BB), in the presence or in the absence of 2 mM H_2SiO_3 (Si). Data are means \pm standard errors (n = 5). Values with different letters are significantly different at $P < 0.05$ according to the Tukey's HSD all-pairwise comparisons.

2.2. Photosynthesis-related parameters

Plant photosynthesis was not significantly influenced by soil contamination (Figures 6, 7). However, for both cultivars grown in CLL soil, net photosynthesis (A) tended to be higher than in BB treatment, while CO_2 in intercellular spaces (C_i) and stomatal conductance (g_s) followed the opposite trend. Moreover, a slight decrease of NPQ was recorded in CLL treatment for Futura 75 cultivar.

Similarly, Si had no significant impact on photosynthesis, but it tended to increase A and to decrease C_i and F_v/F_m in BB and CLL treatments, and for both cultivars. Moreover, it decreased g_s in Futura 75 grown in BB

and CLL treatments, and increased E of Santhica 27 grown in BB or CLL soils.

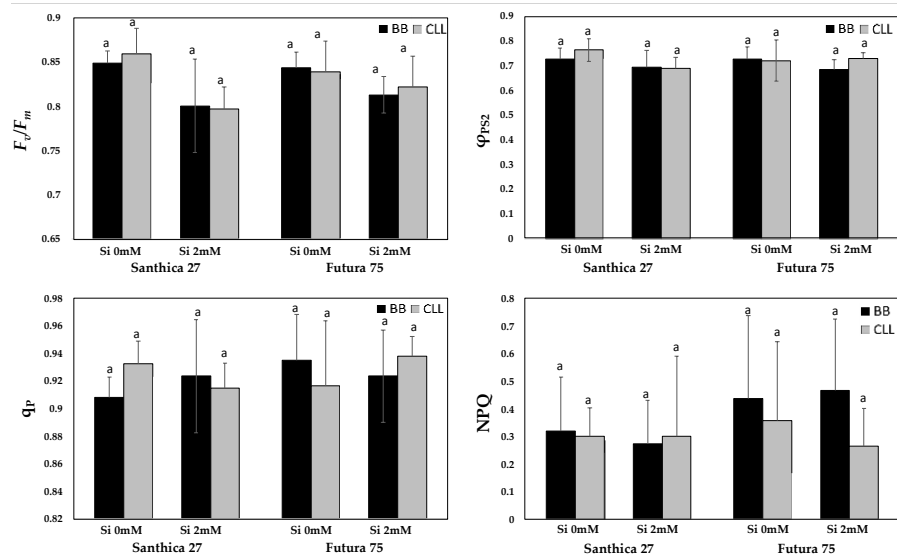


Figure 6: Light-dependent parameters of pphotosynthesis. *C. sativa* cv Santhica 27 and Futura 75 were grown 4 months in 5L pots filled with HM contaminated soil of Courcelles-lès-Lens (CLL) or control soil of Bois-Bernard (BB), in the presence or in the absence of 2 mM H_2SiO_3 (Si). Maximal efficiency of PSII photochemistry in the dark-adapted state (F_v/F_m), actual PSII efficiency (Φ_{PS2}), photochemical quenching coefficient (q_p), non-photochemical quenching (NPQ). Data are means \pm standard errors ($n = 5$). Values with different letters are significantly different at $P < 0.05$ according to the Tukey's HSD all-pairwise comparisons.

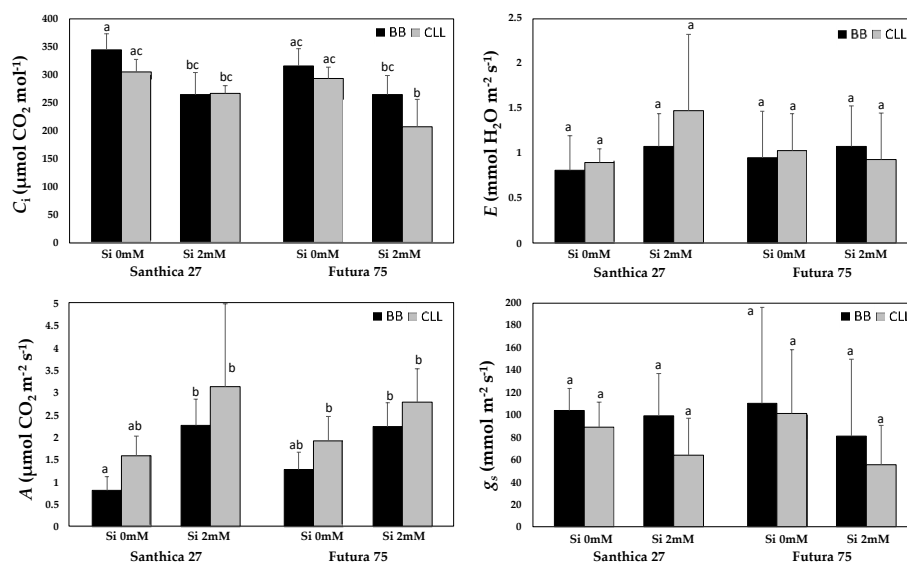


Figure 7: Light-independent parameters of pphotosynthesis. *C. sativa* cv Santhica 27 and Futura 75 were grown 4 months in 5L pots filled with HM contaminated soil of Courcelles-lès-Lens (CLL) or control soil of Bois-Bernard (BB), in the presence or in the absence of 2 mM H_2SiO_3 (Si). CO_2 in intercellular spaces (C_i), instantaneous evapotranspiration (E), net photosynthesis (A), stomatal conductance (g_s). Data are means \pm standard errors ($n = 5$). Values with different letters are significantly different at $P < 0.05$ according to the Tukey's HSD all-pairwise comparisons.

2.3. Plant Cd and Zn content

Cadmium concentrations were under the detection limits of the flame atomic absorption spectrophotometer used, and could not be precisely quantify in our samples. However, Zn was detected in hemp (Santhica 27 and Futura 75) grown on BB and CLL soils (Figure 8). In both treatments, Zn accumulated to higher concentration in leaves and seeds than in the stems. Soil contamination led to a significant increase of Zn leaves concentration for Santhica 27, while it did not significantly impact Zn concentrations in Futura 75.

The additional presence of Si in BB treatment tended to decreased Zn concentration in seeds of Santhica 27, while it tended to increase Zn concentration in stems of Futura 75. In the presence of soil contamination, Si exposure simultaneously significantly decreased Zn concentration in seeds and tended to increase Zn leaves concentrations in Santhica 27, while it tended to increase Zn concentration in seeds of Futura 75.

Besides, Futura 75 tended to be less concentrated in Zn than Santhica 27, especially in CLL treatment.

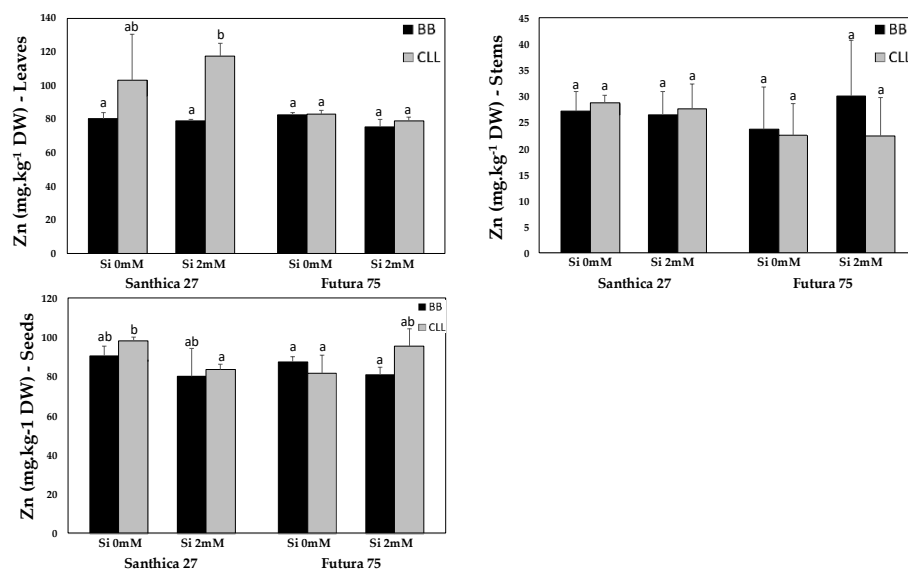


Figure 8: Zinc concentration (in mg.kg⁻¹ DW) in leaves, stems and seeds of *C. sativa* cv Santhica 27 and Futura 75. Plants were grown 4 months in 5L pots filled with HM contaminated soil of Courcelles-lès-Lens (CLL) or control soil of Bois-Bernard (BB), in the presence or in the absence of 2 mM H₂SiO₃ (Si). Data are means ± standard errors (n = 5). Values with different letters are significantly different at *P* < 0.05 according to the Tukey's HSD all-pairwise comparisons.

3. Discussion

Although the two cultivars studied are known to show differences in their cultural cycles, cultivation in 5L pots, in the absence of soil contamination, did not result in significant differences in morpho-physiological parameters, nor Zn accumulation (Figure 9). Only few trends emerged: leaves and stems DW, *q_P*, NPQ and *A* values tended to be higher for Futura 75, while leaves and stems WC and *C_i* followed the opposite trend. Futura 75 started to flower a week after Santhica 27 given more time to the plant for the vegetative growth, which probably explain higher DW values.

When plants were exposed to HM, both cultivars behaved in a similar way, with no major impact of HM on growth and photosynthesis. The only significant difference observed between the two cultivars consisted of an increased Zn accumulation in leaves of Santhica 27. This suggests that the two cultivars may differ in their ability to extract HM from soils. Nevertheless, it

is essential to keep in mind that Zn is essential for plant growth, and its accumulation in Santhica 27 did not lead to the appearance of toxic symptoms. The flame atomic absorption spectrophotometer used in this study did not allowed us to quantify Cd concentrations in plants, although we detected Cd in plants grown in similar conditions (soils from BB and CLL, greenhouses conditions; Appendix 1). In Appendix 1, we quantified ions through Inductively Coupled Plasma-Optical Emission Spectroscopy, with higher sensitivity to low concentrations of Cd in plants, but the machine was not available at the time of the experiment. The precise determination of Cd content in plant samples from the current study will provide more definitive results on the different ability of Santhica 27 and Futura 75 to extract HM from soils.

Parameter	Santhica 27 (S27)			S27 vs F75	Futura 75 (F75)		
	BBSi (vs BB)	CLL (vs BB)	CLLSi (vs CLL)		BBSi (vs BB)	CLL (vs BB)	CLLSi (vs CLL)
Stem length	↗	=	↗	=	↗	=	↗
DW leaves	↘	=	↘	<	=	=	↗
DW stems	=	=	=	<	↘	↘	↗
WC leaves	=	=	=	>	=	=	↘
WC stems	=	↗	↘	>	=	=	=
F_v/F_m	↘	=	↘	=	↘	=	↘
φ_{PSII}	=	=	=	=	=	=	=
q_p	=	=	=	<	=	=	=
NPQ	=	=	=	<	=	↘	=
C_i	↘	↘	↘	>	↘	↘	↘
E	↗	=	↗	=	=	=	=
A	↗	↗	↗	<	↗	↗	↗
g_s	=	↘	↘	=	↘	↘	↘
Zn leaves	=	↗	↗	=	=	=	=
Zn stems	=	=	=	=	↗	=	=
Zn seeds	↘	=	↘	=	=	=	↗

Figure 9: Summary of the results obtained in the current study. *C. sativa* cv Santhica 27 and Futura 75 were grown 4 months in 5L pots filled with HM contaminated soil of Courcelles-lès-Lens (CLL) or control soil of Bois-Bernard (BB), in the presence or in the absence of 2 mM H₂SiO₃ (Si). Significant results are represented by red arrows, non-significant results by black arrows. Similar trends between the two cultivars are colored in green, while opposite trends are colored in orange.

In the present work, foliar application of H₂SiO₃ had no significant impact on Santhica 27 and Futura 75 grown in the absence of soil contamination, and most of the trends observed were similar between both cultivars. However, in the presence of soil contamination, Si exposure induced a significant decrease of Zn concentration in seeds of Santhica 27, while we

observed the opposite trend in Futura 75. As mentioned above, Zn is essential for plant growth, and HM exposure did not lead to a change in Zn concentration in seeds comparatively to controls. Si may act on Zn distribution in Santhica 27 as it decreased Zn accumulation in seeds but increased its accumulation in leaves. Such an increased accumulation in leaves was not observed in Futura 75.

4. Conclusion

To conclude, both cultivars were comparable in terms of growth and photosynthesis parameters. They also both behaved in a similar way when exposed to HM and or Si, except a significant increase of Zn accumulation in leaves in CLL treatment, and a decreased Zn accumulation in seeds in CLLSi treatment, for Santhica 27. Zn is essential for plant growth. Thus the precise quantification of non essential ions (Cd and Pb) is needed to specify if a difference exists in the ability of Santhica 27 and Futura 75 to extract HM, and the consequent effect of Si on their distribution in plants.

Acknowledgement

This work was financed by ADEME (French Agency for the Environment and Energy Management); Convention MisChar n°1672C0044).

References

- Dufey, I., Gheysens, S., Ingabire, A., Lutts, S., & Bertin, P. (2014). Silicon application in cultivated rices (*Oryza sativa* L and *Oryza glaberrima* Steud) alleviates iron toxicity symptoms through the reduction in iron concentration in the leaf tissue. *Journal of agronomy and crop science*, 200, 132-142.
- HEMP-it, Catalogue variétal 2021. Recherche Google. (s.d.). <https://fr.calameo.com/read/0047134055d7ac7fd2049> (Accessed 12 October 2021).